NASA/CP—1998-206958

Minnowbrook II
1997 Workshop on Boundary Layer Transition in Turbomachines

June 1998

The NASA STI Program Office . . . in Profile

Since its founding, NASA has been dedicated to the advancement of aeronautics and space science. The NASA Scientific and Technical Information (STI) Program Office plays a key part in helping NASA maintain this important role.

The NASA STI Program Office is operated by Langley Research Center, the Lead Center for NASA's scientific and technical information. The NASA STI Program Office provides access to the NASA STI Database, the largest collection of aeronautical and space science STI in the world. The Program Office is also NASA's institutional mechanism for disseminating the results of its research and development activities. These results are published by NASA in the NASA STI Report Series, which includes the following report types:

- TECHNICAL PUBLICATION. Reports of completed research or a major significant phase of research that present the results of NASA programs and include extensive data or theoretical analysis. Includes compilations of significant scientific and technical data and information deemed to be of continuing reference value. NASA's counterpart of peer-reviewed formal professional papers but has less stringent limitations on manuscript length and extent of graphic presentations.

- TECHNICAL MEMORANDUM. Scientific and technical findings that are preliminary or of specialized interest, e.g., quick release reports, working papers, and bibliographies that contain minimal annotation. Does not contain extensive analysis.

- CONTRACTOR REPORT. Scientific and technical findings by NASA-sponsored contractors and grantees.

- CONFERENCE PUBLICATION. Collected papers from scientific and technical conferences, symposia, seminars, or other meetings sponsored or cosponsored by NASA.

- SPECIAL PUBLICATION. Scientific, technical, or historical information from NASA programs, projects, and missions, often concerned with subjects having substantial public interest.

- TECHNICAL TRANSLATION. English-language translations of foreign scientific and technical material pertinent to NASA's mission.

Specialized services that complement the STI Program Office's diverse offerings include creating custom thesauri, building customized data bases, organizing and publishing research results . . . even providing videos.

For more information about the NASA STI Program Office, see the following:

- Access the NASA STI Program Home Page at ***http://www.sti.nasa.gov***

- E-mail your question via the Internet to help@sti.nasa.gov

- Fax your question to the NASA Access Help Desk at (301) 621-0134

- Telephone the NASA Access Help Desk at (301) 621-0390

- Write to:
  NASA Access Help Desk
  NASA Center for AeroSpace Information
  800 Elkridge Landing Road
  Linthicum Heights, MD 21090-2934

NASA/CP—1998-206958

Minnowbrook II
1997 Workshop on Boundary Layer Transition in Turbomachines

John E. LaGraff and David E. Ashpis, editors

Proceedings of a workshop
held at the Minnowbrook Conference Center,
Syracuse University
Syracuse, New York
September 7–10, 1997

National Aeronautics and
Space Administration

Lewis Research Center

June 1998

Acknowledgments

Workshop Sponsors

The workshop co-chairs would like to express their appreciation for financial support given to the workshop and to participants by the following groups and individuals:

US Air Force Office of Scientific Research
(Jim McMichael, Mark Glauser, Grant AFOSR-F49620-97-0524)

European Office of Aerospace Research and Development
(USAFOSR-Mark Maurice, Charbel Raffoul, Window-on-Science Program)

NASA Lewis Research Center
(Lou Povinelli, David Ashpis, Grant NASA-NAG3-1982)

Asian Office of Aerospace Research and Development
(USAFOSR-Shiro Fujishiro, Window-on-Science Program)

Syracuse University
Vice President, Research and Computing (Ben Ware)
Dean of Engineering and Computer Science (Edward Bogucz)

Local Organizing Support

Special praise is due to Ms. Vicky McKee-Banas who devoted long hours and great care to the processing of the hundreds of details required for a successful workshop. Acknowledgment for help with logistics by students Leonardo Biagioni and Greg Lisnyczyj is also well deserved.

Proceedings

Special thanks to Lori Feher, Editorial Assistant, and to Caroline Rist, Publishing Coordinator, of LTID Publishing Services at NASA Lewis, for their dedication in producing this volume.

Available from

NASA Center for Aerospace Information
800 Elkridge Landing Road
Linthicum Heights, MD 21090-2934
Price Code: A23

National Technical Information Service
5287 Port Royal Road
Springfield, VA 22100
Price Code: A23

PREFACE

On September 7-10, 1997, over forty attendees participated in a workshop entitled "Minnowbrook II – 1997 Workshop on Boundary Layer Transition in Turbomachines".

Workshop Co-Chairs were:

John E. LaGraff - Syracuse University
Terry V. Jones - Oxford University
J. Paul Gostelow - University of Leicester

The sessions were held at the Syracuse University Minnowbrook Conference Center in Blue Mountain Lake, New York, and followed the theme, venue and format of an earlier workshop in 1993 (Minnowbrook I). The theme focused on improving the understanding of late stage (final breakdown) boundary layer transition. The specific engineering application of improving design codes for turbomachinery was encouraged by the attendance of representatives from gas turbine manufacturers.

The format of the workshop was intentionally kept informal, to encourage presentations which could include a wide range of material spanning a level of formality from previously published work to work-in-progress or even future/proposed work. We did not want to inhibit presentation of relevant material for artificial reasons of normal publication restrictions. Written papers were not requested. Abstracts and copies of figures were the only written record of the workshop aside from a specifically commissioned summation paper prepared after the workshop and transcriptions of the extensive working group reports and discussions that followed on the final morning of the workshop. The format of the workshop was also unusual in that nearly as much time was allowed for discussions as was allowed for the presentations. Groupings of three or four papers were followed by a large block of discussion time.

This volume contains abstracts and copies of the viewgraphs presented, organized according to the workshop sessions. The post-workshop summary and the plenary-discussion transcript clearly highlight the need for continued vigorous research in the technologically important area of transition in turbomachines.

John E. LaGraff

David E. Ashpis

Editors

TABLE OF CONTENTS

MINNOWBROOK I AND AFTER

Roddam Narasimha
Indian Institute of Science
Bangalore, India

CONTENTS

TRANSITION IN TURBOMACHINES

3D (in the mean), compound curvature

Unsteady, with length/time scales >> "large eddy" scales

"Harsh" environment: highly disturbed, in different modes

"Awkward" Reynolds numbers (+/-)

CONSEQUENCES

Separation
Bubbles
Reattachment
Transition
Relaminarization
Retransition ...

⇒ A VERITABLE **B. L. ZOO**

THEMES IN M'B 1

1. SPOTS

"Spot-less" transition relevant?

Spot birth:

non-linear endgames, mechanisms

Kendall : Gaster : Emmons

locations | as affected by
rates | pres. grad. + ...

Spot propagation:

celerities | with pres. grad.
spread rates | - "spotlets" vs. "new vortices"

trajectories (in 3D flows)

Spots vs. "slabs"

- in periodically wake-induced transition

Interacting spots

"Calming":

NASA/CP—1998-206958

MODELLING

With or without streamwise intermittency γ?

- intermittency distributions, with or without "sub-transitions"?

"Best" modifications of $K\varepsilon$, $K\omega$, RST, eddy viscosity ...

More elaborate modelling

DNS

STABILITY

Relevant at all in turbomachines?

"TS waves" vs. "linear response"

"Klebanoff" modes

Receptivity

"Bypass"

PSE ...

Absolute (global) vs. convective

CHAOS

Not relevant or Not fruitful ?

THE STANDARD HYPOTHESIS

SPOTS IN DIVERGING CONSTANT-PRESSURE FLOW

(Jahanmiri, Prabhu & Narasimha 1996 JFM 329:1-24)

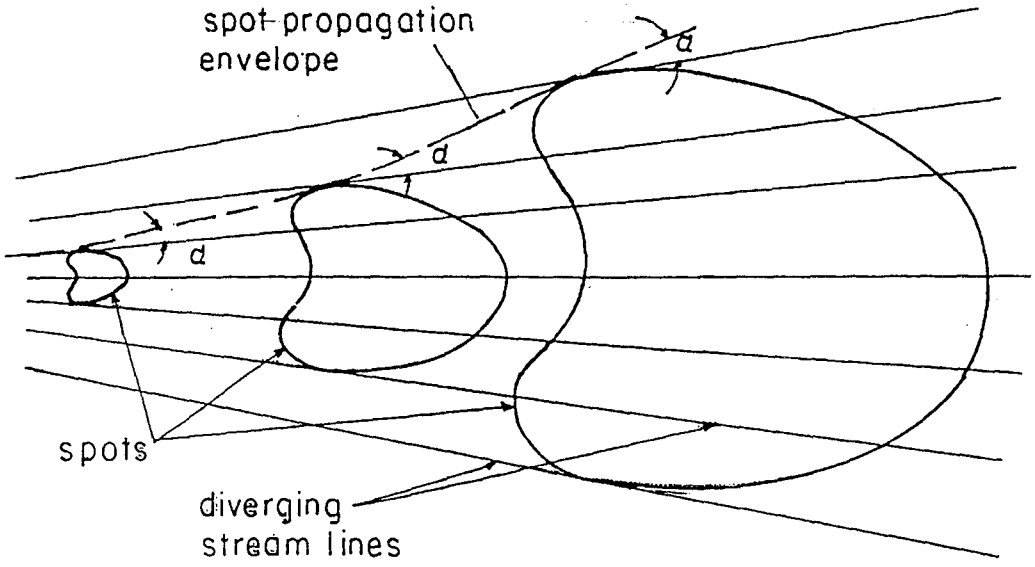

THE EXPERIMENTAL SET-UP

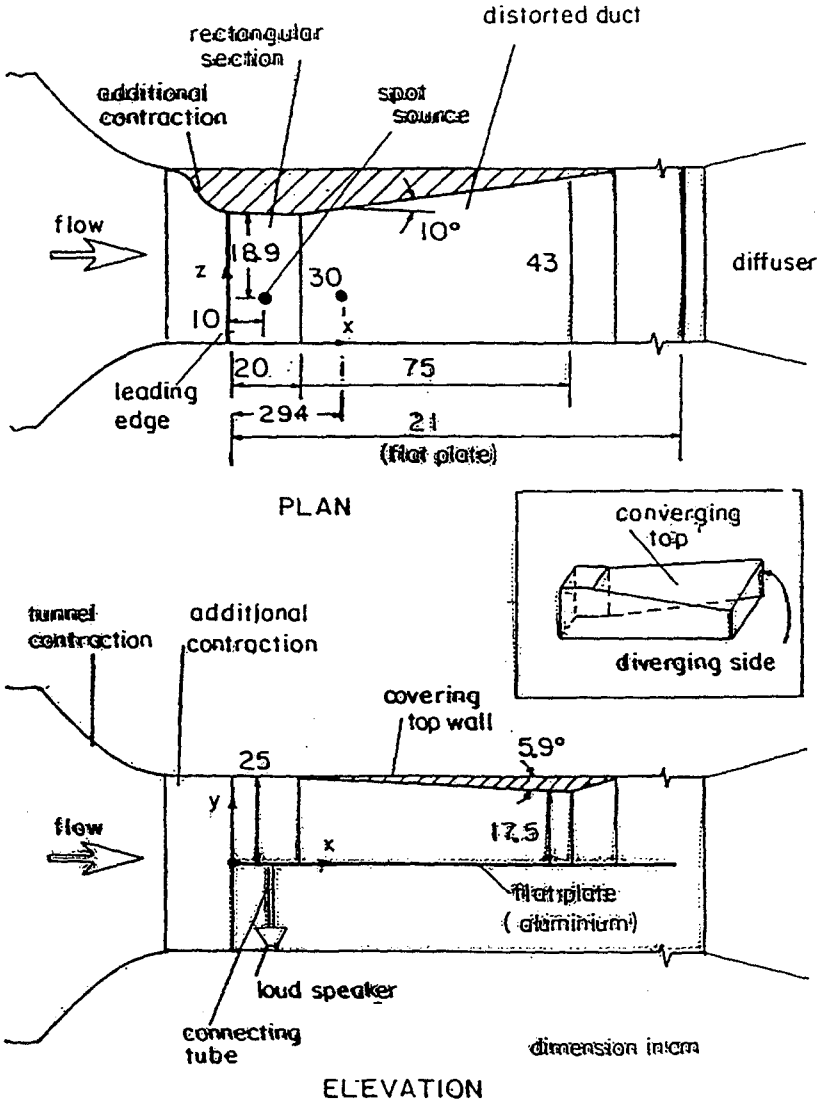

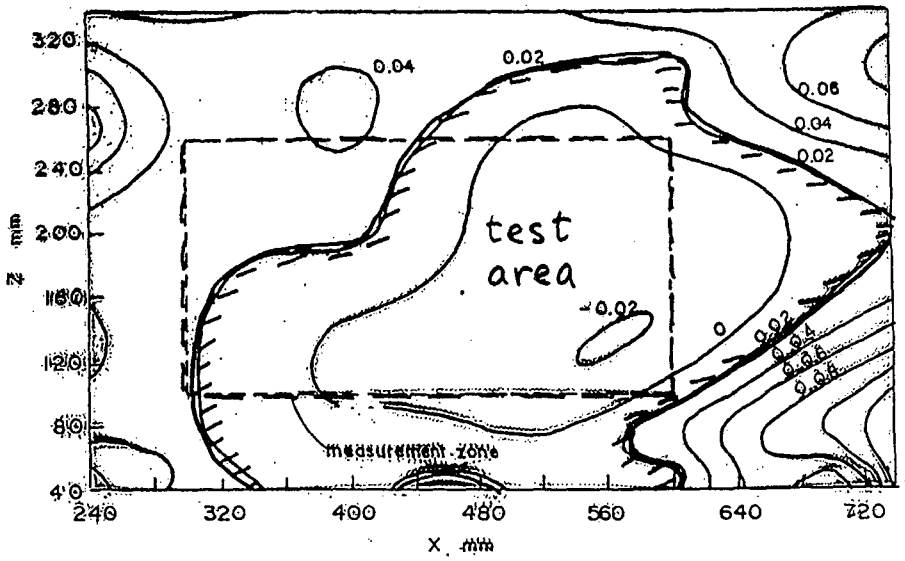

THE PRESSURE DISTRIBUTION ON THE TEST SURFACE

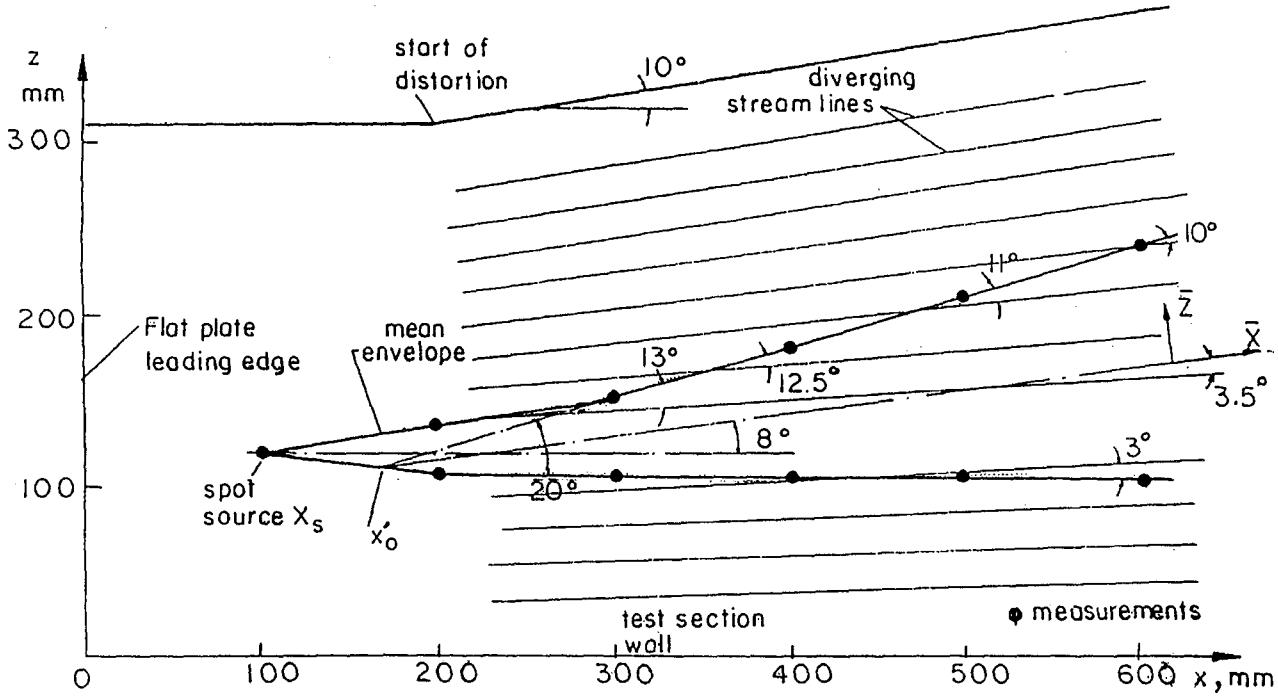

SPOT TRAJECTORY AND ENVELOPE

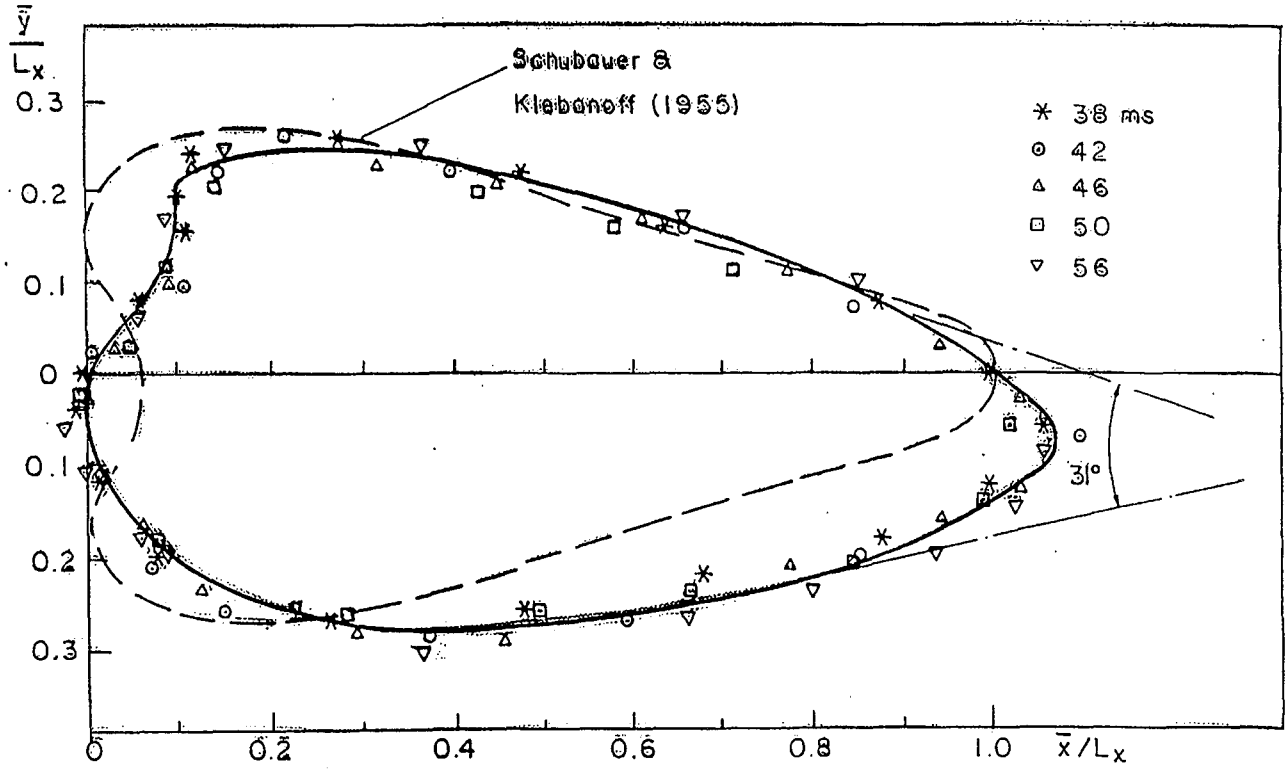

SPOT SHAPE IN DISTORTION DUCT

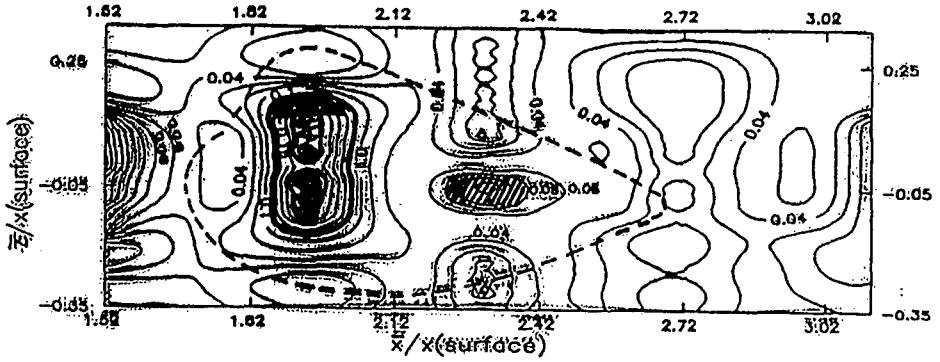

PERTURBATION VELOCITY CONTOURS

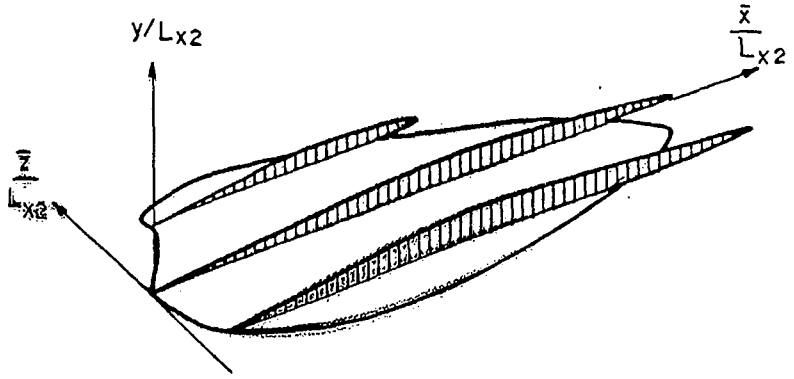

AN ISOMETRIC VIEW OF DISTORTED SPOT

CONCLUSIONS

1. Spots do NOT grow across streamlines at universal angles.
2. Overall spread rate insensitive to flow divergence.
3. Spot shape exquisitely sensitive to flow asymmetries

→ Chief effect, of distortion of coheren structure (Λ- vortex) in spot,

GEOMETRIC, rather than DYNAMICAL,

for the kind of flow divergence used in experiment

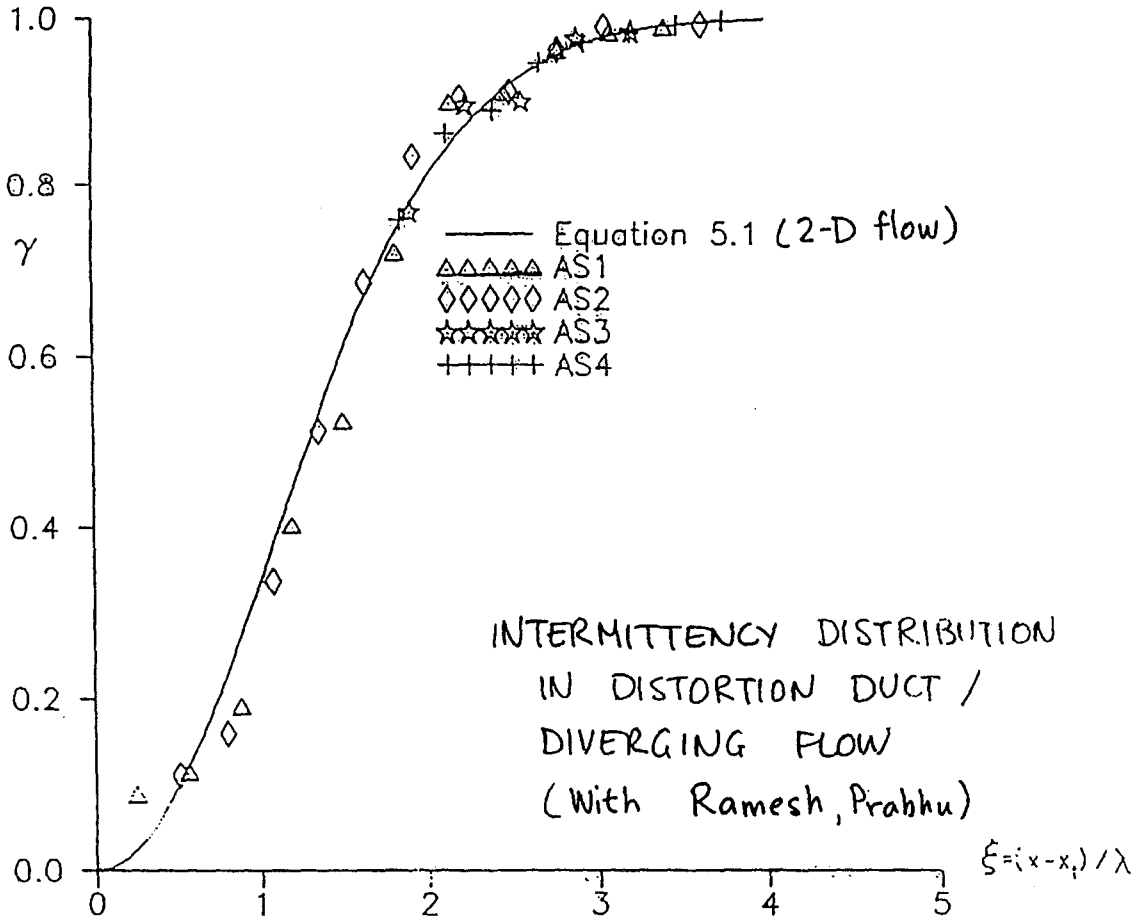

Figure 5.11a Comparison of the measured intermittency data in A with the universal intermittency distribution.

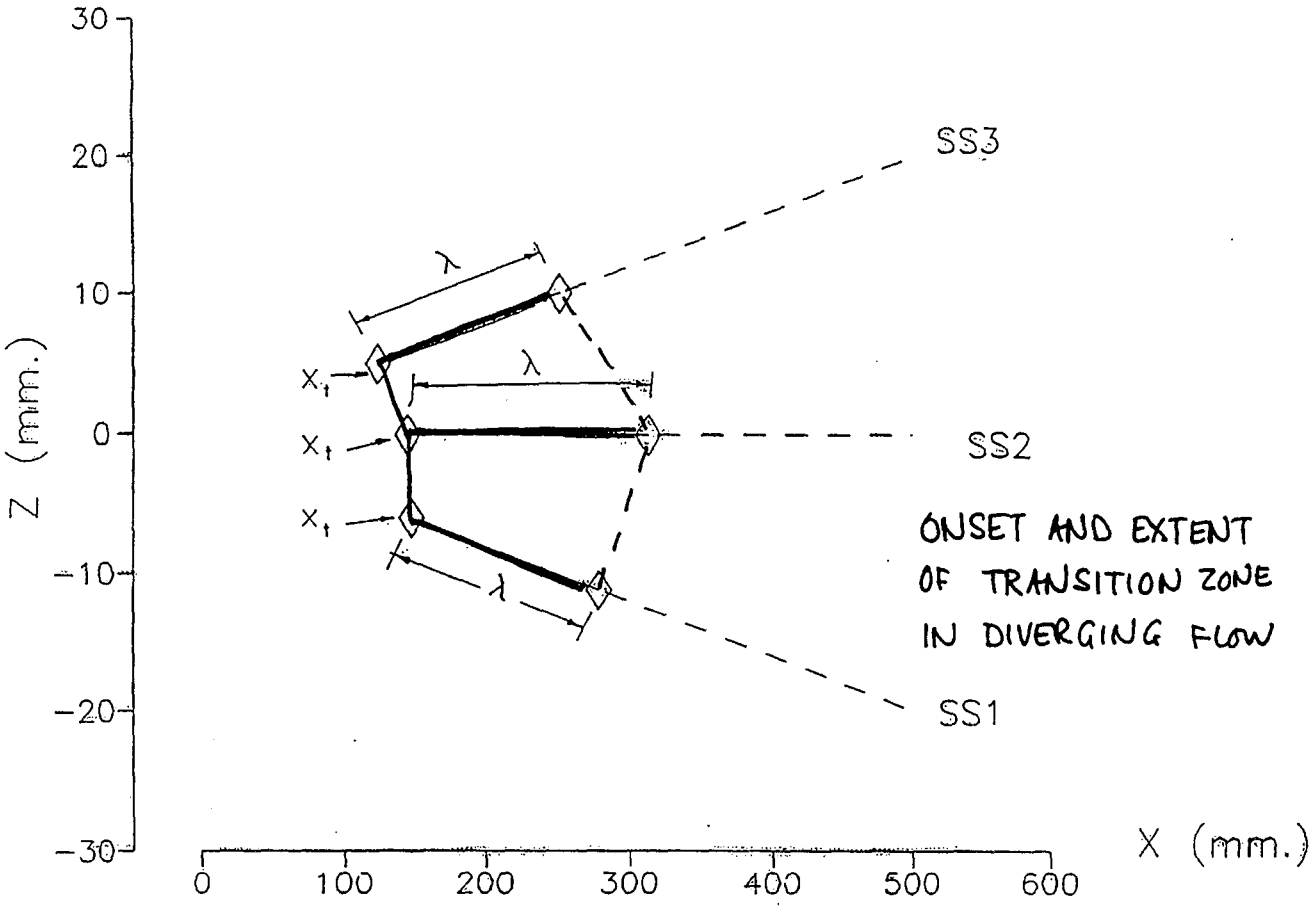

Fig. 5.12 Variation of x_t and λ along $SS1 - SS3$ in S

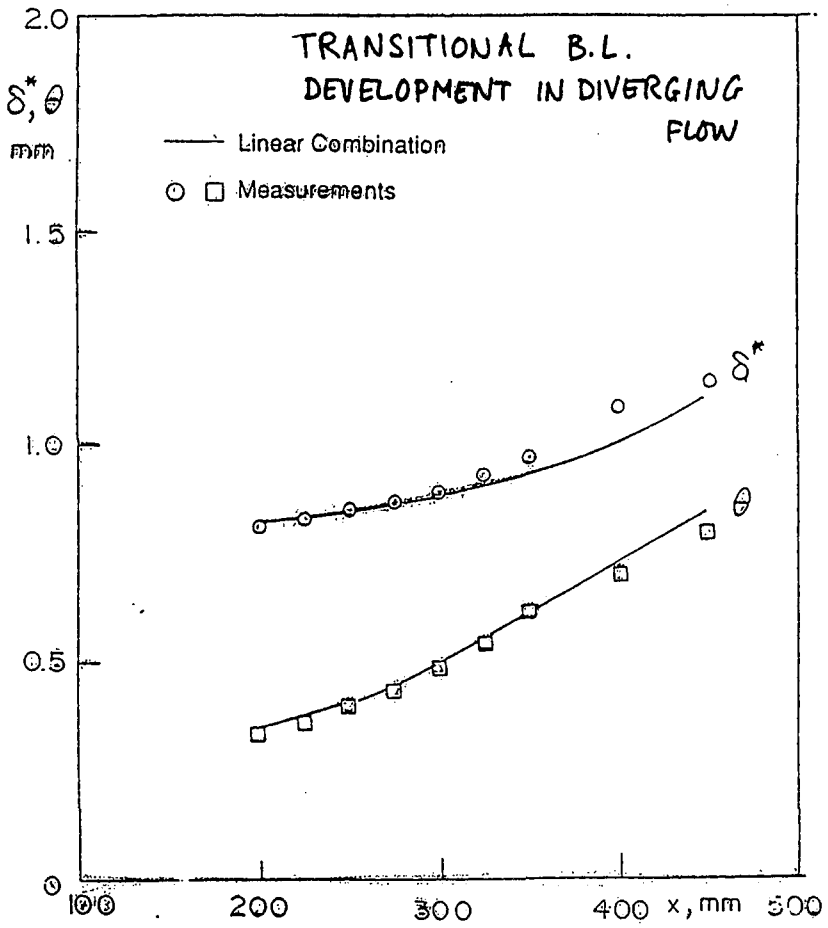

Fig. 5.16a Variation of δ^* and θ along $SS1$

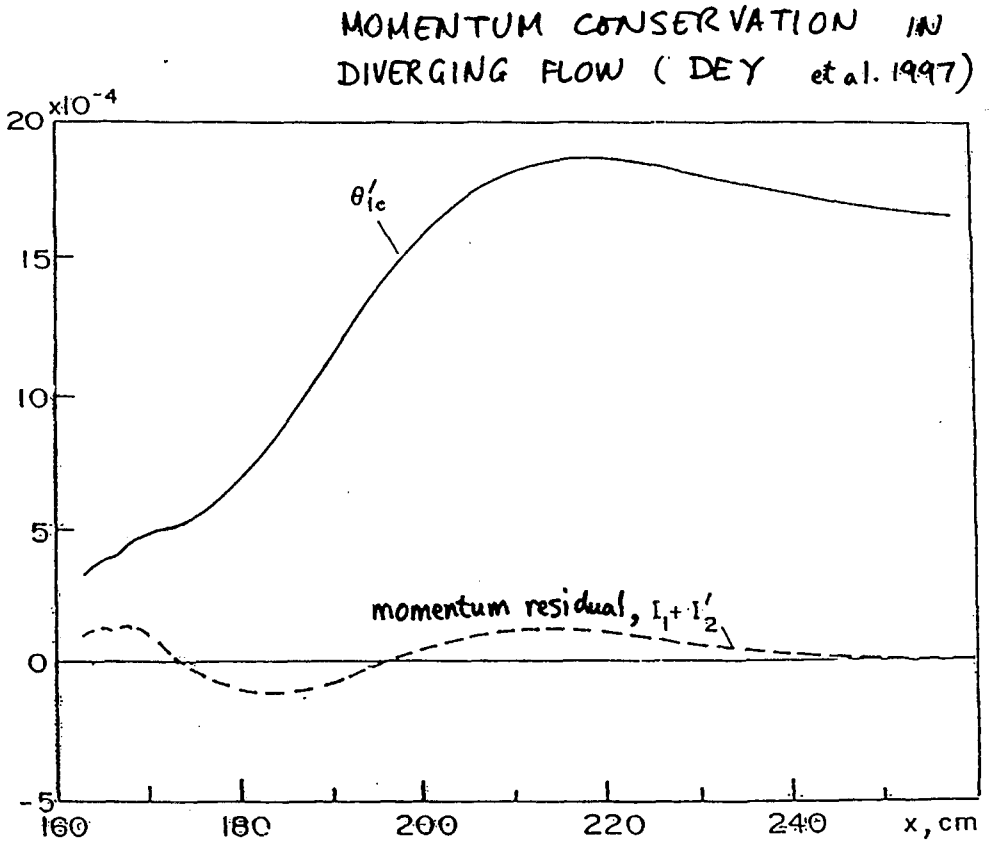
MOMENTUM CONSERVATION IN
DIVERGING FLOW (DEY et al. 1997)
20 x10⁻⁴
15
10
5
0
-5
θ'ic
momentum residual, I1+I'2
160
180
200
220
240
x, cm

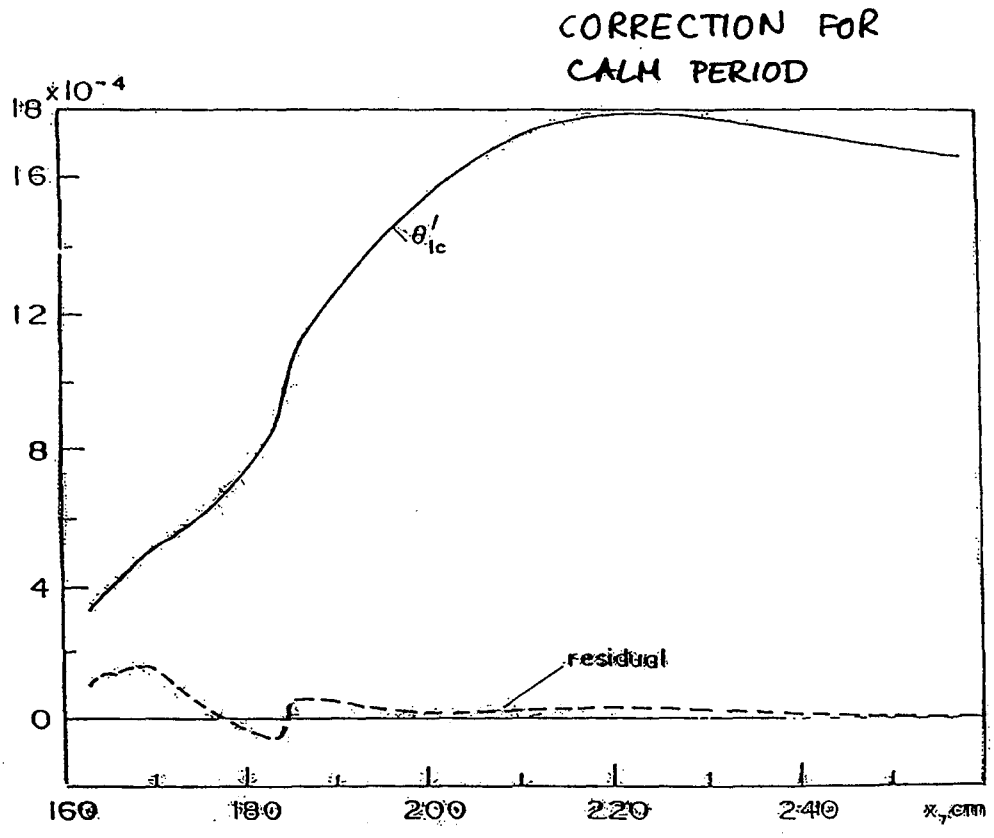
CORRECTION FOR
CALM PERIOD
x10⁻⁴
18
16
12
8
4
0
θ'lc
residual
160
180
200
220
240
x, cm

STABILITY OF NON-PARALLEL 2D FLOWS

(With Rama Govindarajan)

Introduce (Govindarajan & Narasimha 1995*)

$$y_d = \theta_d(x)\cdot y \quad , \quad dx_d = \theta_d(x)\cdot dx$$

$y \sim$ Blasius η

$( )_d$ = dimensional quantity

$$\psi_d = \underbrace{U_d(x_d)\,\theta_d(x_d)}_{\text{local scaling}}\,\psi(x,y)$$

$$\psi(x,y) = \underbrace{\Phi(y,\ldots)}_{\substack{\text{mean flow}\\ \sim \text{F-S f}}} + \underbrace{\phi(x,y)\exp\left[i\int\alpha\,dx - \omega t\right]}_{\text{perturbation}}$$

$$\Phi(y,\ldots) = \underbrace{\Phi_0(y)}_{\substack{\text{Falkner}\\ \text{-Skan}}} + \underbrace{R^{-1}\Phi_1(y,\ldots)}_{\substack{\text{higher order}\\ \text{b. l. theory}}} + O(R^{-2})$$

$$p \equiv R\frac{d}{dx}U\theta = \text{const}, \quad q \equiv R\frac{d\theta}{dx} = \text{const}$$

Note $\dfrac{d\theta}{dx} \sim \theta(R^{-1})$; $\dfrac{\partial\phi}{\partial x} \sim \dfrac{d\alpha}{dx} = O(R^{-1})$

$$\frac{\partial^2\phi}{\partial x^2} = o(R^{-1}), \quad \frac{d^2\alpha}{dx^2} = o(R^{-1}).$$

* JFM 300: 117–147

"FULL NON-PARALLEL" (GN 95)

$$\{[OS] + R^{-1}[NP_1(\Phi_0) + NP_h(\Phi_1)]\}\phi = O(R^{-2})$$

Orr-Sommerfeld — Non-parallel, lowest order b.l. — Non-parallel, higher order b.l.

$$OS \equiv i(\omega - \alpha\Phi_0')(D^2-\alpha^2) + i\alpha\Phi_0'' \quad \text{Rayleigh}$$
$$+ R^{-1}(D^4 - 2\alpha^2D^2 + \alpha^4) \quad \text{viscous}$$

$$NP_1 \equiv p\Phi_0 D^3 + (2q-p)\Phi_0' D^2$$
$$+ \{2yq\alpha(\omega - \alpha\Phi_0') - p\alpha^2\Phi_0 + (2q-p)\Phi_0''\}D$$
$$+ \{(q-2p)\alpha\omega + p\Phi_0'' + 3(p-q)\alpha^2\Phi_0'$$
$$+ (-\omega + 3\alpha\Phi_0')R\alpha'$$
$$+ (\Phi_0''' + 3\alpha^2\Phi_0' - 2\alpha\omega - \Phi_0 D^2)R\frac{\partial}{\partial x}$$

$$NP_h \equiv -i\alpha\{(D^2-\alpha^2)(\Phi_1' - \Phi_1''')\}$$

LOWEST-ORDER PARABOLIC

(~ highest order stability for lowest order mean flow) (GN97b)$^{\triangle}$

$$\left[i(\omega - \alpha\Phi_0')(D^2-\alpha^2) + i\alpha\Phi_0''' + R^{-1}\left(D^4 + p\Phi_0 D^3 + \underbrace{\left\{ -2\alpha^2 + \Phi_0'(2q-p) - \Phi_0' R \frac{\partial}{\partial x} \right\} D^2}_{\text{lowest-order parabolic correction, cf. below} \downarrow} \right] \phi = 0$$

LOWEST-ORDER ORDINARY DIFFL. EQN. (GN97a)*

$$\left[i(\omega - \alpha\Phi_0')(D^2-\alpha^2) + i\alpha\Phi_0''' + R^{-1}\left(\underbrace{D^4}_{\alpha^2 D^2\phi,\ \alpha^4\phi \text{ in OS not required}} + \underbrace{p\Phi_0 D^3}_{\text{from mean wall-normal vel. (reqd. in crit. layer in general)}} \right) \right] \phi = 0$$

Rayleigh

* Proc. Roy. Soc. (in press) $^{\triangle}$ Submitted for pubn

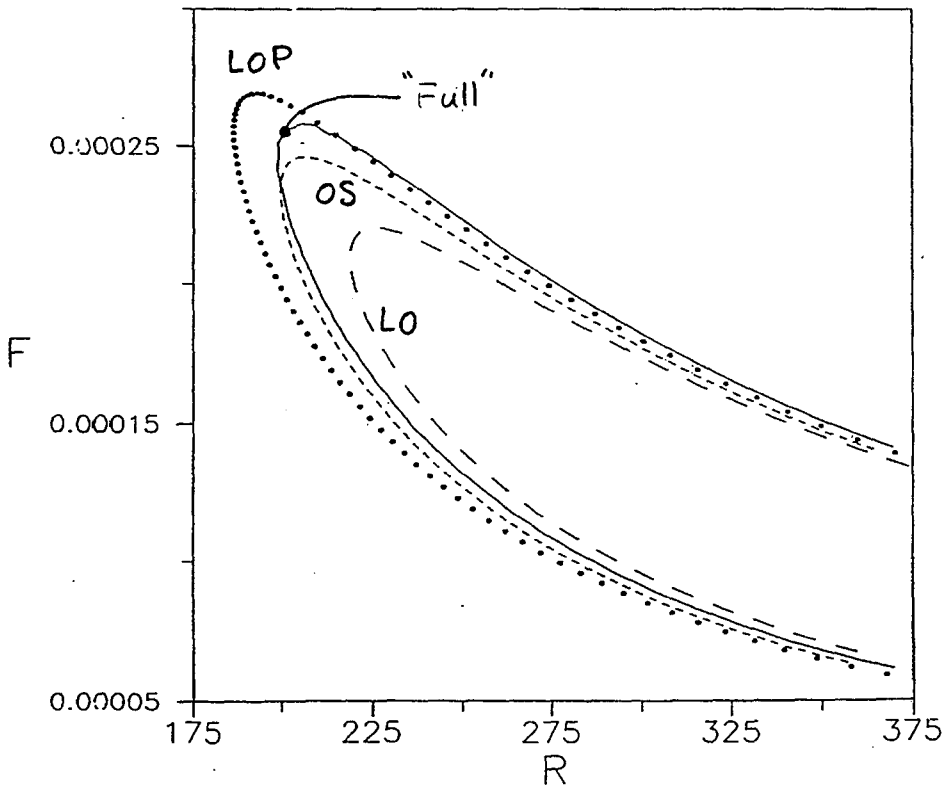

Neutral stability at inner maximum. Symbols: Lowest order parabolic stability equation; solid line: full non–parallel; short dashes: OS; long dashes: lowest order

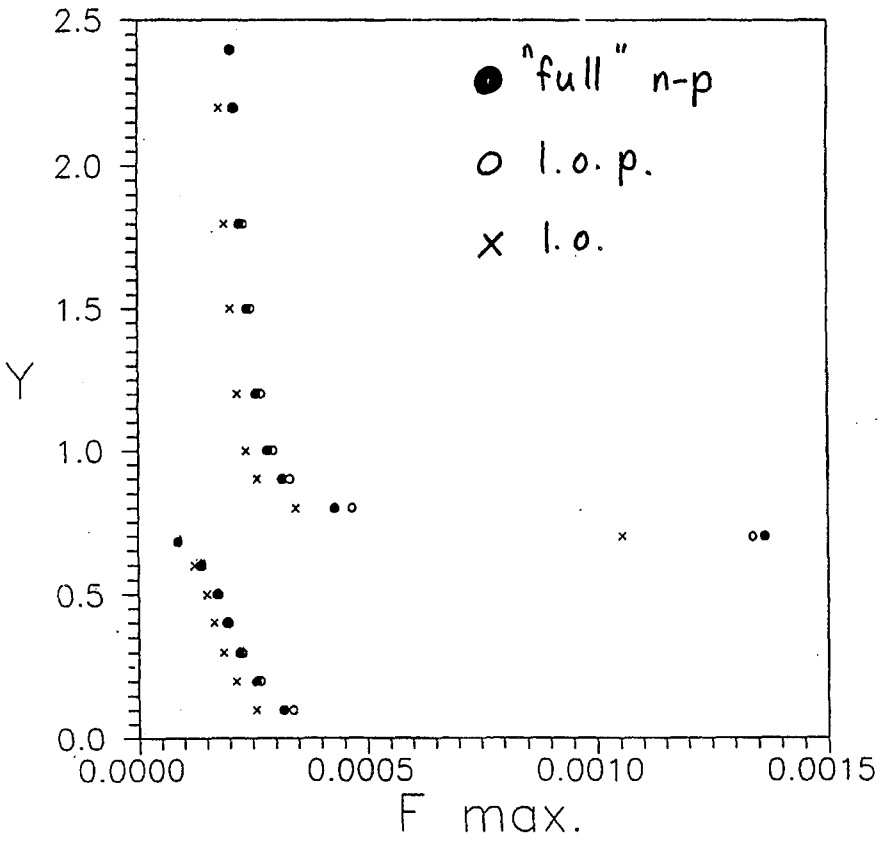

m=c

Fig. : Critical Reynolds number as a function of height open circles: lowest-order parabolic; filled circles: full non-parallel; crosses: lowest order equation.

A MODEST PROPOSAL

Do a DNS

- in "mission" mode
- on a realistic blade
  ("define a "Minnowbrook profile" or blade)
- with progressive "complexification" of geometry, i/b.c. :

  3D
  surface roughness
  FST
  wake impact
  cooling
  compressibility
  tip clearance
  ...

- following agreed data protocols, access rules, credit-sharing norms

+ associated experiments, theory

SESSION 1

TRANSITION IN TURBOMACHINERY

NASA/CP—1998-206958

G.J. Walker
University of Tasmania
Hobart, Australia

WHY STUDY TRANSITION IN TURBOMACHINES ?

Practical importance – turbomachines are used in most energy conversion and propulsion systems

Transition can significantly affect performance (operating range and efficiency) and aeroelastic behaviour of blades

Performance improvements can provide significant economic and environmental benefits

A challenging and stimulating problem

Study has advanced basic understanding of transition physics (calming, concentrated breakdown, pressure gradient effects, sub-transitions)

WHERE IS TRANSITION IMPORTANT ?

Boundary layers a necessary pre-requisite

These can only be identified in predominantly axial flow machines

Embedded stage is the norm – multiple stages needed to achieve practical pressure rise

Relatively high aspect ratio blades of most interest (LP turbine and compressor)

Low aspect ratio blades largely immersed in turbulent annulus wall boundary layer

Flow in radial machines essentially fully viscous

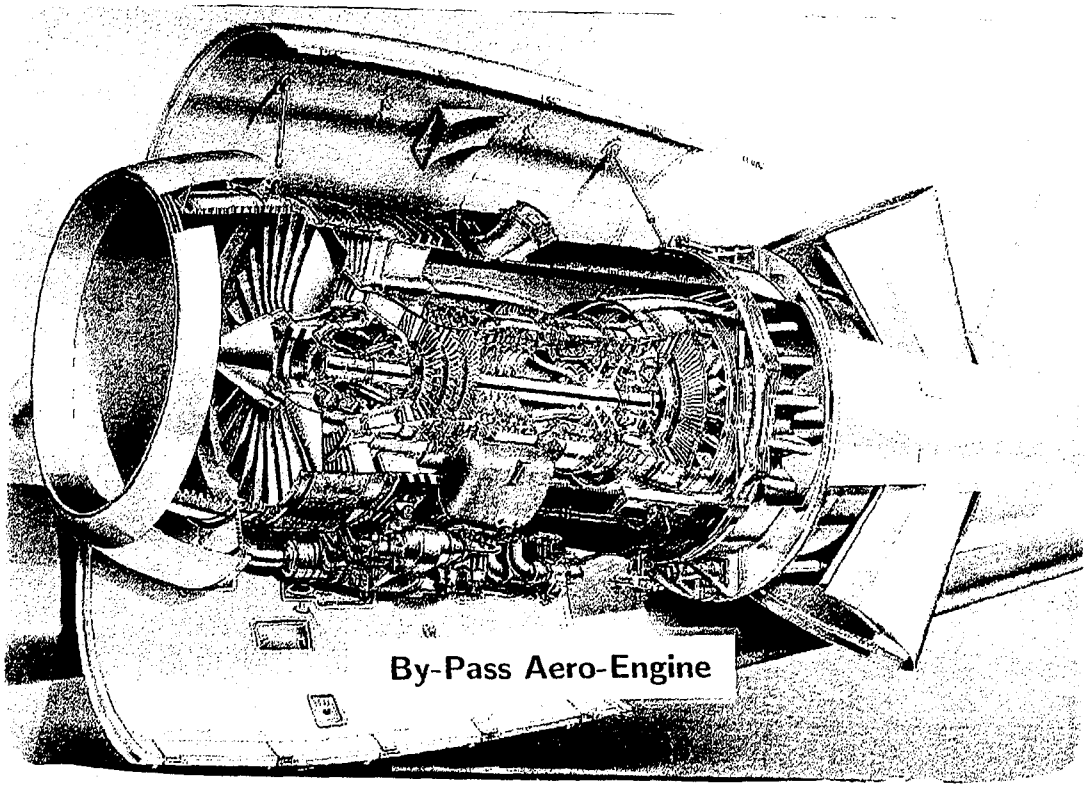

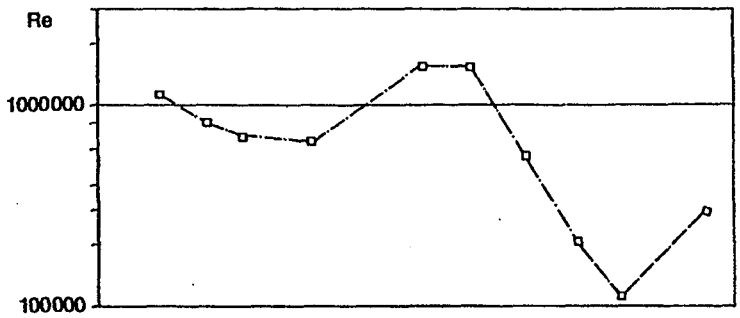

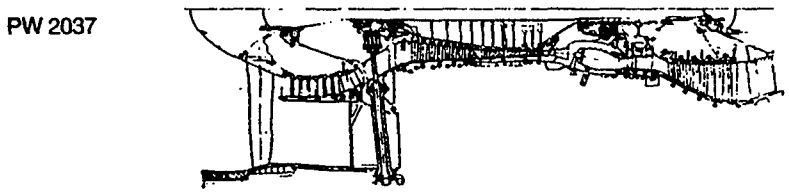

Reynolds Number in a By-Pass Engine – Altitude Cruise (Hourmouziadis)

ENVIRONMENT OF AN EMBEDDED BLADE ROW

- Periodic disturbances
  - potential (neighbouring blade rows)
  - viscous (upstream blade wakes)
- Random disturbances
  - high level (wakes of next upstream row)
  - background (dispersed wakes and inflow turbulence)
- Low Reynolds number, high loading (separation effects important)

(Compare with external aerodynamics problems $\sim$ high Re, low turbulence)

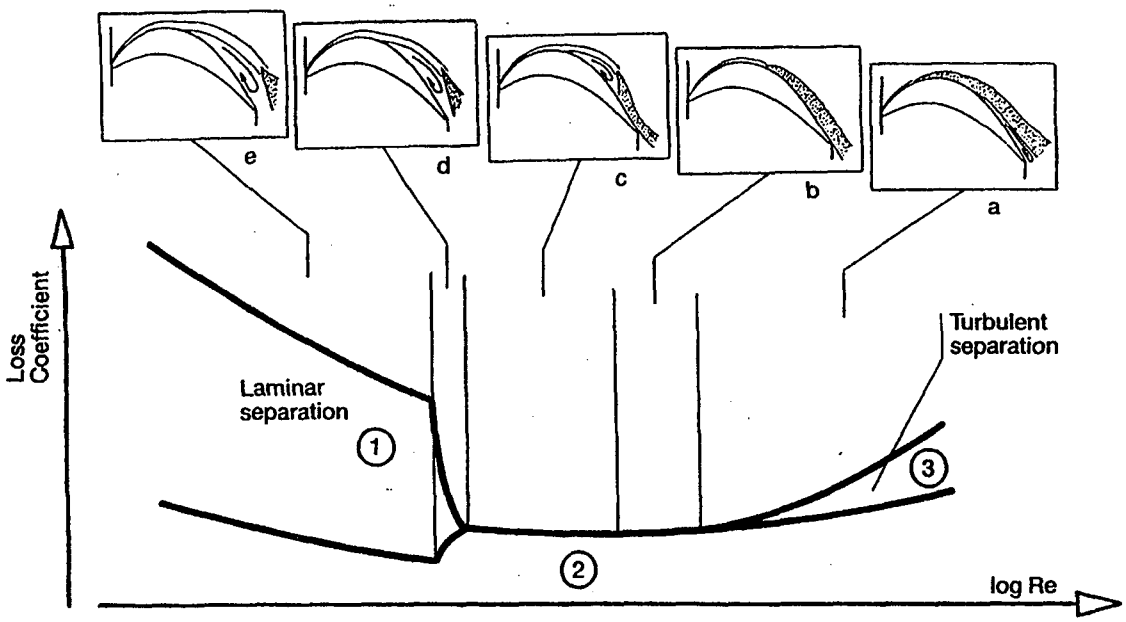

Reynolds Number Effects on Turbine Cascade Performance (Hourmouziadis)

WAKE DISPERSION IN AXIAL MACHINES

Wake chopping by next downstream row

Wake-wake interactions cause circumferential variations in time-mean velocity and periodic disturbance component

Wake-jet effects are opposite for compressor and turbine rows (and for suction and pressure surfaces of blading)

Radial variation of whirl velocity skews wake regions relative to downstream blades

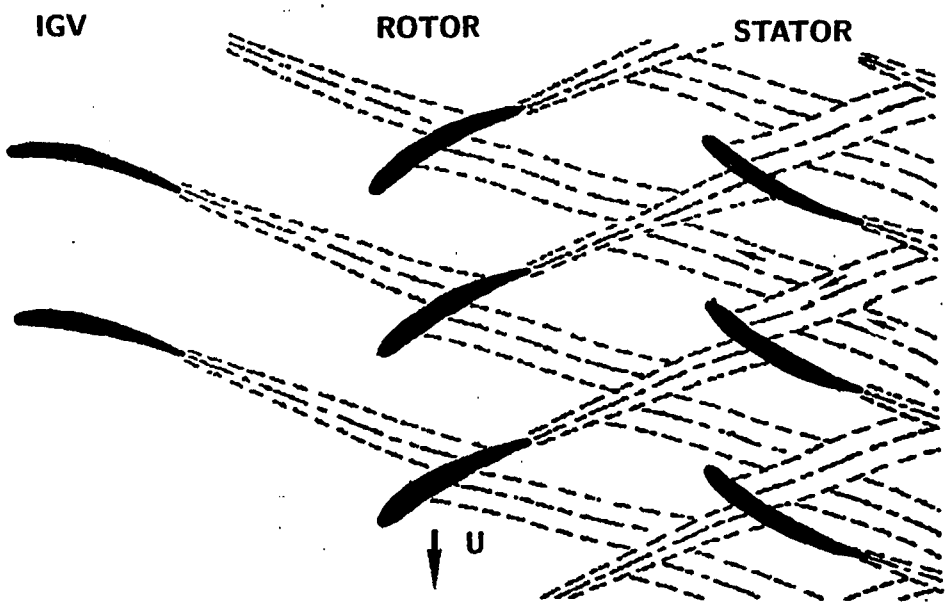

Cross-section of 1.5 stage axial compressor showing typical instantaneous wake dispersion (schematic)

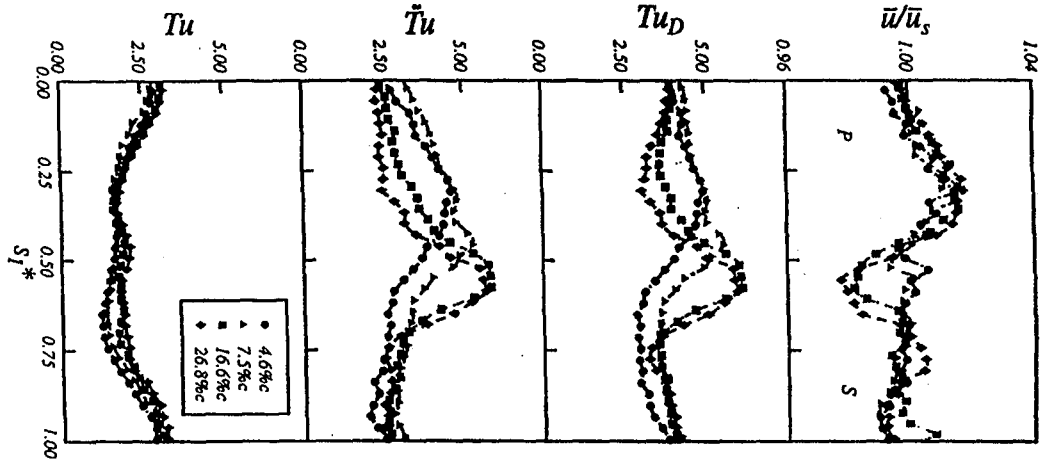

Flow development due to wake interaction downstream of IGV-rotor compressor stage (S_I^* = circumferential distance from local center of IGV wake street)

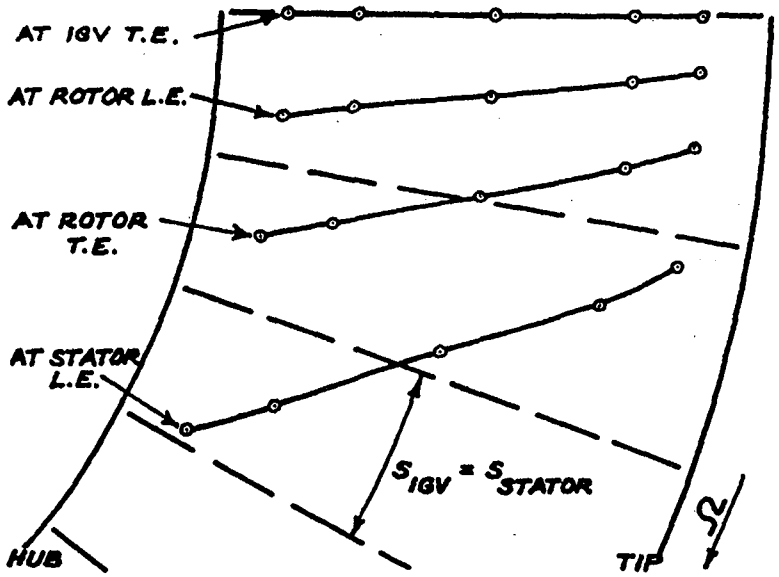

Circumferential transport of IGV wakes in a 1.5-stage axial compressor (design flow)

TRANSITION MODES (Mayle)

Natural transition (T-S waves)

Bypass transition

Separated-flow transition

Periodic-unsteady transition

Reverse transition

FACTORS INFLUENCING TRANSITION IN GAS TURBINE ENGINES (Mayle)

Primary

- free stream turbulence
- pressure gradient
- laminar separation
- wake passing

Secondary

- surface roughness
- concave curvature
- compressibility/heat transfer
- coolant injection

TRANSITION INCEPTION PREDICTION (STEADY FLOW)

Linearised stability analysis (low turbulence)

- doubtful relevance for turbomachinery flows

Parabolised stability analysis (higher turbulence)

- greater potential/needs more testing for turbomachinery cases

Theoretical approaches for bypass transition (Johnson, Mayle)

- encouraging progress, but still some differences to be resolved

Experimental correlations (Mayle, Gostelow)

- current industrial practice

TRANSITION LENGTH PREDICTION (STEADY FLOW)

Transition length correlations based on conditions at transition inception give poor results in rapidly changing pressure gradient

Improved model (Solomon, Walker, Gostelow)

- spot inception rate controlled by conditions at inception (concentrated breakdown)
- local spot spreading rate depends on local Pohlhausen pressure gradient parameter in undisturbed laminar flow
- spot-spreading data from triggered spot studies
- new theory gives good results for turbomachine blade cases and explains sub-transitions

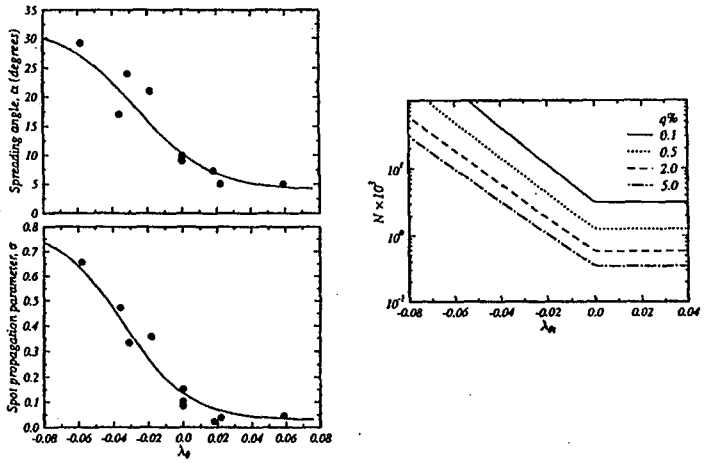

Correlations for spot spreading half angle α spot propagation rate σ and generation rate N. Experimental data from various sources compiled by Gostelow et al.(1995)

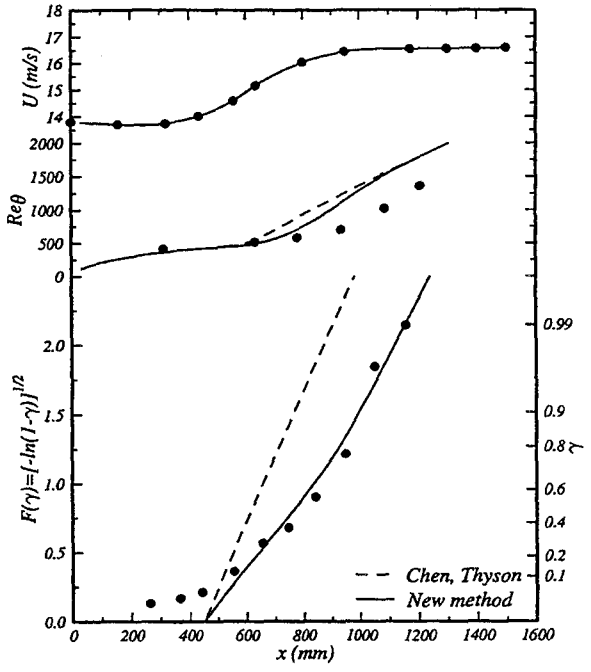

Calculation of transition in flow with a changing pressure gradient. Experimental data from Narasimha et al. (1984)

EXPERIMENTAL INVESTIGATIONS

Flat plate

- imposed surface pressure distribution
- grid turbulence (random disturbances)
- moving bar wakes (periodic disturbances) (Turbulence level must also be correct – Halstead)
- triggered turbulent spots (Gostelow)

2-D cascade

- grid turbulence and bar wakes

Rotating cascade

Blowdown facilities (intermittent)

Engine component tests

MEASUREMENT TECHNIQUES

Boundary layer surveys (difficult in real machines)

- pressure probe
- hot-wire
- LDV

Surface film arrays (film gauges, liquid crystals)

- show instantaneous spatial distributions
- do not see peak turbulence in boundary layer

Data Analysis

- time-mean velocity/wall shear/heat transfer
- periodic fluctuations (ensemble averaging)
- random fluctuations, skew, intermittency
- relaxation parameter (Solomon)

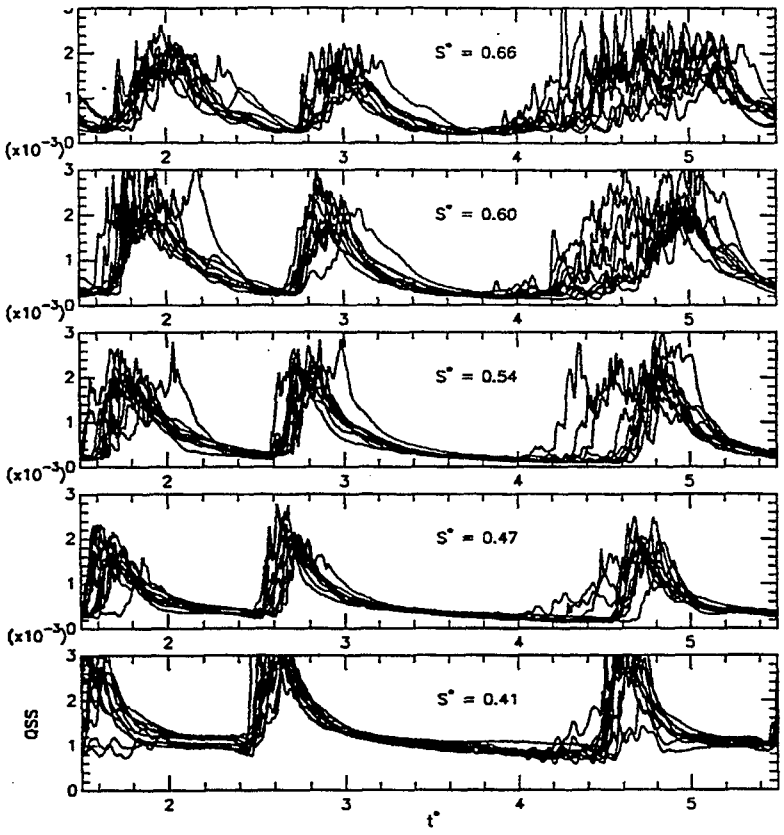

Individual wall shear stress traces at different streamwise positions along the suction surface of a compressor stator blade (10 traces at each position). Single blade removed to vary wake spacing

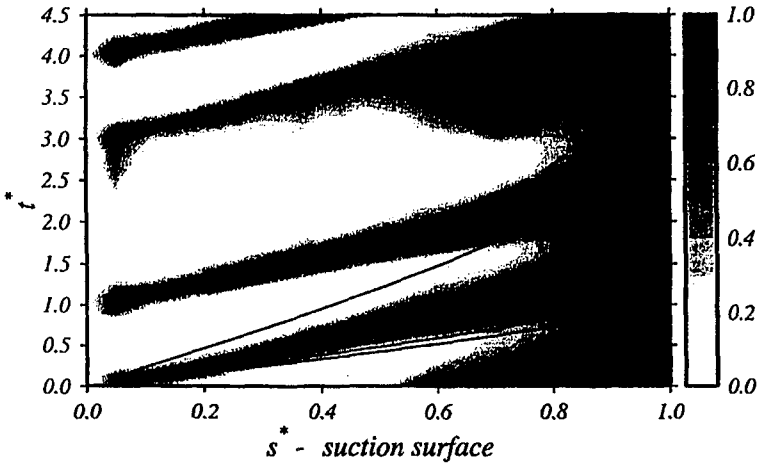

Wake-induced turbulent spots developing on an axial compressor blade. T–S diagram of ensemble averaged intermittency. Wake induced turbulent strip at $t^* = 2$ eliminated by removal of a single upstream rotor blade. Particle trajectories for $1.0U, 0.88U, 0.7U, 0.5U, 0.35U$ overlaid.

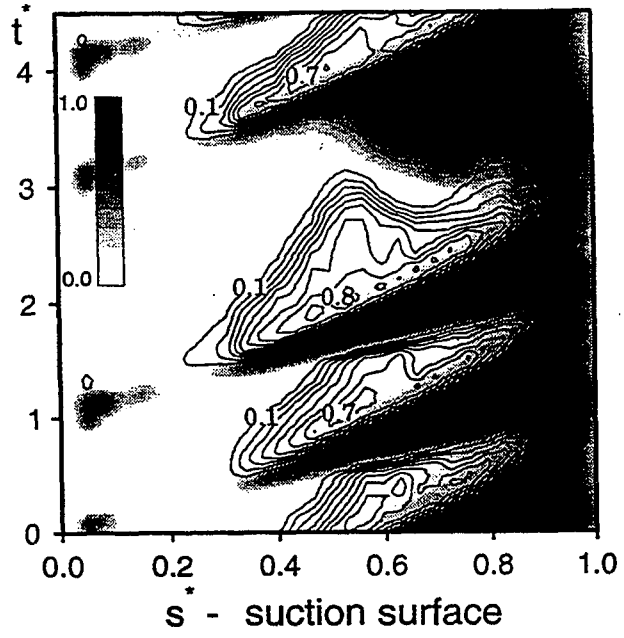

$s^* \sim t^*$ plane distributions of flow state on compressor stator suction surface. Shading indicates the probability , γ, of turbulent flow (intermittency) and contours indicate probability, κ, of relaxing non-turbulent flow. One upstream rotor blade removed to vary wake spacing

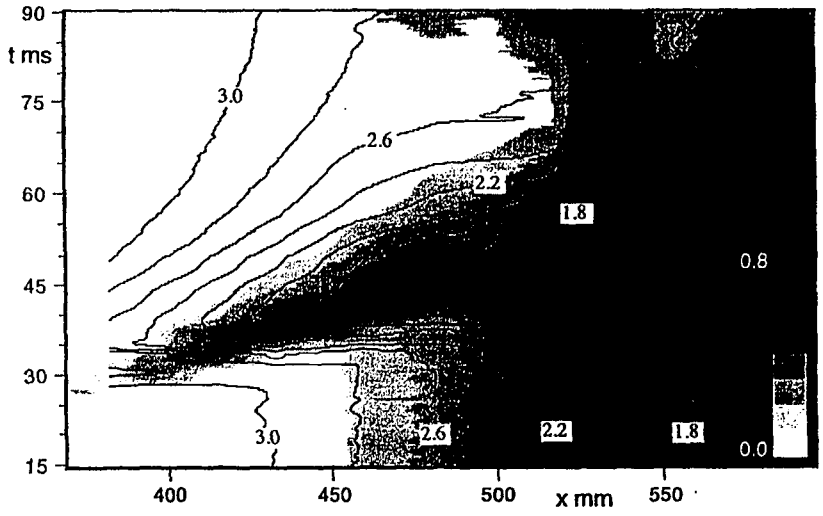

t–x diagram for a triggered spot in an adverse pressure gradient. Shading indicates RMS disturbance level integrated over the boundary layer height. Contours give the shape factor H

MORPHOLOGY OF TRANSITION

GE compressor (Halstead)

- wake-induced transitional and turbulent strips
- calmed regions (relaxing non-turbulent flow)
- other modes between wake-induced strips (bypass, separated flow)
- transitional flow extends over 60% chord

Blade-out studies (Halstead, Solomon)

- confirm above model
- demonstrate suppression of laminar separation by calmed regions

Confirmation of transitional flow

- spanwise film arrays indicate turbulent spots

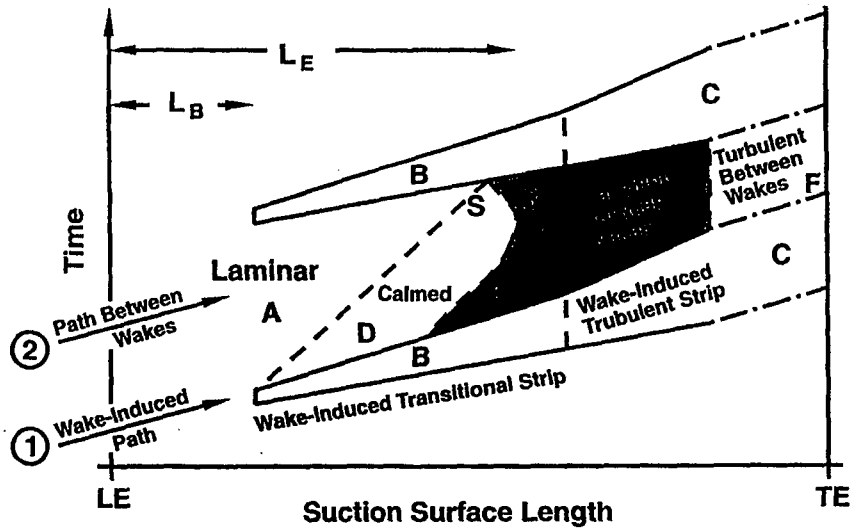

Unsteady boundary layer development on an axial compressor blade (Halstead et al. (1995))

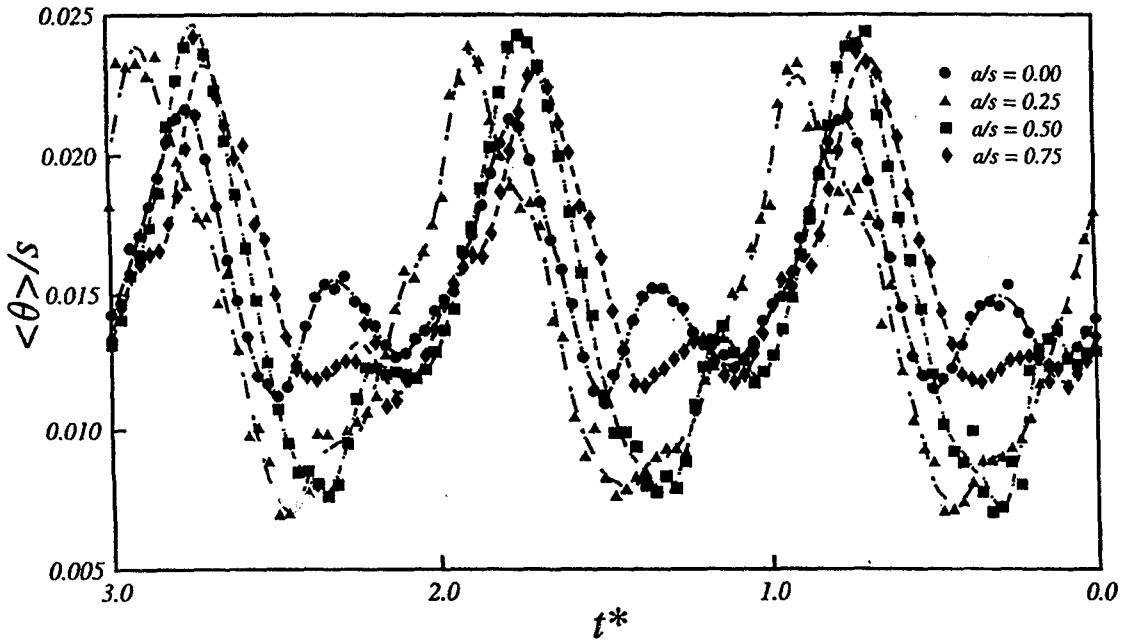

Influence of IGV clocking on temporal variation of ensemble average compressor stator wake momentum thickness (a/s = relative circumferential position)

TRANSITION INCEPTION (PERIODIC FLOW)

Influence of wake-jet direction

- delayed inception when jet is away from surface (Walker, Orth, Funazaki)
- inception coincides with wake passage when jet is toward surface

Relative importance of periodic and random components of wake disturbance ?

Why does wake in free-stream not cause further breakdown after the initial inception ?

- modification of environment by growing transitional strip ?
- turbulence not the primary parameter ?

TRANSITION ZONE CALCULATIONS

Calculation methods with intermittency weighting of parameters (e.g. eddy viscosity or entrainment)

Linear combination integral methods

Backward extrapolation of fully turbulent calculation methods

- does not model physics of breakdown or calmed regions (transition effected by diffusion of turbulence from free-stream)
- does not predict transition length correctly

Intermittency transport approach

Turbomachinery designers need fast robust methods which can be used interactively

- quasi steady integral methods ?

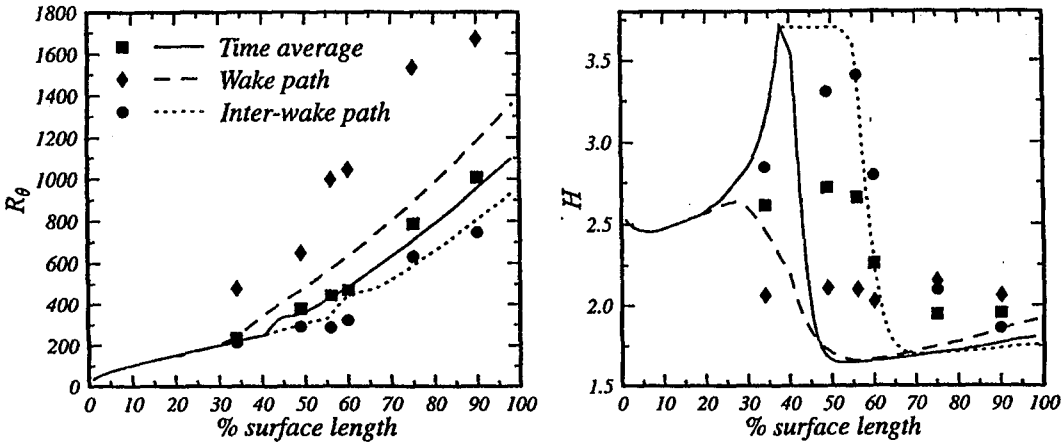

Quasi-steady calculation of the boundary layer development in the unsteady flow on the suction surface of a compressor blade. Symbols are experimental data of Halstead et al. (1995)

APPLICATIONS

Improved LP turbine performance from use of calming effect now demonstrated and in service

Can unsteady transitional flow effects be used to advantage on compressor airfoils ?

Current empirical design techniques based on steady flow calculations may have already factored these in to some extent

Changing inflow disturbance field by blade row clocking certainly alters compressor blade wake thickness fluctuations (Walker et al.)

Strength of turbulent spots and calming regions influenced by blade surface pressure distributions (Solomon)

CURRENT CHALLENGES

Obtain more comprehensive data on turbulent spot breakdown rates and spreading (Re effects ?)

Resolve differences in bypass transition models

Develop accurate prediction of periodic unsteady transition inception

Which freestream disturbance components are effective in promoting transition ?

- periodic versus random disturbance components
- turbulence scale effects

Examine 3-D effects (crossflow, convergence)

Incorporate effects of disturbed laminar boundary layer in turbomachinery blade performance calculations

Examine parabolised stability analysis for turbomachinery flows

Develop a unified prediction of transition in separated and attached flows which avoid current inconsistencies and resulting computational instability

Identify possible design or performance improvements for compressor blades incorporating periodic unsteady transition effects

THE NASA LOW-PRESSURE TURBINE FLOW PHYSICS PROGRAM

David Ashpis
NASA Lewis Research Center
Cleveland, Ohio 44135

ABSTRACT

An overview of the NASA Lewis Low-Pressure Turbine (LPT) Flow Physics Program will be presented. The program was established in response to the aero-engine industry needs for improved LPT efficiency and designs. Modern jet engines have four to seven LPT stages, significantly contributing to engine weight. In addition, there is a significant efficiency degradation between takeoff and cruise conditions, of up to 2 points. Reducing the weight and part count of the LPT and minimizing the efficiency degradation will translate into fuel savings. Accurate prediction methods of LPT flows and losses are needed to accomplish those improvements.

The flow in LPT passages is at low Reynolds number, and is dominated by interplay of three basic mechanisms: transition, separation and wake interaction. The affecting parameters traditionally considered are Reynolds number, freestream turbulence intensity, wake frequency parameter, and the pressure distribution (loading). Three-dimensional effects and additional parameters, particularly turbulence characteristics like length scales, spectra and other statistics, as well as wake turbulence intensity and properties also play a role.

The flow of most interest is on the suction surface, where large losses are generated as the flow tends to separate at the low Reynolds numbers. Ignoring wakes, a common flow scenario there is laminar separation, followed by transition on the separation bubble and turbulent reattachment. If transition starts earlier separation will be eliminated, the boundary layer will be attached leading to the well known bypass transition issues. In contrast, transition over a separation bubble is closer to free shear layer transition and was not investigated as well, particularly in the turbine environment. Unsteadiness created by wakes complicates the picture. Wakes induce earlier transition, and the calmed regions trailing the induced turbulent spots can delay or eliminate separation via shear stress modification. Three-dimensional flow physics and geometry will have strong effects. Altogether a very complex and challenging problem emerges.

The objective of the program is to provide improved models and physical understanding of the complex flow, which are essential for accurate prediction of flow and losses in the LPT. Experimental, computational and analytical work as complementing and augmenting approaches are used. The program involves industry, universities and research institutes, and other government laboratories. It is characterized by strong interaction among participants, quick dissemination of results, and responsiveness to industry's needs.

The presentation will describe the work elements. Highlighting some activities, in progress are experiments on simulated blade suction surface in low-speed wind tunnels, on curved wall, and on a flat-plate, both with pressure gradient. In the area of computation, assessment of existing models is performed using RANS (Reynolds Averaged Navier Stokes) simulations. Laminar flow DNS was completed. Analytical studies of instability and receptivity in attached and separated flows were started. In the near future the program is moving to include wake effects and development of improved modeling. Experimental work in preparation stages are: (1) Addition of wakes to the curved tunnel experiment, (2) Low-speed rotating rig experiment on GE90 engine LPT (3) Transonic cascade. In the area of computation it is expected to move from model assessment towards development of improved models. In addition, a new project of Large Eddy Simulation (LES) of LPT is to begin and will provide numerical data bases. It is planned to implement the emerging improved models in a multistage turbomachinery code and to validate against the GE90 engine LPT

Some Expectations

In addition to the stated workshop goals, we view the workshop also as a peer review for the NASA LPT Program.

Solicit feedback and opinions on program plan and content.

Will use the information to modify the program if needed.

Request to produce a document detailing the challenges and the impact of transition in turbomachines research, to be used for advocacy.

Looking to establish new collaborations and pooling of resources.

Propose to establish an international working group.

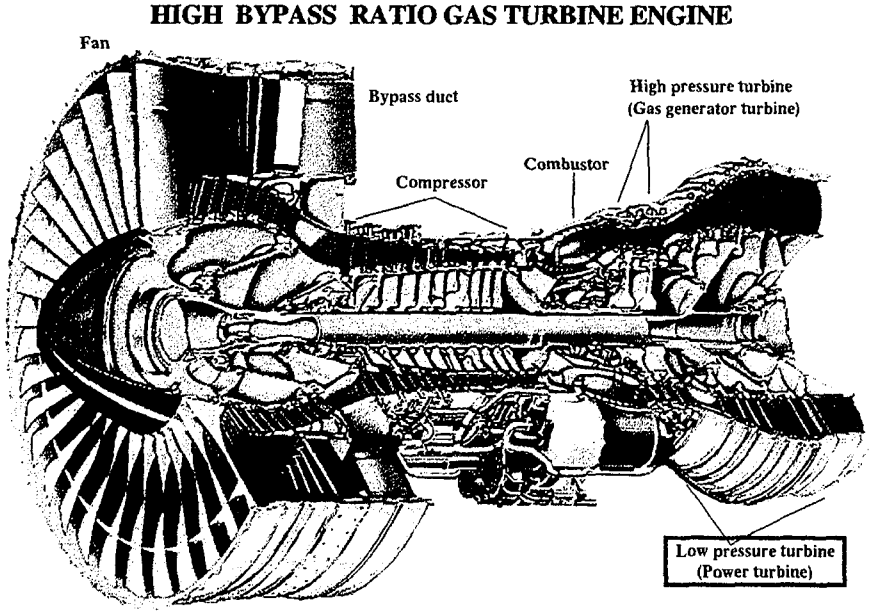

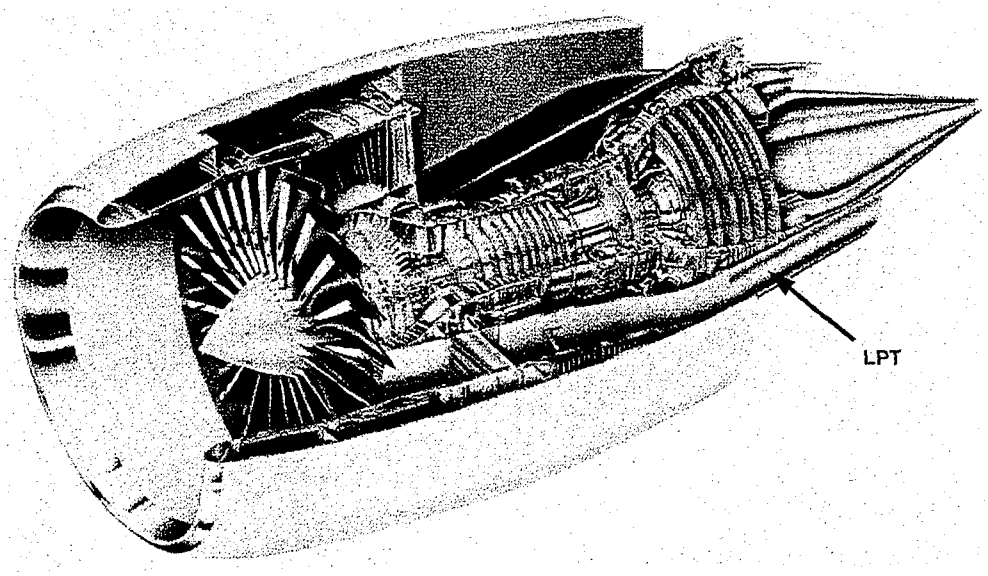

GE90

LPT IMPROVED DESIGN NEEDS

- General design and performance improvements
  - Note that the LPT is a large, 4-7 stages component
  - Need to increase loading, reduce parts count, reduce weight
  - Reduced number of stages will be a revolutionary improvement
- Minimize performance degradation from takeoff to cruise:
  - A significant 2 pts. efficiency loss

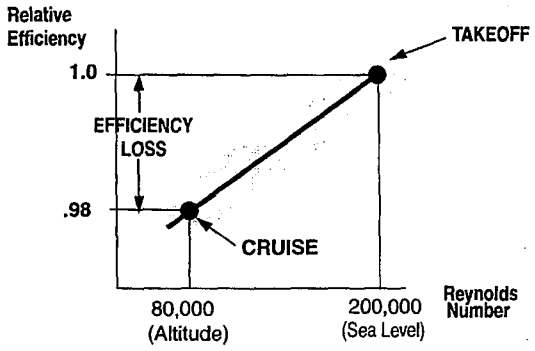

LPT FLOW PHYSICS

- Low Reynolds number flow
- Interplay of the three physical mechanisms determine flow and associated losses

PHYSICAL MECHANISMS:

- ✦ SEPARATION
  - Separation bubbles on the suction surface
- ✦ WAKE PASSING
  - Wake/boundary-layer interaction
- ✦ TRANSITION
  - Bypass transition
  - Transition in separation bubbles
  - Calmed regions & turbulent spot dynamics

Affecting parameters:

- ❑ Reynolds number
- ❑ Freestream turbulence intensity and characteristics (scales etc.)
- ❑ Wake turbulence intensity and characteristics (scales etc.)
- ❑ Pressure gradient (loading)
- ❑ Reduced frequency

GOAL STATEMENT

Provide Fundamental Understanding and Practical Models of Transition/Separation Which Lead to Improved Design and Performance of the LP Turbine

Alignment With NASA's Mission

The Aeronautics Enterprise Program "Pillars"

- ✈ Pillar I. Global Civil Aviation
  - ✈ Affordable Air Travel
    - ✈ Increase Fuel Efficiency
- ✈ Pillar II. Revolutionary Technology Leaps
  - ✈ Innovative Tools & Technology
    - ✈ Reduce Development time to market

Future Vision

- **Zero efficiency degradation between take-off and cruise**
- **Full understanding of LPT flow physics:**
  *** transition * separation * wake interaction * affecting factors**
- **Advanced models of flow phenomena**
- **Unsteady 3-D multistage RANS/LES computational capability**

Payoffs

- **Fuel savings**
- **Improved LPT and overall engine designs**
- **Reduced cost/time of engine design cycle**

Barriers

- **Limited capabilities/high cost of unsteady CFD in engine environment**
- **Cost and complexity of experiments in real engine**
- **Lack of experimental data bases**
- **DNS data bases not yet feasible**
- **3-D effects virtually unknown**

MODELING ISSUES

- Separation/Reattachment
- Effects of wake on attached/separated boundary layers
- Transition onset and extent
  - attached/separated boundary layer
- Turbulent spot physics:
  - Spot dynamics
    - incorporation in models
  - "Calming" (trailing relaxation)
    - effects on separation and transition

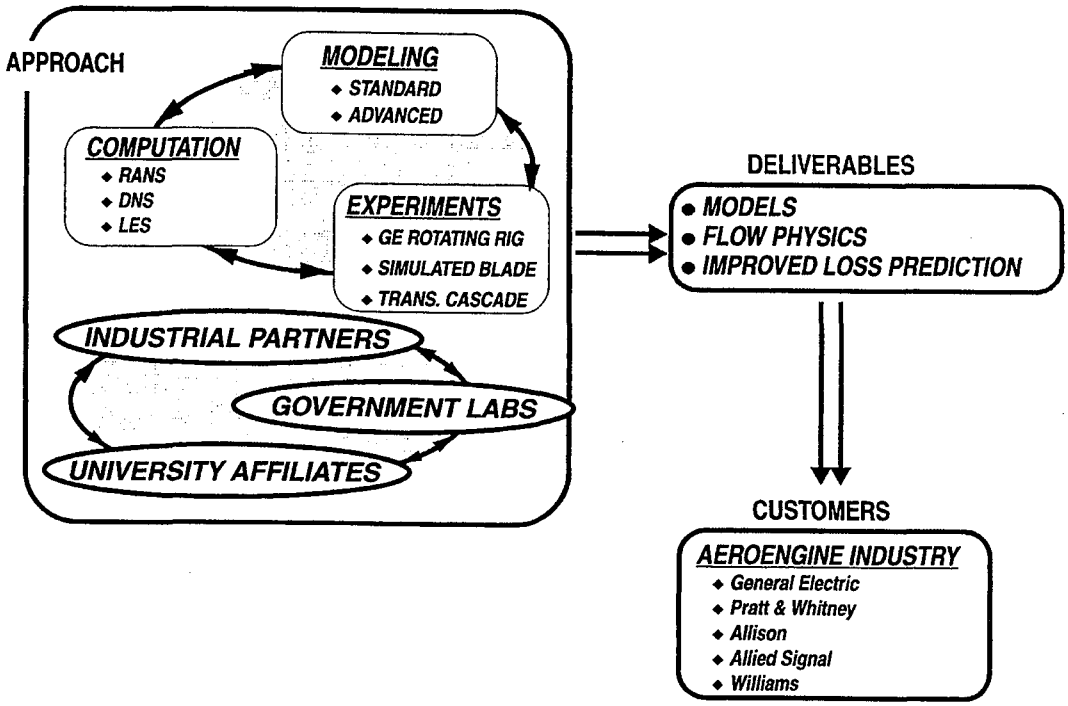

LP TURBINE FLOW PHYSICS PROGRAM

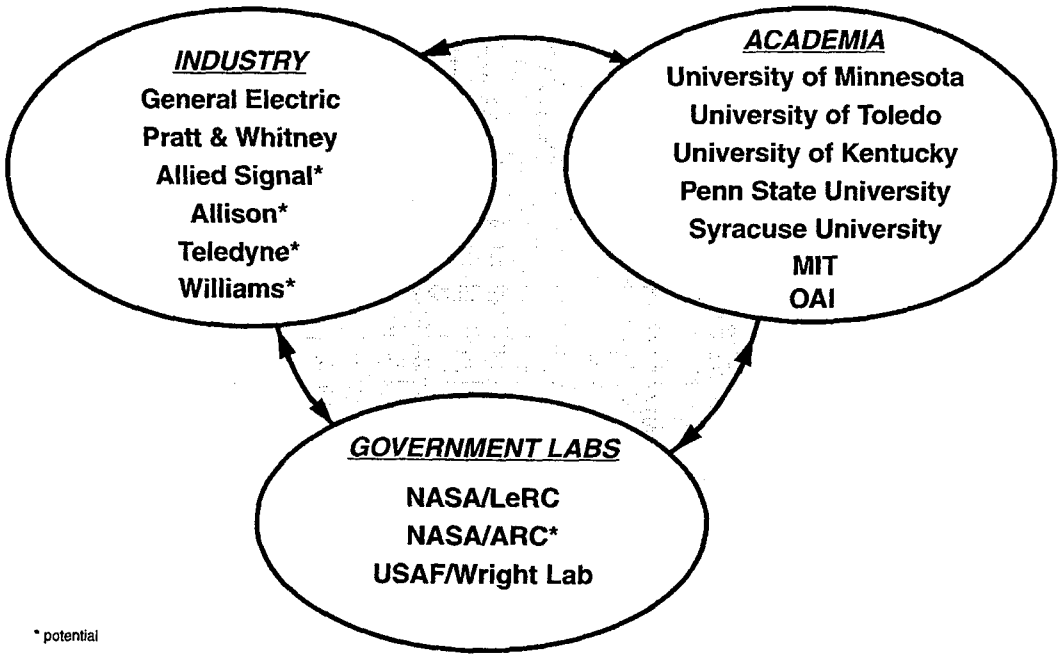

* potential

WORK ELEMENTS

	Task	Org	PI/Investigators	Task Title	Outcome
	EXPERIMENTS				
A	E-1	LeRC/UT	Shyne/Sohn	Simulated Blade With Flat Surface	Surface & Boundary Layer Surveys, Correlations
A	E-2	U. Minnesota	T. Simon/Qiu	Simulated Blade With Curved Surface	
A	E-3	OAI/GEAE	Solomon/Wisler	LSRT GE90 LPT	
A	E-4	LeRC	Boyle/Lucci	Transonic Cascade	
	COMPUTATION				
C	C-1	WMU	Dorney	RANS Analyses	Initial Model Assessment, Major Parameters
	C-4	LeRC	Ashpis/TBD	MSU/AP Code Analysis of GE LSRT Exp.	Integration & Assessment of Models
	C-5	GEAE/LeRC	TBD/Adamczyk	MSU/AP Code Analysis of GE90 LPT Exp.	Code & Model Validation for LPT
C	C-6	MIT/PW/LeRC	Tan/Burry	DNS with SEM code	Laminar Separation Baseline Data Base
S	C-8	U. Kentucky	Huang/Hauser	LES of LPT	Flowfield Data Bases
	MODELING				
D	M-1	OAI	Liou	Assessment of Existing Models	Evaluation of Applicability of Existing Models
A	M-2	LeRC	F. Simon	Development of Flow Physics Models	Models that describe the physics of transition, separation and the "calmed" region
A	M-3	SU/LeRC	Lewalle/Ashpis	Wavelet-Based Modeling and Post-Processing	Models that describe turbulent scales, Improved understanding of flow physics
D	M-5	NYMA-LeRC	W-M To	Assessment of Models Using SEM Code	Accuracy Assessment of New Models
A	M-6	Penn State	Lakshminarayana	Development of New Engineering Models	Models that capture unsteady wake effects on transition, separation and the "calmed" region
A	M-7	U. Kentucky	Huang/Xiong	Development of Advanced Models	
	THEORY				
A	T-1	LeRC	Hultgren	Flow Physics Fundamentals	Improved understanding of receptivity, separation, and wake induced transition

A - Active C - Completed D - Discontinued S - To start 10/97

STATUS SUMMARY

- Good progress in computational and experimental activities
- Blade coordinates provided by P&W and GEAE
- Cooperative work with GEAE in progress
- Mailing list for technology transfer
- Timely dissemination of progress reports
- Continuous improvement of the program
- Several work elements completed, others added, some deleted
- Strong interaction between researchers.

NOMENCLATURE

AP	Average Passage
ARC	Ames Research Center
CMOTT	Center for Modeling of Turbulence & Transition
DNS	Direct Navier-Stokes Simulation
GEAE	General Electric Aircraft Engines
LERC	Lewis Research Center
LES	Large Eddy Simulation
LP	Low Pressure
LPT	Low Pressure Turbine
LSRT	Low Speed Research Turbine
MIT	Massachusetts Institute of Technology
MSU	Mississippi State University
OAI	Ohio Aerospace Institute
P&W	Pratt & Whitney
PostDoc	Post-Doctoral Researcher
RANS	Reynolds-Averaged Navier-Stokes
SEM	Spectral-Element Method
SU	Syracuse University
UM	University of Minnesota
UT	University of Toledo
UK	University of Kentucky
WMU	Western Michigan University

THE TECHNICAL AND ECONOMIC RELEVANCE OF UNDERSTANDING BOUNDARY LAYER TRANSITION IN GAS TURBINE ENGINES

David C. Wisler
GE Aircraft Engines
Cincinnati, Ohio

Abstract

This presentation addresses the technical and economic relevance of understanding boundary layer transition in gas turbine engines from two perspectives. The first is the micro perspective of the technologist and designer whose principal task is to untie (or even cut) the Gordian knot of transition and thus, hopefully, produce better component designs. The second is the macro perspective of overall engine economics and reliability where the benefits of "this better component design obtained from improved understanding of transition" are compared to the benefits that could potentially be realized from improvements in other areas.

From the micro perspective, we have now reached the point where our lack of ability to predict the location of boundary layer transition for components in gas turbine engines is impeding our ability to gain maximum benefit from our design effort. This is especially true for compressor and turbine blade rows with their respective relative motion between rotors and stators. Clearly the numerics for 2-D and 3-D Reynolds-averaged N-S solutions are in hand. So too is CPU computing power. What's missing is an adequate turbulence model, one the provides a practical, CFD design tool that will consistently and accurately predict transition and other boundary layer features for arbitrary flows. This missing link impedes designers in their efforts to tailor airfoil shapes to achieve increased loading and/or increased efficiency. With increased airfoil loading, engine part count can be reduced. With increased efficiency, engine fuel consumption is reduced. The presentation discusses the magnitudes of the benefits one might potentially achieve in these micro endeavors.

From a macro perspective, there are issues that are far more significant to engine economics than those involving the resolution of boundary layer transition. Understanding the relative importance of these issues enables one to get a better understanding of why the gas turbine industry is moving in its current direction. We are approaching a mature technology. Thus we are becoming more of a cost-driven business and less of a technology-driven business, although our product is still "very high tech". With more maturity comes a focus on manufacturing costs, quality, product reliability and total cost of engine ownership. Design for Manufacture, Design for Reliability, Error Proofing Design, and Low Maintenance are heavy hitters economically. This presentation discusses the relative magnitudes of the benefits one might potentially achieve in these macro endeavors.

Understanding transition phenomena is certainly important, but its importance also needs to be viewed in the context of total engine economics. With this understanding, the roles of industry, universities and government laboratories in finding solutions to the transition issue are discussed.

Objectives

- **Examine the Technical and Economic Relevance (Impact) of Understanding BL Transition from Two Perspectives**
  - **– *Micro Perspective* (Technologist Working the Field)**
  - **– *Macro Perspective* (Engine Global Viewpoint)**
- **Provide Some Insights:**
  - **– From Where the Answers Likely Will (and Will Not) Come**
  - **– GEAE's Transition Work**
- **Ask Questions for Later Discussion**

The Micro Perspective

What We Have:

- **3–D, Reynolds–Averaged, N–S Solvers**
- **CPU Computing Power**
- **k–ε, Baldwin–Lomax, etc. Turbulence Models**

What We Need:

- **The Above ... *Plus* ...**
- **Adequate Turbulence Model**
  - **– Predicts Transition and other BL Features Consistently and Accurately for Arbitrary (unsteady) Flows**
  - **– Incorporates Wake–Passing & Calming Effects Accurately**

What We Would Really, Really Like:

- **All of the Above Embodied in a *Practical CFD Design Tool* That Can Be Used to Accurately Compare Designs**

Where Better Understanding of Transition *Could* Be Useful

Component	Application	Benefit
1. Nacelle	Laminar Flow Nacelle	Reduced Drag (?Bugs?)
2. Transonic Fan 3. LP Compressor (Booster) 4. HP Compressor	• Design LE Region • Shock/BL Interaction • C–D/C–T Airfoils • Compare 3–D Designs • Unsteady Wake (Calming) • Stator Indexing	• Small Efficiency Increase • Better Optimization of Design • Predict Speedline (Off Design Tool)
5. HP Turbine (Film Cooled)	Not Much – Film Cooling has Strong Influence	
6. LP Turbine	• Design Loading Distrib. • Unsteady Wake (Calming) • Evaluate High Alt Cruise • Nozzle Indexing • Compare 3–D Designs	• Small Efficiency Increase • Increase Airfoil Loading (Reduce Part Count/Wt) • Better Optimization

But How Large is the Benefit?

Component Sensitivities (Derivatives)†

Cruise @ 35K ft., M = 0.8

1% Change in Efficiency of	Percent Change in Specific Fuel Consumption (SFC)*
• Fan	~ 0.62 %
• Low Pressure Compressor	~ 0.22 %
• High Pressure Compressor	~ 0.66 %
• High Pressure Turbine	~ 0.82 %
• Low Pressure Turbine	~ 0.96 %

† Typical, but value is very sensitive to aircraft, mission, Engine Configuration, etc.

* SFC is in pounds of fuel per hour per pound of thrust

Engine Sensitivities

1000 nm mission with 45,000 Lbs. T/O SLS F_n Engine

3.7% SFC
17% Engine Weight
7.3% Engine Cost
18% Maintenance Cost

⇨ 1% DOC (Direct Operating Cost

Assumptions:

80% Depreciation over 15 yrs.
10% Down, 10% Residual
6% Airframe Spares, 17% Engine Spares
6.0% Interest
25 Year Service Life
Fuel Price = $0.70 USG
1300 Trips/yr

DOC Includes:

- Cash DOC Items:
  - Flight & Cabin Crew
  - Fuel
  - Airframe Maintenance
  - Hull Insurance
  - Landing Fees
- Depreciation:
  - Airframe
  - Engine
- Interest:

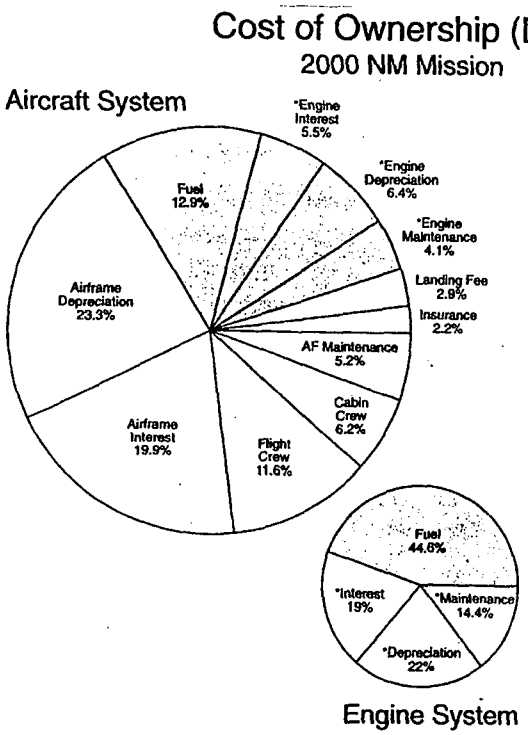

Engine Influences
≈25–30% of
Aircraft DOC

Typical Values of SFC

Engine	Specific Fuel Consumption (SFC)*	
	Cruise	Take–Off
• GE90	0.458	0.288
• CF6–50	0.620	0.377

*** SFC is in pounds of fuel per hour per pound of thrust**

Typical Example

Using the general values given previously, one can compute the savings obtained from a 1% Improvement in LPT Efficiency

A 2000 nm Trip Costs the Airlines $\sim$ $31,000 in DOC
@ 650 Trips/year Costs $\sim$ $ 20 M in DOC

1% improvement in DOC Saves $\sim$ $200,000/ year per aircraft

This means that a

1% improvement in LPT η Saves $\sim$ $52,000/ year per aircraft

Micro Conclusions

Better Transition Technology That Produces Improved Understanding and Better Design Tools Has the Potential to Improve Engine Performance

- **Can Put Design Process on Firmer Physics–Based Grounds**
- **Gains Produced Likely to be Small (But Not Unimportant)**
- **Some General Concepts Already Known so Clever Designers Can Reap Benefits Today**
  - **Can Remove LPT Airfoils Without Penalty–How Many? (We know about calming effects)**
  - **Can Clock Airfoil Rows**
  - **Can Evaluate Loading Distributions**

Beware of the Myth

A Better Understanding of and a Full Accounting for all Features of a Complex Flow Necessarily Lead to

1) Better Design

2) Major Advancement

The Macro Perspective

(Engine Global Viewpoint)

What are the Heavy Hitters Economically?
- **To the Cost of Doing Business**
- **To Our Customers**

What Do Our Customers Actually Want?

How Do We Control Costs While:
- **Satisfying Customers**
- **Providing Safe, Reliable, Easily–Maintained Product**

Aircraft Gas Turbine Engines

A Complex Business

Product Life Cycle > 20 years

Development Costs

- **Derivative Engine ~ $400 – 500 M**
- **New Engine > $1,000 M**

Individual Engine Costs ~ $3M to $10M

Our Business Really Departs from "Toaster" or "Computer Hardware" Business

How Are You Going To Design the Engine?

Design for	**Technology**
"	**Manufacturability (Producibility)**
"	**Reliability**
"	**Ease of Maintenance**
"	**Low Cost**
"	**Ease of Disassembly**
"	**Weight**
"	**Number of Parts**
"	**Reduced Complexity**
"	**Etc.**

One Must Achieve a Proper Balance

Examples of Economic Heavy Hitters

Item	Cost
1. Manufacturing Losses in Internal, Partners, and Suppliers Shops (scrap, rework, repair)	$ Hundreds of Millions
2. Reliability Issues (Warranty Costs, Concessions, Give–aways)	$ Hundreds of Millions
3. Errors (Drive Enormous Cost and Customer Pain) • Missed Operation (Heat Treat) • Missed Non–Destructive Evaluation • Assembly / Maintenance Errors	$ Hundreds of Millions

How Do You Error–Proof the Design?

Business Realities of the '90s

- Fierce competitive pressures have forced GEAE to:
  - Reduce workforce significantly (*21,000 to 8500 at Cincinnati*)
  - Restructure the way of doing business (*emphasize outsourcing*)
  - Reduce cost of products (*more* cost–driven *business, less technology–driven*)
- Business is rebounding strongly but we will NOT return to the ways of the '80s with large research budgets for enabling technology
- Need to resolve complex technical issues within framework of new ways of doing business

When Viewed in the Light of:

1. The Macro Perspective of Economic Heavy Hitters

2. The Business Realities of the '90s

3. The Relatively Small Gains in Performance that can be Achieved by Understanding/Computing Transition Better

One Can See Why Funding for Transition Research by Engine Companies is Low

From Where Will Answers Likely Come?

- **From University Researchers Working in Conjunction with Government Agencies for Funding**
- **Not From GEAE Internal Research**
- **Possibly from Some Small Interactive Research Grants from Gas Turbine Companies**

GEAE's Work in Transition

1. Experimental
   - Low Speed Research Turbine and Compressor Tests *Piggybacked* on Major Research Areas of Interest
     - High Wall Sloped Turbines
     - 3D Aero Designs

2. Numerical
   - Evaluation of Turbulence Models as They are Available
   - Work with GE CR&D

3. University Support
   - Support Limited University Research in Teaming Effort

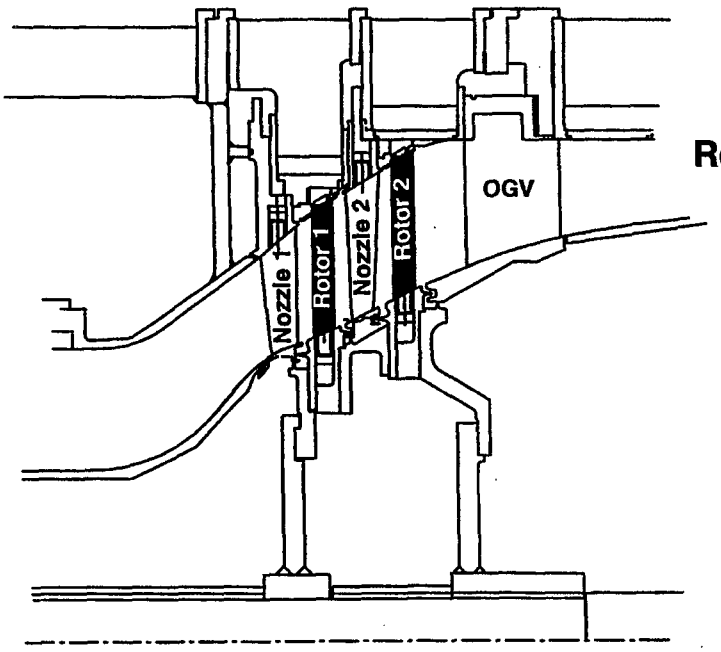

Low Speed Research Turbine

Conclusions

1. Improving Boundary Layer Transition Technology is Relevant to the Gas Turbine Business
   - Could Provide some Product Improvement
   - Would Remove Some Uncertainty in the Design Process

2. For Fair Assessment of its Relevance, One Must View the Benefits of this Relative to the Economic Heavy Hitters
   - Improved Transition Technology Unlikely to Have *Major* Impact on Gas Turbine Engines

3. Universities Should Continue Strong efforts to Develop Improved Transition Technology because
   - Important To Resolve This Issue for General Aerodynamics
   - Gas Turbine Companies Are Not Going To Do It

Questions

1. What facets of BL Transition Research should be conducted?
   - What are the goals of the research?
2. Who will (should) conduct this research?
   - Experimental
   - Numerical / Modeling
3. How detailed of an understanding is necessary (desired)?
4. How will (should) industry participate?
5. How will this research contribute to a design approach?
6. Do the participants understand design or are they linked with a group that does?
7. Who will pay for this?

IMPACT OF REYNOLDS NUMBER ON LP TURBINE PERFORMANCE

Om Sharma
Pratt & Whitney
East Hartford, Connecticut

ABSTRACT

Experimental and numerical methods developed over the past twenty five years have permitted the designs of low pressure turbines, utilized in aircraft gas turbine engines, which yield very high efficiencies at the sea level take off conditions. These turbines, however, encounter large loss in performance at the altitude cruise operating conditions. This loss in performance can be attributed to the impact of Reynolds Number on the behavior of boundary layers on airfoil suction surfaces.

Experimental and analytical results are shown in this paper to elucidate the problem encountered by the turbine design egineers. Experimental data consists of those acquired in an engine and a model rig environment. Analysis of these experimental data demonstrate shortcomings of models, criteria and correlations used in the current design procedures and point towards lack of current understanding of the actual operating environment in the gas turbine engine. Analytical results demonstrate limitations of turbulence / transition models used in a low Reynolds Number environment of low pressure turbines.

Areas of further research are identified to provide support to the design community. Experimental and analytical methods developed over the past twenty five years have permitted.

HIGH LOSSES MEASURED IN CASCADESAT LOW Re

- **LAMINAR SEPARATION BUBBLE RE-ATTACHMENT (TRANSITION) PROCESS CONTROLS LOSS GENERATION**

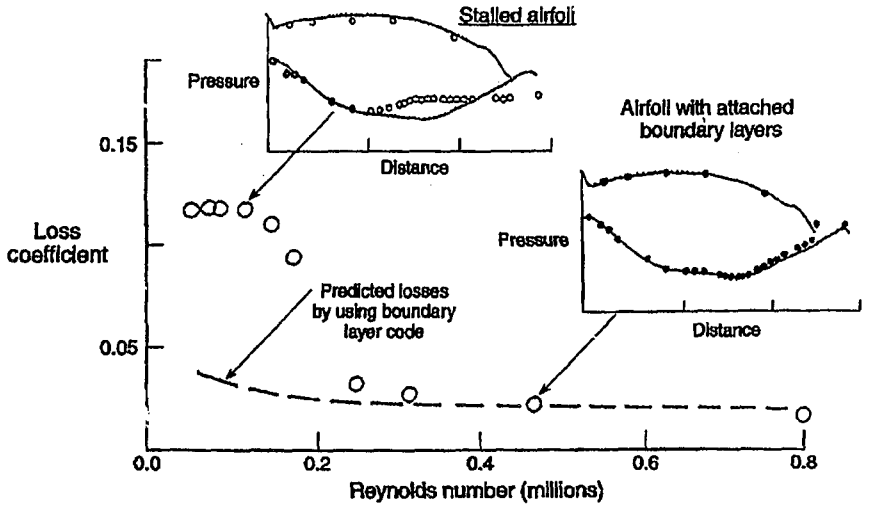

LOW RE # OPERATION CAUSES SIGNIFICANT PERFORMANCE REDUCTION

LOW PRESSURE TURBINES

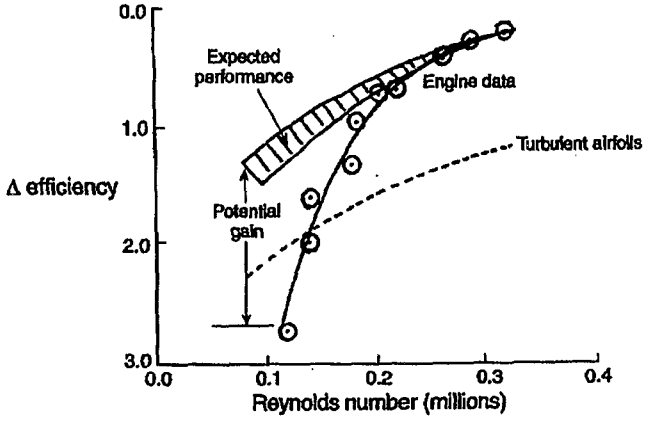

- Loss in performance due to drag on airfoils

SCHEMATICS OF SEPARATION BUBBLES

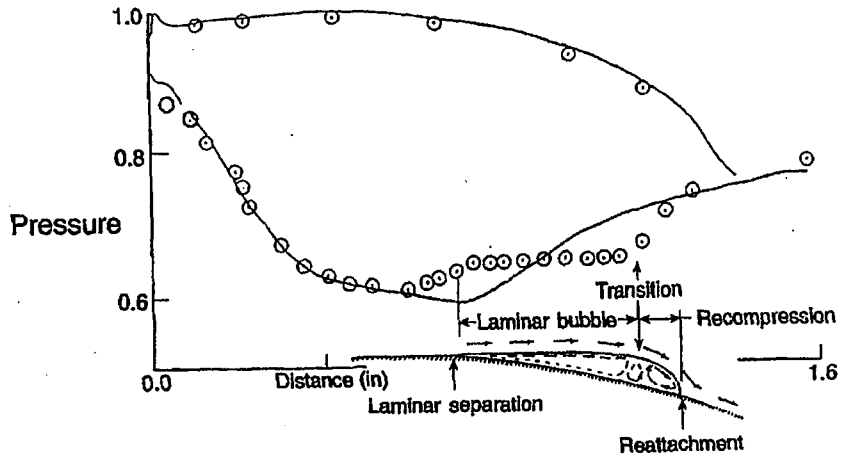

- TURBULENCE/UNSTEADINESS KNOWN TO HAVE SIGNIFICANT IMPACT ON THE BUBBLE SIZE AND TRANSITION ONSET

UNSTEADINESS/TURBULENCE MEASURED IN AN ENGINE

- SEA LEVEL TAKE OFF (SLTO) CONDITIONS AT INLET & EXIT OF A LOW PRESSURE TURBINE

- ALTITUDE CRUISE CONDITIONS AT THE EXIT OF THE SAME TURBINE

SUMMARY OF ENGINE EXIT MEASUREMENTS

	Sea level takeoff	Altitude cruise
Turbulence – random fluctuations		
Turbulence (RMS-intensity)	$\frac{\sqrt{\frac{[Mx]'^2+[My]'^2+[Mz]'^2}{3}}}{[\bar{M}_{Exit\ 60\%\ span}]}$	$\frac{\sqrt{\frac{[Mx]'^2+[My]'^2+[Mz]'^2}{3}}}{[\bar{M}_{Exit\ 60\%\ span}]}$
Wake	17%	21%
Average	12%	15%
Free Stream	8%	10%
Unsteadiness – periodic fluctuations		
Periodic unsteadiness (RMS-intensity)	$\frac{\sqrt{\frac{[\bar{M}x]'^2+[\bar{M}y]'^2+[\bar{M}z]'^2}{3}}}{[\bar{M}_{Exit\ 60\%\ span}]}$	$\frac{\sqrt{\frac{[\bar{M}x]'^2+[\bar{M}y]'^2+[\bar{M}z]'^2}{3}}}{[\bar{M}_{Exit\ 60\%\ span}]}$
Average	6%	16%

COMPARISON OF INLET AND EXIT AT SLTO

	Inlet	Exit
Turbulence – random fluctuations		
Turbulence (RMS-intensity)	$\frac{\sqrt{\frac{[Mx]'^2+[Mz]'^2}{2}}}{[\bar{M}_{Inlet\ 60\%\ span}]}$	$\frac{\sqrt{\frac{[Mx]'^2+[Mz]'^2}{2}}}{[\bar{M}_{Inlet\ 60\%\ span}]}$
Wake	16%	23%
Average	14%	16%
Free Stream	11%	11%
Unsteadiness – periodic fluctuations		
Periodic unsteadiness (RMS-intensity)	$\frac{\sqrt{\frac{[\bar{M}x]'^2+[\bar{M}z]'^2}{2}}}{[\bar{M}_{Inlet\ 60\%\ span}]}$	$\frac{\sqrt{\frac{[\bar{M}x]'^2+[\bar{M}z]'^2}{2}}}{[\bar{M}_{Inlet\ 60\%\ span}]}$
Average	3%	8%

SUMMARY

- SIGNIFICANT LOSSES GENERATED ON AIRFOILS DURING THE LAMINAR SEPARATION AND TURBULENT RE-ATTACHMENT PROCESS
- HIGH LEVELS OF TURBULENCE MEASURED IN AN ENGINE ENVIRONMENT
  - ➡ INDICATIONS ARE THAT THE VISCOUS FLOW IS STILL CONTROLLED BY THE LAMINAR SEPARATION/TURBULENT RE-ATTACHMENT PROCESS
- PHYSICS BASED MODELS & DESIGN GUIDELINES NEEDED
- DIRECT NUMERICAL SIMULATION (DNS) SHOULD BE EXPLORED TO HIGHLIGHT PHYSICS OF LOSS GENERATION MECHANISMS AT LOW Re #

SESSION 2

TURBULENT SPOT CALMED REGION

NASA/CP—1998-206958

BENEFICIAL EFFECTS OF THE CALMED REGION ON FLAT PLATE AND BLADE BOUNDARY LAYERS

J.P. Gostelow
University of Leicester
Leicester, England

Abstract

The calmed region behind triggered wave packets and turbulent spots on a flat plate under a strong controlled diffusion adverse pressure gradient is investigated The results are compared with equivalent transition behavior resulting from incident wakes on the suction surface of a turbine cascade blade. Comparisons are also made with measurements from the stator blades of an axial flow compressor, where turbulent spots are induced by the passing of rotor wakes. The purpose is to gain an appreciation of turbulent spot behavior under an adverse pressure gradient as a foundation for the more accurate modeling of spots and their environment in predictions of transitional boundary layer flows.

Under a strong adverse pressure gradient the calmed region behind a triggered turbulent spot is extensive; its interaction with the surrounding natural boundary layer is complex and its behavior is dependent on whether that boundary layer is laminar or turbulent.

Conditional intermittency profiles are used to investigate the spot and its calmed region in more detail. In particular a new relaxation parameter is used to quantify and describe the calmed region behind the triggered spots and on the compressor blading. Wavelet analysis of triggered spots and wake-induced turbulent patches demonstrates similar calmed region behavior. Boundary layer profiles are also presented through the triggered spot in order to validate the author's modeling of transition based on the physics of turbulent spots.

The calmed region has benefical effects in delaying both laminar separation and transition in wind tunnel flows and on the blade surfaces of turbomachinery. In the calmed region the boundary layer velocity profiles are more stable than those of the laminar boundary layer. This has the effect of delaying laminar separation. The amplitude of Tollmien-Schlichting instabilities is reduced in the calmed region and the consequent progression to harmonic breakdown and transition to turbulence are delayed in that region.

Basis of New Method

n spot formation rate
σ spot propagation parameter = $\tan\alpha\,(1/b - 1/a)$
G $= n\sigma = n\tan\alpha\,(1/b - 1/a)$

Narasimha intermittency distribution is
$\gamma = 1 - \exp[-(x-x_t)^2 n\sigma/u]$.
Chen and Thyson generalised this for varying u
$\gamma = 1 - \exp[-\sigma(x-x_t)\int_{x_t}^{x} (dx/u)]$.

This assumes that n, σ are fixed at flat plate, zero pressure gradient values - i.e. classical Emmons spot. We will demonstrate that under variable pressure gradient the spot varies substantially from the classical Emmons model. In particular n and σ vary with pressure gradient parameter, λ_θ, and free stream turbulence level, q. We need correlations for these which can be incorporated into the integral,

$$\gamma = 1 - \exp[-n \int_{x_t}^{x} (\sigma/\tan\alpha).(dx/u) \int_{x_t}^{x} \tan\alpha\, dx]$$

These have been provided through experimentally-determined correlations for:

$N = n\sigma\theta_t^3/\nu = f_1(\lambda_\theta, q)$, $\sigma = f_2(\lambda_\theta)$ and $\alpha = f_3(\lambda_\theta)$.

The correlations are:

$$N = f_1(\lambda_\theta, q) = 0.86\times10^{-3}\exp[2.134\lambda_{\theta t}\ln(q) - 59.23\lambda_{\theta t} - 0.564\ln(q)]$$

$$\sigma = f_2(\lambda_\theta) = 0.03 + (0.37/(0.48 + 3.0\exp(52.9\lambda_\theta)))$$

$$\alpha = f_3(\lambda_\theta) = 4.0 + (22.14/(0.79 + 2.72\exp(47.63\lambda_\theta))).$$

This is the basis of the new integral method which takes into account local pressure gradient variations through the transition region.

TABLE I Turbulent Spot Spreading and Celerities, $0.05<y/\delta_L<0.35$.

	β	λ_θ	a	b	α^o	σ
Present work	-0.223	-0.0573	0.872	0.431	29.2	0.656
van Hest (1994)	-0.14	-0.036	0.92	0.38	17.0	0.472
Gostelow *et al.* (1993)	-0.173	-0.031	0.8	0.5	24.0	0.334
Seifert and Wygnanski (1994)	-0.1	-0.018	0.9	0.49	21.0	0.357
Sankaran *et al.* (1986)	0.0	0.0	0.74	0.53	9.0	0.084
Wygnanski *et al.* (1982)	0.0	0.0	0.89	0.57	9.2	0.102
Schubauer and Klebanoff (1956)	0.0	0.0	0.88	0.5	10.0	0.152
Sankaran *et al.* (1986)	0.095	0.018*	0.79	0.69	7.3	0.024
Wygnanski (1981)	0.12	0.022*	0.98	0.68	5.0	0.039
Katz *et al.* (1990)	1.0	0.059	0.9	0.61	5.0	0.04

*assumes global similarity

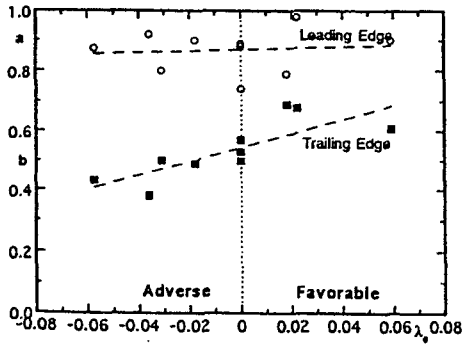

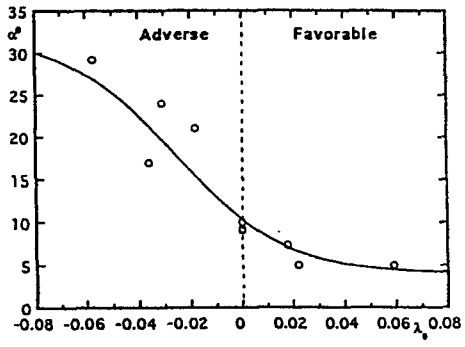

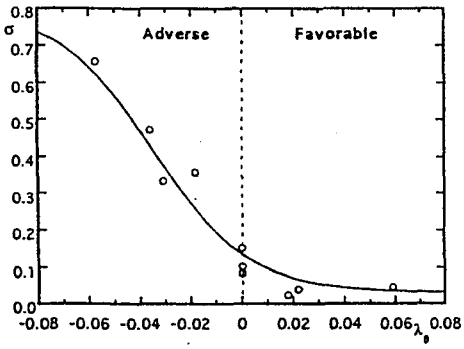

Amplitude reduction and suppression of harmonic development behind a triggered wave packet and spot. Hot wire traces near wall. Three successive streamwise locations. Behavior is illustrated by wavelets.

Wave packet initially has pure T-S wavelength. This develops a harmonic. Meanwhile ambient boundary layer oscillates at this wavelength.

Finally spot develops with high frequency content. Natural boundary layer develops the second (harmonic) phase but in the calmed region the amplitude is attenuated and harmonic development delayed.

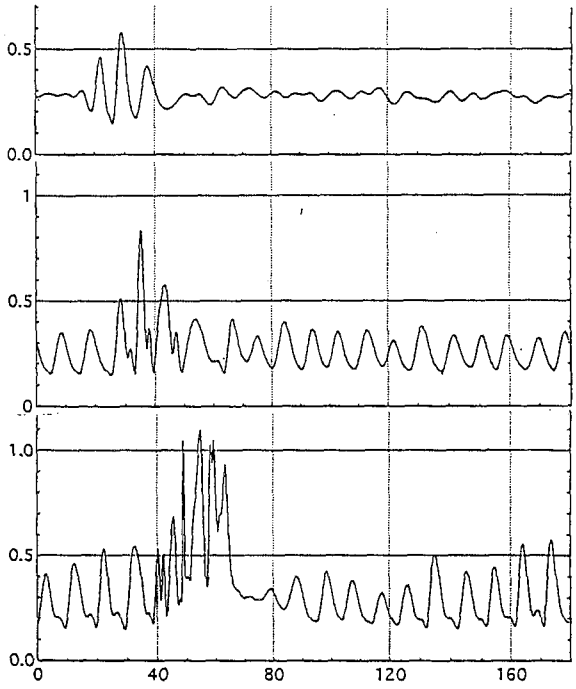

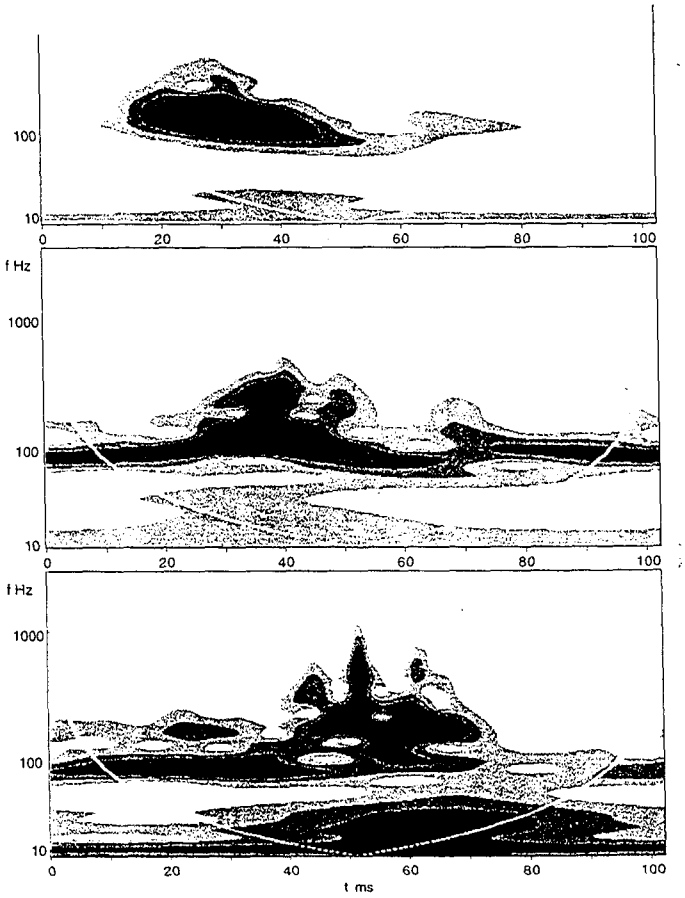

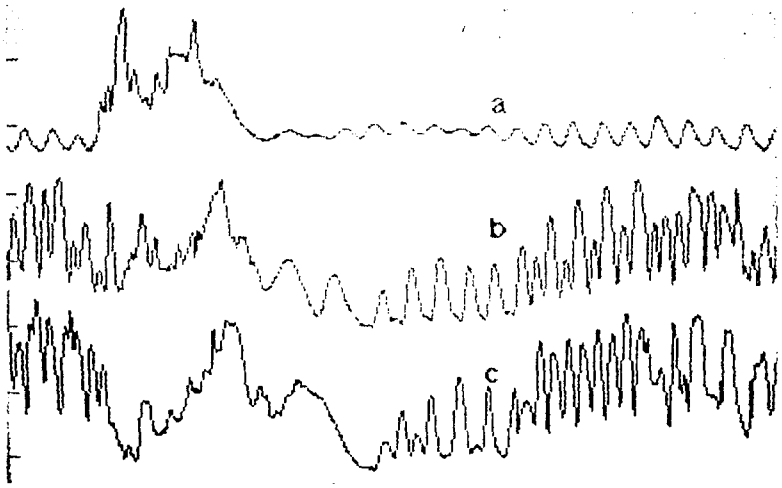

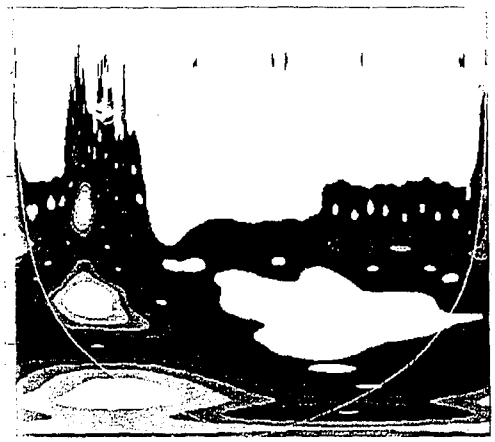

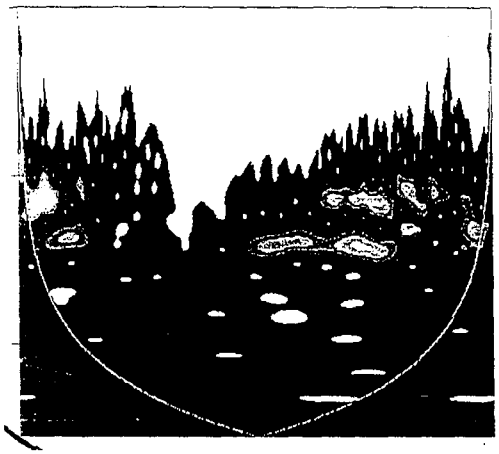

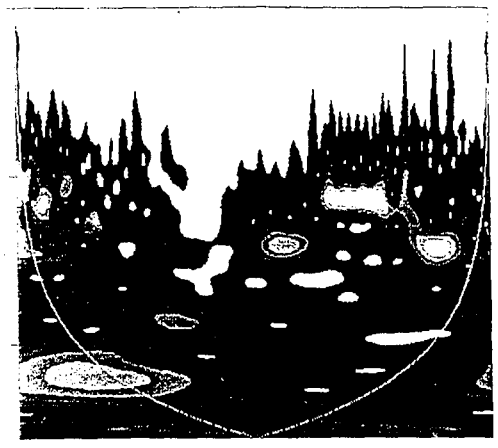

Thin film traces of Schulte and Hodson show similar tendencies. Instead of a triggered spot we are looking at effects of an impinging wake at three streamwise locations.

In 'a' the natural boundary layer displays strong T-S activity which is attenuated in the calmed region. In 'b' the amplitude in the calmed region has grown whilst significant harmonic activity has developed in the natural boundary layer. In 'c' the natural layer is undergoing transition and the calmed region displays harmonic activity.

These behavior modes of a boundary layer affected by wake interaction are similar to those of the triggered spot. This shows that the calmed region prevails behind any such disturbance whether 2-D or 3-D. It is therefore important in the wake interactions of turbomachinery.

G.E. work predicted behavior shown in s~t cartoon. Between the wakes are a laminar region, a calmed region, a transitional region and a turbulent region.

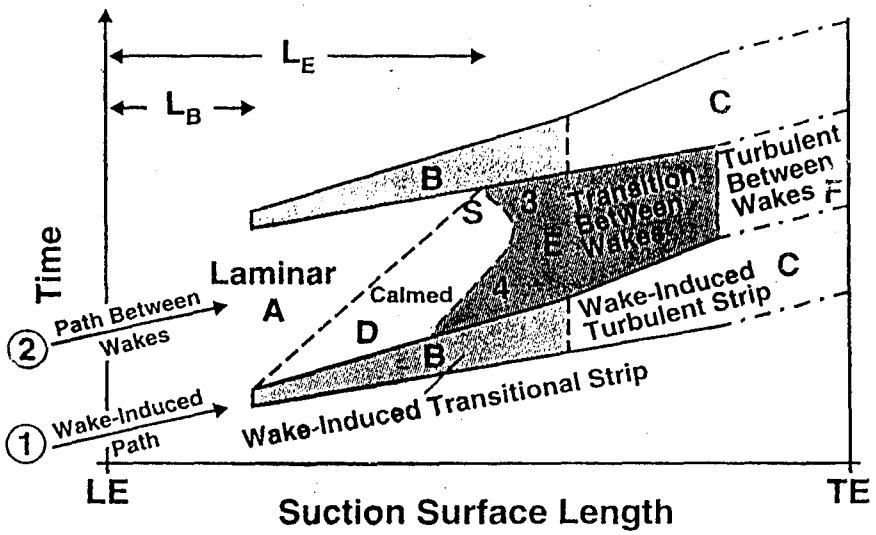

University of Tasmania film gage data for wakes passing over stator blades show these regions. Removal of one wake (i.e. one rotor blade) showed that calmed region no longer was able to hold off the natural transition. Plotted are rms (greyscale) and relaxation parameter (contours).

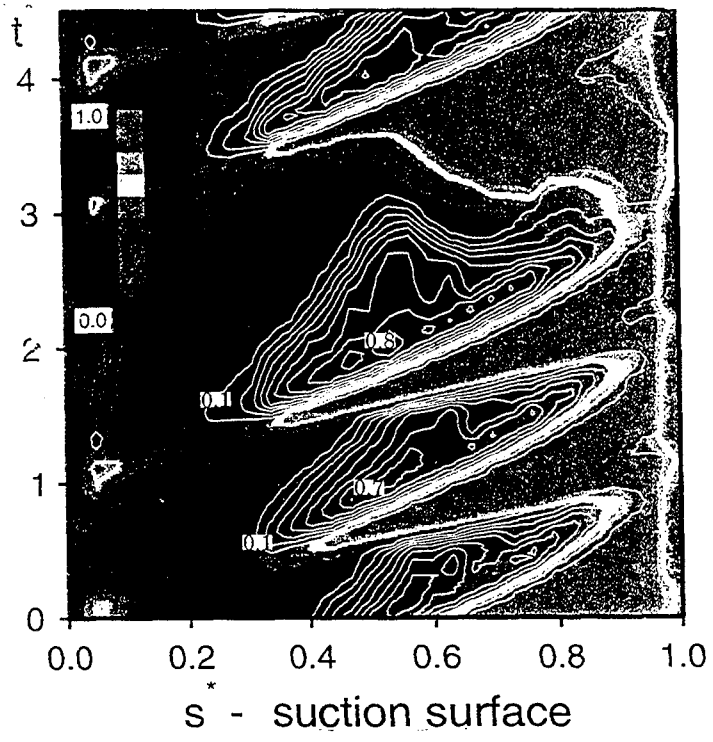

Top elevation shows rms variation of spot and calmed region in a turbulent layer. Second elevation shows how κ varies behind spot. Note that it is only really useful near the wall.

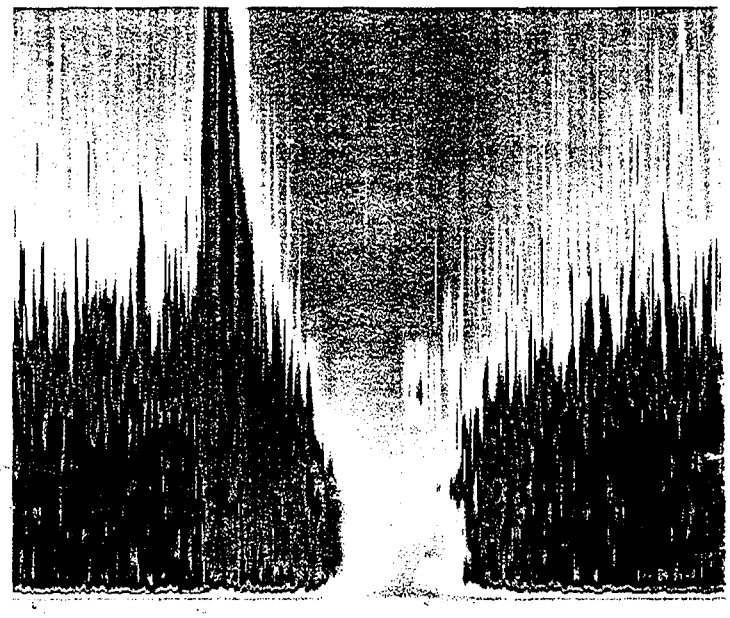

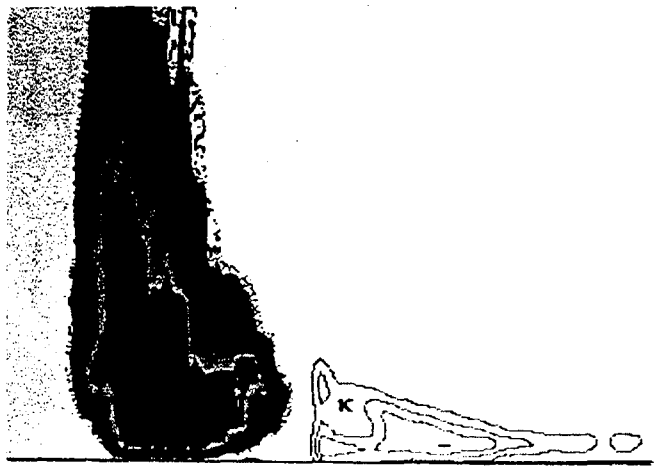

To quantify extent of calmed region a new relaxation parameter κ is introduced. Defined as probability that, following a reduction of intermittency below unity, the flow remains in a relaxing state.

Typical behavior of various parameters through triggered spot and calmed region given below. Main indicators for spot are intermittency, γ, and Blackwelder rms (disturbance integrated over height of spot). For calmed region H and relaxation (calmed) parameter are used.

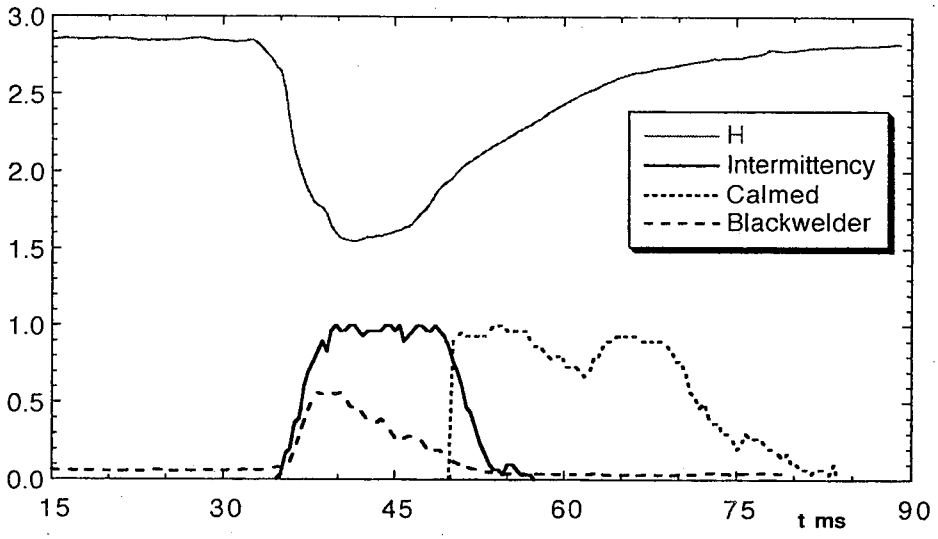

γ and κ are most sensitive. Nevertheless Blackwelder disturbance can be sensitive as shown by this plan view of spot and calmed region.

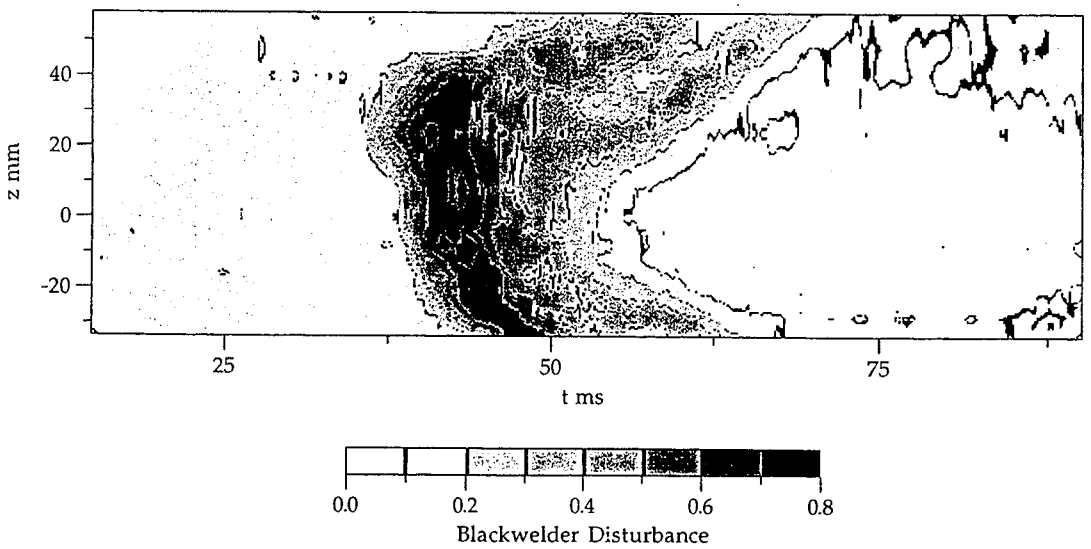

These x-t results show similar effects for a triggered spot under adverse pressure gradient. Plotted are Blackwelder rms as greyscale and H as contours. Transition of natural layer is suppressed by the injection of a spot and its calmed region.

From results such as these the celerities of spot and calmed region may be plotted. Note that trailing edge of calmed region is gradually affected by boundary layer turbulence.

Boundary layer velocity profiles through triggered spot shown in laminar layer and calmed region. Hartree curves are for reference. Initial layer represented by β of -0.14, obviously susceptible to laminar separation. At beginning of calmed region it has changed to very stable profile represented β of 0.6. One third of way through calmed region something like Blasius profile is attained. Clearly the calmed region reduces susceptibility to laminar separation.

The calmed region, whether behind a triggered spot on a flat plate, induced by a wake on a turbine blade in cascade, or measured on a compressor stator blade, has similar beneficial effects. It reduces amplitude of T-S waves and delays the onset of harmonics and turbulence. It delays the onset of laminar separation and stall. The calmed region occurs not simply behind individual spots but also behind a 'two-dimensional' strip of wake sweeping over a blade. It is extensive in most wake-blade interactions and therefore has a beneficial effect on turbomachinery performance.

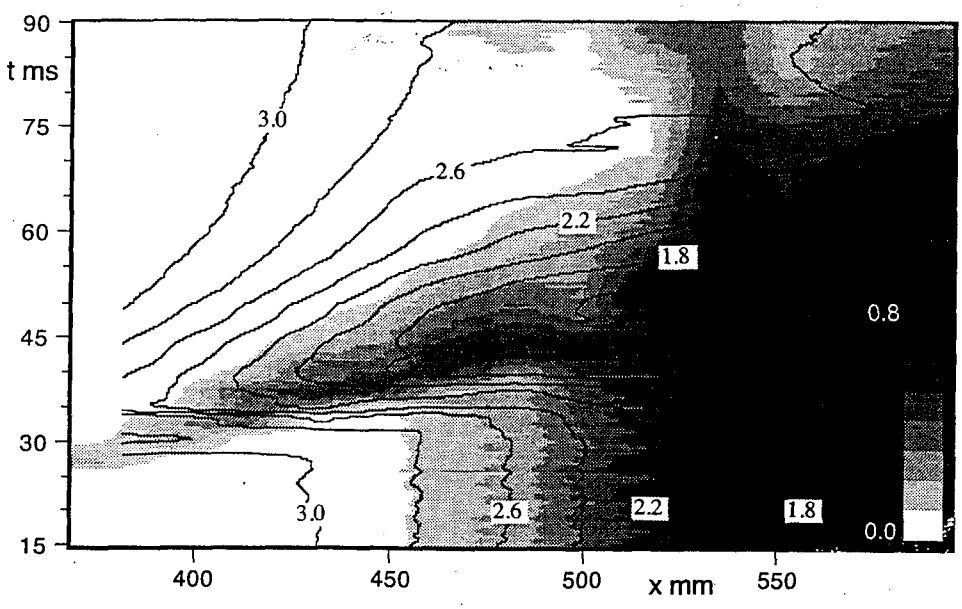

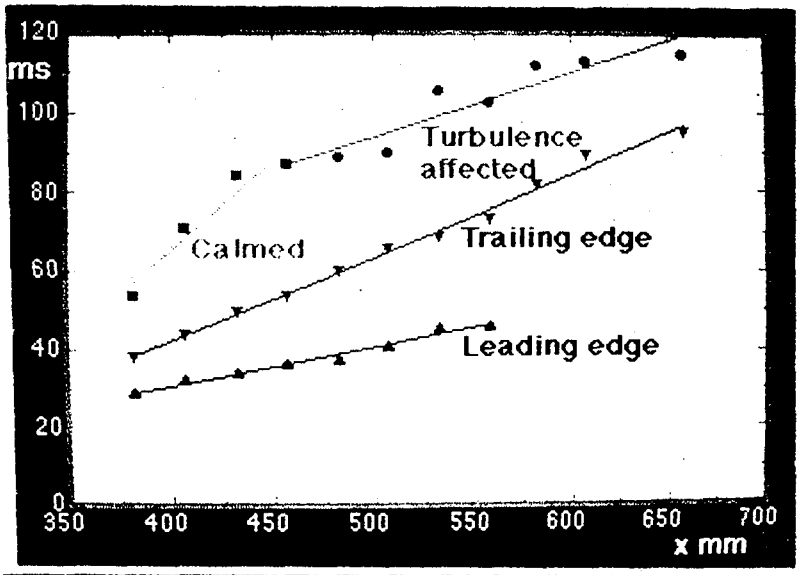

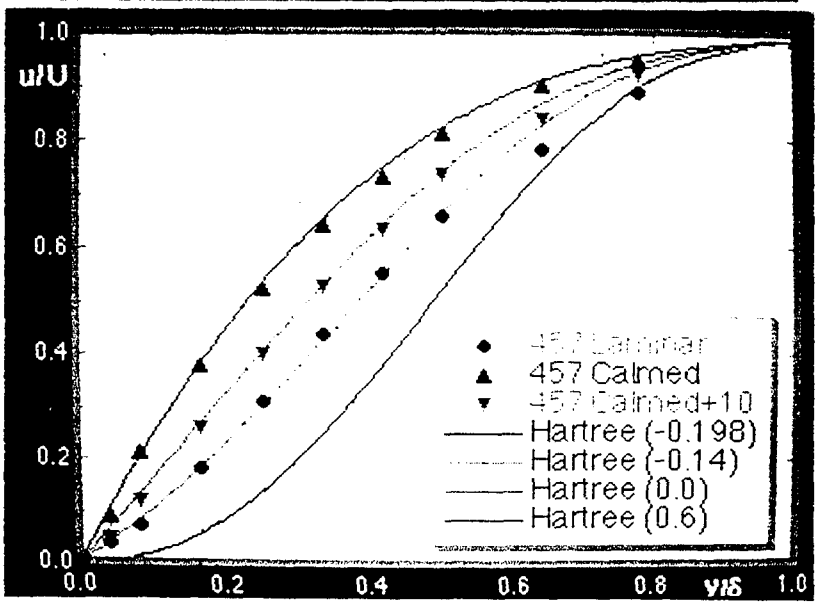

THE CALMED REGION AND ITS SIGNIFICANCE IN LOW PRESSURE TURBINES

H.P. Hodson, V. Schulte,
and R.J. Howell
Cambridge University
Cambridge, England

ABSTRACT

This paper will describe progress in understanding and modelling of some of the important details of the flow and the loss generation processes that arise in low pressure turbines. Particular emphasis will be placed on the unsteady transitional and separated flows that arise in these turbines. It will be shown how their effects may be exploited in controlling the laminar-turbulent attached and separated flow transition processes to the benefit of the design. It is argued that in many low pressure turbines, transition to turbulent flow takes place via the formation of turbulent spots. Recent attention has focused on the so called 'calmed region' that follows the turbulent spots that have observed inside the boundary layers of turbomachinery blading. The nature and the significance of the calmed region are examined using experimental observations and computational studies. It is shown that the calmed region may be modelled using the unsteady laminar boundary layer equations. It is found that the calmed region produces about the same amount of entropy as would a laminar boundary. Because the becalmed region is less prone to separation than a conventional laminar boundary layer, it may be exploited to increase the lift of low pressure turbine blades by preventing boundary layer separation and the increase in loss that this entails. A spot-based unsteady intermittency model is proposed with an extension allowing for the 'calming effect' of passing wakes. Predictions of the effect of the calmed region are obtained using a well known blade-blade flow solver. The predictions utilize an algebraic turbulence model in conjunction with the prescribed unsteady intermittency model. Comparisons are made with experiments using surface mounted hot-film measurements from unsteady cascade as well as full scale rig testing in an Altitude Test Facility. Comparisons with data on the profile losses low pressure turbine blades at low Reynolds-numbers suggests that the method is capable of predicting the variation of loss with Reynolds-number and with wake-passing frequency.

Overview

- "Traditional" cost of unsteady wake induced transition
- Benefits of unsteady wake induced transition
  - entropy production in the calmed zone
- Prescribed Unsteady Intermittency Models
- Examples
- Conclusions

Effect of wakes on profile loss: Datum (Curtis et al, 1997)

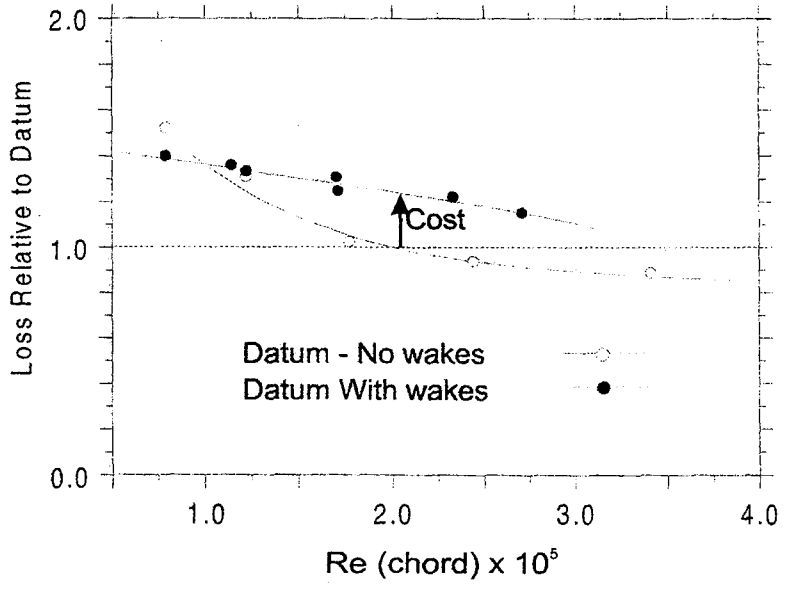

Effect of wakes on profile loss: +20% lift (Curtis et al, 1997)

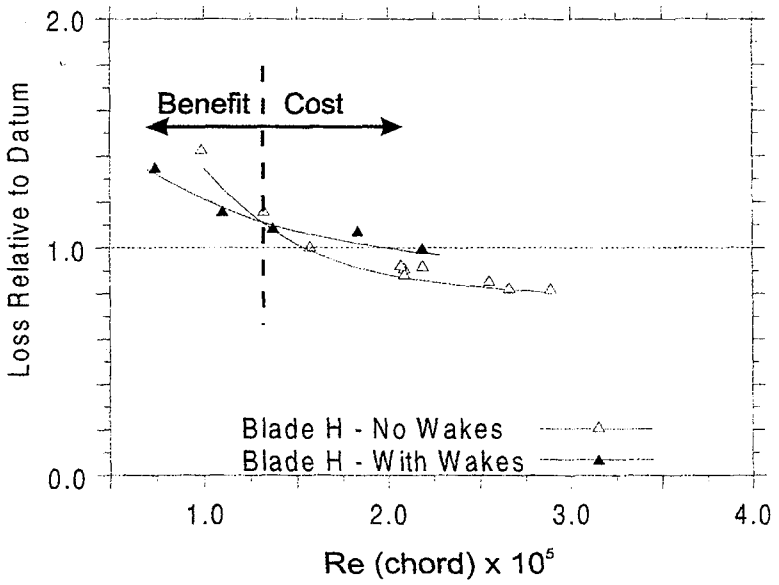

The Benefits of Calming

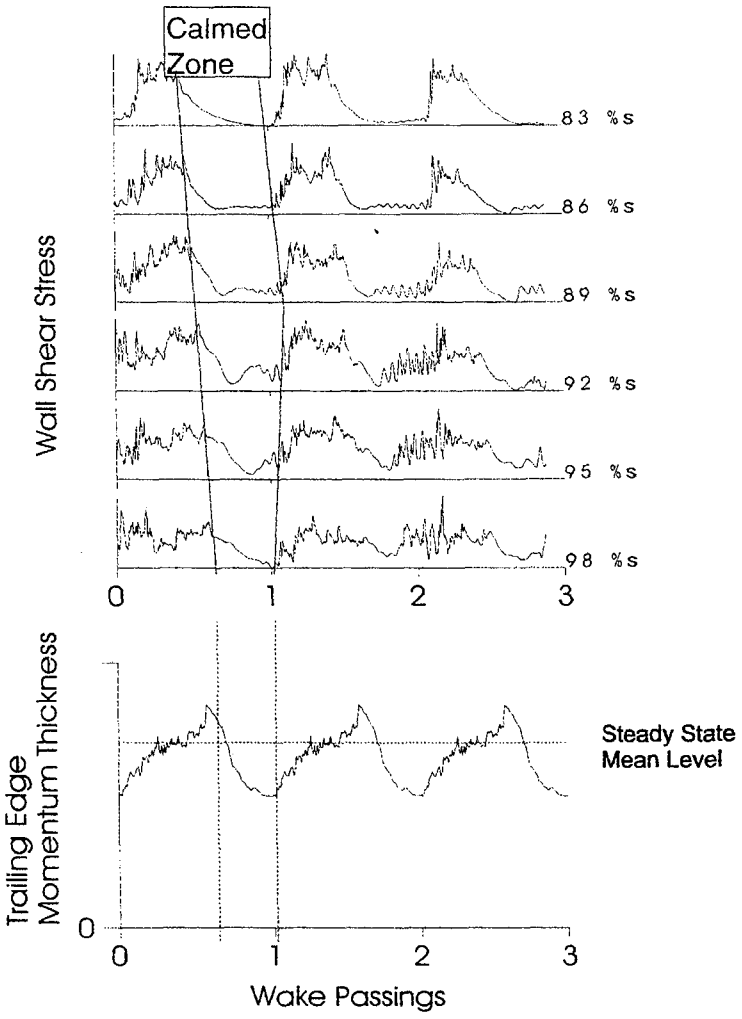

Schematic Interpretation

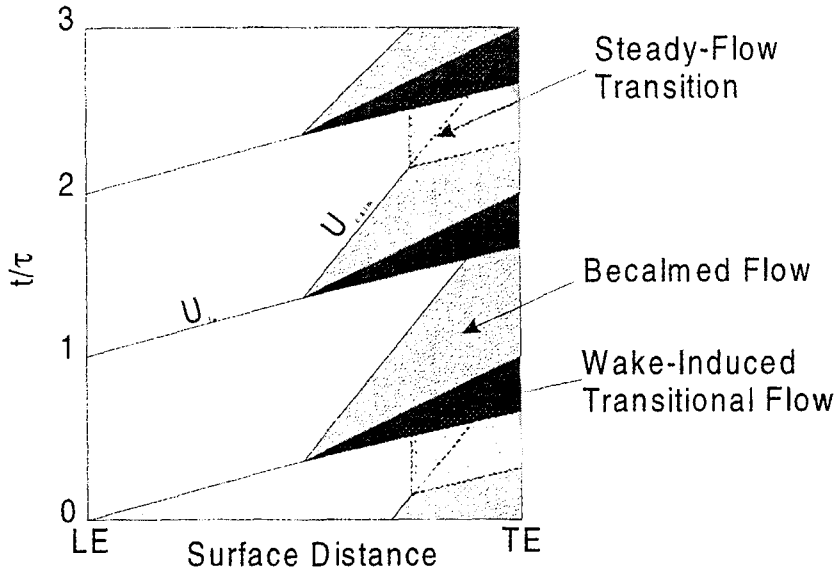

Predicted Entropy Production for Siefert's experiment

C_d = *dissipation integral*

where

$$\frac{d}{dx}\left(U^3\varepsilon\right) = 2\int_0^{\delta} \upsilon\left(\frac{\partial u}{\partial y}\right)^2 dy = 2C_d U^3$$

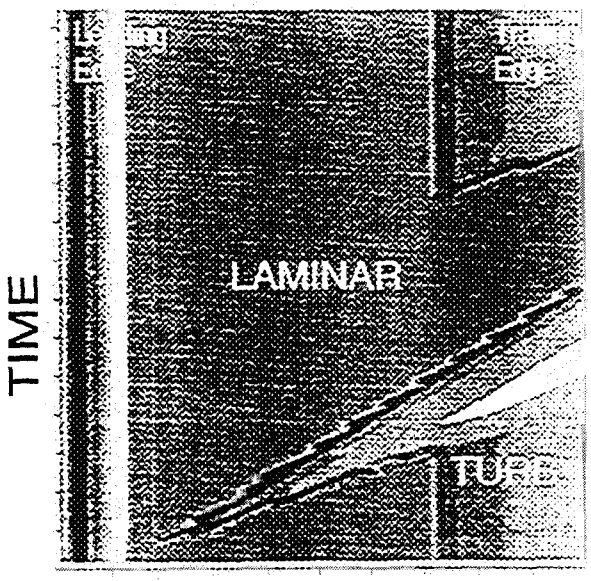

Predicted/Measured (Siefert) Spot-Boundary Layer Interaction

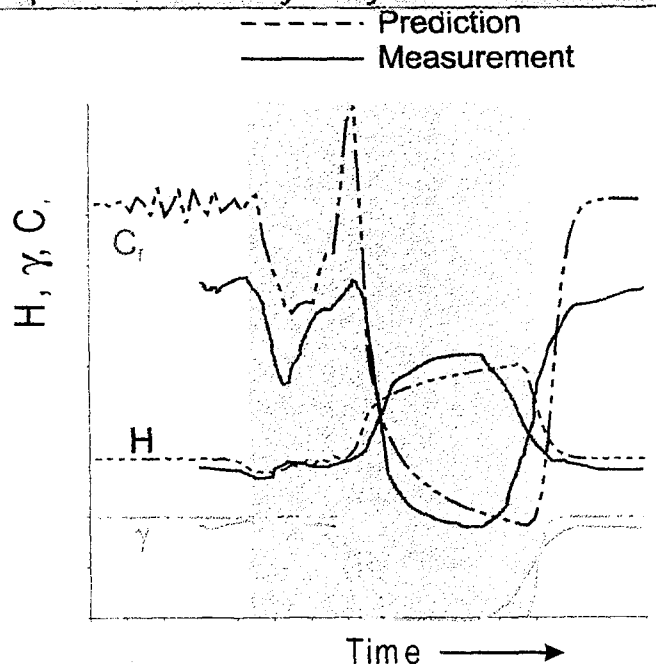

Comparison of BR710 LP Turbine and Whittle Data

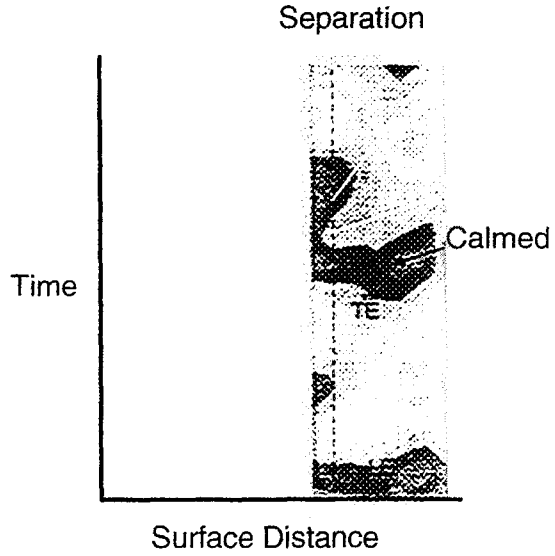

BR 710 Hot film data

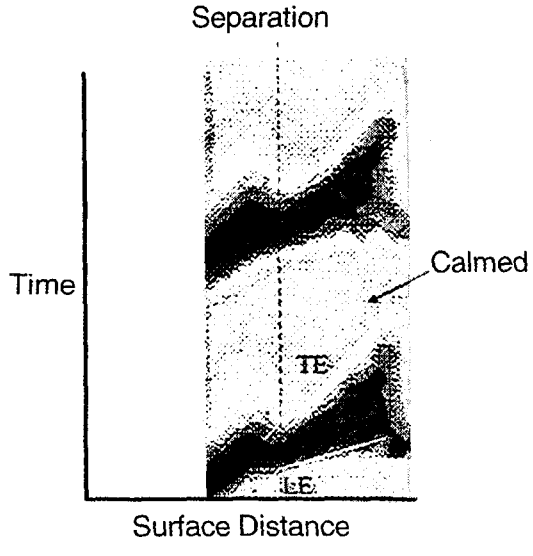

Cascade Hot film data

Prescribed Unsteady Intermittency Model

Inputs

- Steady Flow Solution
- Onset correlations
- Spot formation correlations
- Freestream Turbulence

Output

- Intermittency distribution $\gamma(s,t)$

UNSFLO/PUIM mode

- $\upsilon_{eff} = \upsilon_{lam} + \gamma(s,t)\ \upsilon_t$

Modifying spot production rates - effects of calming

Probability that the point $P(x,z,t)$ is calmed or turbulent

$$\gamma_{corr}(P) = 1 - \exp\left(- \int_{V_{inter}+V_{calm}} g_{corr}(P_0) dV_0 \right)$$

Corrected production rate given by

$$g_{corr}(P_0) = (1 - \gamma_{corr}) g(P_0)$$

Intermittency given by

$$\gamma(P) = 1 - \exp\left(- \int_{V_{inter}} g_{corr}(P_0) dV_0 \right)$$

Predicted γ(s,t)

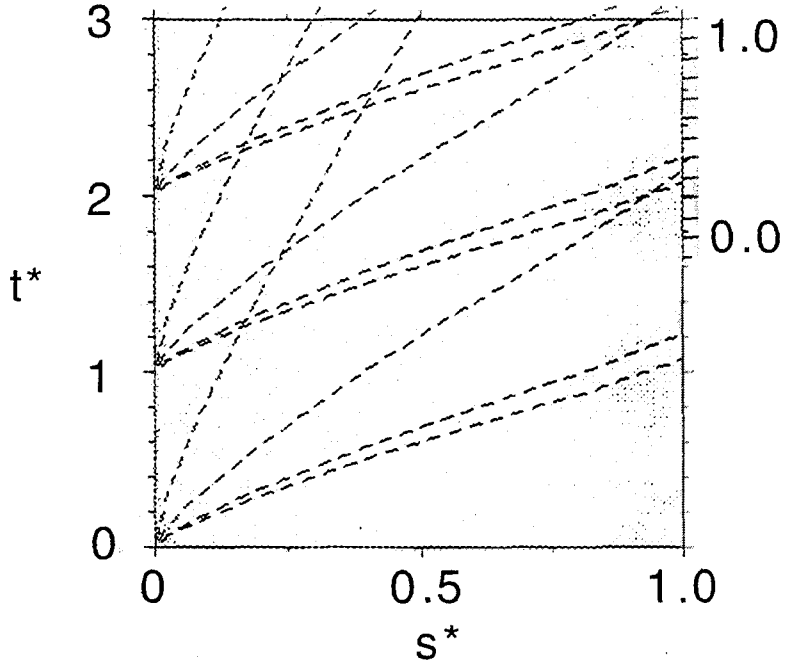

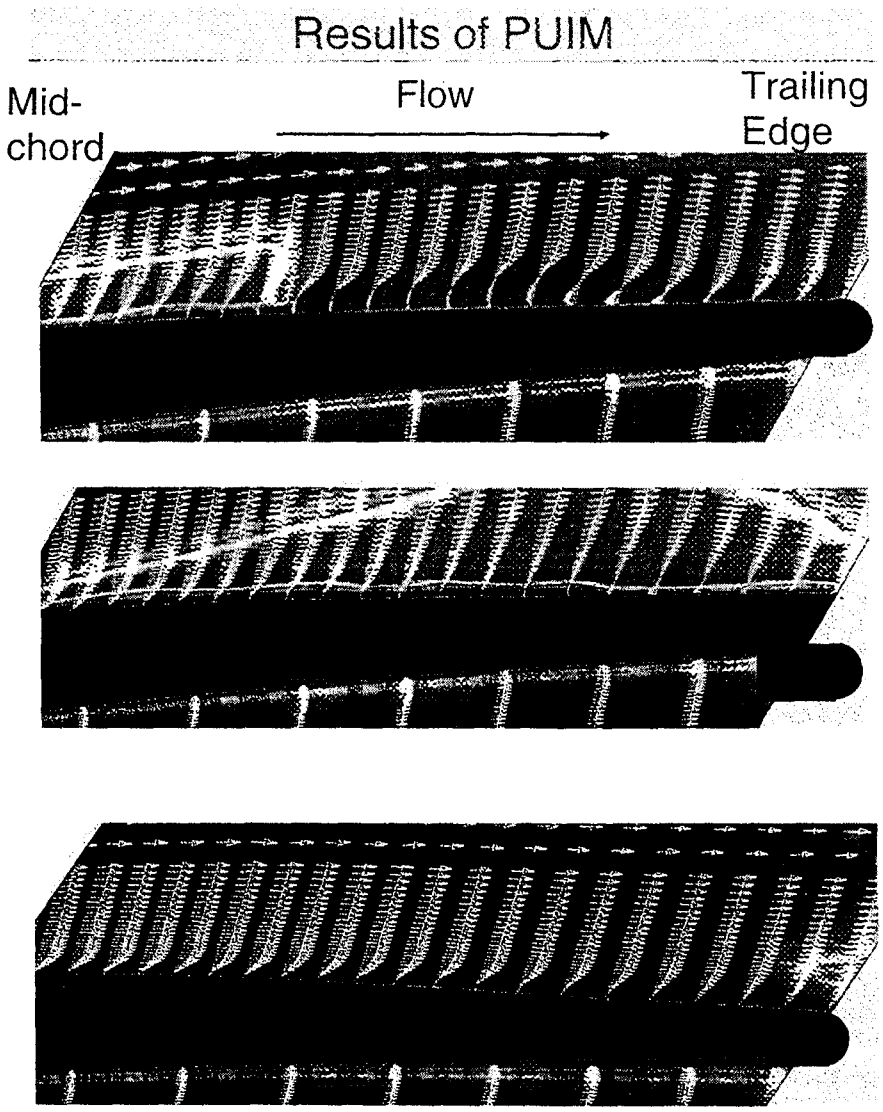
Results of PUIM
Mid-
chord
Flow
Trailing
Edge

Predicted/Measured Trailing Edge Momentum Thickness

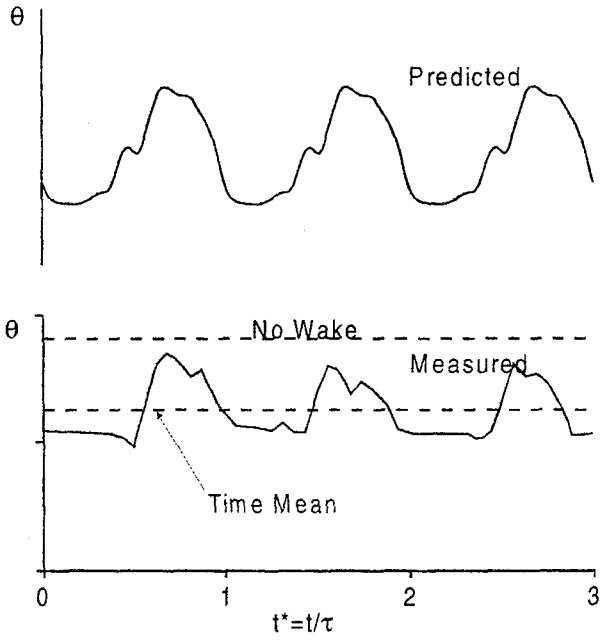

Benefits of Calming

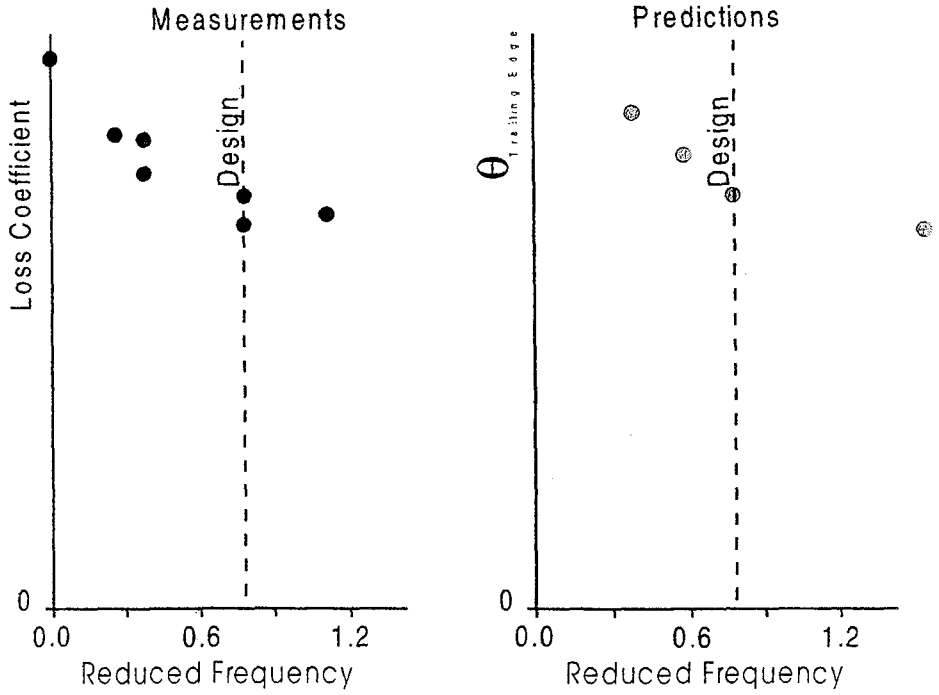

Summary

- Traditional models deny benefit of unsteadiness
- Calming benefit depends on frequency, Re, level of diffusion
- Industry wants fewer blades/higher blade loadings
- Possible to achieve with unsteady flow methods

And finally .....

In 1955, Schubauer & Klebanoff wrote

'... turbulence injected at proper time intervals can in principle alleviate the severity of the turbulence "disease"..... Our difficulty here is ..... if the periods of immunity are too short.'

THE BECALMED REGION IN TURBULENT SPOTS

Albert Hofeldt and John Clark
Oxford University
Oxford, England

John LaGraff
Syracuse University
Syracuse, New York

Terry Jones
Oxford University
Oxford, England

ABSTRACT

A series of detailed turbulent spot experiments were conducted in two facilities. The freestream pressure gradient and Mach number was varied over a wide range. A theory was developed which explains the properties of the becalmed region of the turbulent spot as the regrowth of a disturbed laminar boundary layer. The time for which the becalmed region persists may be predicted and the heat transfer rate within the region calculated using time dependent CFD. Experimental results for unsteady heat transfer are presented and are used to substantiate the theory.

LAMINAR BOUNDARY LAYER
ESTABLISHMENT TIME t_F

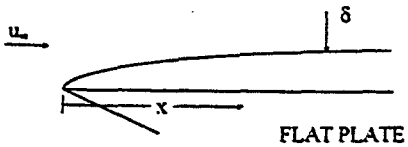

FLAT PLATE

$$t_F \sim \frac{x}{u_\infty} = T$$

FLOW TRANSIT TIME

DIFFUSION OF SHEAR LAYER

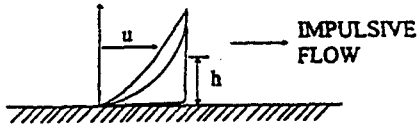

$$\frac{vt}{h^2} \sim 1$$

$$\therefore t_F \sim \frac{\delta^2}{v}$$

as $\frac{\delta}{x} \sim Re_x^{-\frac{1}{2}}$ FLAT PLATE LAMINAR B.L.

$$\delta \sim \left(\frac{vx}{u_\infty}\right)^{\frac{1}{2}}$$

and $t_F \sim \frac{x}{u_\infty}$

RESULTS FROM DIMENSIONAL ARGUMENTS FOR A FLAT PLATE

FOR A FLAT PLATE IN ZERO PRESSURE GRADIENT

DIMENSIONAL REASONING GIVES SURFACE HEAT FLUX AS

$$\frac{Nu_x}{Re_x^{1/2}} = f\left(\frac{t}{T}, Pr\right)$$

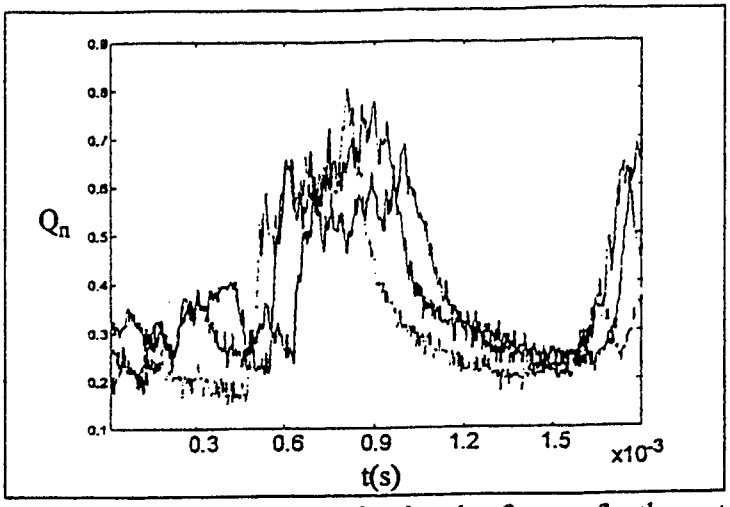

FIGURE 5.30. Normalized heat transfer signals of a spot for three streamwise TFGs. This spot is fully developed as demonstrated by the uniform time difference between the leading and trailing edges. Also note the slight increase in heat transfer at the rear of the spot which is typical of this region.

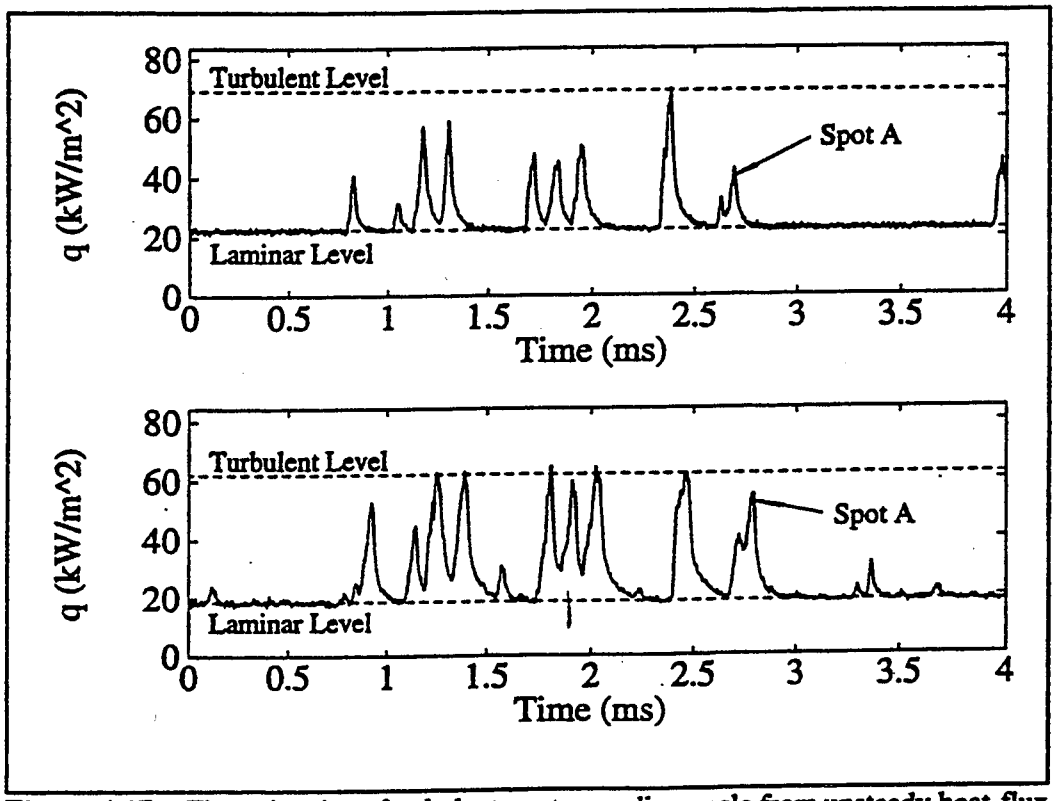

Figure 4.17- The estimation of turbulent-spot spreading angle from unsteady heat-flux traces. The upper and lower traces are from gauges 8 and 14 of Figure 4.1, respectively (Δx=12.0mm and α=7.6°).

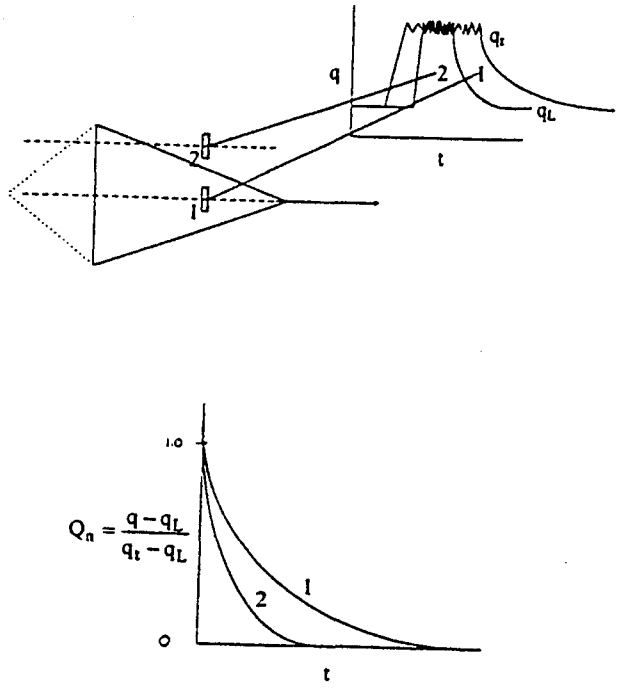

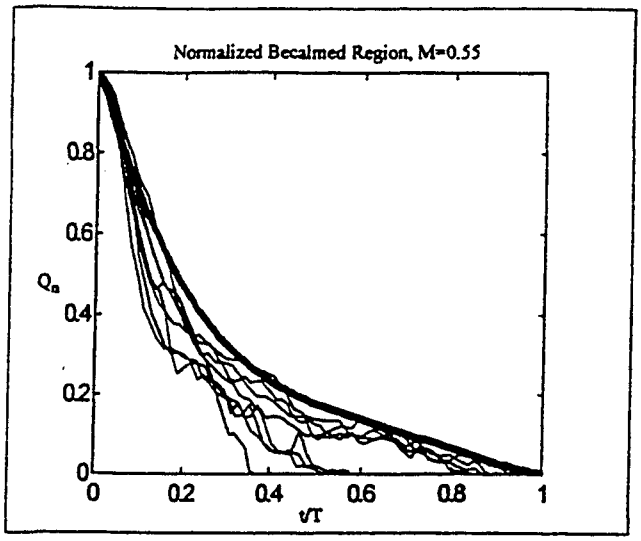

FIGURE 5.21. The decay of heat transfer in the becalmed region for runs in the ILPT at M=0.55, T_g/T_w=1.5. The variation of t/T corresponds to the spanwise variation of the becalmed region. The Point where Q_n=1corresponds to the trailing edge of the turbulent spot. Similarly, the point where Q_n=0 corresponds to the trailing edge of the becalmed region.

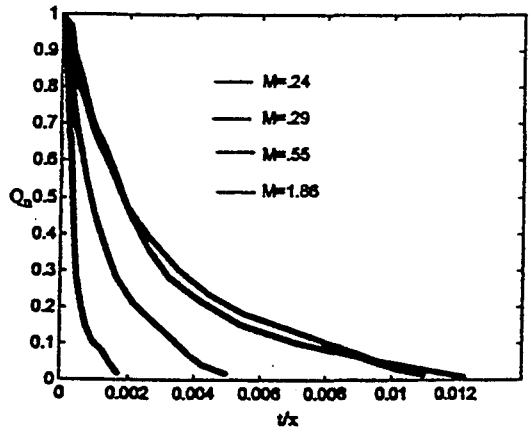

FIGURE 5.20. A summary of the centreline cases of the becalmed region for runs in the ILPT and suction tunnel at M=0.24, 0.29, 0.55, and 1.86.

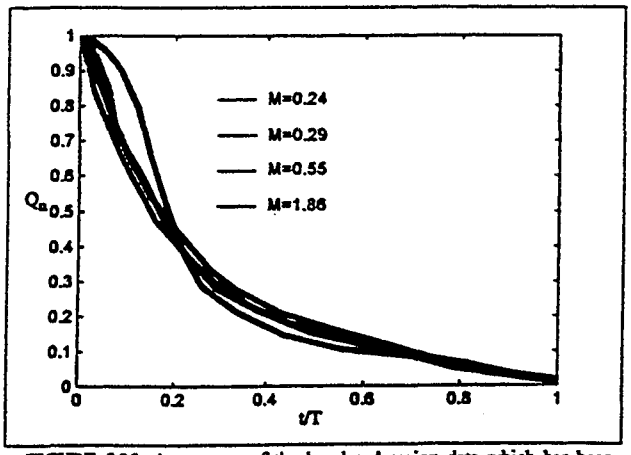

FIGURE 5.25. A summary of the becalmed region data which has been normalized by the time required for the regrowth of a laminar boundary layer from the inception point of the turbulent spot.

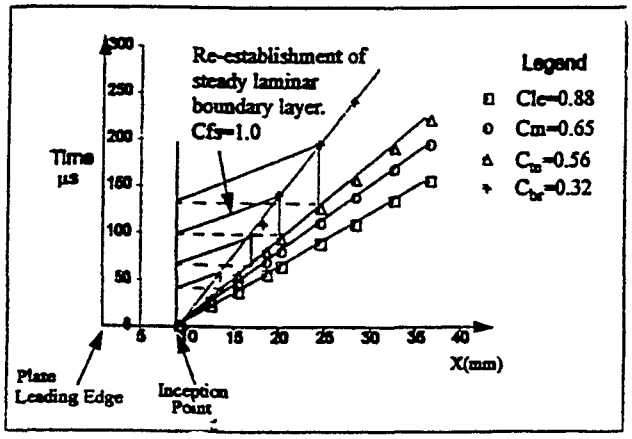

FIGURE 5.19. An X-T plot for the propagation of the turbulent spot boundaries (leading and trailing edges), the becalmed region, and the regrown laminar boundary layer from the turbulent spot inception point. The freestream propagation of a regrown laminar boundary layer dictates the time over which the becalmed region trailing edge will exist. The rate at which the becalmed region travels (32%U), is defined by (and equivalent to), the time for a new boundary layer to grow from the point where the spot was 'born'. Due to this fact, the time over which the becalmed region exists should be normalized by the flow transit time.

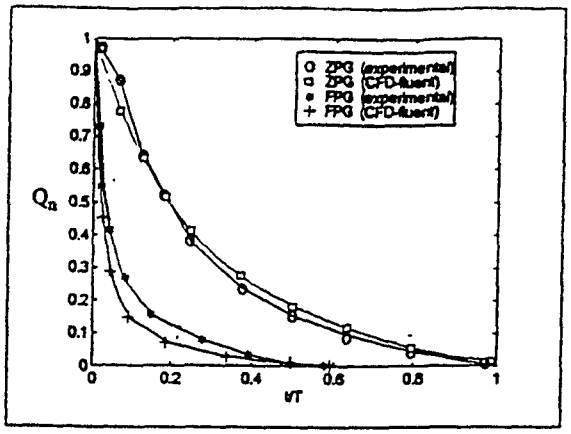

FIGURE 5.46. Combined results of the experimental and CFD cases for both ZPG and FPG heat transfer decay behaviour resulting from the passing of the becalmed region over one point along a flat plate.

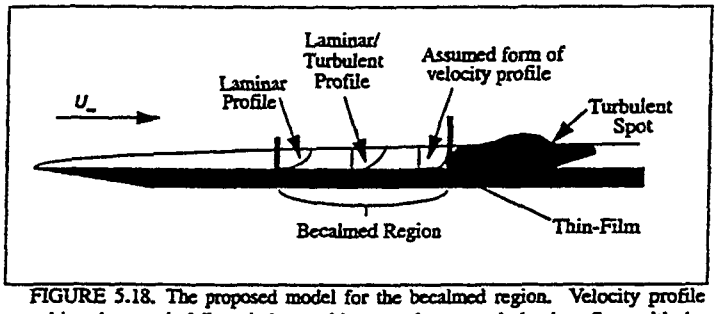

FIGURE 5.18. The proposed model for the becalmed region. Velocity profile exiting the spot is fully turbulent and is merged to a steady laminar flow with the passing of the becalmed region trailing edge.

ASSUMPTIONS FOR BECALMED REGION

1. MAY BE CONSIDERED TO BE LAMINAR
2. AFTER THE TRAILING EDGE OF THE SPOT VELOCITY PROFILE APPROXIMATES TO A TURBULENT PROFILE
3. SUBSEQUENTLY GROWS BACK TO A STEADY STATE LAMINAR PROFILE.

* WITNESS HEAT TRANSFER LEVELS

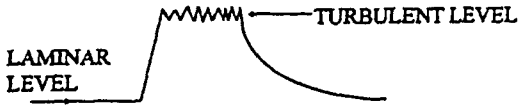

DIFFUSION TIME IN ACCELERATING FLOW T_D

$$T_D \sim \frac{\delta^2}{\nu}$$

δ - LOCAL BOUNDARY LAYER THICKNESS

THWAITES APPROXIMATION GIVES

$$\theta^2 \sim \frac{\nu \int u_\infty^5}{u_\infty^6}$$

HENCE ASSUMING $\delta^2 \propto \theta^2$

$$T_D = \frac{\int_{x_i}^{x} u_\infty^5 dx}{u_\infty^6}$$

UNIFORM FLOW $T_D = \frac{x}{u_\infty}$ = TransitTime = T

WEDGE FLOW $u_\infty = ax$

$$T_D = \frac{T}{6 \ln \frac{u_\infty}{u_i}}$$

WHERE GENERALLY $T = \int_{x_i}^{x} \frac{dx}{u_\infty}$

BECALMED HEAT TRANSFER DECAY IN A PRESSURE GRADIENT SCALED WITH DIFFUSION TIME

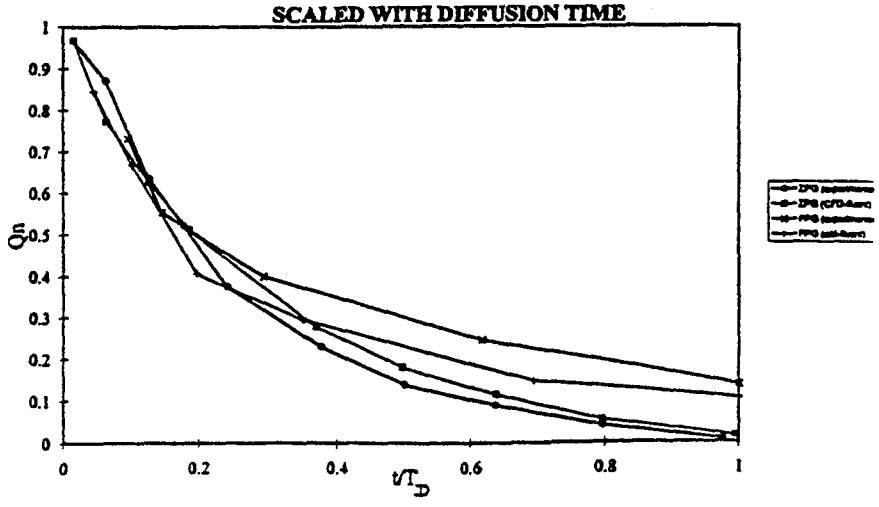

SPOT CALMING EFFECT ON BOUNDARY LAYER TRANSITION

A. Seifert
Tel-Aviv University
Tel-Aviv, Israel

Abstract

A turbulent spot, triggered in a laminar boundary layer, was followed into the transitional and turbulent regions of the boundary layer. It was found experimentally that its calming region is manifested as an island of laminar flow in an otherwise turbulent surrounding. This region is maintained for hundreds of boundary layer thickness downstream of natural transition. Assumptions concerning the production and maintenance of the calming region are presented. Possible means of using it for transition management were tested. It was found that transition length could be tripled and phase locked laminar periods could be maintained further downstream of mean transition location.

Nomenclature

C_f	skin friction
dT	duration of spot disturbance [ms]
H	BL shape factor, δ^*/θ
$R_{\theta p}$	Reynolds number, $Ur * \theta p / \nu$
T	$T*U_e/X_S$
U_e	local free stream velocity
Ur	free stream velocity at X=50cm
X	streasmwise distance from LE
Y	distance normal to wall
Z	span wise distance from spot source
abbreviations	
BL	boundary layer
CR	calmed region
LBL	laminar boundary layer
LE	spot leading interface
LAM	LBL values
TBL	turbulent boundary layer
TE	spot trailing interface
UND	undisturbed BL values
Greek	
β	Falkner-Skan parameter
γ	intermittency factor
δ^*	BL displacement thickness [mm]
ΔT_+	spot repetition rate [ms]
ΔT	$\Delta T*U_e/X_S$
ΔZ	distance between spot sources
θ	BL momentum thickness
subscript	
s	distance from spot source
t	transition location
p	spot source location

1. Introduction

The "calming" effect of a turbulent spot, convected in a transitional BL, was discovered by Schubauer and Klebanoff (1956). They observed (their Fig. 9) that when a patch of turbulence occurs in a BL which undergoes *natural* transition , the spot wake attenuates transitional disturbances for a considerable period of time. This "calmed region" (CR) was observed also when the spot turbulence was indistinguishable from the highly intermittent or even turbulent flow. The physical mechanism causing this stabilizing effect is not fully understood. It is probably generated by the blockage the slow spot imposes outside the BL and the low pressure caused by the faster spot near the wall. Both effects cause the fluid to accelerate behind the spot, either towards the wall and into it or away from the wall at the outer edge of the BL. Wygnanski et al. (1976) investigated the evolution of a turbulent spot generated in a LBL. They presented ensemble averaged velocity profiles (their Fig. 16) corresponding to times before the arrival of the spot and after its passage. It appeared that the shape of the transient velocity profile behind the spot, is significantly fuller than the undisturbed Blasius velocity profile. The shape of the mean velocity profile is the most sensitive indication of the LBL stability to low amplitude disturbances. Fuller velocity profiles are more stable to weak disturbances. This consideration should hold also for high amplitude disturbances, since turbulent spot spreading rates in an accelerated BL (Katz et al, 1990) are about half those found in Blasius flow.

A number of experimental investigations were performed during the seventies and early eighties on the structure and evolution of a "synthetic" TBL (Savas,1979, Coles and Savas, 1985). This flow is generated by actively tripping an LBL by dense formations of turbulent spots. It was suggested (Coles and Barker, 1975) that the *natural* TBL consists of overlapping and interacting spots and that the orderly production of spots in the "synthetic" TBL would permit easier pattern recognition of the turbulent structures. Many patterns of interacting spots were described in the Ph.D. thesis of Savas (1979). A unique pattern was formed due to the *simultaneous*

production of rows of turbulent spots, generated at small spanwise separation in comparison to their duration and at low repetition rate. This mode of disturbance formed a turbulent "strip" (or a 2D spot, Savas' Fig. 33) which was found to persist over a considerable distance downstream without elongation or distortion. It is assumed that the 2D CR, formed by one strip inhibits the elongation rate of the next strip. The absence of unstable "wing tips" of the isolated spot eliminates spanwise spreading and therefore also reduces the spot elongation. Savas' data could not reveal much about transition delay since his BL did not undergo natural transition in the absence of the forced disturbances. The flow structure was only partially studied since his measurements included only intermittency at a single plane parallel to the wall.

The present work follows the path suggested by Schubauer and Klebanoff in studying the spot calming effect on a transitional and turbulent BL. In section 3.1 we describe the evolution of an isolated spot calming region, where the spot was generated in an LBL and convected into a TBL. In section 3.2 we study the evolution of a train of spots entering a TBL and present some guidelines for using this stabilizing effect for generating a transition delay mechanism. Finally, in section 3.3, we present results where arrays of spots were introduced close to and upstream of the BL transition location. The relevance of the present research to turbomachines will be discussed.

2. The experiment

The experiment was conducted in the closed loop, low turbulence wind tunnel located at Tel-Aviv University (see Seifert & Wygnanski, 1995, for a complete description). Measurements were carried out in an adverse pressure gradient BL. The significance of the adverse pressure gradient in the present experiment is twofold. First, due to the short transition length, it enables one to study the whole transition process in a single experimental set-up, and second it is similar to the aft portion of the suction side of airfoils and turbo machinery blades. 2D laminar flow existed until the initialization of transition at R_X*10^{-6}=0.5-0.6. The measurements agree with the theoretical predictions of β=-0.1±0.02 in the range $0.23>R_X*10^{-6}<0.53$ (50<X<120 cm). At X>120 cm and Ur=7.2 m/s transition takes place. Since θ is a smooth function of X even through transition, while δ^* is not, θ was chosen as a scaling length for distances.

Table 1 summarizes the test conditions.

3. Discussion of results

3.1) The calming region of an isolated spot

Figure 1 presents contours of velocity perturbation measured on the centerline of a spot in an LBL. The insert on the left hand side of this Figure presents the undisturbed ***laminar*** velocity profile. The velocity perturbation due to the passage of the spot was computed with respect to this mean velocity distribution. Time is made dimensionless using the conical transformation of Cantwell et al (1978). The convection distance $TsUe$, is divided by Xs. The spot shape is self-similar under constant spreading rates. Therefore, key features and changes in the shape or convection velocities, as the spot it enters the TBL should be easily identifiable. The spot turbulent activity is constrained inside the thick solid line, γ=0.5. The -2% velocity perturbation contour corresponds rather closely to γ=0.5, outside the edge of the LBL ($Y\geq 7\theta$). The maximum velocity perturbations are -30% at the LBL edge and +42%, near the wall at $T^+\approx 1.8$, implying of increased skin friction. The CR can be easily detected as a positive velocity perturbation trailing the spot, inside the BL ($Y<7\theta$ and $T^+>1.9$). Its duration, measured from the spot TE to the closing of the +2% perturbation near the wall, is $\Delta T^+\approx 2.6$ or 3.5 times the spot duration.

The BL integral parameters of the data described in Figure 1 are presented in Figure 2. The vertical dotted lines indicate the spot LE (γ=0.5 at $Y/\theta\sim 6$), the spot TE (γ=0.5 at $Y/\theta\sim 1$), and the CR termination (when $H=0.98H_{UND}$). The undisturbed, laminar shape factor of an LBL with β=-0.1 is 2.8, as shown in Figure 2 before and after the spot. As the spot arrives ($T^+\approx 1$), the displacement (and momentum) thickness increase due to the spot turbulence and H decreases to obtain a minimum of 1.65 at $T^+\approx 1.8$. The accepted value for H, in zero pressure gradient, low Re, developed TBL, is 1.5 (Coles and Hirst, 1968). A turbulent wedge measured downstream of a 3D roughness element (a sphere, $d/\theta p$=4), located at the same Xp as our spot generator, triggered a TBL with H=1.55. Therefore, H=1.65 for the spot indicates that the flow inside it does not yet resemble a fully developed TBL. The calming effect of the spot becomes evident when observing the reduction of R_δ. and H, trailing the spot. Linear stability analysis (Wazzan et al, 1968) indicates that as H decreases, the LBL becomes more stable. When H remains below 2.8 for a long time (at $T^+>2.0$), and the flow is laminar, the BL is more stable than the undisturbed LBL. The

displacement thickness returns to its undisturbed value only at $T^+>4.5$, therefore the CR duration is equivalent to 3.5 times the spot duration.

The velocity perturbation caused by the spot in the ***turbulent*** region of the BL is presented in Figure 3. These data were measured 25 cm downstream of the BL natural transition location. The velocity perturbation was computed with respect to the undisturbed *turbulent* mean velocity profile, which is represented by the insert on the left hand side of Figure 3 (8). The arrival of the spot leading interface is marked by the -2% perturbation at $T^+ \approx 1.25$. The negative velocity perturbation reaches the wall (Fig. 3, $1.2<T^+<1.8$), in contrast to the spot in the LBL (Figure 2). This implies that skin friction should be reduced by a spot passing in a TBL. The laminar part of the CR is associated with a negative velocity perturbation near the wall ($Y/\theta<3$ and $2.0>T^+>3.2$), and a positive velocity perturbation away from it ($3<Y/\theta<9$ and $1.9>T^+>3.3$). These changes are in accordance with a change from turbulent to laminar velocity distribution.

Figures 4a and 4b present the BL integral parameters of the data presented in Fig. 3. The undisturbed BL intermittency ($T^+<1$) indicates that the flow is turbulent at this X station. The remnants of the spot turbulence are easily detectable by the turbulent activity outside the undisturbed TBL (Fig. 3), appearing as a sharp increase of R_{δ^*} and R_θ at $T^+\approx1.4$. The cause of this effect is the significantly upstream origin of the spot with respect to the TBL origin. The arrival of the spot turbulence is also marked by a decrease in the shape factor from 1.5 to 1.4 at $T^+\approx 1.4$. Lower turbulent H is, again, an indication of a more developed TBL. It can be seen that the relative skin friction (U/U_{UND} near the wall, Fig. 4b) shows a 30% reduction at $T^+\approx1.4$ (spot) and 60-70% reduction at $T^+\approx3$ (CR). It was calculated as the ratio between the transient and undisturbed velocity gradient near the wall (where $Y\approx10$ in the undisturbed flow) and is not very sensitive (± 5%) to the precise initial distance from the wall (± 0.1mm), but Y was maintained fixed during the A/D period. The intermittency begins to decrease at $T^+>2$, accompanied by an increase in the shape factor from 1.5 to 2.3 during the laminarization period. Thereafter, the flow remains laminar between $2.3<T^+<2.8$. As the flow adjusts to the laminar state, the shape factor increases further from 2.3 to H=2.7 (Fig. 4a). This shape factor of an LBL is appropriate for the slight adverse pressure gradient present at that location. Transition to turbulence takes place at $T^+>3$.

Up to this stage we have compared the spot in a TBL with the spot in an LBL. Now we shall examine the near wall evolution of the spot as it is convected through the natural transition region of the background BL (Figures 5a-c). Please note that the intermittency ordinate is on the right hand side of these plots. As the spot just enters the transition region (Fig. 5a, Xs=80 cm, $\gamma_{UND}\approx5\%$), its LE and TE are clearly seen at $T^+\approx1.2$ and 2.2, respectively. The CR begins at the spot TE and persists until the velocity decreases to its undisturbed value, at $T^+\approx5$.

The spot interfaces are also clearly visible further downstream (Xs=90 cm, Fig. 5b), where $\gamma_{UND}\approx$ 20%. The intermittency vanished between $T^+\approx2.3$ to 3.5, returning to its undisturbed value at $T^+\approx5$. It is interesting to note that the velocity decreases below its undisturbed value at $3.7<T^+<5$.

Further downstream (Xs=100 cm, Fig. 5c), where the transition process of the background BL is almost complete, and $\gamma_{UND}\approx55\%$ (visible at $T^+<1$), the spot LE and TE appeared again at $T^+\approx$ 1.2 and 2.2. The velocity perturbation associated with the spot is initially positive, forming a fuller turbulent velocity profile. The flow inside the CR is laminar between $2.3<T^+<3$. A negative velocity perturbation is detected at $2.2<T^+<5$, with a minimum of -15% at $T^+\approx3.5$ and the CR terminates also here at $T^+\approx5$. The most striking change in the spot as it is convected into the TBL is the reduction of the near wall velocity inside the CR, contrary to the velocity excess which marks the spot CR whenever it is convected in an LBL. This is an indication of the change in the shape of the transient velocity profile from turbulent to laminar. In the following section we shall compare this aspect of the spot.

As the spot turbulence is convected downstream in an LBL ($T^+>2.0$), the transient velocity profile becomes "fuller" than the undisturbed velocity profile ($T^+=2.3$ in Fig. 6), and R_{δ^*} reaches a minimum (Fig. 2). The difference in the *shape* of these two laminar velocity profiles was emphasized because we normalized each profile by its *own* δ^*. Besides the decrease in R_{δ^*} (from 1230 at $T^+<1$ to 880 at $T^+\approx2.3$, Fig. 2) and in H (from 2.8 to 2.3), the best fitted β (based on the shape of the entire velocity profile), increases from -0.1 to 0.4. As a result the critical R_{δ^*} increases from 200 in to 6230 !

The spot effect on the transient velocity profiles in the TBL is presented in Fig. 7. The turbulent activity, which is convected from the laminar region of the BL, thickens the TBL

considerably and reduces the velocity gradient near the wall (Fig. 7, T^+=1.4). As γ decreases to 50% and R_{δ^*} attains a minimum (Fig. 2), the shape of the velocity profile is appropriate to an accelerated laminar velocity profile (e.g., H≈1.7 at T^+=2.0, Fig. 7). The outer region of this transient velocity profile is much fuller than the outer region of the undisturbed TBL velocity profile. ***This also suggests that a possible generation mechanism of the spot calming effect is the flow acceleration towards the spot summit, outside the BL edge. This happens since the flow inside the spot, at the BL edge, is slower than the flow behind it. The maintenance of the calming effect in the TBL is probably caused by the same mechanism, which is getting weaker as the difference between the spot summit height and the TBL edge decreases with increasing X.*** At T^+ ≈2.3 the flow is laminar, γ=0 and H=2.3. This transient shape factor corresponds to a steady self-similar laminar velocity profile with β≈0.4 and causes a significant reduction of the skin friction estimation, which is reduced further during the laminar period of the flow, as R_{δ^*} increases (Fig. 4b, as happens in a streamwise evolution of self-similar LBLs). The transient velocity profile at T^+ ≈2.8, resembles that of a laminar mean velocity profile with H=2.7 and is accompanied by an estimated skin friction reduction of 70% (Fig. bb). During the transition to turbulence (T^+≈3.3, Fig. 7), the outer part of the transient velocity profile resembles the TBL undisturbed velocity profile, but the inner part of the BL has not yet recovered from the spot calming effect. Due to the reduction in the near wall velocity, R_{δ^*} attains a local maximum (Fig. 4a). The TBL returns to its undisturbed velocity profile, relative skin friction and integral parameters at T^+≈4. The total duration of the spot effect on the TBL is about ΔT^+≈2.5 while the spot turbulent activity, as estimated from the increase in R_{δ^*} and R_θ above the TBL value (Fig. 4a), is ΔT^+≈0.7. During most of this period the relative skin friction was reduced (Fig. 4b), due to two effects: first, the spot turbulent activity (centered around T^+≈1.4), is more developed than the TBL due to an upstream location of the spot virtual origin, and secondly, the flow inside the CR is laminar and the skin friction corresponds to that of an LBL with R_θ≈ 400 (Fig. 4a). It is emphasized that this local effect does not imply a net drag reduction. Further upstream, in the laminar region of the BL, the skin friction is increased due to the presence of the spot. Considering the data presented, it is shown that the effect of a developed spot, entering the transition region of an LBL is *reversed* in many aspects when compared to the spot effect on an LBL.

Clearly, the transition process is three dimensional and one should be interested in the spanwise structure of the CR as it enters the TBL. Figure 8a presents contours of the intermittency factor in the *Y-T* plane corresponding to the data presented in Figures 3,4 and 7. The TBL is about 9θ thick before the arrival of the spot; this thickness doubles as the spot turbulence arrives, based on γ =0.5 (Fig. 8a) or -2% perturbation (Fig. 3). The near wall intermittency of the TBL decreases to 0 between T^+=2.0 to 2.2, γ<0.5 for 2.1>T^+>3.3, about twice the spot duration, as estimated from the -2% velocity perturbation contour at 3<Y/θ<6 (Figure 3).

To efficiently generate 2D spots, or "turbulent strips", one would have to know the spanwise extent of an isolated turbulent spot CR in a *TBL*. This width depends on the distance from the spot origin and on the distance from the location of natural transition. The width of the CR shrinks in the TBL as X increases, due to turbulent diffusion, entrainment and "growth by destabilization" (Gad-El-Hak et al., 1982) similar to that which is partly responsible for the spot spanwise spreading in an LBL. This assumption needs to be verified. The spanwise extent of a spot CR is presented in Figure 8b by contours of intermittency (at Y corresponding to U/Ue≈0.4). Only one side of the spot centerline is presented. The CR total width, based on γ=0.5, is 62 θ. The CR duration shrinks to half its centerline value at Z_S/θ≈46. This data allows us to estimate the maximum ratio between the spot generator spanwise separation, ΔZp, and the streamwise distance between the spot generators, Xp and the transition location, Xt, [i.e. $\Delta Zp/(Xt-Xp)$=0.15]. Please note that this value is about half the spot spanwise spreading rate in an LBL. Seifert and Wygnanski (1995) found that the spanwise extent and strength of the CR are proportional to the duration and strength of the disturbance generating the spot. Therefore, it is desirable to use somewhat long disturbances, of the order $dTUe/\theta p$=150, in order to generate a strong and wide CR.

3.2) Calming region of a train of spots

A train of spots, generated at different repetition rates, was studied in order to understand its effect on the BL transition process. We have chosen the minimum near wall intermittency as our criterion and attempted to minimize it by varying the spot production rate. Representative ensemble

averaged velocity perturbation and intermittency factor were calculated. Figure 9 presents two cycles of a train of spots, measured at Y of $0.4Ue$. It can be seen that the intermittency vanishes for about 30% of the period. The near wall velocity decreases with γ, due to laminarization, as shown also in Figures 3,4,5 & 8. The optimization was performed by altering the spot production rate, measuring the velocity and calculating the average intermittency of an integer number of cycles of the ensemble averaged intermittency (Figure 10). Spot production rate is made dimensionless using the conical transformation. The data presented in Fig. 10 shows that the average intermittency in the presence of a train of spots decreases from 1 in the undisturbed TBL to less than 50% for all the spot production rates tested. The lowest averaged intermittency is found at a dimensionless interval of $Ue\Delta T/\theta p \approx 4700$ or $\Delta T^+ = U_e \Delta T / X_S \approx 2$ and is about 43%.

The reason for obtaining a minimal averaged intermittency at $\Delta T^+ \approx 2$ is explained as follows: it takes about $0.8T^+$ from the spot LE appearance until the laminar period begins, independently of the production rate. The normalized duration of the calmed region is $\Delta T^+ \cong 1.2$. The addition of these two times determines the beneficial production rate. It is not desirable to use smaller ΔT^+ since in this case the laminar period would be overtaken by the next spot LE. On the other hand, higher ΔT^+ would allow a development of a turbulent period before the next spot arrives.

3.3) Turbulent strips in a transitional BL

To fully explore the effects of the spot CR on the BL transition process, 2D turbulent strips should be produced as close as possible to, and upstream of, the BL transition at an optimal rate. Production of spots upstream of the BL natural transition is necessary in order to allow the spot to develop a CR before entering the TBL. On the other hand, it should be as close as possible to transition location since in the LBL the spots increase the skin friction. A higher reference velocity, Ur=8.6 m/s, was used in order to shorten the transition length. Nevertheless, natural transition took place only at $R_{ex} > 0.55*10^6$ (X>100 cm), which was not desirable since the closest spot generator was located at X=50 cm. To shorten the transition length, a gentle tripping device was located at 42<X<49 cm ($R_{ex}*10^{-6} \approx 0.25$) and transition moved 20 cm upstream.

Optimization of the spots production rate was performed at $(X-Xt)/\theta t$=210 ($R_{ex}*10^{-6}$=0.48, Xs=50 cm), directly downstream of the spot generator. This location was chosen because on the one hand the transition process terminated there, anon the other, visual survey of hot-wire traces showed that the spot CR disappears by $R_{ex}*10^{-6}$>0.63 (X>130 cm).

An interval of $\Delta T^+ \approx 2$ was found to be optimal, also in the new configuration with an averaged γ of 62%. This value is considerably higher than the lowest intermittency (43%) measured when a train of spots was produced at an interval of $\Delta T^+ \approx 2$ at $R_{\theta p}$=240 (Fig. 10). The difference probably stems from the fact that spots produced at $R_{\theta p}$ =240, travel 1800 θp (90 cm) in the LBL and are fully developed as they enter the TBL. In the tripped BL, the spots travel only 520 θp in the LBL and develop as the BL undergoes accelerated transition. Thus, their CR is not as developed as that of a spot generated further upstream. For the turbulent strip test, an interval of ΔT^+=2.45 was chosen, in spite the somewhat higher average intermittency measured for this production rate (67%). The expectation was that when spots are produced in side by side formation, the calming effect would be stronger, since 3D effects which usually erode the CR spanwise extent are weaker. The spot generators spanwise separation chosen for the side-by-side spot formation is $\Delta Z / (X_t - X_p) \approx 0.13$, in accordance to the values recommended in section 3.1.

Figure 11 presents the train of spots interface detection times at $Z^+ \equiv Z/\theta p$ =0 and 34.5 (Z=4 and 6 cm) when two side by side spots were generated at $R_{\theta P}$ =320, $Zp/\theta p$ =0 and 69 (Zp=4 and 8 cm) and at intervals of

ΔT^+=2.45 ($\Delta TU_e/\theta_p \approx 2200$, $dTU_e/\theta_p \approx 150$).

This spanwise separation was chosen on the expectation that the spot spanwise spreading will fill the gap between the two spots before entering the TBL, forming effectively a 2D spot. At $Xs/\theta p$ <620, the spots travel in an LBL. The spot turbulence arrives earlier at the probe located at Z^+=0, since it is directly downstream of the one of the sources . The difference between the leading interface detection times at Z^+=0 and 34.5, (half the spanwise separation between the two sources) decrease as X increases, since the spots spread in the spanwise direction. The TE detection times are identical for the two spanwise locations. This means that a uniform CR was produced even between the two spot sources as a result of the selected spanwise separation. At $Xs/\theta p$>620 the spots travel in a TBL. The interface detected at $Ts/\Delta T \approx 0.25$ and $Xs/\theta p \approx 620$ does not

correspond to the spot leading interface any longer, but to the termination of the CR. One can note that the major feature of this flow is the presence of phase locked laminar periods at otherwise TBL, downstream of steady-undisturbed BL transition. It was observed that the CR detection times form a straight line in the *X-Ts* plane. The slope of this line, dX/dTs, marks a convection velocity of approximately $0.55Ue$.

In order to asses the gross effect included in the X-T plot, an averaged (both in Z and in time) intermittency factor was calculated for the steady and forced BL (Fig. 12). In the steady BL, transition takes place at $620>Xs/\theta p>340$. The average intermittency of the forced BL is somewhat higher than that of the steady BL for $Xs/\theta p<480$, due to the introduction of spots into an LBL, but is lower for $1400>Xs/\theta p>480$ since a fraction of every cycle was maintained laminar. The first obvious result of forcing the BL is a significant increase in the transition length, from 400 θp to 1200 θp. Secondly, a phase locked fraction of the cycle was maintained laminar at locations in which the flow is otherwise turbulent. This could be important for many engineering applications. Estimations about the shape of the near wall, transient velocity profile should be made in order to extract the approximate skin friction from our indirect data. These estimations are not accurate enough to make a clear argument. However, our finding that reduction of the near wall velocity (where $U/Ue=0.4$ in the undisturbed TBL), even in the turbulent periods of the forced flow (e.g. see $T^+ \approx 1.5$ in Fig. 3) and the laminarization of the flow at a significant fraction of the cycle, downstream of steady transition, encourage further study. The generation of only two side-by-side spots instead of a turbulent "strip" is another shortcoming.

As the laminar CR is convected into the TBL, its size shrinks, as observed already by Schubauer and Klebanoff. The rate at which this region shrinks depends on many parameters such as: the size of the CR as the spot enters the TBL (which depends on the spot generation location, duration and strength of the disturbance), the Re number, the pressure gradient and the distance the laminar CR traveled downstream of the average BL transition location. An attempt was made to collapse all these parameters in order to scale the CR decay rate.

Fig. 13a presents the duration of the laminar CR in the TBL (corresponding to the data of Fig. 11). It was found that the data collapses to a single curve if the CR length (ΔT_{Lam}*Ue) is normalized by the distance traveled in the TBL ($X-X_t$) and the streamwise parameter is the ratio between the distance the CR traveled in the TBL and the distance it traveled in the LBL (X_t-X_p). In these coordinates, the CR decays exponentially. Fig. 13b contains the data from Fig. 11 (for a "2D spots") along with the data corresponding to a train of isolated spots (described in Figs. 5c and 8) and also data extracted for the work of Schubauer and Klebanoff (in Blasius BL).

4. Conclusions

It was found that a developed turbulent spot that enters the transition region of a BL keeps the flow in its wake laminar for a considerable distance downstream of the steady transition location. The width of this laminar region shrinks as the isolated spot enters the TBL. There is some evidence that the spot calming region is generated due to flow acceleration at the outer edge of the BL, toward the spot summit. A train of spots generated ***upstream*** of the transition region, can reduce the average intermittency to less than half its stationary value. When spots were generated in side-by-side tandem and at the same dimensionless intervals ($\Delta T^+ \approx 2$) ***inside*** the transition region, the transition length was tripled and phase locked laminar periods were maintained 800 θp downstream of steady transition. The possibility of achieving also some drag reduction as a result of the delayed transition requires further experimentation.

The author would like to thank Messes B. Margaliot, Y. Mytnik and D. Heifetz for their assistance in gathering, processing and presenting the data.

References

Cantwell, B., Coles, D. and Dimotakis, P. 1978 Structure and entrainment in the plane of symmetry of a turbulent spot. *J. Fluid Mech.* **87**, pp. 641.

Coles, D and Barker, S.J., 1975, Some remarks on the synthetic turbulent boundary layer. In *Turbulent Mixing in Nonreactive and Reactive Flows* (ed. S.N.B Murphy), pp. 285-292. Plenum.

Coles, D. and Hirst, E.A. 1968 *Proceedings of the computations of turbulent boundary layers AFOSR-IFP-Stanford conference.*

Gad-El-Hak, M., Blackwelder, R.F., and Riley, J.J. 1982 On the growth of turbulent regions in laminar boundary layers, *J. Fluid Mech.* **110**, pp. 73-96.

Katz, Y., Seifert, A., and Wygnanski, I., 1990, On the evolution of a turbulent spot in a laminar

boundary layer in favorable pressure gradient, *J. Fluid Mech.* **221**, 1-22.

Savas, O. 1979 Some measurements in synthetic turbulent boundary layers. Ph.D. thesis, California Inst. of Tech.

Savas, O and Coles, D. 1985 Coherence measurements in synthetic turbulent boundary layer. *J. Fluid Mech.* **160**, pp. 421-446. 1985

Schubauer, G. B. and Klebanoff, P.S., 1956 Contributions to the mechanics of boundary layer transition, *NACA Report* number 1289.

Seifert, A. and Wygnanski, I.J., 1995, On turbulent spots in a laminar boundary layer subjected to a self-similar adverse pressure gradient . *J. Fluid Mech.*, 296, Aug. 10, p. 185-209.

Wazzan, A.R., Okamora, T.T. and Smith, A.M.O. 1968 Spatial and temporal stability charts for the Falkner-Skan velocity profiles. *McDonnel Douglas Corp. Rep* DAC 67086

Wygnanski, I., Sokolov, M., and Friedman, D. 1976 On a turbulent spot in a laminar boundary layer, *J. Fluid Mech.* **78**, 785-819.

Baseline Boundary Layer

Free StreamVelocity

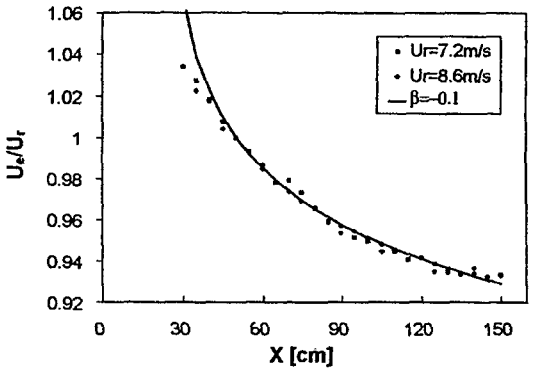

Velocity Profiles

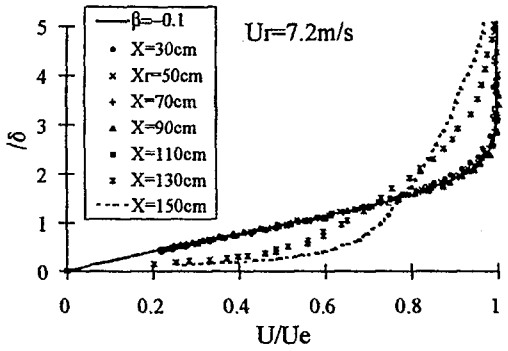

Integral Parameters

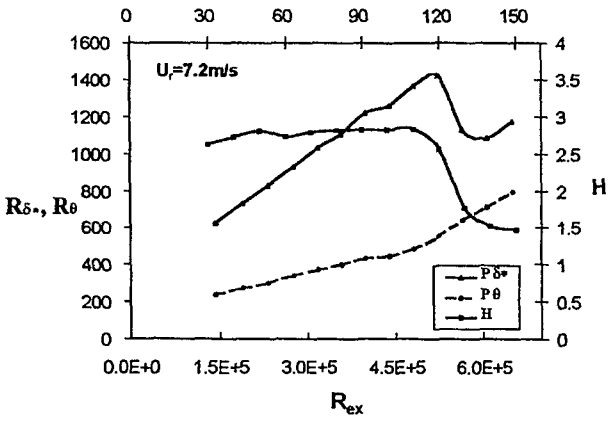

Law of the wall

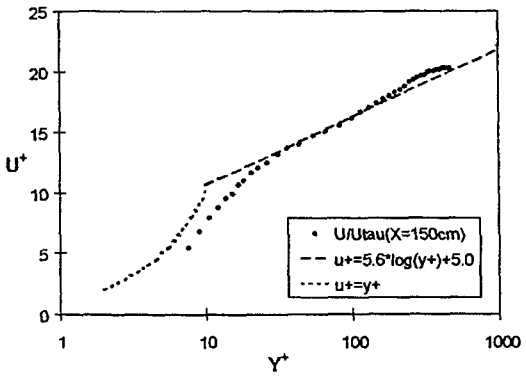

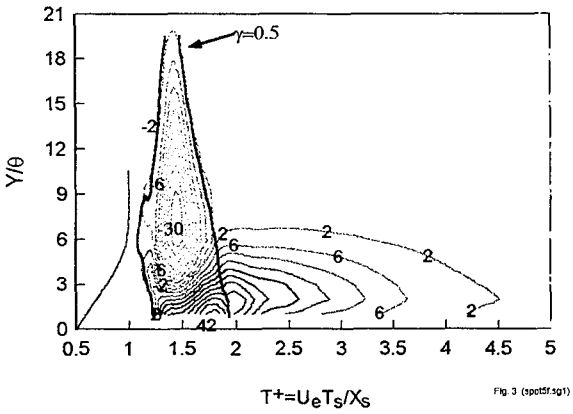

Fig. 1. Contours of velocity perturbation [%*Ue*], due to a spot in an LBL and on the spot centerline, (*Xs*=50, $R_{\theta P}$=240, R_{θ}=450).

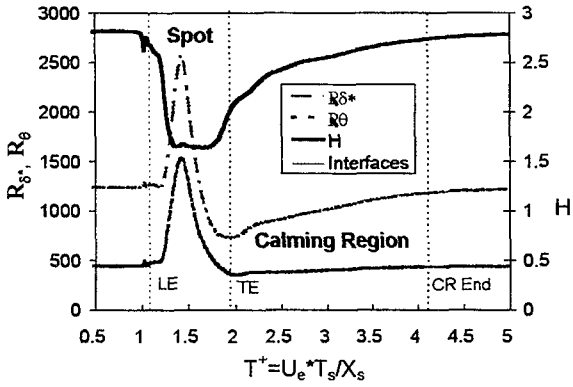

Fig. 2. BL integral parameters as a turbulent spot is convected in an LBL (data of Fig. 1).

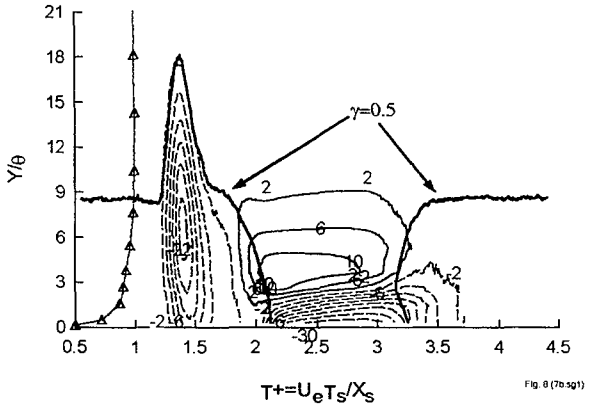

Fig. 3. Contours of velocity perturbation [%*Ue*], due to a spot in the TBL, on the centerline, (*Xs*=100cm, $R_{\theta P}$=240, R_{θ}=790).

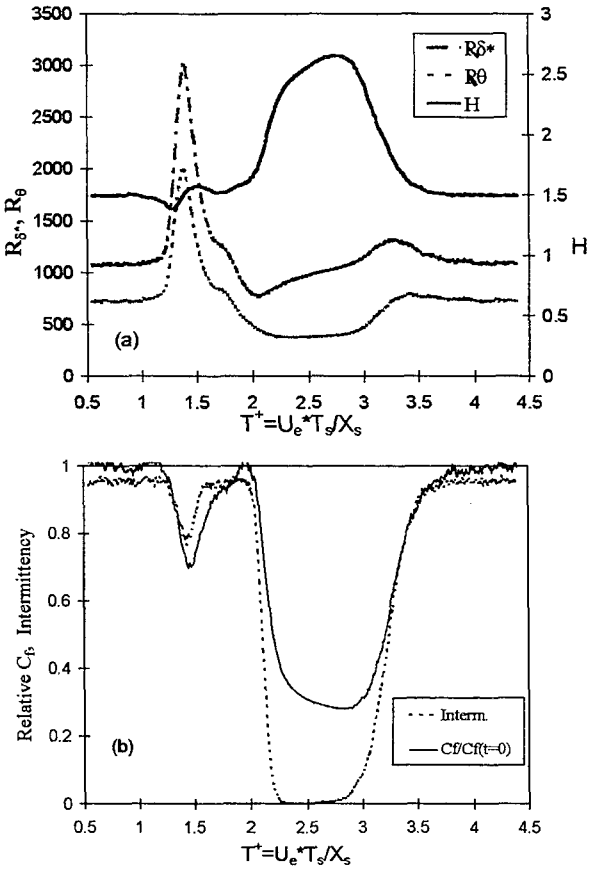

Fig. 4. BL integral parameters (a); and skin friction estimation and intermittency factor near the wall (b); for a turbulent spot convected into a TBL (data of Fig. 3).

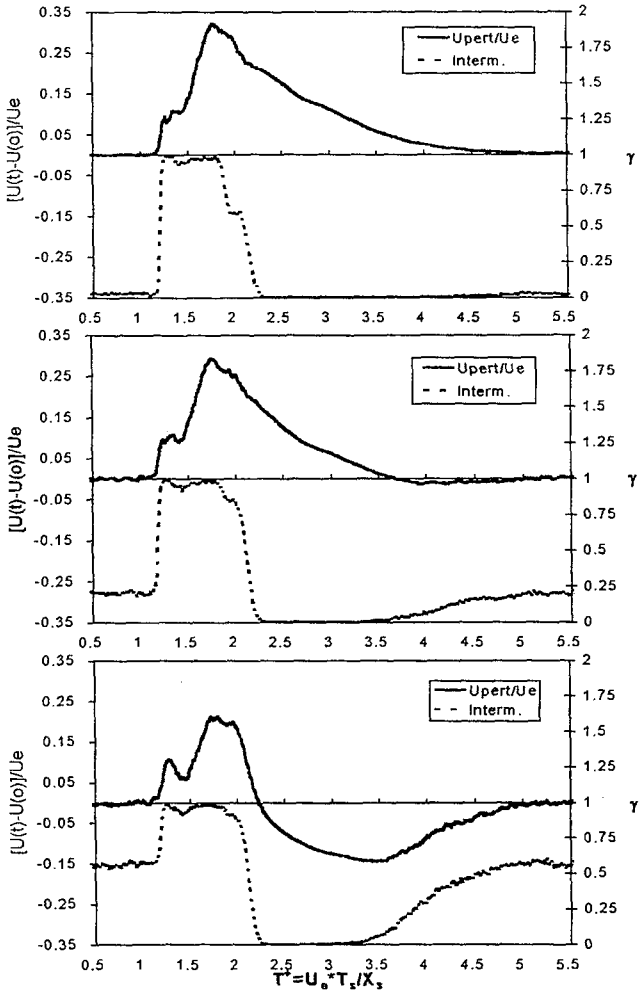

Fig. 5. Velocity perturbation and intermittency factor as spots are convected into the transition region, $R_{\theta P}$=240: (a) Xs=60cm; R_θ=480, (b) 70; 550, (c) 80; 640.

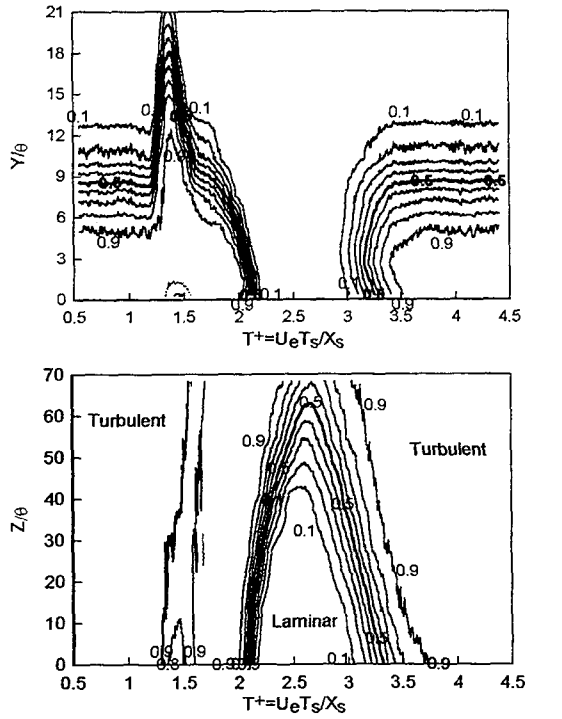

Fig. 8 Contours of intermittency factor due to a spot in a TBL, (a) Y-T plane (data of Fig. 3), (b) Z-T plane ($R_{\theta P}$=240, R_θ=790).

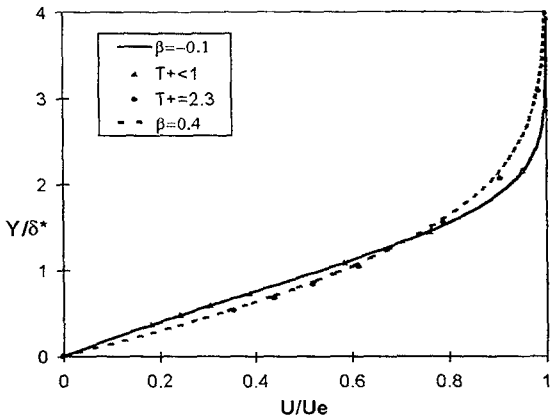

Fig. 6. Laminar transient velocity profiles as a turbulent spot is convected in an LBL (data of Fig. 1), Y normalized by corresponding transient δ*.

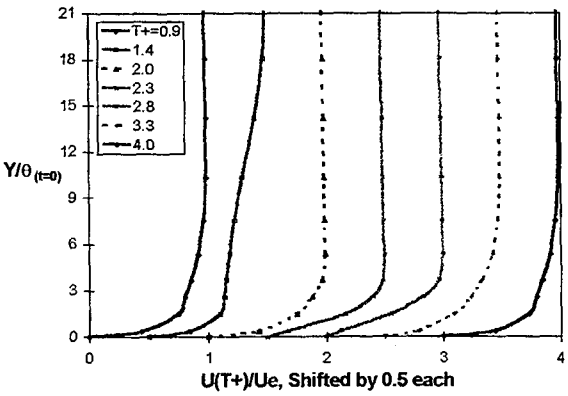

Fig. 7. Transient velocity profiles as a turbulent spot is convected in a TBL (data of Fig. 3 & 4).

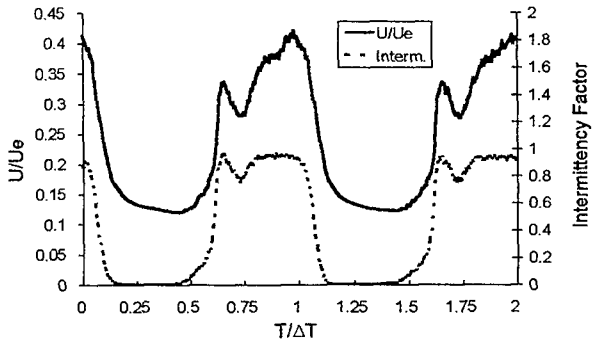

Fig. 9. Velocity and intermittency due to a train of spots in a TBL (Xs=100cm, $R_{\theta P}$=240, R_{θ}=790, $\Delta T^{+}\approx 2$).

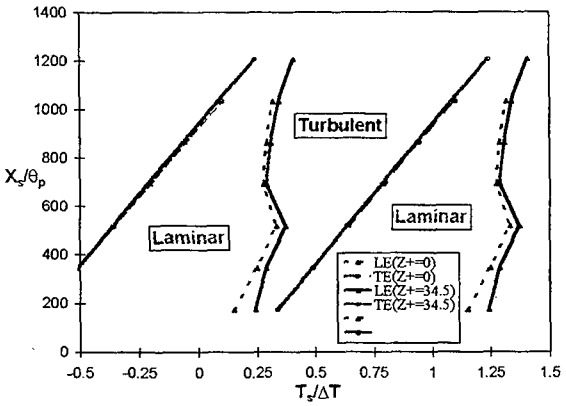

Fig. 11. Interface detection times of a train of two side by side spots, $R_{\theta P}$=320, tripped boundary layer, $\Delta T^{+}\approx 2.45$.

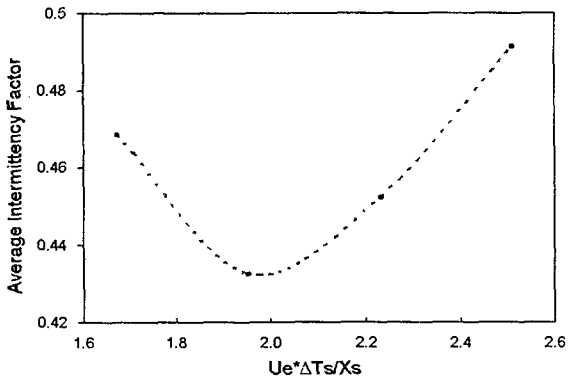

Fig. 10. Averaged intermittency factor of a train of spots (same X as Fig. 9).

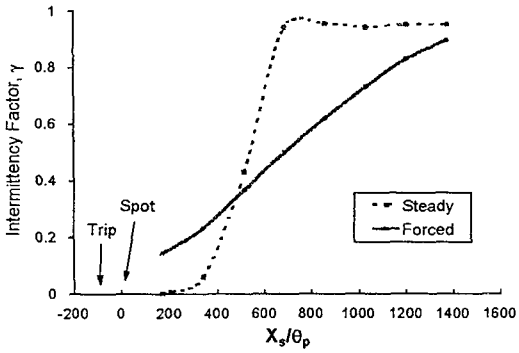

Fig. 12. Steady and forced averaged intermittency factor (conditions as in Fig. 11)

Variable	U_r	X_p	θ_p	$R_{\theta p}$	X_S	X_t	θ_t	ΔT	ΔT^{+}	Note
Units	m/s	cm	mm	none	cm	cm	mm	msec	none	
sec. 3.1	7.2	30	0.50	240	70-120	125	1.37	∞	∞	isolated spot (Fig. 3-12)
sec. 3.2	7.2	30	0.50	240	120	125	1.37	300-450	1.7-2.5	train of spots (Fig. 13)
sec.3.3	8.6	50	0.58	320	10-80	80	0.96	100-165	1.6-2.7	train of spots tripped BL

Table 1 Summary of important variables and test conditions

Calmed Region Decay Rate in TBL

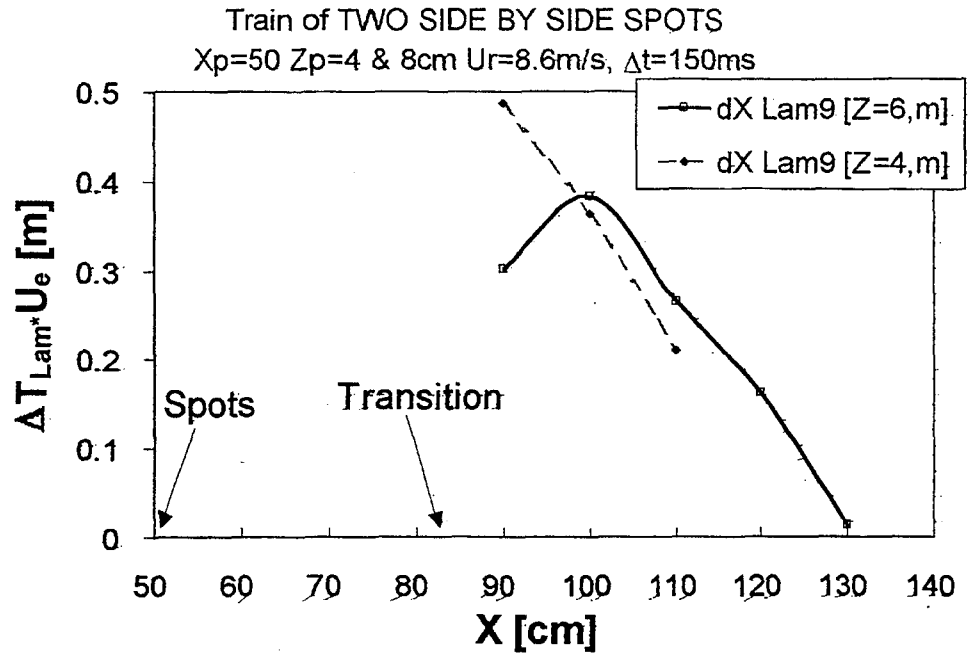

Fig. 13a

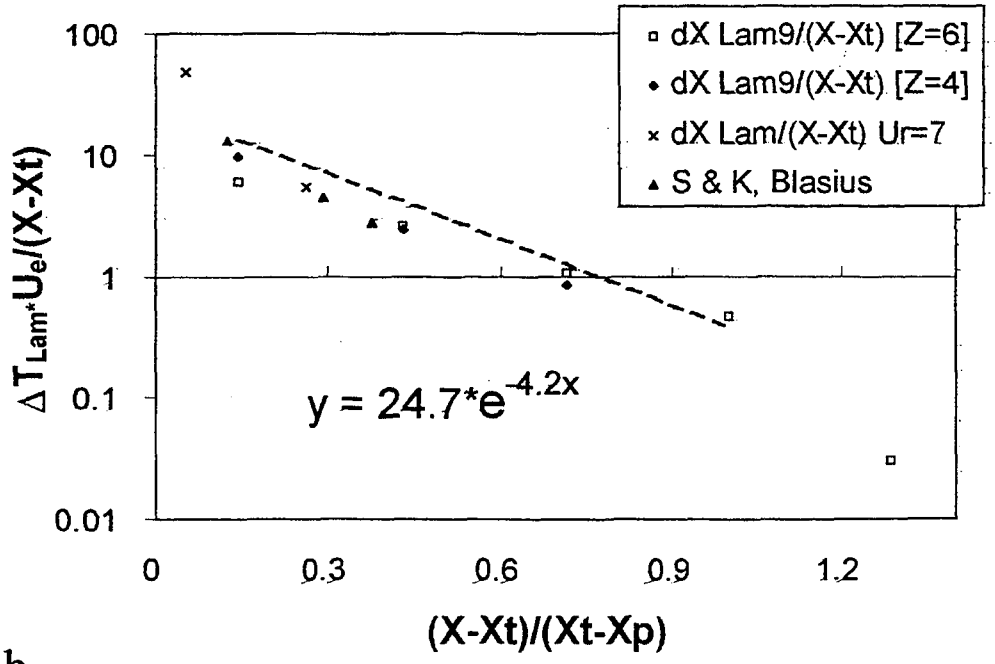

Fig. 13b

SESSION 3

BYPASS TRANSITION—
EXTERNAL EFFECTS

ROUGHNESS-INDUCED TRANSITION

Eli Reshotko
Case Western Reserve University
Cleveland, Ohio

ABSTRACT

Surface roughness can have a profound effect on boundary layer transition. The mechanisms associated with single roughness elements are only partially understood while those responsible for transition with distributed roughness are not yet known. This has led to a large body of empirical information in the literature that is not fully consistent. These correlations are generally based on two-dimensional parameters such as Re_k , k/δ^*, k/δ whereas the distributed roughness is inherently three-dimensional. The three-dimensionality is introduced by providing separate curves for each three-dimensional shape and distribution. Nevertheless, these correlations are still the operative data base for dealing with distributed roughness.

Experimental studies by Reshotko & Leventhal 1981, Corke, Bar Sever & Morkovin 1986, and Tadjfar et al 1985, have elucidated some of the physical observations of flow over distributed roughness. It is generally agreed that roughness displaces the mean flow outward affecting profiles only within the roughness height. Subcritical amplification is observed principally at low frequencies and the growth can easily reach nonlinear levels quickly. It is suspected that in common with single 3D roughness elements, the distributed roughness gives rise to vortex structures emanating from the elements. Aside from a weak horseshoe vortex in front of each element, there are chimney vortices arising behind each element that are turned horizontally at the crests of the roughness and lead to an upwash or lift of the vortices. These vortices are primarily streamwise. Papers summarizing these observations are by Reshotko 1984, and Morkovin 1990a, 1990b.

A possible unifying explanation for these observations is in the mechanism of transient growth. Transient growth arises through the coupling between slightly damped, highly oblique (nearly streamwise) Orr-Sommerfeld and Squire modes leading to algebraic growth followed by decay outside the T-S neutral curve. A weak transient growth can also occur for two-dimensional or axisymmetric modes since the Orr-Sommerfeld operator is not self-adjoint, therefore its eigenfunctions are not strictly orthogonal. Transient growth is certainly a candidate mechanism for many examples of bypass transition. While it may be difficult to quantify its influence, the qualitative trends are consistent attesting to the possible role of transient growth in roughness-induced transition.

References

Corke, T.C., Bar Sever, A. & Morkovin, M.V. 1986: "Experiments on transition enhancement by distributed roughness." Phys. Fluids, vol. 29, pp. 3199-3213

Morkovin, M.V. 1990a: "Panel Summary: Roughness," in M.Y. Hussaini, R.G. Voight, eds., *Instability and Transition, Vol I,* Springer-Verlag, 1990, pp. 265-271

Morkovin, M.V. 1990b: "On Roughness-Induced Transition: Facts, Views & Speculation," in M.Y. Hussaini, R.G. Voight, eds., *Instability and Transition, Vol. I,* Springer-Verlag, 1990, pp.281-295

Reshotko, E. 1984: "Disturbances in a laminar boundary layer due to distributed surface roughness," in *Turbulence and Chaotic Phenomena in Fluids,* T.Tatsumi, ed., Elsevier Sci. Publishers B.V. (North Holland) pp. 39-46

Reshotko, E. & Leventhal, L. 1981: "Preliminary experimental study of disturbances in a laminar boundary layer due to distributed surface roughness," AIAA Paper 81-1224

Tadjfar, M., Reshotko, E., Dybbs, A. & Edwards, R.V.1985: "Velocity Measurements Within Boundary Layer Roughness Using Index Matching," in *International Symposium on Laser Anemometry,* A. Dybbs and P.A. Pfund, eds., FED Vol. 33, pp. 59-73, ASME Press (Book #G00328)

How smooth is smooth?

To be hydraulically smooth

$$Re_k \equiv \frac{u_k k}{\nu}$$

$$= \left(\frac{\partial u}{\partial y}\right)_w k^2/\nu$$

$$< 25$$

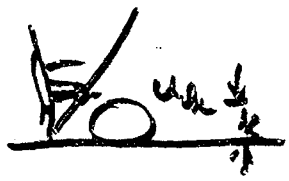

$$Re_k = (k^+)^2$$

When $Re_{k_{rms}} < 25$, surface still seems rough

When using abrasives to polish

$$\boxed{k_{max} \sim 10\, k_{rms}}$$

EMPIRICAL CORRELATIONS

Parameters

$Re_{x_{tr}}$ $\quad Re_k, \frac{k}{\xi^*}, \frac{k}{\delta}$

Re_{x_k}

These are 2D parameters for a phenomenon that is inherently 3D!

Example Correlations

Dryden

Tani

Smith & Clutter

& many others

Morkovin

Leventhal & Reshotko
Corke, Bar Sever & Morkovin

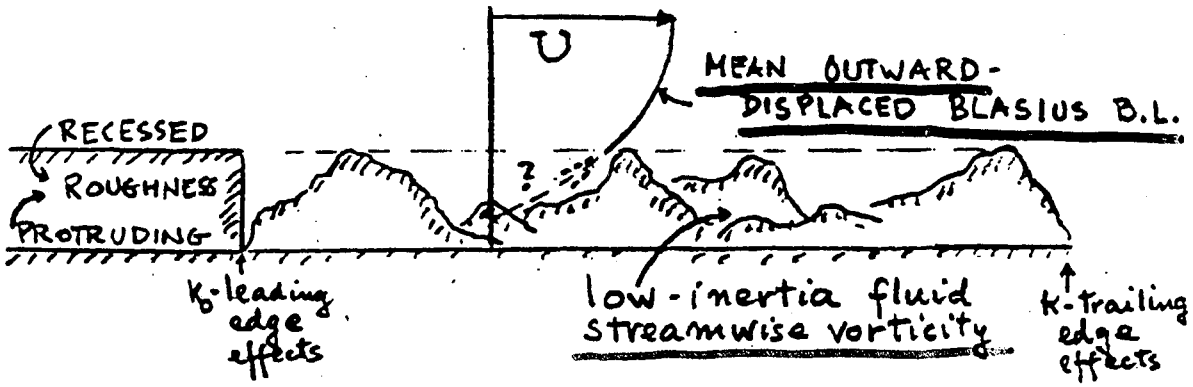

BYPASS REGIME (possibly triggered by highest-k population)

{higher Re_K^* ; smaller $x_{K_0} < x_{crTS}$}

*exceptions $x_{K_0} \ll x_{crTS}$?

Steady growth of low f spectra (below TS) as sensed by hot wire

No high f of hairpin eddies has been seen

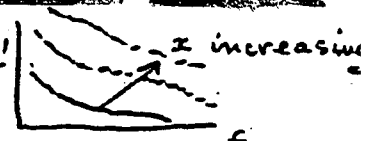

For high Re_{δ^*} peaks of near TS upper neutral curve do occur.

$150 \lesssim Re_K \lesssim 300$?

{lower $Re_K \lesssim 150$; $x_{K_0} \sim x_{crTS}$; $\lambda_{TS} \sim 50\text{-}60\, k_{nom}$} {Rapid growth rate of quasi-2DTS and 3DTS waves past Re_{crTS} of Blasius profile. early onset of Craik & Herbert secondary instabilities and breakdown.}

---

u_{TS} in complex notation: wave no $= k_{TSr} + ik_{TS}$; angular frequency ω_r

$$u_{TS}(x) = u_{TS}(x_0)\exp i\{k_{TSr}(x-x_0) - \omega_r t\}\exp\{-k_{TSi}(x-x_0)\} + \text{TABULATED TS GROWTH, homogeneous soln.}$$

$$+ \int_{x_0}^{x} \Delta u_{TS}(x')\exp i\{k_{TSr}(x-x') - \omega_r t\}\exp\{-k_{TSi}(x-x')dx'$$

RECEPTIVITY NON-HOMOGENEOUS SEEDING with account of phase interaction

For unsteady pressure-gradient disturbances non-homo contribution far in excess of homo rate has been measured, Nishioka+Morkovin 1986.
This probably true for roughness-enhanced receptivity.
Also k_{TSi} of BL could possibly exceed k_{TSi} BLASIUS.

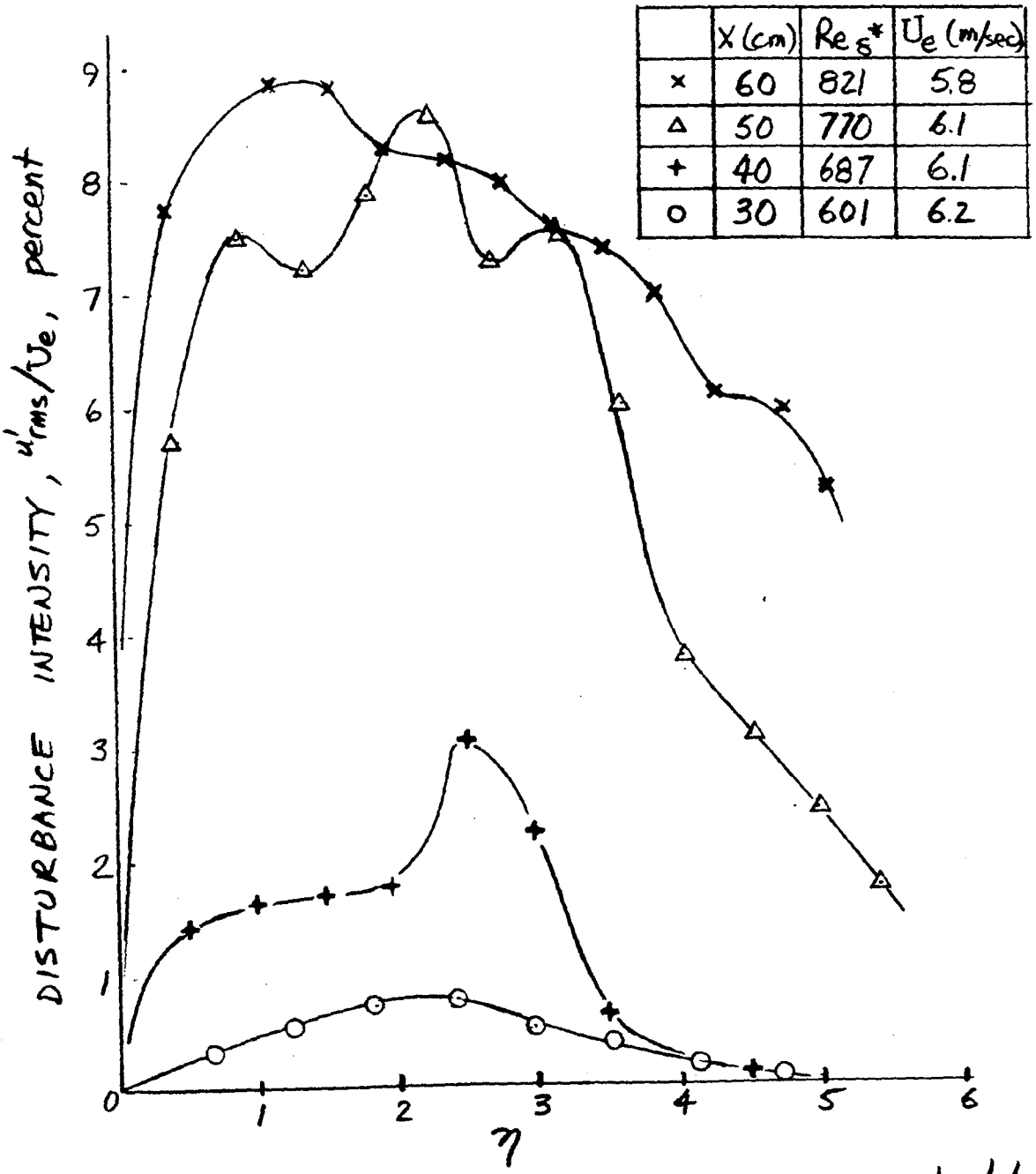

	X (cm)	Re_{δ^*}	U_e (m/sec)
×	60	821	5.8
△	50	770	6.1
+	40	687	6.1
o	30	601	6.2

Figure 5. Disturbance intensity profiles for a rough plate.
Re_x (X=30 cm) = 155

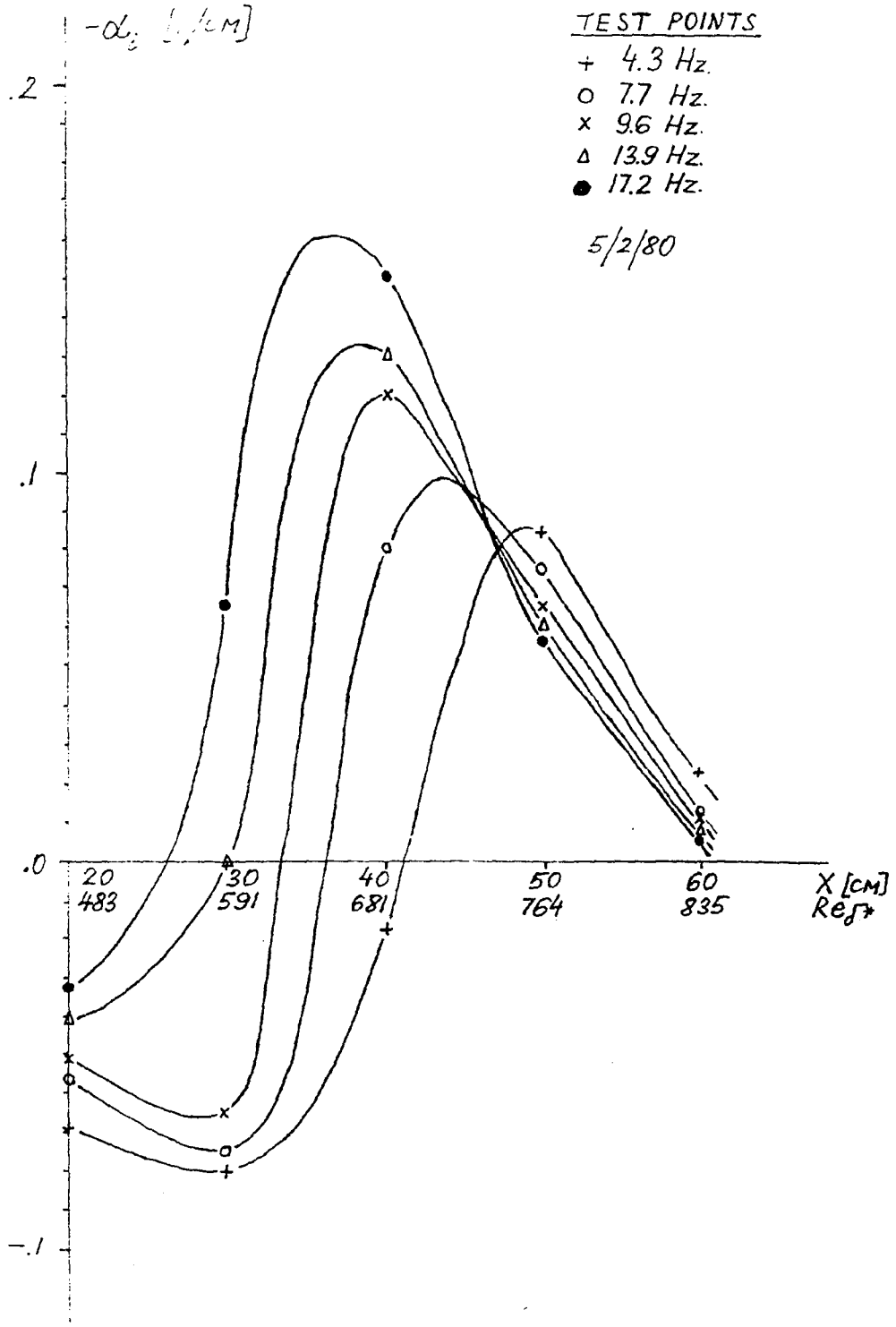

Fig. 41. Amplification rates for disturbances with frequencies from 4.3 Hz to 17.2 Hz; Re_k (X = 30 cm) = 155.

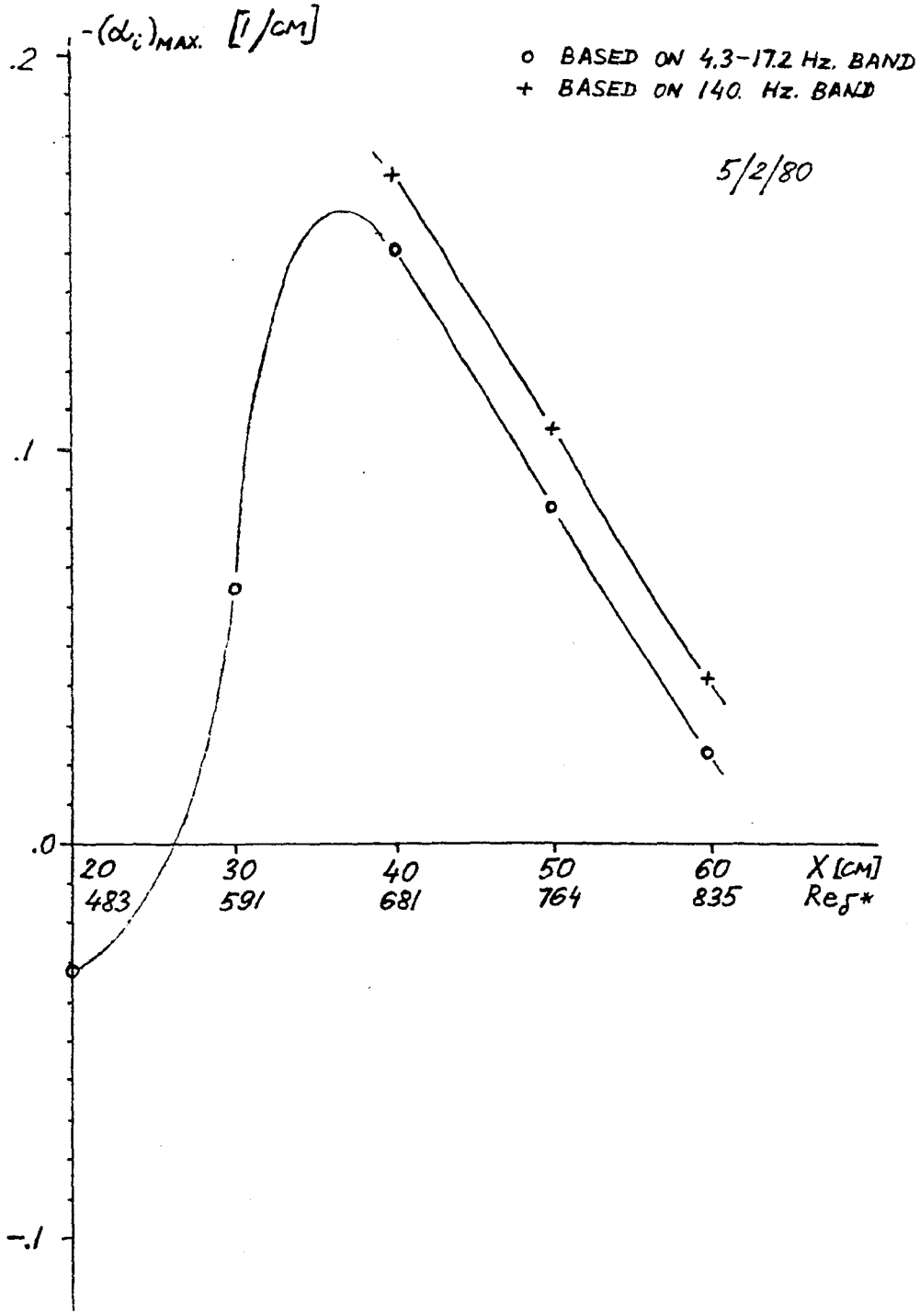

Fig. 43. The highest amplification rate versus X. Re_k (X = 30 cm) = 155.

Morkovin

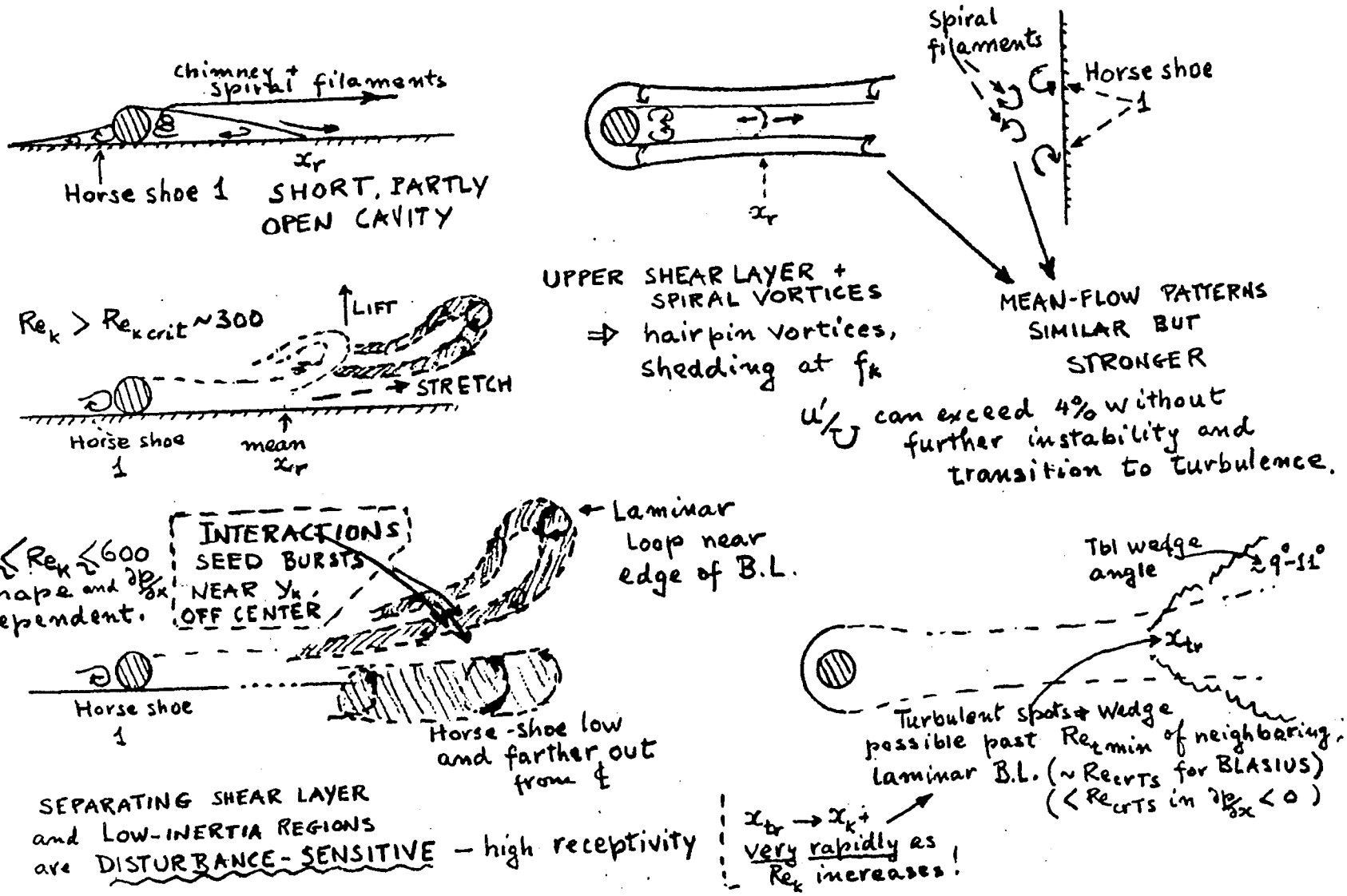

FIG 2 FLOWS AROUND 3D SINGLE-ROUGHNESS ELEMENTS

Tadjfar, Reshotko, Dybbs, & Edwards, 1985

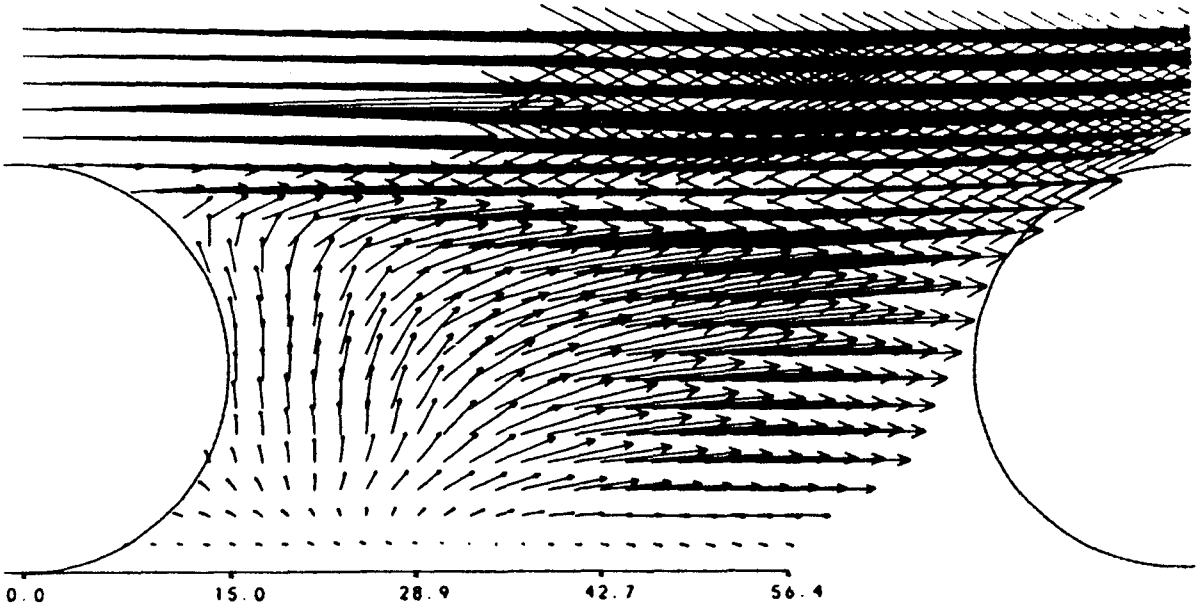

CONCLUSIONS

1. All measurements above beads consistent with prior investigations: Kendall, Leventhal & Reshotko, Shin et al., Morkovin et al.

2. Within bead array, profiles depend on location within bead array and upon Re_k

3. In vicinity of transition ($Re_k \approx 315$) oscillations observed at Strouhal numbers ≈ 0.1 with velocity patterns consistent with Machinki's observations about a single sphere.

4. No evidence of T-S waves.

TRANSIENT DISTURBANCES

Emanate from Landahl's "LIFT-UP" (1980) mechanism — localized 3D up-down motions in regions of high mean shear

Boberg & Brosa	1988
Schmid, Henningson et al	1993
Trefethen, et al	1993
Butler and Farrell	1992

Coupling between slightly damped, highly-oblique Orr-Sommerfeld and Squire modes leads to algebraic growth followed by decay outside the T-S neutral curve.

(O-S equation NOT self-adjoint, therefore eigenfunctions are not strictly orthogonal)

Morkovin - Disturbances must be environmentally realizable. In absence of definitive localized sources, relevant 3D seeding and receptivity mechanisms not obvious.

TRANSIENT DISTURBANCES

A MODEL PROBLEM (Boberg/Brosa. 1988) (Waleffe, 1993)

Orr-Sommerfeld/Squire System:

$$\frac{\partial}{\partial t}\begin{pmatrix}\mathcal{J}\\ \eta\end{pmatrix} = \begin{pmatrix}\mathcal{L}_{OS} & 0\\ \gamma & \mathcal{L}_S\end{pmatrix}\begin{pmatrix}\mathcal{J}\\ \eta\end{pmatrix}$$

$\mathcal{J}$ is disturbance vorticity in x-z plane normal to direction of wave propagation

η is disturbance vorticity normal to the bounding surface

$\mathcal{L}_{OS}, \mathcal{L}_S$ are homogeneous Orr-Sommerfeld and Squire operators respectively.

γ is the coupling coefficient.
For 2D boundary layer, $\gamma \sim \beta \bar{u}'$
where β is the spanwise wave number,
$\bar{u}'$ is the mean shear $\left(\frac{\partial \bar{u}}{\partial y}\right)$

Model System: Replace operators by eigenvalues

$$\frac{d}{dt}\begin{pmatrix} \xi \\ \eta \end{pmatrix} = \begin{pmatrix} -\lambda & 0 \\ \gamma & -\mu \end{pmatrix}\begin{pmatrix} \xi \\ \eta \end{pmatrix} \qquad \lambda, \mu > 0$$

$$\xi(0) = \xi_0 \qquad \eta(0) = \eta_0$$

$$\xi = \xi_0 e^{-\lambda t}$$

$$\boxed{\eta = -\xi_0 \gamma \left(\frac{e^{-\lambda t} - e^{-\mu t}}{\lambda - \mu} \right) + \eta_0 e^{-\mu t}}$$

For $\lambda = \mu$

$$\eta = (\eta_0 + \gamma \xi_0 t) e^{-\mu t}$$

$$\eta_{max} = \left(\frac{\gamma \xi_0}{\mu} + \eta_0 \right) e^{-\left(1 + \frac{\mu \eta_0}{\xi_0}\right)}$$

$$\text{at} \quad t = \frac{1}{\mu} + \frac{\eta_0}{\xi_0}$$

If additionally $\eta_0 = 0$

$$\eta_{max} = \frac{\gamma \xi_0}{e \mu} \qquad \text{at} \quad t = \frac{1}{\mu}$$

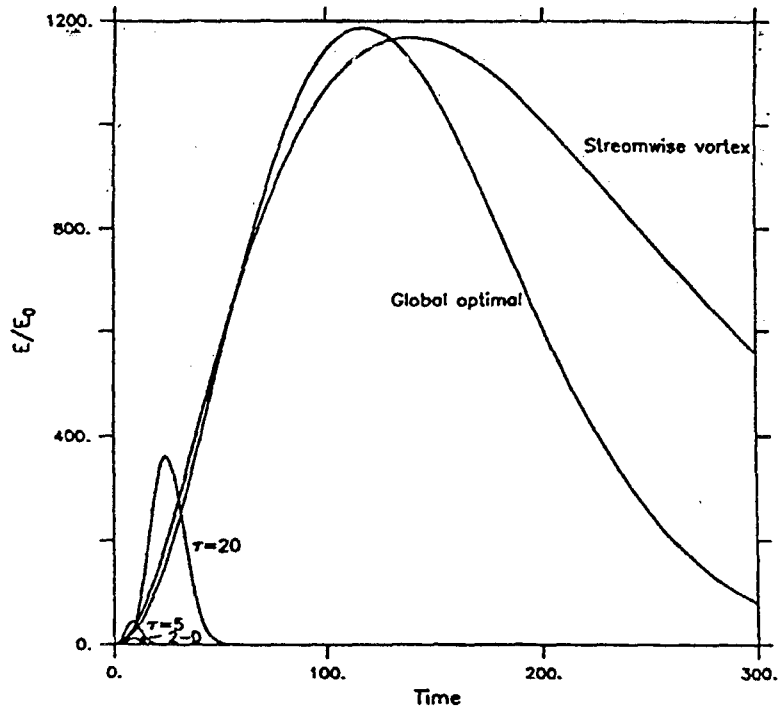

FIG. 8. Energy growth versus time for the global optimal, the streamwise vortex, and 2-D perturbation which grow the most, and perturbations which grow the most in 5 and 20 advective time units in Couette flow with $R = 1000$

OPTIMAL PERTURBATIONS

Butler and Farrell, 1992

TABLE I. Optimal perturbations in Couette flow at $R=1000$.

	τ	α	β	E_τ/E_0
Global optimal	117	0.035	1.60	1185
Best streamwise vortex	138	0	1.66	1166
Best optimal at $\tau=20$	20	0.46	1.9	312
Best optimal at $\tau=5$	5	1.6	2.9	26.4
Best 2-D optimal	8.7	1.21	0	13.0

TABLE II. Global optima for Couette flow.

R	τ	α	β	E_τ/E_0
4000	467	0.0088	1.60	18 956
2000	234	0.0175	1.60	4739
1000	117	0.035	1.60	1184.6
500	59	0.067	1.60	296.0
250	30.2	0.12	1.61	73.9
125	16.1	0.144	1.63	18.55
62.5	8.2	0.0024	1.65	4.87
31.25	3.21	0	1.62	1.50

TABLE III. Optimal perturbations in Poiseuille flow at $R=5000$.

	τ	α	β	E_τ/E_0
Antisymmetric global optimal	379	0	2.044	4897
Gustavsson—antisymmetric peak	420	0	1.98	4448
Symmetric global optimal	270	0	2.644	2819
Gustavsson—symmetric peak	286	0	2.60	2708
Best optimal at $\tau=20$	20	0.93	3.1	512
Best optimal at $\tau=5$	5	3.6	7.3	49.1
Best 2-D optimal	14.1	1.48	0	45.7

TABLE IV. Optimal perturbations in Blasius flow at $R_\delta=1000$.

	τ	α	β	E_τ/E_0
Global optimal	778	0	0.65	1514
Best optimal at $\tau=100$	100	0.15	0.96	652
Best optimal at $\tau=20$	20	0.87	1.7	78
Best 2-D optimal	45	0.42	0	28

Evidence for Transient Growth in a 1961 Pipe Flow Experiment

Ernst Mayer & Eli Reshotko

1996
(Physics of Fluids, Jan. 1997)

Kaskel, A. (J. Laufer) JPL Tech. Report 32-138, 1961

Reshotko, E. (J. Laufer) JPL Progress Report 20-364, 1958

Kaskel, 1961

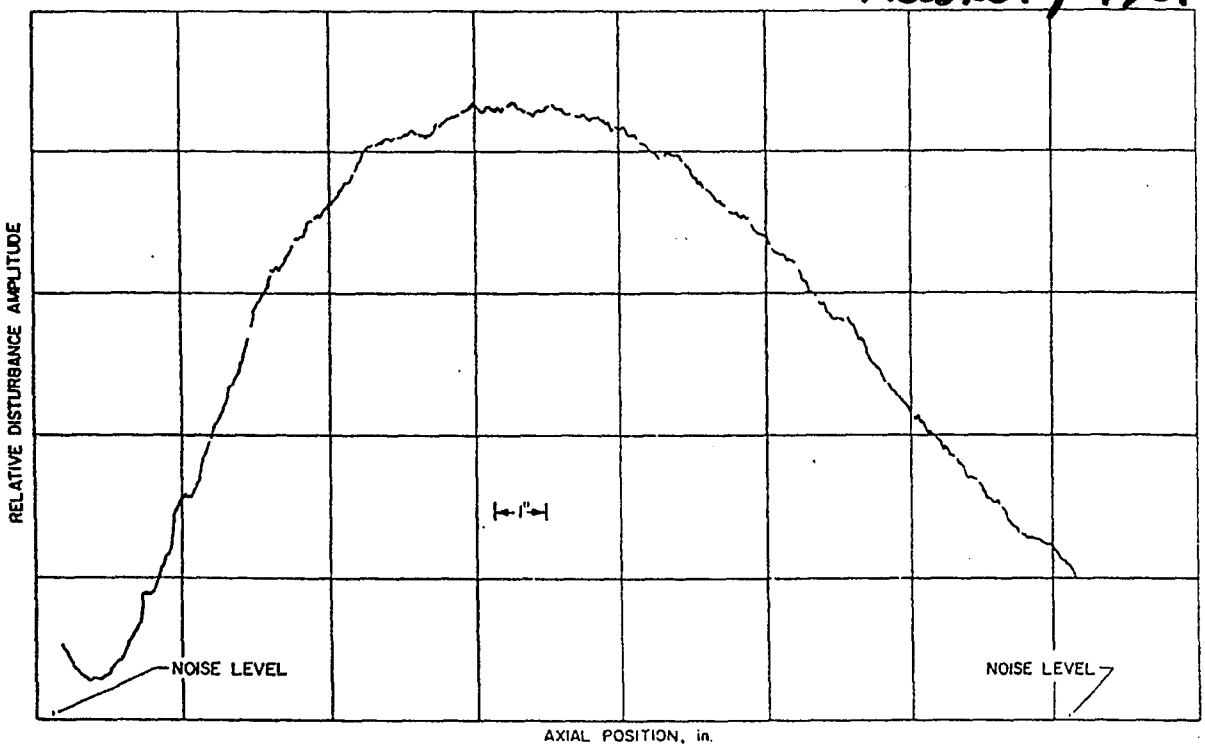

Fig. 13. Decay profiles, frequency = 10 cps

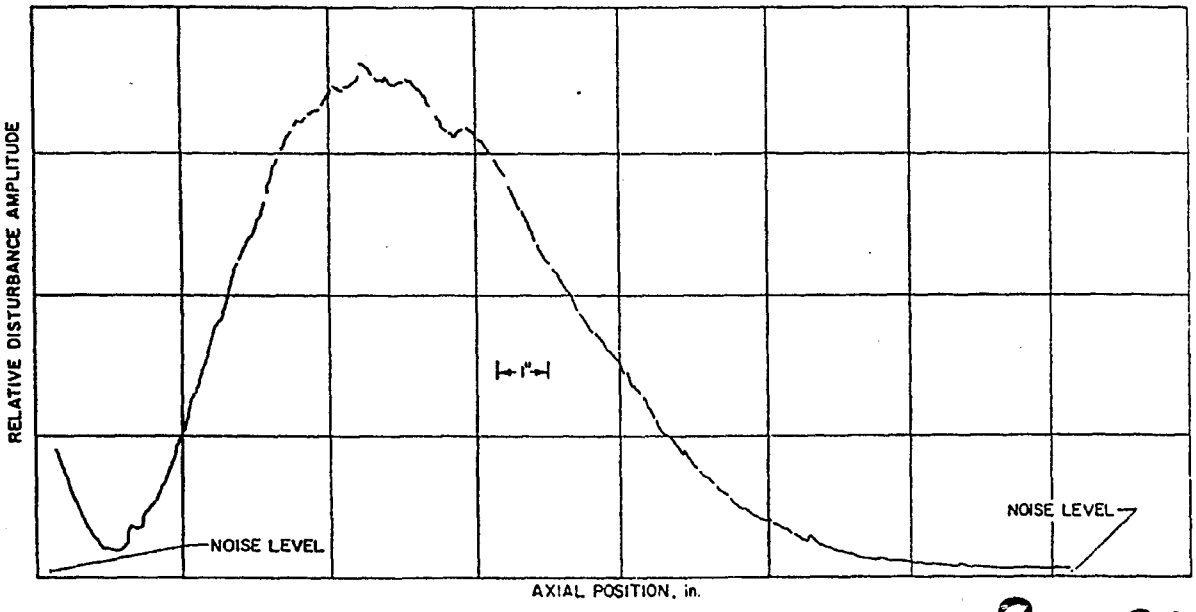

Fig. 14. Decay profiles, frequency = 15 cps

$Re_D = 7600$

$n = 0$:	$n = 1$:	$n = 2$:	$n = 6$:
w-modes:			
1.0856641969888 $-i$0.03450085564279	1.0611163132 $-i$0.02751620273	1.045687715 $-i$0.04008288198	0.17167147 $-i$0.09871350
1.0513283939735 $-i$0.0688366586554	1.09224614238 $-i$0.05878973387	0.3049381953 $-i$0.0678818281	0.28465728 $-i$0.10135200
0.3360305703154 $-i$0.090366295802	0.3236543770 $-i$0.05886525857	1.008847729 $-i$0.072414365	0.98013457 $-i$0.10486589
1.016992590793 $-i$0.1031724615698	1.0234851163 $-i$0.0592837405	1.0798142780 $-i$0.0744577016	0.9446064 $-i$0.1381439
0.98265678682 $-i$0.137508259116	0.986964733 $-i$0.091750950	0.17227814448 $-i$0.0947372444	1.01522142 $-i$0.14007073
0.94832106125 $-i$0.17184397481	0.17297331236 $-i$0.095715576277	0.97275850 $-i$0.10524301	0.909280 $-i$0.171588
0.51391902785 $-i$0.193211881469	1.0602393414 $-i$0.09610472398	1.047335562 $-i$0.111240717	0.29636902 $-i$0.17428392
0.9139871906 $-i$0.206179924	0.95096823 $-i$0.12457267	0.93707760 $-i$0.1383568	0.9819209 $-i$0.1756065
0.87966529 $-i$0.240538230	1.027514552 $-i$0.1322845008	1.014356474 $-i$0.14727062	0.87409 $-i$0.20515
0.270460993828 $-i$0.244038011176	0.480503128 $-i$0.156973999	0.301010659 $-i$0.168060640	0.9484547 $-i$0.210940
0.658609876 $-i$0.265002374	0.9152641 $-i$0.1576086	0.90164888 $-i$0.1716564	0.455118 $-i$0.215532
0.84521113 $-i$0.275158725	0.3010542588 $-i$0.16629884668	0.46798785 $-i$0.1809063	0.400576 $-i$0.2160195
0.8070032 $-i$0.31051374	0.994406150 $-i$0.167913609	0.98108555 $-i$0.18289014	0.30077606 $-i$0.220815043
0.7821618 $-i$0.32058167	0.879735 $-i$0.1907875	0.866387 $-i$0.205089	0.8391 $-i$0.2389
0.4719505762 $-i$0.3237878080	0.96105084 $-i$0.203220515	0.40176946 $-i$0.21207254	0.914870 $-i$0.246127
0.7756150 $-i$0.3712267	0.402318415 $-i$0.2129997690	0.9476210 $-i$0.21825497	0.483540 $-i$0.262971
0.633425116 $-i$0.38139632	0.844320 $-i$0.224076	0.2629488251 $-i$0.2248569862	0.804 $-i$0.272
0.7558902 $-i$0.4146450	0.25570019720 $-i$0.23136830750	0.83126 $-i$0.23861	0.88118 $-i$0.2812
0.7534788 $-i$0.4584174	0.609286 $-i$0.237686	0.9140176 $-i$0.2534494	0.5679 $-i$0.2896
0.7537500 $-i$0.5140457	0.92751888 $-i$0.2383190	0.490169 $-i$0.2611181	0.59960 $-i$0.2971
0.7529491 $-i$0.57273295	0.80900 $-i$0.25760	0.60798 $-i$0.26294	0.511719 $-i$0.30104
0.752161185 $-i$0.63365426	0.49112575 $-i$0.25887299	0.7960 $-i$0.2725	0.77 $-i$0.308
0.75148356 $-i$0.69685108	0.8938521 $-i$0.2732751	0.571106 $-i$0.287701	0.8475 $-i$0.3162
0.75090553 $-i$0.76236465	0.571529 $-i$0.289060	0.88031 $-i$0.288525	0.636 $-i$0.326
0.750411313 $-i$0.83022811	0.7727 $-i$0.2926	0.4709382 $-i$0.29950974	0.73 $-i$0.33
v-modes:	0.7278 $-i$0.3009	0.759 $-i$0.306	0.70 $-i$0.35
1.0856641969889 $-i$0.0345008556427	0.45959539 $-i$0.304962005	0.725 $-i$0.322	0.8133 $-i$0.351
1.051328393977 $-i$0.068836658654	0.860077 $-i$0.308137	0.84652 $-i$0.323524	0.674 $-i$0.355
0.1738444674500 $-i$0.0976664873763	0.64380 $-i$0.32439	0.64129 $-i$0.32635	0.74 $-i$0.38
1.016992590967 $-i$0.103172461665	0.82616 $-i$0.34296	0.714 $-i$0.344	0.78 $-i$0.387
0.982656787955 $-i$0.137508264675	0.7163 $-i$0.3449	0.63846 $-i$0.355800	0.75 $-i$0.40
0.300749160839 $-i$0.16451971343	0.737 $-i$0.347	0.8125 $-i$0.3585	0.751 $-i$0.43
0.9483209849 $-i$0.17184406769	0.624808 $-i$0.359377	0.738 $-i$0.374	0.750 $-i$0.454
0.9139851818 $-i$0.2061798707	0.791688 $-i$0.37745	0.777 $-i$0.393	0.750 $-i$0.484
0.40265575265 $-i$0.21510912667	0.7443 $-i$0.3934	0.751 $-i$0.408	0.748 $-i$0.510
0.879649380 $-i$0.240515673	0.7594 $-i$0.40794	0.754 $-i$0.4304	0.749 $-i$0.541
0.491286581 $-i$0.256517661	0.7537 $-i$0.4309	0.754 $-i$0.457	0.747 $-i$0.5685
0.84531363 $-i$0.274851582	0.754431 $-i$0.45715	0.7536 $-i$0.4853	0.7490 $-i$0.600
0.57119413 $-i$0.291506657	0.7540 $-i$0.4854	0.753 $-i$0.5134	0.746 $-i$0.629
0.8109672 $-i$0.3091893	0.753536 $-i$0.513985	0.7528 $-i$0.5430	0.748 $-i$0.662
0.64477025 $-i$0.32152282	0.7531 $-i$0.54288	0.7522 $-i$0.5720	0.746 $-i$0.692
0.7768072 $-i$0.3428031	0.752599 $-i$0.572729	0.75195 $-i$0.6028	0.7482 $-i$0.726
0.7134939 $-i$0.3473997	0.75225 $-i$0.60268	0.7514 $-i$0.6329	0.7457 $-i$0.75762
0.757182 $-i$0.378733	0.7518066 $-i$0.633671	0.75129 $-i$0.6648	0.7478 $-i$0.7927
0.755428 $-i$0.430060	0.75148 $-i$0.66473	0.7507 $-i$0.6961	0.7457 $-i$0.8254
0.754215 $-i$0.485480	0.7511390 $-i$0.696890	0.75071 $-i$0.72916	0.7476 $-i$0.8613
0.7531689 $-i$0.5430774	0.75085 $-i$0.729098	0.7501 $-i$0.7616	0.7453 $-i$0.8957
0.7522802 $-i$0.6028933	0.750574 $-i$0.7624240	0.75022 $-i$0.79584	0.74750 $-i$0.9327
0.7515255 $-i$0.6649713	0.75030 $-i$0.79580	0.7496 $-i$0.8295	0.7452 $-i$0.9683
0.75088391 $-i$0.729350164	0.7500962 $-i$0.8303055	0.74981 $-i$0.864871	0.7474 $-i$1.0063
0.75033772 $-i$0.79606393			

Table II: Best approximation (using 64-bit real arithmetic) to the 50 least-damped eigenvalues for pipe Poiseuille flow with $\alpha = 1.12$ and $Re = 7600$, for various azimuthal wavenumbers.

INNER PRODUCTS MATRIX (n=1)

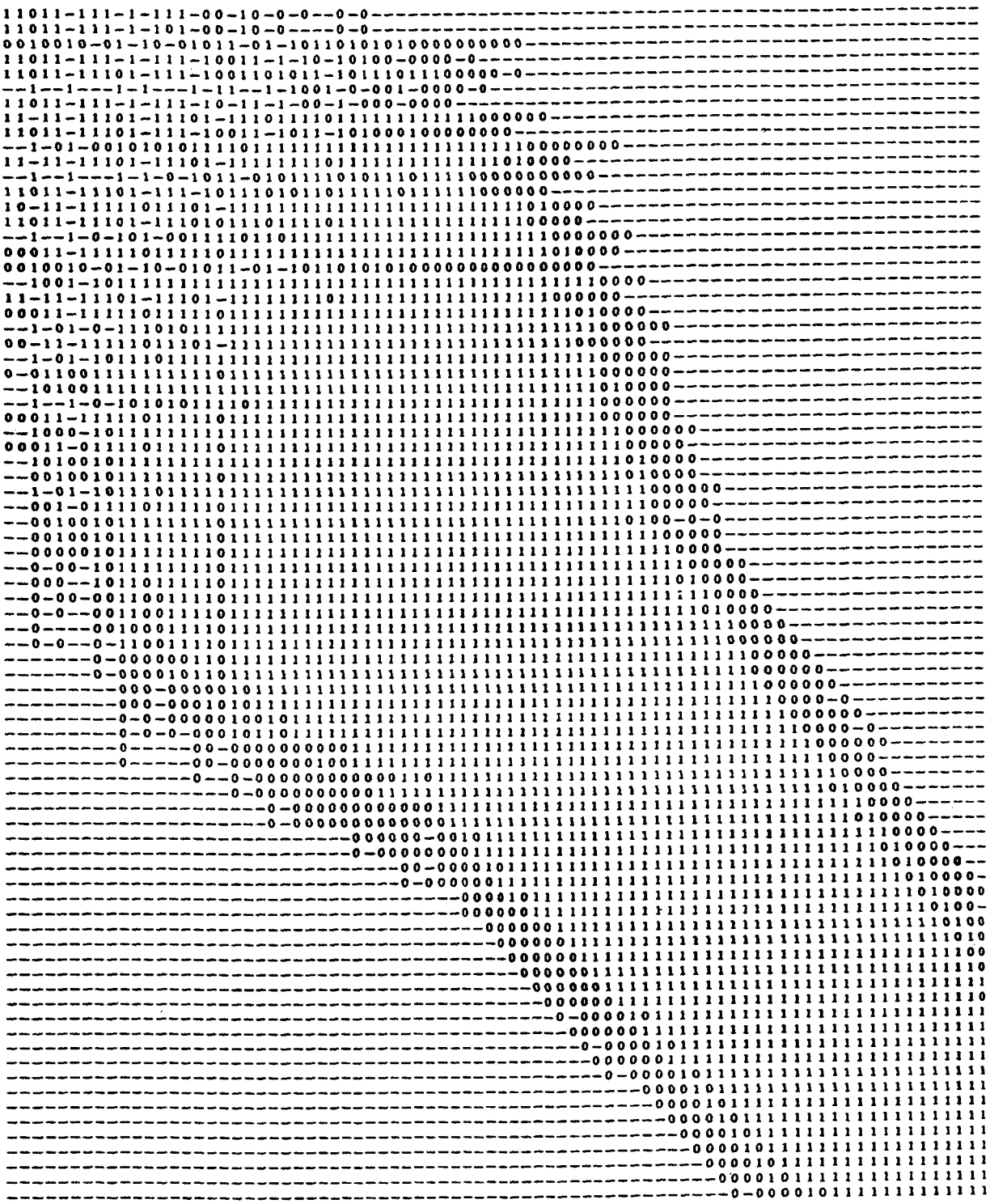

Figure 1: 80-eigenfunction inner products matrix (symbolic form) for pipe flow at $Re = 7600$, $n = 1$ and $\alpha = 1.12$. (10 Hz)

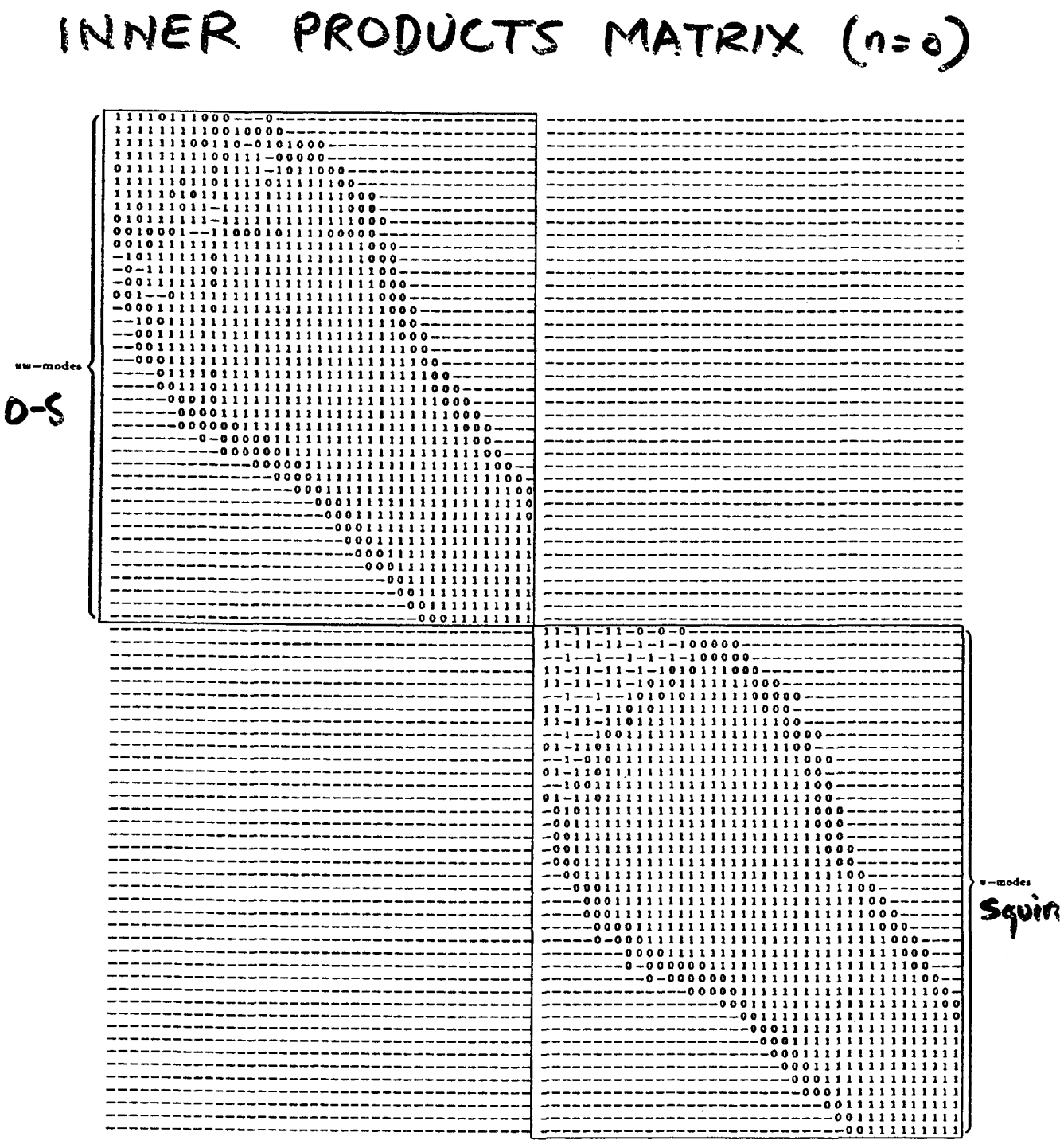

Figure 2: 80-eigenfunction inner products matrix (symbolic form) for pipe flow at $Re = 7600$, $n = 0$ and $\alpha = 1.12$.

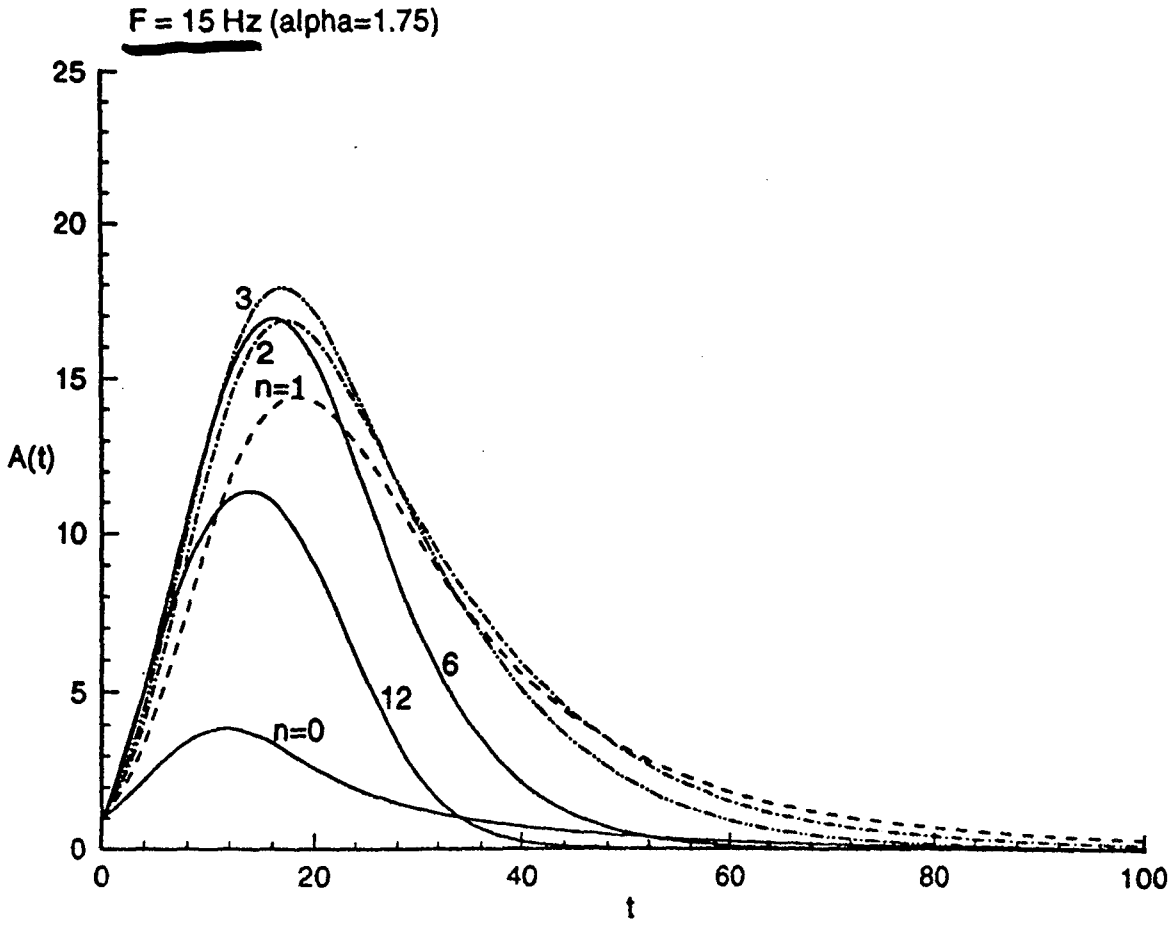

Figure 4: Nondimensional amplitude growth for pipe flow at $Re = 7600$, $\alpha = 1.75$ (F=15 Hz), at various azimuthal disturbance wavenumbers.

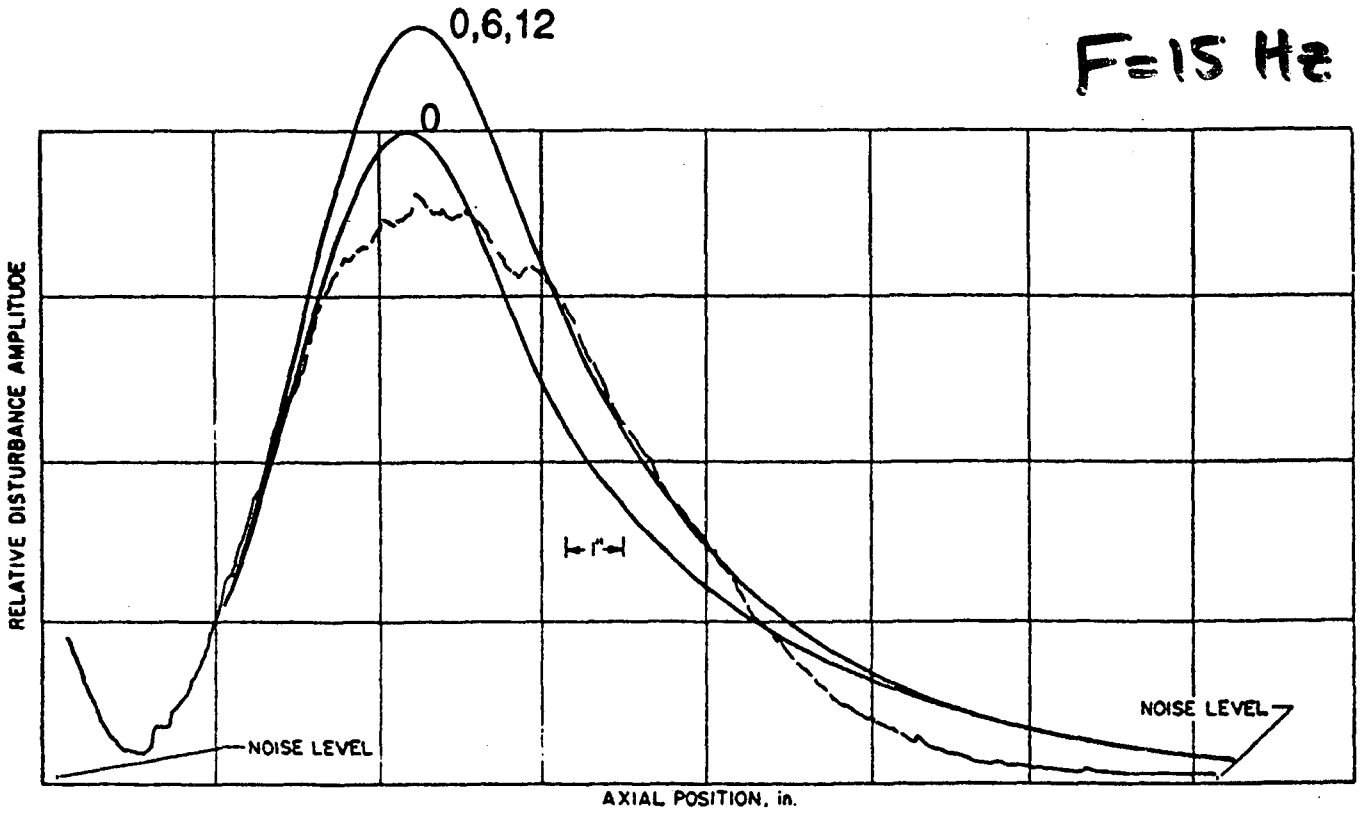

Figure 6: Experimental traces vs. theoretical predictions of amplitude growth, F=15 Hz.

Disturbance Generator Influence Coefficients

n=0	0.955
n=6	0.055
n=12	-0.013
	0.997

PATHS TO TURBULENCE IN WALL LAYERS - TRADITIONAL VIEW

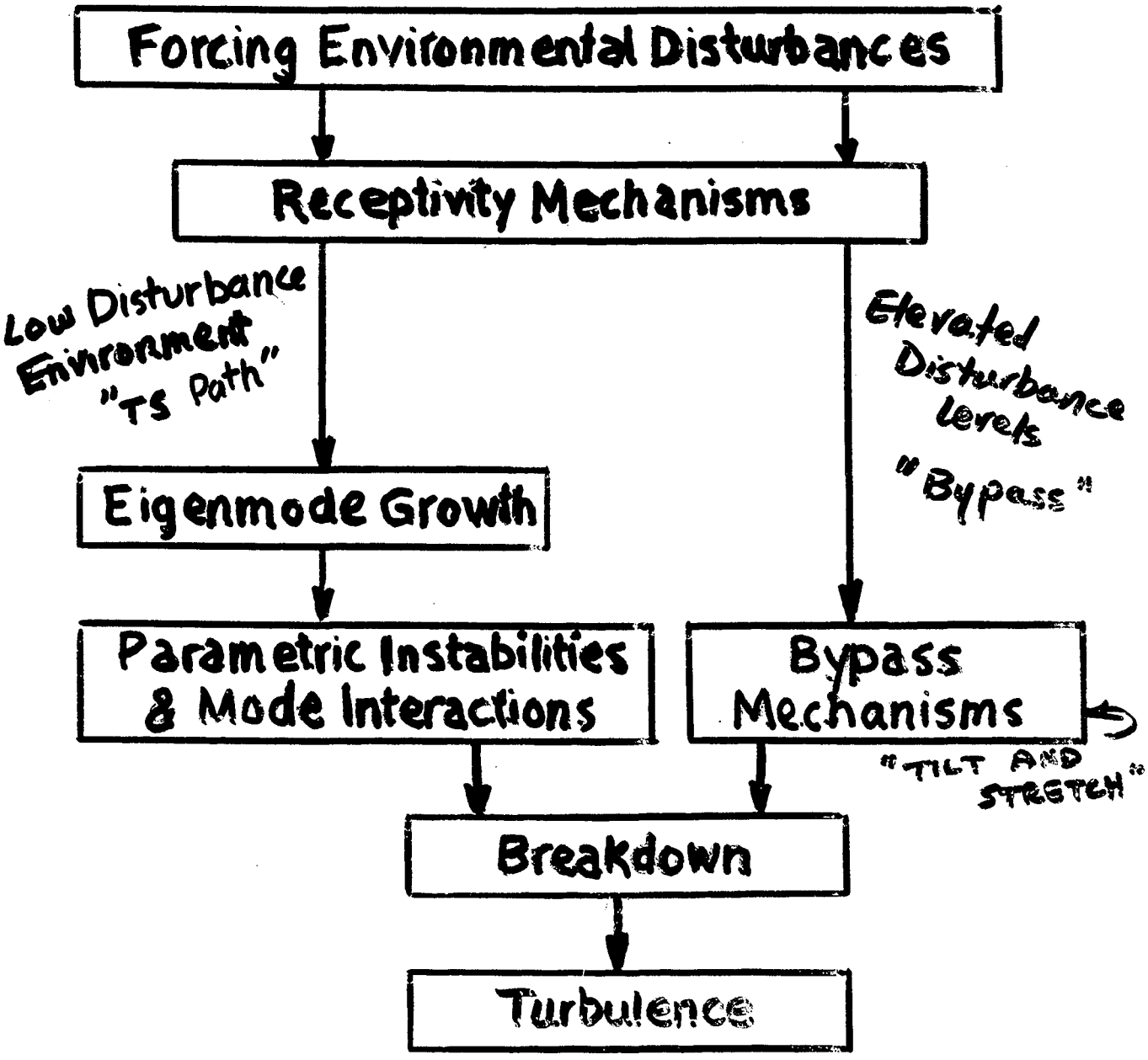

PATHS TO TURBULENCE IN WALL LAYERS

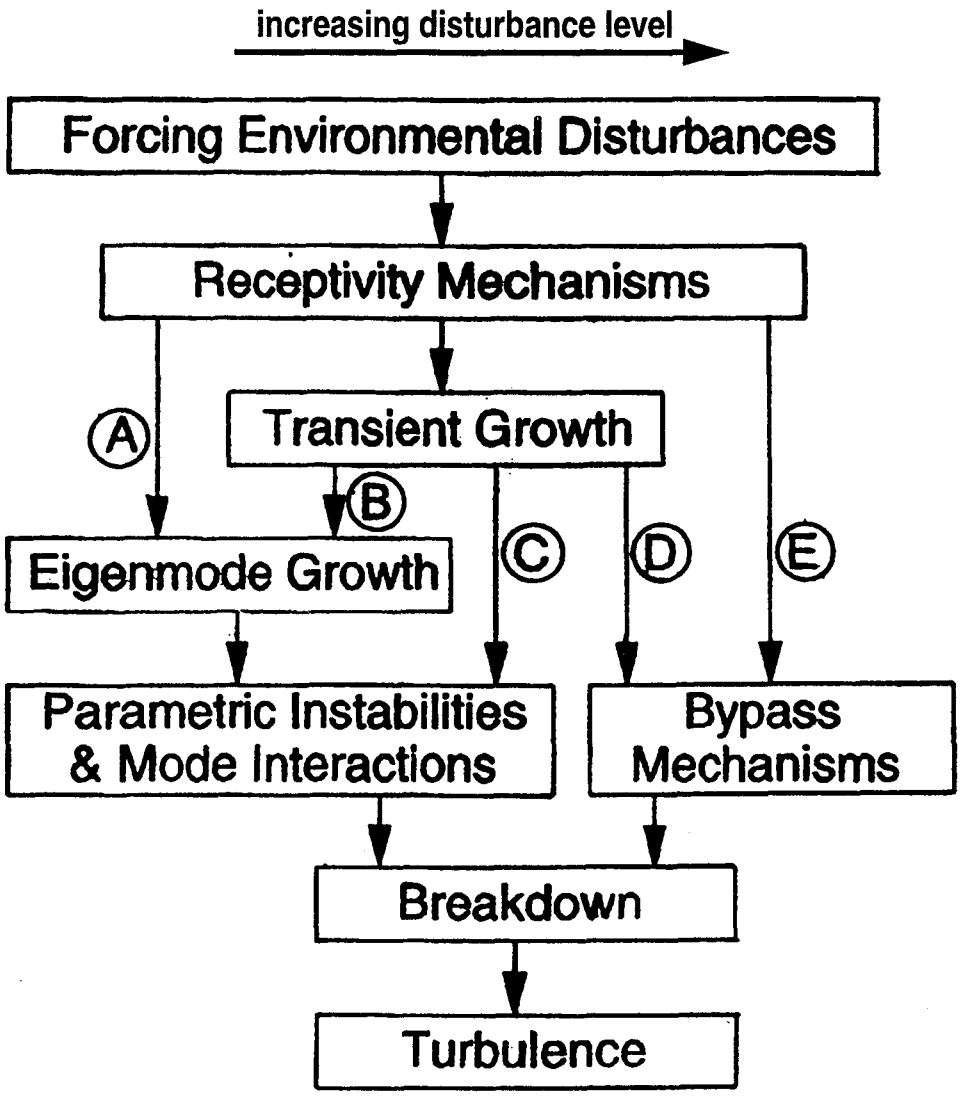

- (A) - Transient growth benign - insignificant
  Traditional T-S (or Goertler) path
- (B) - Some transient growth providing higher amplitude input to eigenmode growth when disturbance crosses Branch I
- (C) - Transient growth large enough to directly excite secondary instabilities and mode interactions
- (D) - Spectrum of disturbances is full - looks like a turbulent spectrum with all the interactions so implied
- (E) - Very large amplitude forcing - like through a chopper.
  Crazy spectrum!

More examples, experimental and otherwise, are needed to refine this speculative picture

EXPERIMENTAL INVESTIGATION OF BY-PASS TRANSITION IN THE INSTITUTE OF THERMOMECHANICS IN PRAGUE

Pavel Jonas
Institute of Thermomechanics
Czech Republic

ABSTRACT

Rather pure is the knowledge on the effect of mixed disturbances (turbulent and periodic) on the by-pass transition. This encouraged to arrange experiments to compare the boundary layer transition in a facility with an invariable configuration of walls surrounding the flow field, with a given value of time averaged free stream velocity (Ue~ 10 m/s) and with independently acting generators of the outerstream velocity disturbances (random, harmonic, mixed). The investigated flat-plate boundary layer develops itself in flow with either natural turbulence (intensity 0,12 percent) or with grid-turbulence (intensity amplified up to 4 percent). By means of a rotating flap inserted into the sonic throat, the periodic pulsations are generated. The frequency and the amplitude have been chosen so, as to reach low subcritical (1200 and 3000) and high supercritical (~50000) values of the non-steady Reynolds number (OBREMSKI & FEJER [1967]). It has been observed that periodic disturbances cause the alterations of the velocity gradient in space and during every period of oscillations even though the time-mean velocity is constant. Owing to this are the alterations of turbulence production and decay inside the of oscillations. Consequently the time-averaged turbulence intensity amplifies; above all in the arrangement without turbulence generator. The courses of the skin-friction coefficient Cf reveal that the flows with turbulent or harmonic or mixed disturbances force the onset of transition sooner than an undisturbed flow. Also the final stage of the transition process is carried out more quickly. The alterations of turbulence production and decay manifest themselves in the alterations of the phase-averaged valued of Cf mentioned and further effects are more important of supercritical non-steady Reynolds number and in the case without turbulence generator. There are known the fact about the effect of the wall constraint and the viscous sticking of the fluid to the surface on the structure of the external turbulent flow and the fact that the effect of outer stream turbulence on turbulent boundary layer depend not only on the intensity but also on the length scale of outer stream turbulentc. From this follows: to a certain degree the length scale should influence the by-pass transition. To examine the above mention notion and to assemble the data of the Test Case T3A+ specified by the COST-ERCOFTAC Special Interest Group on Transition the effect of variable dissipative length scale Le (from~3 to ~40 mm) and 3 percent turbulence level of the incoming flow (Ue = 5 or 10 m/s) on a zero pressure gradient boundary layer has been investigated. From the measured distributions of the shape parameter H12 and of the skin-friction coefficient CF it is obvious that the dissipative length scale Le influence the by-pass transition. At the given turbulence level of the incoming flow the onset of the last stage of the transition is coming later in the fine-grain turbulence. The length of the last part of transitional layer appears to be independent on Le. An attempt to study the modification of the turbulence structure of the investigated layers, namely of the bursting phenomenon has been done.

Further effort should be devoted to precise the investigated effect, especially the receptivity of a boundary layer to disturbance near the region where is the layer loosing the stability.

Synopsis:

1. *"former"*: Effect of mixed (turbulent and periodic) disturbances in the incoming stream on the by-pass transition in a facility with an invariable configuration of walls surrounding the flow field;
2. *"current"*: Effect of the length scale of the incoming turbulence on flat plate boundary layer transition - Test Case T3A+ of the COST/ERCOFTAC SIG on Transition;
3. *"proposed"*: Receptivity of a boundary layer to the action of a given kind of turbulence disturbances in various distances from the leading edge.

Acknowledgements

The investigation was accomplished in the period 1992 - 1997 and funded by grants from the Grant Agency of the Academy of Sciences of the Czech Republic (Projects No.27612 and No.A2076602), from the budged of the CR by means of the Ministry of Education, Youth and Physical Training of the CR (Project No. OC F1. 10) and with the financial support from the European Communities: Action for Co-operation in Science and Technology with Central and Eastern Countries (Project No.121180, COST Action F1).
The attendance at the Workshop is accomplished as the WOS visit to the United States, received through the European Office of Aeronautical Research and Development.
All these supports are gratefully acknowledged.

Motivation

- conclusions of the investigation of turbulent boundary layer perturbed by the outer stream turbulence;
- several private talks (Novosibirsk - transition school, M.V.Morkovin, O.Zeman);
- published reviews e.g. GREK et al.[1991]; MAYLE [1991]; MORKOVIN et al.[1973]; MORKOVIN & RESHOTKO [1990]; MORKOVIN [1992]; PFEIL & HERBST [1979]; SAVILL [1991]; WALKER [1992]

⇓

MORE investigated the effect of Tu_e and introductory phases of the process;
LESS data about: the response to periodic disturbances; the final part of the transition region
($x_p \rightarrow$ turbulent spots start to produce, grow, propagate downstream; $x_t \rightarrow$ t.b.l. become selfsustaining)
RARELY fully described all the factors influencing the transition
(is ever possible to do this completely ?)
NEED of original experiments at well defined boundary conditions, completely described features of the incoming flow etc.

⇓

PROJEKT:

A Comparison of Transitional Boundary Layers in Streams with Different Flow Structures

AIM: To compare most important features of transitional boundary layers in a facility

- with a permanent configuration of walls surrounding the flow field,
- with a possibility to generate well defined free-stream disturbances of different kind (turbulent, periodical and mixed) at sub- and super- critical „non-steady Reynolds number"

OBREMSKI & FEJER [1967]: b.l. transition characterized with $\mathrm{Re}_t = \frac{x_t . \overline{U_e}}{\nu}$ depends on the non-steady Reynolds number

$$\mathrm{Re}_{NS} = \frac{\Delta U_e \ell}{2\pi\nu}; \quad \ell = \frac{\overline{U}_e}{f};$$

critical value $(\mathrm{Re}_{NS})_C = 25000$ to 27000

e.g. LOEHRKE, MORKOVIN, FEJER [1975]:

$$\mathrm{Re}_{NS} > (\mathrm{Re}_{NS})_C \rightarrow \mathrm{Re}_t \approx F(\Delta U_e);$$
$$\mathrm{Re}_{NS} < (\mathrm{Re}_{NS})_C \rightarrow \mathrm{Re}_t \approx \text{const.}$$

Experimental Set Up:

- *small wind-tunnel vacuum storage drive (on the schematic picture are exhibited details);*
- *test section 0,1 x 0,1 m^2 and 2 m length;*
- *adjustable sonic throat controls the mass-flow;*
- *rotating flap inserted into critical section creates the periodic oscillations of velocity:*
  $U_e(t) = \overline{U}_e + \Delta U_e . \sin 2\pi f . t$; $[m/s]$; $[f] = Hz$
- *square mesh plane grid* (porosity 60.5%) *across the stream in the entrance of the test section* (x=0) *is producing turbulence fluctuations*
  u is the longitudinal component of velocity fluctuations;
  $Iu = \frac{\sqrt{\overline{u^2}}}{\overline{U}}, Su = \frac{\overline{u^3}}{\left(\overline{u^2}\right)^{3/2}}, Fu = \frac{\overline{u^4}}{\left(\overline{u^2}\right)^2}$ are intensity, skewness and kurtosis;
- *investigated boundary layer develops itself on a smooth steel plate-wall*
  $K = \frac{\nu.\left(d\overline{U}_e/dx\right)}{\overline{U}_e^2}$ is the free stream velocity gradient;
- *suction of boundary layers arising on remaining walls ensures the 2D-flow*

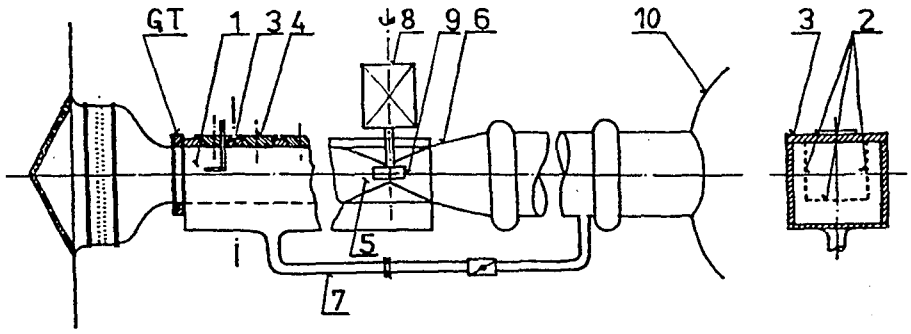

1 test section (0,1m x 0,1m)
2 porous sucked walls
3 steel flat plate with the investigated b.layer
4 interchangeable lids with probes etc.
5 adjustable sonic throat
6 diffuser
7 suction system
8 generator of oscillations - el.motor
9 rotating flap
10 vacuum tank: 6500m^3
GT turbulence generator - grid/screen - if necessary

A survey of the important flow characteristics of the channel
(x=0.086m; $U_e \approx 8{,}5$ m/s; hydraulic Reynolds number = 54000)

Turbulence generator	$10^7.K$	f [Hz]	$(\Delta U/U)_e$	$10^3.Re_{NS}$	Iu_e [%]
no	-1.0	0	0	0	0.12
grid*) (β=60%)	-1.1	0	0	0	4.0
no	1.5	10.2	0.67	50.8	9.0
grid (β=60%)	1.1	10.2	0.60	45.5	6.5
no	0.7	54.8	0.27	3.0	0.71
grid (β=60%)	-0.8	54.8	0.24	3.0	4.0
no	0.7	80	0.07	1.2	0.65

*) biplane grid: 3 x 3 mm^2 rods, 13,5 mm mesh
The dimensions of the sonic throat, rotating flap and number of the motor's revolutions i.e. frequency f and the amplitude ΔU have been chosen so as to reach low subcritical (1200 and 3000) and high supercritical (~50000) values of the "nonsteady Reynolds number" Re_{NS}.

Measurement technique and methods:

- HW-probes (tungsten wire 2,7 μm diameter; 0,8 mm long);
- HF-wall probes (platinum 0,4mm long; 5mm width);
- DANTEC CTA System (3 channels; t.55M and 56N);
- MAUER Transient Recorder (t.ADAM; 4 channels S/H 10 bit);
- data acquisition rate: 32 data points per period;
- data ensemble ≥ 160 000 samples per channel;
- averaging procedures: time- , statistical- , phase- averaged quantities;

Estimate of the measurement errors:
(derived from the recurrent observations)
averaged velocity U: ±0,5 %
variance u: ± (3÷5) %
skewness u: Su: ±0,05
kurtosis u: Fu: ±(0,10÷0,15)
wall friction coefficient Cf: ± (2÷3) %
frequency f: ± (1÷2) %

Generating an oscillating flow:

- travelling and standing waves are provoked in the channel
- alternations of the flow acceleration and deceleration
- variation of the amplitude and the phase shift with the streamwise distance x
- increased frequency provokes oscillations with a shorter wave-length, however, with a smaller amplitude
- the courses of the velocity distributions in time and space are very similar in both arrangements with or without the turbulence generating grid
- in the grid turbulence are phase averaged velocity distributions more smooth

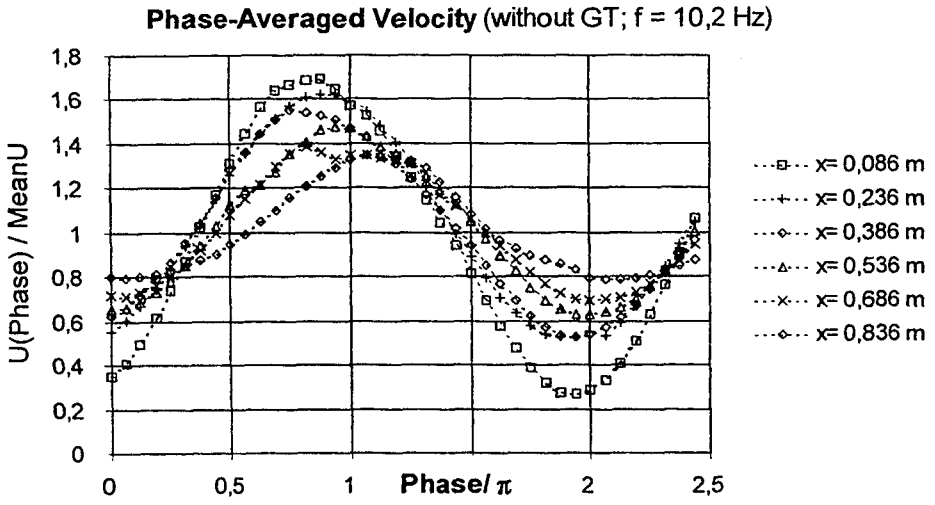

- Owing to the alterations of the acceleration period and the deceleration one, in the channel without a turbulizing grid occur both the dissipation of turbulent energy as well as the turbulent production. At supercritical Re_{NS} the intensity $Iu = \sqrt{\overline{u^2}}/\overline{U}$ considerably increases even though the channel remains in the state which produces a low turbulence level (~ 0,15%) when f=0.

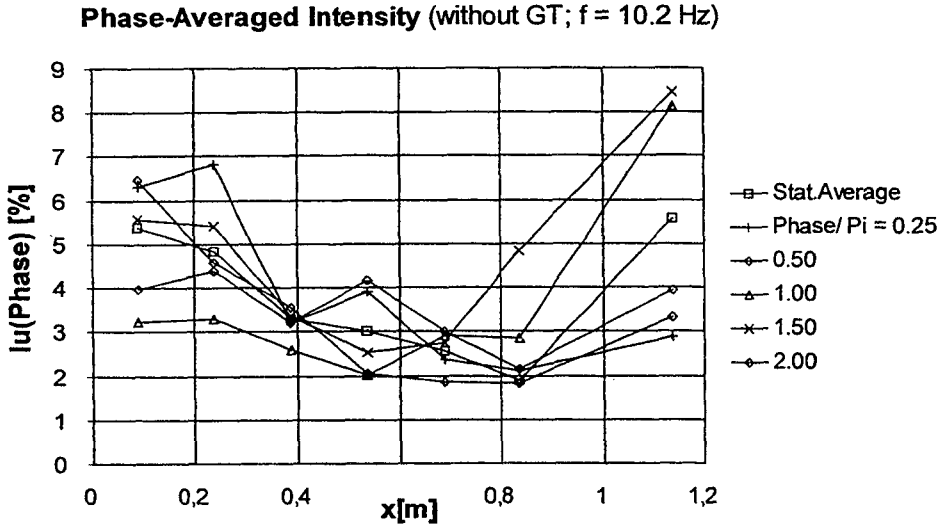

- **In a Grid-Turbulence** at roughly the same Re_{NS} the turbulence level is similar but the dissipation remains dominant - during the period the Iu remains largely diminishing.
- Oscillations characterized by the subcritical Re_{NS} cause smaller changes of the intensity during a period in configuration without grid and even more smaller in grid turbulence

Phase-Averaged Intensity (Grid Turbulence; f= 10.2 Hz)

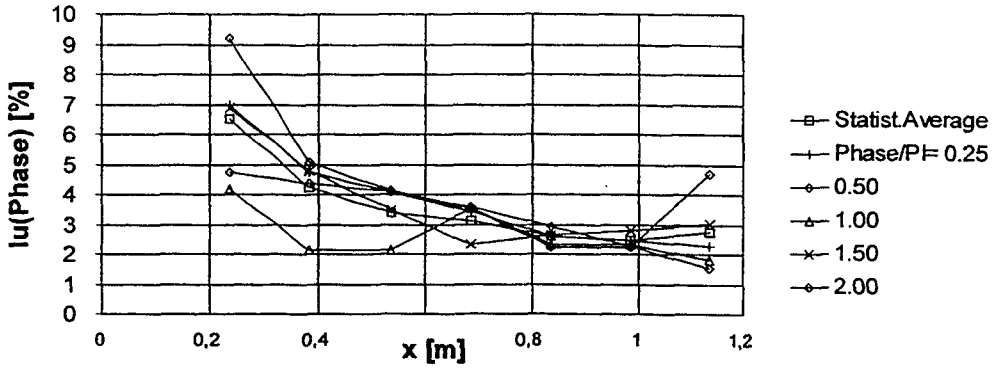

Decay of the grid turbulence reveals:

•almost negligible departures are between the decay at zero and subcritical Re;

•at supercritical Re_{NS} the turbulence energy is considerably amplified; the production predominates at x > 0,8 m

Decay of the Grid Turbulence:
Statistically Averaged Quantities; Reh = 68900; f = ~

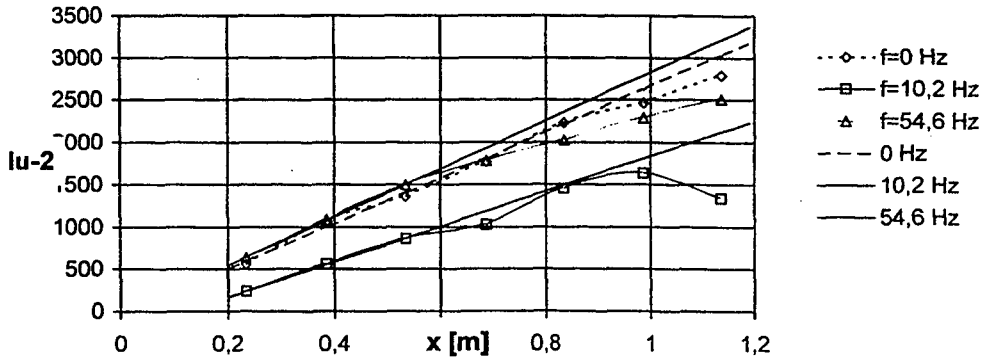

Skin Friction Coefficient:
proof of the experimental set-up and measuring methods;
f = 0 Hz; Re_h=127600; suction of b.l. at the entrance of the test section

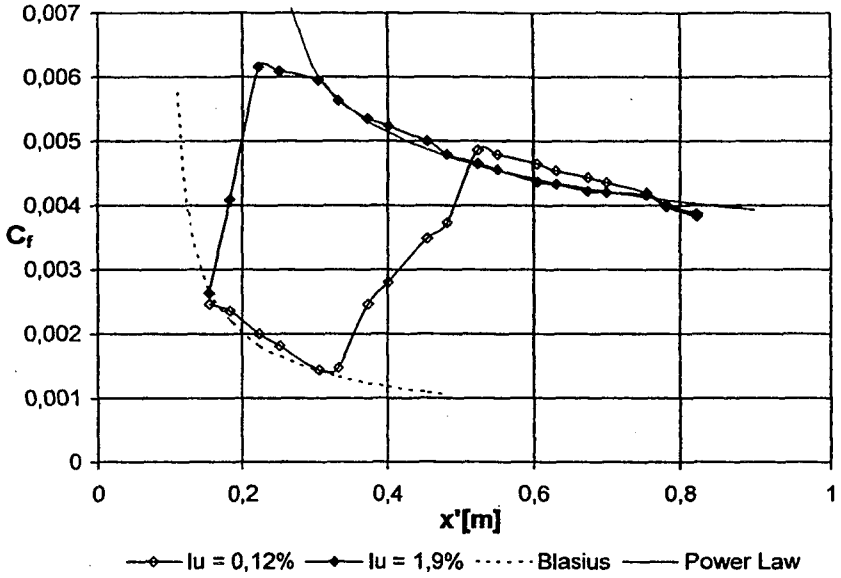

The locations x_p and x_t of the final part of the transition region are most distinct from the plot of C_f

Skin Friction Coefficient: Time Average;
Natural Turbulence; Re_h = 68900; f = ~

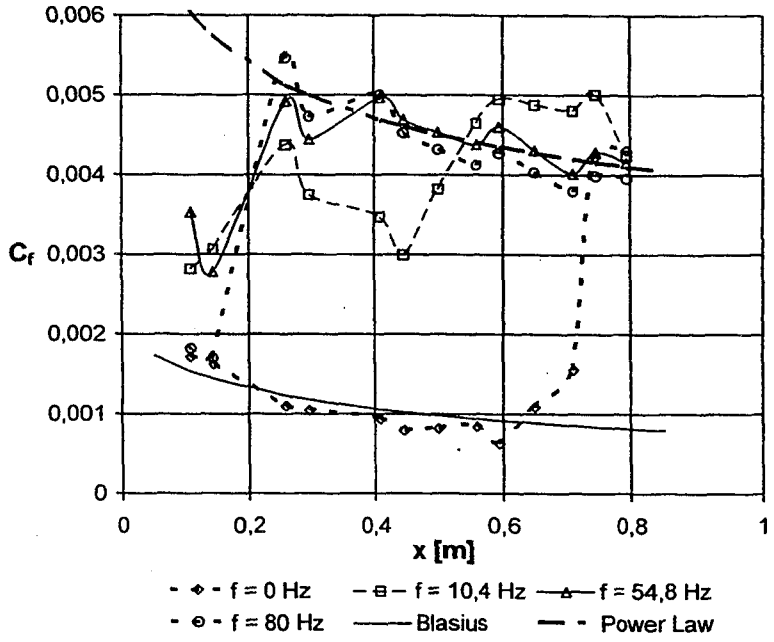

Oscillating flows force the onset of transition after a shorter distance downstream from the channel entrance than the undisturbed flow

Courses of Phase Averaged Nondimensional Velocity and Skin Friction Coefficient:
Natural Turbulence; Re_h = 68900; f = 10,4 Hz

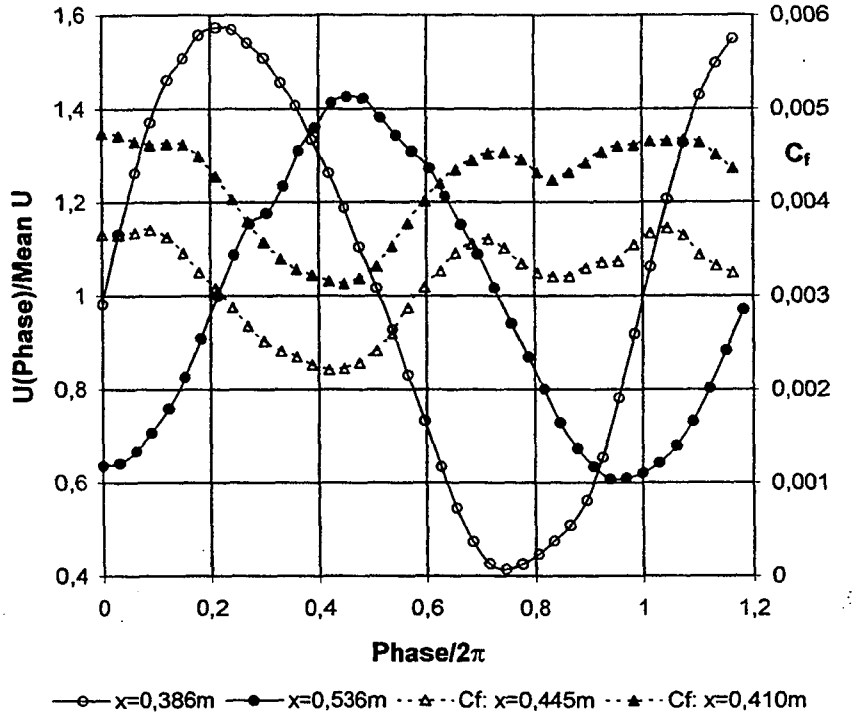

Temporal as well as spatial acceleration of the phase averaged free stream velocity results in the decrease of the phase averaged coefficient Cf and on the contrary.

Skin Friction Coefficient: Phase Average;
Natural Turbulence; Reh = 68900; f = 80 Hz

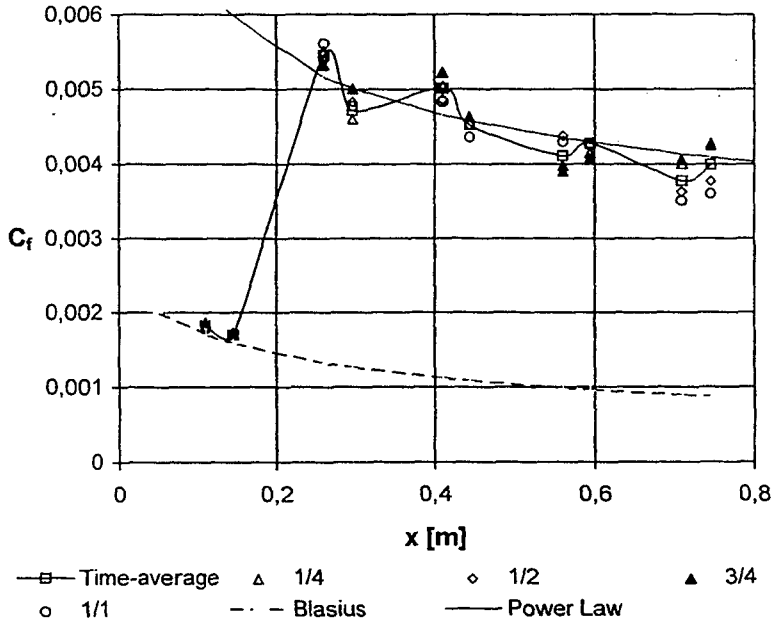

At higher frequencies (subcritical Re_{NS}) of the free stream oscillations, the transition process is executed very quickly likewise as in turbulent free stream.

Skin Friction Coefficient: Phase Average; Natural Turbulence;
Reh = 68900; f = 10,4 Hz

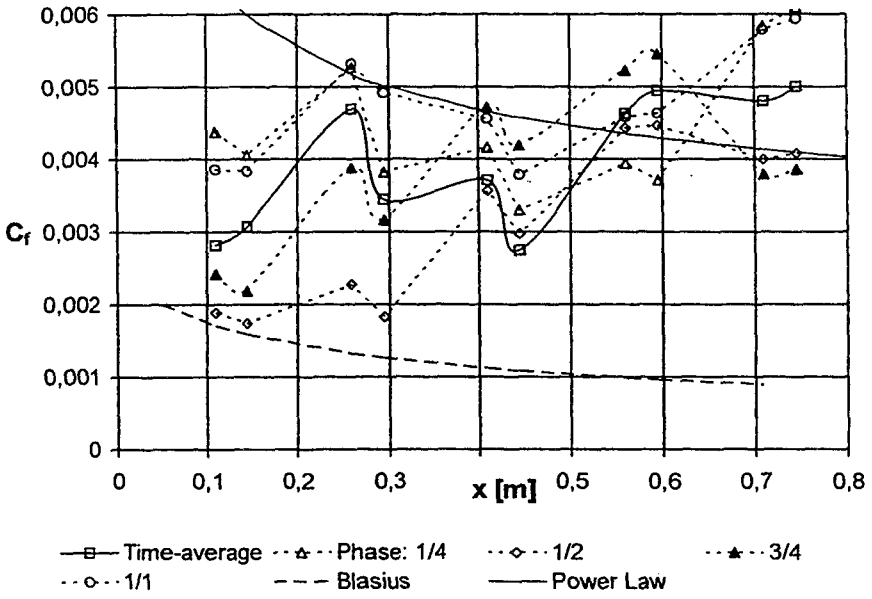

Temporal and spatial alteration of the turbulence production and damping, caused by the free stream oscillations at low frequency (supercritical Re_{NS}) manifests itself in an extended region of the final part of transition.
Transitional features of the boundary layer are distinct from the apparently chaotic distribution of the phase-averaged values of the skin friction coefficient C_f.

Current investigation:

Study of the role of the length scale in by-pass transition

Why should the free stream turbulence length scale influence the laminar to turbulent transition of a boundary layer ?

1. This effect follows from the fundamental features of the turbulence dynamics (dimensional estimates e.g. TENNEKES & LUMLEY [1974]);
2. Because of the wall constraint and the influence of the viscous boundary conditions on the grid-turbulence convected by a free stream past a rigid surface (experiments and theoretical solution e.g.UZKAN & REYNOLDS [1967], THOMAS & HANCOCK [1977], HUNT & GRAHAM [1978]);
3. Because this effect on a turbulent boundary layer in a turbulent outer stream has been proved (HANCOCK [1981], HANCOCK & BRADSHAW [1983], JONÁŠ [1977 and 1992])

execution

- **experiments** carried out by author & Oton MAZUR & Václav URUBA
- **modelling** accomplished by Tomáš HLAVA & Zbyněk JAŇOUR & Jaromír PŘÍHODA

Experimental Set Up

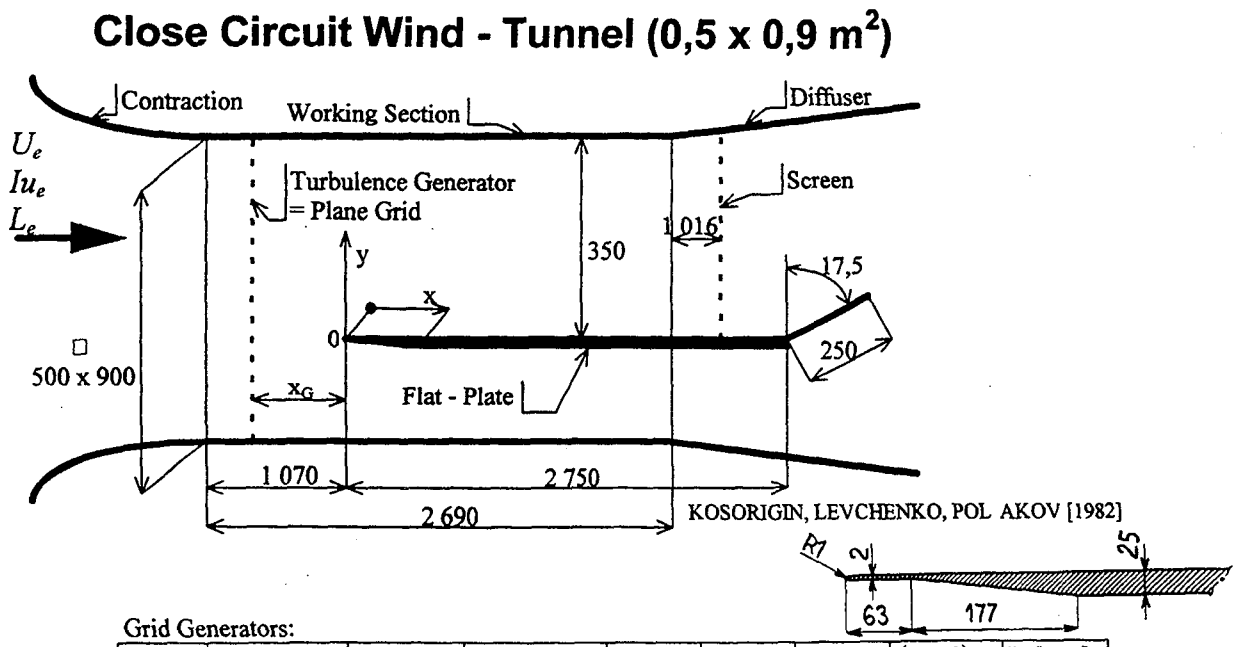

Grid Generators:

title	mesh [mm]	dia [mm]	porosity[%]	Δx_G [m]	Iu_e [%]	$(Iv/Iu)_e$	$\left(\overline{uv}/\overline{U}^2\right)_e$	L_e [mm]
GT 1	20	3	72	-0,445	3,0	1,02	-2.10^{-5}	6,8
GT 3a	40	6	72	-1,087	3,0	1,.05	$-2,1.10^{-5}$	16,1
GT 3b	40	6	72	-1,076	3,0	1,.05	$-2,1.10^{-5}$	15,7
GT 5	35	10	51	-1,350	3,0	1,03	$-1,6.10^{-5}$	34,5
GT 9	5	1	64	-0,123	3,0			2,3

Δx_G is the distance of the grid plane from the leading edge of the plate (x=0);
all turbulence characteristics have been measured in plane x=0 (y= 1÷150mm) at U_e= 5m/s

Measurement method

COST/ERCOFTAC SIG on Transition Test Case T3A⁺:

mean free-stream velocity U_e= 5 m/s ⟶ CTA (single and „X" hot-wire)

Hot-wire is calibrated in the range 0,2 to 10 m/s
special calibration set up with a metering nozzle - „amplification" 1:10
(individual components DANTEC or home production.

Measuring system consists of: anemometer DANTEC 55M01;
signal conditioners etc. DANTEC 56N;
PC Pentium EISA 133 MHz.

Data acquisition:
PC is equipped with the Data Acquisition System of National Instruments (EISA A-2000) controlled by the software LabVIEW (sampling rate 25 kHz; 0,75 millions samples; 12 bit).

Relations to derive the fluctuation velocities:

$$Nu\left(\frac{T_m}{T}\right)^M = A + B.\mathrm{Re}^N ; Nu \sim E^2 ; \mathrm{Re} \sim U_{ef} ; U_{ef}^2 = W^2\left(1 + k\cos^2\right.$$

Correction: the effect of the wall proximity on the HW-reading (JONÁŠ & ŘEHÁK[1983]).

Accuracy estimates (relative errors):
mean velocity ~ 0,5%; < 0,3 %
skin-friction coefficient ~ 2%;
variance u- component ~ 4%; etc.

Definitions:

$$\frac{U^2}{\overline{u^2}} = Iu^{-2} = C.(x - x_0)^m ; L = -\frac{Iu^3}{dIu^2 / dx}$$

Outer Stream Turbulence - Intensity of Streamwise Fluctuations

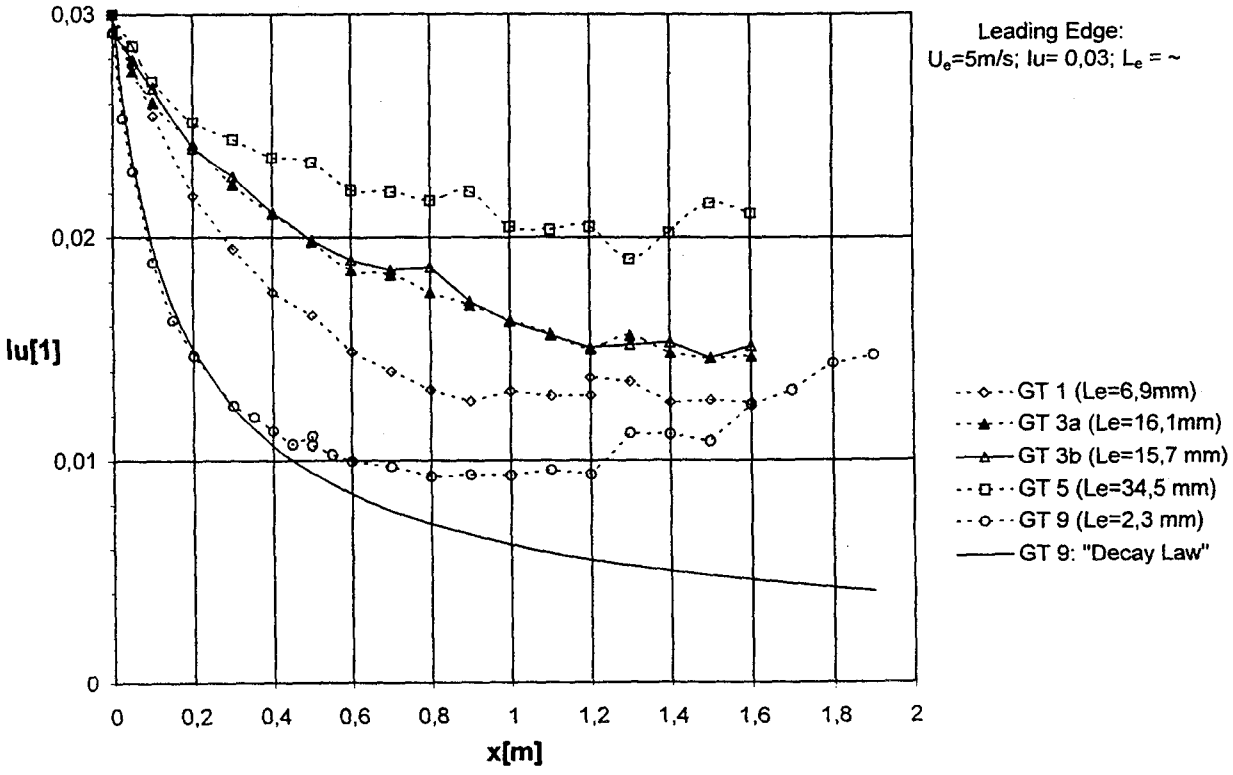

Outer Stream Turbulence :
Dissipative Length Scale/Thickness (99,5%)

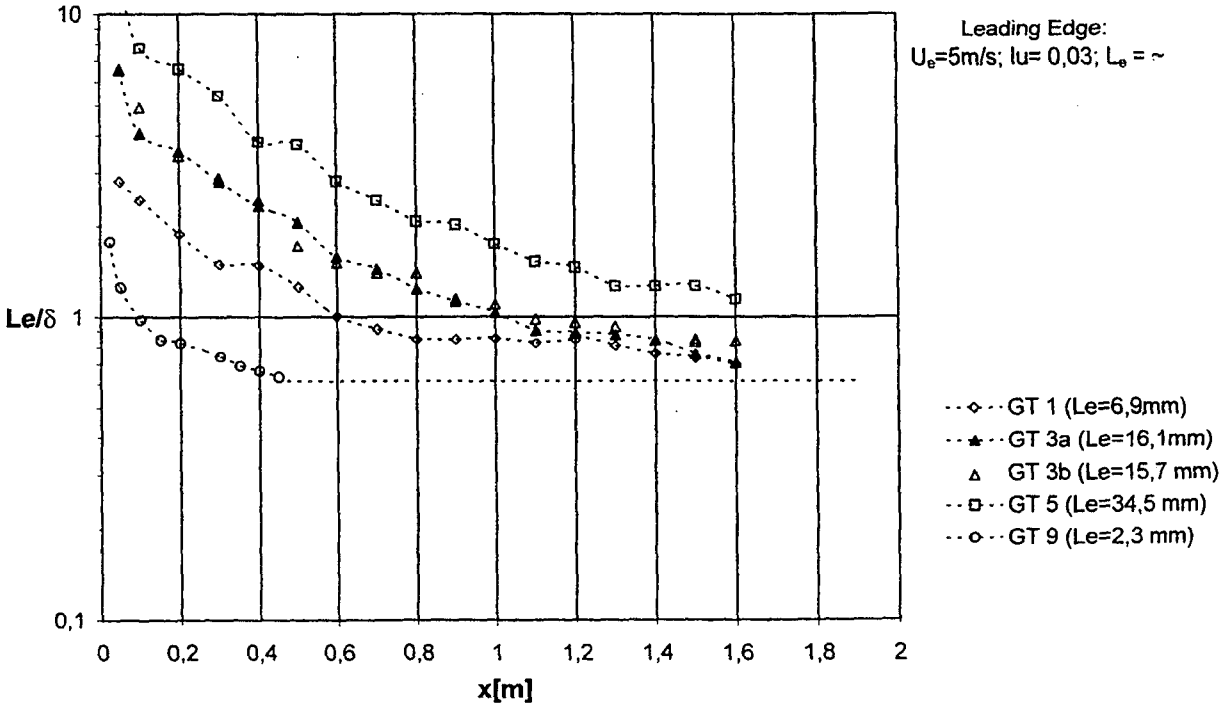

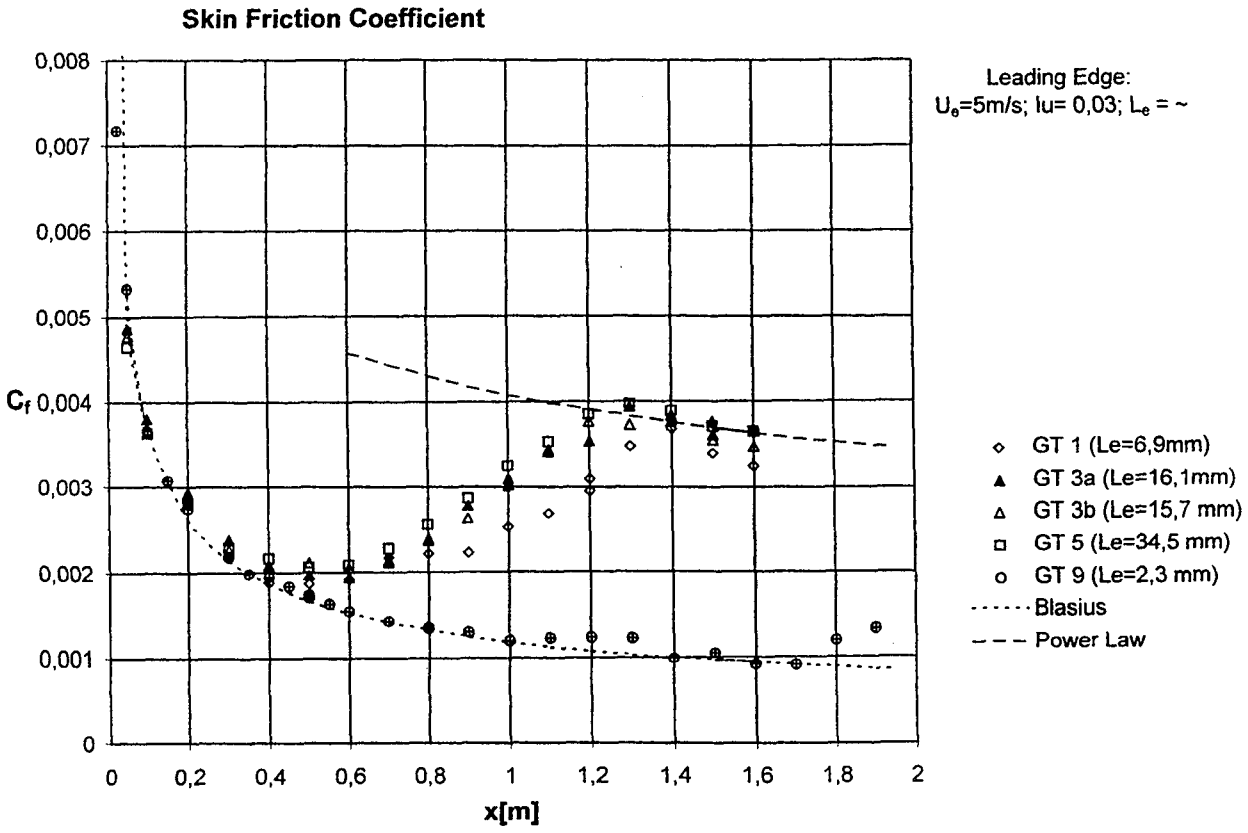
Skin Friction Coefficient
0,008
0,007
0,006
0,005
0,004
0,003
0,002
0,001
0
C_f
0
0,2
0,4
0,6
0,8
1
1,2
1,4
1,6
1,8
2
x[m]
Leading Edge:
U_e=5m/s; Iu= 0,03; L_e = ~
GT 1 (Le=6,9mm)
GT 3a (Le=16,1mm)
GT 3b (Le=15,7 mm)
GT 5 (Le=34,5 mm)
GT 9 (Le=2,3 mm)
Blasius
Power Law

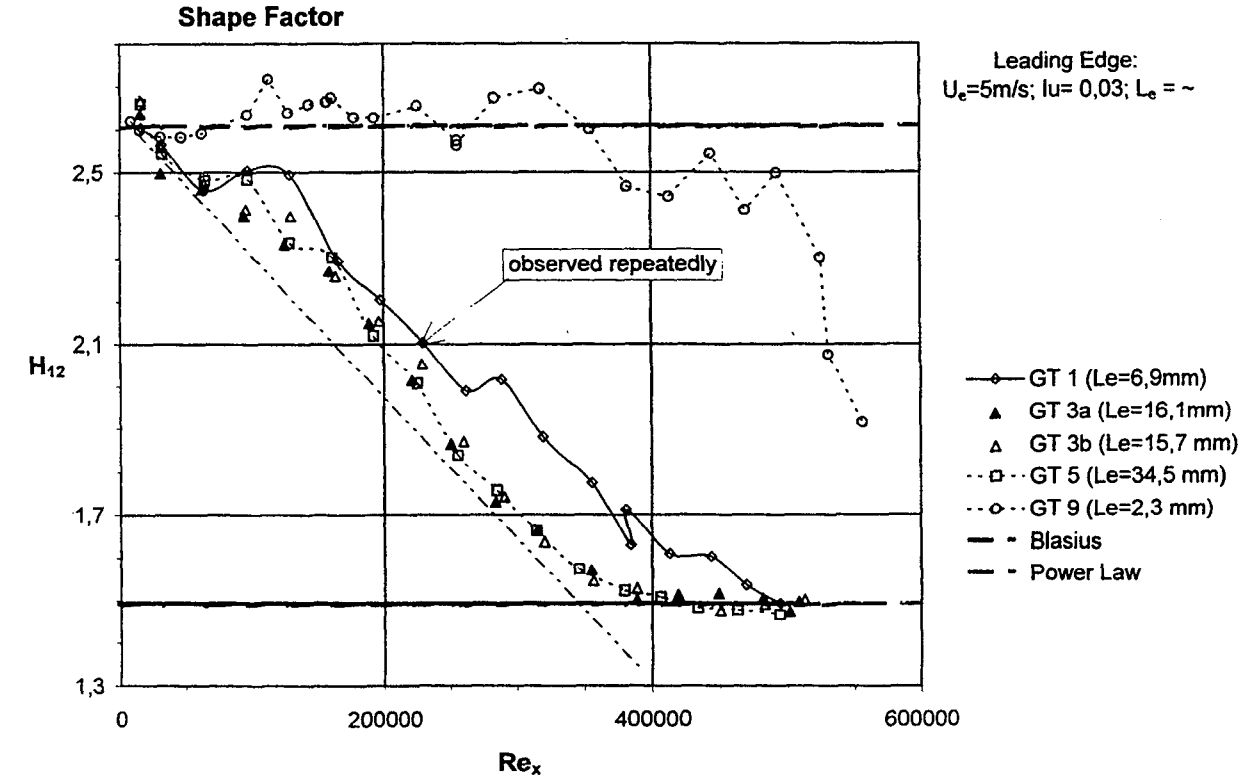
Shape Factor
2,5
2,1
1,7
1,3
H_{12}
observed repeatedly
0
200000
400000
600000
Re_x
Leading Edge:
U_e=5m/s; Iu= 0,03; L_e = ~
GT 1 (Le=6,9mm)
GT 3a (Le=16,1mm)
GT 3b (Le=15,7 mm)
GT 5 (Le=34,5 mm)
GT 9 (Le=2,3 mm)
Blasius
Power Law

The Effect of the Turbulence Grid Mesh on the Onset of Transition
(supplied Fig.12 in Mayle [1991])

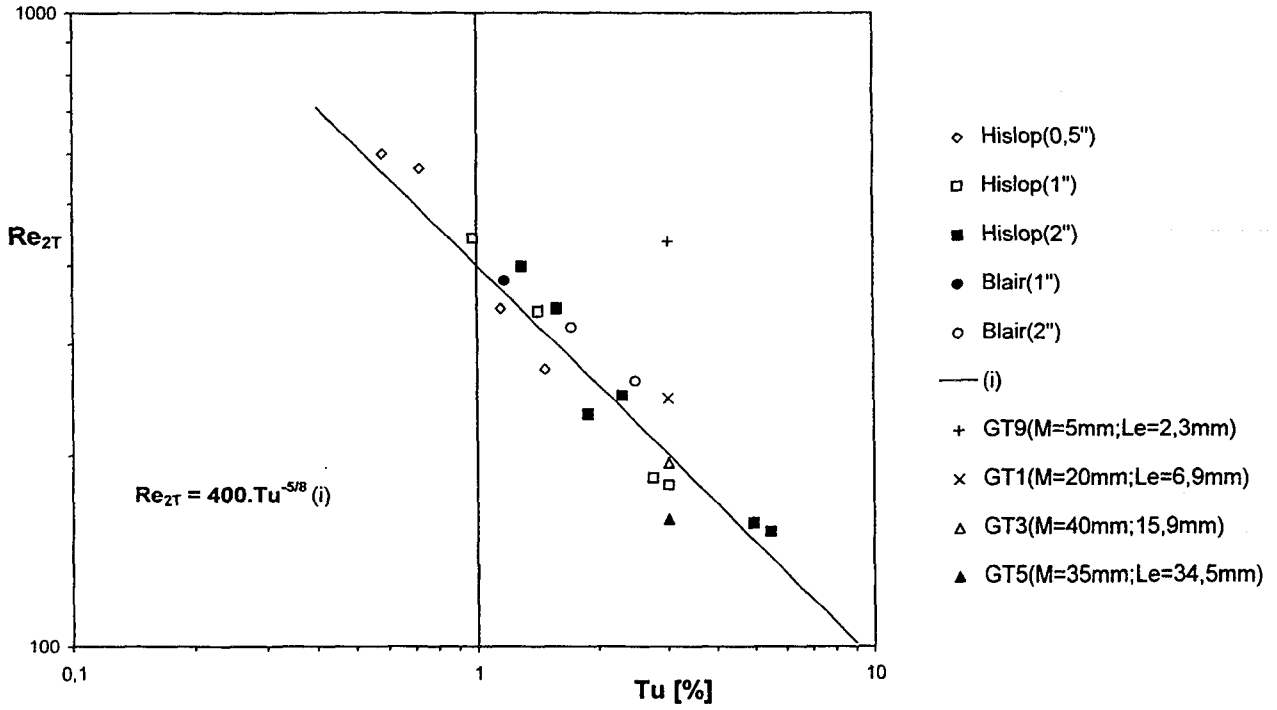

Intermittence Factor

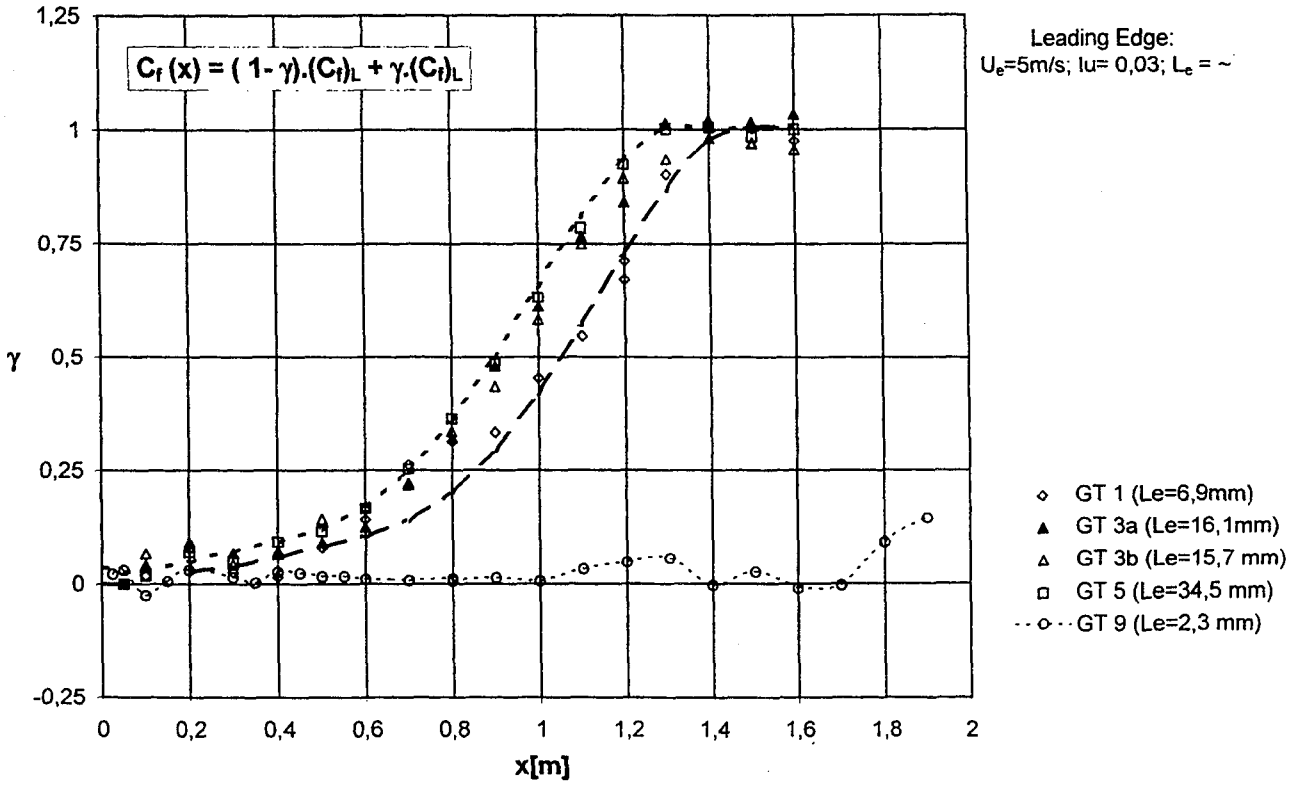

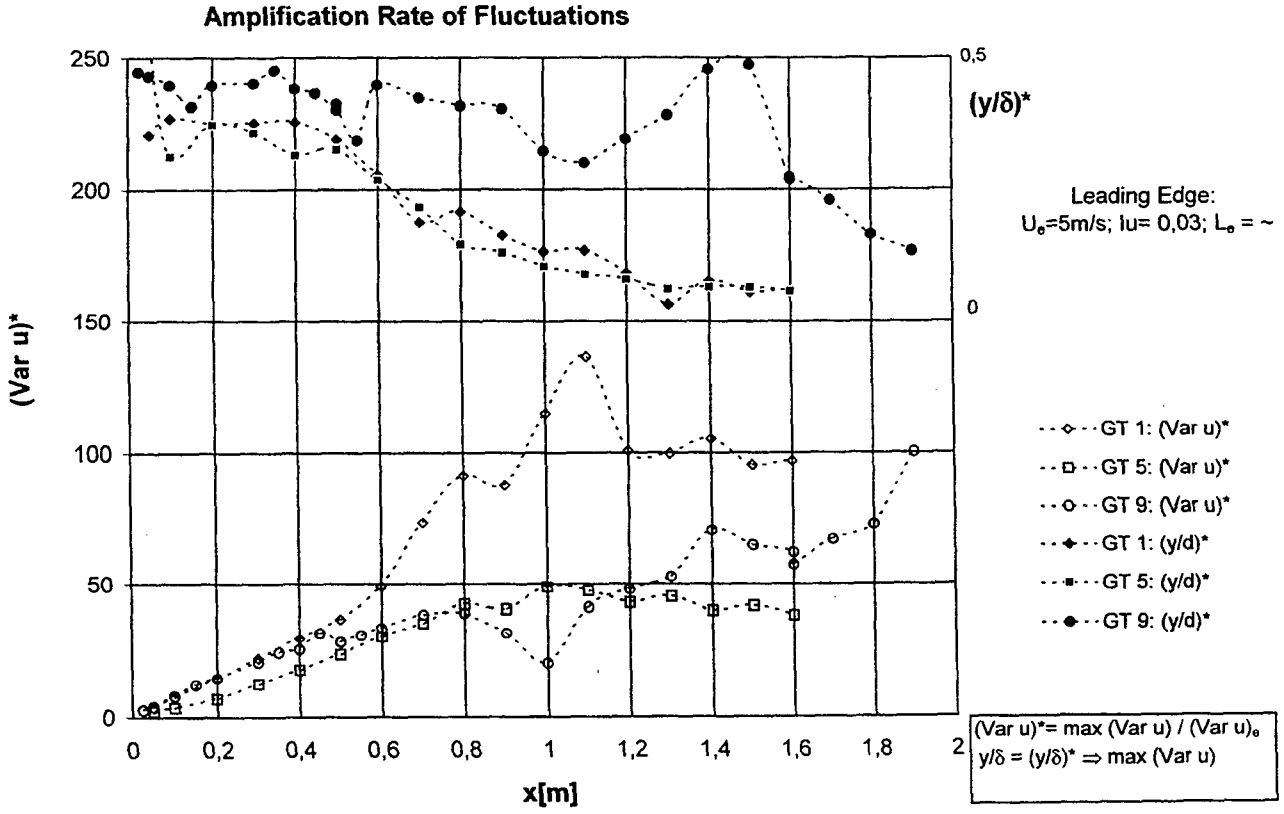
Amplification Rate of Fluctuations
(Var u)*
(y/δ)*
x[m]
Leading Edge:
Ue=5m/s; Iu= 0,03; Le = ~
GT 1: (Var u)*
GT 5: (Var u)*
GT 9: (Var u)*
GT 1: (y/d)*
GT 5: (y/d)*
GT 9: (y/d)*
(Var u)*= max (Var u) / (Var u)e
y/δ = (y/δ)* ⇒ max (Var u)

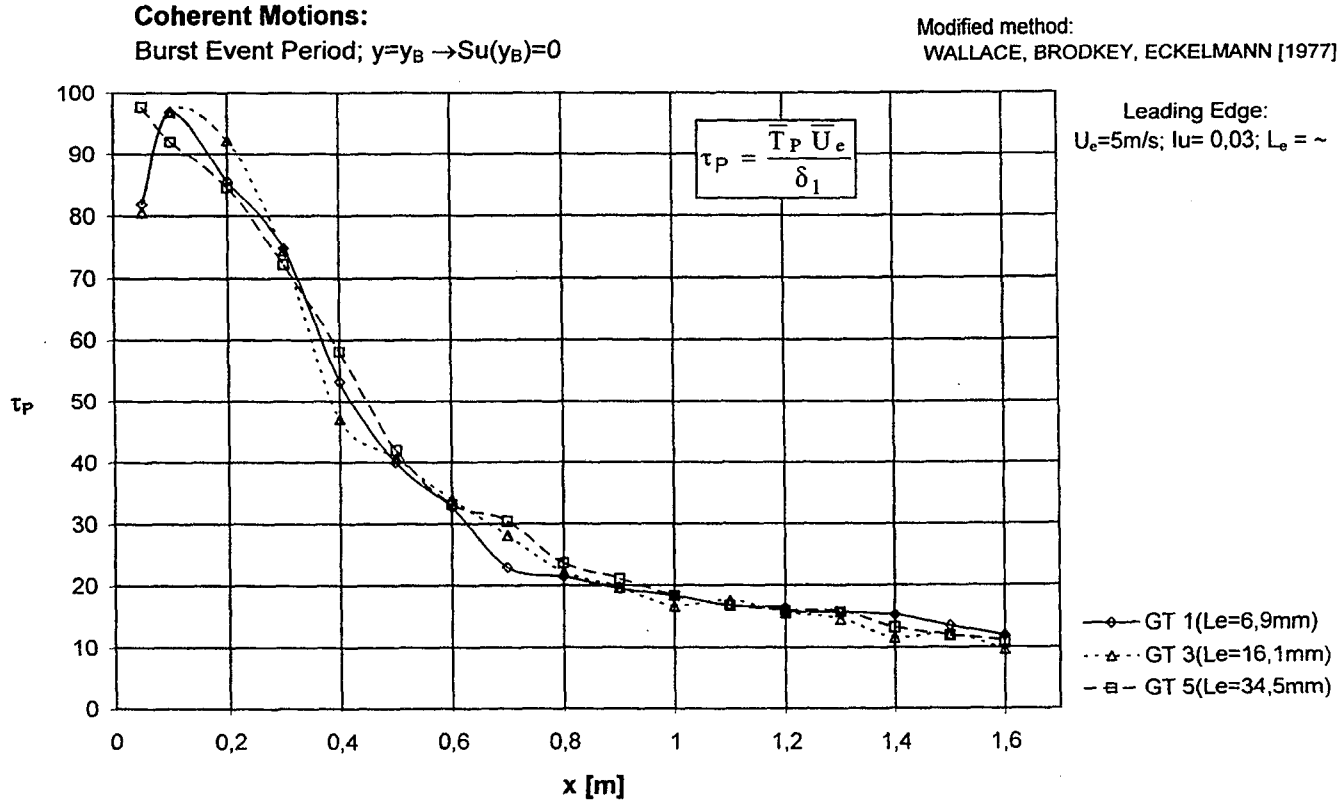
Coherent Motions:
Burst Event Period; y=yB →Su(yB)=0
Modified method:
WALLACE, BRODKEY, ECKELMANN [1977]
τP
x [m]
Leading Edge:
Ue=5m/s; Iu= 0,03; Le = ~
GT 1(Le=6,9mm)
GT 3(Le=16,1mm)
GT 5(Le=34,5mm)

CONCLUSIONS

Courses of the fundamental parameters of boundary layer (C_f, H_{12}, . . .) as well as the distributions and profiles of statistical characteristics (Iu, Su, Fu, Amplification Rate, Bursting etc.) imply:

- length scale influences the laminar/turbulent transition;
- at the given intensity Iu(x=0) the onset of the last stage of the process is coming later and probably last longer in a boundary layer perturbed by a fine grain outer stream turbulence (small length scale);
- the universal features of the flow structure (bursting) seem to be independent on the length scale.

The data for validation of the transition prediction methods for boundary conditions prescribed by the COST/ERCOFTAC Special Interest Group on Transition for the Test Case T3A+ (at the leading edge plane: Iu=3%, L_e= ~) have been received.

Further effort should be devoted to the investigation of broader turbulence length scale band, to the receptivity of boundary layer to the action of a given kind of disturbances in different positions and to a deeper analyse of the flow structure in the region of the last stage of transition.

INFLUENCE OF HIGH-AMPLITUDE NOISE ON BOUNDARY-LAYER TRANSITION TO TURBULENCE

William S. Saric
Arizona State University
Tempe, Arizona

ABSTRACT

This work continues detailed experiments of boundary layers undergoing transition to turbulence with the major effort directed toward the most important issue facing the understanding of fundamental causes of transition, i.e., the receptivity to freestream disturbances. This problem is described in detail by Saric et al. (1994). The present effort concentrates on effects of large-amplitude freestream noise that are characteristic of gas turbine engines. As such, it is a significant departure from the usual linear receptivity mechanisms. Oblique and broad-band sound waves are used along with 3-D roughness elements to determine how the unstable waves are initiated. Techniques for control and cancellation of the unstable waves will be developed as part of this work. The experiment utilizes multiple hot-wire measurements in combination with recently developed flow-visualization and computational techniques. The use of in-house developed phase-correlated and conditionally-sampled measurements permits the separation of the acoustic signals from the unstable waves. The goal is to establish the framework for the active control of such fluid motions and to provide the initial conditions for computational modeling.

Recent work

A typical hot-wire signal at the driving frequency is composed of the T-S wave, the Stokes wave within the acoustic boundary layer, and probe vibrations. Therefore, hot-wire measurements taken directly within a narrow band-pass produce a signal that does not resemble a T-S amplitude profile. The complex-plane signal-separation technique used in previous experiments used a process that requires an extremely time consuming data-sampling process since the method requires that hundreds of streamwise scans be taken so that one T-S wavelength is covered. Although the technique is successful, typically over 500 measurements are required to obtain a single T-S wave amplitude. This technique was rejected along with differential microphones, multiple microphones, and adaptive filtering. Wlezien (1994) and Saric (1996) present critical reviews of these techniques. A new technique is now implemented to measure the amplitude of the T-S wave. From linear theory, the maximum of the T-S wave propagates at approximately one third the speed of the freestream speed (about 1% of the speed of downstream-traveling sound wave). Using this fact, the traveling T-S wave can be isolated from the acoustic disturbance and associated Stokes wave by sending bursts of sound into the test section. The initial sound burst is first measured and fractions of a second later after the sound wave has passed, the slower-traveling T-S wave initiated by the sound burst is measured. An ensemble average of the bursts are taken to account for any low-frequency oscillations in the test section and to minimize error. This technique is useful for noise and large amplitude

signals. All of the work is conducted in the ASU Unsteady Wind Tunnel (Saric 1992) and the basic experiment is described in Saric et al. (1995). We are now in the process of reducing data and extending the receptivity data base. The data that will be presented at the meeting include: Normalized T-S amplitude as a function of forcing amplitude is measured to document the departure from linearity. Since large-amplitude sound in the freestream may itself contain harmonics of the fundamental, the appearance of harmonics within the boundary layer is not prima facie evidence of nonlinear receptivity. Receptivity coefficients for nonlinear T-S waves with planar sound are found. Using the appropriate separation techniques, the T-S wave can be traced back to Branch I in order to obtain a receptivity coefficient. Nonlinear interactions of waves with broad-band input is attempted. The broad-band input may produce different wave interactions within the receptivity zone as well as downstream locations.

Acknowledgment

This work was sponsored (in part) by the Air Force Office of Scientific Research, USAF, under grant number F49620-96-1-0369.

References

Saric, W.S. 1992. The ASU Transition Research Facility. (Invited) AIAA Paper No. 92-3910.

Saric, W.S., Reed, H.L., and Kerschen E.J. 1994. Leading-Edge Receptivity to Sound.

(Invited) AIAA Paper No. 94-2222.

Saric, W.S., Wei, W., Rasmussen, B.K. and Krutckoff, T.K. 1995. Experiments on Leading-Edge Receptivity to Sound. (Invited) AIAA Paper No. 95-2253.

Saric, W.S. 1996. Low-Speed Boundary Layer Transition Experiments.

Transition: Experiments, Theory & Computations. Eds. T.C. Corke, G. Erlebacher, M.Y. Hussaini, pp. 61-178, Oxford.

Wlezien, R.W. 1994. Measurement of acoustic receptivity. AIAA Paper No. 94-2221.

PURPOSE

PROVIDE INITIAL CONDITIONS FOR TRANSITION COMPUTATIONS

- RECEPTIVITY COEFFICIENTS FOR ACOUSTIC DISTURBANCES
  - LEADING EDGES
  - ROUGHNESS

EXTEND TO LARGE AMPLITUDE DISTURBANCES

- SINGLE MODE versus BROAD BAND
- THRESHOLD FOR NONLINEAR RECEPTIVITY
  - DONE FOR ROUGHNESS HEIGHT (1991, 1994)
  - DO FOR DISTURBANCE AMPLITUDE
- DATA BASE FOR THEORY/CODE VALIDATION

DNS OF L.E. RECEPTIVITY (HELEN REED)

- WEAK NONLINEAR BEHAVIOR OBSERVED AT 1% FREESTREAM FORCING
- RECEPTIVITY COEFFICIENT

  F = 85 X 10-6 AT TUNNEL CONDITIONS AND MODEL GEOMETRY

  EXP: 0.038
  DNS: 0.05
  Theory: 0.13

- OBLIQUE WAVES CALCULATED AND COMPARED WITH THEORY

  DNS K = 1/4 THEORY

Leading-Edge Receptivity Coefficients

$$K_S = \frac{\left(u'_{TS}\right)_I}{\left(u'_{AC}\right)_{LE}}$$

$$\left(u'_{TS}\right)_R = \left(u'_{TS}\right)_I e^N$$

$$N = 2\int_{R_I}^{R}\left(-k_i\right)dR$$

Receptivity Coefficients for Different Speed/Frequency Combinations

Previous Results (Saric et. al 1995)

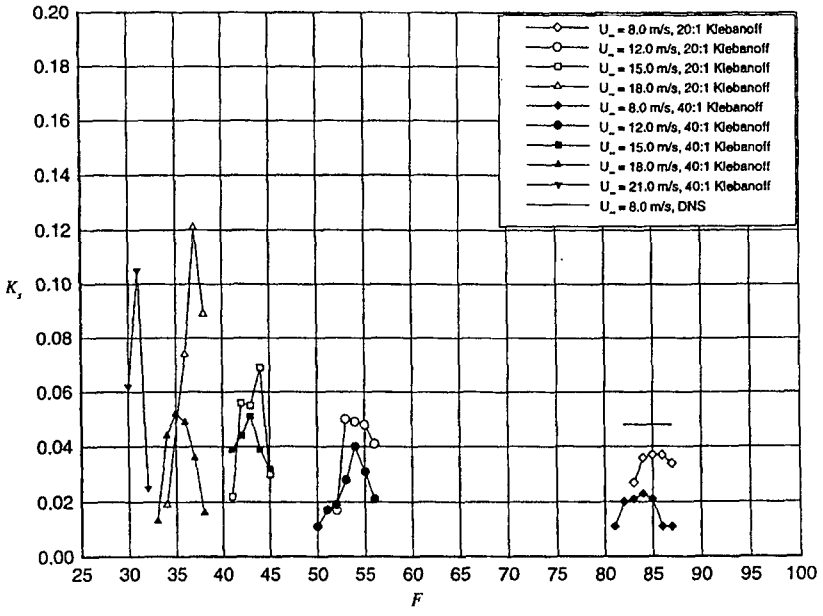

$(u'_2 - u'_1)_{rms}$

$U_\infty = 12$ m/s, $x = 1.7$ m, $Re_x = 1.14 \times 10^6$, $T = 304.4$ K

$V_{sp_{rms}} = 0.5$ volts, Band Pass 40–120 Hz

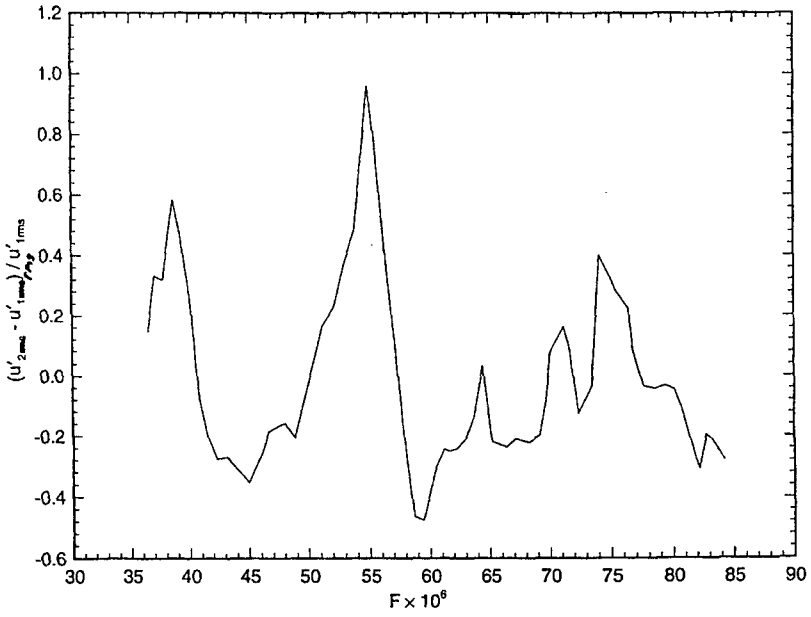

$(u'_2 - u'_1)_{rms}$

$U_\infty = 18$ m/s, $x = 1.7$ m, $Re_x = 1.52 \times 10^6$, $T = 303.9$ K

$V_{sp_{rms}} = 0.5$ volts, Band Pass 30–130 Hz

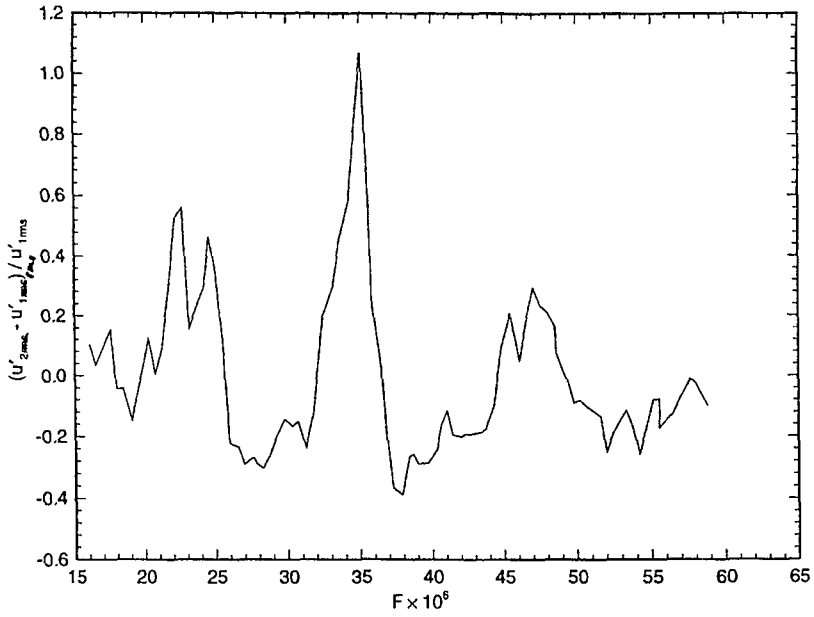

Signal/Noise Separation

1. Complex-Plane Technique

   - Tedious, slow
   - Requires narrow band-pass filter

2. Kendall Gauge

   - Differential Pressure

3. Multi-Signal Analysis

4. Differential Phase Speed

   C_{ac} = 350 m/s

   C_{TS} = 4 m/s

   Δx = 1.8 m

   Time Delay ≈ 250 ms

   1. "Chirp" Acoustic Signal (Kendall)

      - Ramp Frequency
      - Narrow Band-Pass
      - Works for Single Frequency

   2. "Burst" Acoustic Signal

      - $\Delta t \approx 50$ ms
      - Conditional Sampling

Time Trace Using the Sound-Burst Technique

$R = 1140$, $F = 56$, $f = 80$ Hz, $\hat{x} = 1.8$ m

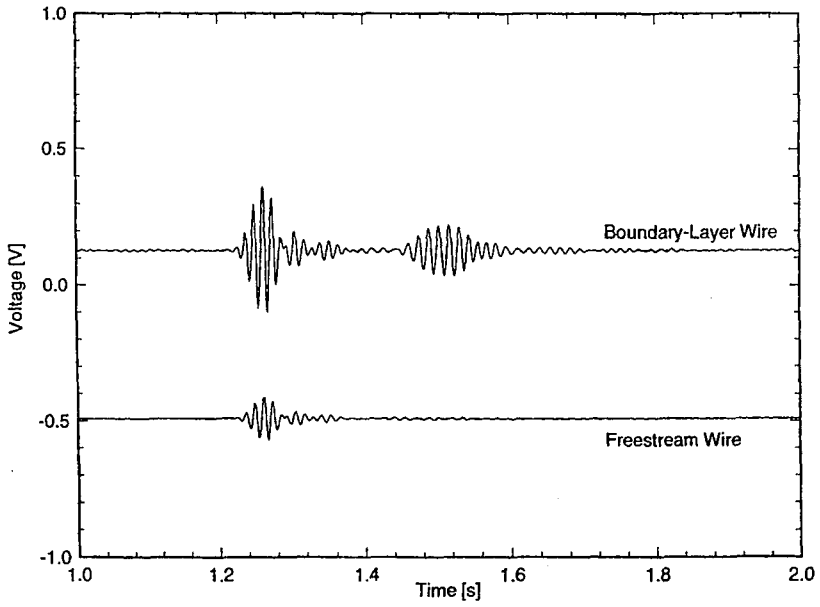

Flat-Plate Acoustic Amplitude Sweep

$U_\infty = 15$ m/s, $x = 1.50$ m

White noise forcing, 50–200 Hz bandpass
10–200 Hz hot-wire bandpass

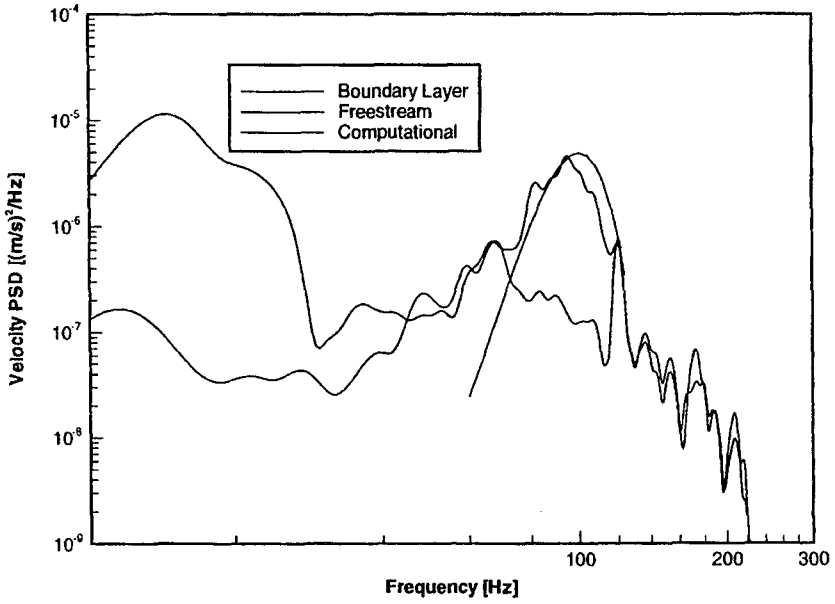

CONCLUSIONS 1

LEADING-EDGE RECEPTIVITY

- SHARP FREQUENCY FOCUSING OF SINGLE MODE IS DUE TO COMPLICATED DUCT ACOUSTICS. ACTUAL RECEPTIVITY IS LOWER. CORRECT MEASUREMENTS MADE WITH SOUND BURSTS AND CONDITIONAL SAMPLING.

- AGREEMENT BETWEEN THEORY, DNS, AND EXPERIMENTS IS GOOD WHEN RESULTS ARE EXTENDED TO BRANCH I. MISLEADING TO SAY L.E. RECEPTIVITY INCREASES WITH NOSE RADIUS BECAUSE OF PRESSURE RECOVERY REGION ON ELLIPSE. MUST BE CAREFUL IN DEFINITION OF RECEPTIVITY COEFFICIENT.

2-D ROUGHNESS

Place 45 micron thick strips at Branch I. Width is 1/2 T-S wavelength

Flat-Plate Acoustic Amplitude Sweep

$U_\infty = 12.75$ m/s, $x = 1.60$ m

White noise forcing, 20–150 Hz bandpass
10–200 Hz hot-wire bandpass
45 μm 2-D roughness at $x = 0.62$ m

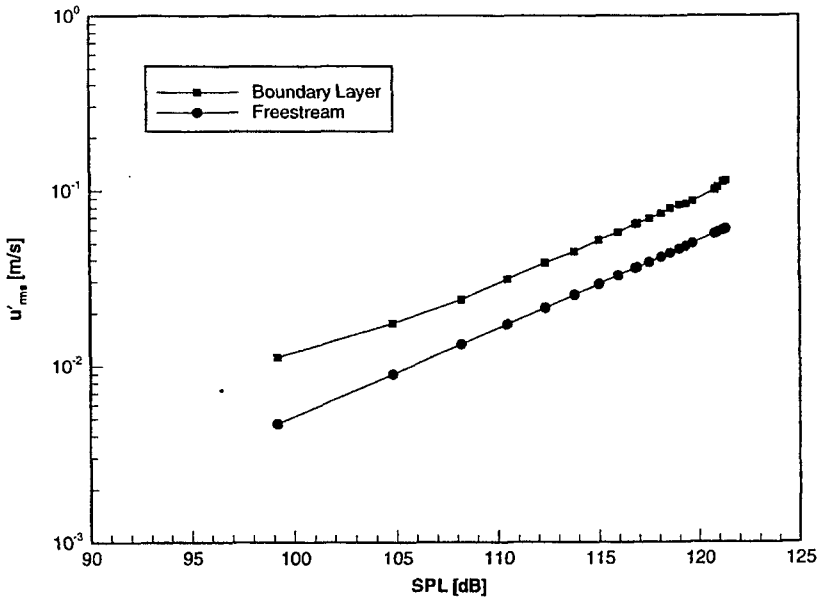

Flat-Plate Acoustic Amplitude Sweep

$U_\infty = 12.75$ m/s, $x = 1.60$ m

White noise forcing, 20–150 Hz bandpass
10–200 Hz hot-wire bandpass
45 μm 2-D roughness at $x = 0.62$ m

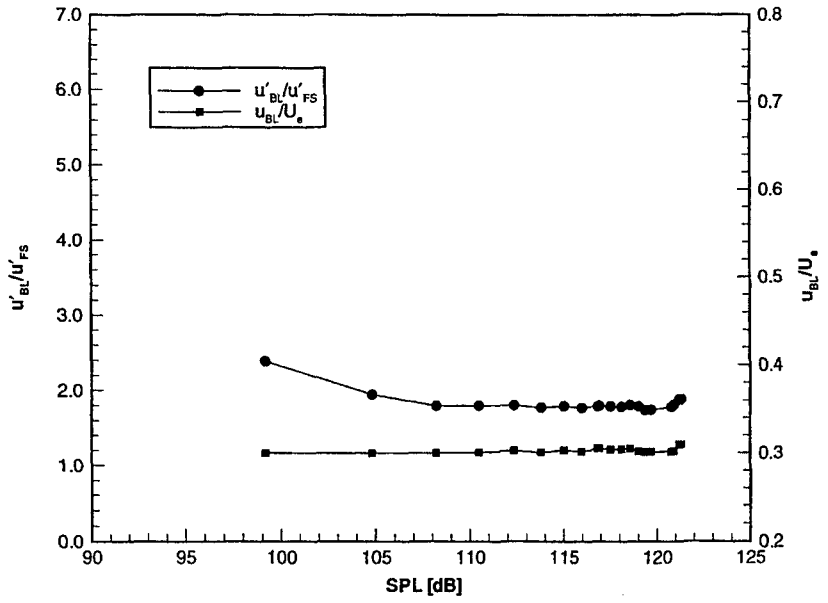

Flat-Plate Acoustic Amplitude Sweep

$U_\infty = 12.75$ m/s, $x = 1.80$ m

White noise forcing, 20–150 Hz bandpass
10–200 Hz hot-wire bandpass
45 μm 2-D roughness at $x = 0.62$ m

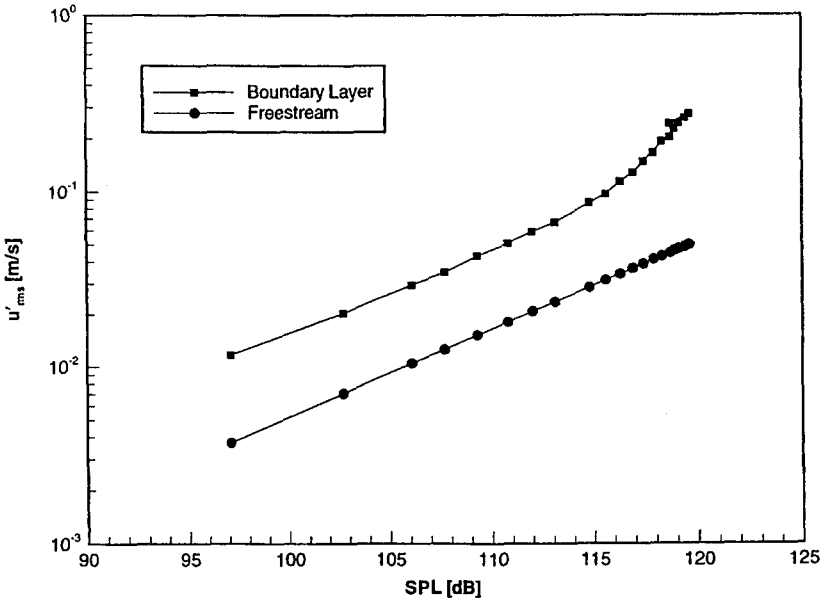

Flat-Plate Acoustic Amplitude Sweep

$U_\infty = 12.75$ m/s, $x = 1.80$ m

White noise forcing, 20–150 Hz bandpass
10–200 Hz hot-wire bandpass
45 μm 2-D roughness at $x = 0.62$ m

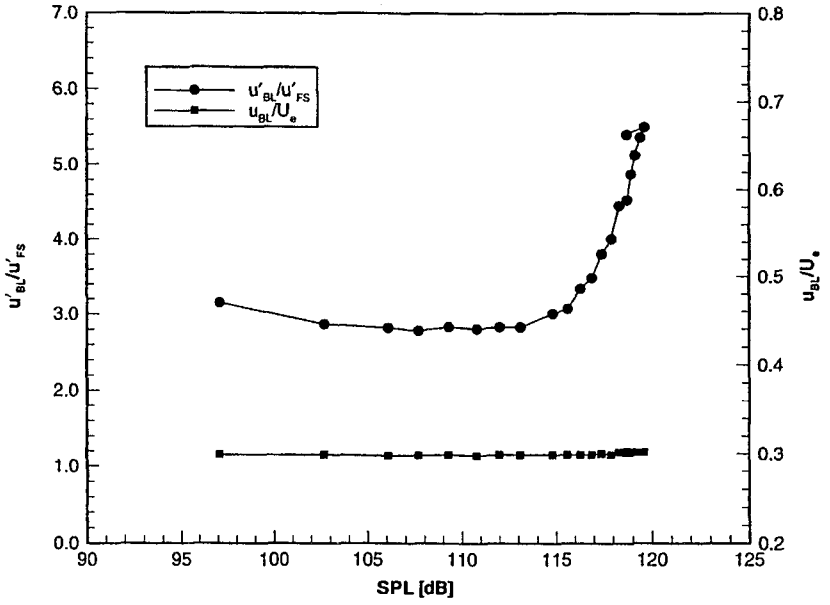

Flat-Plate Acoustic Amplitude Sweep

$U_\infty = 12.75$ m/s, $x = 1.80$ m

White noise forcing, 20–150 Hz bandpass
10–200 Hz hot-wire bandpass
90 μm 2-D roughness at $x = 0.62$ m

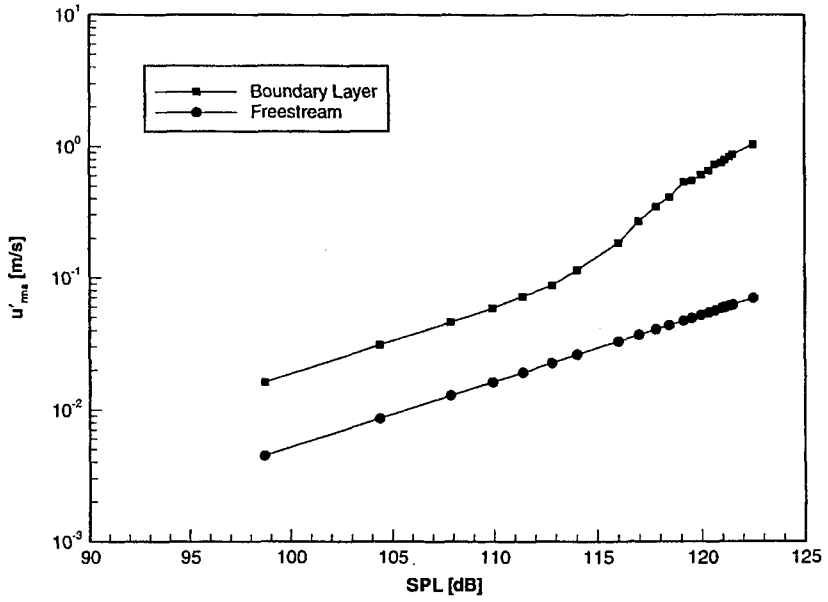

Flat-Plate Acoustic Amplitude Sweep

$U_\infty = 12.75$ m/s, $x = 1.80$ m

White noise forcing, 20–150 Hz bandpass
10–200 Hz hot-wire bandpass
90 μm 2-D roughness at $x = 0.62$ m

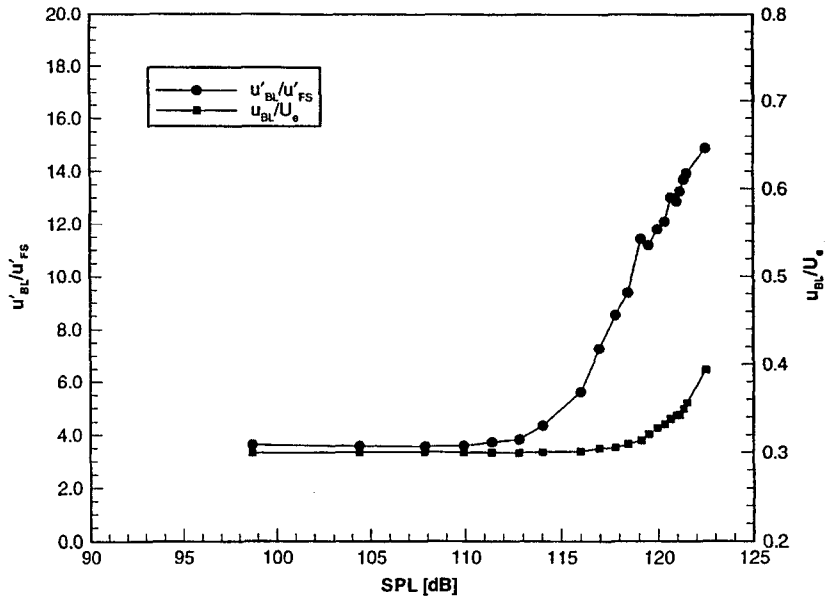

Flat-Plate Acoustic Amplitude Sweep

$U_\infty = 12.75$ m/s, $x = 1.60$ m

Sine wave forcing, $f = 75.8$ Hz

10–300 Hz hot-wire bandpass

45 μm 2-D roughness at $x = 0.62$ m

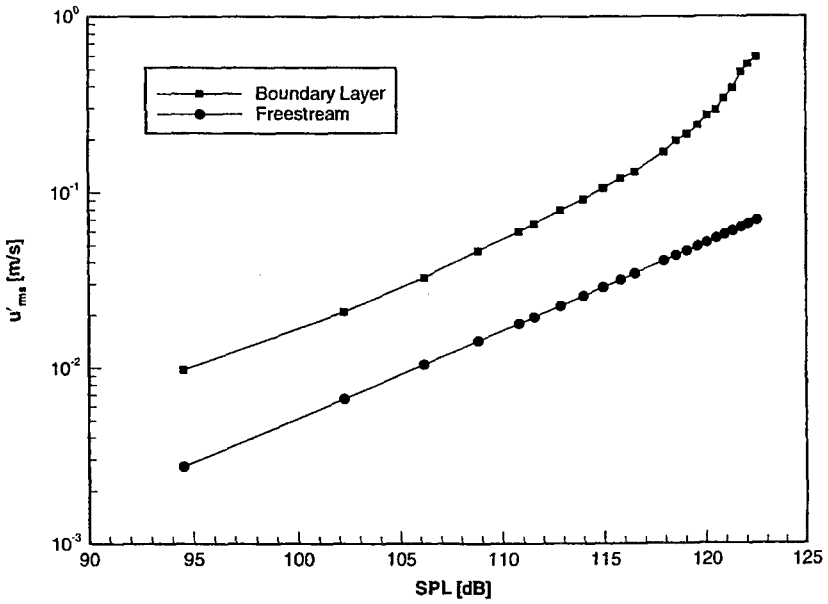

Flat-Plate Acoustic Amplitude Sweep

$U_\infty = 12.75$ m/s, $x = 1.60$ m

Sine wave forcing, $f = 75.8$ Hz

10–300 Hz hot-wire bandpass

45 μm 2-D roughness at $x = 0.62$ m

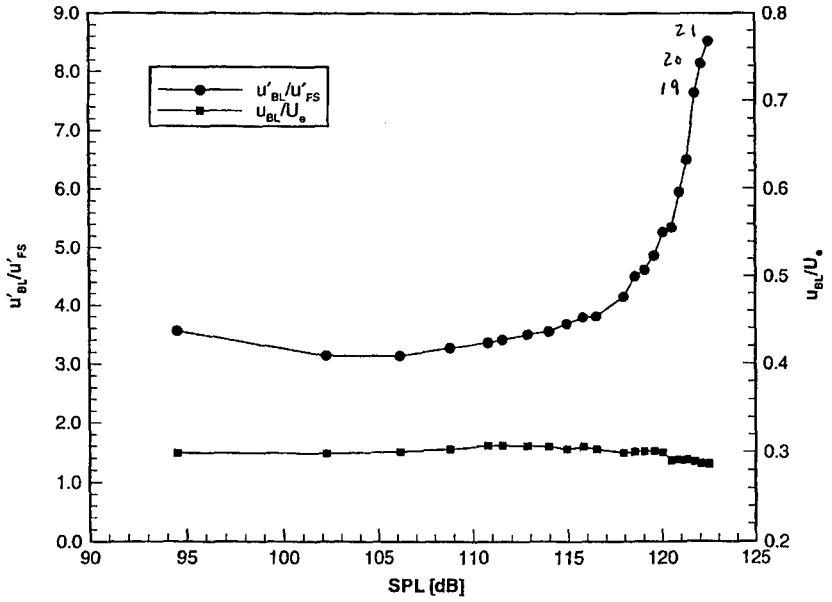

Flat-Plate Acoustic Amplitude Sweep

$U_\infty = 12.75$ m/s, $x = 1.60$ m

Sine wave forcing, $f = 75.8$ Hz
10–300 Hz hot-wire bandpass
45 μm 2-D roughness at $x = 0.62$ m

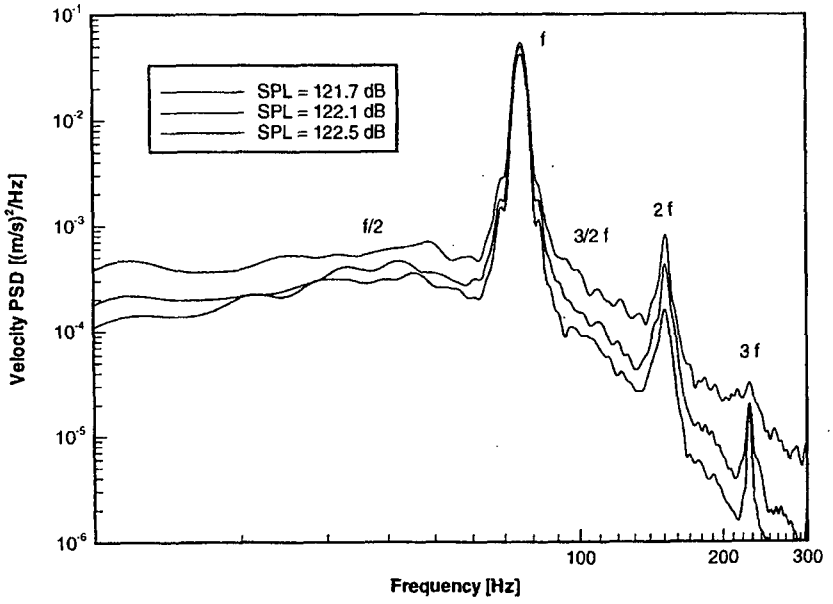

Flat-Plate Acoustic Amplitude Sweep

$U_\infty = 12.75$ m/s, $x = 1.80$ m

Sine wave forcing, $f = 75.8$ Hz
10–300 Hz hot-wire bandpass
45 μm 2-D roughness at $x = 0.62$ m

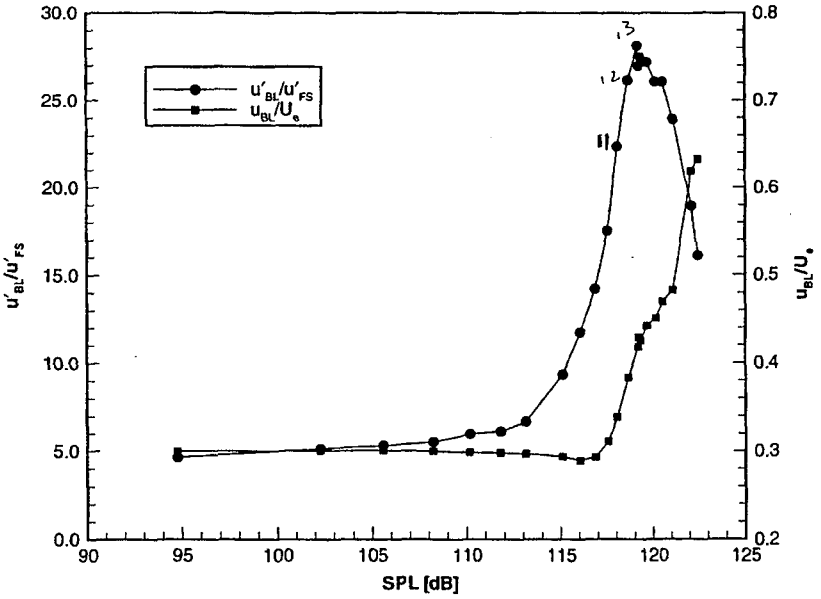

Flat-Plate Acoustic Amplitude Sweep

$U_\infty = 12.75$ m/s, $x = 1.80$ m

Sine wave forcing, $f = 75.8$ Hz

10–300 Hz hot-wire bandpass

45 μm 2-D roughness at $x = 0.62$ m

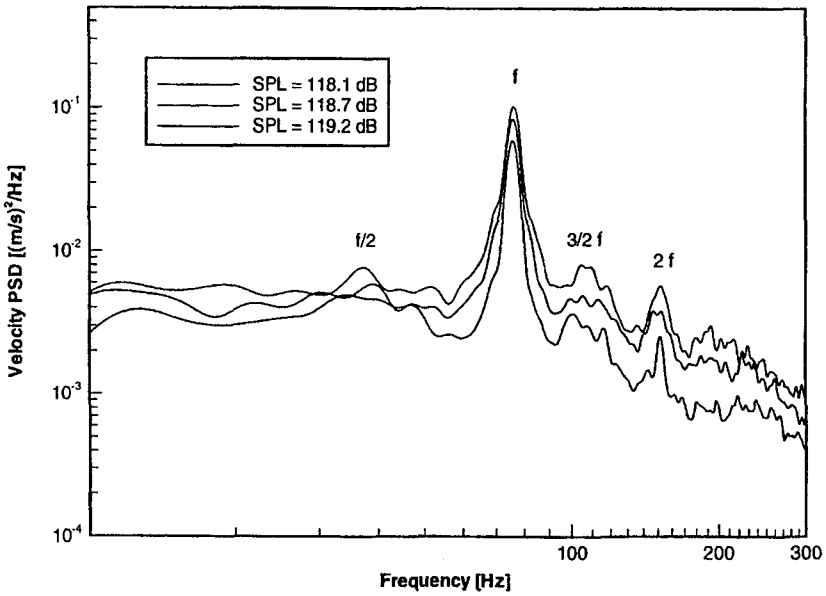

CONCLUSIONS 2

NO ESSENTIAL DIFFERENCE BETWEEN BROAD BAND AND SINGLE MODE

- **FOR GIVEN SOUND PRESSURE LEVEL SINGLE-MODE AMPLITUDE IS MUCH HIGHER THAN BROAD BAND (T-S BAND). NEED A 30 DB INCREASE IN BROAD BAND TO APPROACH EFFECTS OF SINGLE MODE.**

MULTIPLE 2-D ROUGHNESS

Place 45 micron and 90 micron at Branch I and also at 1 T-S wavelength downstream.

Combinations of (45,0); (90,0); (90,45); (90,90)

Measure at u' max $u/U_0 = 0.2$

Flat-Plate Acoustic Amplitude Sweep

$U_\infty = 12.75$ m/s, $x = 1.60$ m

Sine wave forcing, $f = 75.8$ Hz

10–300 Hz hot-wire bandpass

45 μm 2-D roughness at $x = 0.62$ m

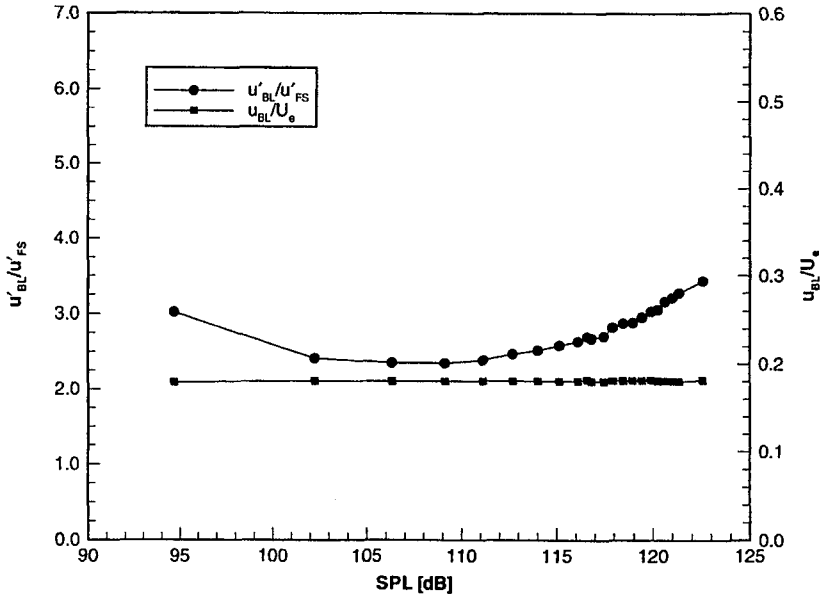

Flat-Plate Acoustic Amplitude Sweep

$U_\infty = 12.75$ m/s, $x = 1.60$ m

Sine wave forcing, $f = 75.8$ Hz

10–300 Hz hot-wire bandpass

90 μm 2-D roughness at $x = 0.62$ m

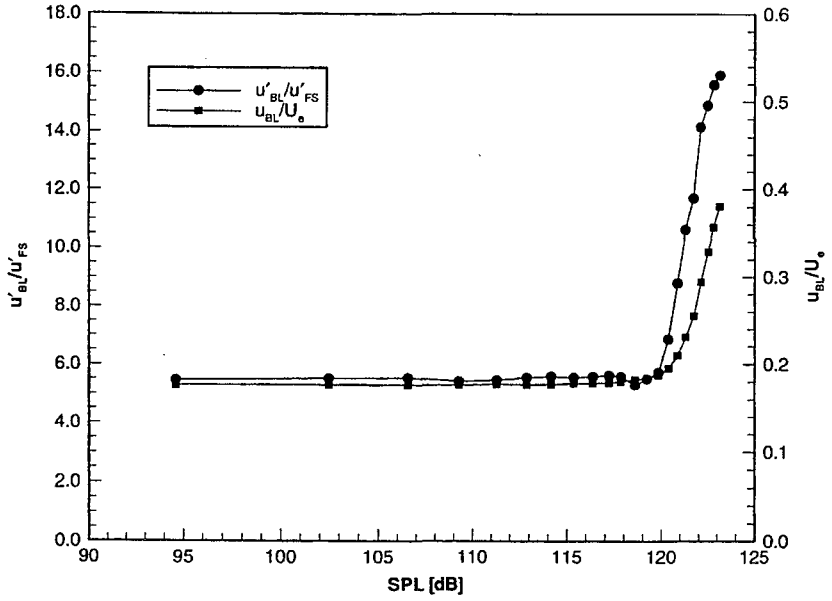

Flat-Plate Acoustic Amplitude Sweep

$U_\infty = 12.75$ m/s, $x = 1.60$ m

Sine wave forcing, $f = 75.8$ Hz

10–300 Hz hot-wire bandpass

(90,45) μm 2-D roughness at $x = (0.62, 0.65)$ m

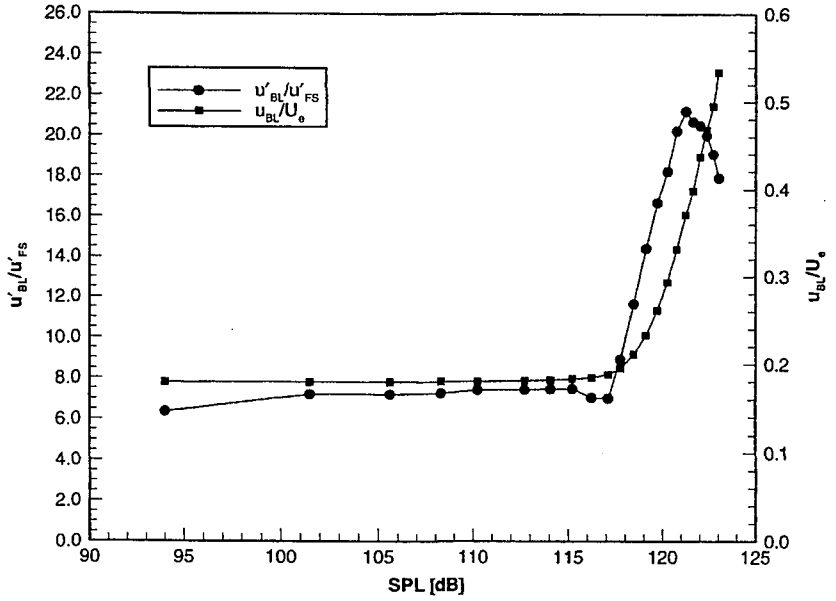

Flat-Plate Acoustic Amplitude Sweep

$U_\infty = 12.75$ m/s, $x = 1.60$ m

Sine wave forcing, $f = 75.8$ Hz
10–300 Hz hot-wire bandpass
(90,90) μm 2-D roughness at $x = (0.62, 0.65)$ m

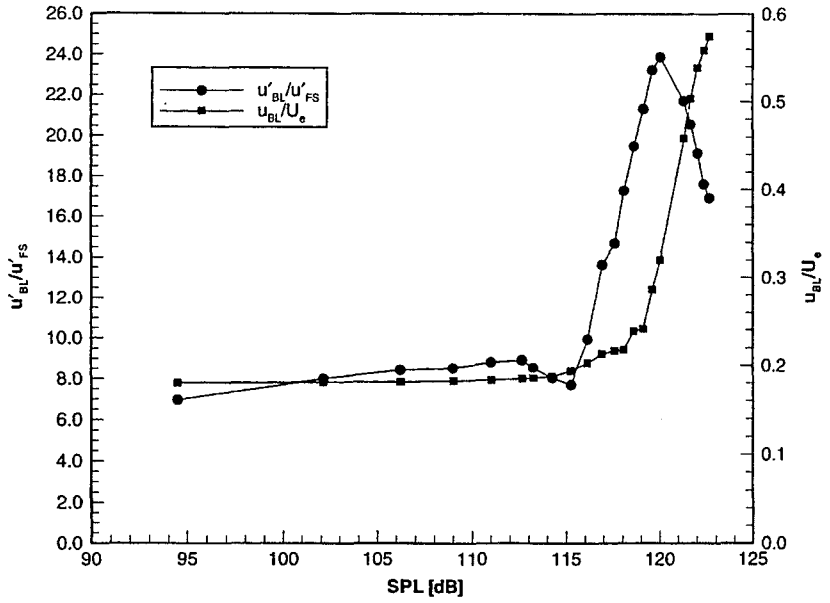

Flat-Plate Acoustic Amplitude Sweep

$U_\infty = 12.75$ m/s, $x = 1.60$ m

White noise forcing, 20–150 Hz bandpass
10–300 Hz hot-wire bandpass
45 μm 2-D roughness at $x = 0.62$ m

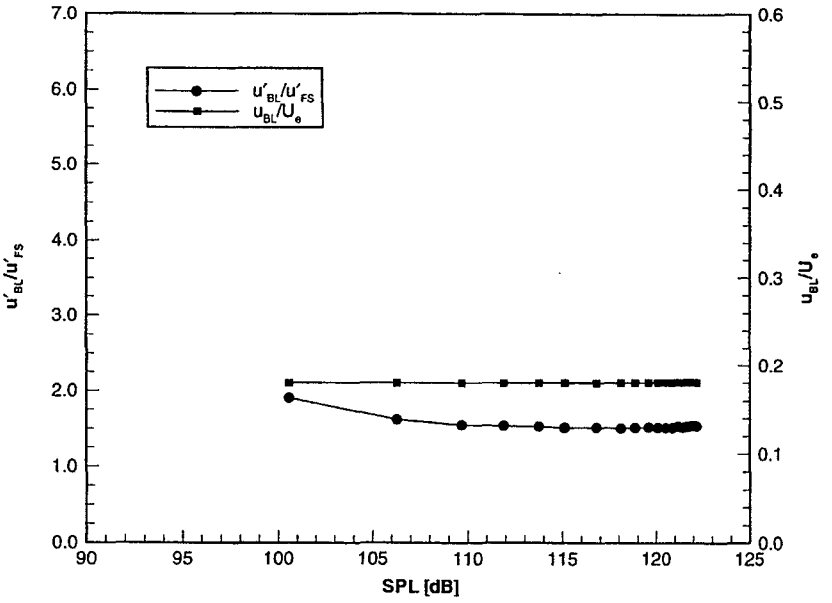

Flat-Plate Acoustic Amplitude Sweep

$U_\infty = 12.75$ m/s, $x = 1.60$ m

White noise forcing, 20–150 Hz bandpass
10–300 Hz hot-wire bandpass
90 μm 2-D roughness at $x = 0.62$ m

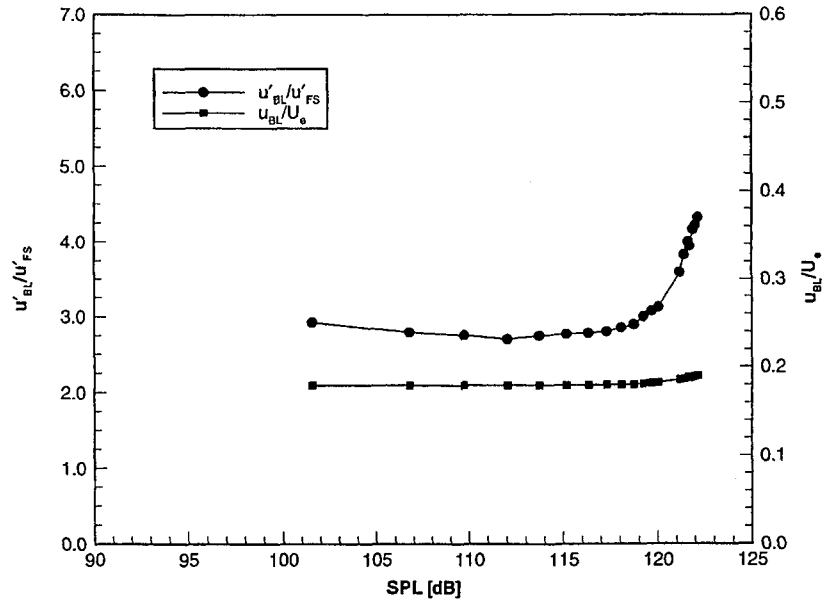

Flat-Plate Acoustic Amplitude Sweep

$U_\infty = 12.75$ m/s, $x = 1.60$ m

White noise forcing, 20–150 Hz bandpass
10–300 Hz hot-wire bandpass
(90, 45) μm 2-D roughness at $x = (0.62, 0.65)$ m

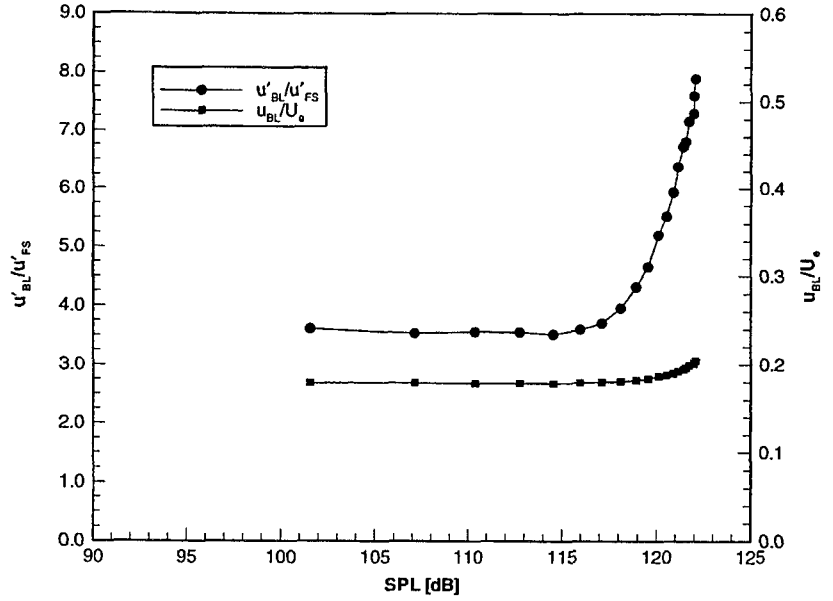

Flat-Plate Acoustic Amplitude Sweep

$U_\infty = 12.75$ m/s, $x = 1.60$ m

White noise forcing, 20–150 Hz bandpass
10–300 Hz hot-wire bandpass
(90, 90) μm 2-D roughness at $x = (0.62, 0.65)$ m

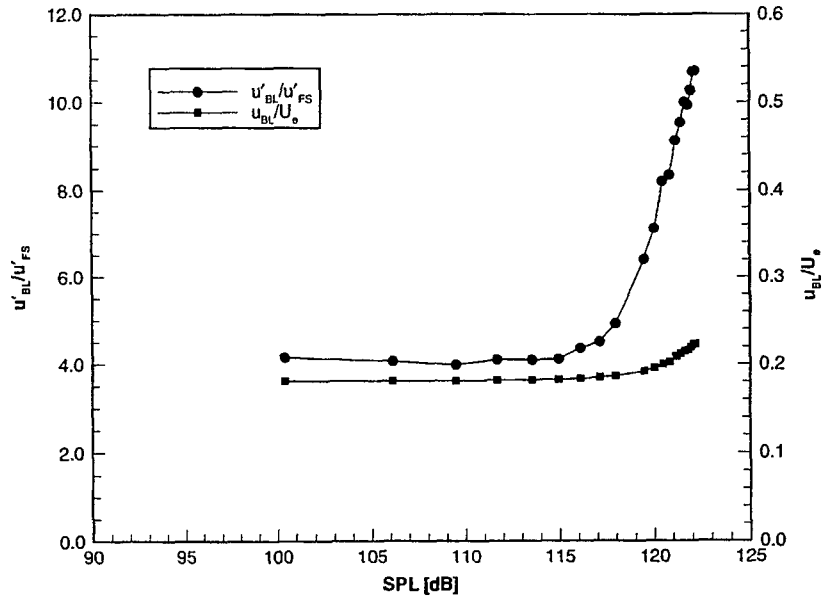

CONCLUSIONS 3

2-D ROUGHNESS

- **LEADING EDGE RECEPTIVITY IS MUCH WEAKER THAN ROUGHNESS AT 45 MICRON (Rek < 1).**
- **NONLINEAR RECEPTIVITY IS OBSERVED BEFORE TRANSITION.**
- **BREAKDOWN APPEARS TO BE VIA SUBHARMONIC TYPE.**
- **NONLINEAR DATA SET FOR Rek = 0.75 and 3.0**

CONCLUSIONS - 4

NO BYPASS OBSERVED UP TO 125 DB

REMAINING WORK

- DOCUMENT QUANTITATIVE L.E. RECEPTIVITY COEFFICIENTS USING BURSTS
- EXTEND DATA BASE FOR 2-D ROUGHNESS
- PROVIDE DATA BASE FOR 3-D ROUGHNESS
  - MUST MEASURE CLOSE TO ROUGHNESS
  - PREVIOUSLY LIMITED BY LOW SOUND AMPLITUDE
- EXTEND TO FORCING TO 135 DB FOR BYPASS
- TRANSITION WITH UNSTEADY BASIC STATE
  - U' IN ACCELERATED FREESTREAM FLOW
  - LOW-FREQUENCY SINUSOIDAL MODULATIONS
    - LOW TO LARGE AMPLITUDE
  - GUSTS AND LULLS

CONTROL OF CROSSFLOW INSTABILITY FIELD BY SELECTIVE SUCTION SYSTEM

Yasuhiro Egami and Yasuaki Kohama
Tohoku University
Sendai, Japan

ABSTRACT

A full turbulent transition process is created on a yawed flat plate using a displacement body system in a wind tunnel. It was found that high frequency secondary instability drives the crossflow dominant boundary layer into a full turbulent state as shown in Figure 1(a). Taking into account such transition structures, effective control of the flow field to delay the transition is possible. That is, by placing grooving line suction holes along each streamwise crossflow vortex, and as is causing selective suction in the low-momentum flow, the appearance of the secondary instability is successfully delayed turbulent transition as seen in Figure 1(b),(c). Figure 1 (b) shows the condition without suction.This suction system also has an advantage over a uniform suction system in that the amount of suction air volume required to control the flow field is much less than in uniform suction. Thus, a great deal of energy needed for flow control is saved. We also attempted to determine the most appropriate condition for selective suctioning.

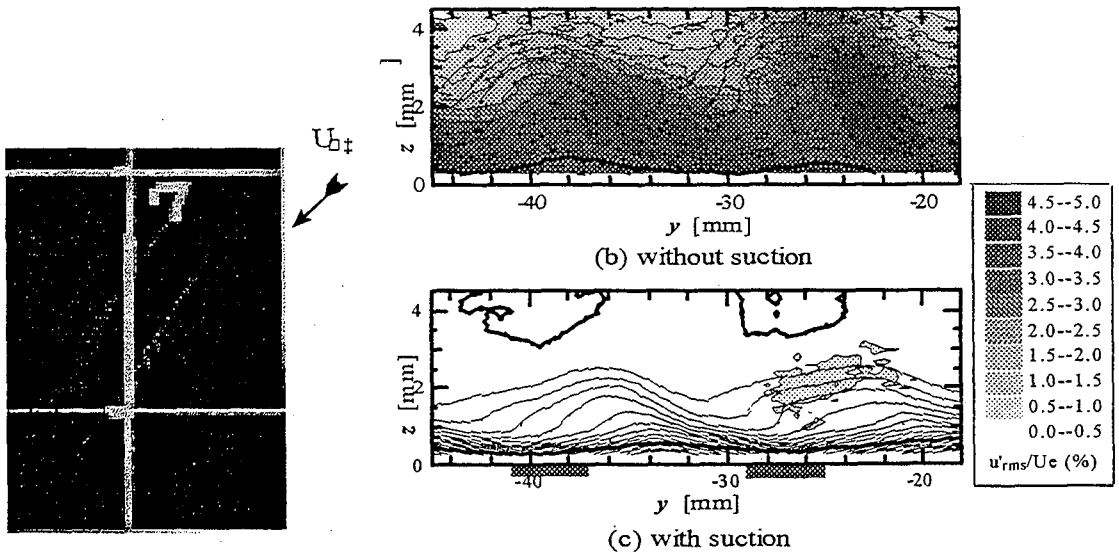

(a) Smoke visualization of the flow field.
(Ue = 10m/s, $Re_C = 5.3\times10^5$)

(velocity contour line step: 5% ofUe,
Bandpass filter range : 1.25-3kHz for disturbance f_2,
x/C=0.79, Ue=12.3m/s, Suction volume 0.045m^3/m s,
▩ indicates suction positions)

Figure 1. Crossflow turbulent field on a swept flat plate with displacement body boundary layer.

1. Back Ground

Transition mechanism in 3D boundary layer is still unclear

Complex structure, thin boundary layer,

curved wall, relatively high velocity

" One of the important issue remained in the aerodynamics field"

" It is still difficult problem approaching from CFD method"

2. Motivation

★ **Drag reduction by developing Laminar Flow Control technique**

for the next generation large subsonic aircraft is

one of the important research topics in the aircraft industry

★ **Transition region can be utilized for the purpose of**

enhancement of the mixing, reaction, and heat transfer

3. Objective

First,
to make it clear the transition mechanism,

and then,
to find out the possible way to control Three-Dimensional boundary layer on a swept wing,

the transition mechanism of which is considerably different from 2D case, and uniform suction system is difficult to apply

★ Idea of the LFC in 3D boundary layer case :

Steady nature of the streamwise vortex is one of the key

for the transition control

4. State of the art of present research field

1) streamwise vortex system appears as primary instability

2) relatively low frequency traveling instability appears

3) about one order higher frequency traveling instability appears as the secondary instability

4) is crossflow instability absolute or convective in its nature?

5) existence of the streamline curvature instability?

5. Experimental condition

☆ Experiment is conducted using low turbulence wind tunnel equipped at the Institute of Fluid Science, Tohoku University, Sendai Japan.

☆ The turbulence level of the tunnel is less than 0.02 % in the wind speed range 20-50 m/s

☆ Swept flat plate with displacement body system is developed and full boundary layer condition from laminar to turbulent is created on the flat plate

☆ This system is originally introduced by Prof. W. S. Saric

☆ Hot wire system and flow visualization technique are being used

6. Results and discussion

6.1 Base flow structure

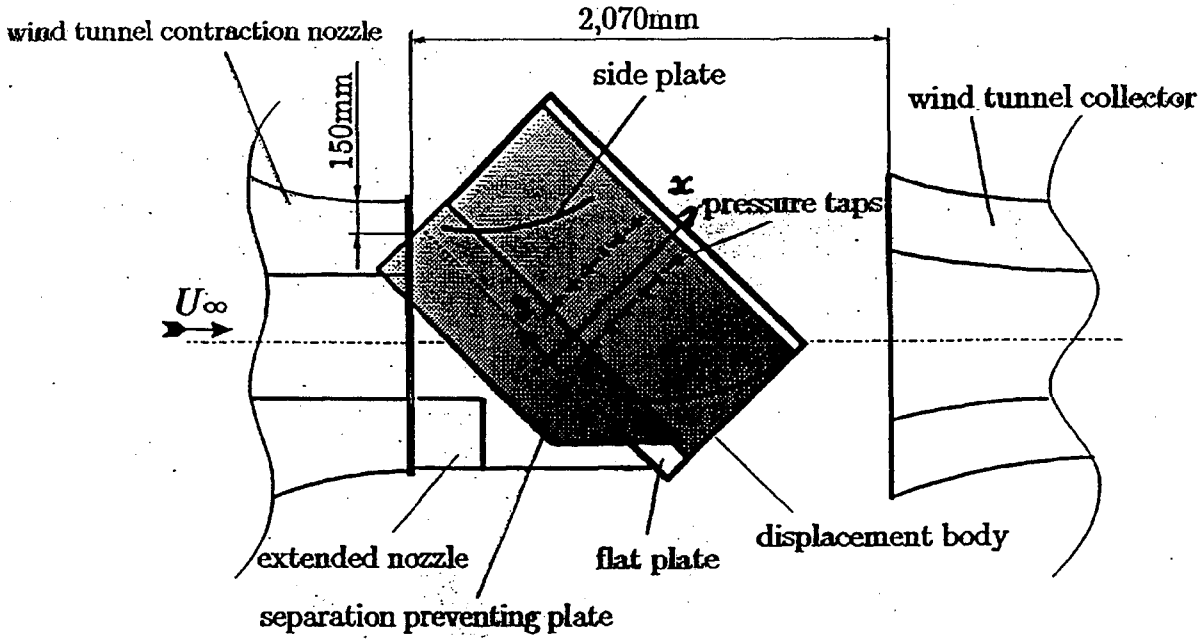

Plane view

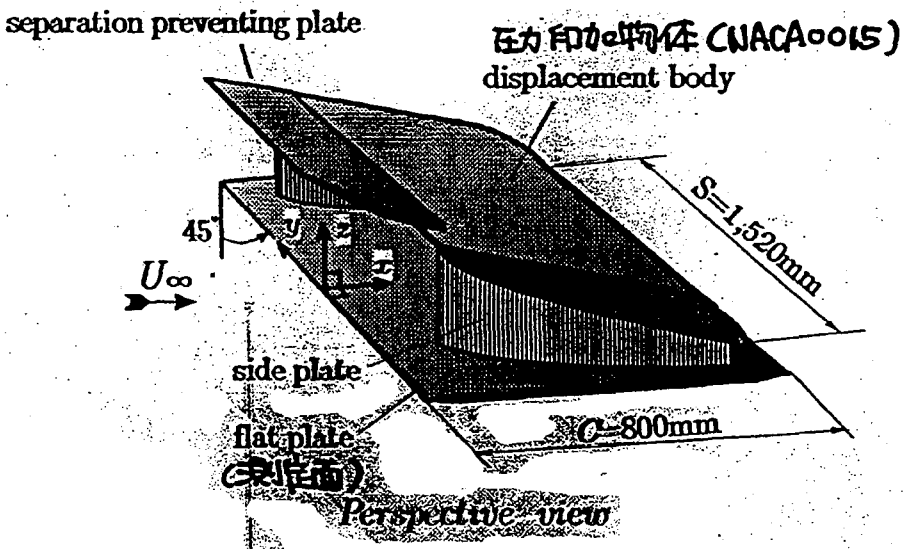

Perspective view

Figure 2-3. Experimental set-ups and coordinate system.

$Re \leq 5.3\times10^5 \sim 1.1\times10^6$

主流速度 U_∞=10-20m/s, u'_{rms}/U_∞=0.07%

平板の平均粗さ 0.576μm

(cf. Dryden等(1936) 1.8μm)

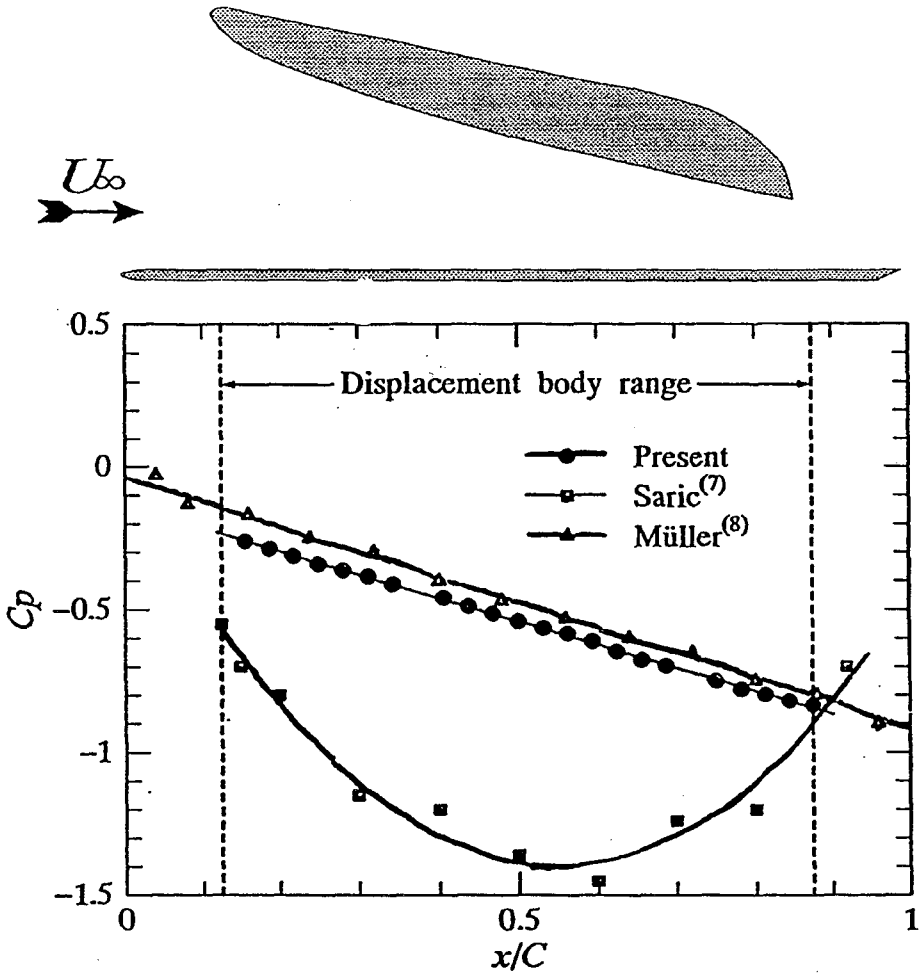

Figure 3. Chordwise pressure distribution on a 45° swept flat plate

(g) Flow visualization by Stage-smoke method of high frequency secondary instability and its sketch.
(Side view, U_∞=10m/s, $Re_c = 5.3 \times 10^5$,
nozzle position x/C =0.35, $y = \pm$100mm)

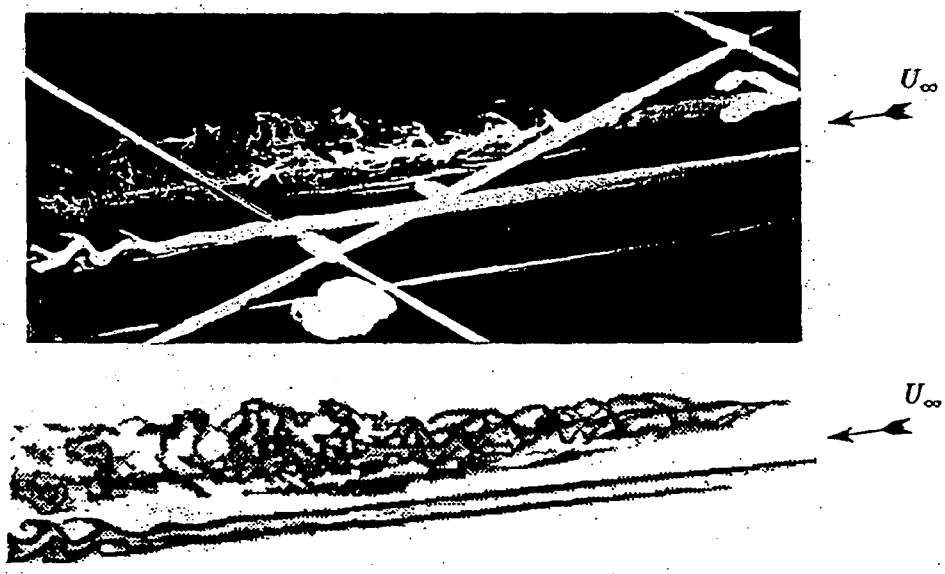

(h) Flow visualization by Stage-smoke method of high frequency secondary instability from diagonally above view and its sketch.
(Perspective view, U_∞=10m/s, Re_c=5.3×10^5,
nozzle position x/C =0.35, $y = \pm$100mm)

Figure 3-2. Flow visualizations.

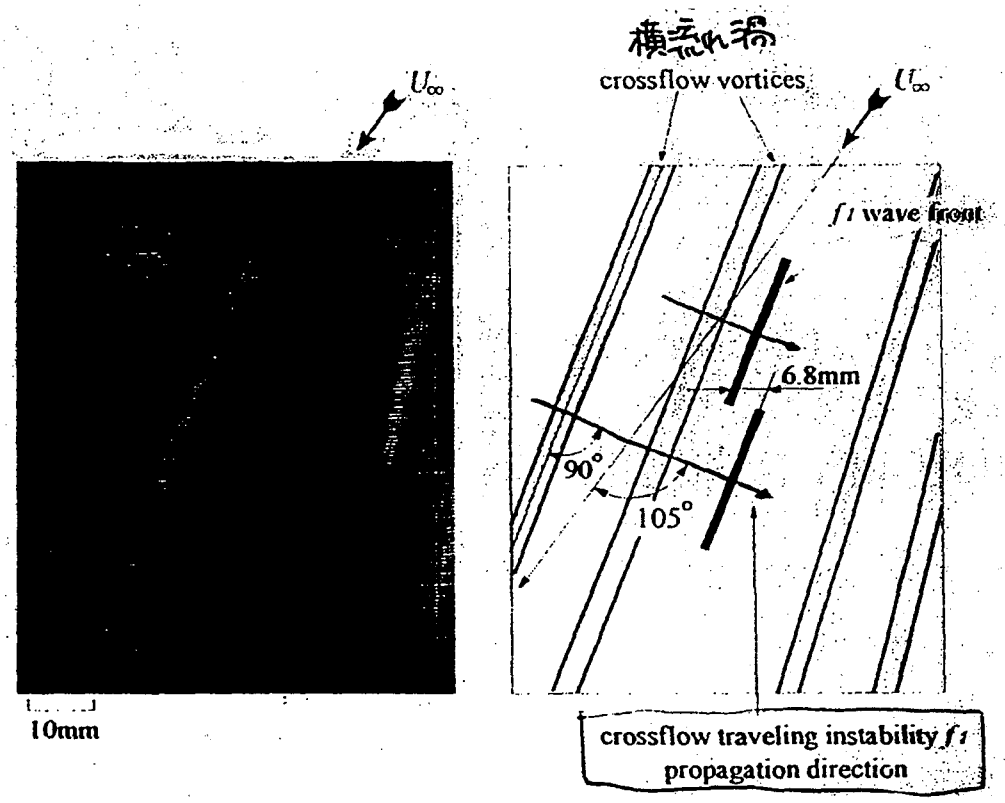

Figure 3-5. Flow visualization by Stage-smoke method of crossflow traveling instability and its sketch..

(U_∞ = 10m/s, $Re_c = 5.3 \times 10^5$, nozzle position x/C =0.35, $y = \pm 100$mm)

(1) $U_\infty = 8$ m/s, $Re = 3.4 \times 10^5$

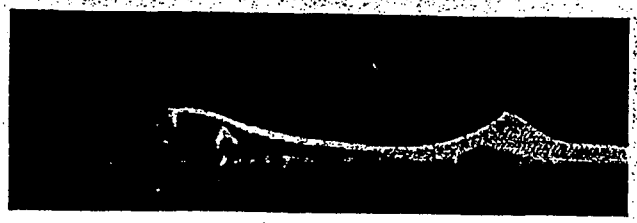

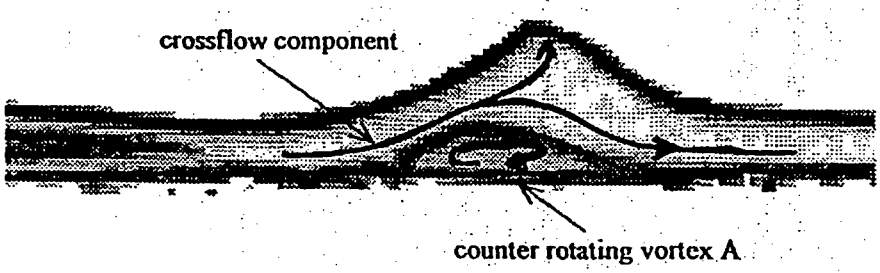

(2) $U_\infty = 9$ m/s, $Re = 3.8 \times 10^5$

(3) $U_\infty = 10$ m/s, $Re = 4.3 \times 10^5$

Figure 3-3 Depelopment of crossflow vortices taken by high speed video camera ($x/C = 0.80$)

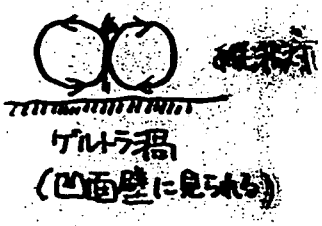

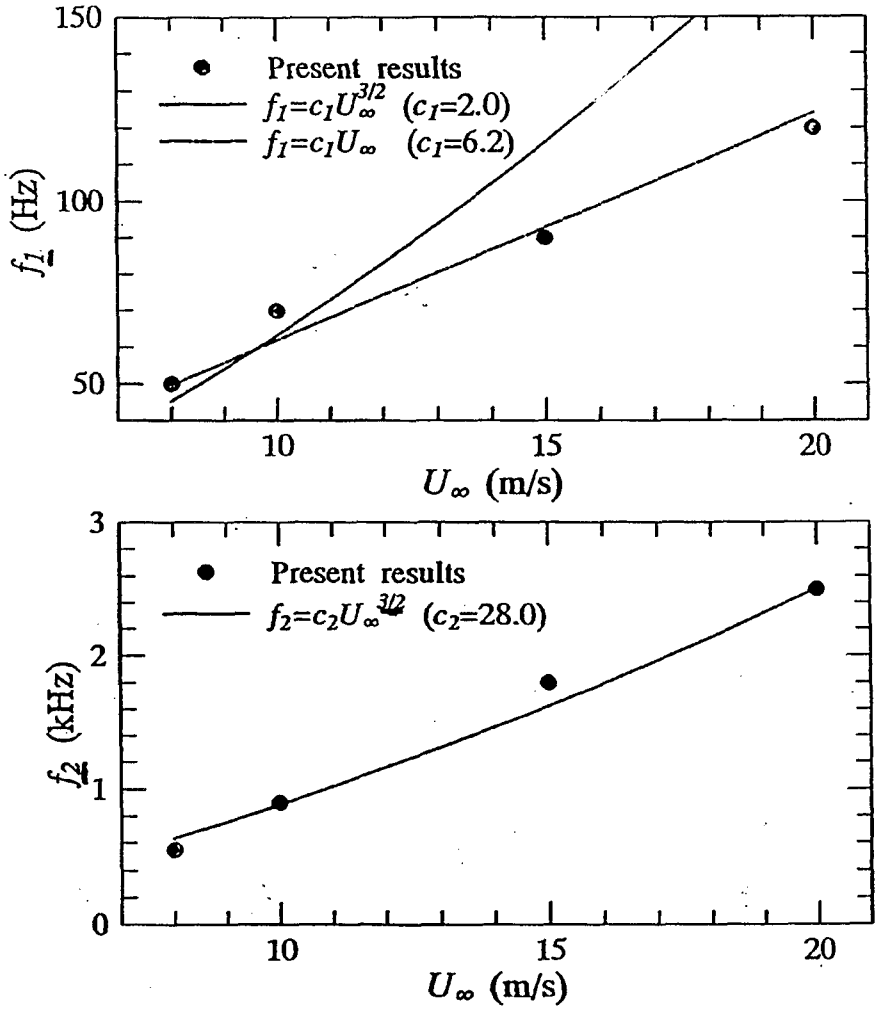

Figure 8 Frequency characterics of unstedy disturbances (c) with respect to flow velocity

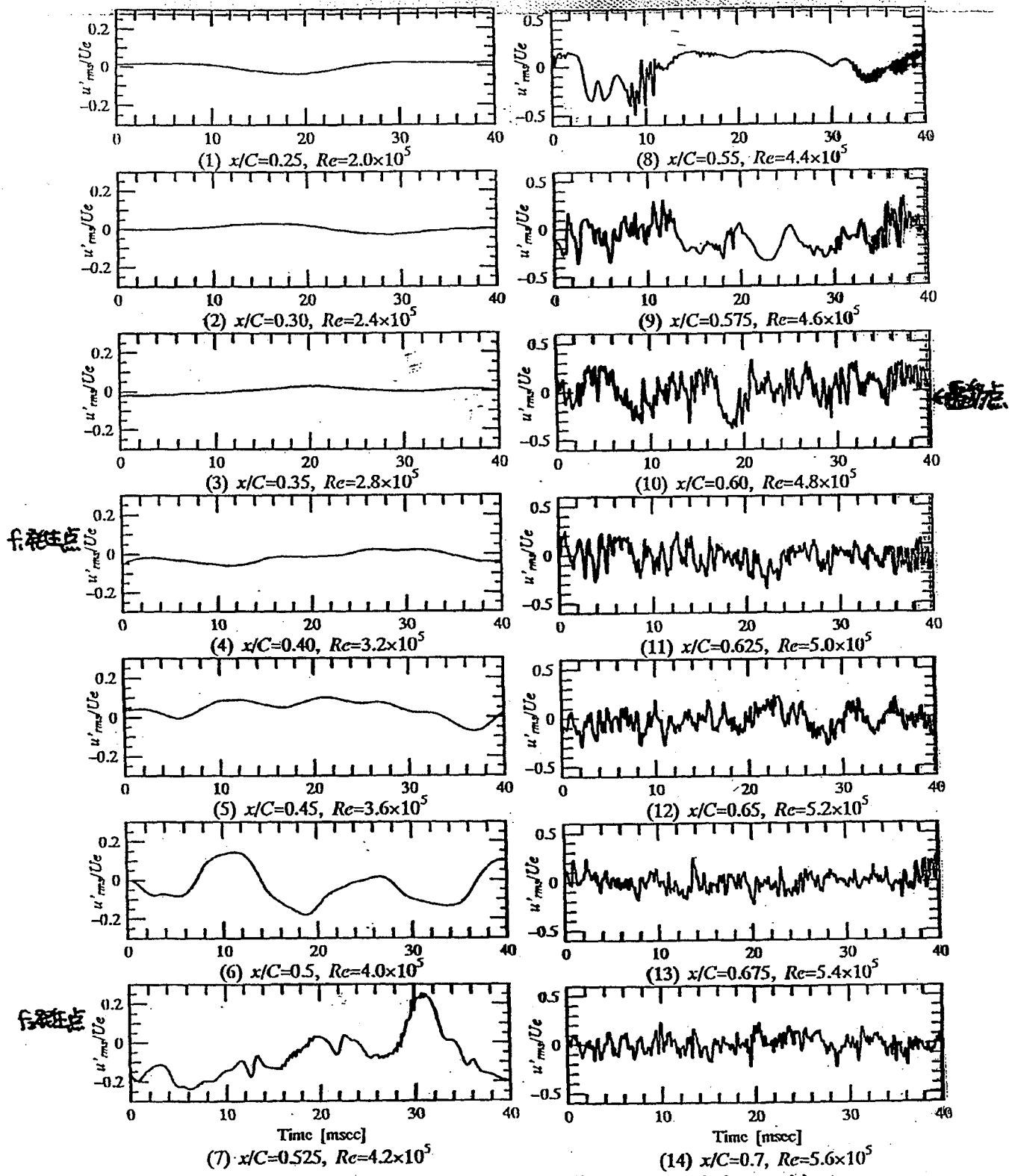

Figure 4–5. Time signals $u'(t)$ at different chordwise positions (U_∞=15m/s, z=0.8mm)

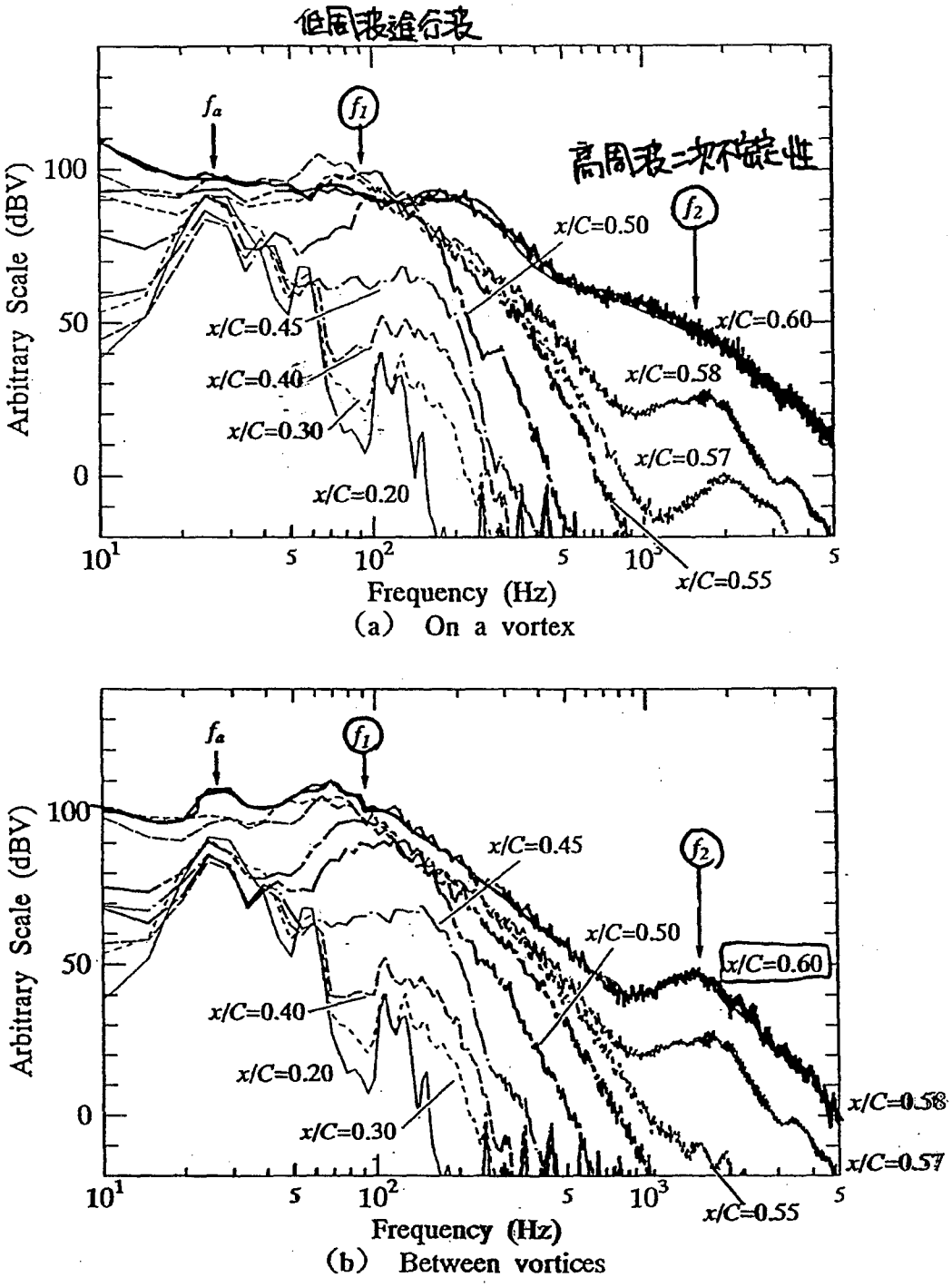

Figure 4–6. FFT analysis results of velocity fluctuations at different chord positions. (U_∞=15m/s, z=0.8mm)

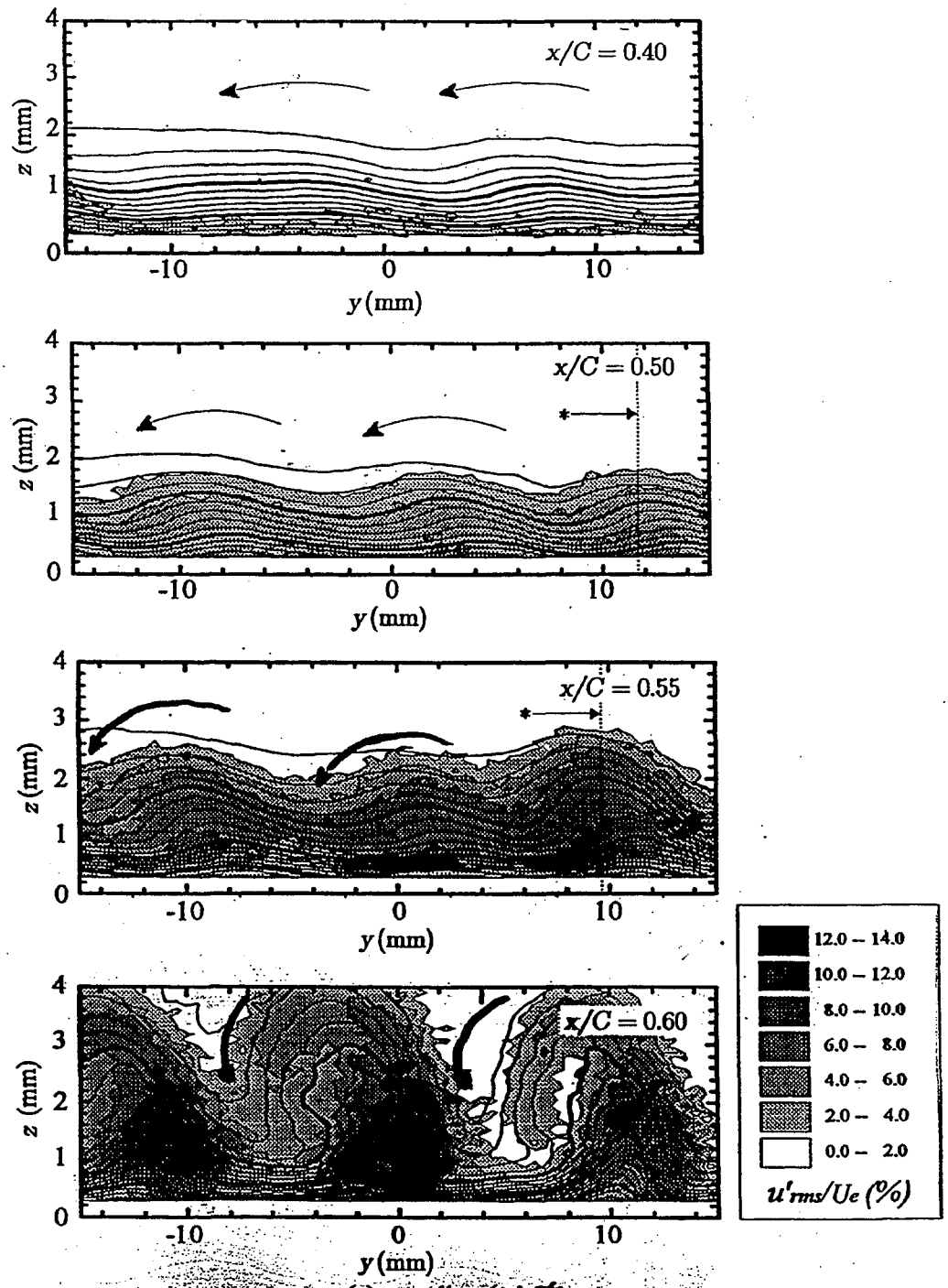

(a) overall

Figure 4-14. Cross section mesh measurement of velocity and turbulence intensities at different chord positions. (velocity contour line step : 5% of *Ue*, U_∞=15m/s)

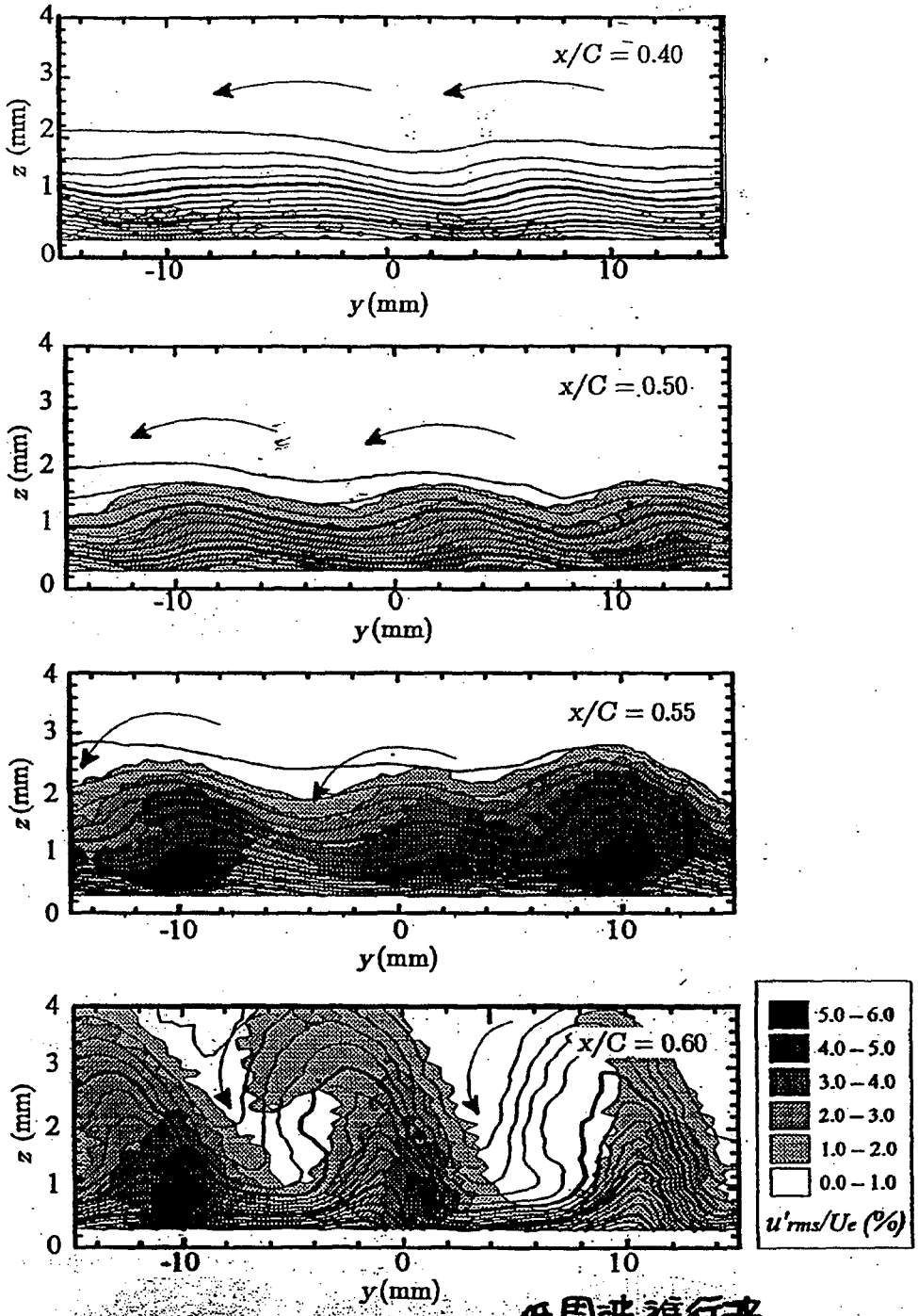

(b) Bandpass filter range : 80-100Hz, for disturbance f_1

Figure 4-14. Cross section mesh measurement of velocity and turbulence intensities at different chord positions. (velocity contour line step : 5% of Ue, U_∞=15m/s)

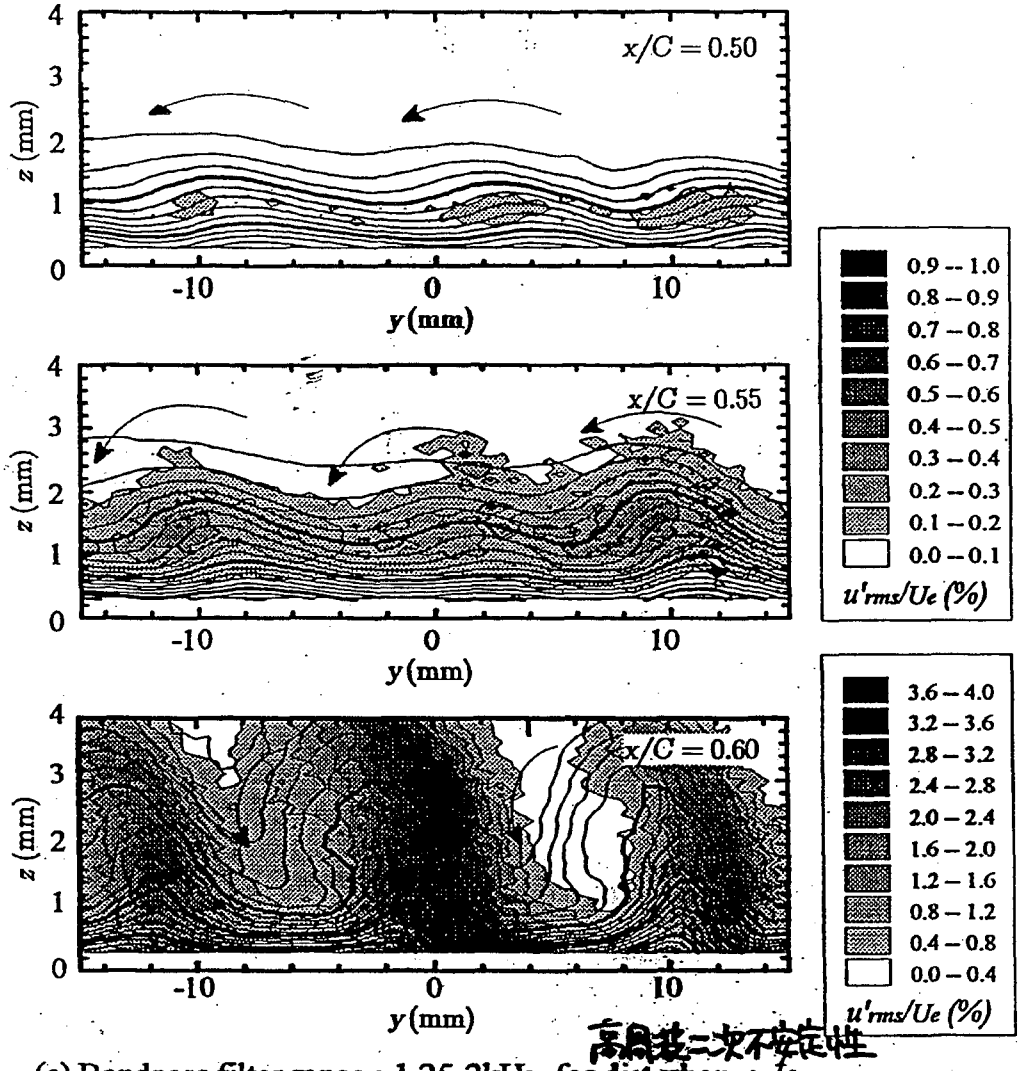

(c) Bandpass filter range : 1.25-2kHz, for disturbance f_2

Figure 4-14. Cross section mesh measurement of velocity and turbulence intensities at different chord positions. (velocity contour line step : 5% of Ue, U_∞=15m/s)

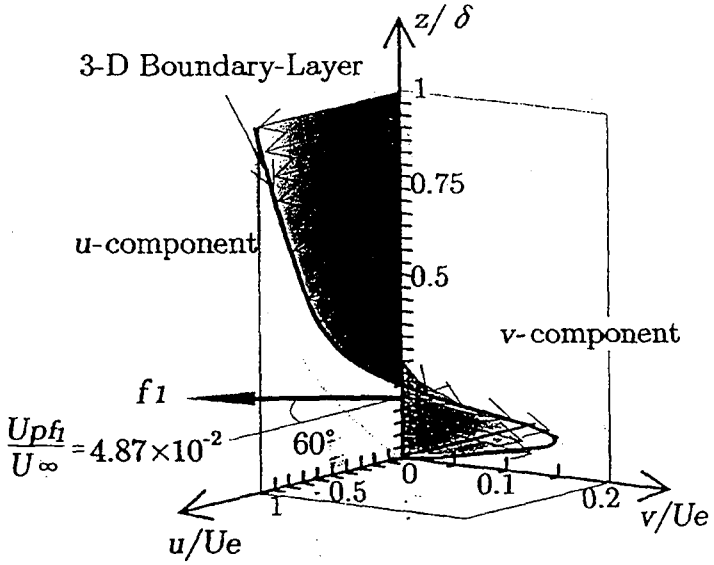

(a) Crossflow disturbances unsteady mode f_1
(x/C=0.50)

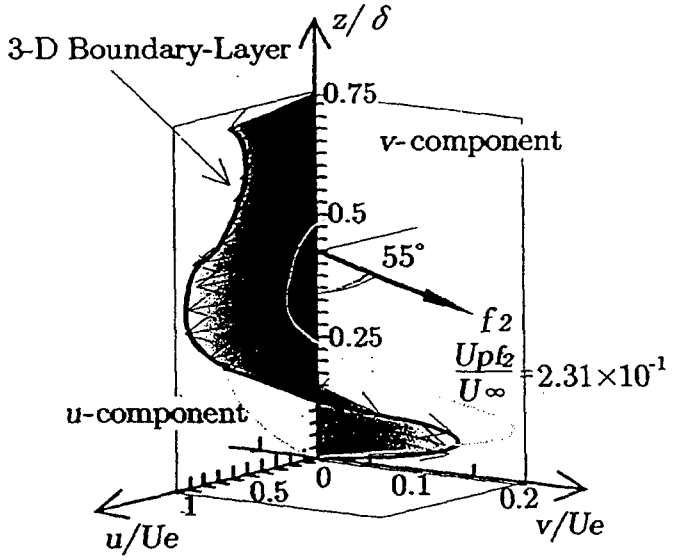

(b) High frequency secondary instability f_2
(x/C=0.60)

Figure 11. Schematic sketch of the obtained velocity profiles and nature of unsteady disturbances

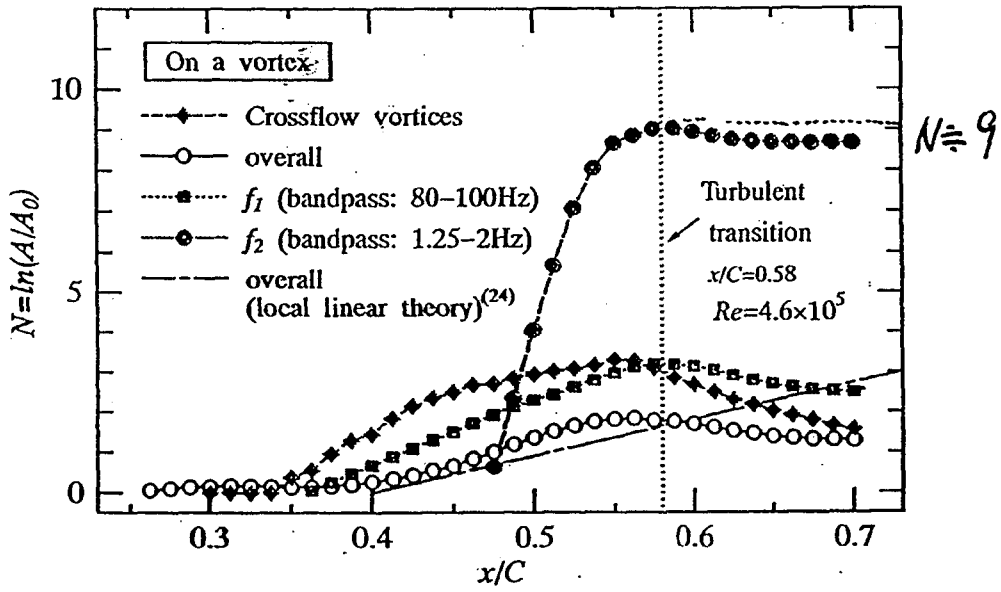

(b) Amplitude

Figure 4–11. Chordwise growth rate of disturbances.
(U_∞=15m/s, Re_c=8.0×10^5, z=0.8)

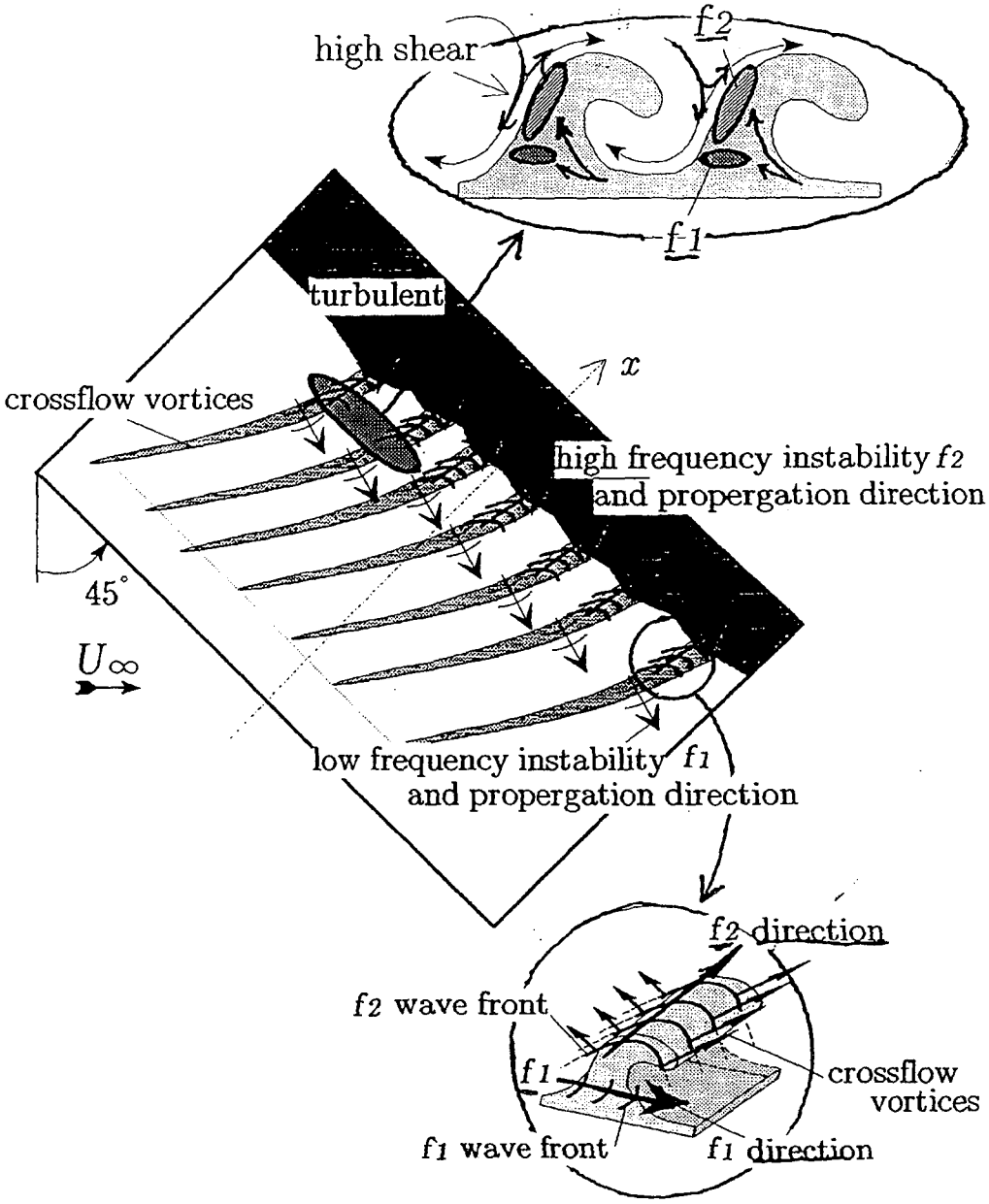

Figure 10. Crossflow instability on the swept back flat plate boundary layer

6. Results and discussion

6.2 Control of the transition

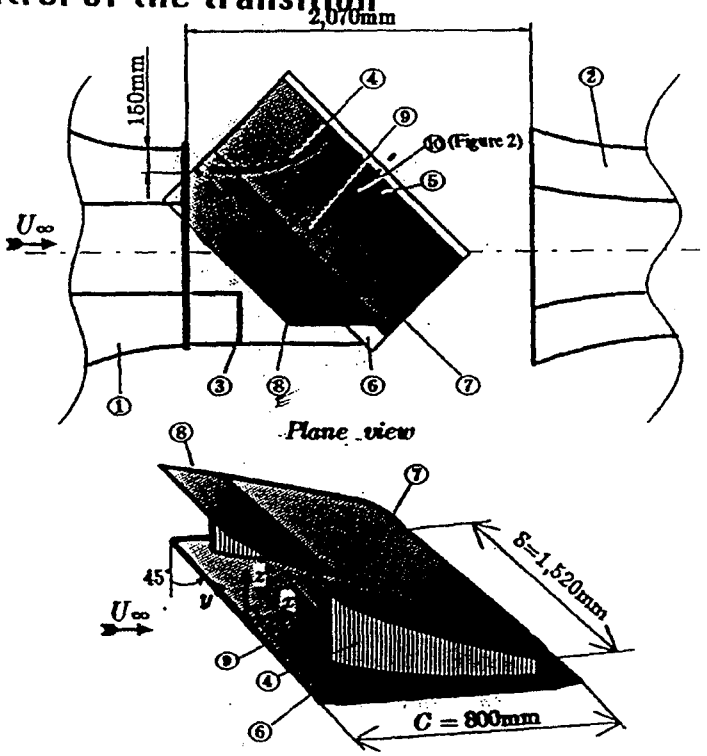

① wind tunnel contraction nozzle ② wind tunnel collector
③ extended nozzle ④ side plate ⑤ pressure taps ⑥ flat plate
⑦ displacement body ⑧ separation preventing plate
⑨ smoke visualization slit ⑩ suction slits

Figure 1. Experimental set-ups and coordinate system

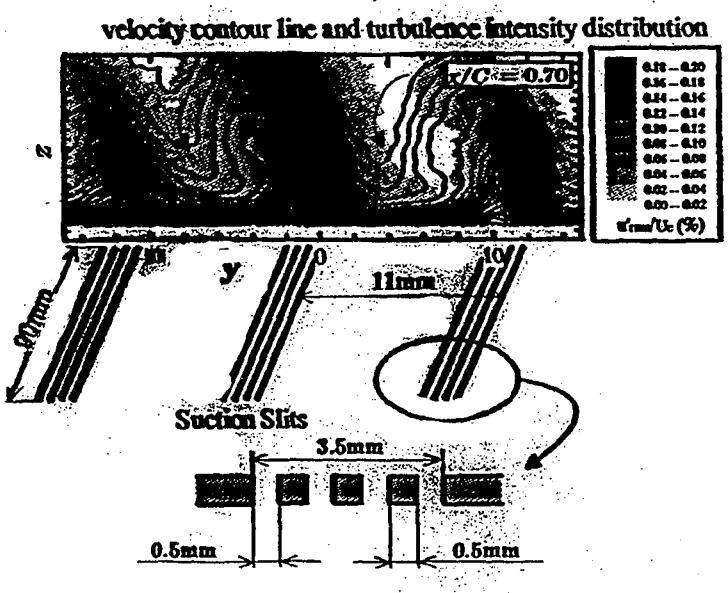

Figure 2. Detail of the suction slits

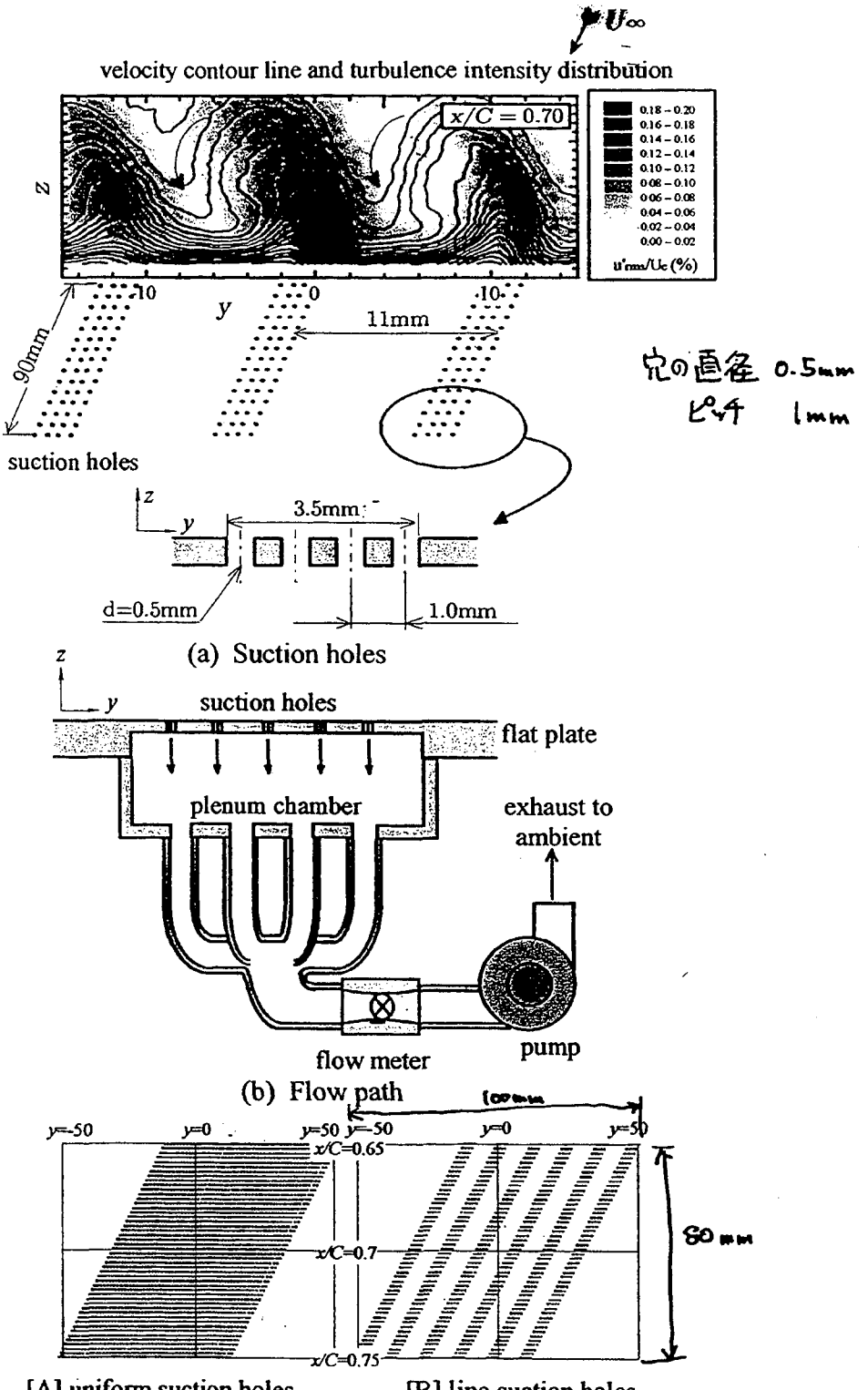

Figure 2. Details of the suction system

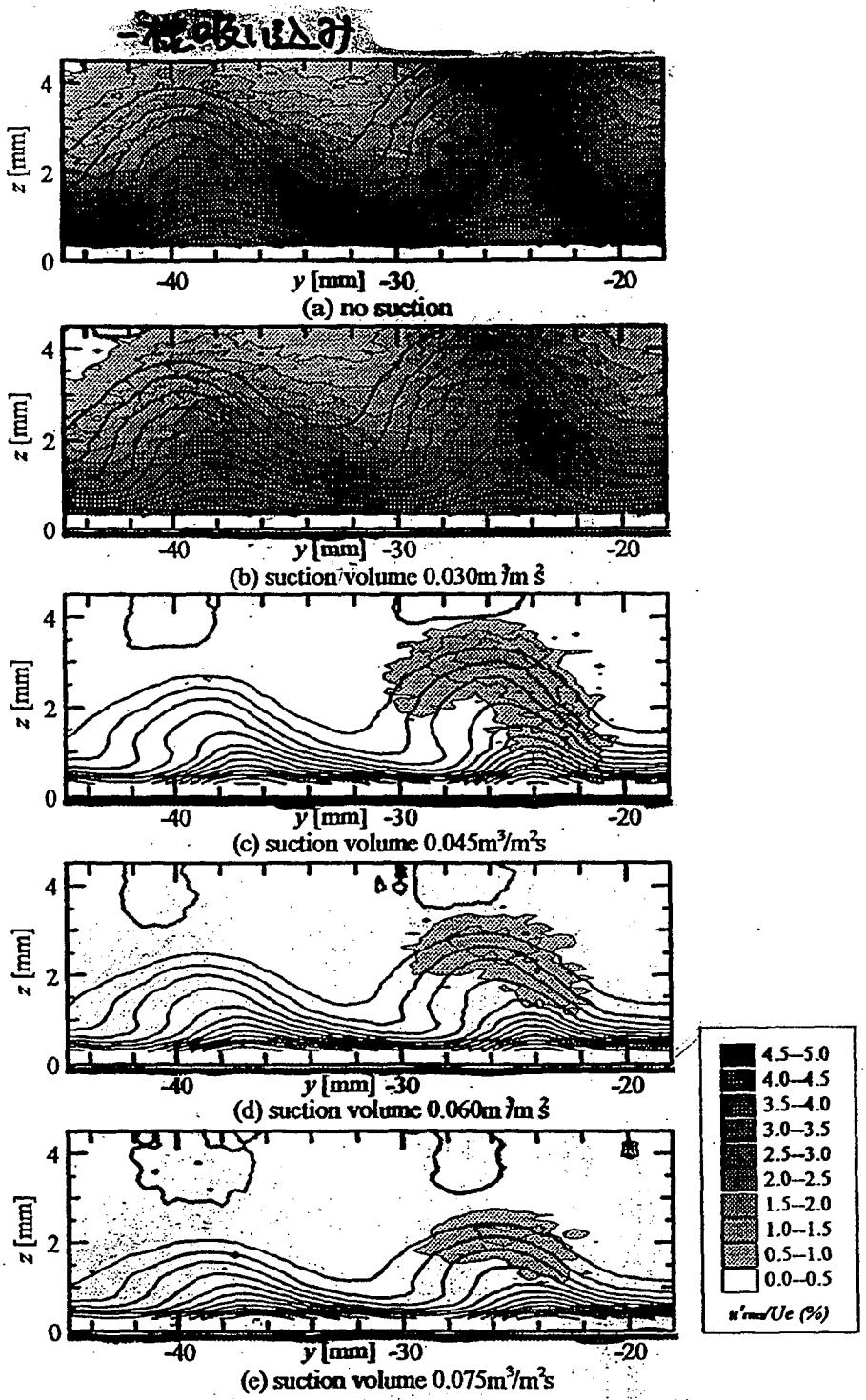

(3) f_2 (bandpass filter range : 1.25- 2kHz)

Figure 5-3. Cross sectional measurement of velocity and turbulence intensity for distributed suction using uniform suction holes.
(x/C=0.79, U_∞=12.3m/s, Re=5.2×10^5,
suction position: x/C=0.65-0.75, ▬▬ indicates suction position,
velocity contour line step: 5% of Ue)

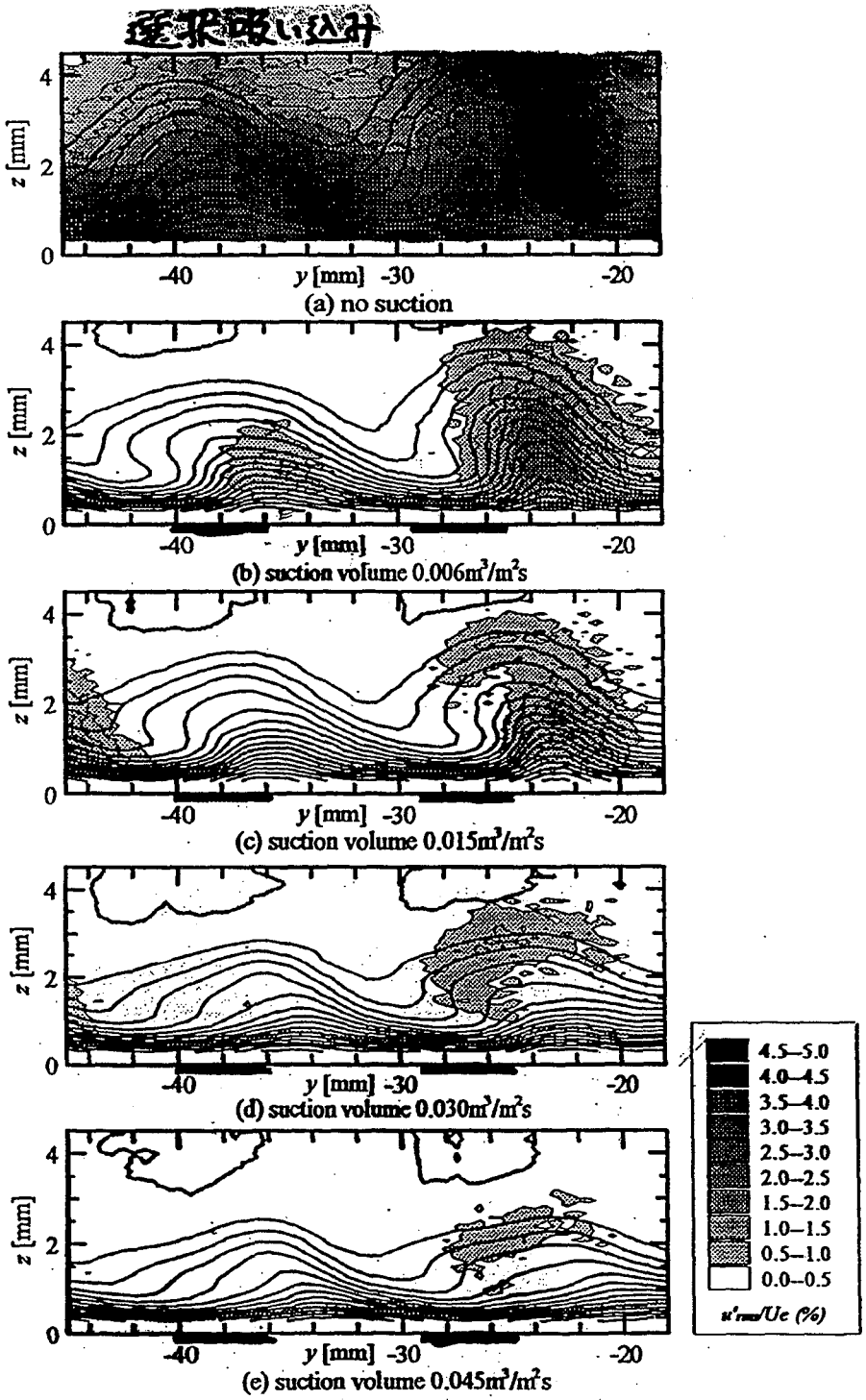

(3) f_2 (bandpass filter range : 1.25-2kHz)

Figure 5-4. Cross sectional measurement of velocity and turbulence intensity for distributed suction using line holes suction.
(x/C=0.79. U_∞=12.3m/s, Re=5.2×10^5,
suction position: x/C=0.65-0.75, ▬ indicates suction position,
velocity contour line step: 5% of Ue)

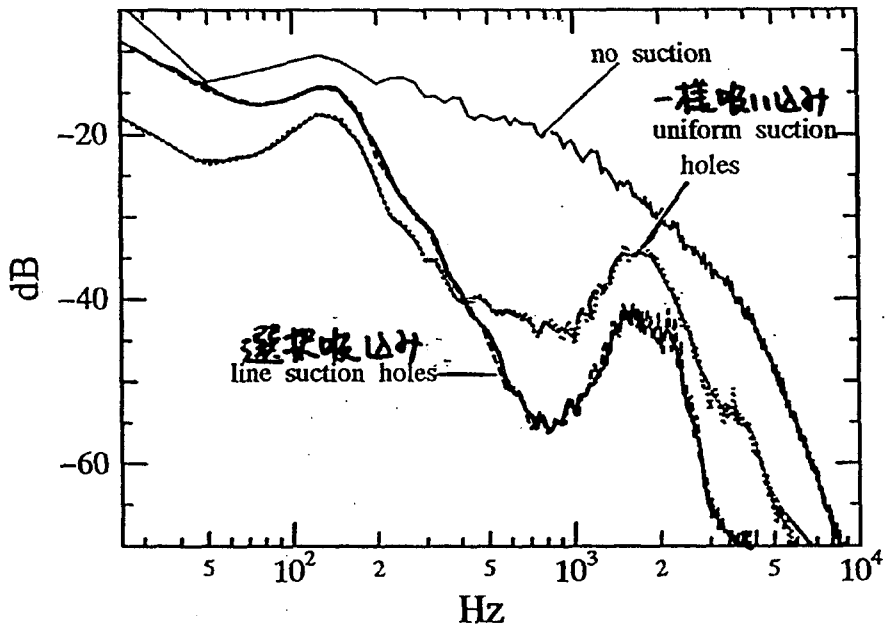

Figure 5–5. FFT analysis results of velocity fluctuations. at a crossflow vortex
(U_∞=12.3m/s, x/C=0.79, Re=5.2×10^5, z/δ=0.35
suction volume s=0.045m^3/m^2s)

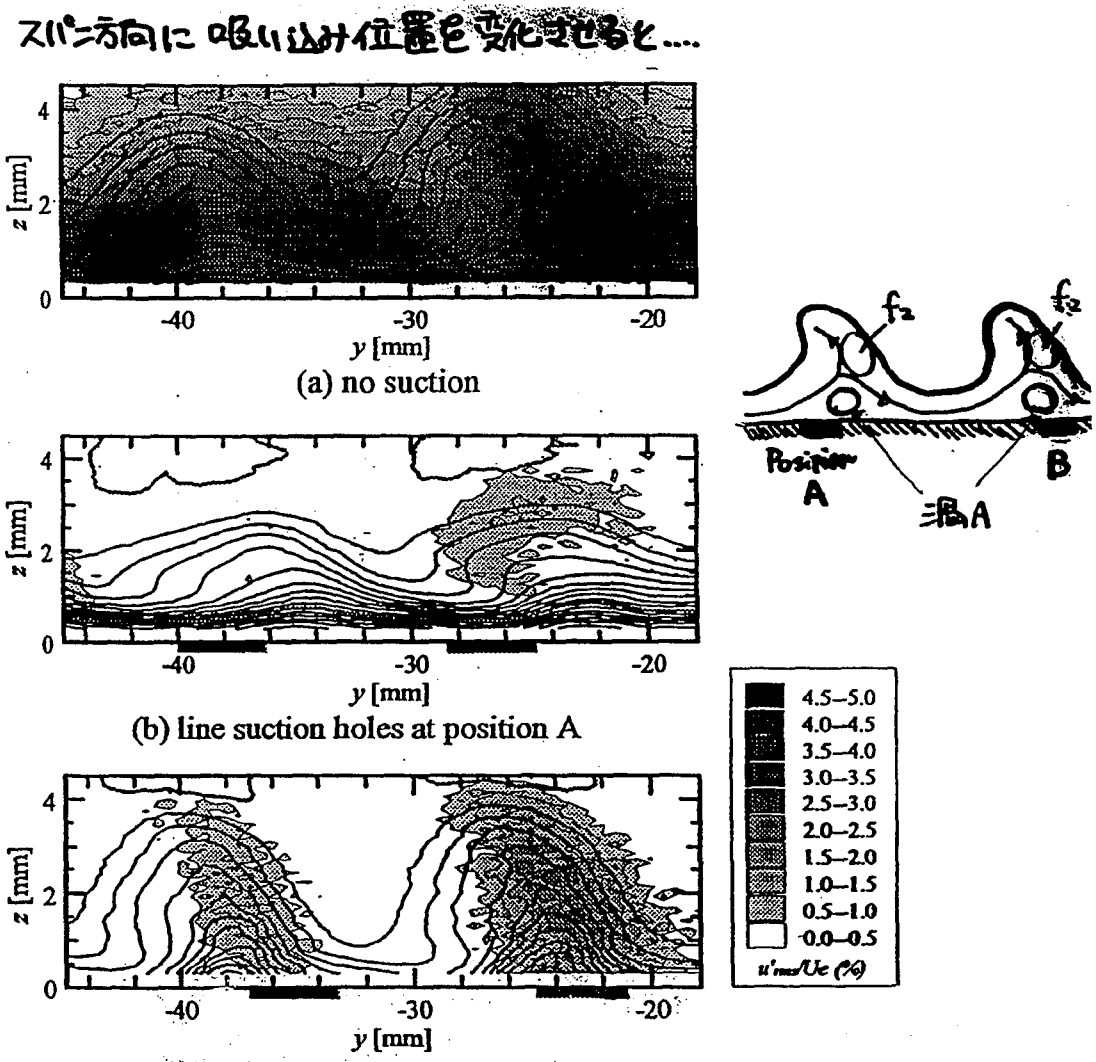

Figure 5-12. Cross sectional measurement of velocity and turbulence intensity profiles for different spanwise suction positions.

(Bandpass filter range : 1.25-2kHz for disturbance f_2,
Re=5.2×10^5, x/C=0.79, U_∞=12.3m/s,
suction volume 0.03m^3/m^2・s, suction position : x/C=0.65-0.75,
▬ indicates suction positions,
velocity contour line step: 5% of Ue)

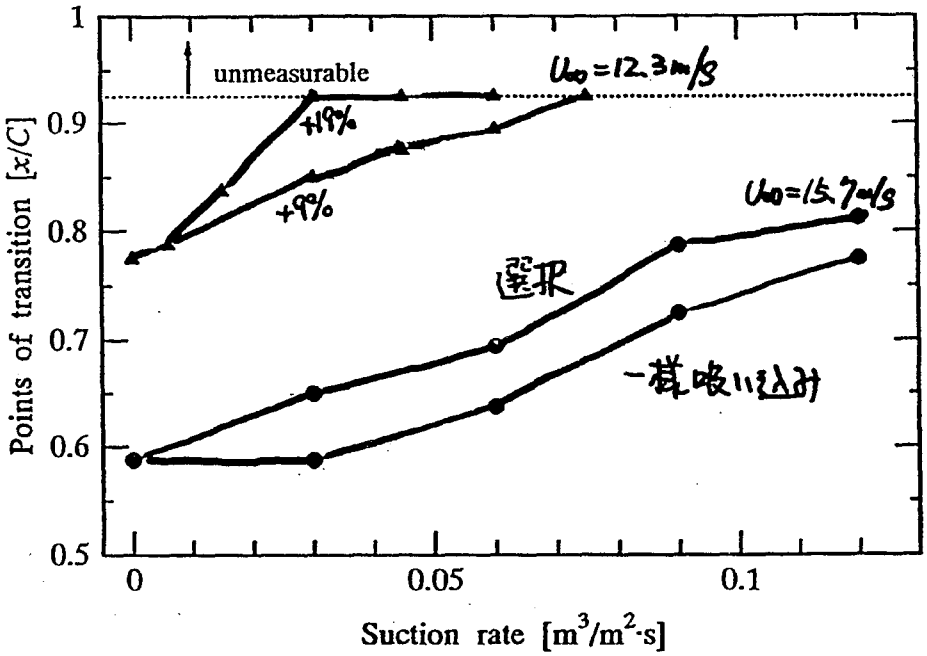

Figure 5–10. Transition characteristics for different distributed suctions

U_∞=12.3m/s
- uniform suction holes
- line suction holes

(suction point: x/C=0.65~0.75)

U_∞=15.7m/s
- uniform suction holes
- line suction holes

(suction point: x/C=0.475~0.575)

吸い込みを遷移過程のどの段階で行うと良いか？

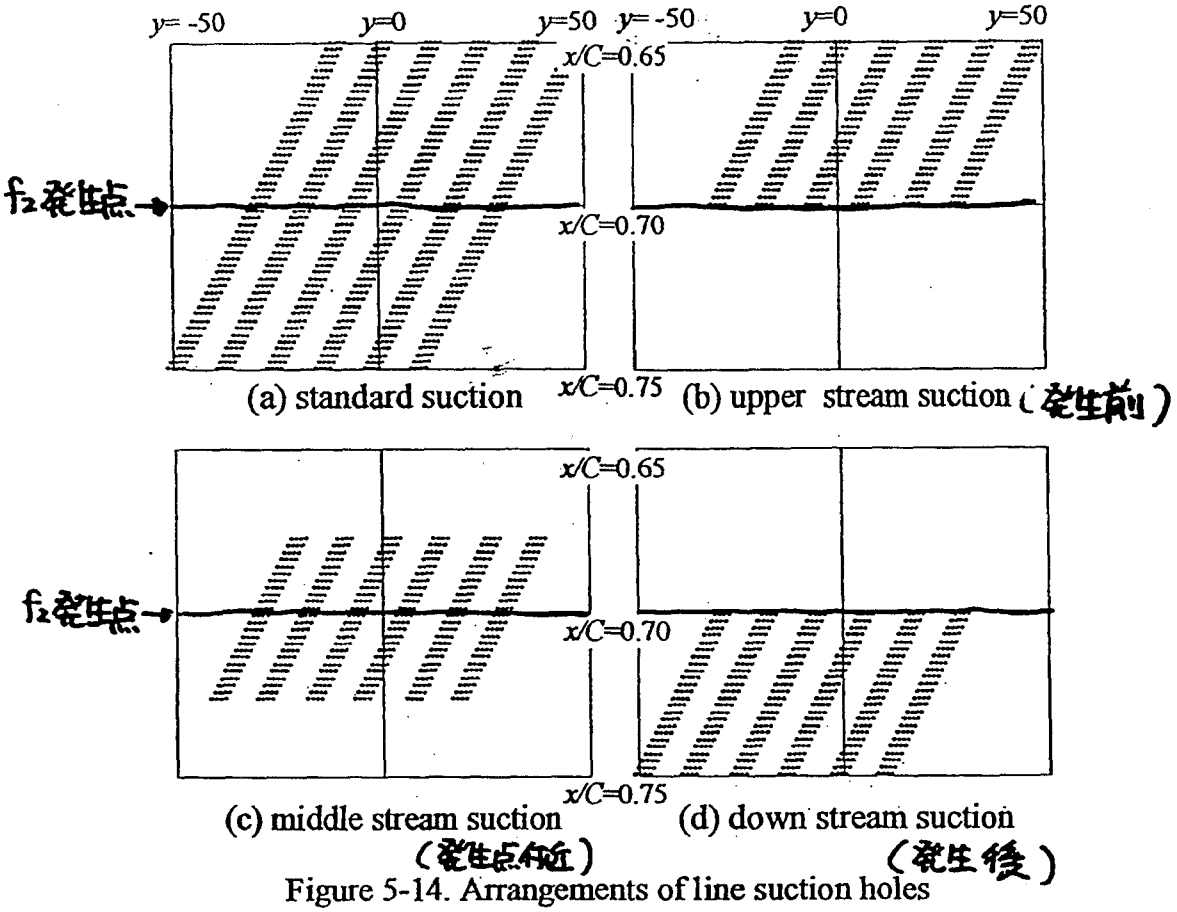

Figure 5-14. Arrangements of line suction holes

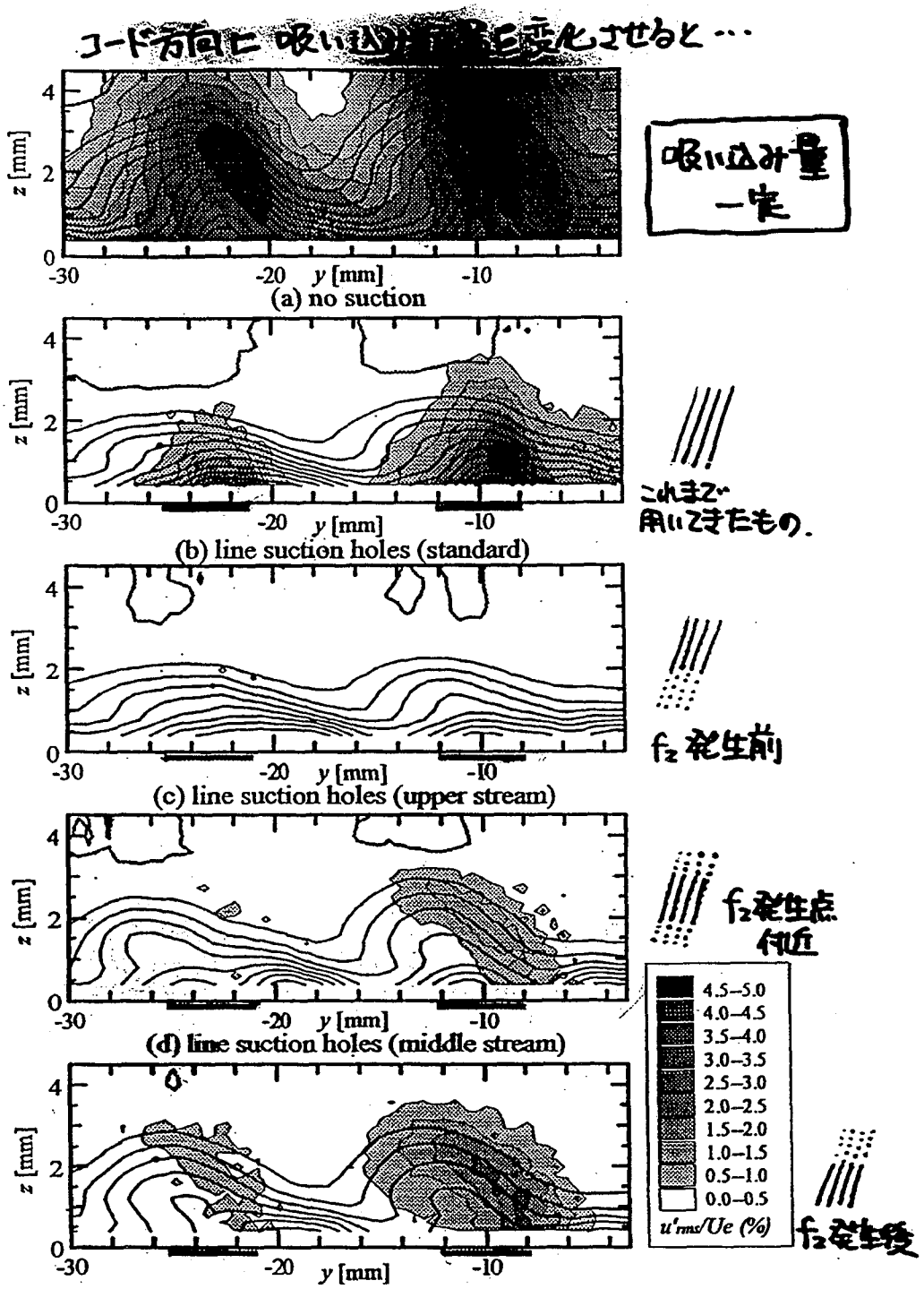

Figure 5-15. Cross sectional measurement of velocity and turbulence intensity profiles for different chordwise suction positions.
(Bandpass filter range : 1.25-2kHz for disturbance f_2,
$Re = 5.2\times10^5$, x/C=0.76, U_∞=13.5m/s, suction volume 0.06m^3/m^2・s,
▬▬ indicates suction positions, velocity contour line step: 5% of Ue)

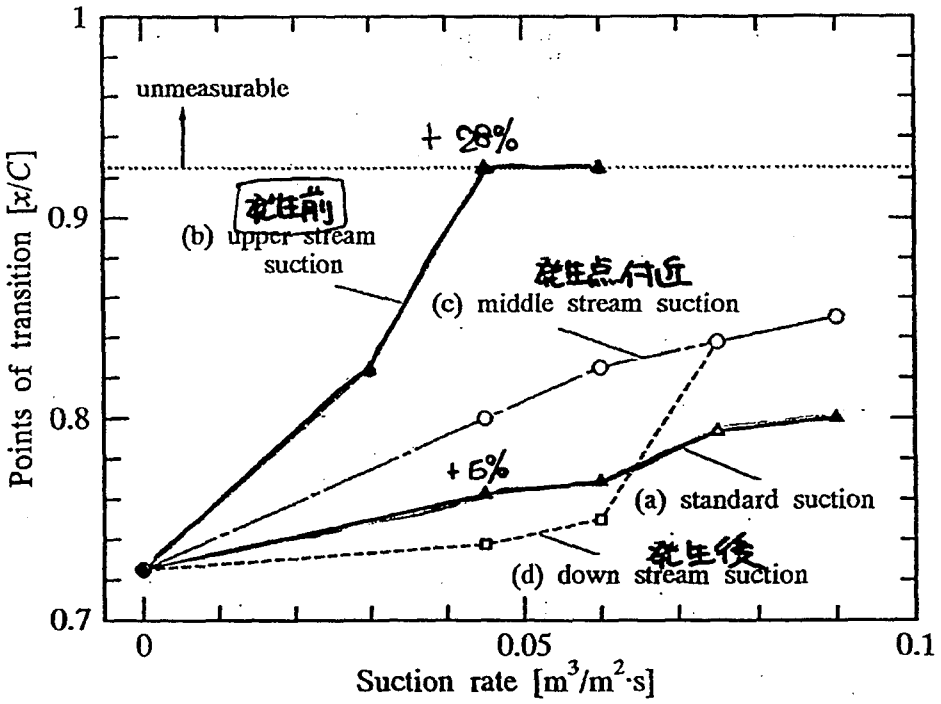

Figure 5–16. Transition characteristics for several line suction holes. (U_∞=13.5m/s, suction position x/C=0.65~0.75)

高周波二次不安定性の発生する前の
線形成長段階で吸い込むと良い

7. Concluding remarks

1) Full turbulent transition process, from onset of the instability to full turbulent state, is successfully generated on the swept flat plate boundary layer

2) High frequency secondary instability f2 is visualized by smoke visualization method, and spetial structure of the sppearance of this instability is clarified

3) In the boundary layer three different instabilities, namely crossflow primary instability (stationary crossflow vortices), crossflow instability unsteady mode f1 and high frequency secondary instability f2 are measured

4) By using rotatable parallel hot wire probe, travel directions and phase velocities of the unsteady disturbances are measured. These are shown in Figure 11.

5) It is found out that turbulent transition is triggered by high frequency secondary instability f2 and therefore, turbulent wedge starts from the middle height of the boundary layer on each crossflow vortex. This results isdifferent from conventional understanding concerning "turbulent wedge" obtained in wall flow visualization

SESSION 4

MODELING

A LAYER AVERAGED TWO-EQUATION MODEL FOR THE PREDICTION OF BOUNDARY LAYER TRANSITION ONSET

C.J. Fraser
University of Abertay
Dundee, Scotland

Abstract

Current industrial practice in the UK makes use of relatively simplistic empirical correlations to predict the onset of the breakdown to fully developed turbulent flow in the boundary layer. While these methods work after a fashion, they still do little more than correlate the original experimental data on which they are based. When applied to other cases there is often considerable error between predicted and actual transition onset position. This is particularly the case when laboratory based experimental correlations are used to predict transition onset in industrial gas turbine blade flows.

Recent research work has been concentrated on the development of a two-equation transition model where the production and dissipation rates of turbulent energy have been expressed in the forms of ordinary non-linear differential equations. These equations were formulated from the classic turbulence energy equations which are obtained by multiplying the Navier-Stokes equations by the fluctuating velocity in the main flow direction. An order of magnitude analysis eliminates the lesser terms and integration across the boundary layer produces a set of layer averaged ordinary differential equations. Within these equations a considerable amount of further simplification and empirical modelling results in the particular forms that are currently being investigated.

The basic concept being tested is that the intensity of the turbulent energy associated with the velocity fluctuations will grow or decay depending upon the prevailing influences like the external freestream turbulence intensity and the streamwise pressure gradient. In all cases the general tendency is that the intensity of the turbulent energy will grow, but that the growth rate will be limited or enhanced by these external influences. The current transition onset model makes use of the assumption that when the turbulent energy reaches a maximum critical value then the final breakdown process, in the form of turbulent spot generation, will be initiated.

Implementation of a Transition Model Within the PHOENICS Software Package

- **Laminar Layer:- Thwaites method**
- **Turbulent Layer:- White's Integral method**
- **Transition Region:- Linear intermittency weighted combination**
- **The above is computed as a satellite subroutine in PHOENICS**
- **The boundary layer is modelled as a retarding force at the wall where:-**

$$\tau_w = -\frac{C_f}{2}\rho U^2$$

- **Transitional boundary layer properties are evaluated e.g.**

$$C_f = (1-\gamma)C_{fl} + \gamma C_{ft}$$

Correlations for Start of Transition

$$Re_{\theta_s} = \left[163 + \exp\left[g(m)\left[1 - \frac{t}{6.91} \right] \right] \right]$$

$$Re_{\theta_s} = 400t^{-5/8} \qquad (t \geq 3\%)$$

where: t freestream turbulence intensity

m pressure gradient parameter = $(\theta^2/\nu)(dW/dz)$

Experimental Test Data

European Research Community on Flow Turbulence and Combustion (ERCOFTAC)

Special Interest Group on Transition

Flat plate transitional boundary layer flow test cases in varying pressure gradients

Data supplied by Rolls Royce PLC, Derby

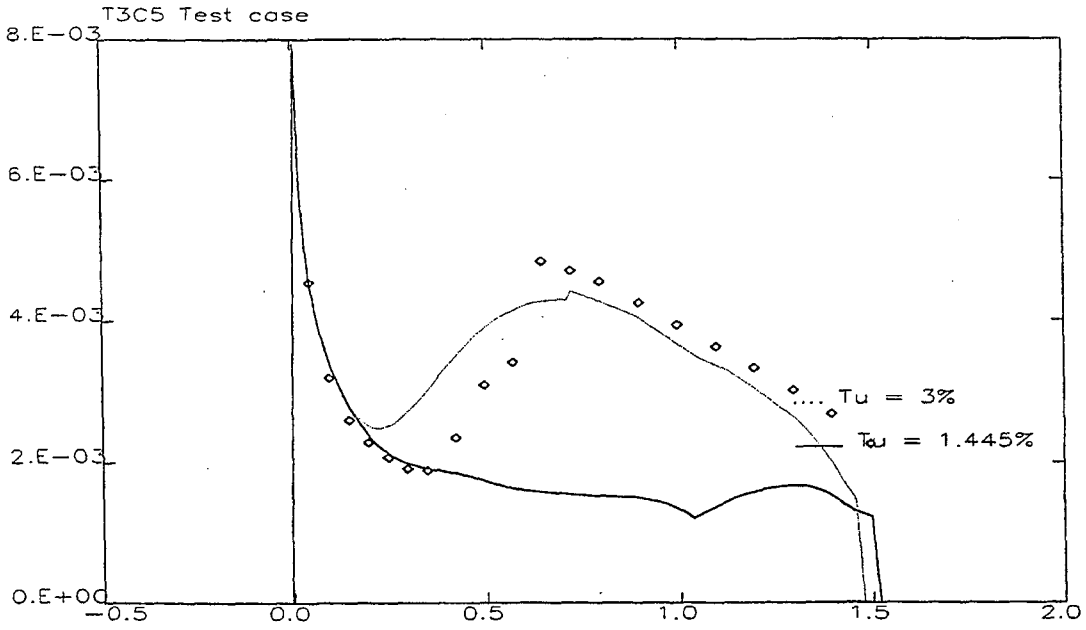

Integral Turbulent Energy Equation

The equations for kinetic energy and dissipation can be written as:-

$$\rho\bar{w}\frac{\partial k}{\partial z}+\rho\bar{u}\frac{\partial k}{\partial x}=\frac{\partial}{\partial x}\left[\left(\mu+\frac{\mu_t}{\sigma_k}\right)\frac{\partial k}{\partial x}\right]+\mu_t\left(\frac{\partial\bar{w}}{\partial x}\right)^2-\rho\varepsilon$$

$$\rho\bar{w}\frac{\partial \varepsilon}{\partial z}+\rho\bar{u}\frac{\partial \varepsilon}{\partial x}=\frac{\partial}{\partial x}\left[\left(\mu+\frac{\mu_t}{\sigma_\varepsilon}\right)\frac{\partial \varepsilon}{\partial x}\right]+C_1\mu_t\left(\frac{\partial\bar{w}}{\partial x}\right)^2\frac{\varepsilon}{k}-C_2\rho\frac{\varepsilon^2}{k}$$

Freestream Turbulence

The equations for turbulent kinetic energy and its dissipation rate in the freestream are :-

$$W\frac{dk}{dz} = -\varepsilon$$

$$W\frac{d\varepsilon}{dz} = -C_{2\varepsilon}\frac{\varepsilon^2}{k}$$

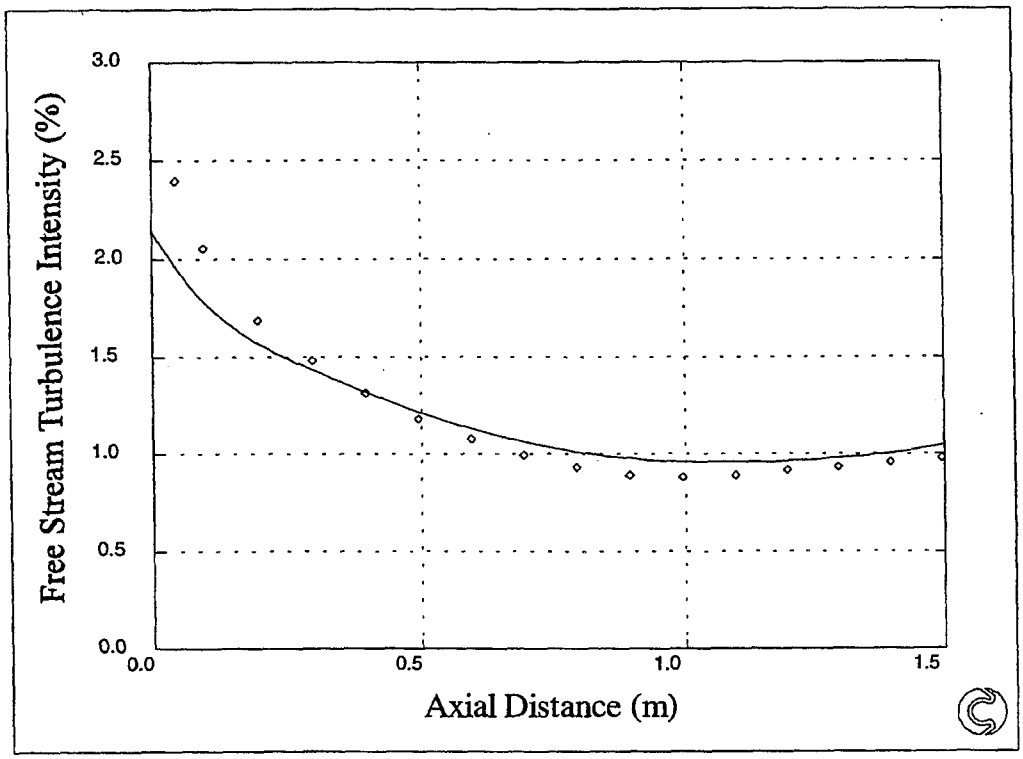

T3C2 Freestream Turbulence Intensity Profile

Integrated forms of the turbulent kinetic energy and its dissipation rate

$$\frac{d}{dz}\left(\int_0^\infty \bar{w}k\,dx\right) = \int_0^\infty \tau_t\left(\frac{d\bar{w}}{dx}\right)dx - \int_0^\infty \varepsilon\,dx$$

$$\frac{d}{dz}\left(\int_0^\infty \bar{w}\varepsilon\,dx\right) = C_1\int_0^\infty a\varepsilon\left(\frac{d\bar{w}}{dx}\right)dx - C_2\int_0^\infty \frac{\varepsilon^2}{k}dx$$

where

$$a = \frac{\tau_t}{\rho k}$$

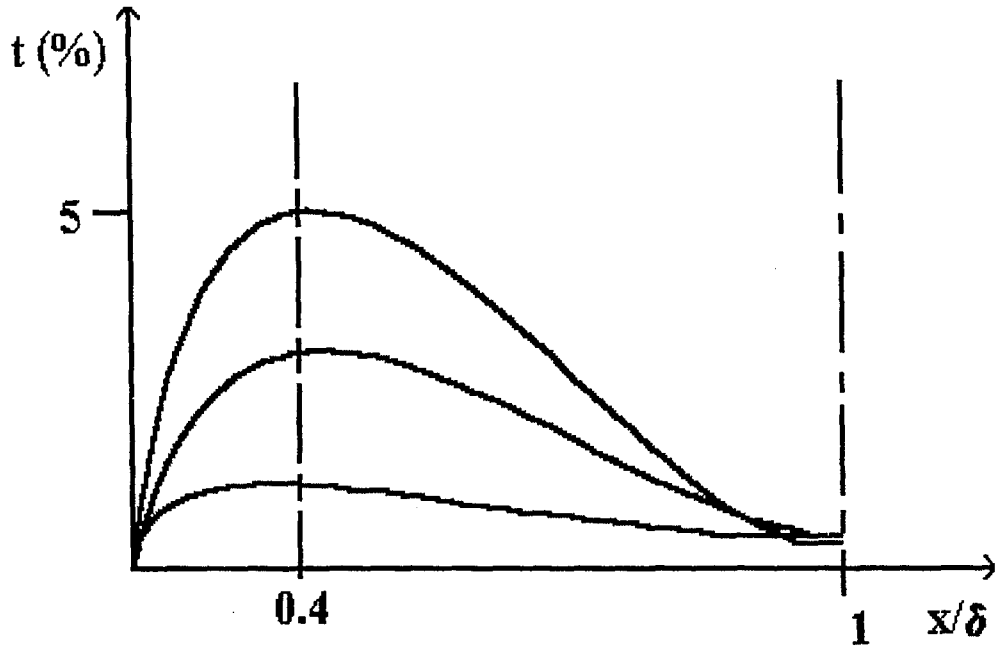

Turbulence Intensity Profiles Across the Boundary Layer

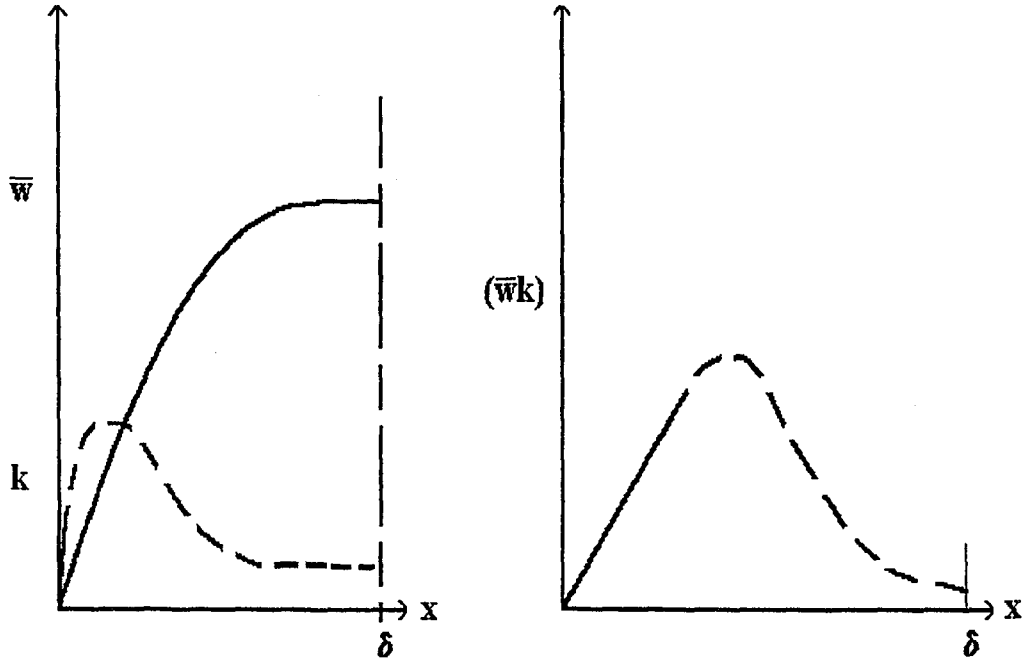

Reduced Form of the Turbulent Energy Equations

$$\frac{d\hat{k}}{dz} = \hat{k}\left[\frac{a\tau_0}{W_\infty \mu} - \frac{1}{W_\infty}\frac{dW_\infty}{dz} - \frac{1}{\delta}\frac{d\delta}{dz}\right] - 2.86\frac{\overline{\varepsilon}}{W_\infty}$$

$$\frac{d\overline{\varepsilon}}{dz} = \overline{\varepsilon}\left[\frac{1.04\,a\tau_0}{W_\infty \mu} - \frac{1}{W_\infty}\frac{dW_\infty}{dz} - \frac{1}{\delta}\frac{d\delta}{dz}\right] - \frac{5.486\,\overline{\varepsilon}^2}{W_\infty \hat{k}}$$

Proposed Function for 'a'

$$a = \exp\left[\left(\frac{-19}{t}\right)\left(\frac{L_e}{0.004}\right)(1-5.3m)^2\right]$$

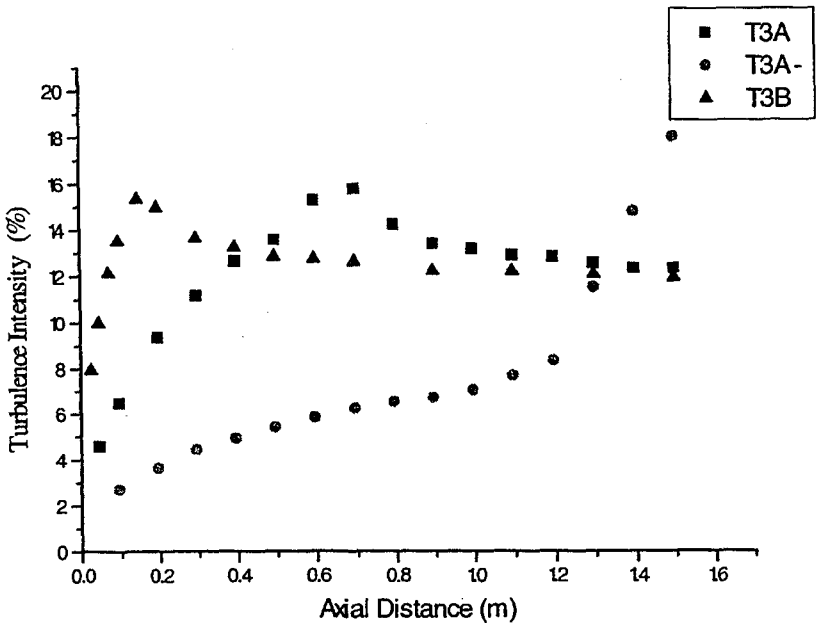

Plot of Maximum Turbulence Intensity in Boundary Layer

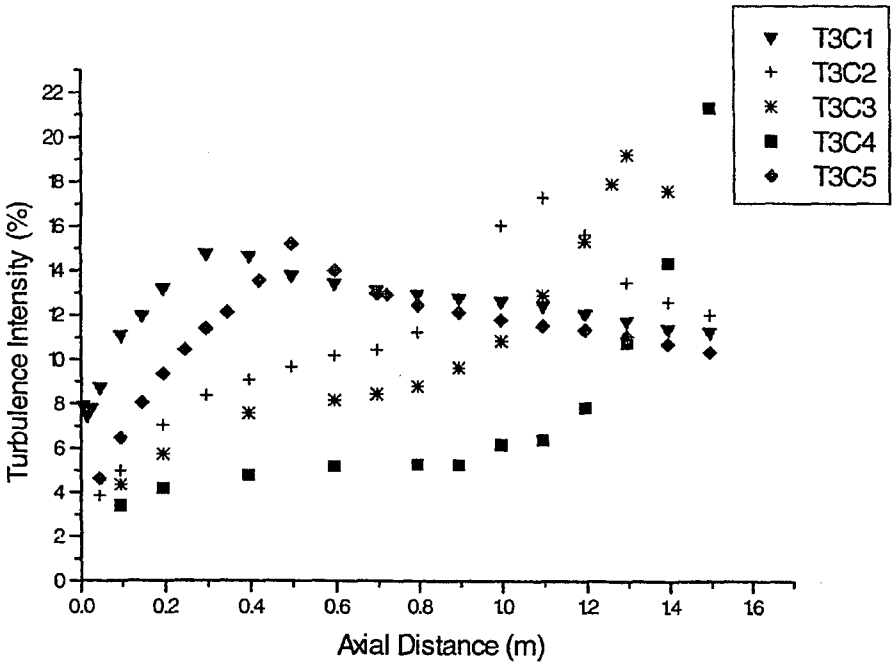

Plot of Maximum Turbulence Intensity in Boundary Layer

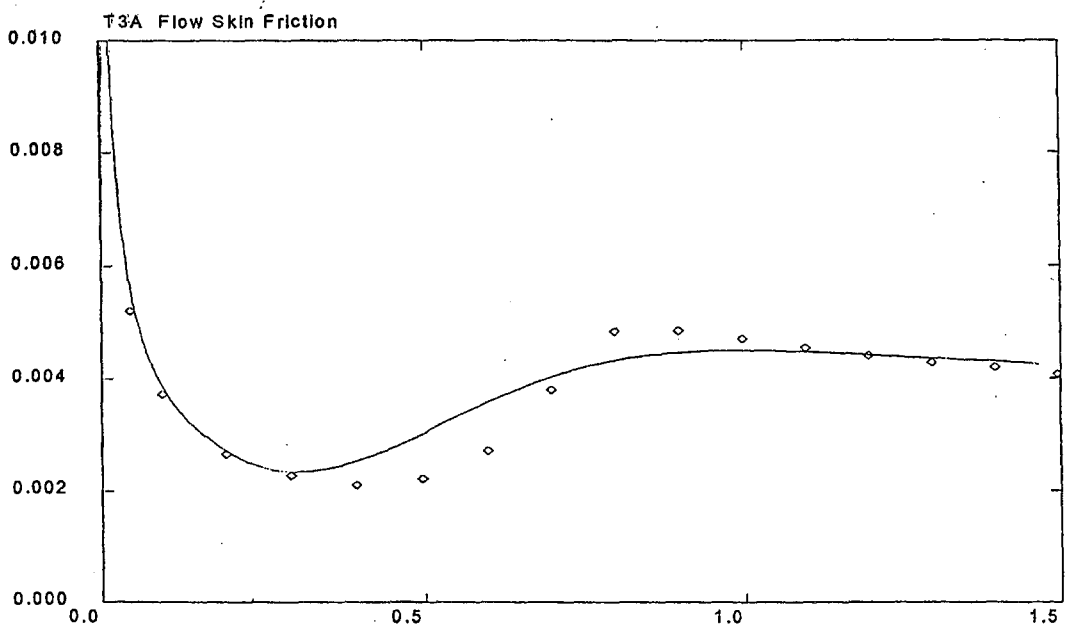

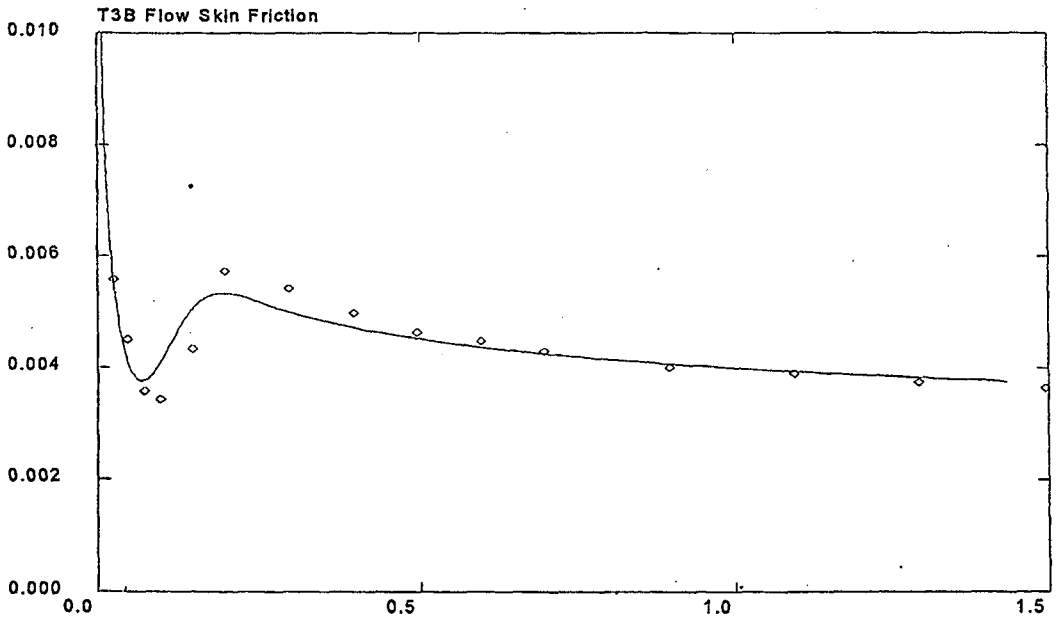
T3B Flow Skin Friction
0.010
0.008
0.006
0.004
0.002
0.000
0.0
0.5
1.0
1.5

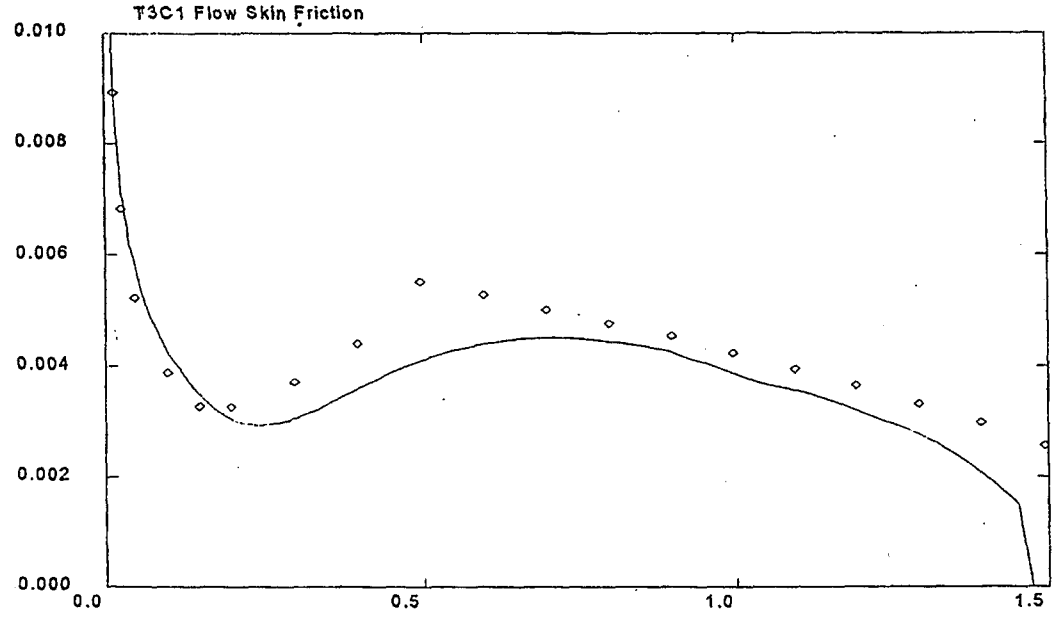
T3C1 Flow Skin Friction
0.010
0.008
0.006
0.004
0.002
0.000
0.0
0.5
1.0
1.5

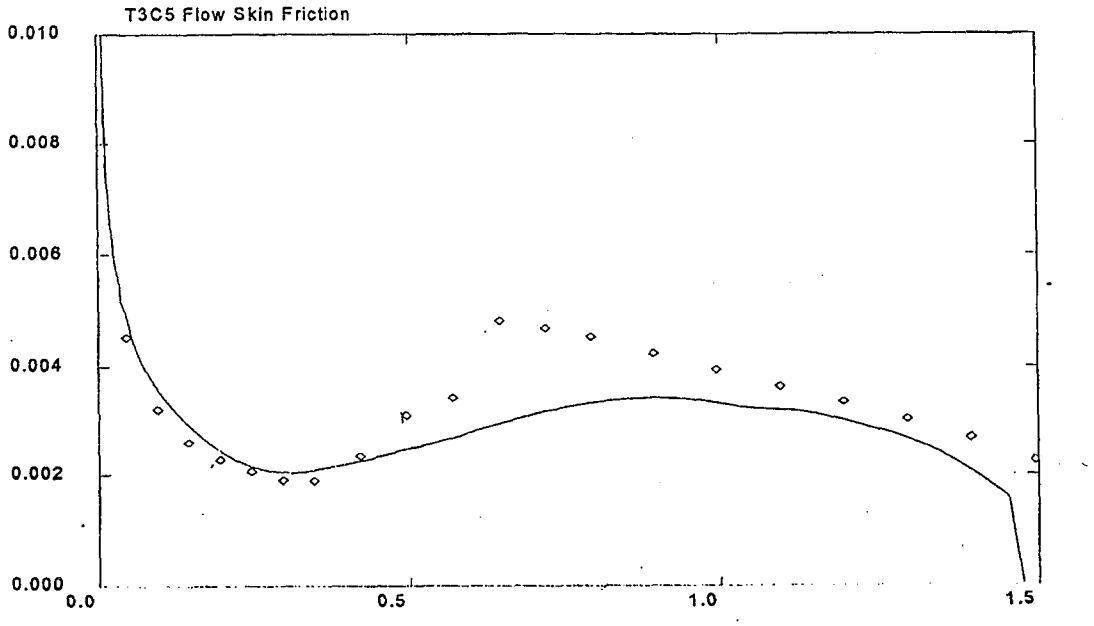

Conclusions

- **The method successfully predicted the transion point for many of the flows under consideration**
- **The method removes many of the ambiguous boundary conditions**
- **computational cells in the transverse direction are minimised**
- **increased cell density in the flow direction is facilitated**

PHYSICAL MODELLING OF BYPASS TRANSITION

Mark W. Johnson
The University of Liverpool
Liverpool, England

ABSTRACT

Empirical correlations are used extensively for predicting transition in turbomachines. A disadvantage of such correlations is that they only account for some of the factors affecting transition (typically freestream turbulence level and streamwise pressure gradient), but other important factors are neglected (e.g., turbulent length scale, blade curvature and blade sweep). The formulation of correlations which will accurately account for all such factors would seem implausible.

The objective of the work at Liverpool has been to improve the understanding of how freestream turbulence induces turbulent spots within a transitional boundary layer and to utilise this knowledge to derive a physical model of the transition process. This alleviates the need for empirical correlation and hence simplifies the task of predicting transition accurately in complex turbomachinery geometries. To this end, extensive wind tunnel experiments on flat plates have been performed. These experiments have established that freestream turbulence induces velocity fluctuations in the near wall region ($y/\delta < 0.2$) of the laminar boundary layer primarily through the unsteady pressure field. These fluctuations increase in strength as the laminar boundary layer develops until the instantaneous velocities minima are sufficiently low to induce transient local separation of the flow. This separation, which has also been predicted elsewhere through Direct Numerical Simulation, is believed to be the mechanism through which turbulent spots are induced. This mechanism has been modelled and incorporated within a simple boundary layer integral code, which has been successfully used for predicting many of the ERCOFTAC test cases (T3A-, T3A, T3B, T3C1-5) and also the measurements of Gostelow and co-workers.

Currently, experimental work is in progress on concave surfaces and future work is planned on swept surfaces. The model will also be developed to predict transition in these flows. Work is also in progress in measuring and predicting relaminarising boundary layers.

OUTLINE

1. **Transition modelling philosophy**

2. **Intermittency - Distributed versus concentrated breakdown models**

3. **Model predictions**

4. **Future modelling and experimental work**

5. **Other boundary layer work at Liverpool**

How does freestream turbulence induce velocity fluctuations near the wall?

Total pressure fluctuations decay rapidly due to shear

Static pressure fluctuations induce 'local' near wall velocity fluctuations

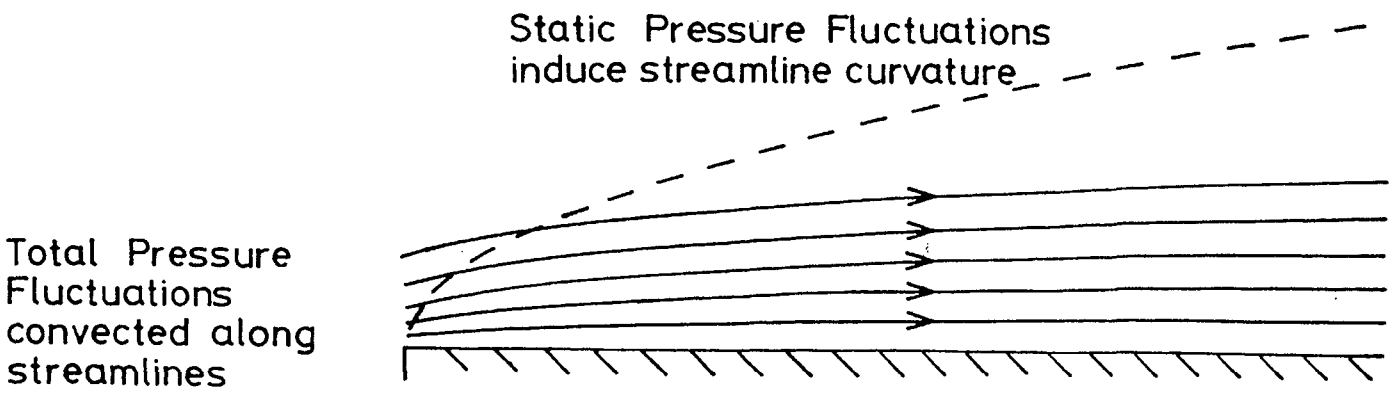

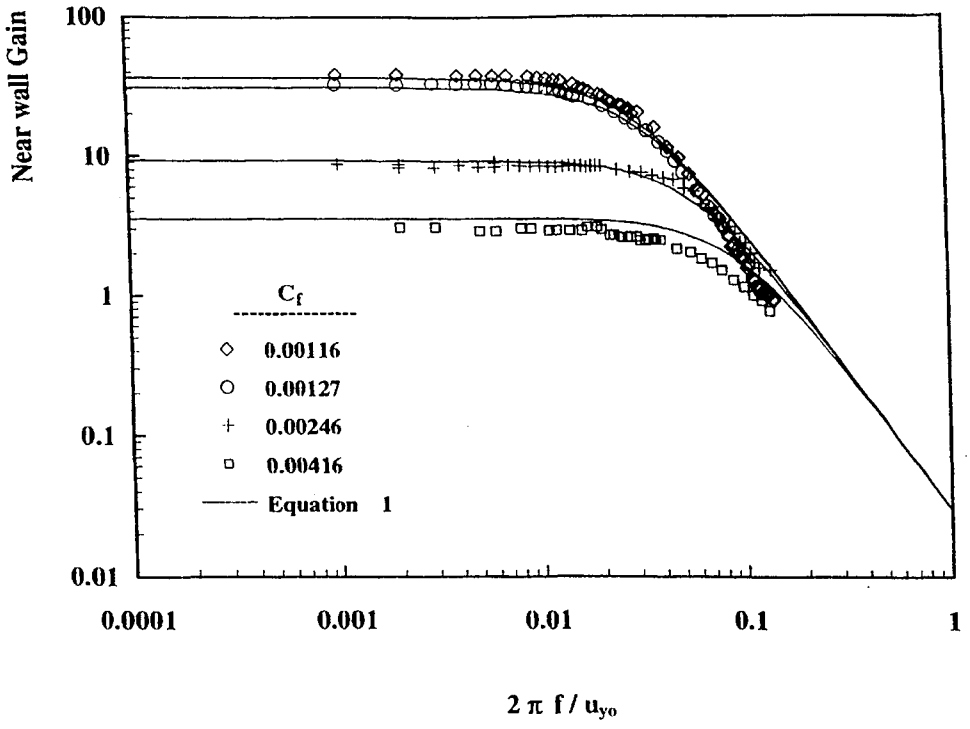

Empirical correlation for near wall gain
(= Near wall turbulence level/freestream turbulence level)

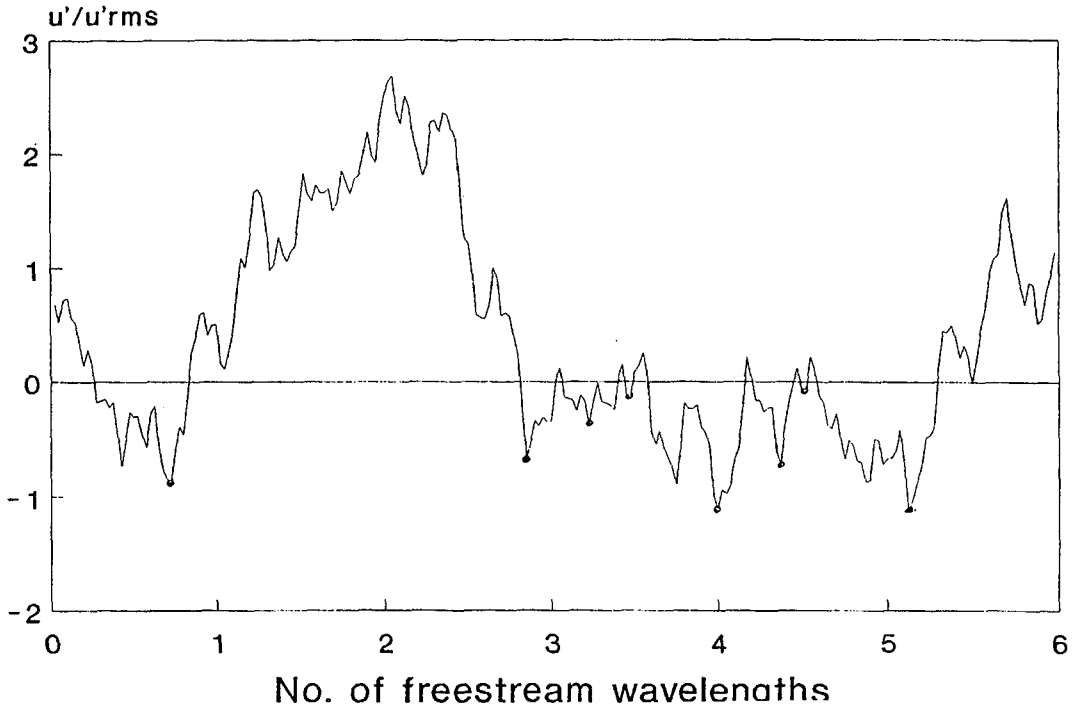

Turbulent spots are induced whenever the instantaneous velocity drops below 50% of the time mean velocity

INTERMITTENCY

$$\frac{dN}{dt} = \underbrace{(1-\gamma)\left[\frac{U_{LE} - U_{TE}}{U_{LE}}\right]\int_0^x PU\left[\frac{z}{\ell}\right]^3 dx}_{\text{spot generation rate}} - \underbrace{\frac{2U_{TE}\,N^2\,\text{Tan}\alpha}{(1-\gamma)}}_{\text{spot merge rate}}$$

where P = Proportion of minima that induce spots

$\frac{z}{\ell}$ = Minima per local wavelength

Also

$$\frac{d\gamma}{dt} = \underbrace{2N\,U_{TE}\,\text{Tan}\,\alpha}_{\text{Spread rate of spots}}$$

and $$\frac{dx}{dt} = U_{TE}$$

Therefore $$\frac{dN}{dx} = \frac{(1-\gamma)\sigma}{U\,\text{Tan}\,\alpha}\int_0^x PU\left(\frac{z}{\ell}\right)^3 dx - \frac{2N^2\text{Tan}\,\alpha}{(1-\gamma)} \qquad (18)$$

and $$\frac{d\gamma}{dx} = 2N\,\text{Tan}\alpha \qquad (19)$$

The current model uses this distributed breakdown model, i.e., $\int_0^x PU\left(\frac{z}{\ell}\right)^3 dx$ varies continuously with x.

NARASIMHA CONCENTRATED BREAKDOWN MODEL

$$\int_0^x PU \left(\frac{z}{\ell}\right)^3 dx = 0 \qquad \text{for} \quad x < x_s$$

$$\int_0^x PU \left(\frac{z}{\ell}\right)^3 dx = n \qquad \text{for} \quad x \geq x_s$$

when substituted into equations (18) and (19) leads to the Narasimha equation for intermittency

$$\gamma = 1 - \exp\left(\frac{-\sigma n (x-x_s)^2}{U}\right)$$

The Narasimha model can be used to predict turbulent spot size distributions through transition, but these differ from the experimental ones.

(See Johnson and Fasihfar, Int. J. Heat and Fluid Flow, Vol. 15, No. 4, August 1994, pp. 283-290.)

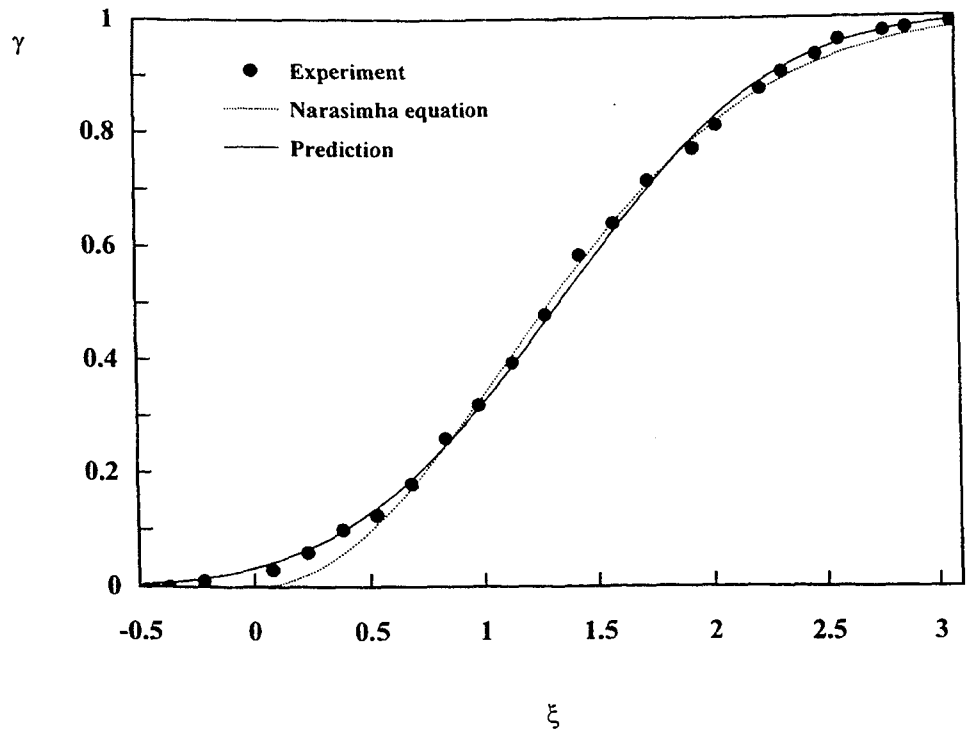

Intermittency model prediction and Narasimha equation for Gostelow Tu = 2.1% zero pressure gradient

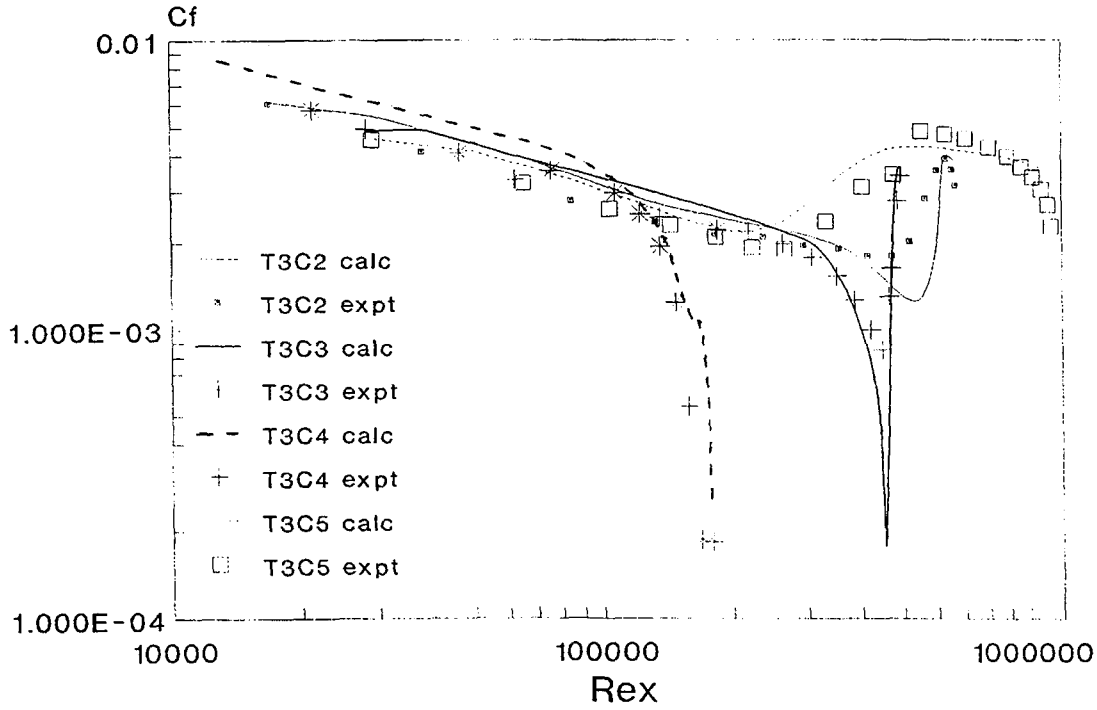

ERCOFTAC Pressure gradient cases T3C2-5

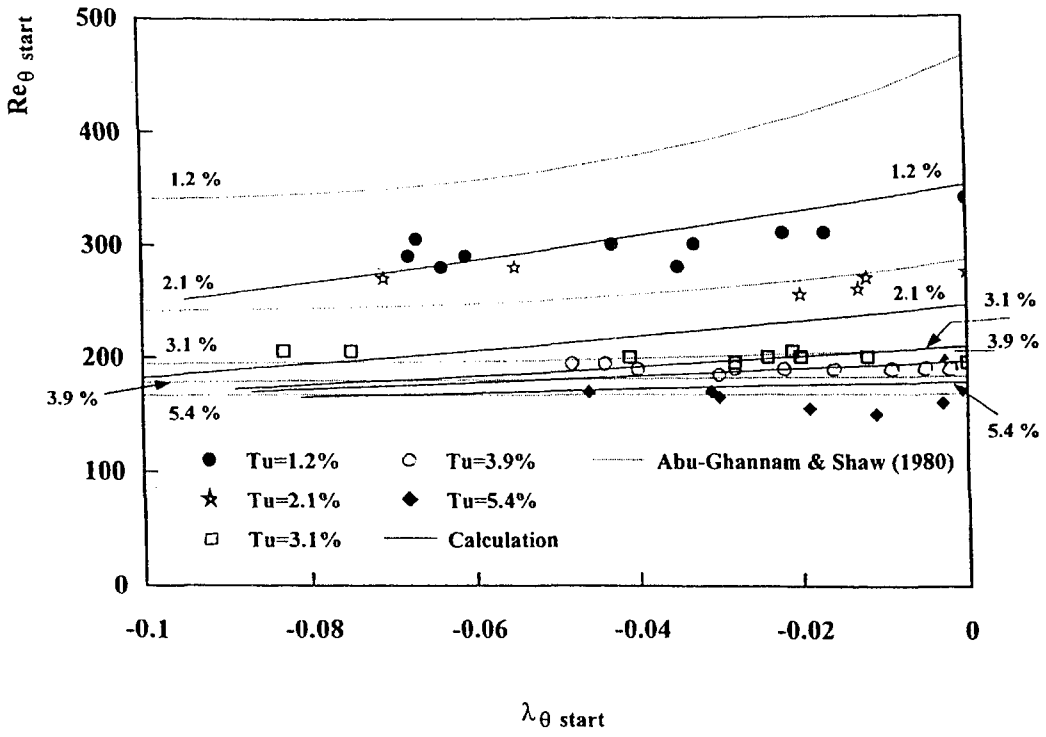

Start of transition, model prediction, Abu Ghannam and Shaw prediction and Gostelow experimental data

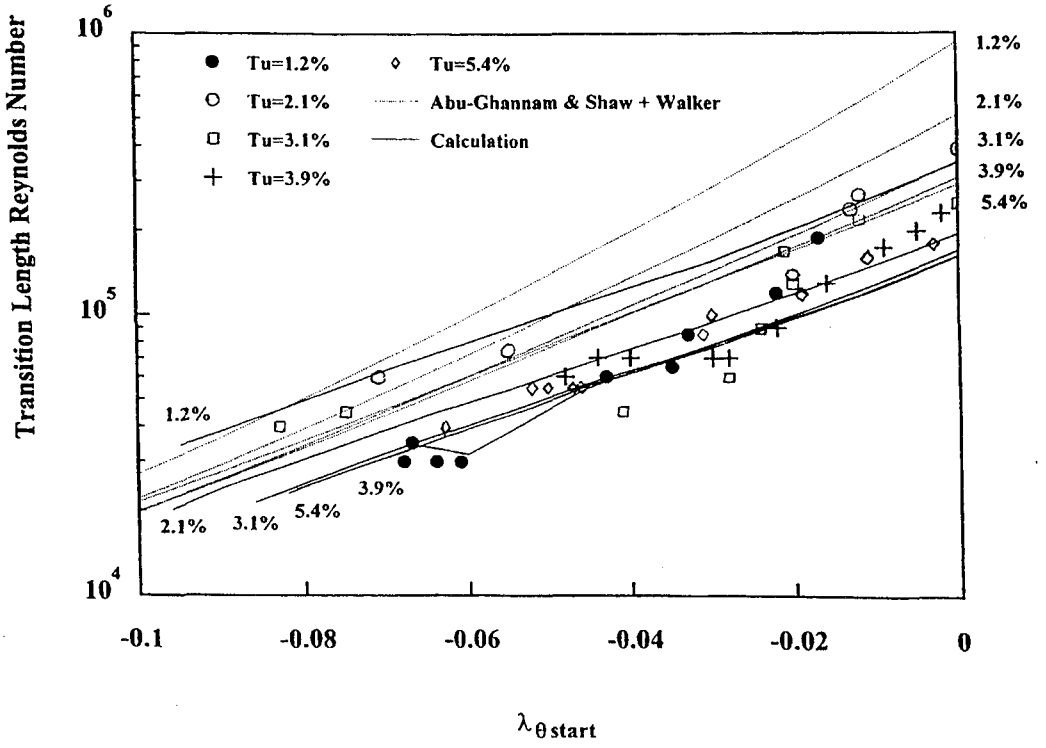

Transition length. Model prediction, Abu-Ghannam and Shaw and Walker length prediction and Gostelow experimental data

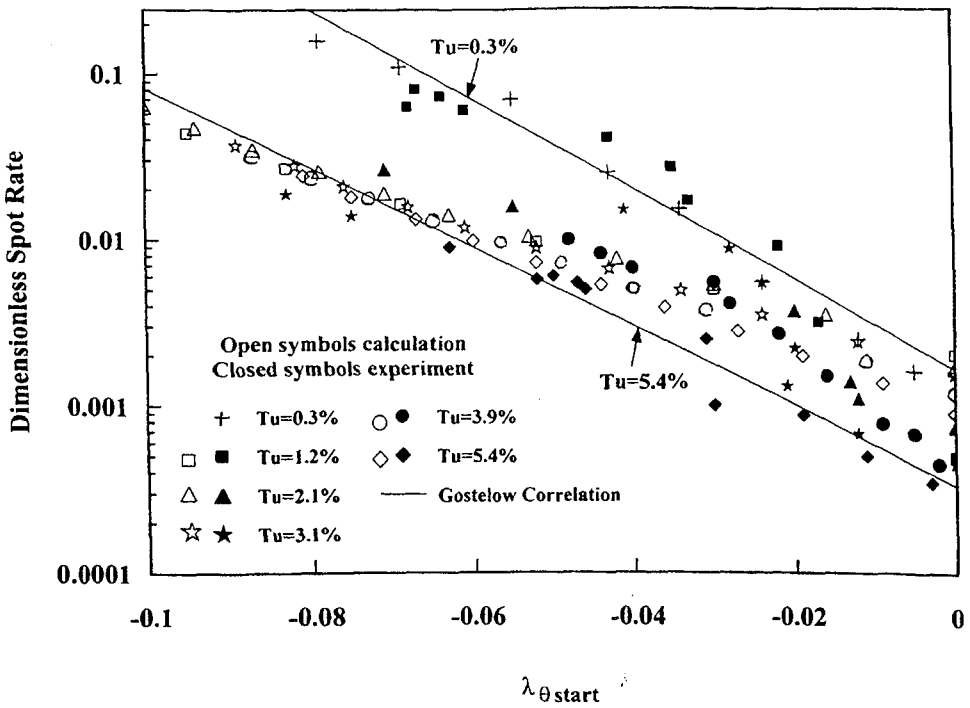

Narasimha spot parameter. Model prediction, Gostelow experimental data and empirical correlation

BOUNDARY LAYER WORK AT LIVERPOOL

1. **Relaminarisation due to rapid acceleration with blade sweep.**

2. **Compliant surface drag reduction for turbulent flow.**

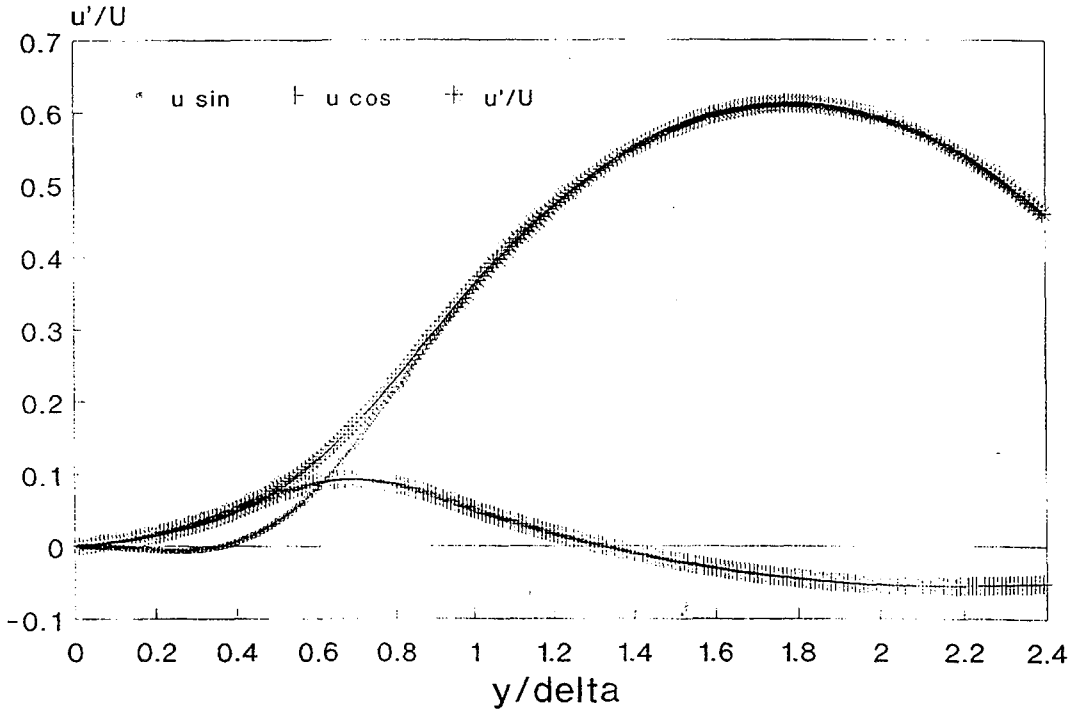

B.l. receptivity. Low frequency.

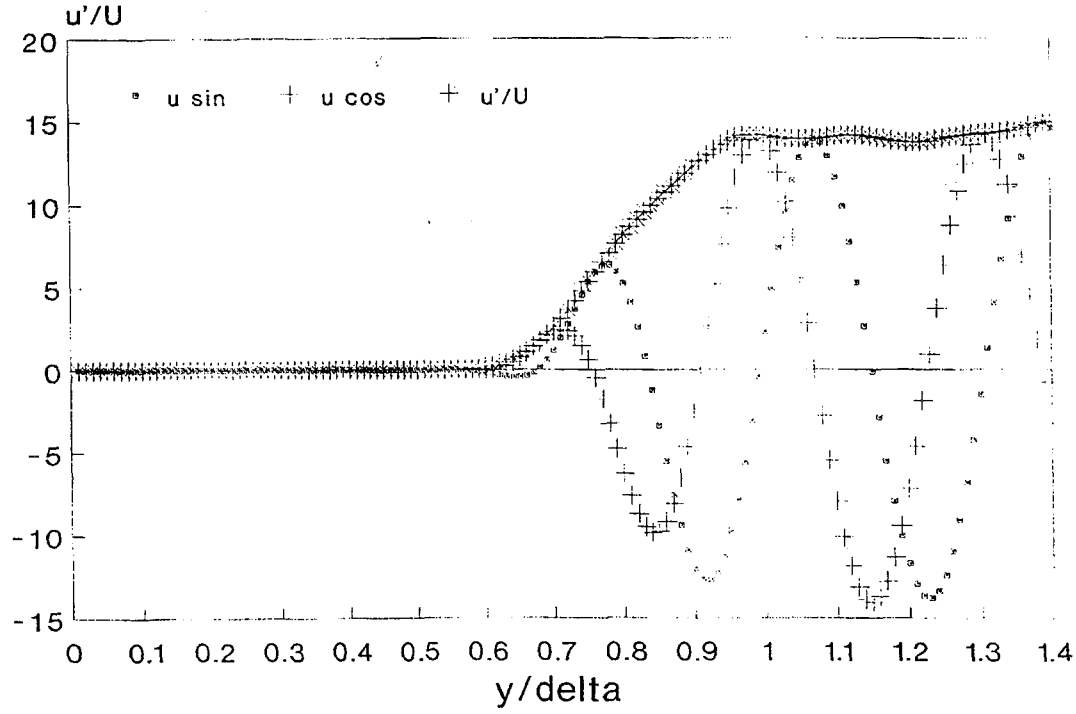

B.l. receptivity. High frequency

FUTURE WORK

Modelling

1. **Elimination of 3 empirical coefficients for near wall gain by solving unsteady Navier Stokes equations (currently 2-d).**

2. **Elimination of empirical coefficients for spot development (leading and trailing edge velocities and spreading angle).**

3. **Incorporation of model in CFD code (i.e., differential rather than integral procedure).**

Experimental

1. **Concave surface curvature**
   (a) **Laminar boundary layer profiles**
   (b) **Receptivity**

2. **Effect of blade sweep**

FORCED TRANSITION MEASUREMENTS IN THE NEW INEEL MATCHED-INDEX-OF-REFRACTION FLOW SYSTEM

Donald M. McEligot
Idaho National Engineering and
Environmental Laboratory
Idaho Falls, Idaho

A joint project is underway to measure the structure of the laminar-to-turbulent transition induced by roughness elements. A goal is provide benchmark data for the assessment and guidance of numerical predictive techniques for the effects of two- and three-dimensional geometries in inducing transition. In addition to applications to enhance heat, mass and momentum transfer, to assist in controling lift and drag on laminar airfoils and to improve fundamental understanding, the geometries can provide qualitative simulation of the effects of injection of fluid into laminar boundary layers on turbine blades (film cooling).

Preliminary data have been obtained in the wind tunnel at the Lehrstuhl für Strömungsmechanik (LSTM) using a two-dimensional rectangular rib roughness element on a flat plate with a NACA 0009 airfoil shape as the leading edge. Angle-of-attack was adjusted to yield a negligible streamwise pressure gradient. Benchmark data will be obtained in the liquid tunnel of the new Matched-Index-of-Refraction (MIR) flow system at the Idaho National Engineering and Environmental Laboratory (INEEL).

The INEEL MIR flow system is considerably larger than other MIR facilities; the square cross section is 60 cm on each side and about 2-1/2 meters long. Its low velocity and large size give good spatial resolution at a given Reynolds number and, in turn, good temporal resolution. Refractive-index-matching leads to reduction of noise in near-wall laser Doppler velocimeter measurements, a key benefit in the present program. In addition to flows in internal or external turbine blade passage configurations, experiments that can benefit from use of the MIR facility include complex flows in engine compartments, in electronic assemblies, in tube bundles, near sharply-concave surfaces, through porous media and in or around other complicated geometries plus two-phase particulate flow.

The initial experiments, preliminary results, ongoing studies and plans will be discussed.

Forced transition measurements in the new INEEL Matched-Index-of-Refraction(MIR) flow system

Donald M. McEligot, Idaho National Engineering and Environmental Laboratory
and
Stefan Becker and Franz Durst, Lehrstuhl für Strömungsmechanik, Uni. Erlangen

Ultimate *goal* ----> Reliable predictive techniques for transitional behavior in turbomachine passages -- based on benchmark measurements

Transition problems in turbomachines

- o Laminar ---> turbulent transition in external boundary layers of blades
- o Internal cooling passages -- laminarization due to heating ?

The work reported was partly supported by the Deutsche Forschungsgemeinschaft (DFG) and by the Long Term Research Initiative Program of the Idaho National Engineering and Environmental Laboratory / Lockheed Martin Idaho Technologies Company under DOE Idaho Field Office Contract DE-AC07-94ID13223

Structure of transition due to roughness elements

Applications of induced transition

- o Enhanced heat, mass and momentum transfer
- o Lift and drag control on laminar airfoils
- o Flow over small airfoils
- o Fundamental understanding
- o (Very) qualitative simulation of transition due to a row of jets (e.g., film cooling)

Approach

Obtain *careful, high precision measurements* in the INEEL MIR flow system (Durst, McEligot) (Condie, McEligot)

for assessment and guidance in the

development of *numerical predictive techniques* ( )

2-D ------> 3-D

Initial objectives -- 2-D element

- o Conduct measurements of the structure of the transition process
- o Evaluate the effects of Reynolds number on the resulting near-wall turbulent flow, negligible pressure gradient (i.e., separate effects)
- o Develop numerical predictions - DNS, other

Preliminary measurements

Wind tunnel at LSTM, Uni. Erlangen, with a hot wire sensor

INEEL Matched-Index-of-Refraction system

Goal = *versatile* system with good temporal and spatial resolution *for complex flows*

Characteristics: *Internationally unique facility*
- Resolution, H/d_{meas} ---> 2×10^4, ~ 5-10 x typical
- Reynolds number, ~ 5 x typical

Permits optical measurements otherwise impossible
Pump designed for 340 lps, 3 m head; current contraction ~ 4:1
Test sections to 1.3 x 1.3 m^2, 2D or circular/annular,
currently 60 x 60 cm^2, length ~ 2.5 m
Velocity to ~ 2 m/sec, Re' —> ~ 1.7×10^5/m
Temperature control to match refractive index

Experiments that will benefit: Complex geometries
- Curved surfaces (turbine blade passages), flow junctions
- Unsteady flows induced inside building and vehicle models
- Flow in porous media, such as core debris; particulate flows
- Enhanced internal cooling passages
- Near wall turbulence (viscous layer $y^+ < 50$)
- Active control of turbulent flows, scaled MEMS models
- Rod bundles for Spent Nuclear Fuel drying and storage

Instrumentation: LDV, flow vis, HFA, PDA, Δp, p(t)

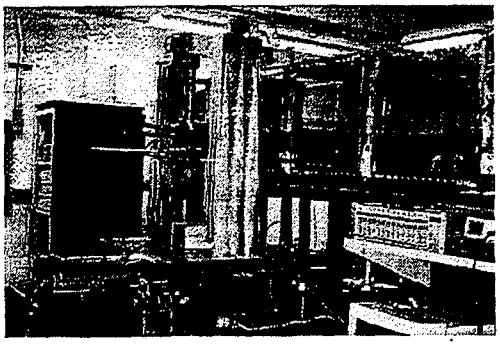

Potential experiments

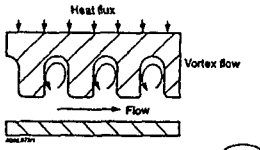

- Flow field in a Hypervapotron
- Particulate transport in tubular swirl flow

- Impinging jets, with and without particles

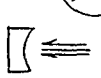

- o Flow through film cooling holes

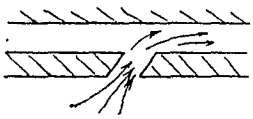

- o TBL on riblet-modified surfaces
- Turbulence modification by particles
- o Velocity and concentration measurements in static mixers
- Flow through tube bundles and arrays of elements

FY-98 experimental concept

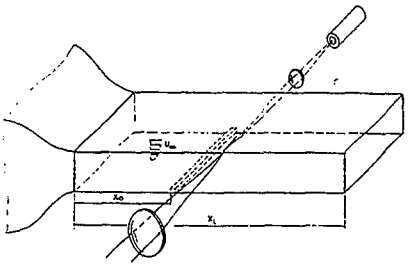

Advantages of INEEL MIR flow sys

o Low velocity ——> Re' ≈ 1.7 x 10^5 1/m ------> large size

-------> Good spatial resolution

o Large size + low velocity ($t^+ = t\,V / L$ —> $t = t^+ L / V$)

-------> Good temporal resolution

o Refractive-index-matching and forward scattering ---> reduction of noise in near-wall data ----> "high" signal-to-noise ratio

-------> Benchmark data

Model

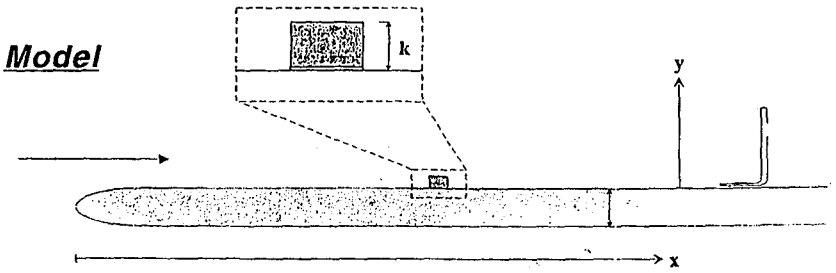

- o Flat plate, negligible dp/dx, NACA 0009 leading edge
- o Roughness element, 2 x 1 cross section, $k \approx \delta / 2$

Conditions

- o $U_{\infty} \approx 0.5$ ---> 2 m/s, L ---> ~ 6 ft ≈ 2 m
- o Re_L ---> ~ 3×10^5, Re_k variable
- o Sensor size $d+ \approx 0.03$ Positioning $\delta y+ \approx 0.001$

FY-98 measurements (winter/spring)

- o Check laminar boundary layer
- o Effects of plate thickness ?
- o Effects of k and Re
  - u{x,y,t}, v{x,y,t} ---> U{x,y}, V{x,y}
  - Disturbance growth vs Re_x
  - Spectra vs Re_x

Future plans

- o Transition behavior for 3-D geometries
- o Turbine blade "cascade"
- o Effect of injection (film cooling) and pressure gradient on transition
- o Other suggestions ?

SESSION 5

TRANSITION IN TURBOMACHINES—II

NASA/CP—1998-206958

FLOWFIELD UNSTEADINESS AND TURBULENCE IN MULTISTAGE LOW PRESSURE TURBINES

David E. Halstead
GE Aircraft Engines
Cincinnati, Ohio

ABSTRACT

Experiments were conducted to measure flowfield unsteadiness and turbulence in a multistage, axial–flow, low pressure turbine. Measurements were obtained at inter– bladerow stations extending from the inlet to exit of the machine. The streamwise and transverse velocity components were resolved using an X hot–film probe. Characteristics of the turbulence environment are quantified in terms of intensity, length scale, and the turbulence energy spectrum. For the first time, measurements of length scale from a low pressure turbine are reported. A procedure to calculate turbulence length scale based on the frequency–averaged spectra is presented.

In the low pressure turbine, levels of turbulence intensity are found to increase progressively across the two stages of blading. Length scales measure nominally thirty percent of the throat width of the upstream bladerow. The complexity of the time–unsteady flowfield between bladerows is shown to increase markedly through the turbine. At the inlet to the second stage nozzle, the unsteadiness correlates directly to the circumferential clocking position of the upstream nozzle bladerow. At the exit of the turbine, there is no discernible "freestream" region in the time–varying distribution of turbulence intensity. This suggests simulation experiments carried out using wake generators upstream of an airfoil cascade or using a single stage turbine will not simulate many features of the flowfield in multistage machines.

The measurements are presented in a manner that they can be used readily to establish relevant inlet conditions for experimental facilities and for CFD analyses.

- **Objectives**
- **Test Facility and Instrumentation**
- **Calculation of Turbulence Quantities**
- **LSRT Measurements**
- **Concluding Observations and Thoughts**
- **Nomenclature**

Objectives

- Determine the nature of the disturbance environment in multi–stage LP turbines.
  - What magnitudes of turbulence intensity and length scale are found in actual LP turbines?
  - How does the disturbance environment develop from bladerow to bladerow?
  - How does bladerow clocking impact the disturbance environment?
- Establish a standard approach by which turbulence measurements from turbomachines are acquired and reported.

Why is this important?
- Accurate boundary conditions for model development and CFD
- Relevant test conditions for multi–stage simulation experiments (i.e., cascades, single stage machines, etc.)

Low Speed Research Turbine

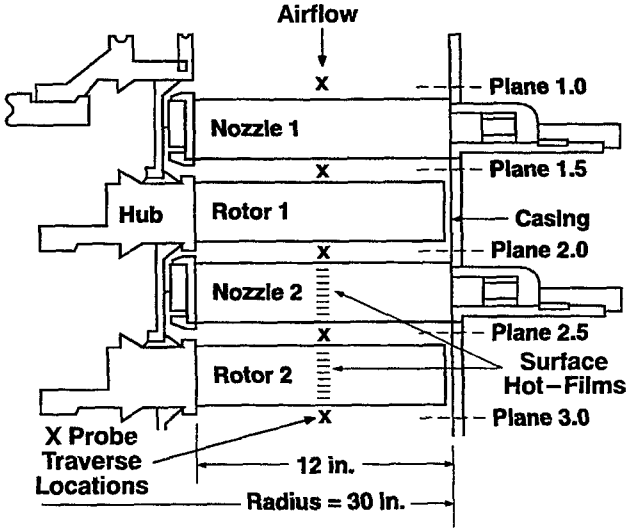

- Models low–pressure turbine blading of a commercial GEAE engine family.
- Instrumentation
  - X hot–film probe in axial–tangential plane
  - midspan only
  - supports modified to mitigate prong vibration
- Nominal Design Point:
  RPM=600 U_{mid}=126 ft/s
  ϕ=1.03 ψ=1.17
  k_{rotor}=1.3 k_{nozzle}=0.75
  Re_{SSL}=100k–500k

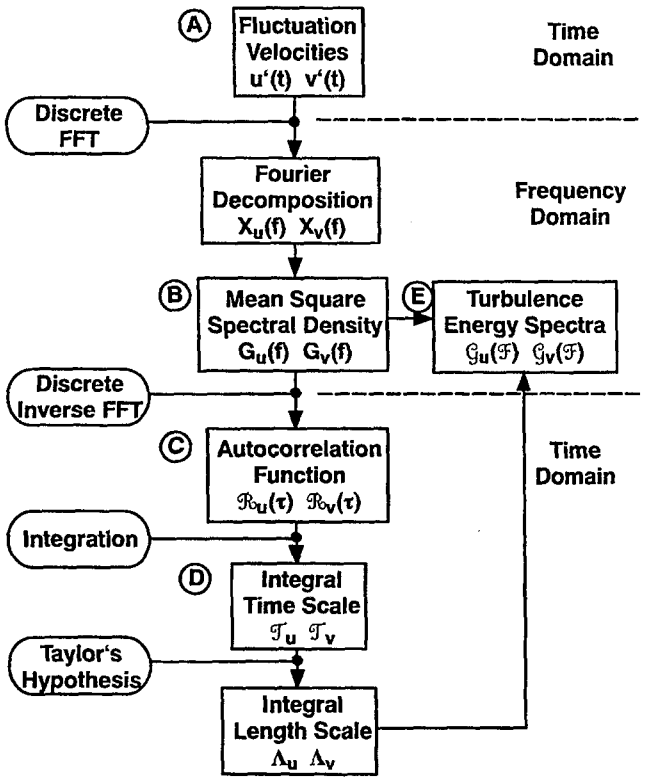

Calculation of Turbulence Parameters

- "Conventional" approach applied to periodically unsteady flowfield.
- Periodic and "random" unsteadiness decomposed via ensemble averaging.
- Spectral analyses based on frequency average of data ensemble.

A) Instantaneous Time Traces of Fluctuation Velocity

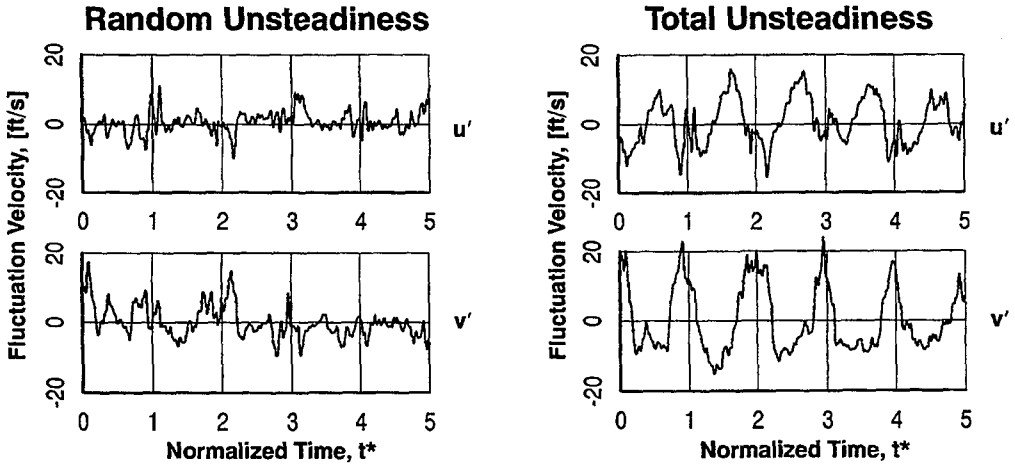

- Data set acquired at exit of Nozzle 2, Plane 2.5, N2 at 68% pitch
  - Velocity trace n=1 of 300
  - u=streamwise component, v=transverse component

B) Mean Square Spectral Density

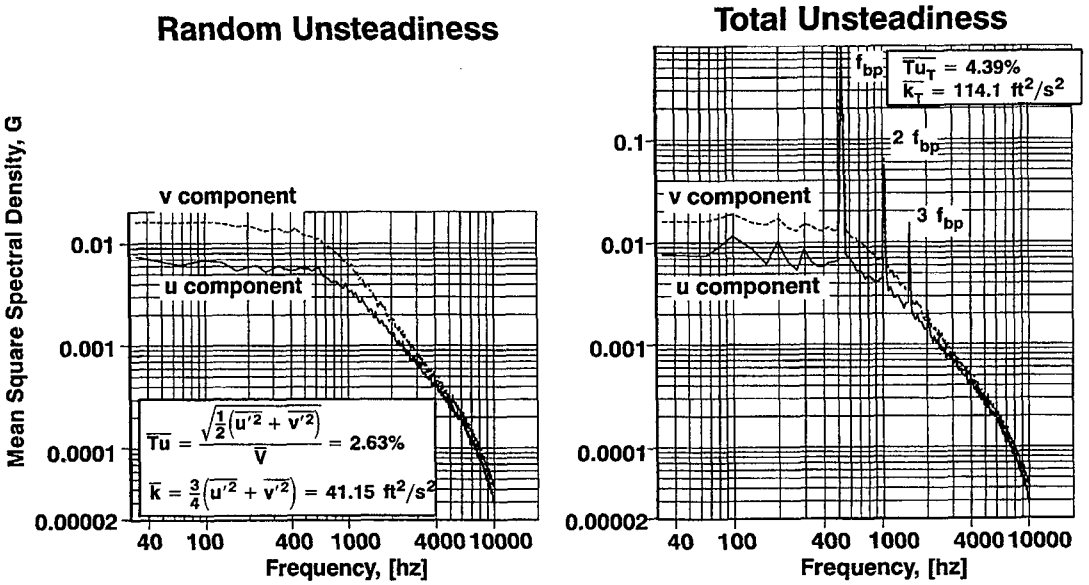

- Frequency average of 300 individual spectra
- Data set acquired at exit of Nozzle 2, N2 at 68% pitch

C) Auto Correlation Functions

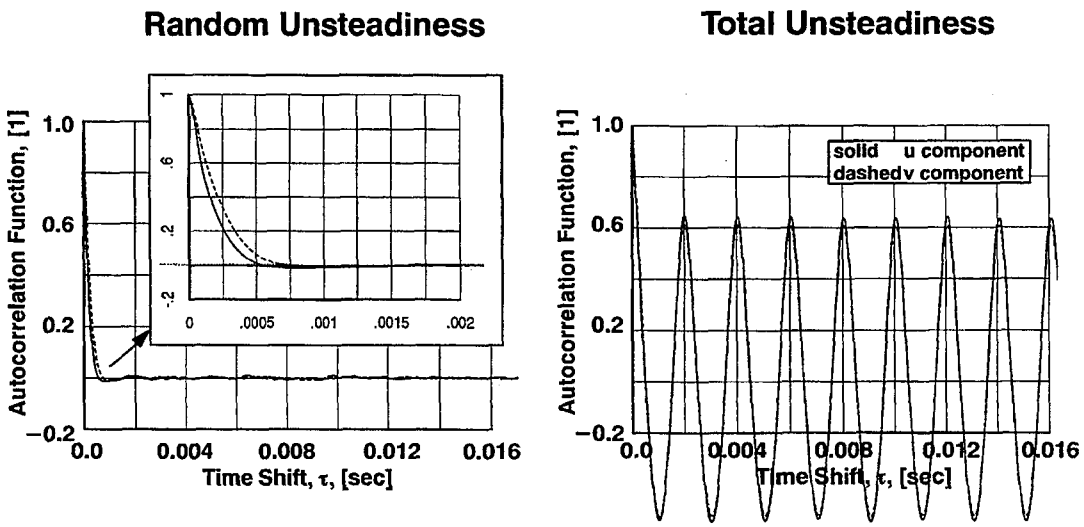

- Data set acquired at exit of Nozzle 2, N2 at 68% pitch

D) Integral Time Scale

Cumulative Integral Summation
(Random Components Only)

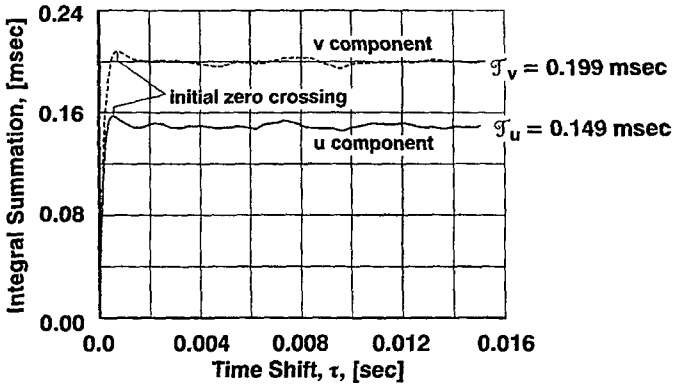

• Data set acquired at exit of Nozzle 2, N2 at 68% pitch

E) Turbulence Energy Spectra

Streamwise Component

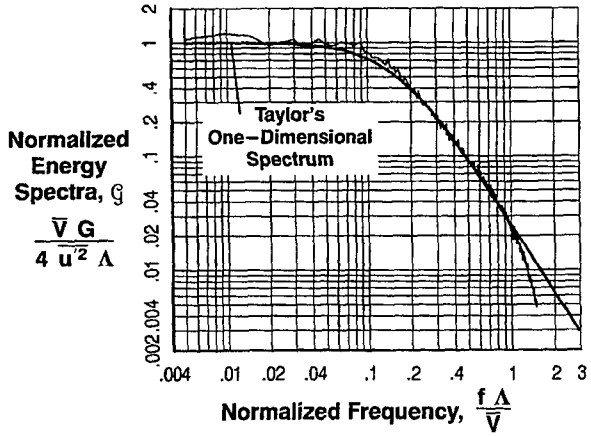

• Data set acquired at exit of Nozzle 2, N2 at 68% pitch

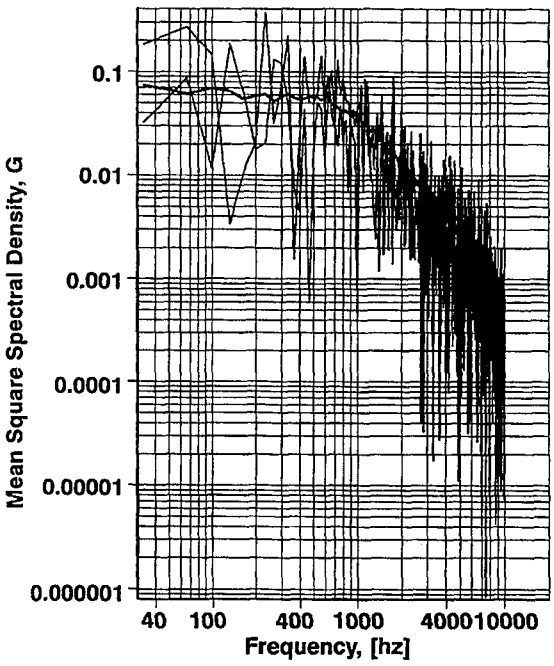

Comparison of Individual and Frequency Averaged Spectra

- Individual–trace MSSD's: light weight lines
- Frequency–Averaged MSSD: heavy weight line
- Data set acquired at exit of Nozzle 2, N2 at 68% pitch, streamwise component

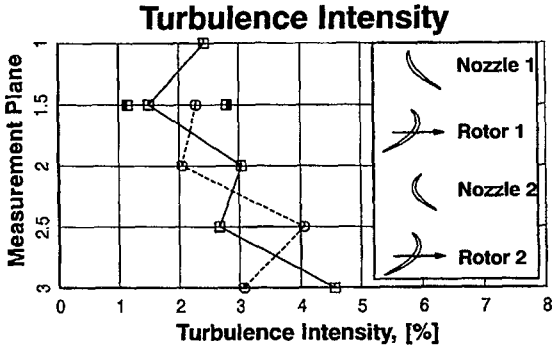

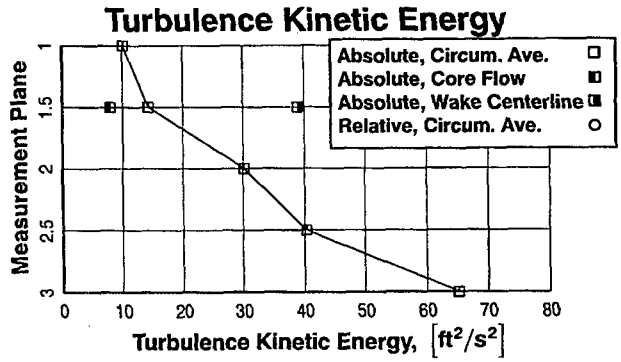

Averaged Turbulence Characteristics

- Midspan
- Averaged temporally and spatially across airfoil pitch
- Inlet conditions to turbine:
  - flat P_t profile
  - isotropic turbulence
- Tu and TKE increase continuously across turbine

∴ *"MULTI–STAGE ENVIRONMENT" LIKELY NOT ACHIEVED WITH RESPECT TO TURBULENCE*

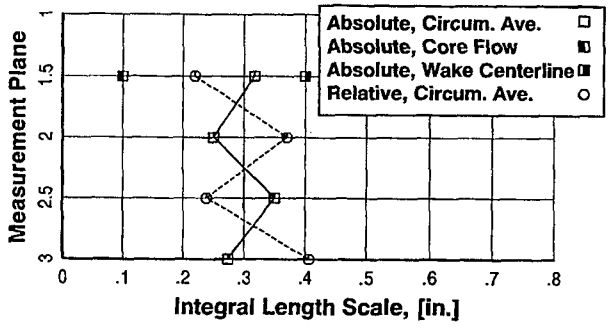

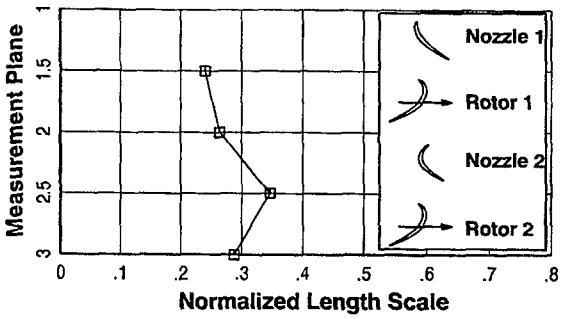

Averaged Turbulence Characteristics

Integral Length Scale

- Midspan
- Averaged temporally and spatially across airfoil pitch
- Length scales do not change significantly across turbine
- Normalized scales:
  - throat of upstream bladerow
  - reference of frame of downstream bladerow

∴ *LENGTH SCALES ~30% THROAT WIDTH OF UPSTREAM BLADEROW.*

Circumferential Variation of Turbulence Intensity

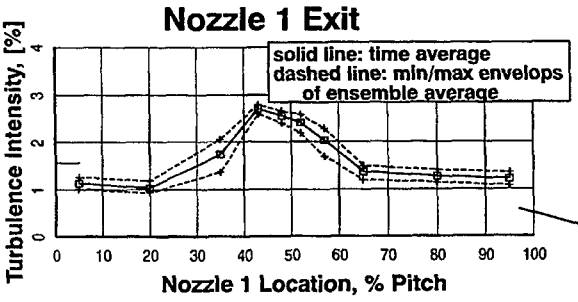

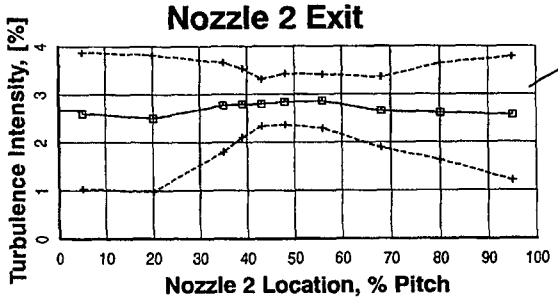

- Nozzle 1 Exit
  - Conventional turbulence signature
    - highest in wake
    - lowest between wakes

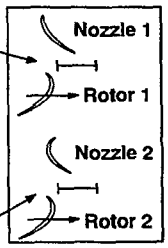

- Embedded Nozzle 2 Exit
  - N2 wake not distinguishable by time–average turbulence intensity
  - Modulation of min / max turbulence occurs across nozzle pitch

Wake Interaction in a Multi–Stage LP Turbine

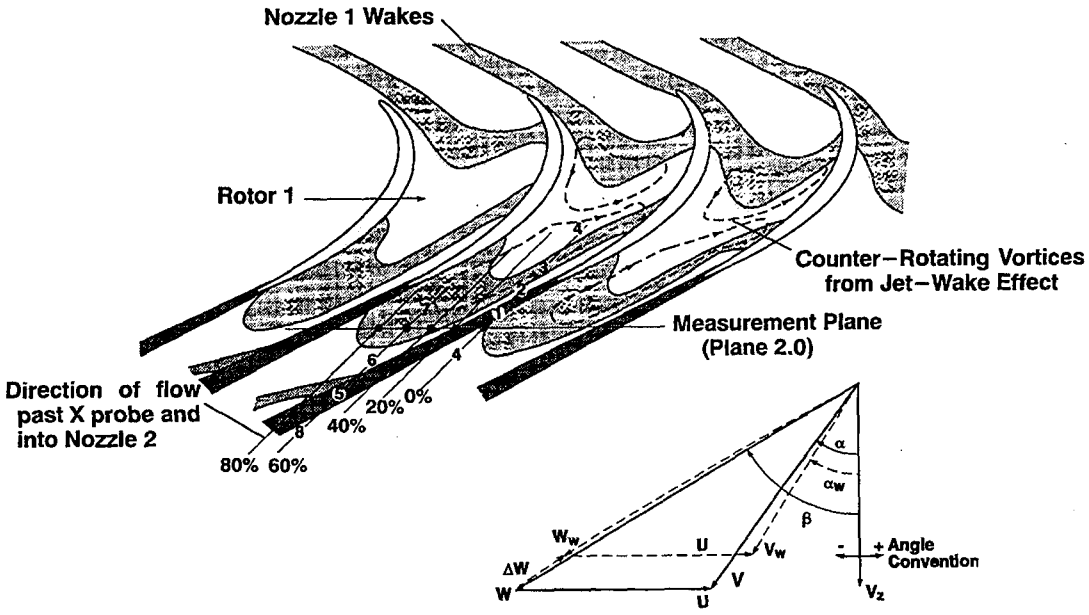

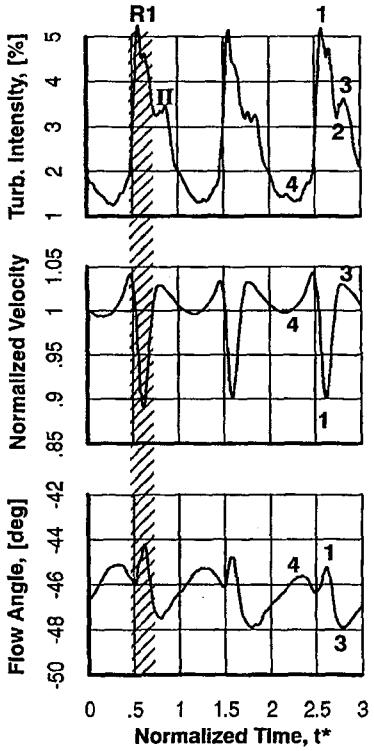

Time Unsteady Flow Inlet to Nozzle 2

Nozzle 1 at 0% Pitch

- Ensemble averages
- Region 1) Rotor 1 Wake
  – highest Tu, lowest velocity, underturned
- Region 3) Nozzle 1 Wake Segment
  – local Tu peak, overturned
- Region 4) Between Wakes/Wake Segments
  – lowest Tu, underturned

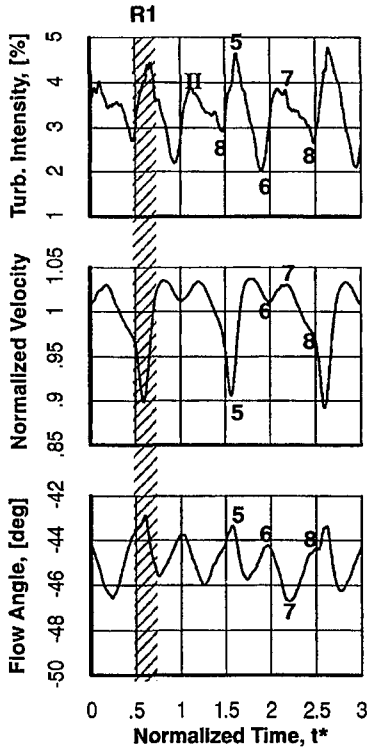

Time Unsteady Flow Inlet to Nozzle 2

Nozzle 1 at 60% Pitch

- Ensemble averages
- Region 5) Rotor 1 Wake
  - highest Tu, lowest velocity, underturned
- Region 7) Nozzle 1 Wake Segment
  - local Tu peak, overturned
- Tu of N1 wake segment nearly equal to that of R1 wake

Effect of Nozzle 1 Clocking on Nozzle 2 Boundary Layer Development

Description of s–t diagrams

- Random unsteadiness of surface shear stress from hot–film sensors
  - red: highest
  - blue: lowest
- Regions:
  - A) laminar
  - B) wake–induced transitional strip
  - C) wake–induced turbulent strip
  - D) calmed region
  - E) transition between wakes
  - F) turbulent flow between wakes
  - G) calmed region

∴ *BOUNDARY LAYER DEVELOPMENT IS RELATED DIRECTLY TO INLET DISTURBANCE ENVIRONMENT. ADDED COMPLEXITY FROM BLADEROW INDEXING NOT CAPTURED BY CASCADE+ROD AND SINGLE STAGE TURBINE FACILITIES.*

Effect of Nozzle 1 Clocking on Nozzle 2 Boundary Layer Development

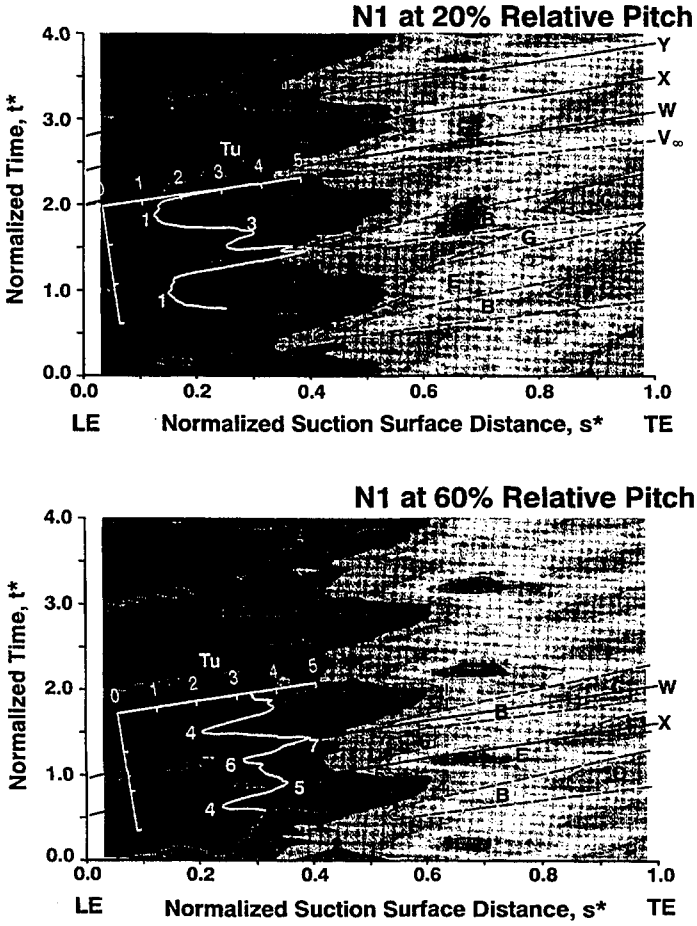

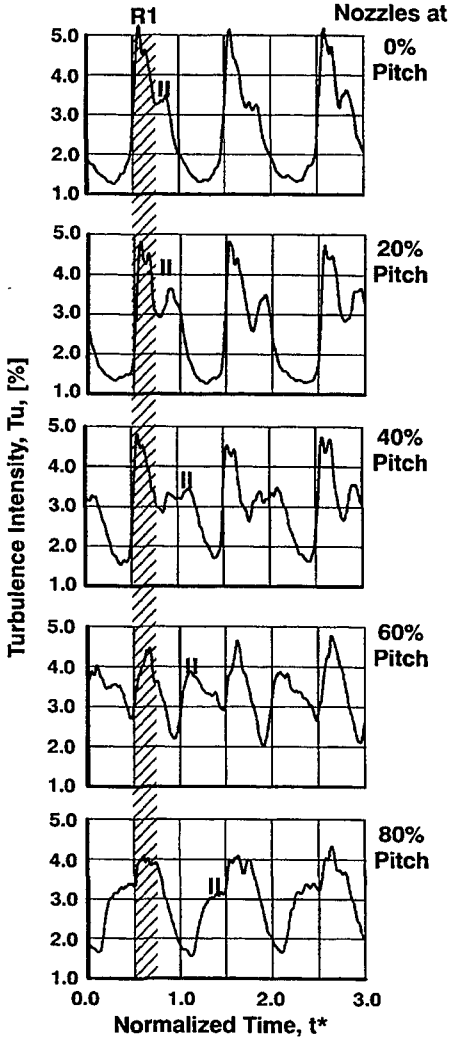

Time Unsteady Flow Inlet of LSRT Nozzle 2

- Ensemble average turbulence intensity
- Absolute reference frame
- Migration of N1 wake segment evident between R1 wakes
- Tu of N1 wake segment nearly equal to that of R1 wake for some clocking orientations
- Character of N1 wake segment varies significantly with clocking

∴ *CONVENTIONAL "FREESTREAM" BETWEEN ROTOR WAKES DOES NOT EXIST IN THE MULTI–STAGE ENVIRONMENT.*

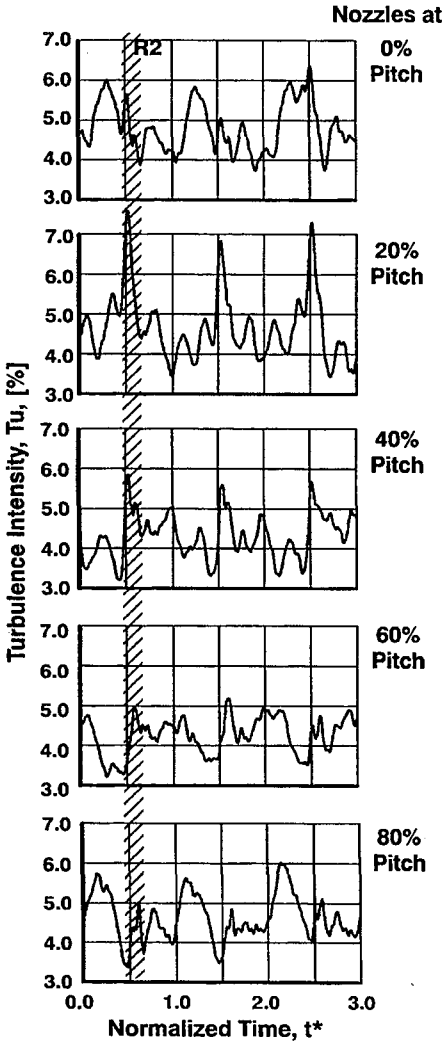

Time Unsteady Flow Exit of LSRT Rotor 2 (Inlet of Nozzle 3)

- Ensemble average turbulence intensity
- Absolute reference frame
- Nozzles 1 and 2 indexed in tandem
- Significantly higher Tu levels than behind Rotor 1
- Highest Tu occurs between R2 wakes for 0% and 80% clocking orientations
- Distinct $4f_{bp}$ variation at 20% and 40% clocking orientations

Concluding Observations and Thoughts

In the Two–Stage LSRT:

- **Turbulence intensities range from up to 5–7+% in wakes and well over 3% between wakes.**
  - **– may be conservative relative to engine environment**

- **The disturbance environment is impacted significantly by wake interaction and bladerow indexing.**
  - **– For embedded bladerows, the conventional model of wake flow superimposed with a "freestream" flow is not valid.**
  - **– This interaction can not be simulated in single stage or cascade+rod facilities and is not accounted for in the "classical" s–t diagrams of boundary layer development.**

- **Integral length scales measured ~30% of upstream blade-row throat. More data needed from other facilities.**

Comments on simulation experiments:

- **Will continue to play an important role in turbomachine boundary layer research.**

- **Experiments must be carried out with relevant test conditions:**
  - **– wake and between–wake turbulence intensity.**
  - **– length scale.**

- **Great care must be excerised when extrpolating these findings to the engine environment.**

∴ UNCERTAINTY REMAINS ABOUT THE DISTURBANCE ENVIRONMENT IN MULTI–STAGE LP TURBINES. INDUSTRY MUST TAKE THE LEAD IN ADDRESSING THIS ISSUE.

NOMENCLATURE

f, f_{bp}	frequency, blade–passing frequency, [hz]
$\mathcal{F}_k$	dimensionless wave number, $f\Lambda/\overline{V}$
G	mean square spectral density, [ft^2/s^2/hz]
$\mathcal{G}_k$	dimensionless turbulence energy spectrum, $\frac{G_i\overline{V}}{4\overline{u_i'^2}\Lambda_i}$, ith coordinate direction
k	turbulence kinetic energy, TKE
	reduced frequency, $f_{bp}s/V_{ex}$, where s is surface length
Re	Reynolds number based on suction surface length, SSL, and bladerow exit conditions, $V_{ex}SSL/\nu$
$\mathcal{R}(\tau)$	auto–correlation coefficient with respect to time shift, τ
s^*	normalized surface distance
t^*	time normalized by blade passing period
Tu	turbulence intensity
$\mathcal{T}$	integral time scale, $\int_0^\infty \mathcal{R}(\tau)d\tau$
U_{mid}	midspan blade speed
u', v'	fluctuation velocities in streamwise and transverse directions
X	Fourier coefficients
Λ	integral length scale, $\mathcal{T}\overline{V}$
ϕ	specific flow, V_z/U_{mid}
ψ	specific work, $\frac{\Delta H_t}{2U_{mid}^2 N_{stages}}$
	where ΔH_t = change in total enthalpy across turbine

AN EXPERIMENTAL INVESTIGATION OF TRANSITION AS APPLIED TO LOW PRESSURE TURBINE SUCTION SURFACE FLOWS*

Songgang Qiu and Terrence W. Simon
University of Minnesota
Minneapolis, Minnesota

ABSTRACT

Results of an experimental study of flow separation and transition in either attached boundary layers or separated shear layers over the suction surface of a simulation of a low-pressure turbine airfoil flow are presented. Detailed velocity profiles were measured with the hot-wire technique. Static pressure distributions are also presented. Flow transition is documented using measured intermittency distributions in the boundary layer and the separated shear layer. Cases for Reynolds numbers of 50,000, 100,000, 200,000 and 300,000 are reported. These Reynolds numbers are based on suction surface length and exit velocity. Three Free Stream Turbulence Intensity values, 0.5%, 2.5% and 10%, are represented. Flow separation is observed for all the low-FSTI cases. Of these, the lowest Reynolds number case was not able to complete transition of the shear layer and the separation bubble persisted over the entire blade surface. For the other low-FSTI cases, transition is observed in the shear layer over the separation bubble. This transition proceeded quickly, spreading rapidly toward the wall. Elevated FSTI drives an earlier transition than in the low-FSTI cases and the separation bubbles are smaller. For the highest Reynolds number cases with 2.5% and 10% FSTI, transition is of the attached boundary layer and no separation exists. Flow separation with shear flow transition is observed for the lower-Re cases. Models for intermittency and transition length and location from the modern literature are assessed.

OBJECTIVES:

TO DOCUMENT TRANSITION AND SEPARATION BEHAVIOR IN FLOWS WHICH ARE REPRESENTATIVE OF SUCTION SURFACE LAYERS ON LOW-PRESSURE GAS TURBINE AIRFOILS.

THE STUDY IS DONE WITH REPRESENTATIVE:
- ACCELERATION PROFILES
- CURVATURE PROFILES
- FREE-STREAM TURBULENCE INTENSITIES

TO ASSESS MODELS FOR:
- TRANSITION INCIPIENCE
- TRANSITION LENGTH
- INTERMITTENCY
- SEPARATION LOCATION
- REATTACHMENT LOCATION

* Work supported by NASA Lewis Research Center (Grant no. NAG3-1732).

AIRFOIL SURFACE FLOWS

BACKGROUND:

- A substantial fraction of the boundary layer on a gas turbine airfoil is transitional (Mayle 1991)

- Understanding and utilizing separated-flow transition can easily increase low-pressure turbine efficiency by several percentage points (1991 Mayle)

SEPARATION OF BOUNDARY LAYERS ON AIRFOIL SUCTION SIDES

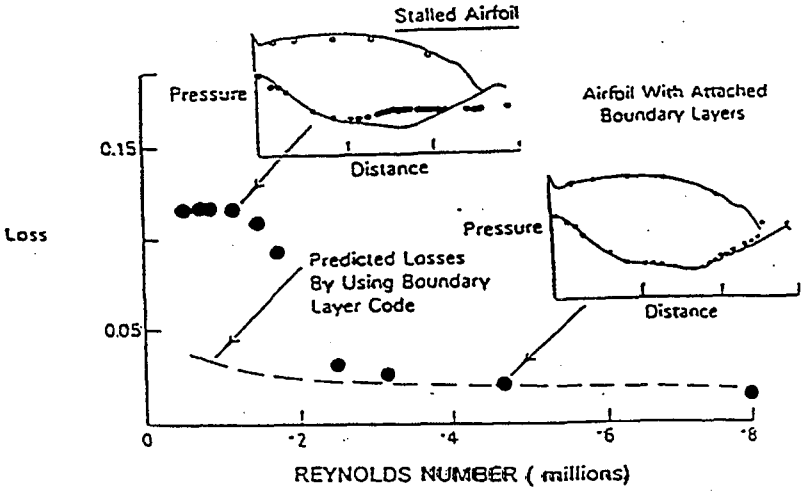

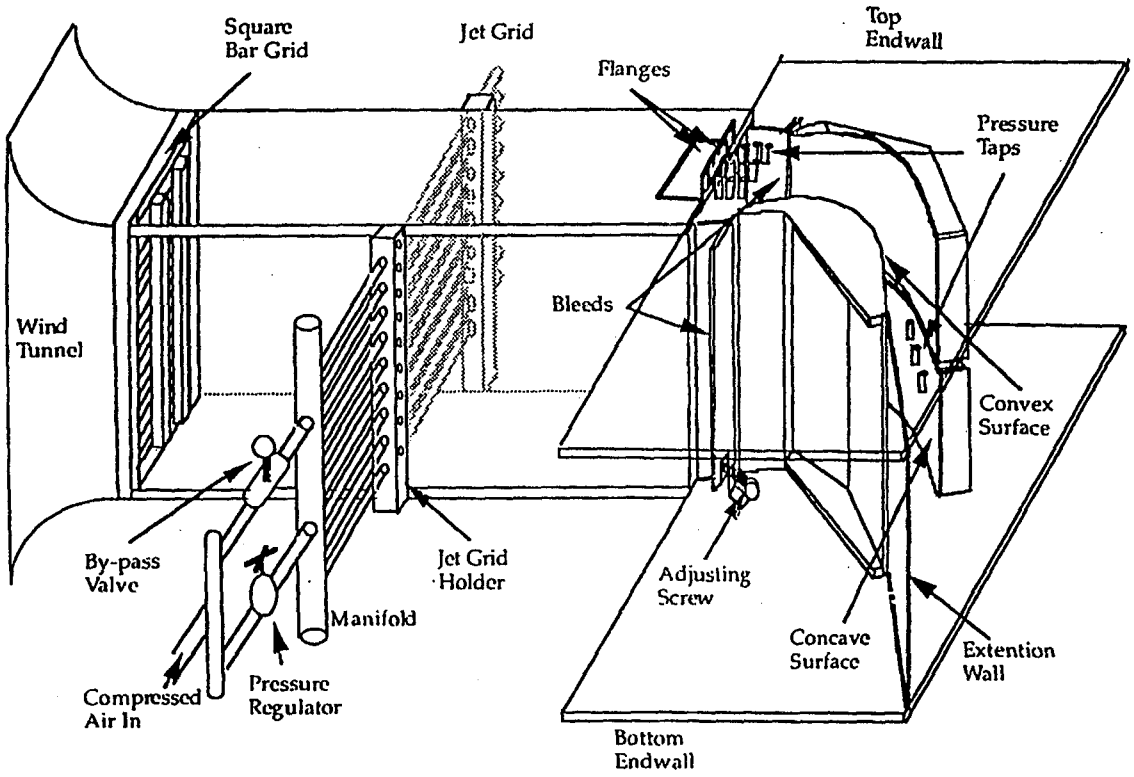

Setup of the turbulence genarators and the test section

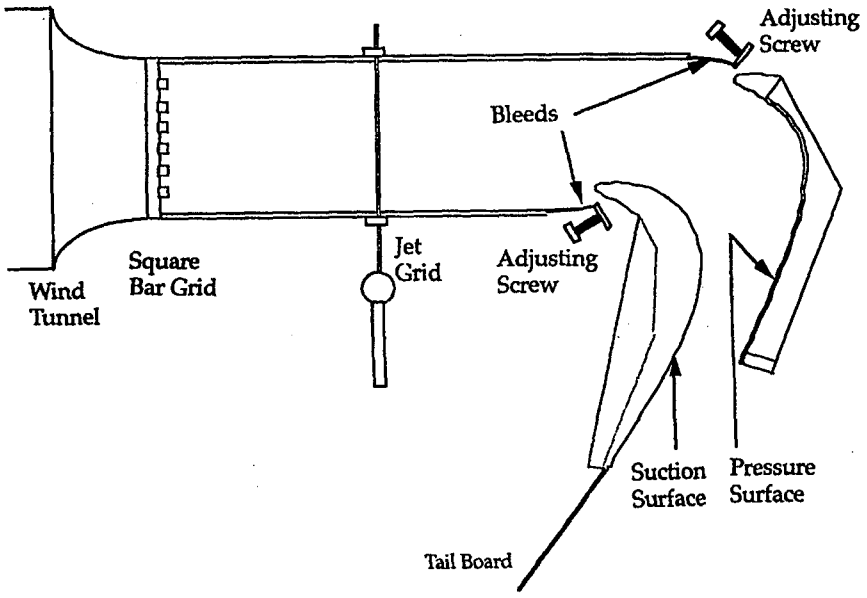

A top view of turbulence generation and test section

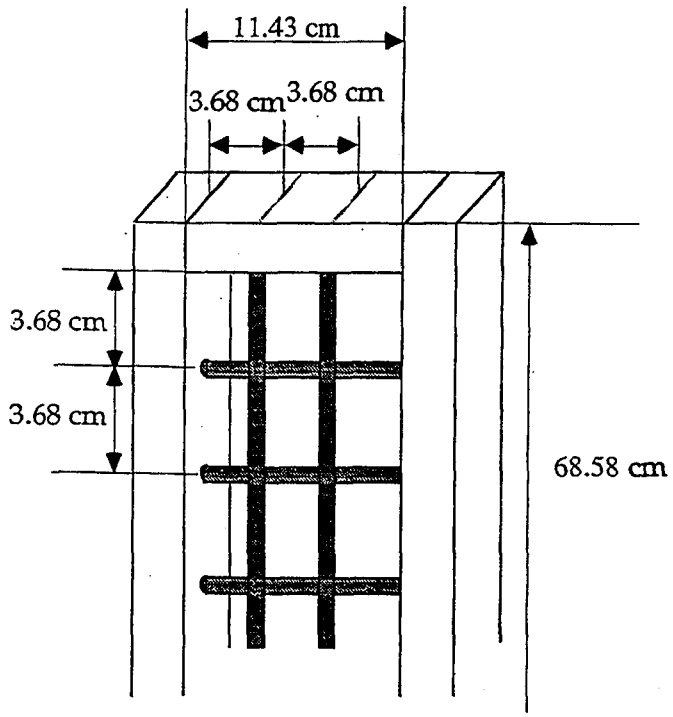

Cylinder-bar grid

FOR GENERATING THE NOMINALLY 2.5%
TURBULENCE INTENSITY CASE

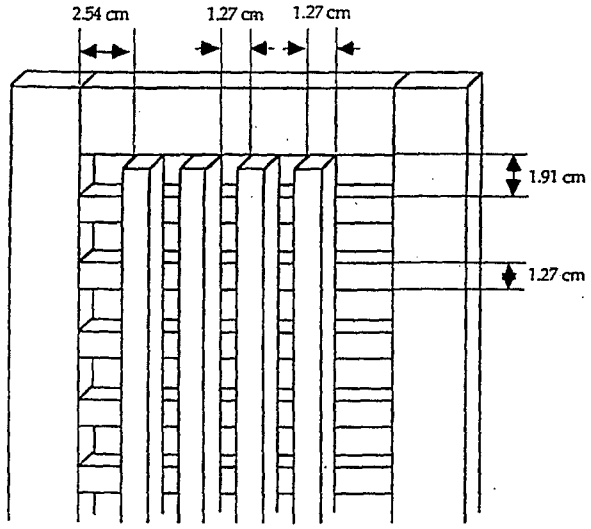

Square-bar grid

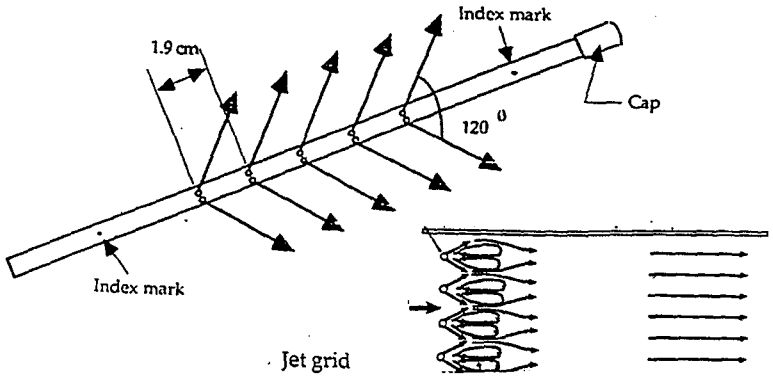

FOR GENERATING THE NOMINALLY 10%
TURBULENCE INTENSITY CASE

NOMENCLATURE

$Cp=2(pt-p)/\rho U_e^2$	static pressure coefficient
FSTI	free stream turbulence intensity
Lx	axial chord length
Lss	suction surface length
$Re=L_{ss}U_e/\nu$	Reynolds number based on suction surface length and exit velocity
U_∞	free-stream velocity
x	axial position
y	normal distance from the wall
γ	intermittency (fraction of time flow is turbulent)

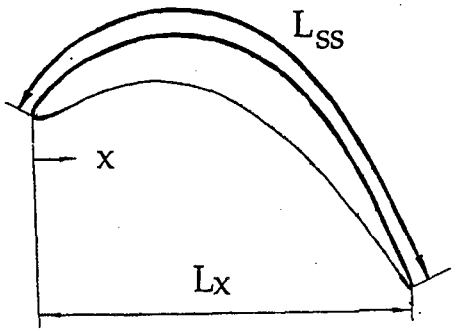

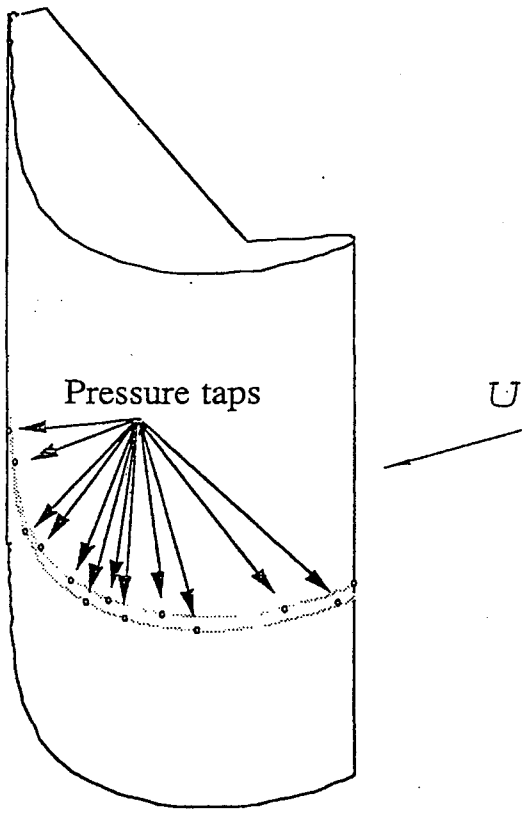
Pressure taps
U
Suction surface

Intermittency circuit performance in a transitional boundary layer

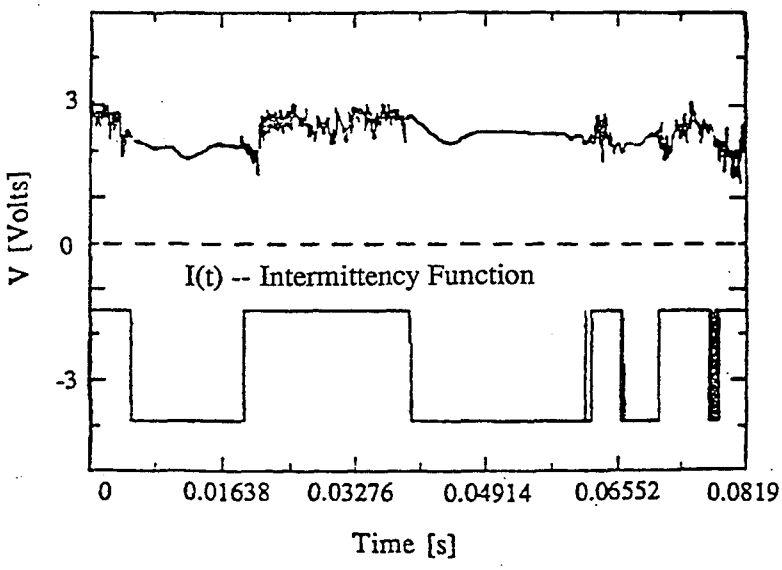

$$\gamma = \frac{1}{T}\int_0^T I(t)dt$$

SIGNAL IS TURBULENT IF EITHER $\frac{du}{dt}$ OR $\frac{d^2u}{dt^2}$ EXCEEDS A THRESHOLD VALUE

CASES INVESTIGATED

	FSTI=0.5%	FSTI=2.5%	FSTI=10%
Re=50,000	S	S, T	S, T
Re=100,000	S, T	S, T	S, T
Re=200,000	S, T	S, T	T, S
Re=300,000	S, T	T, S	

S: SEPARATION

T: TRANSITION

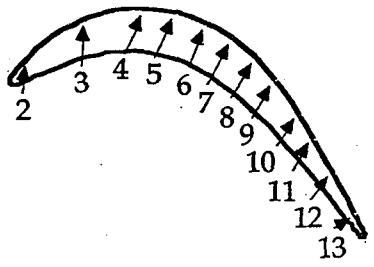

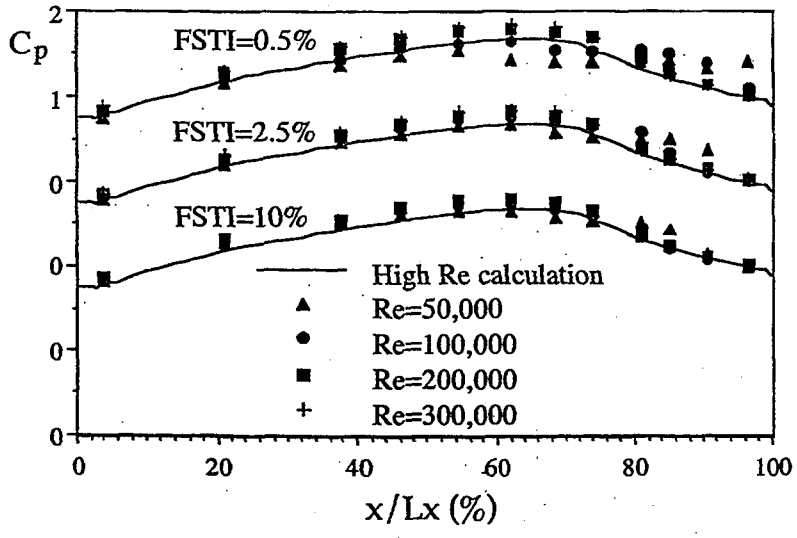

Pressure distributions on suction surface

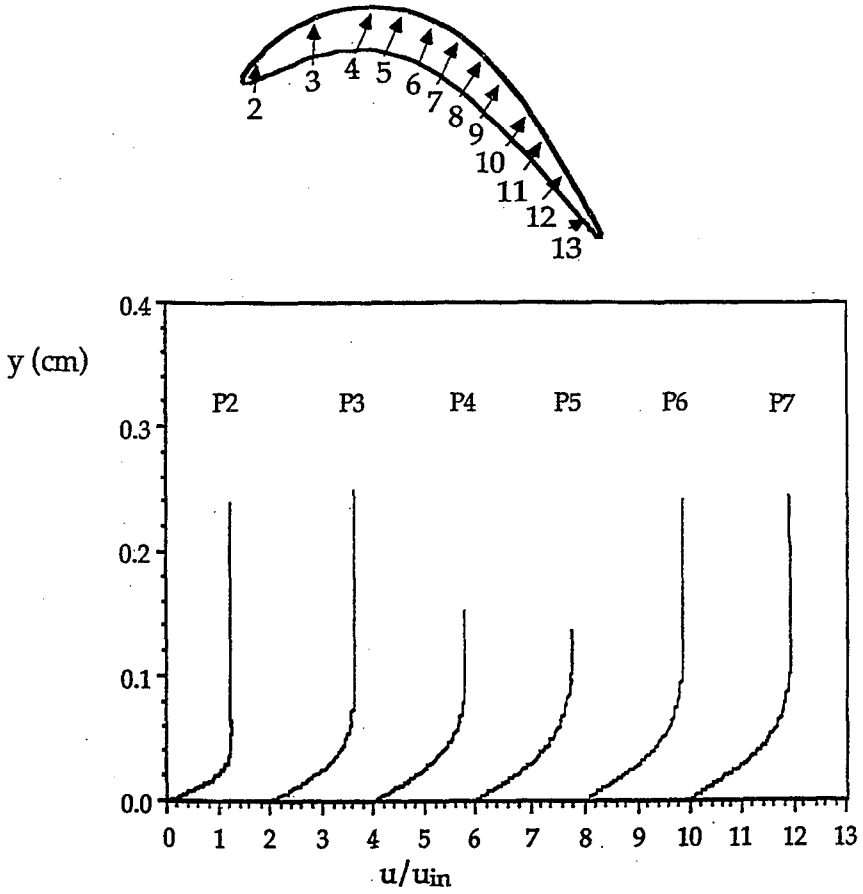

Velocity profiles at p2 - p7, Re=100,000, FSTI=2.5%

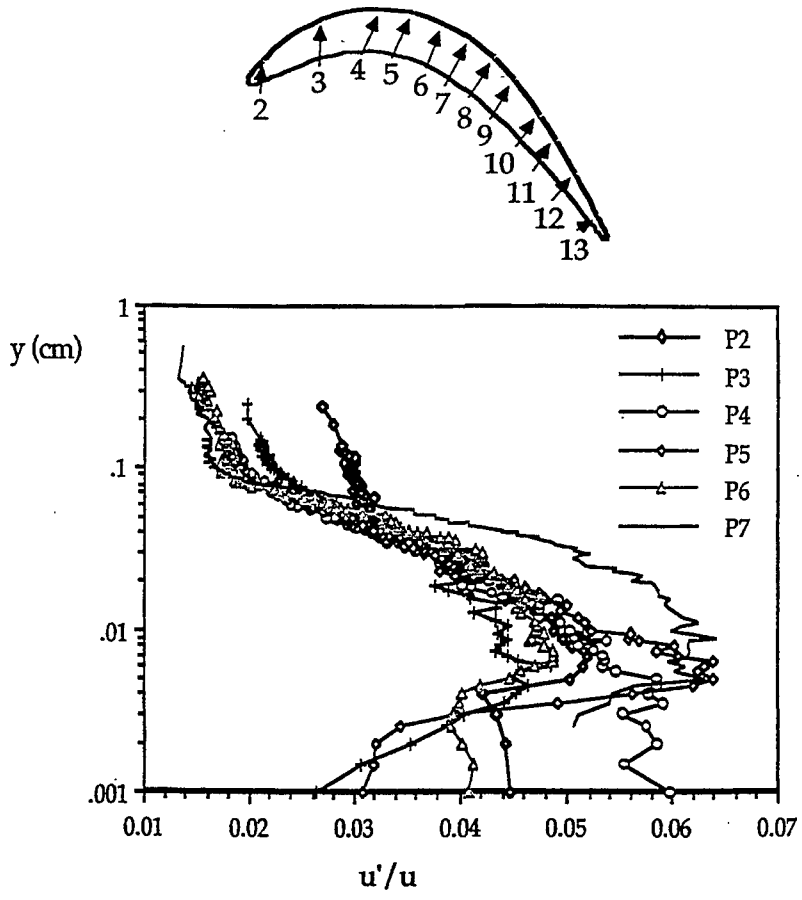

Turbulence intensity at P2 to P7, Re=100,000, FSTI=2.5%

P7=7.17cm, P8=8.08cm, P9=9.00cm, P10=10.37cm, P11=11.28cm, P12=11.54cm, P13=14.14cm

Re=50k S_s=8.07cm
S_r=13.77
Re=100k S_s=8.10cm
S_r=12.24
Re=200k S_s=8.32cm
S_r=10.77cm
Re=300k S_s=8.32cm
S_r=10.27cm

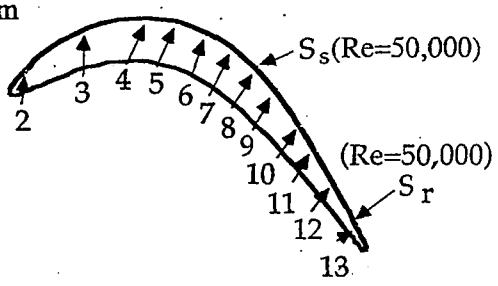

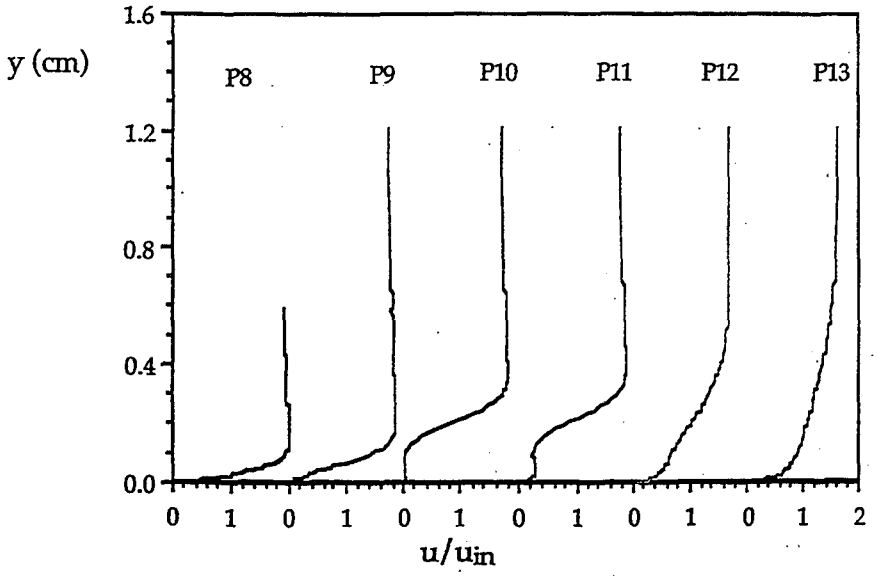

Velocity profiles at p8 - p13 for Re=100,000, FSTI=2.5%

P7=7.17cm, P8=8.08cm, P9=9.00cm, P10=10.37cm, P11=11.28cm, P12=11.54cm, P13=14.14cm

Re=50k S_S=8.07cm
S_r=13.77
Re=100k S_S=8.10cm
S_r=12.24
Re=200k S_S=8.32cm
S_r=10.77cm
Re=300k S_S=8.32cm
S_r=10.27cm

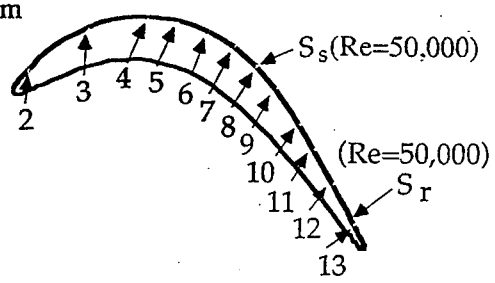

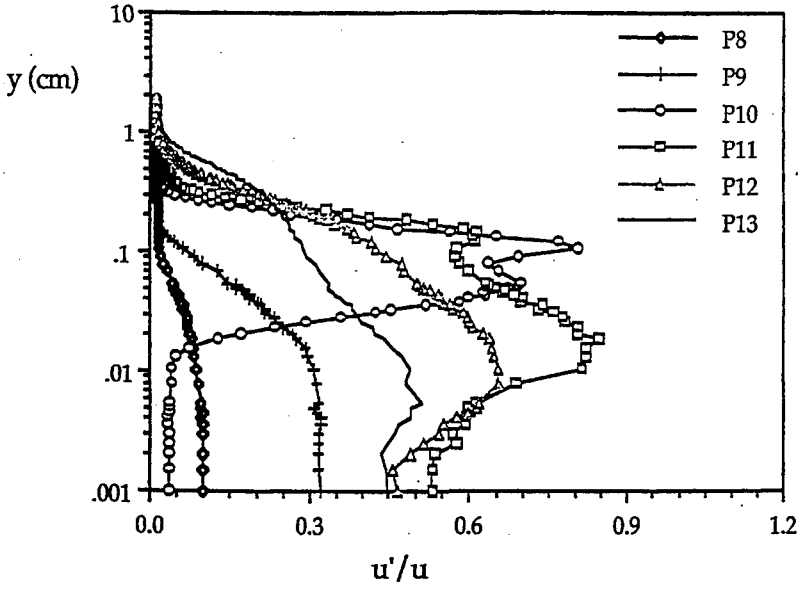

Turbulence intensity at P8 to P13, Re=100,000, FSTI=2.5%

P7=7.17cm, P8=8.08cm, P9=9.00cm, P10=10.37cm, P11=11.28cm, P12=11.54cm, P13=14.14cm

Re=50k S_S=8.07cm
S_r=13.77
Re=100k S_S=8.10cm
S_r=12.24
Re=200k S_S=8.32cm
S_r=10.77cm
Re=300k S_S=8.32cm
S_r=10.27cm

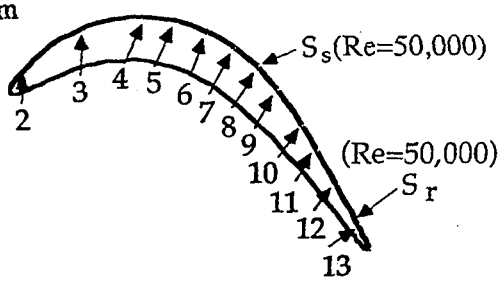

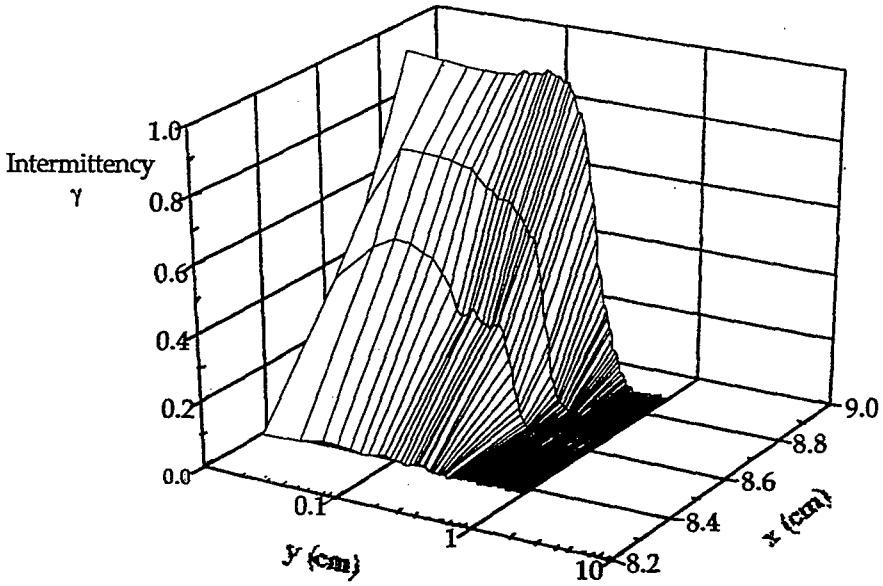

Intermittency distributions for Re=100,000, FSTI=2.5%

P7=7.17cm, P8=8.08cm, P9=9.00cm, P10=10.37cm, P11=11.28cm, P12=11.54cm; P13=14.14cm

Re=50k S_s=8.07cm
S_r=13.77
Re=100k S_s=8.10cm
S_r=12.24
Re=200k S_s=8.32cm
S_r=10.77cm
Re=300k S_s=8.32cm
S_r=10.27cm

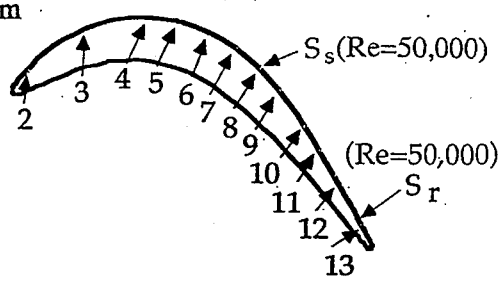

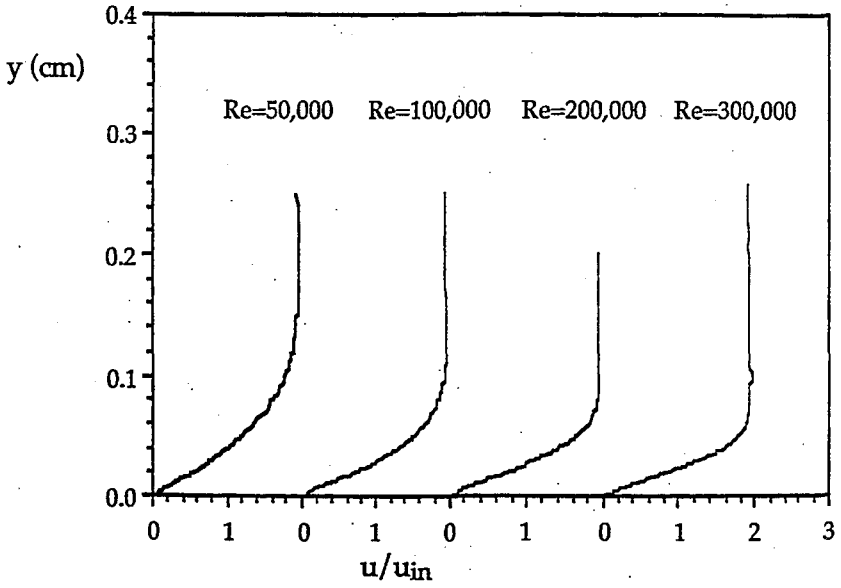

Velocity profiles at p7 for FSTI=2.5%

P7=7.17cm, P8=8.08cm, P9=9.00cm, P10=10.37cm, P11=11.28cm, P12=11.54cm, P13=14.14cm

Re=50k S_s=8.07cm
S_r=13.77
Re=100k S_s=8.10cm
S_r=12.24
Re=200k S_s=8.32cm
S_r=10.77cm
Re=300k S_s=8.32cm
S_r=10.27cm

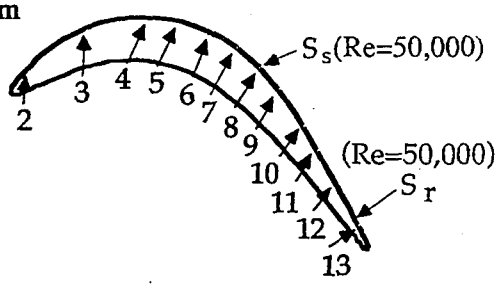

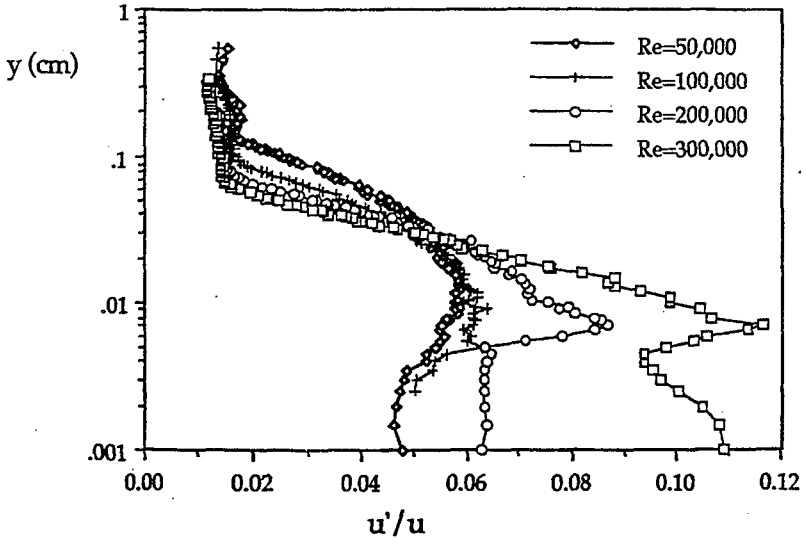

Turbulence intensity at P7, Re=100,000, FSTI=2.5%

P7=7.17cm, P8=8.08cm, P9=9.00cm, P10=10.37cm, P11=11.28cm, P12=11.54cm, P13=14.14cm

Re=50k S_s=8.07cm
S_r=13.77
Re=100k S_s=8.10cm
S_r=12.24
Re=200k S_s=8.32cm
S_r=10.77cm
Re=300k S_s=8.32cm
S_r=10.27cm

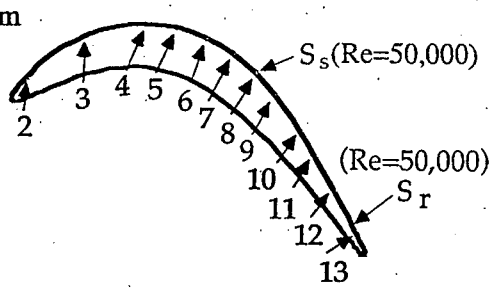

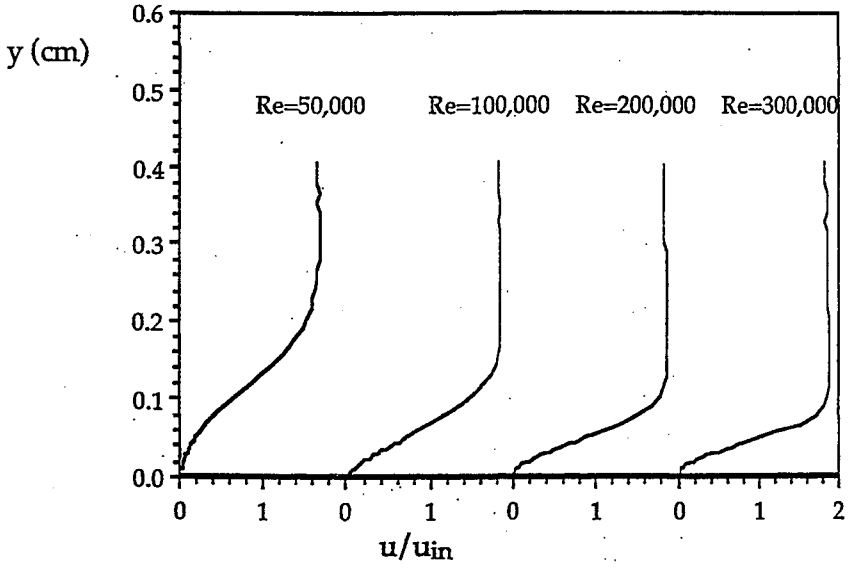

Velocity profiles at station p9 (x/Lx=74.09%), FSTI=2.5%

P7=7.17cm, P8=8.08cm, P9=9.00cm, P10=10.37cm, P11=11.28cm, P12=11.54cm, P13=14.14cm

Re=50k S_S=8.07cm
S_r=13.77
Re=100k S_S=8.10cm
S_r=12.24
Re=200k S_S=8.32cm
S_r=10.77cm
Re=300k S_S=8.32cm
S_r=10.27cm

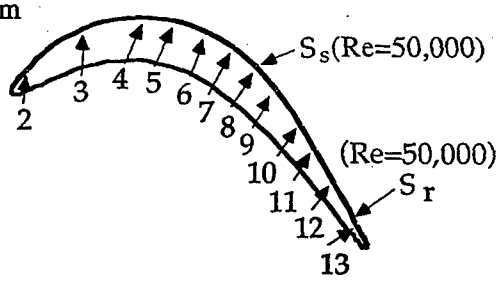

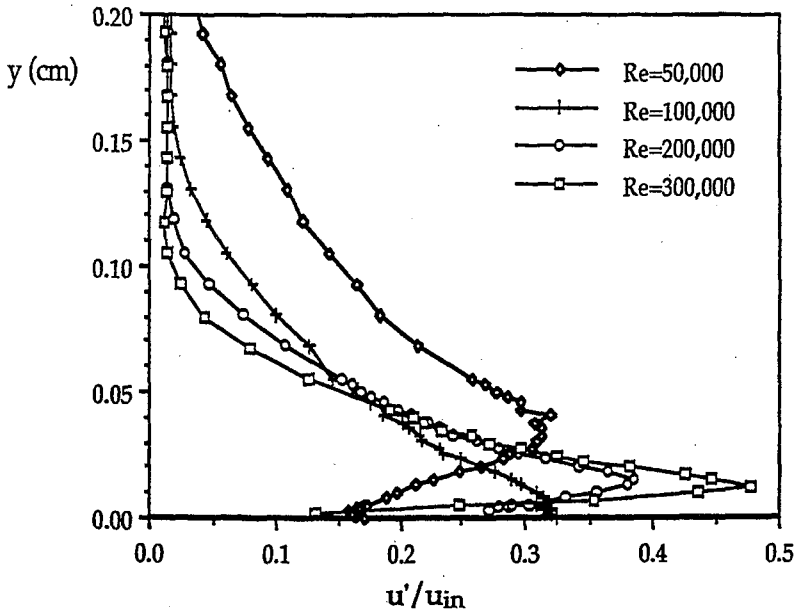

Turbulence intensities at station p9 (x/Lx=74.09%), FSTI=2.5%

P7=7.17cm, P8=8.08cm, P9=9.00cm, P10=10.37cm, P11=11.28cm, P12=11.54cm, P13=14.14cm

Re=50k S_s=8.07cm
S_r=13.77
Re=100k S_s=8.10cm
S_r=12.24
Re=200k S_s=8.32cm
S_r=10.77cm
Re=300k S_s=8.32cm
S_r=10.27cm

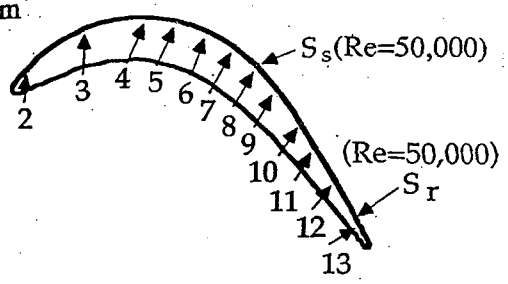

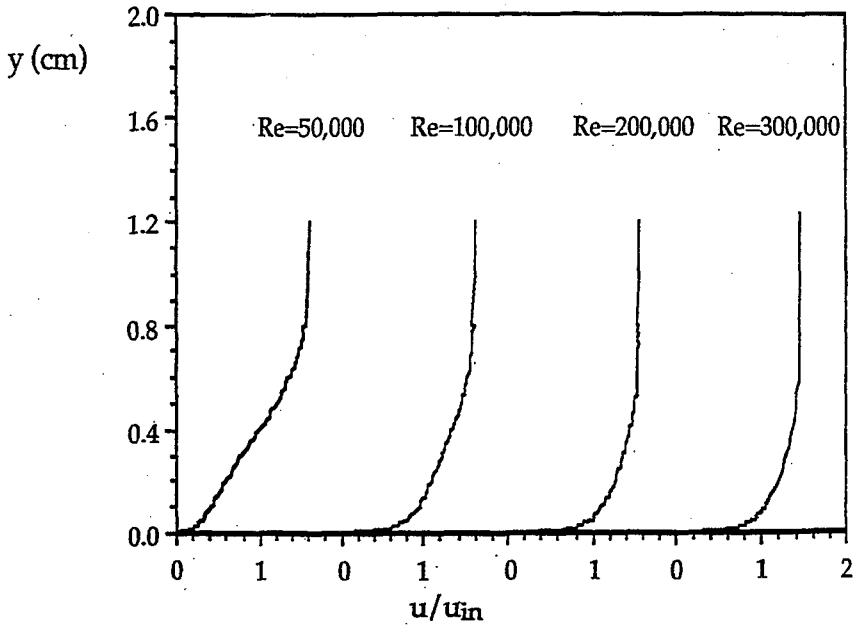

Velocity profiles at station p13 (x/Lx=96.73%), FSTI=2.5%

P7=7.17cm, P8=8.08cm, P9=9.00cm, P10=10.37cm, P11=11.28cm, P12=11.54cm, P13=14.14cm

Re=50k S_s=8.07cm
S_r=13.77
Re=100k S_s=8.10cm
S_r=12.24
Re=200k S_s=8.32cm
S_r=10.77cm
Re=300k S_s=8.32cm
S_r=10.27cm

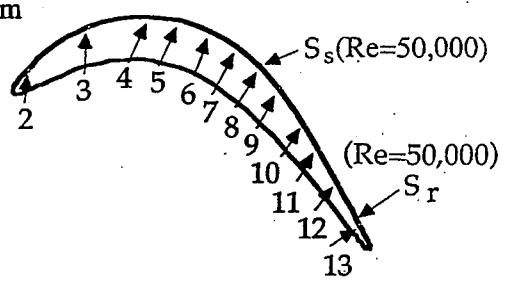

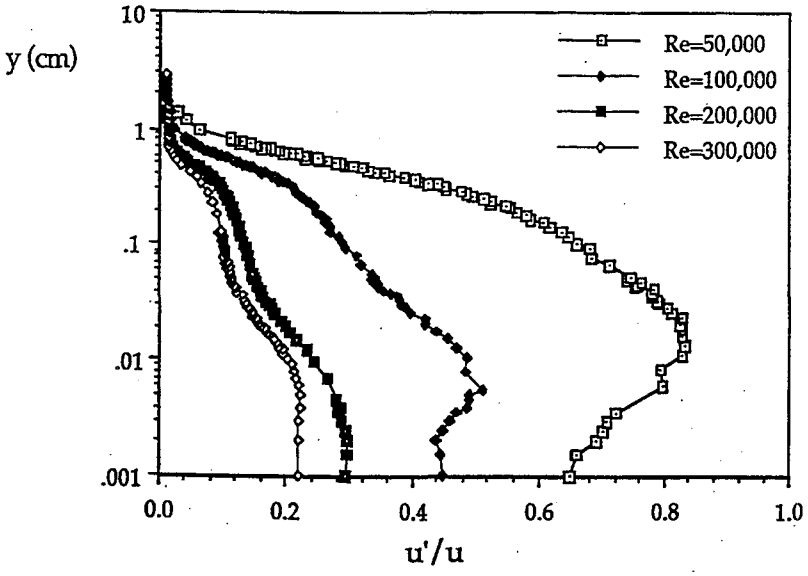

Turbulence intensities at station p13 (x/Lx=96.73%), FSTI=2.5%

P7=7.17cm, P8=8.08cm, P9=9.00cm, P10=10.37cm, P11=11.28cm, P12=11.54cm, P13=14.14cm

Re=50k S_s=8.07cm
S_r=13.77
Re=100k S_s=8.10cm
S_r=12.24
Re=200k S_s=8.32cm
S_r=10.77cm
Re=300k S_s=8.32cm
S_r=10.27cm

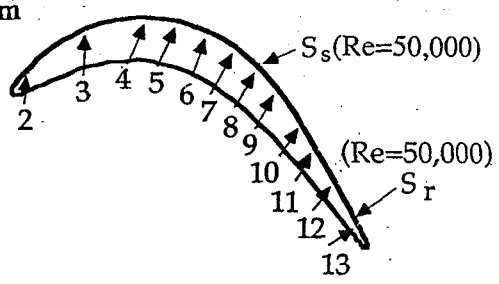

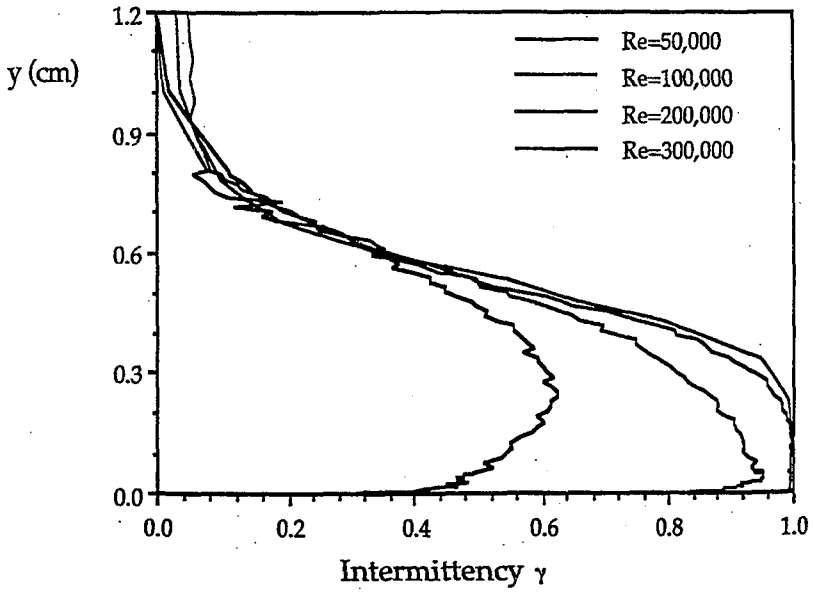

Intermittency distributions at station p13
(x/Lx=96.73%), FSTI=2.5%

P7=7.17cm, P8=8.08cm, P9=9.00cm, P10=10.37cm, P11=11.28cm, P12=11.54cm, P13=14.14cm

Re=50k S_s=7.57cm
S_r> P13
Re=100k S_s=7.77cm
S_r> P13
Re=200k S_s=8.17cm
S_r=12.02cm
Re=300k S_s=8.27cm
S_r=10.97cm

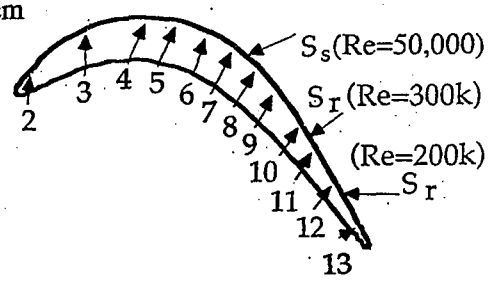

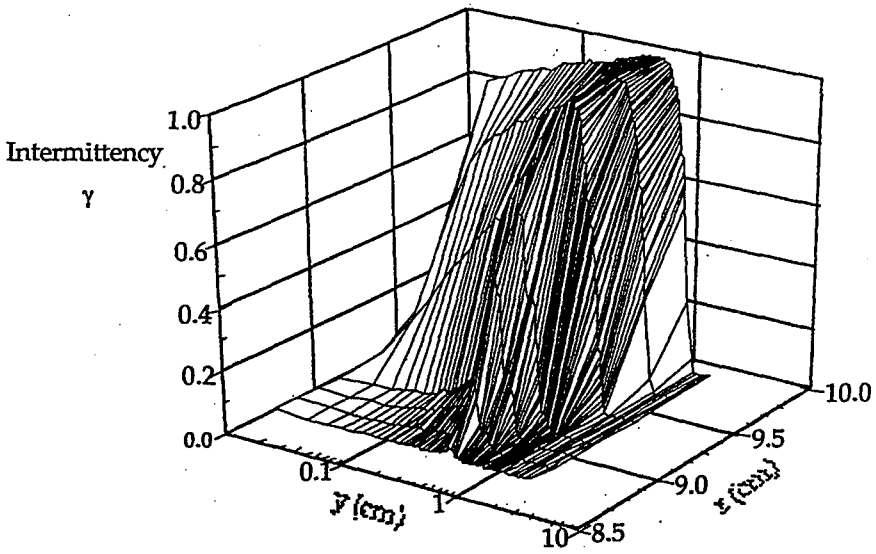

Intermittency distributions for Re=100,000, FSTI=0.5%, constructed from profiles at p10a, p11a, p11b, p11c, p12a, p12b, and p12c

P7=7.17cm, P8=8.08cm, P9=9.00cm, P10=10.37cm, P11=11.28cm, P12=11.54cm, P13=14.14cm

Re=50k S_S=8.27cm
S_r=12.67
Re=100k S_S=8.37cm
S_r=11.47
Re=200k S_S=8.47cm
S_r=10.42cm

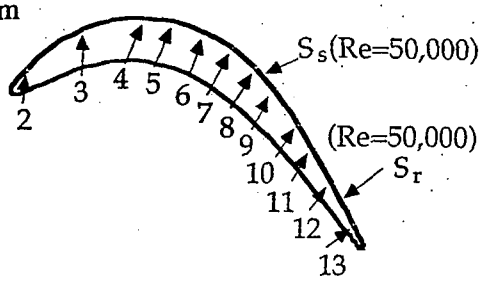

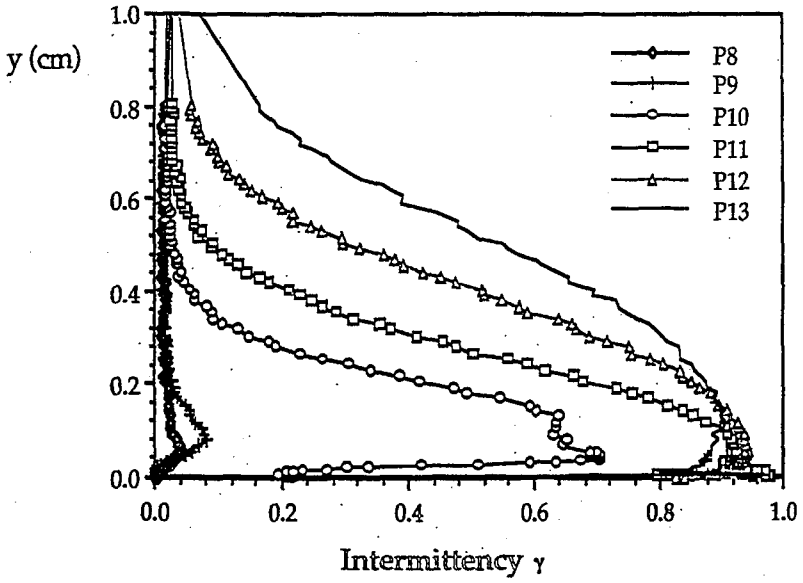

Intermittency distributions for Re=100,000, FSTI=10%

P7=7.17cm, P8=8.08cm, P9=9.00cm, P10=10.37cm, P11=11.28cm, P12=11.54cm, P13=14.14cm

Re=50k S_s=8.27cm
S_r=12.67
Re=100k S_s=8.37cm
S_r=11.47
Re=200k S_s=8.47cm
S_r=10.42cm

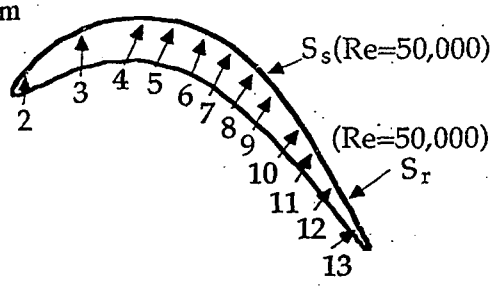

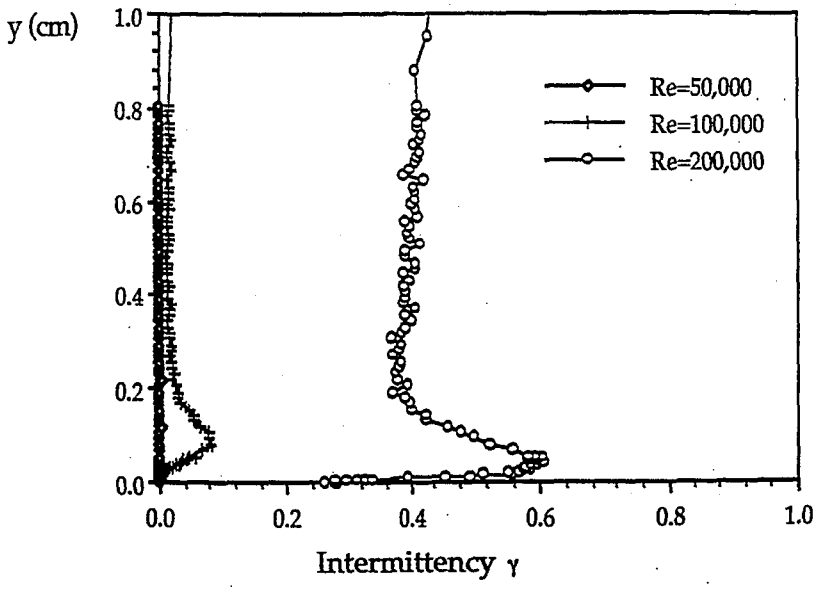

Intermittency distributions at station p9 (x/Lx=74.09%), FSTI=10%

P7=7.17cm, P8=8.08cm, P9=9.00cm, P10=10.37cm, P11=11.28cm, P12=11.54cm, P13=14.14cm

Re=50k S_s=8.27cm
S_r=12.67
Re=100k S_s=8.37cm
S_r=11.47
Re=200k S_s=8.47cm
S_r=10.42cm

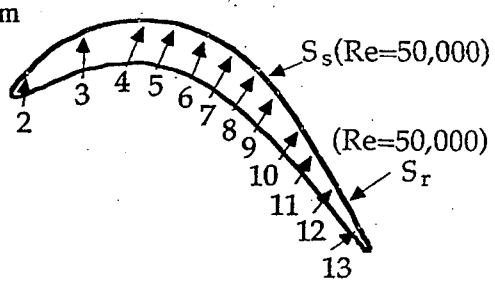

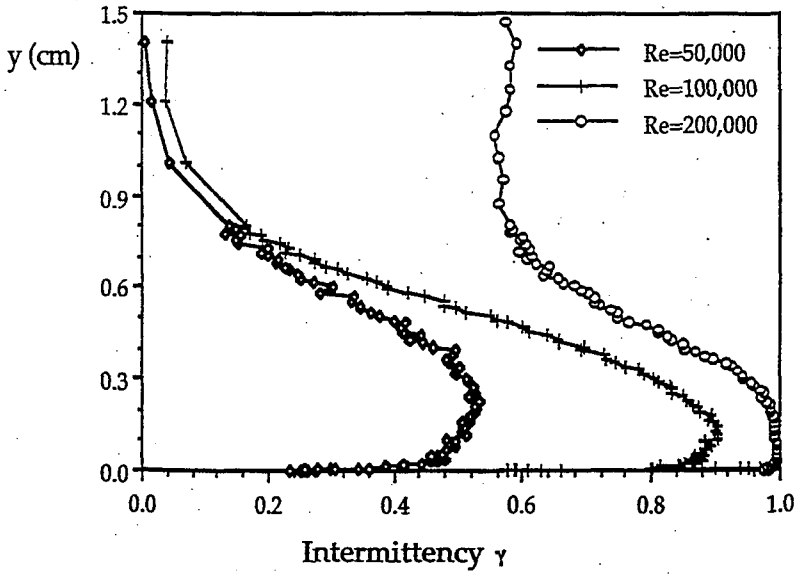

Intermittency distributions at station p13
(x/Lx=96.73%), FSTI=10%

CONCLUSIONS

	Re=50K	Re=100k	Re=200k	Re=300k
FSTI=0.5%	S	S, T	S, T	S, T
FSTI=2.5%	S, T	S, T	S, T	T, S
FSTI=10%	S, T	S, T	T, S	

• Separated boundary layers with transition on the suction surface followed the same path:

1) laminar boundary layer development,
2) strong growth rate as a laminar boundary layer when the adverse pressure gradient section is nearly reached,
3) laminar separation,
4) transition of the free shear layer,
5) turbulent flow throughout the shear layer and near-wall region,
6) reattachment, and
7) growth as an attached turbulent boundary layer.

The speed with which it proceeds through these steps and the degree to which it completes these steps increase as Re or FSTI increases.

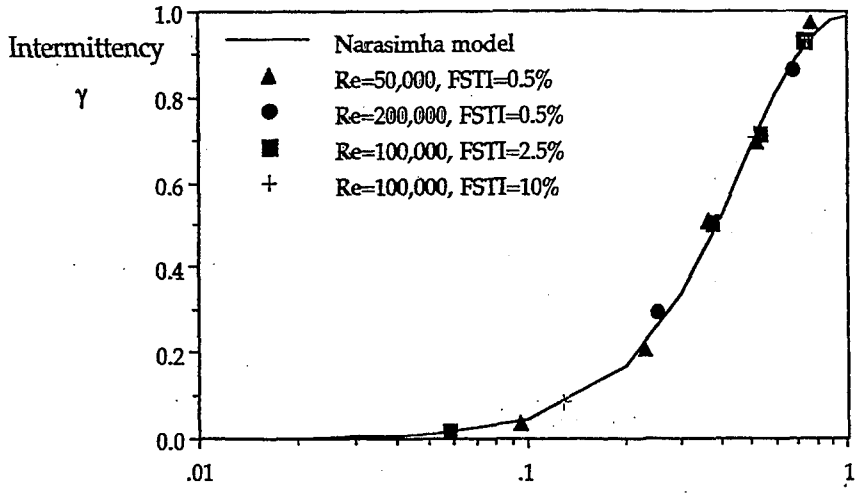

Intermittency distributions through transition

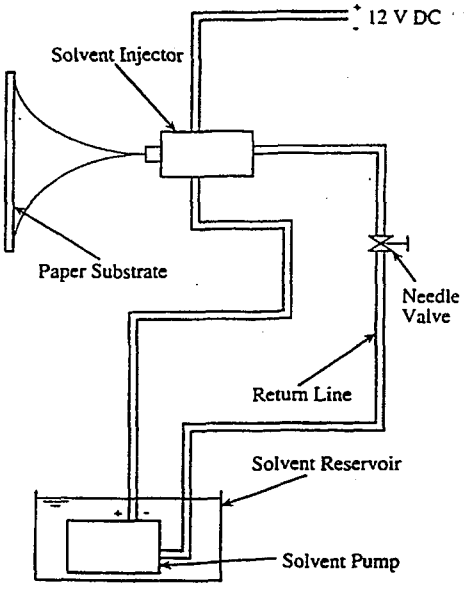

SOLVENT INJECTOR FOR THE SHEAR STRESS

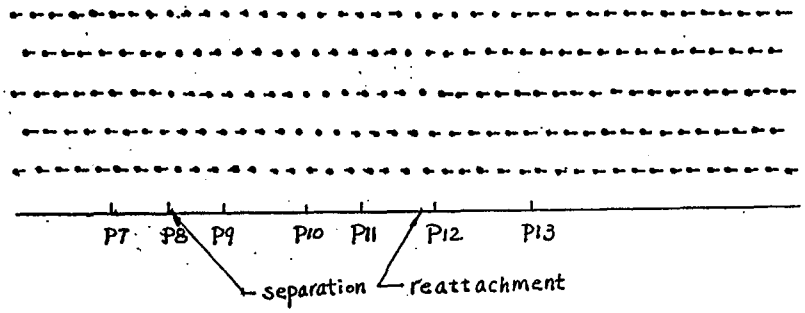

SHEAR STRESS DIRECTION, AS INTERPRETED, FOR THE RE=100,000, TI=2.5% CASE

FLOW SEPARATION AND REATTACHMENT POINTS

	FSTI=0.5%		FSTI=2.5%		FSTI=10%	
	Ss (cm)	Sr (cm)	Ss (cm)	Sr (cm)	Ss (cm)	Sr (cm)
Re=50,000	7.57	18.32	8.07	13.77	8.27	12.67
Re=100,000	7.77	15.72	8.10	12.14	8.37	11.47
Re=200,000	8.17	12.02	8.32	10.77	8.47	10.42
Re=300,000	8.27	10.97	8.32	10.27		

P7	P8	P9	P10	P11	P12	P13
7.17	8.08	9.00	10.37	11.28	12.54	14.14

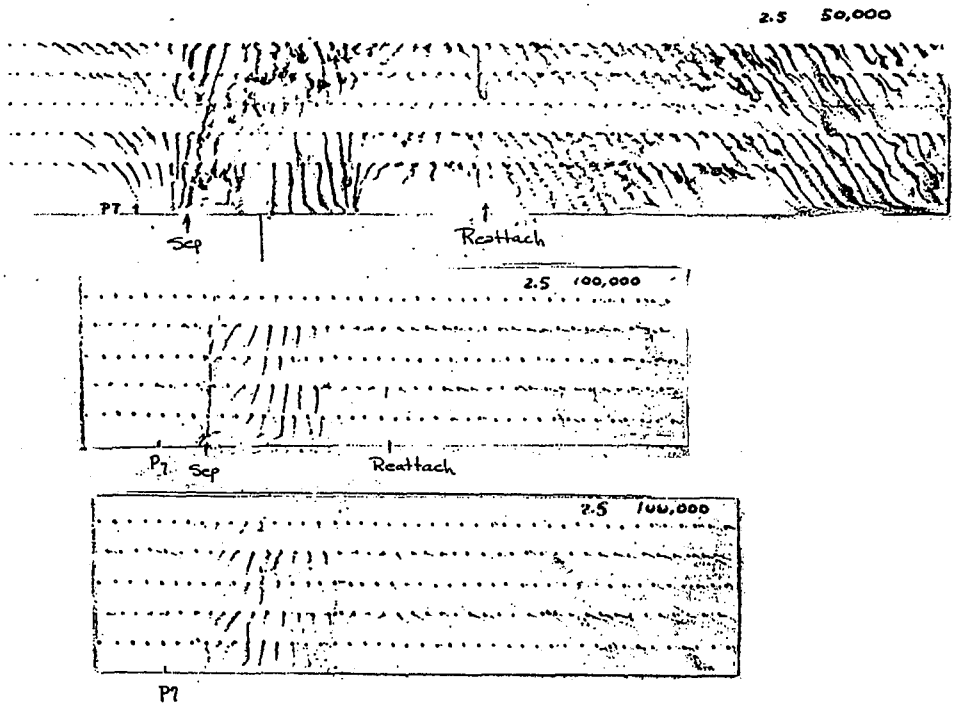

SHEAR STRESS DIRECTION -- RAW TRACES. IN VERY LOW SHEAR STRESS REGION, THE INK FLOWS DOWNWARD.
TOP--RE=50,000, TI=2.5%;
CENTER AND BOTTOM--TWO RUNS OF RE=100,000, TI=2.5%

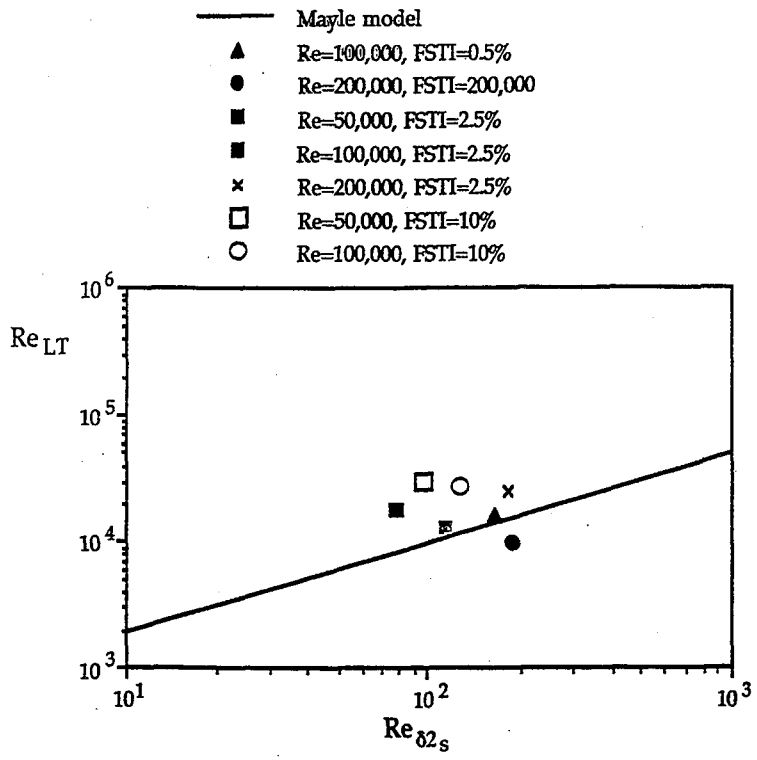

Transition length Reynolds number in the separation bubbles vs. separation momentum thickness Reynolds number

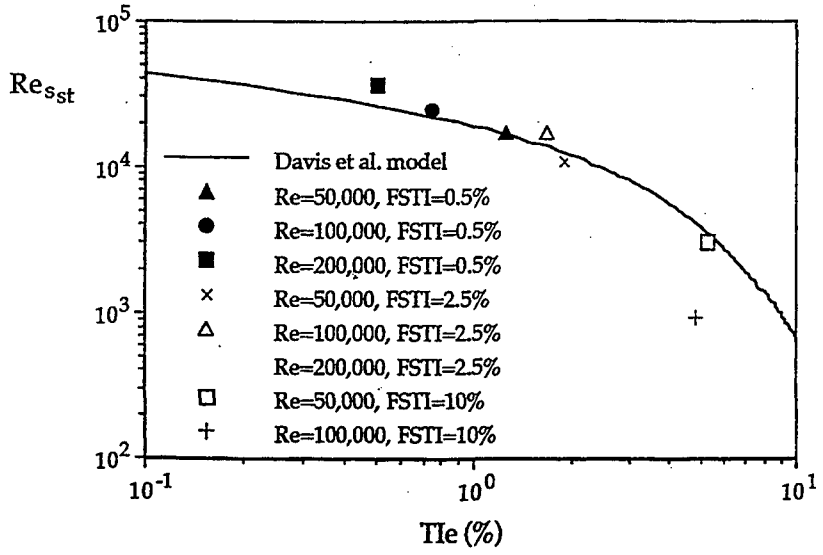

Comparison of momentum thickness Reynolds number to Davis et at. model (1985)

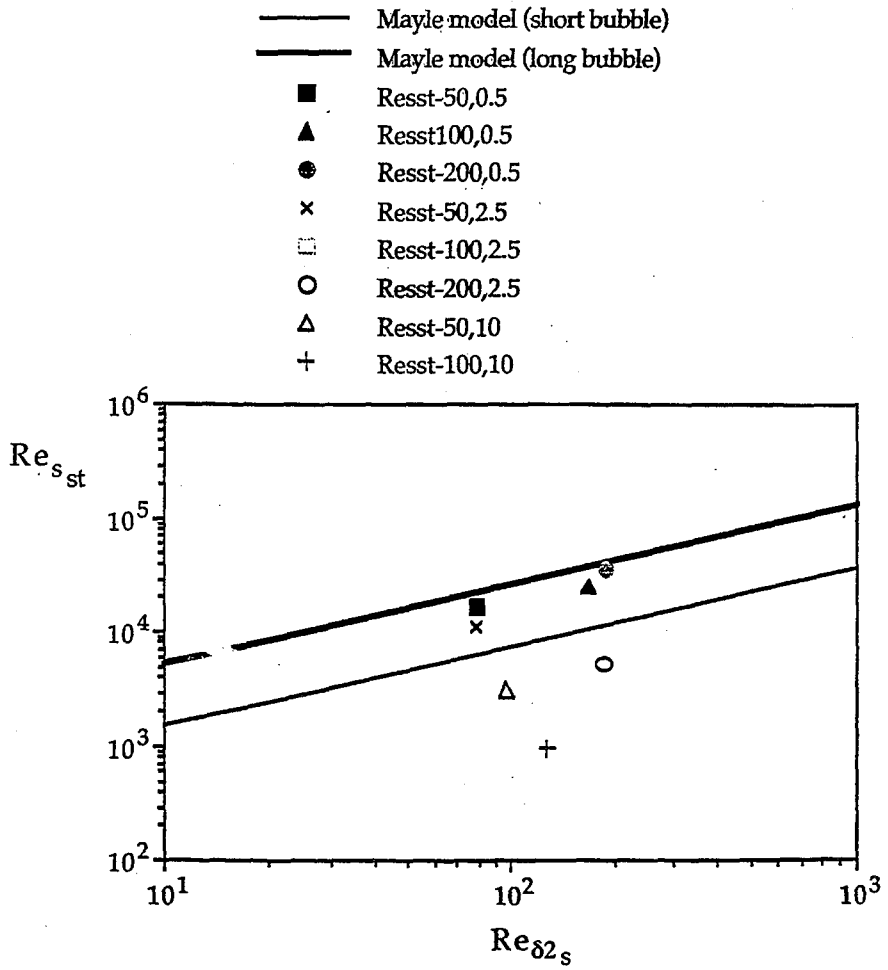

Reynolds number based on distance between separation and transition versus separation Reynolds number

NUMERICAL SIMULATIONS OF STEADY AND UNSTEADY TRANSITION IN LOW-PRESSURE TURBINE BLADE ROWS*

Daniel Dorney
GMI Engineering and Management Institute
Flint, Michigan

Abstract

Transition plays an important role in the prediction of losses and performance in low-pressure turbines. The transition location on a turbine blade may vary significantly because of the wakes from upstream blade rows, and intermittent flow separation can also affect the transition process in an unsteady flow environment. In the present investigation, an unsteady Navier-Stokes analysis is used to predict transition in a low-pressure turbine cascade and a low-pressure turbine stage. The numerical flow analysis is third-order spatially accurate and second-order temporally accurate, and the equations of motion are integrated using an implicit time-marching procedure. The Baldwin-Lomax and $k-\epsilon$ turbulence models, in conjunction with several algebraic transition models, have been used to predict the location of transition. Predicted results include unsteady blade loadings, time-histories of the pressure, transition locations and boundary layer quantities, as well as performance quantities and comparisons with the available experimental/design data.

*Work supported by NASA Lewis Research Center (Grant no. NAG3-1668).

Overview

- Motivation
- Numerical procedure
- Numerical Simulations
  - PAK-B cascade
  - PAK-B stage
- Summary
- Work in progress

Motivation

- Identify loss mechanisms in low-pressure turbines
- Quantify low Reynolds number effects
- Evaluate turbulence and transition models

Transition Model Notes

- Abu-Ghannam & Shaw model produces most reasonable results
- Algebraic models can give poor results for high-turning blades
- Bubble transition predominant at low Reynolds numbers
- Transition point movement can get trapped in a limit cycle

Transition Models

- Natural transition
  - Abu-Ghannam and Shaw
  - Dunham
  - Seyb and Singh
  - Hall and Gibbings
- Bubble Trasnsition
  -Roberts correlation (modified by Davis & Carter)

Turbulence Models

- Baldwin-Lomax
  - conventional
  - modified
- k-e-equation model
  - Chien's low Reynolds number formulation
- q-w two-equation model

Numerical Procedure

- Implicit, full or thin-layer Navier-Stokes
- Newton sub-iterations
- 3rd order accurate inviscid fluxes
- 2nd order accurate viscous fluxes
- 2nd order temporal accuracy
- O-H grid topolgy

Test Article

- PAK-B geometry
  - M1=0.093 Re=40,000 P2/Pt1=0.9844
- Cascade simulations
  - 25,000 grid points y+=0.10
- Stage simulations
  - 1-vane/2-rotor using PAK-B geometry
  - 80,000 grid points y+=0.10

Cascade Simulations

PAK-B Cascade Grid

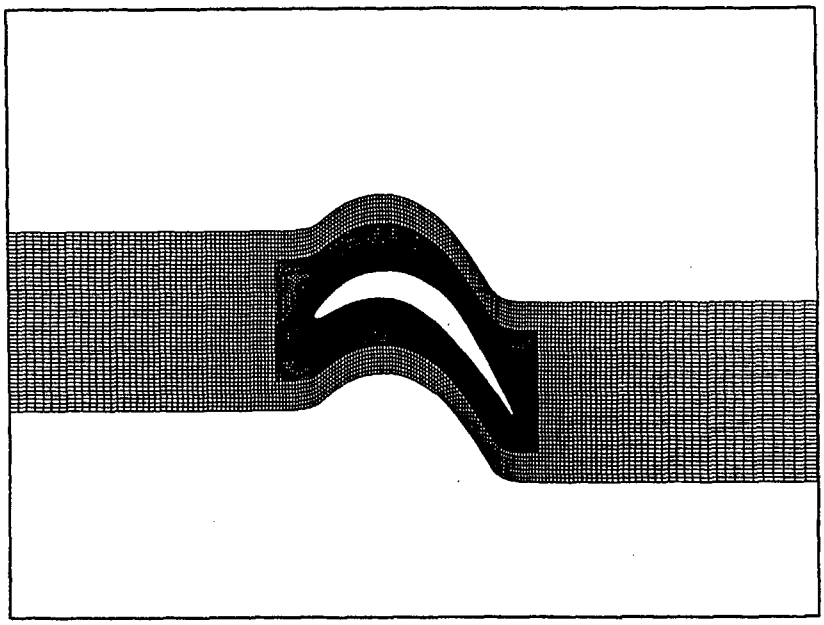

Laminar Flow at Re=40,000

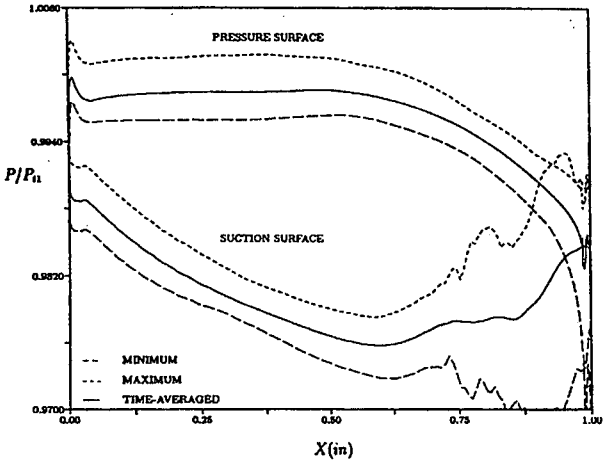

Pressure

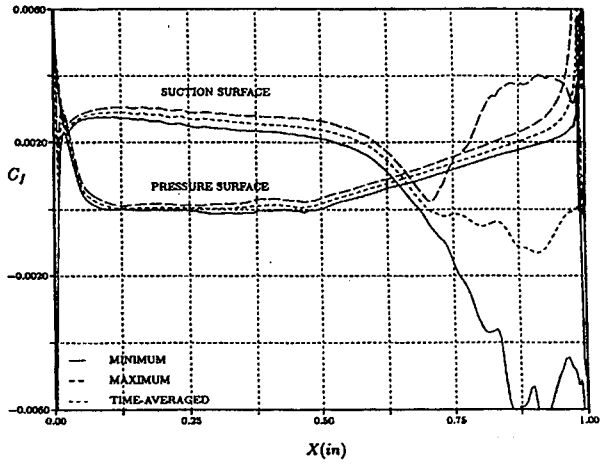

Skin Friction

Laminar Flow at Re=40,000

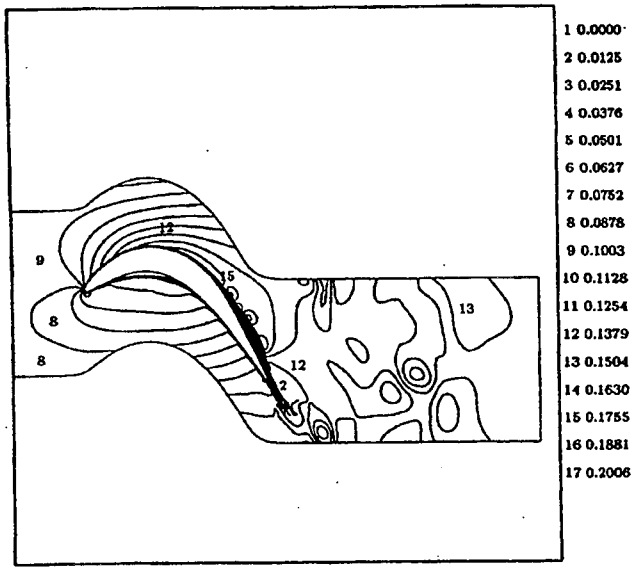

Mach Number

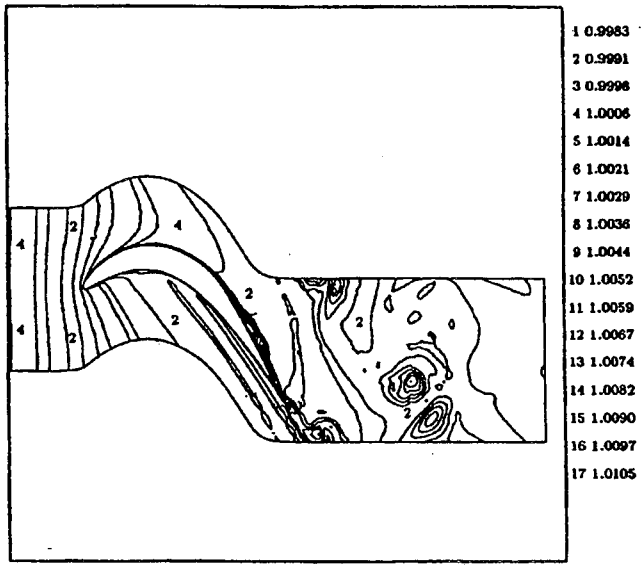

Entropy

Laminar Flow at Re=40,000

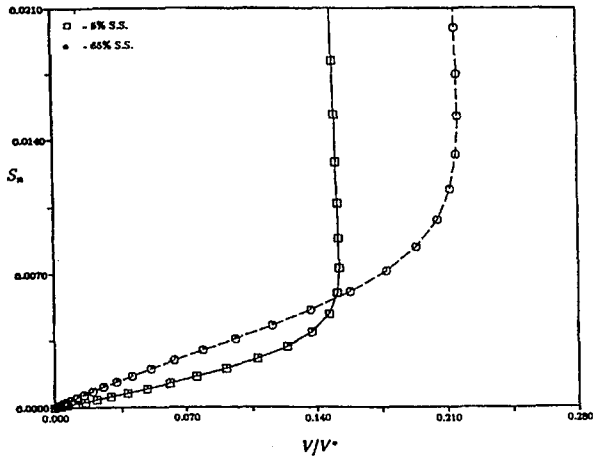

Suction Surface
Velocity Profiles

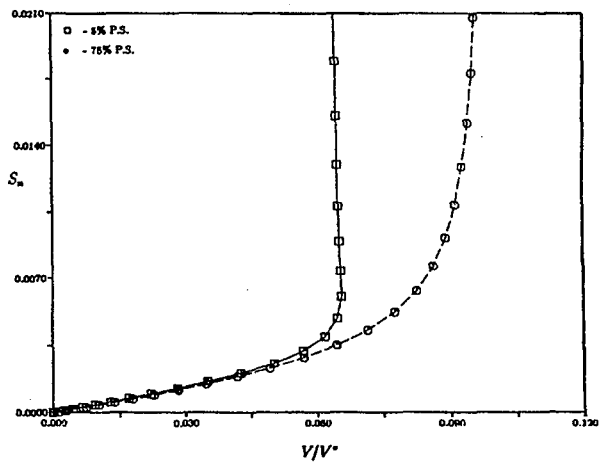

Pressure Surface
Velocity Profiles

Transitional Flow at Re=40,000

Baldwin-Lomax

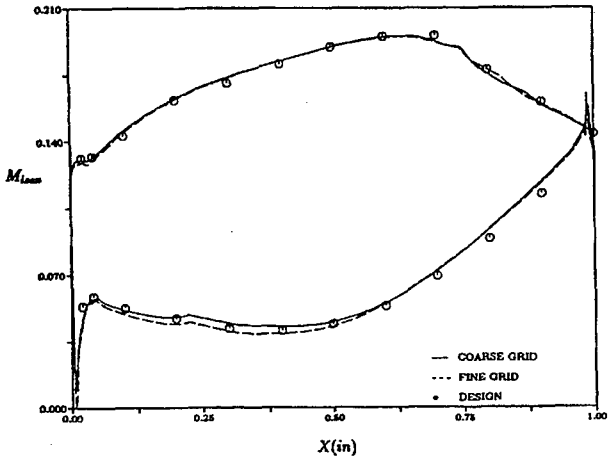

Mach Number

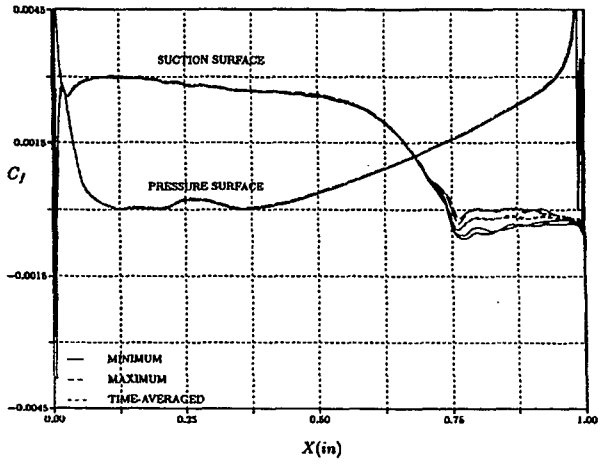

Skin Friction

Transitional Flow at Re=40,000

Baldwin-Lomax

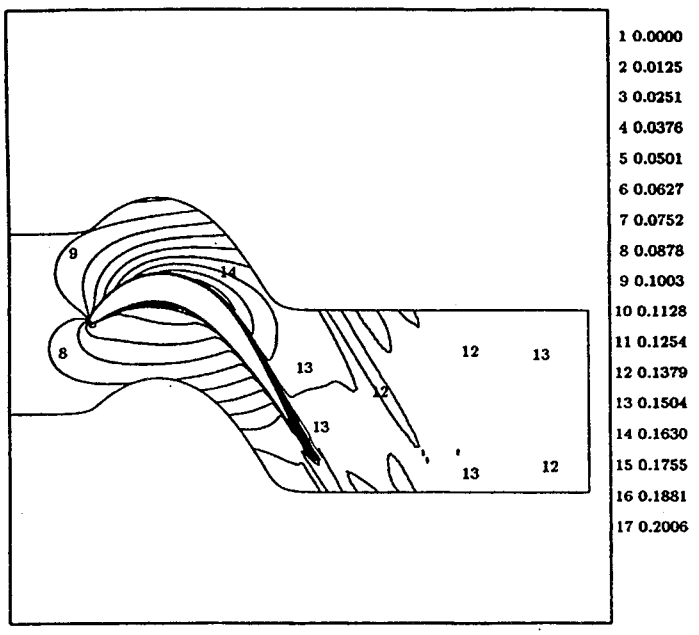

Mach Number

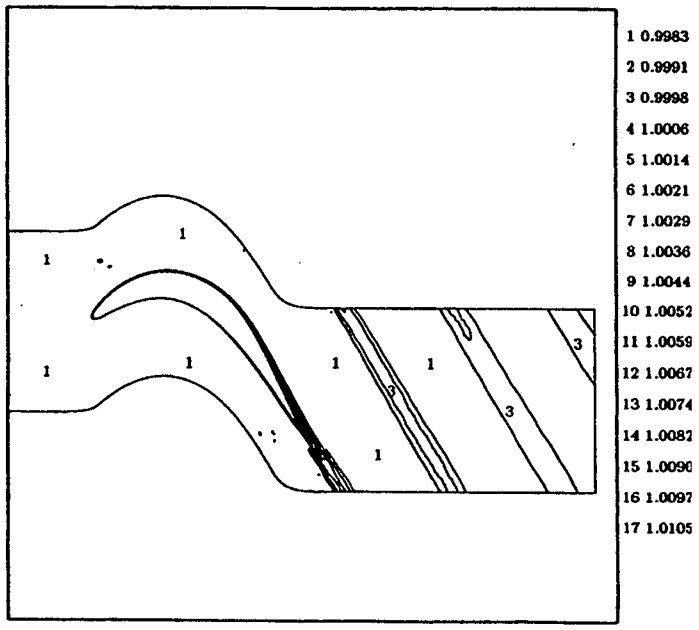

Entropy

Transitional Flow at Re=40,000

Baldwin-Lomax

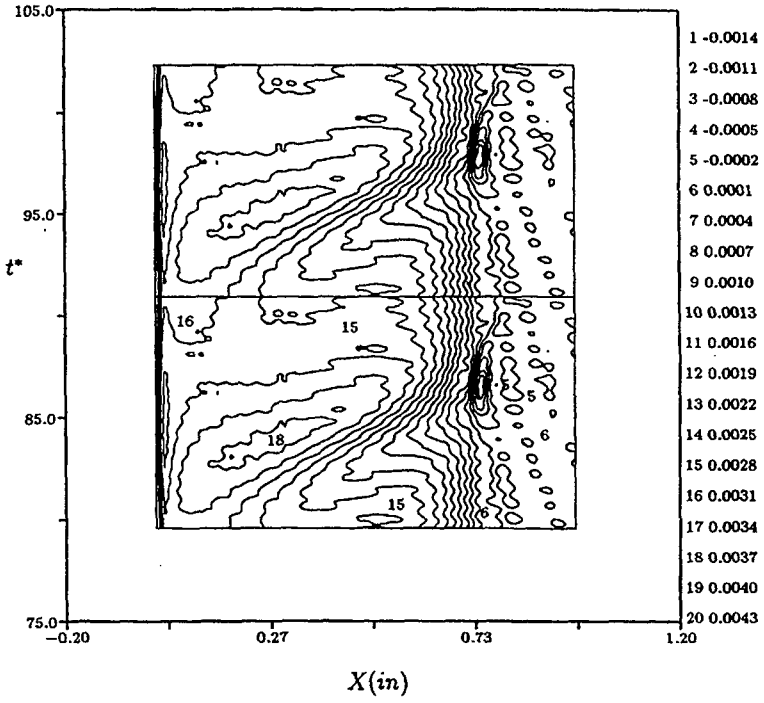

Skin Friction History

Turbulent Flow at Re=40,000

Baldwin-Lomax

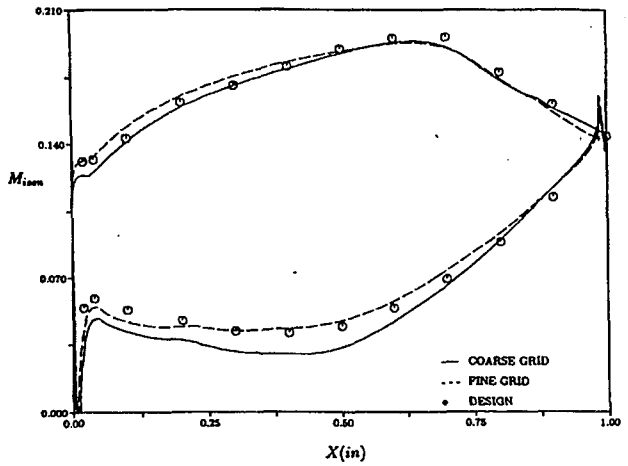

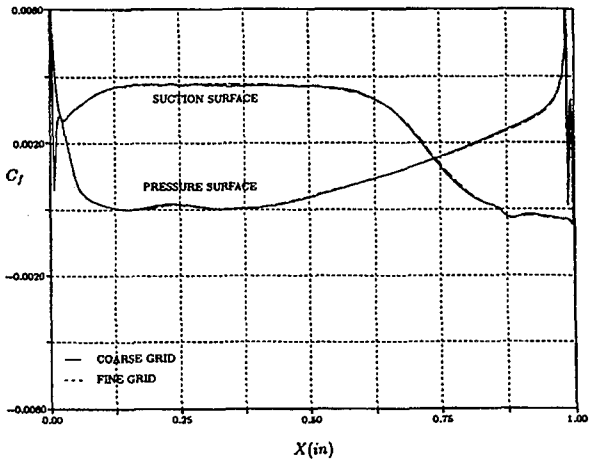

Mach Number

Skin Friction

Transition Limit Cycle
Re=80,000

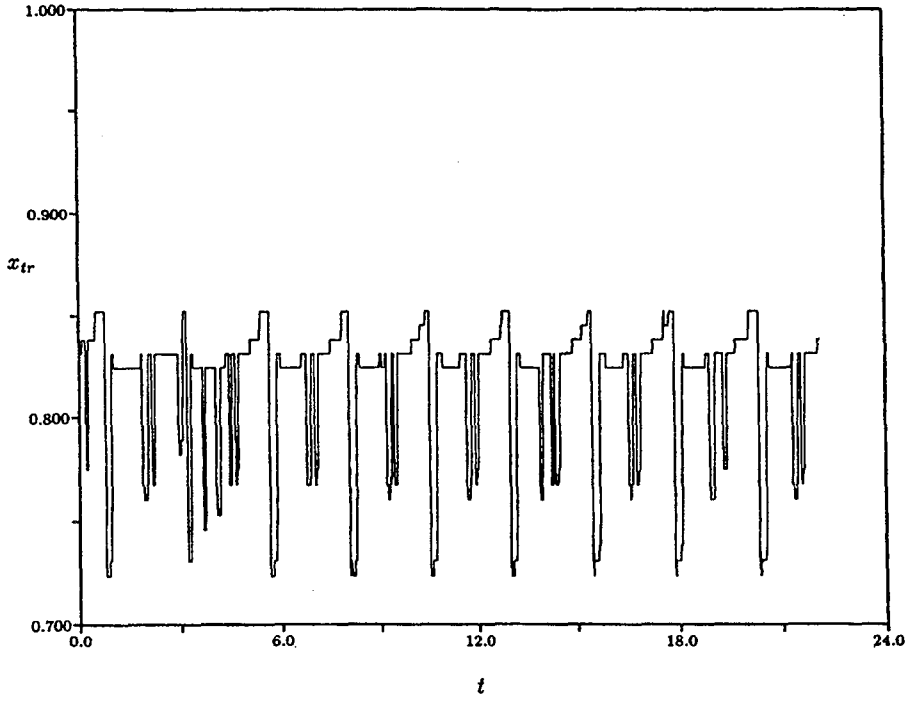

k-e Turbulence Model Effects
Re=80,000

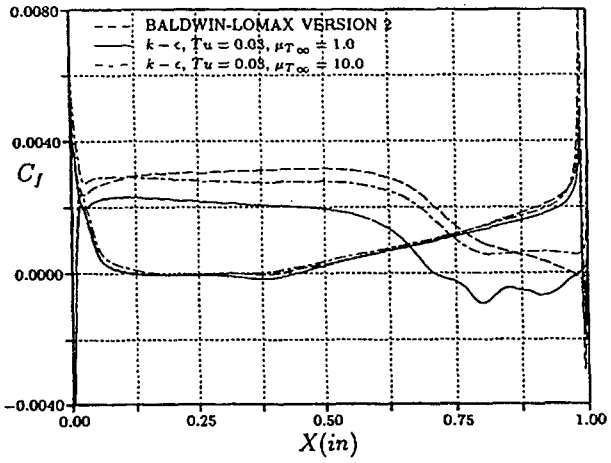

Length Scale

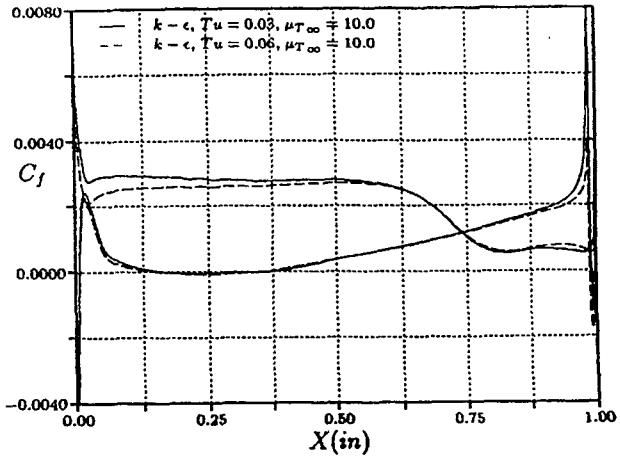

Tu Level

k-e Turbulence Model Effects
Re=80,000

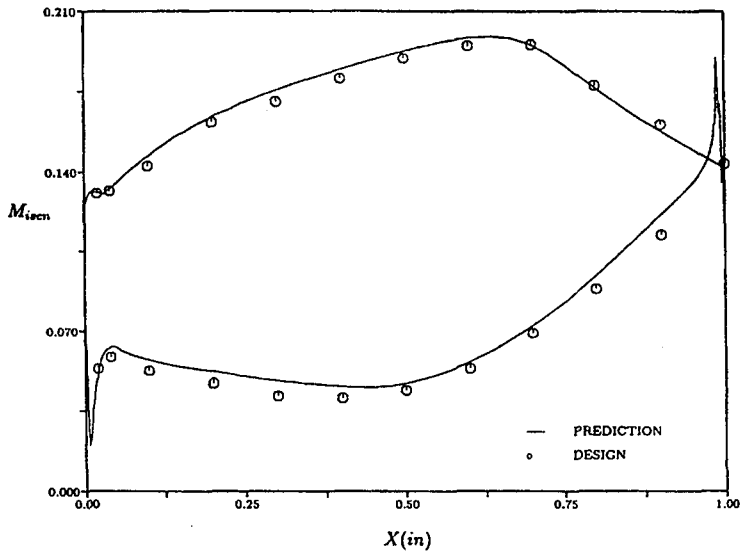

Mach Number

Transitional Flow at Re=120,000

Baldwin-Lomax

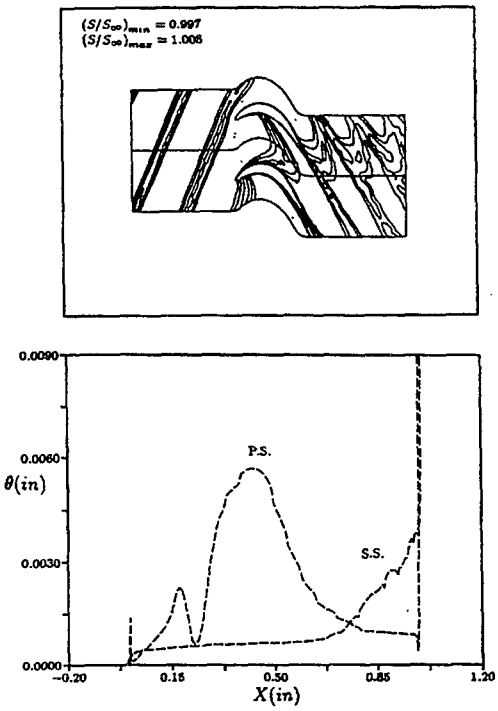

0% Cycle

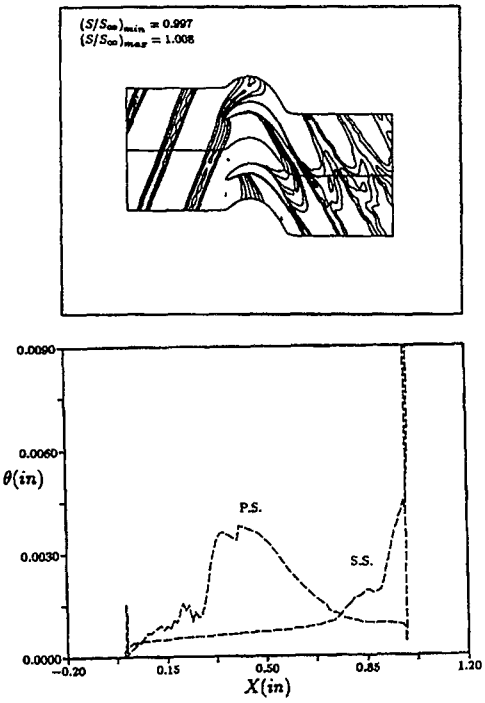

25% Cycle

Transitional Flow at Re=120,000

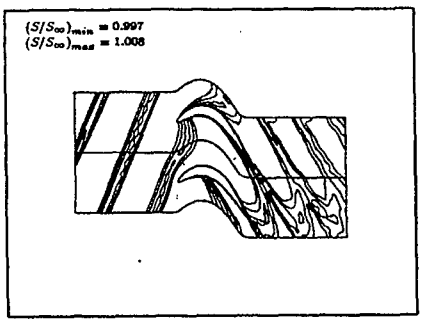

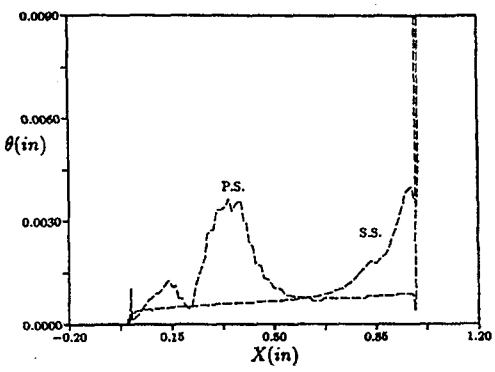

50% Cycle

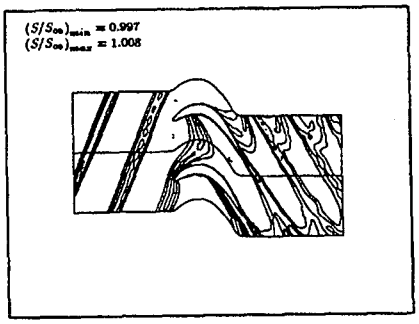

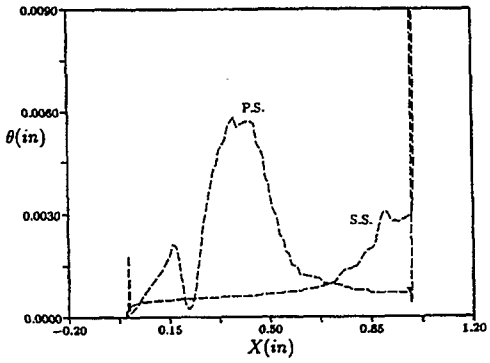

75% Cycle

Stage Simulations

PAK-B Stage Grid

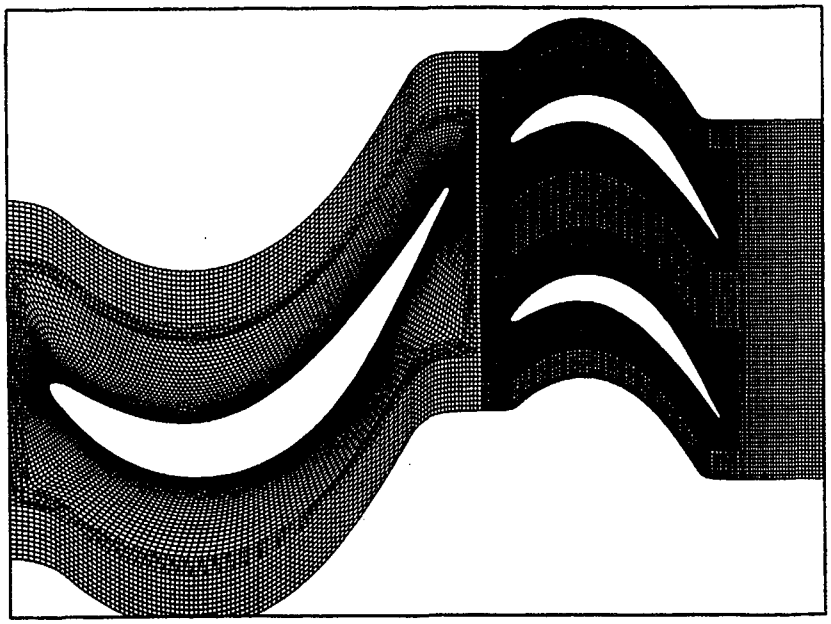

Transitional Flow at Re=40,000

Baldwin-Lomax

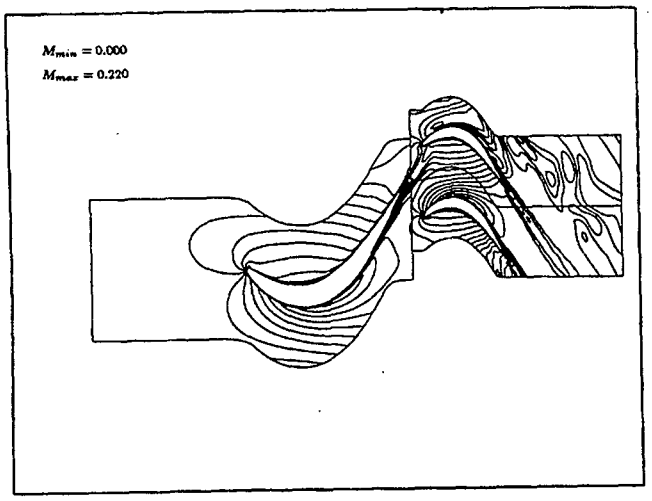

Mach Number

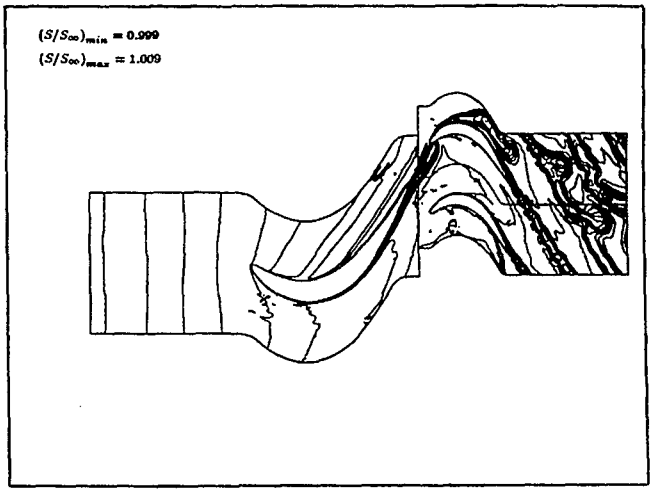

Entropy

Flow at Re=40,000

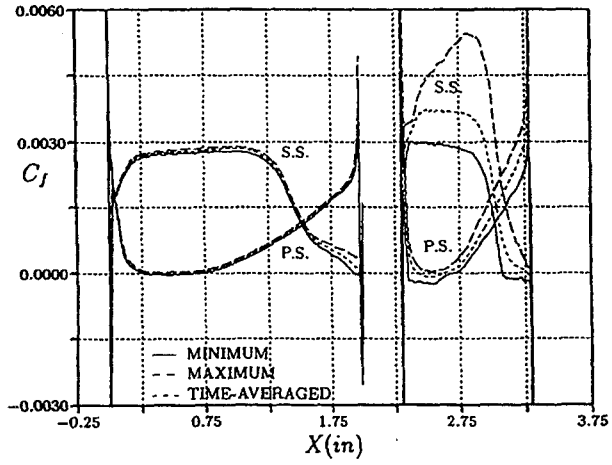

Turbulent - BL

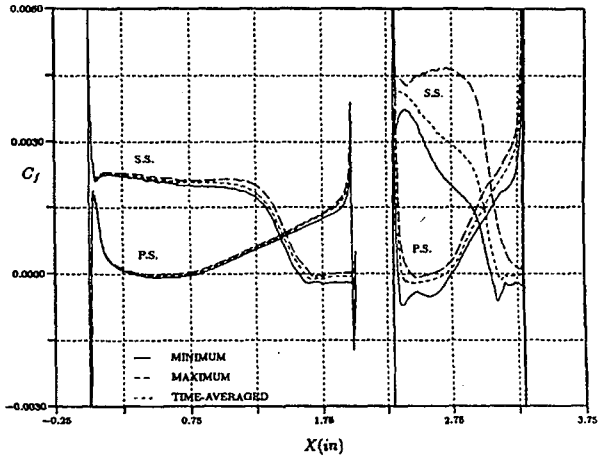

k-e

Flow at Re=40,000

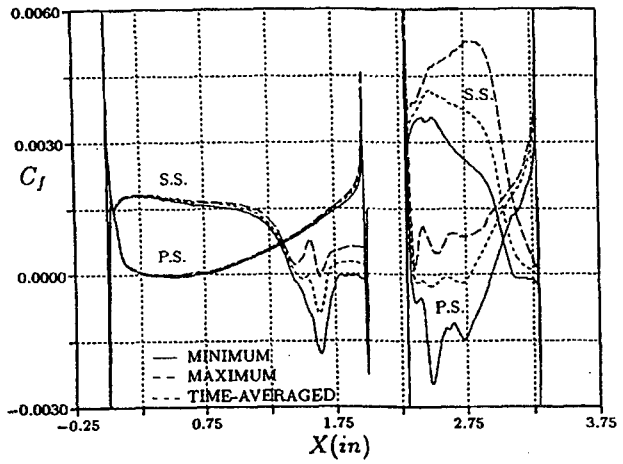

Fixed Trans. - BL

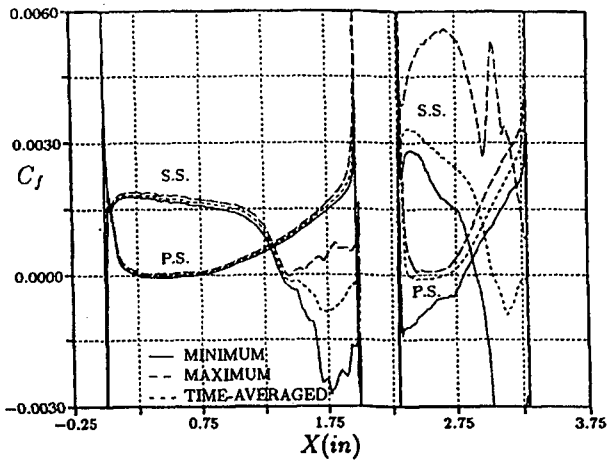

Floating Trans. - BL

Summary

- Cascade simulations
  - Transition model needed to accurately capture losses
  - BL and k-e models give similar results
- Stage simulations
  - Transition location varies significantly
  - Efficiency changes 1.5% with transition modelled

Work in Progress

- Incorporating more recent transition models
- Three-dimensional simulations of the PAK-B geometry

WAVELET ANALYSIS OF TURBULENT SPOTS AND OTHER COHERENT STRUCTURES IN UNSTEADY TRANSITION*

Jacques Lewalle
Syracuse University
Syracuse, New York

ABSTRACT

This is a secondary analysis of a portion of the Halstead data. The hot-film traces from an embedded stage of a low pressure turbine have been extensively analyzed by Halstead et al. In this project, wavelet analysis is used to develop the quantitative characterization of individual coherent structures in terms of size, amplitude, phase, convection speed, etc., as well as phase-averaged time scales. The purposes of the study are (1) to extract information about turbulent time scales for comparison with unsteady model results (e.g. k/epsilon). Phase-averaged maps of dominant time scales will be presented; and (2) to evaluate any differences between wake-induced and natural spots that might affect model performance. Preliminary results, subject to verification with data at higher frequency resolution, indicate that spot properties are independent of their phase relative to the wake footprints: therefore requirements for the physical content of models are kept relatively simple. Incidentally, we also observed that spot substructures can be traced over several stations; further study will examine their possible impact.

Overview

Purpose: modeling

- **Unsteady RANS**

  phase-dependent time scale (κ/ε)

- **Spot properties**

  properties of wake-induced vs. natural spots

The data

- **Halstead et al**

  The GE research turbine, point 5A

- **Past work:**

  Time scales in freestream

- **This work:**

  Focus on hot film data

The tool: wavelets

* Work supported by NASA Lewis Research Center (Contract no. C-76220-D).

Wavelet transforms

Time-frequency decomposition

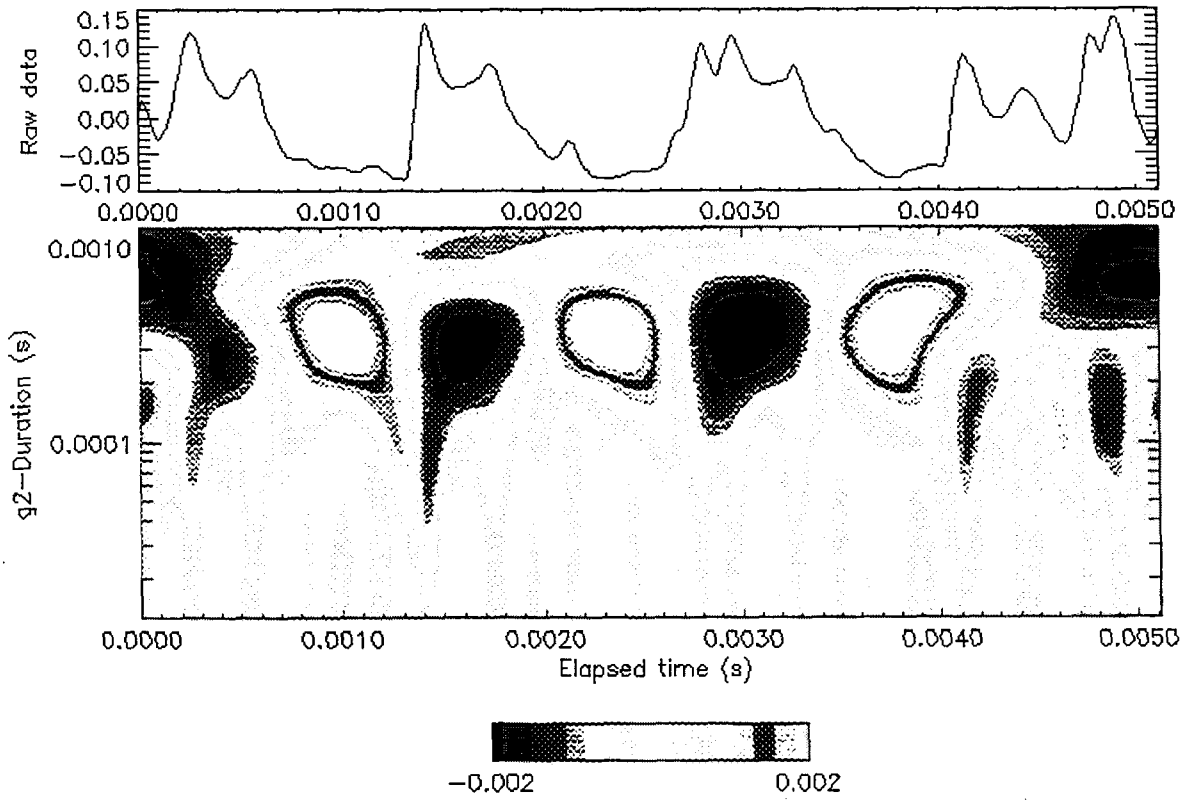

Figure1: Time trace at the beginning of transition (station 8) and Mexican Hat wavelet map, showing wake-related periodicity as well as one-time shorter events}

The time scales

- Phase relative to the wake passing
- Evolution of phase-dependent dominant scales
- Phase determination
  - At the best section (s* = .32), wake footprints are not periodic
  - Flapping?....
  - Morlet wavelet: instantaneous phase at the wake-passing frequency
  - Successive stations: cross-correlation with the previous station
  - We are NOT tracking the wake, but the structures

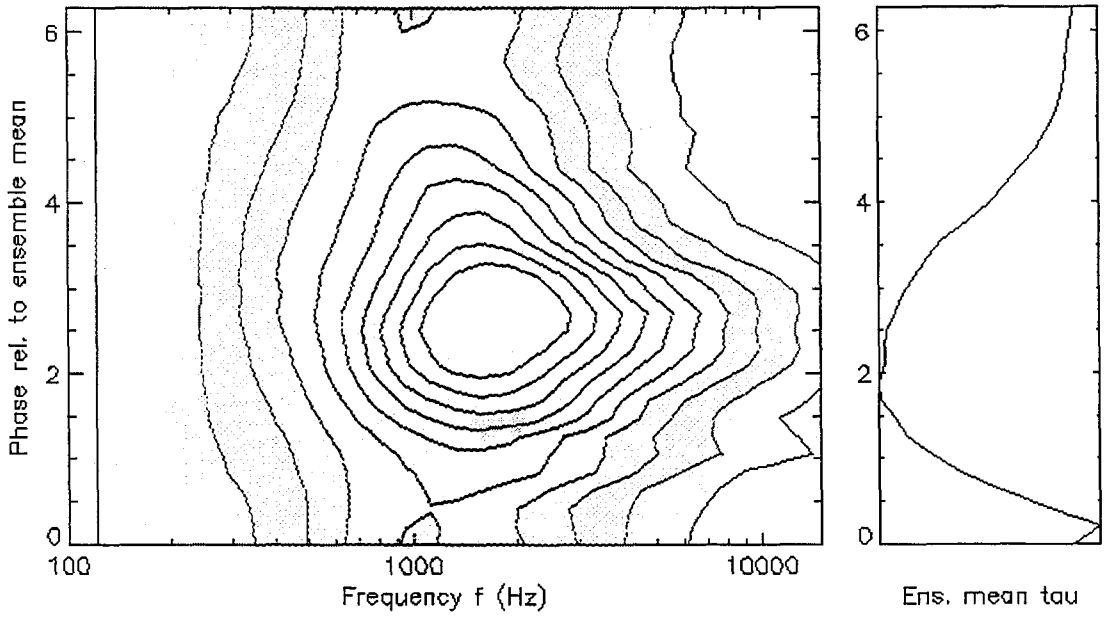

Figure 2: Phase dependence of the power spectrum at station 8. The dominant scales, fluctuating around 1000 Hz, vary with the phase relative to wake passings

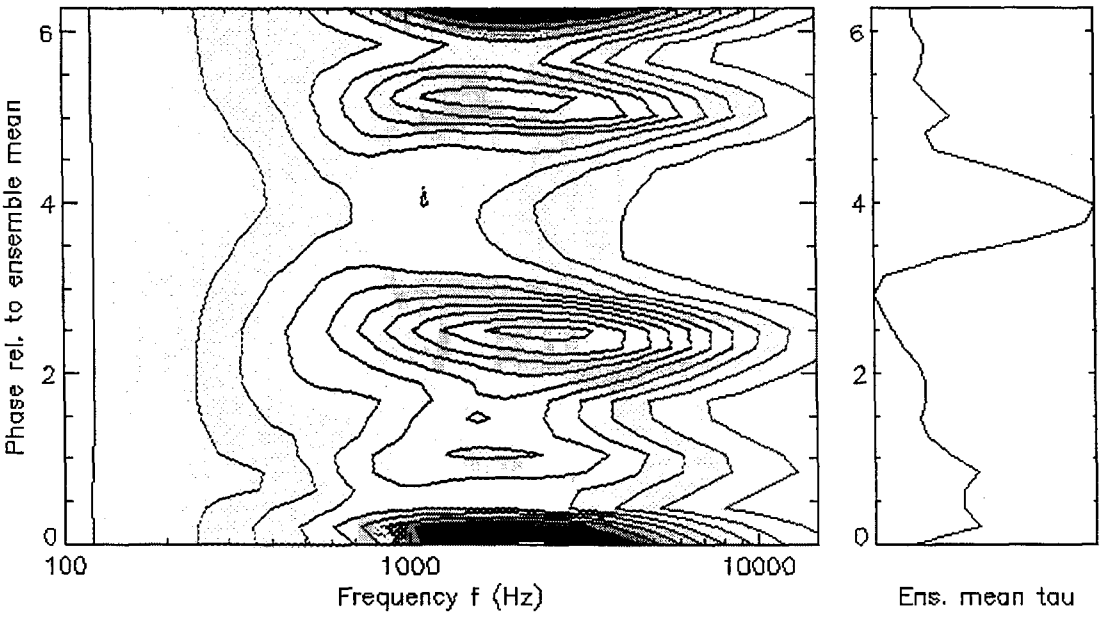

Figure 3: As figure 2, station 10

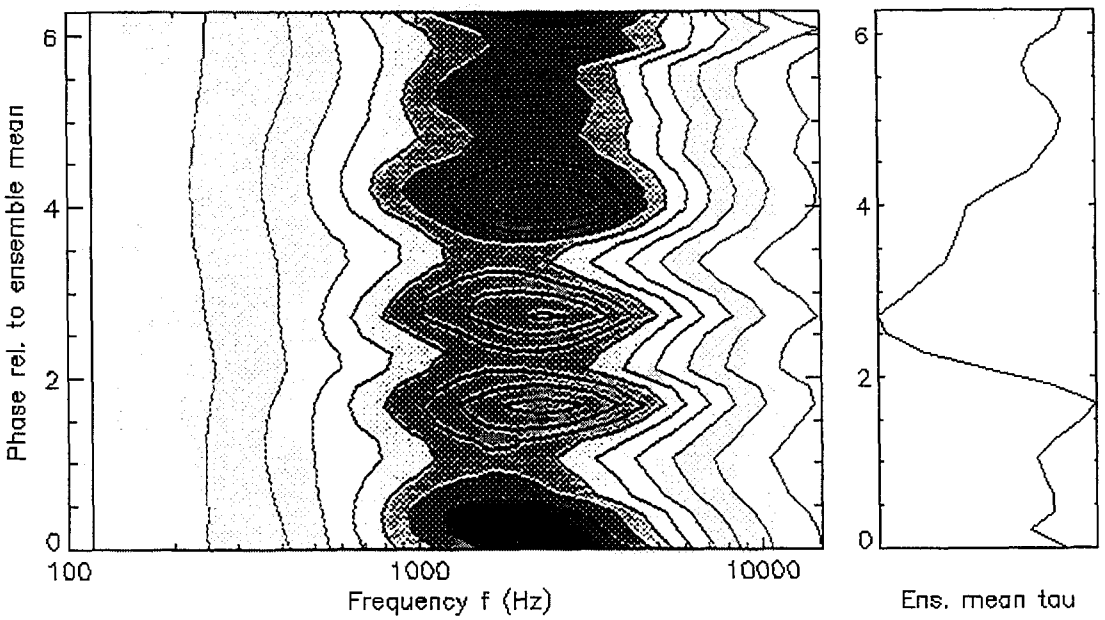

Figure 4: As figure 2, station 12

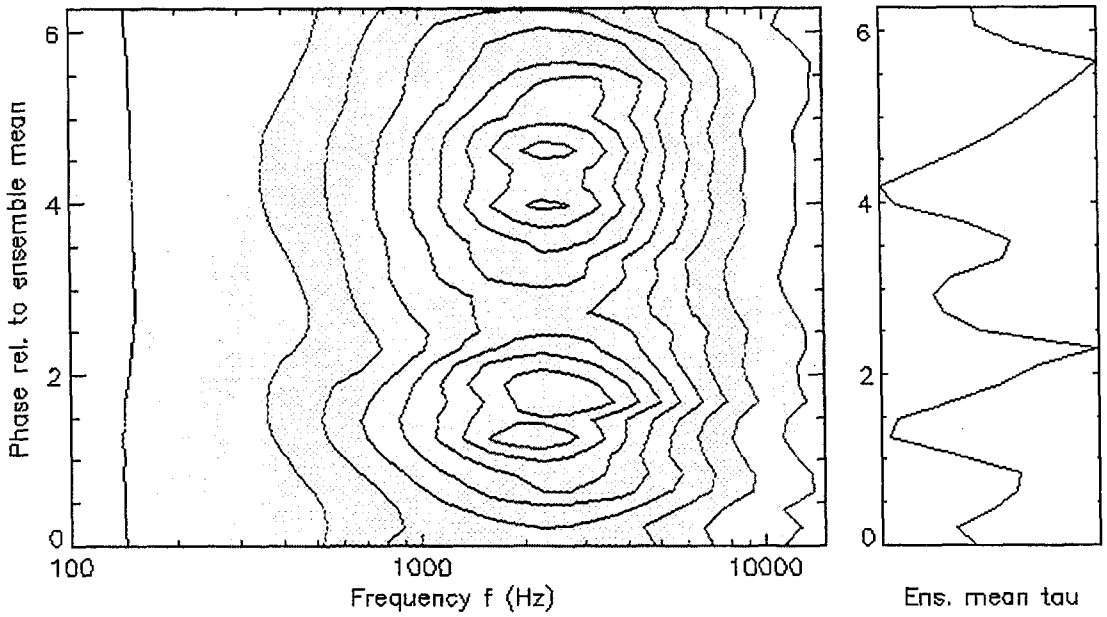

Figure 5: As figure 2, station 14. The rapid evolution of the dominant time scales, presumably associated with turbulent transport properties, is obvious from Figures 2-5.

Tracking coherent structures

- One can track coherent structures
    1. Local maxima of a (filtered) signal
    2. A reasonable tracking algorithm
    3. Variants
- Not all structures are spots
    1. What are they?
    2. Characterization: convection speed, growth,...
- Not all structures are wake-induced
    1. Calmed regions
    2. Natural transition
- Differences in structure properties
- Spots/others
- Wake gets ahead of spots: destabilize the front?
- Event amplitudes, size, growth,...
- Wavelet characterization of structures

Wake passing unsteady filtering

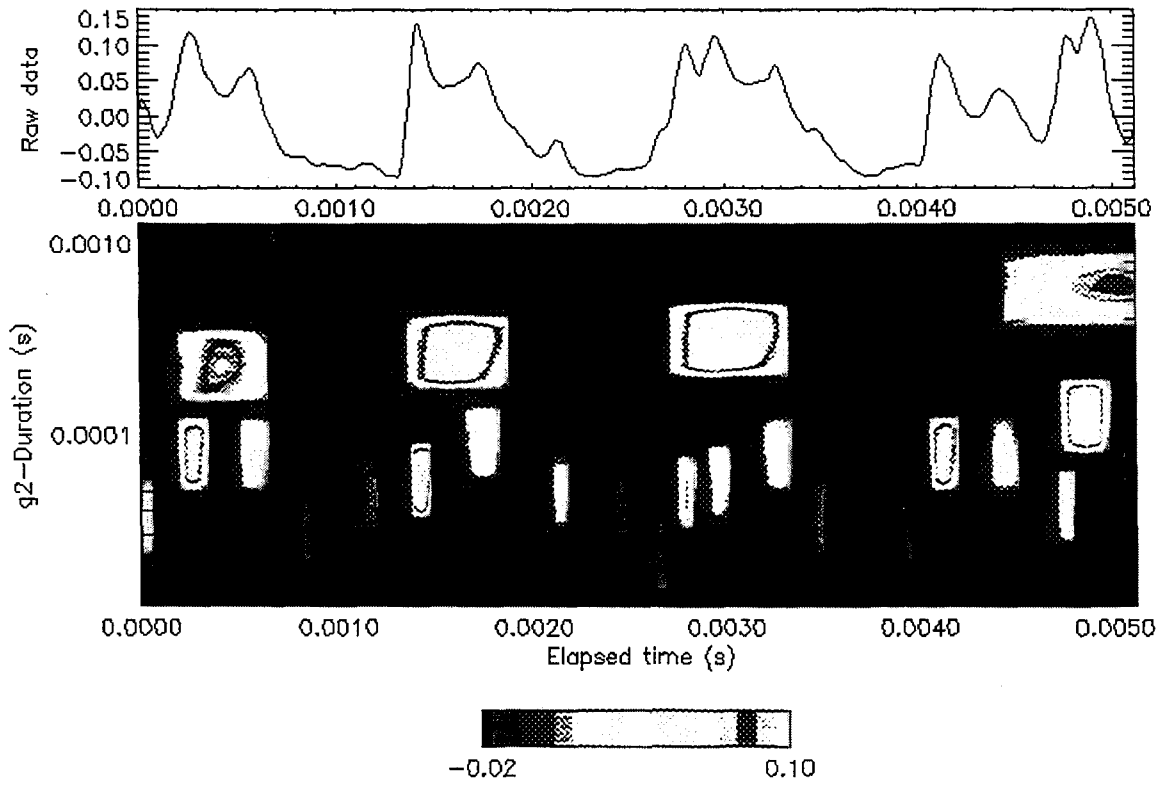

Figure 6: Marking of dominant events (energy scale) prior to filtering of wake-passing events.

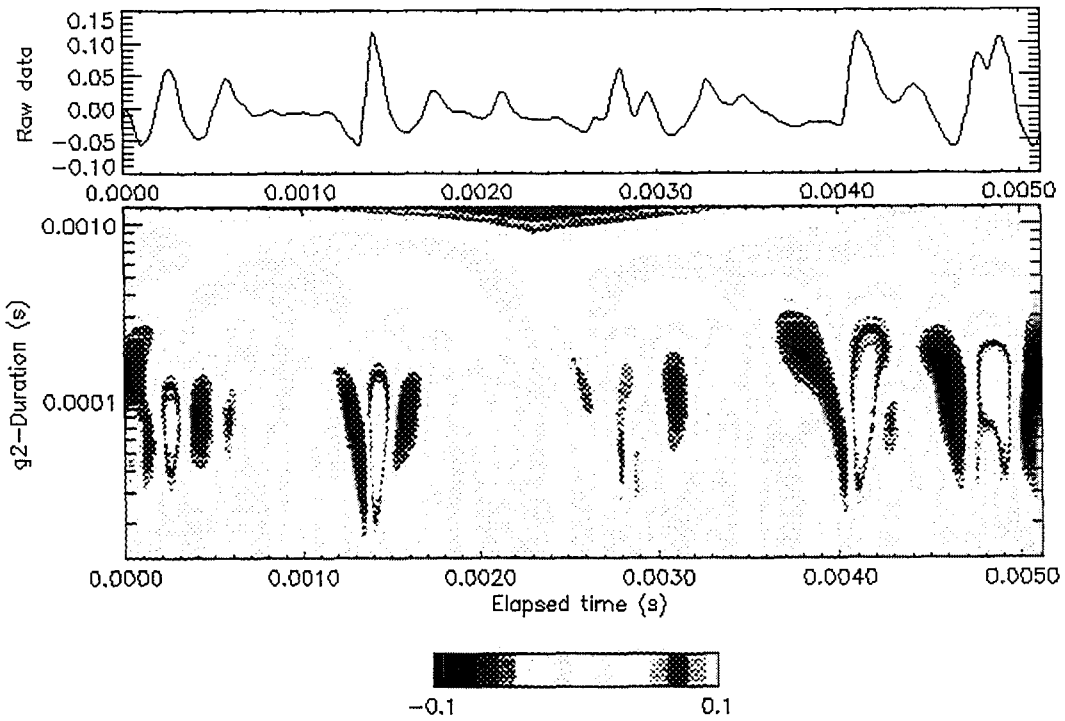

Figure 7: Filtered trace corresponding to Fig.1, and its wavelet map. Spot candidate events are more easily recognizable.

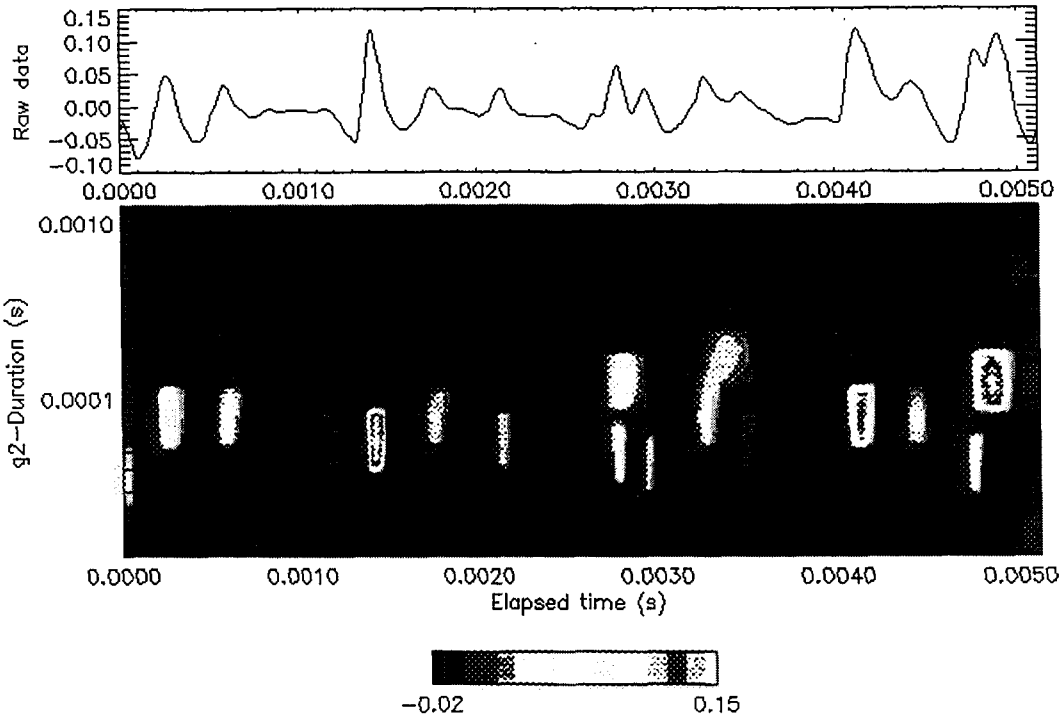

Figure 8: Identification of candidate events from the filtered energy content.

The algorithm

1. Individual event characterization

(a) Candidate events

- maximum of pwss (pseudo wall shear stress)
- maximum negative curvature of pwss (bumps)
- not too close to each other

(b) Wavelet events

- maxima of spectral energy density
- spectral separation
- event removal, spurious events

(c) Matching candidate events to dominant wavelet events

(d) Characterization of 80% of events.

2. Tracking events downstream

- expected location, size, energy content
- define a *distance* between expected events and actual events
- match them to minimize distance
- unmatched events are deleted
- deleted events account for about 30% of events
- remaining events are `coherent'

3. Joint event statistics

Tracking

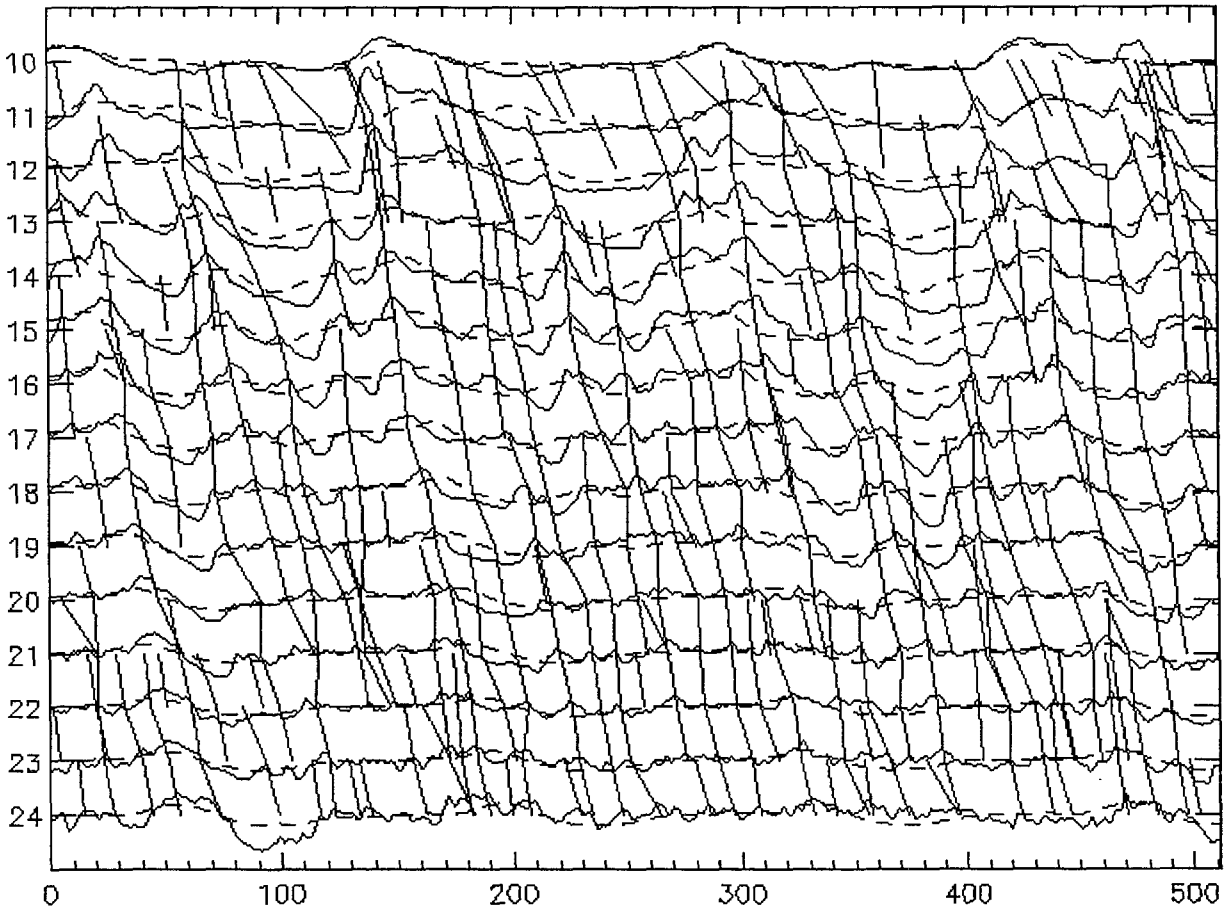

Figure 9: Event matching from trace to trace identifies spot trajectories in the space/time domain. Raw traces are also shown. Only spots that can be tracked are analyzed in the following.

Structure properties

Quantitative values

1. time of occurrence
2. chord value
3. time scale
4. energy content
5. age
6. convection speed
7. leading and trailing edge locations
8. size
9. edge convection speeds

Typical Results

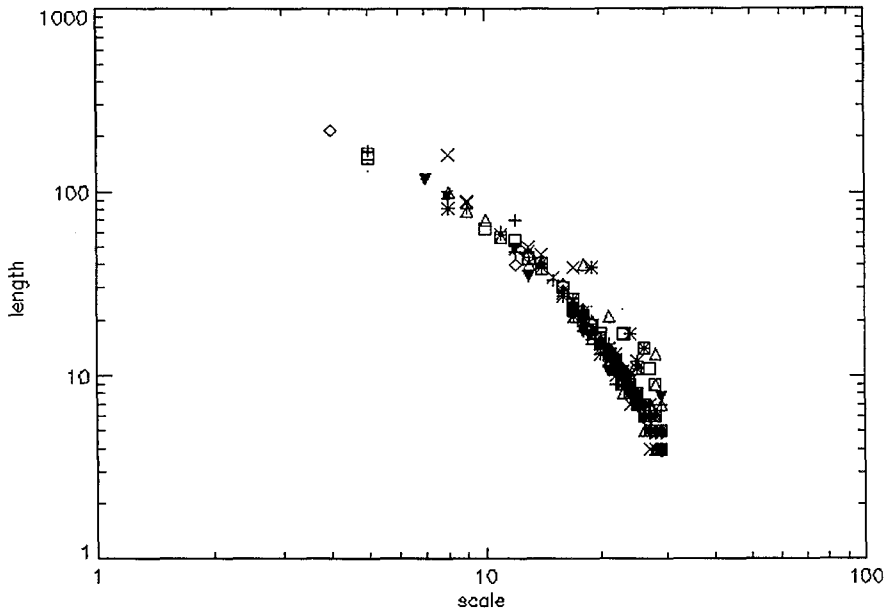

Figure 10: Spot length (difference between leading and trailing edge occurrence time) versus dominant frequency. The near-proportionality of length and inverse frequency for the longer events shows that the energy-dominance is associated with spot occurrence rather than with turbulence inside the spots.

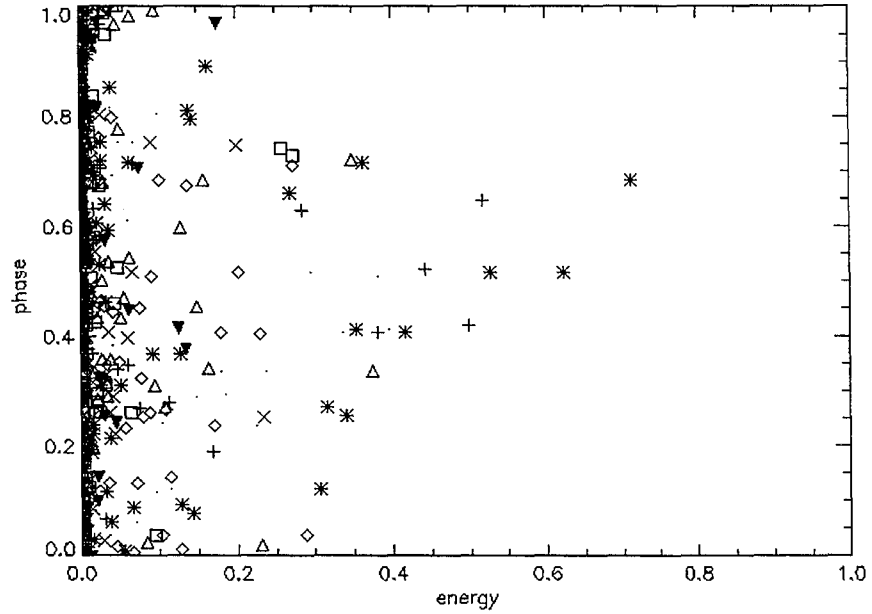

Figure 11: Event energy versus relative phase, at stations 10-13. The most energetic spots occur around 0.6 relative phase.

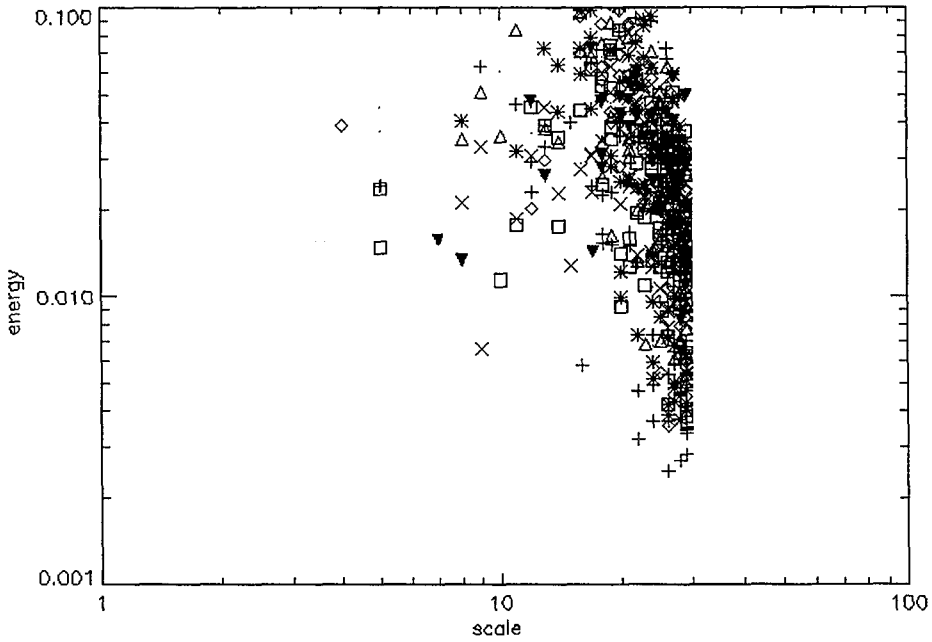

Figure 12: Event energy versus dominant frequency. Two populations may be identified, energetic low-frequency events scattered on the left, and higher frequency events at all energy levels to the right.

Conclusions

- Unsteady time scales
- Event characterization, tracking
- Flexibility of wavelet processing

SESSION 6

LAMINAR SEPARATION AND SPOTS

NASA/CP—1998-206958

TRANSITION IN LEADING-EDGE SEPARATION BUBBLES

Rajesh Khan and Nick Cumpsty
Cambridge University
Cambridge, England

ABSTRACT

Separation bubbles are very common near the leading edge of airfoils. Although extending over a few percent of chord (normally less than 5 percent) they are of technological importance because they can determine the development of the boundary layer over the remainder of the chord. Measurements have shown that freestream turbulence has a very large effect on the nature of the bubble, with raised levels of turbulence leading to a pronounced shortening of the bubble. Quite different transition processes appear to be involved, depending of the level of turbulence and the incidence onto the airfoil. At low incidence no evidence of spot transition could be seen, but at higher incidence and low freestream turbulence spots are clearly visible in the bubble shear layer.

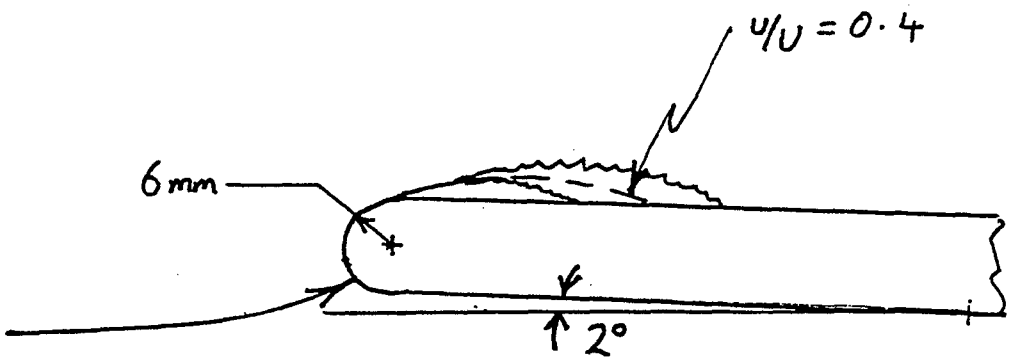

Grid Parameters				Measurements		Predictions	
Grid #	U_∞ (m/s)	x (mm)	d (mm)	Tu (%)	l (mm)	Tu (%)	l (mm)
0	9.01	N/A	N/A	0.1	53.2	N/A	N/A
3	9.13	525	3.2	2.3	10.8	2.1	8.2
3	2.37	525	3.2	2.3	10.9	2.1	8.2
4	8.79	525	12.7	6.2	18.4	5.6	16.3
4	2.59	525	12.7	6.2	17.4	5.6	16.3
1*	8.87	220	6.3	7.2	10.9	6.3	7.4
1*	2.53	220	6.3	7.5	8.4	6.3	7.4

Table 1: Turbulence intensity and integral lengthscale of grids.

Run #	Grid #	Re_r	i (°)
44	0	3500	0
45	0	3500	2
43	3	3500	0
42	3	3500	2
46	4	3500	0
47	4	3500	2
48	4	3500	4
49	1*	3500	2
50	1*	3500	4
51	1*	1000	0
52	1*	1000	2

Table 2: Experimental test matrix.

i = 0°, Re = Ur/ν = 3500

Static pressure distributions.

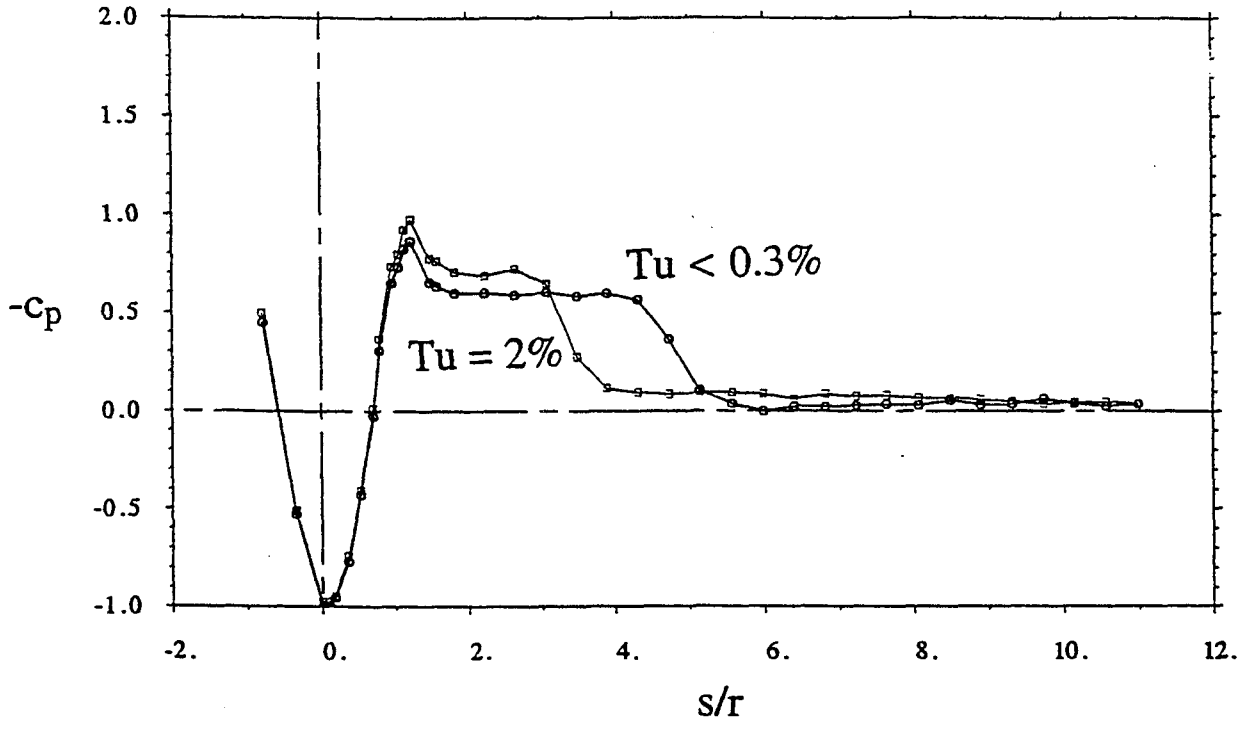

Velocity contours at u/Uref = 0.4

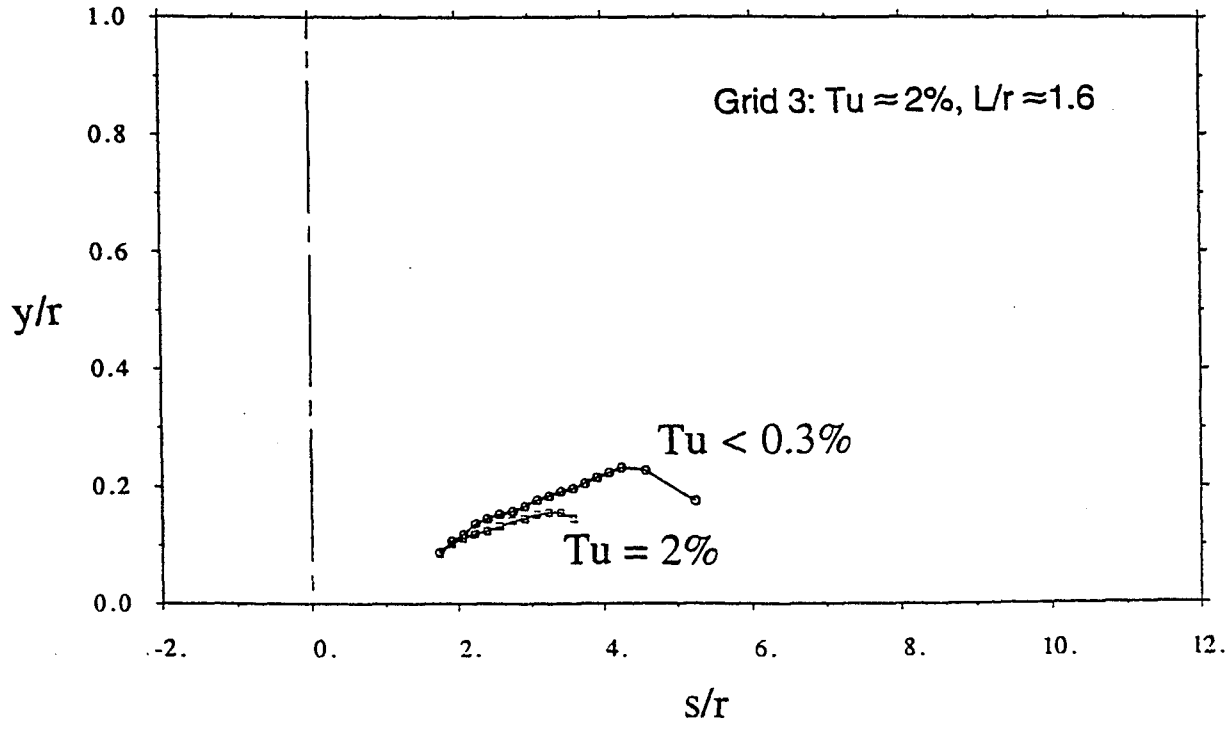

i = 2°, Re = Ur/ν = 3500

Static pressure distributions.

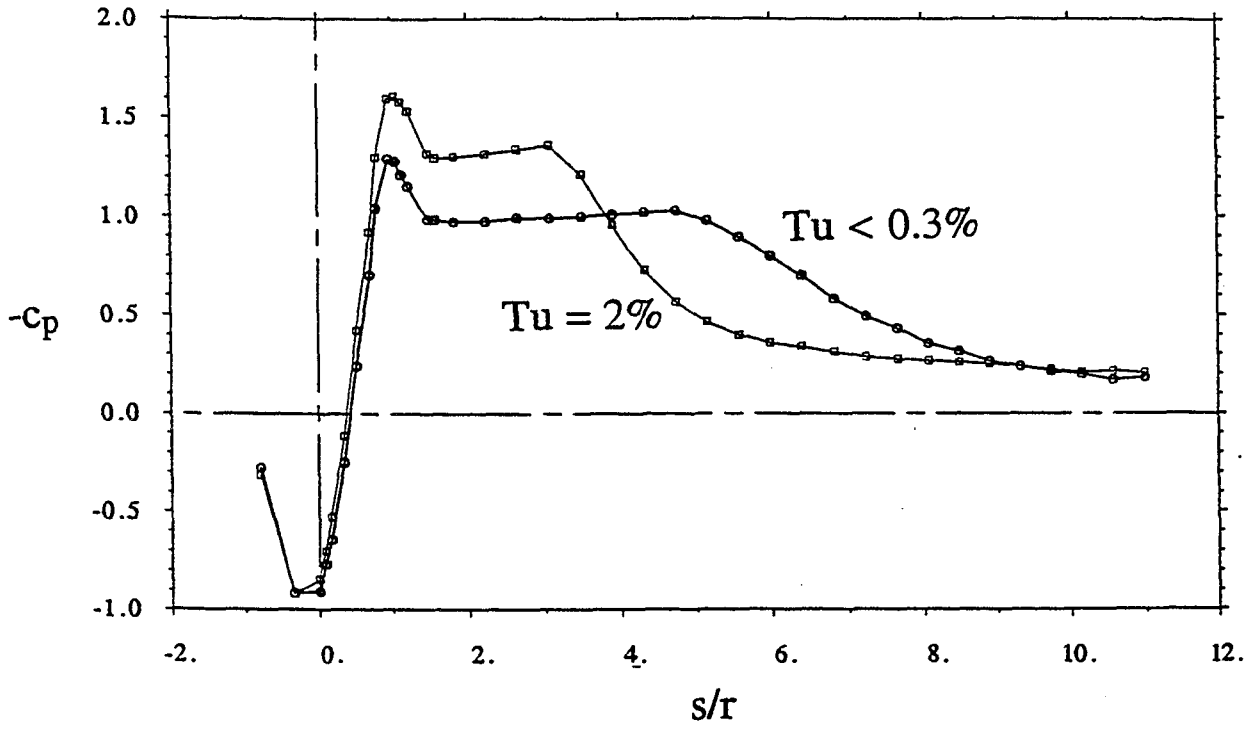

Velocity contours at u/Uref = 0.4

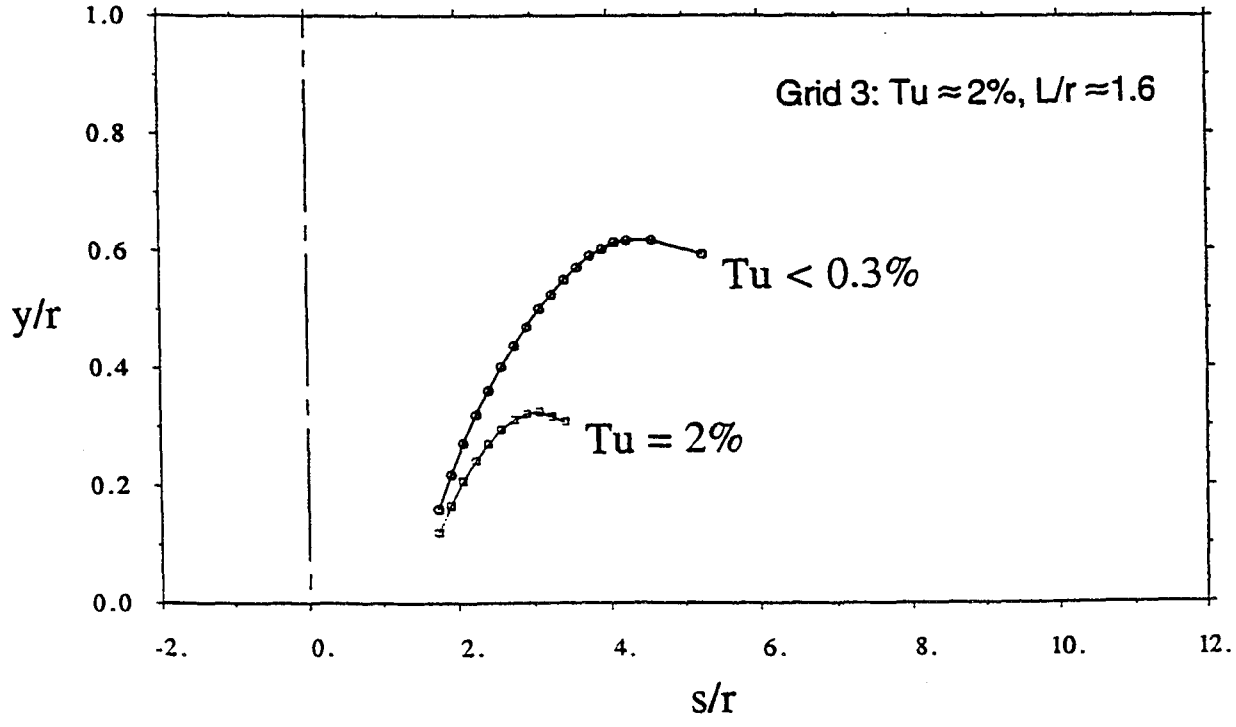

i = 2°, Tu = 6%

Static pressure distributions.

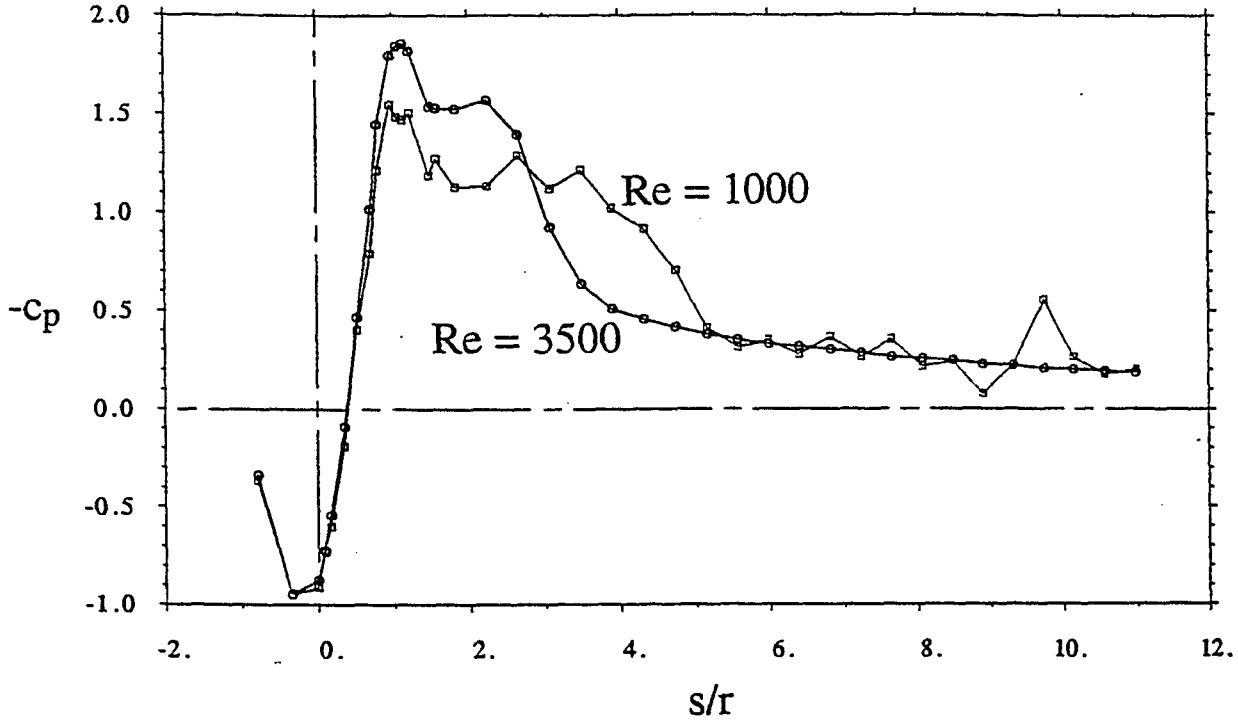

Velocity contours at u/Uref = 0.4

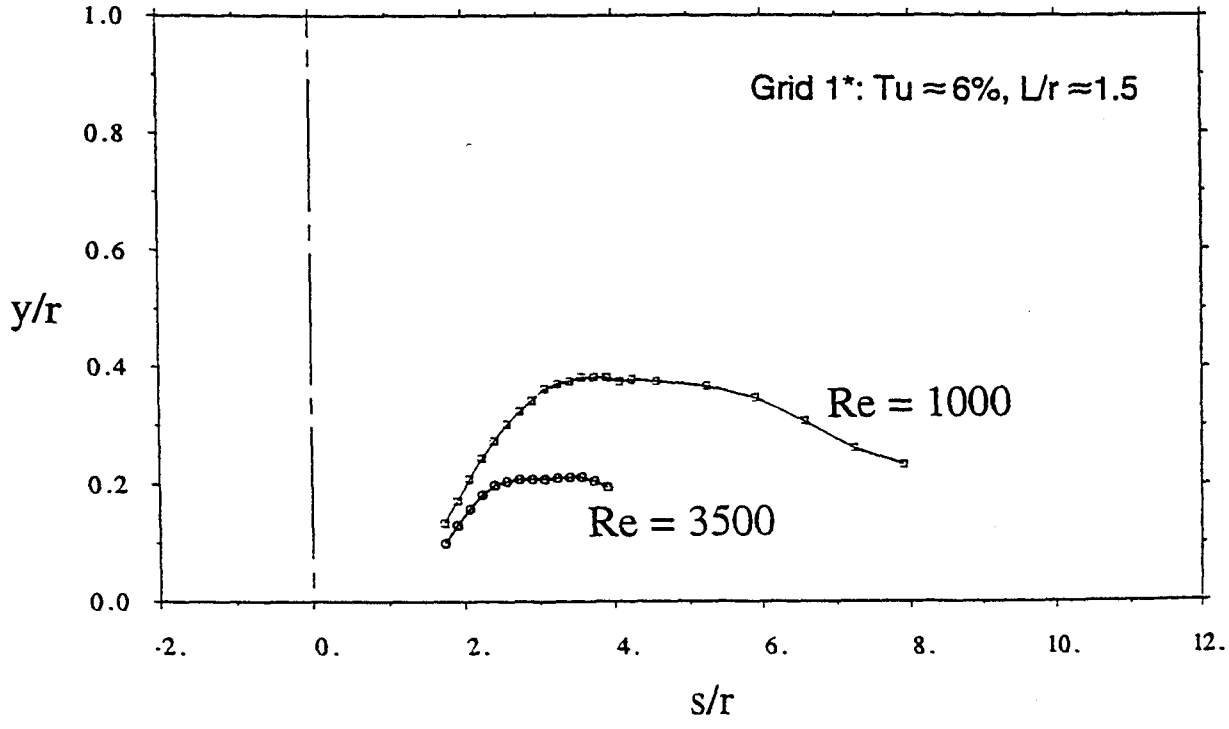

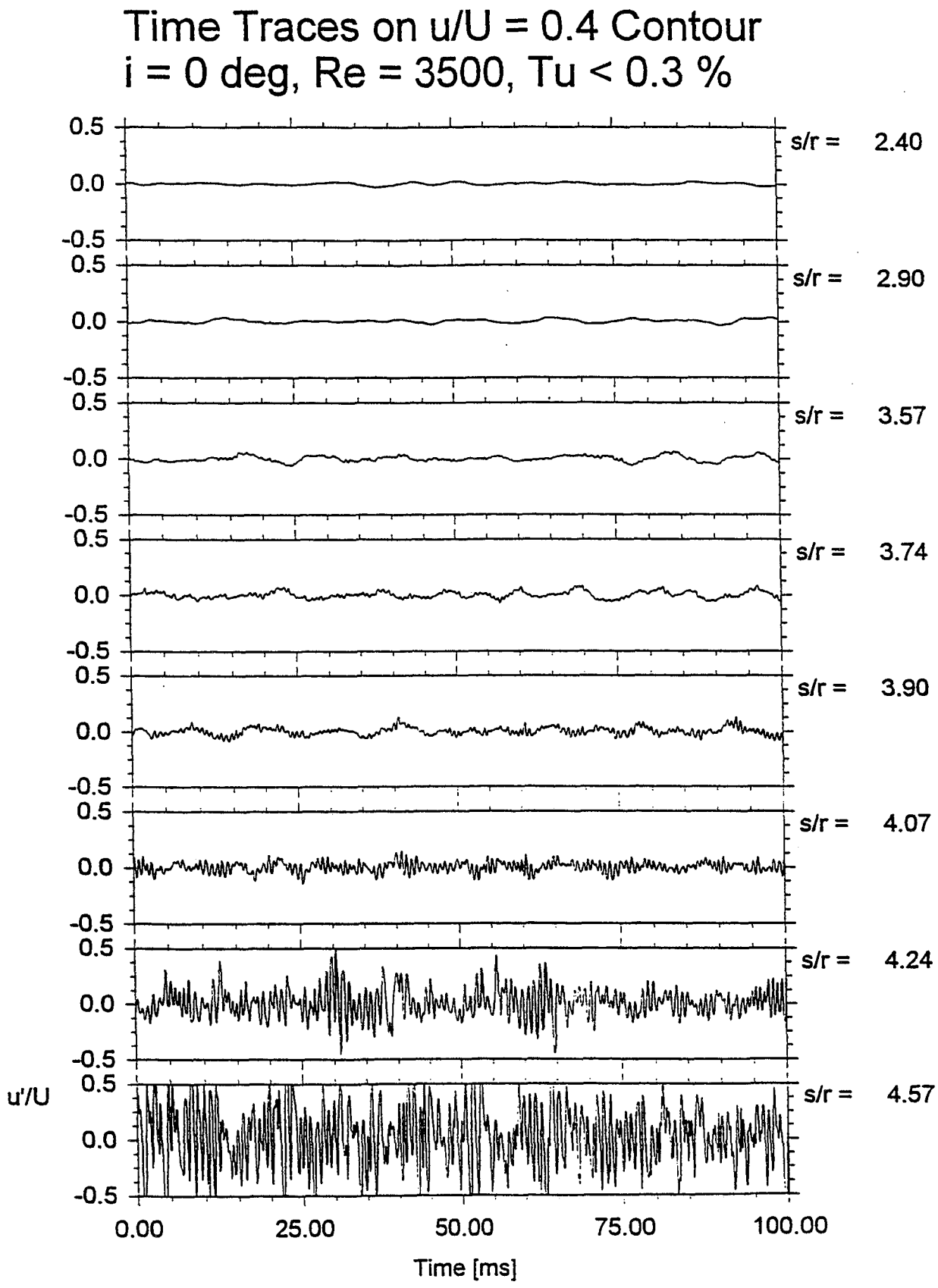
Time Traces on u/U = 0.4 Contour
i = 0 deg, Re = 3500, Tu < 0.3 %
s/r = 2.40
s/r = 2.90
s/r = 3.57
s/r = 3.74
s/r = 3.90
s/r = 4.07
s/r = 4.24
s/r = 4.57
u'/U
0.5
0.0
-0.5
0.00
25.00
50.00
75.00
100.00
Time [ms]

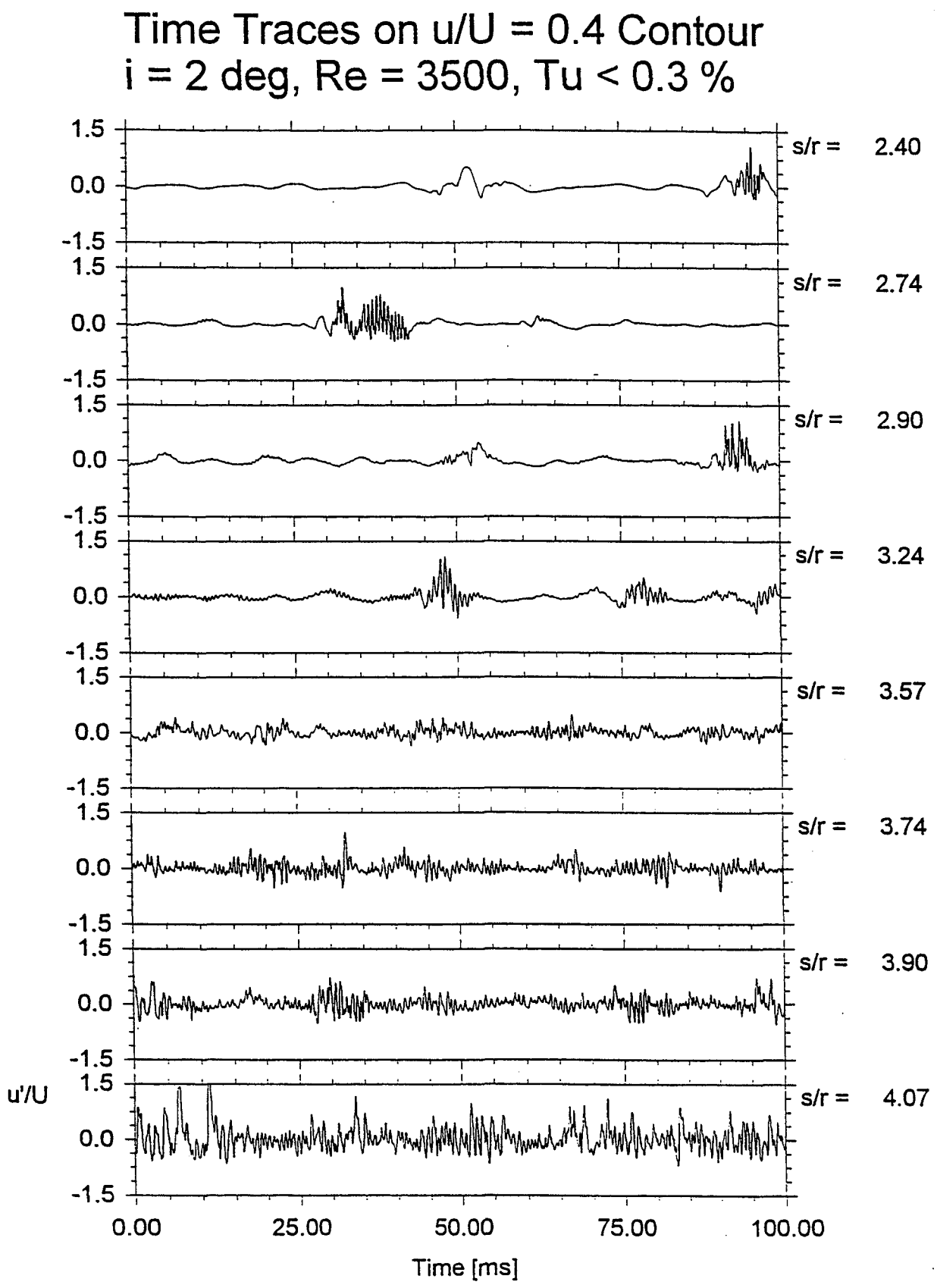
Time Traces on u/U = 0.4 Contour
i = 2 deg, Re = 3500, Tu < 0.3 %
s/r = 2.40
s/r = 2.74
s/r = 2.90
s/r = 3.24
s/r = 3.57
s/r = 3.74
s/r = 3.90
s/r = 4.07
1.5
0.0
-1.5
u'/U
0.00
25.00
50.00
75.00
100.00
Time [ms]

LAMINAR-TURBULENT TRANSITION IN SEPARATED BOUNDARY LAYERS

Ting Wang
Clemson University
Clemson, South Carolina

ABSTRACT

Experiments were conducted to investigate the laminar-turbulent transition process in separated boundary layers. Fifteen different cases of separated-flow transition have been analyzed in detail. The objectives were to (a) clarify the confusing and inconsistent views of short and long separation bubbles, (b) clearly distinguish the difference of the short laminar bubble and the transitional separation bubble, (c) establish new criteria to describe separation flow structure, and (d) provide new empirical correlations for predicting various modes of separation bubbles.

In this study, **laminar separation** is defined as the separation which starts in the laminar boundary layer and transition occurs between the separation point and the reattachment point but outside the dividing streamline. The reattachment of a laminar separation bubble is usually attributed to the completion of the transition process when the mixing of turbulent flow overcomes the adverse pressure gradients. Therefore, the laminar separation bubble is usually completed with a turbulent flow reattachment. The **turbulent separation** is defined as a separation which starts in the turbulent boundary layer, and reattachment is usually attributed to reduced adverse pressure gradients. The **transitional separation** is defined as the separation which starts in the transitional boundary layer and the reattachment occurs while still in the transitional boundary layer or in the fully turbulent boundary layer.

The overall outlook of the configuration of the laminar bubble is almost identical to that of the transitional bubble; however, their structures are different and the flow conditions (such as Reynolds numbers and pressure gradient parameters) in which they occur are very different. A hypothesized model for transition process in different modes of separation bubbles is proposed, as shown in Figs. 4-6. The definitions and notations for separated flows used in these figures are explained in Table 1.

It can be seen that the structure of the laminar short bubble is different from the transitional separation bubble. For example, in the laminar short bubble, the onset of transition occurs near the maximum displacement location, and the maximum turbulence energy (u') occurs near the reattachment point. However, in the transitional separation bubble, the transition starts upstream of the separation point and the maximum u' occurs near the maximum displacement point.

The prediction model to be developed would specifically identify the regions in which various separation models prevail. Fig. 11 shows a preliminary attempt to develop a separation prediction model. The data points shown in Fig. 11 are compiled from the open literature. It can be seen from Fig. 11 that the combination of the pressure parameter at separation (Ks) and various Reynolds numbers, namely at separation point (Re_s), at the maximum displacement point (Re_{MD}), and at the reattachment point (Re_R), constitute specific relations for various separation modes. For example, the reattachment Reynolds number (Re_R) is greater than the separation Reynolds number (Re_s) in laminar long bubble mode, whereas $Re_R < Re_s$ in the transitional separation mode even though the reattachment point is downstream of the separation point. It must be noted that the pressure parameter (K) alone cannot determine the separation mode.

Spectra and wavelet analyses were also performed to study the unsteady features of the bubble pulsation, vortex shedding, and bubble ejections.

Table 1 Definitions and Notations for Separated Flow Transition Model

Start of transition	X_t	The location where the flow structure of the boundary layer, or of the separated shear layer, deviates from the laminar behavior, the signal modifies and the dissipation sprectrum shows an increae in magnitude at selective frequencies. For attached flows the behavior of wall related parameters such as heat transfer and wall shear can be used as precise indicators of start of transition.
Early transition		The early portion of the transition process, where the attached boundary layer or the shear layer is characterized by strong turbulence production in mean flow direction and cross-stream Reynolds transports and by drastic changes in all variables.
Mid-transition	X(u'max)	The border between early and late transition, identified as the location of maximum (u').
Late transition		The late portion of the transition process where the shear layer is characterized by weaker turbulence production, stronger dissipa-tion, and redistribution of turbulence energy toward isotropic turbulence. In this region (u') decreases asymptotically toward the fully-turbulent flow value.
End of transition	XT	The location where the global behavior of the boundary layer or the separated shear layer matches that of a fully turbulent flow.
Separation	Xs	The location where the boundary layer detaches from the wall and the boundary layer displacement thickness begins to increase rapidly.
Maximum displacement location	Xsh	The location where the time-averaged height of the separation bubble, y_D, attains a maximum value. It is believed to coincide with the location of reverse flow vortex shedding.
First reattachment (for long bubbles)	Xr1	The region in which the periodic inflow towards the wall between two shedding vortices, locally modifies the mean velocity profile into a reattached-like flow.
Reattachment	Xr	The region where the time-averaged flow rejoins the surface.

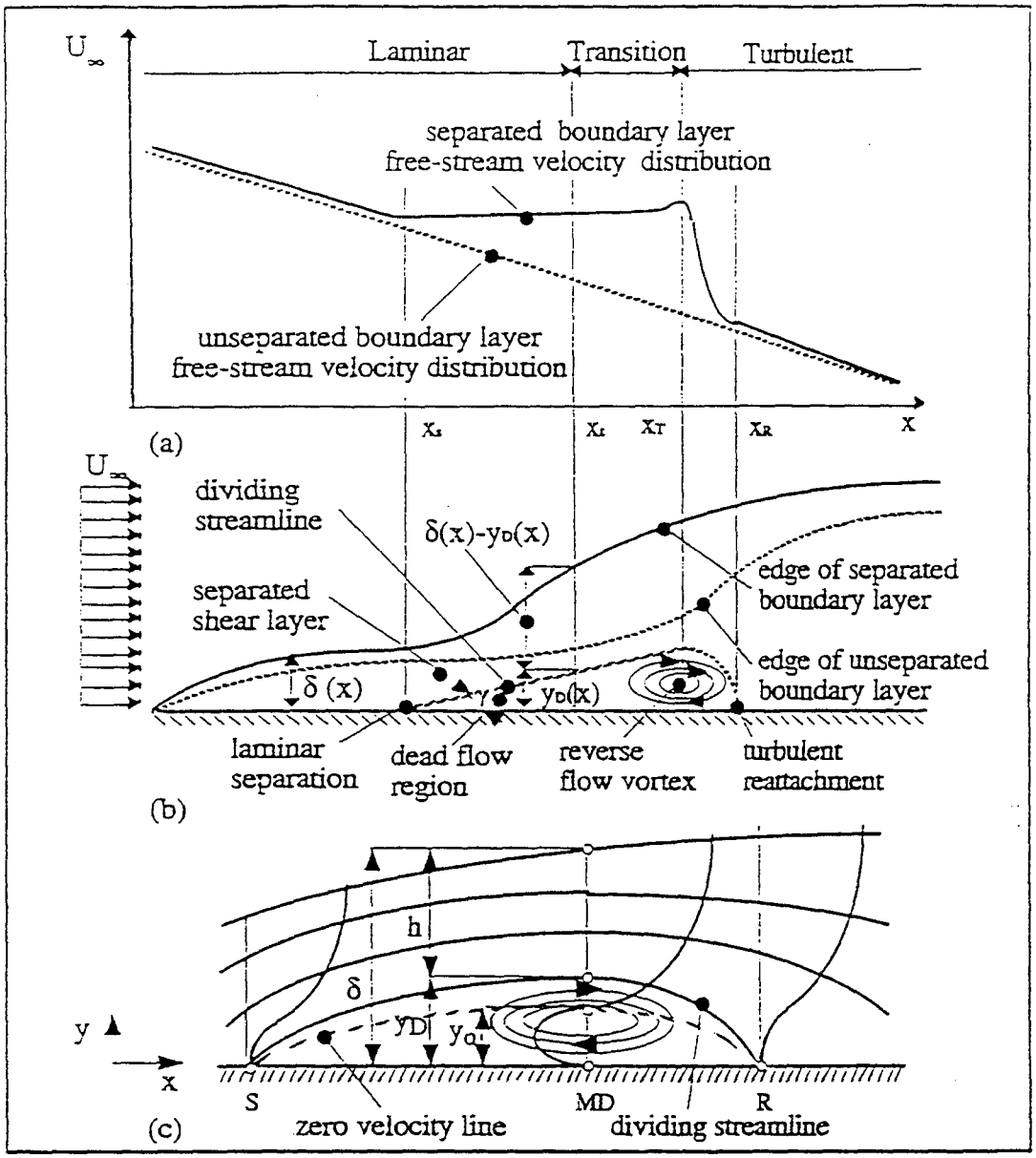

x_t - onset of transition;
x_T - end of transition;
x_s - separation point;
x_R - reattachment point;
h - shear layer thickness;
$\delta(x)$ - boundary layer thickness;
γ - separation angle;
$y_D(x)$ - dividing streamline elevation;
$y_o(x)$ - zero velocity line elevation

A conventional view of a 2-D laminar boundary layer separation:
(a) streamwise free-stream velocity distribution;
(b) boundary layer development and separation bubble elevation;
(c) velocity profiles along separation bubble.

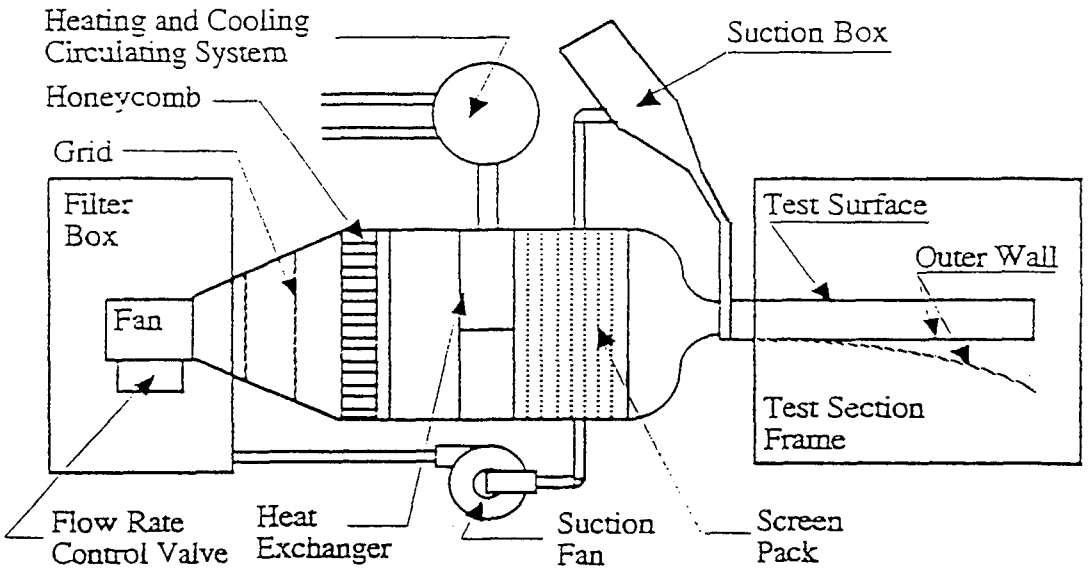

Figure 2.2 Plane view of the low-speed 2-D boundary layer wind tunnel facility.

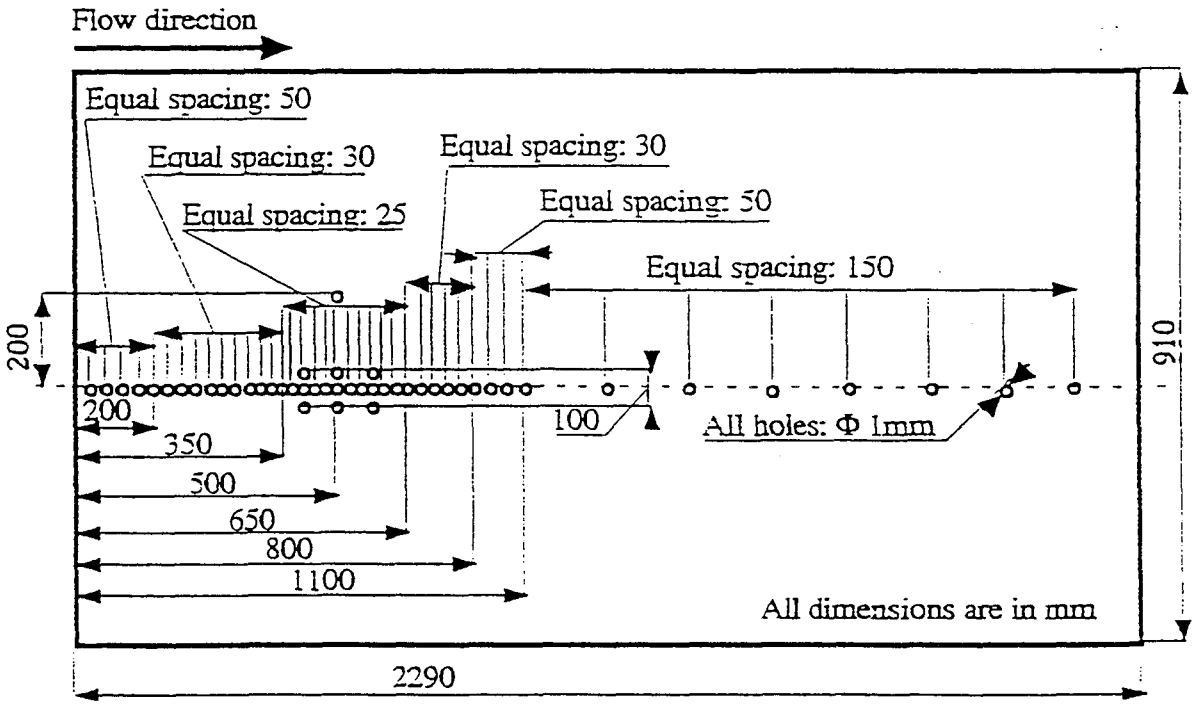

Layout of static pressure taps on the test surface.

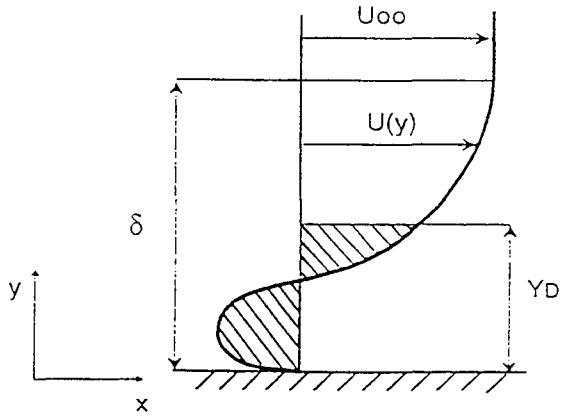

Figure 3 (a) A typical mean velocity profile of a separated boundary layer flow

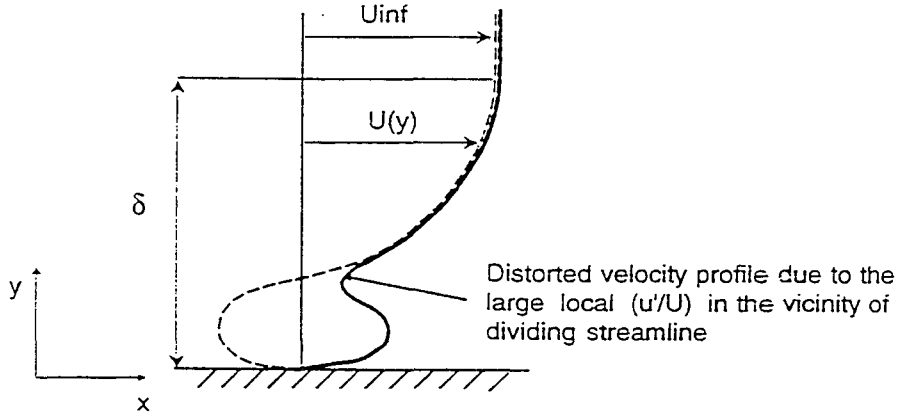

Figure 3 (b) Mean separated flow velocity profile measured with a hot wire

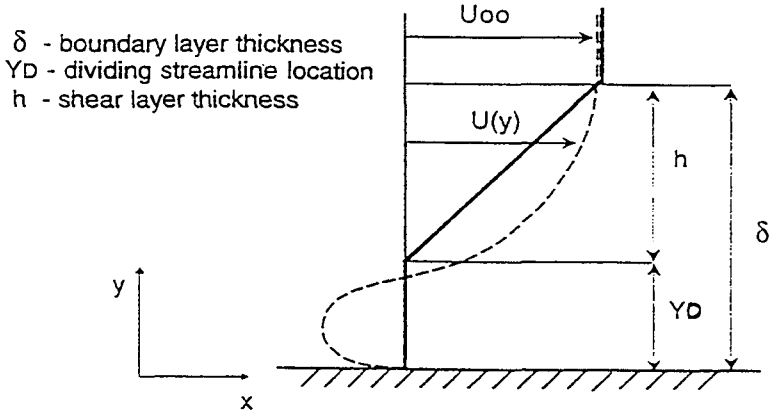

Figure 3 (c) Rayleigh broken line instability profile for separated boundary layer

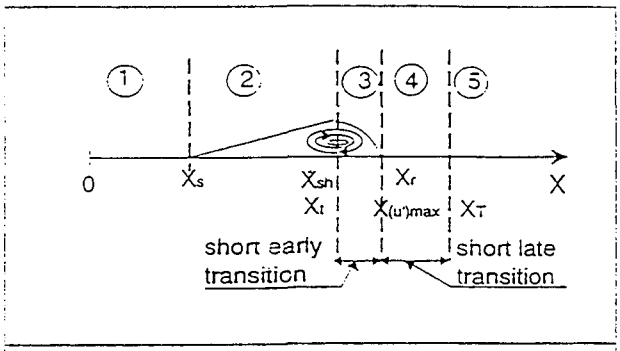

LAMINAR SEPARATION: SHORT BUBBLE MODE

Fig.4 Hypothetical Transition Process in Laminar Separated Boundary Layers at Low Reynolds Numbers, Mild Adverse Pressure Gradient

REGION 1	[0, Xs]	Attached, stable, laminar flow.
REGION 2	[Xs, Xt] [Xs, Xsh]	Stable, laminar, detached shear layer. Close to the separation location the low-frequency oscillations, too low to be subject of amplification, are dominant. The oscillations are mainly induced by the downstream periodic bubble "breathing". Inflexional instability sets in.
REGION 3	[Xt, X(u')max] [Xsh, Xr]	The onset of transition is induced by the shedding of the reverse flow vortex into the detached shear layer. The transition onset is characterized by high turbulent energy production in the low frequency range and it is clearly marked by local high dissipation rates at some discrete frequencies (e.g. f = 40 ~ 45 Hz) from those which are characteristic for the entire separated bubble. These frequencies are characteristic for the eddies size not for the unsteady motion. The primary vortex breaks down abruptly. The short early transition induces high r.m.s. streamwise velocity fluctuation (u'/U_∞ ~ 0.18). The vigorous mixing in the region of maxima (u') leads to reattachment.
REGION 4	[X(u')max, XT] [X>Xr]	The rapid coalescence into turbulence takes place within the reattaching boundary layer. The short late transition is caused by high dissipation rates at high frequencies (f > 70 Hz). The flow is still dominated by high turbulent energy content in the same low frequencies range.
REGION 5	[X>XT] [X>Xr]	Attached, non-equilibrium turbulent boundary layer.

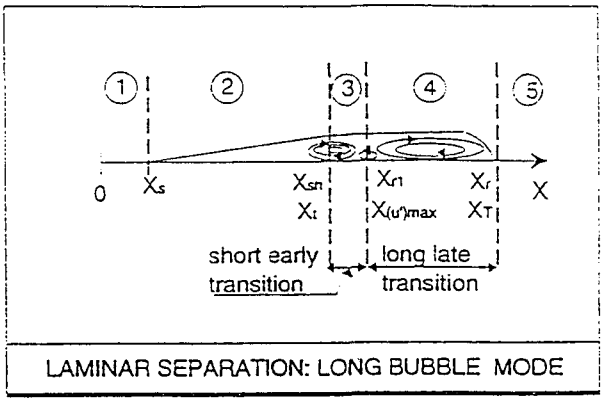

Fig.5 Hypothetical Transition Process in Laminar Separated Boundary Layers at Low Reynolds Numbers, Strong Adverse Pressure Gradient

REGION 1	[0, Xs]	Attached, stable, laminar flow.
REGION 2	[Xs, Xt] [Xs, Xsh]	Stable, laminar, detached shear layer. Low frequency oscillations, induced by the periodic bubble "breathing" are dominant. Far downstream separation, inflexional instability sets in.
REGION 3	[Xt,X(u')max] [Xsh,Xr1]	Similarly to the "short bubble mode" of transition, the onset of transition is induced by the shedding of the primary vortex into the detached shear layer. The transition onset is characterized by significant, but not so high, energy content in the low frequencies range, and it also produces local high dissipation rates at a discrete low frequency. Characteristic for the "long bubble mode" is the fact that the shedding process is accompanied by relatively high dissipation rates at high frequencies, and some strong, large eddy structures survive the early transition and preserve downstream. The high streamwise r.m.s. velocity fluctuations in the maxima (u') region ($u'/U_\infty \sim 0.15$) and the high rate of momentum transport inward and towards the wall leads to the first "reattachment" type behavior.
REGION 4	[X(u')max,XT] [Xr1, Xr]	Due to the outer flow strong adverse pressure gradient and relative reduced mixing, the shear layer fails to remain attached, the bubble "bursts" and a "long bubble" results. Another distinct low frequency activity within the shear layer, related to the secondary vortex, delays the completion of transition. The coalescence into turbulence forces the turbulent reattachment and a closed long bubble results.
REGION 5	[X>XT]; [X>Xr)	Attached, turbulent boundary layer. Large 2-D structures are still present far downstream, embedded within the small scale 3-D turbulence.

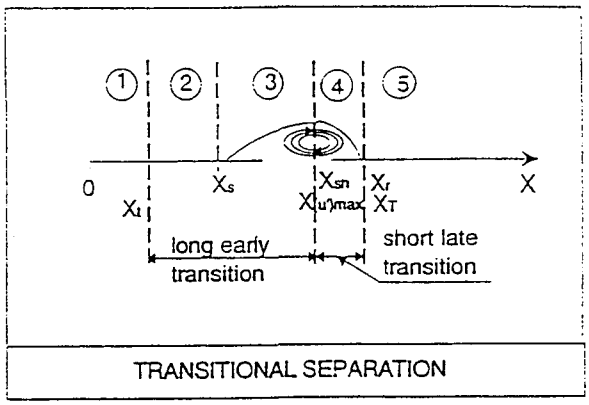

Fig.6 Hypothetical Transition Process in Transitional Separated Boundary Layers at High Reynolds Numbers, Mild Adverse Pressure Gradient

REGION 1	[0, Xt]	Attached, stable, laminar flow.
REGION 2	[Xt, Xs]	Natural transition takes place in the attached boundary layer: 2-D T-S instability waves appear, the spanwise 3-D waves evolve, then breakdown and eventually turbulent wave packets form. As the separation point is approached, the energy content in the low frequency domain (f < 10 Hz) increases. High dissipation occurs in the low frequencies range.
REGION 3	[Xs, X(u')max] [Xs,Xsh]	The turbulent wave packets spread within the detached shear layer, which oscillates due to the periodic bubble "breathing". The early transition takes place slower than expected for the overall adverse gradient flow condition, due to the existence of the "zero" pressure gradient plateau induced by the separation bubble stagnant flow region. The r.m.s. streamwise velocity fluctuation reaches its maxima value (u'/U_∞ ~ 0.16) in the middle of the separated shear layer. The end of the early transition, which coincides with the vortex shedding location, is characterized by an increase in energy production at low frequency (f = 10 ~ 70 Hz) and leads to a sudden reduction of dissipation in the low frequencies range.
REGION 4	[X(u')max,XT] [Xsh, Xr]	The active interactions between the transitional shear layer and the periodic ejections of turbulent fluid in the reverse flow vortex shedding region, accelerates the coalescence into turbulence, resulting in a short late transition. The flow adjusts rapidly to an almost uniform turbulent energy distribution at all frequencies, and the dissipation shifts to higher frequencies (f > 90 Hz). The periodic ejections with subsequent upstream flow sweeping and the turbulent mixing forces the shear layer to reattach.
REGION 5	[X>XT] [X>Xr]	Attached, non-equilibrium turbulent boundary layer. For sufficiently strong adverse pressure gradients, turbulent separation may occur in the immediate vicinity of the first reattachment

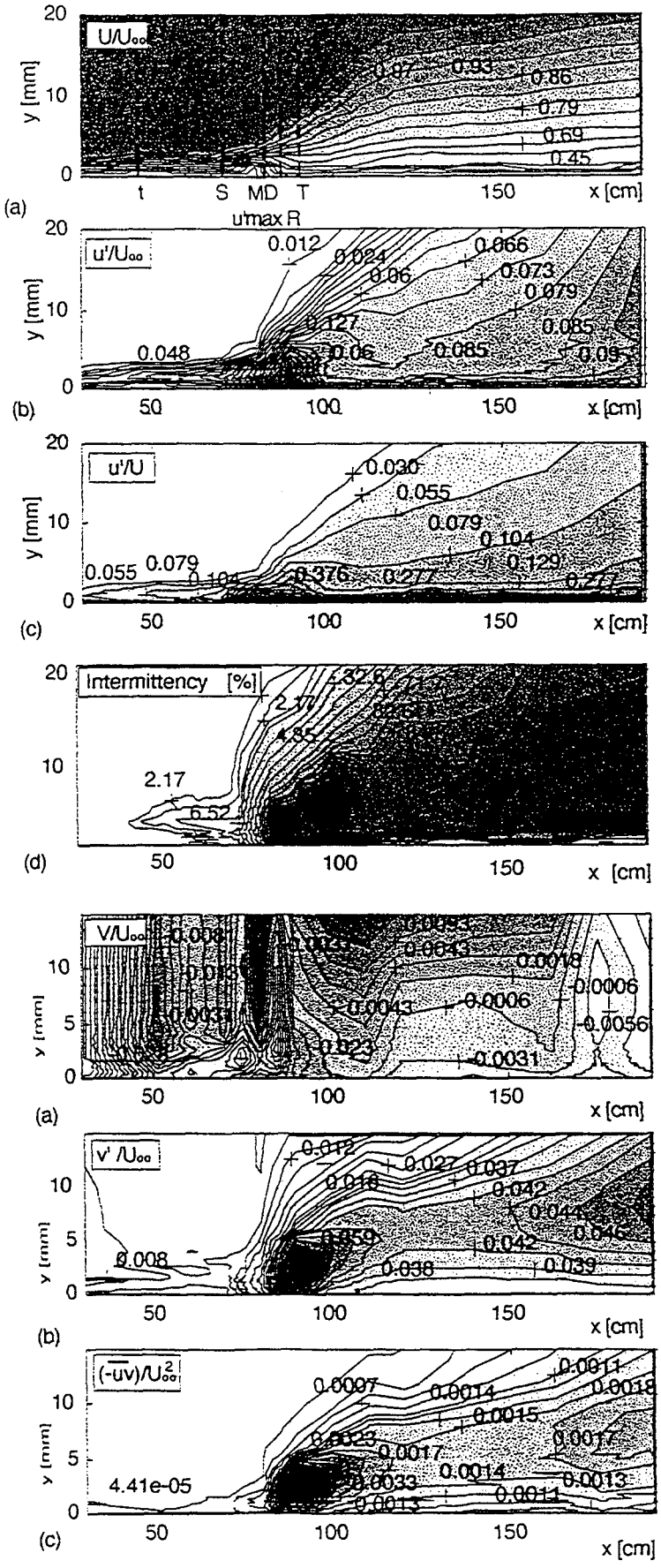
U/U∞
0.97
0.93
0.86
0.79
0.69
0.45
y [mm]
t
S
MD
T
150
x [cm]
(a)
u'max R
u'/U∞
0.012
0.024
0.06
0.066
0.073
0.079
0.085
0.09
0.127
0.048
0.06
0.085
(b)
50
100
150
u'/U
0.030
0.055
0.079
0.104
0.129
0.277
0.055
0.079
0.104
0.376
0.277
(c)
Intermittency [%]
2.17
6.52
(d)
V/U∞
0.0043
0.0018
0.0006
0.0056
0.0031
0.023
(a)
v' /U∞
0.012
0.027
0.037
0.042
0.046
0.039
0.008
0.038
(b)
(-uv)/U∞²
0.0007
0.0014
0.0011
0.0018
0.0015
0.0017
0.0023
0.0017
0.0033
0.0014
0.0013
4.41e-05
(c)

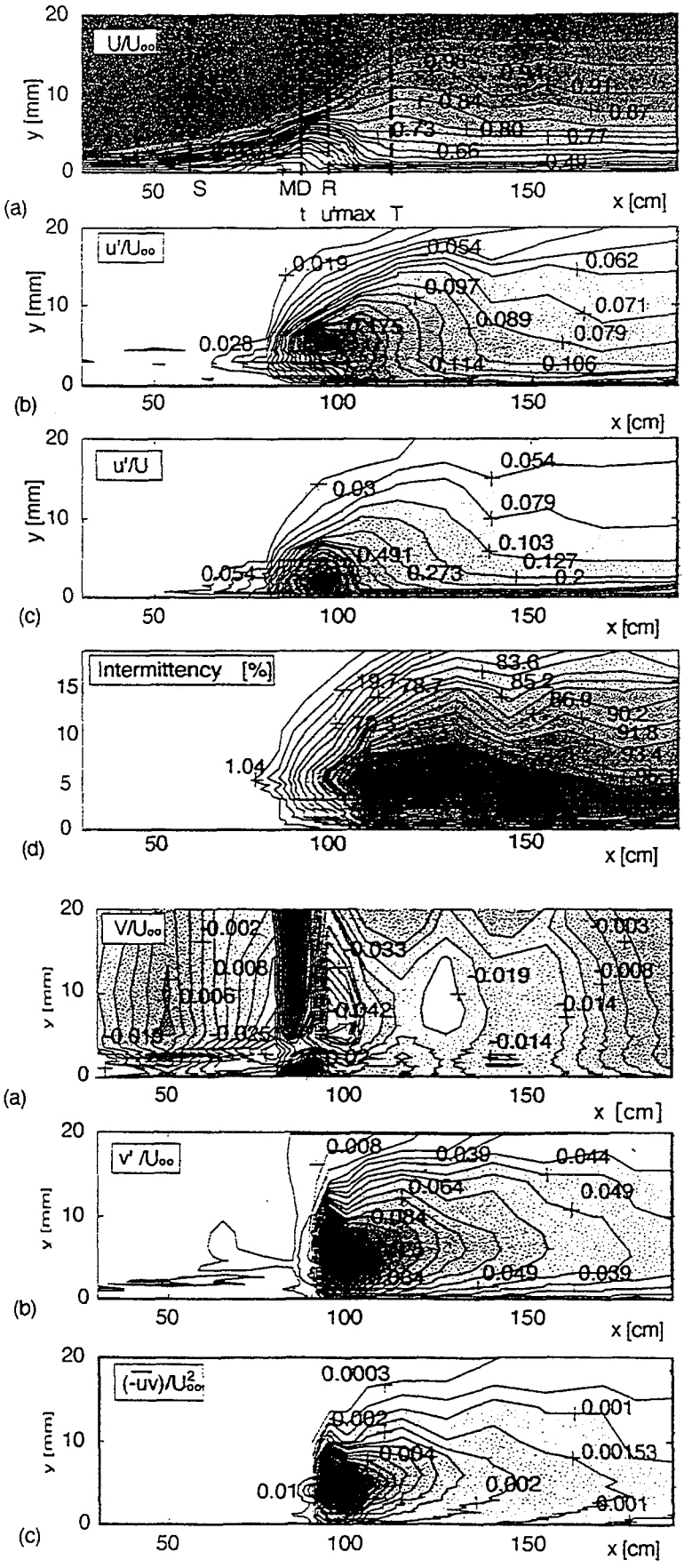
U/U∞
y [mm]
x [cm]
S
MD
R
t
u'max
T
(a)
u'/U∞
(b)
u'/U
(c)
Intermittency [%]
(d)
V/U∞
(a)
v' /U∞
(b)
(-uv)/U²∞
(c)

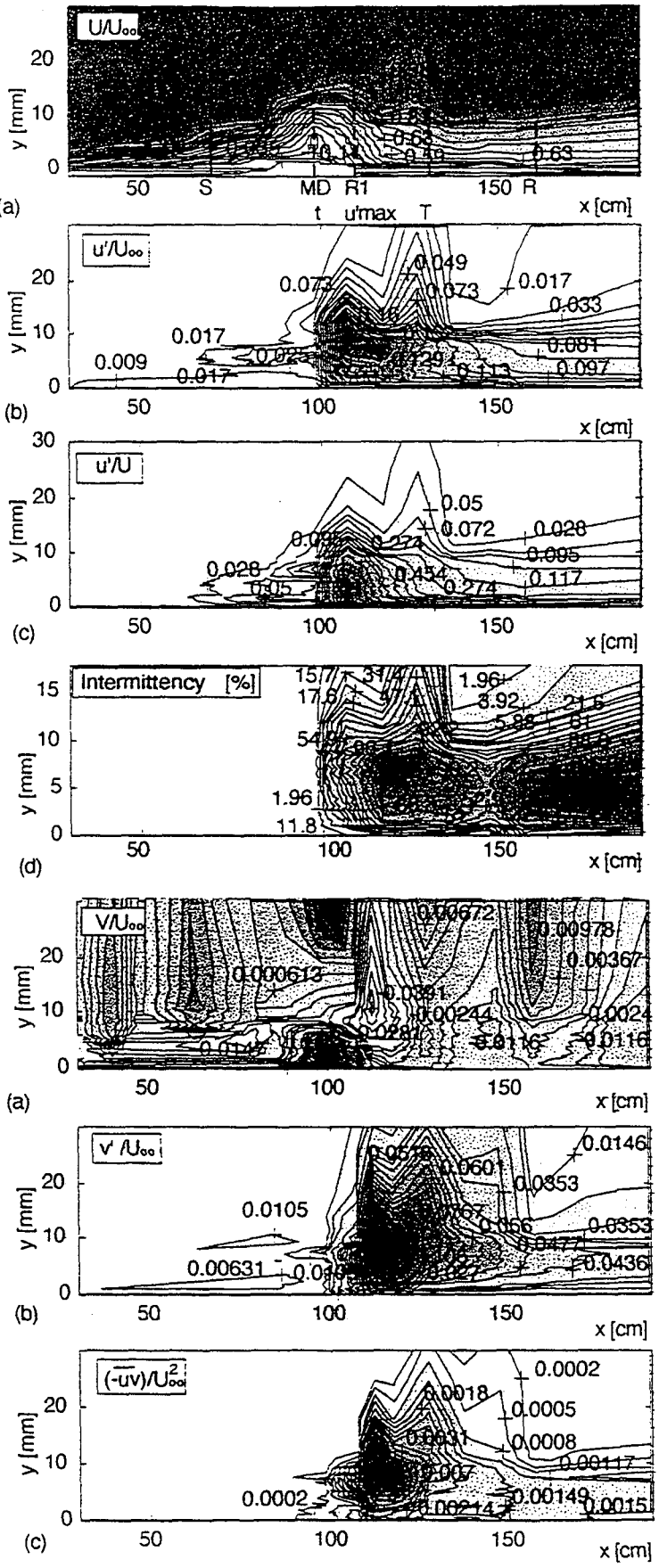
U/U∞
y [mm]
x [cm]
S
MD
R1
R
t
u'max
T
(a)
u'/U∞
(b)
u'/U
(c)
Intermittency [%]
(d)
V/U∞
(a)
v' /U∞
(b)
(-uv)/U∞²
(c)

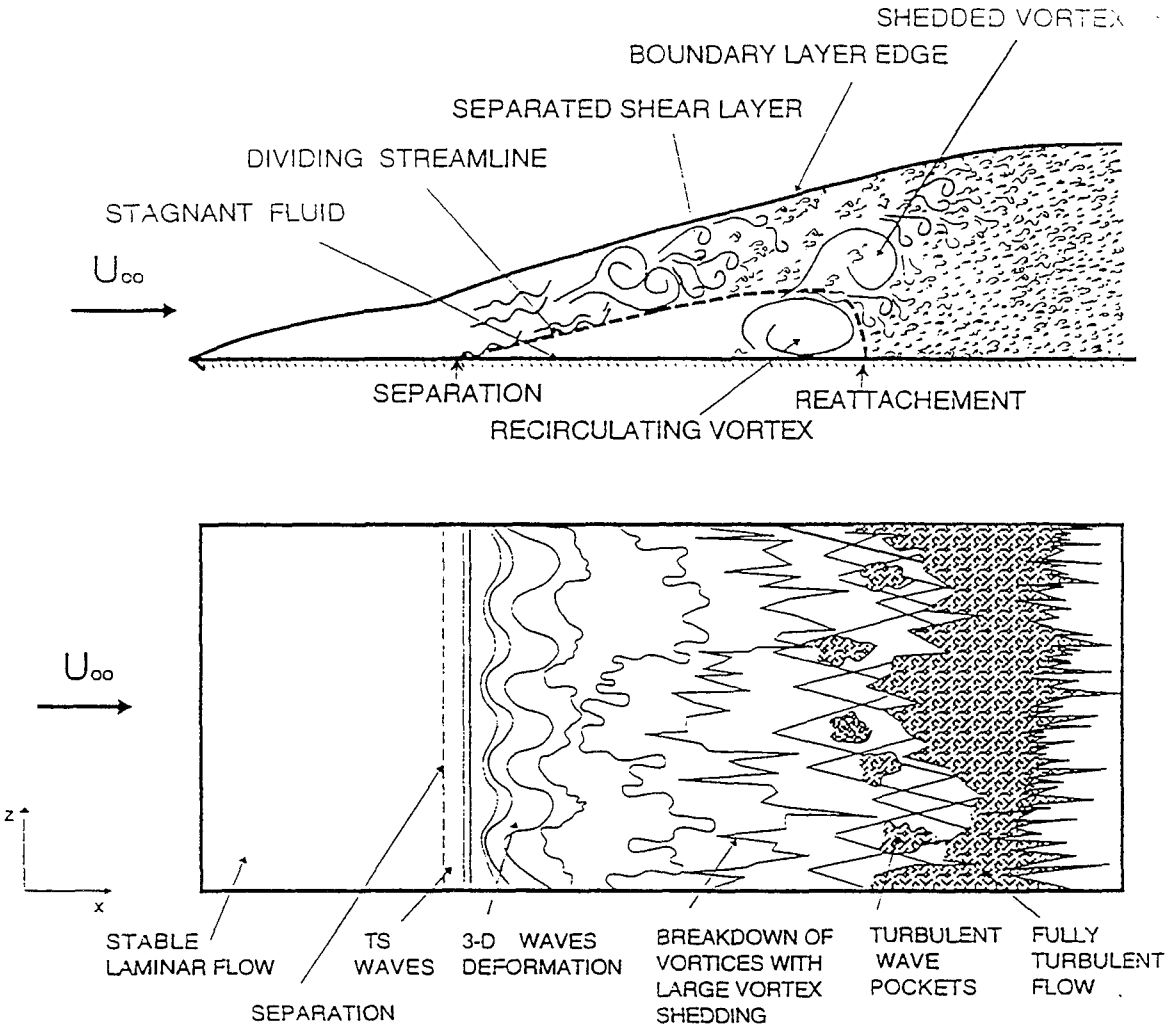

BASIC REGIONS OF TRANSITION PROCESS, SHORT BUBBLE CASE:

(1) - 2-D TOLLMIEN-SCHLICHTING INSTABILITY WAVE FORMATION

(2) - SPANWISE 3-D WAVES DEFORMATION

(3) - BREAKDOWN OF 3-D VORTICES AND REVERSE FLOW VORTEX SHEDDING

(4) - TURBULENT WAVE POCKETS PRODUCTION AND SPREADING

(5) - COALESCENCE OF TURBULENT WAVE POCKETS INTO FULLY TURBULENT FLOW

Figure 9 HYPOTHETICAL TRANSITION PROCESS IN SEPARATED BOUNDARY LAYER OVER A SHORT BUBBLE

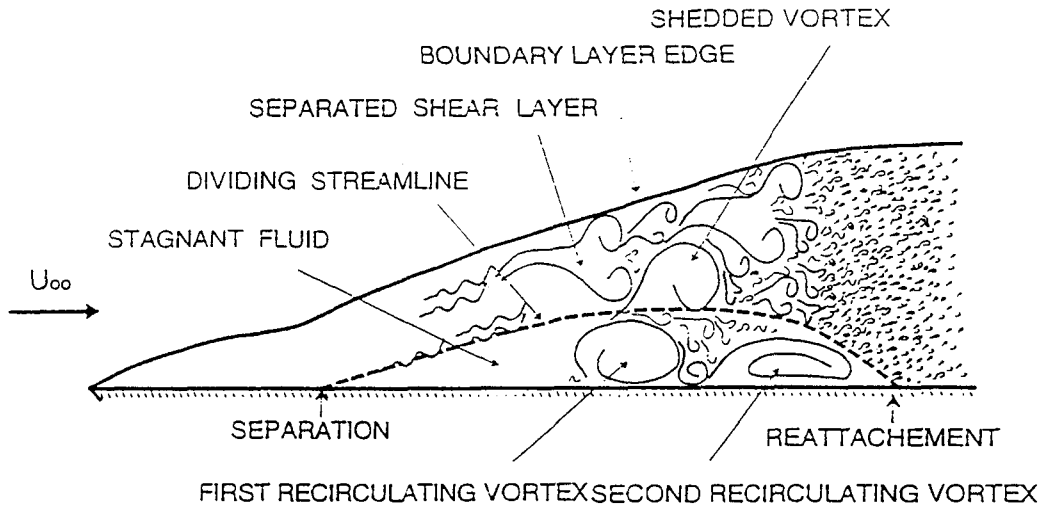

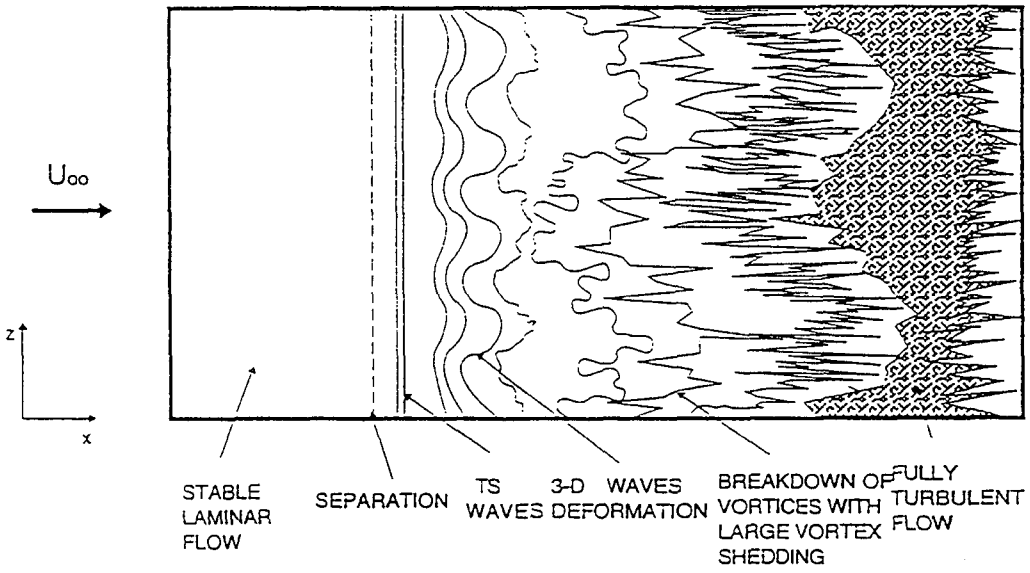

BASIC REGIONS OF TRANSITION PROCESS, LONG BUBBLE CASE:
(1) - 2-D TOLLMIEN-SCHLICHTING INSTABILITY WAVE FORMATION
(2) - SPANWISE 3-D WAVES DEFORMATION
(3) - LOCAL BREAKDOWN OF 3-D VORTICES AND REVERSE FLOW VORTEX SHEDDING
(5) - UNIFORM BREAKDOWN INTO FULLY TURBULENT FLOW

Figure 10 HYPOTHETICAL TRANSITION PROCESS IN SEPARATED BOUNDARY LAYER OVER A LONG BUBBLE

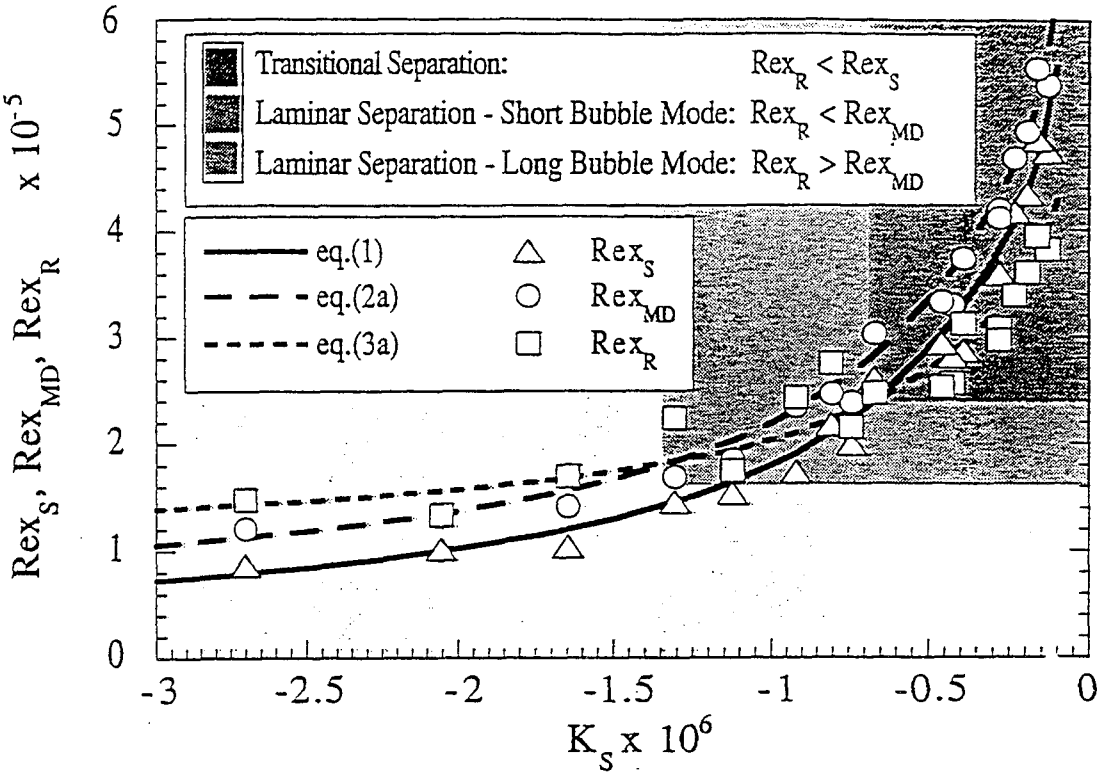

$$Rex_S = 5700 - 215000 / (K_S \times 10^6) - 46000 / (K_S \times 10^6)^2 - \\ - 5000 / (K_S \times 10^6)^3 - 200 / (K_S \times 10^6)^4 \quad (1)$$

$$Rex_{MD} = 1.0594\, Rex_S + 29140 \quad (2)$$

$$Rex_{MD} = 35180 - 227770 / (K_S \times 10^6) - 48730 / (K_S \times 10^6)^2 - \\ - 5300 / (K_S \times 10^6)^3 - 212 / (K_S \times 10^6)^4 \quad (2a)$$

$$Rex_R = 0.59812\, Rex_S + 96259 \quad (3)$$

$$Rex_R = 99670 - 128600 / (K_S \times 10^6) - 27510 / (K_S \times 10^6)^2 - \\ - 2990 / (K_S \times 10^6)^3 - 120 / (K_S \times 10^6)^4 \quad (3a)$$

Figure 11. Chart for determining the (K_S-Rex_S) regions for the separated-flow transition modes.

FREE TRANSITION ONSET IN SEPARATIONS OR WAKES

Frank T. Smith
University College
London, England

ABSTRACT

This is current work aimed at further theoretical and physical understanding of transition in the approach to separation, within separation itself, and in near-wakes. The common theme is the onset of effectively inviscid inflectional growth and the associated influence of nonlinear effects then, in two or three dimensions.

The research starts with transition near a wall. Here three-dimensional nonlinear initial-value (spot) problems are derived concerning the onset of transition, in inflectional flow over a surface roughness buried within a boundary layer and in many related flow configurations. This is for the free evolution of general disturbances rather than forced, fixed frequency or fixed wavelength evolutions. An integral criterion of earlier nonlinear work holds at leading order. The nonlinear amplitude-evolution equation then obtained at the next order is for quite general initial conditions of the disturbance, not just wave packets. Three or four such initial-value problems are developed, along with analytical and computational solution properties which include nonlinear bounded behaviour leading to persistent vortex effects as time increases, or quasi-linear decay, or nonlinear finite-time blowups of the disturbance amplitude. Overall, the spot behaviour depends on local conditions, e.g. whether adverse or not, but also on the incident disturbance size. Induced longitudinal vortices play a key role. The discussion includes the connections between the different cases present, and the links with roughness-transition experiments.

Recent study has begun on inflectional onset for an entire boundary layer at or near the start of a section of adverse pressure gradient on an airfoil. Again the nonlinear initial-value or spot problem is of concern. Work is also in progress on short-scale and fast-time transition at the start of a separation or a wake, from the initial-value viewpoint. Developments will be described as appropriate at the workshop.

Areas currently being investigated in this theoretical research are on transitions in (i) near-wakes, (ii) adverse-pressure-gradient boundary layers, (iii) roughness flows, (iv) larger-scale separating flows. All these are addressing initial-value problems, producing spots. Area (ii) will be mentioned in section 5; (iii) has connections with (ii); and (iv) is partly related to (i). Here the main focus is on area (i), for the incompressible range.

NEAR WAKES : SPOT TRANSITIONS

Rowena Bowles & Frank Smith (UCL) with Simon Clarke (Monash).

1. BACKGROUND
2. LINEAR RESPONSES
3. FIRST NONLINEAR RESPONSES
4. STRONGER NONLINEAR RESPONSES
5. CONCLUSIONS / QUESTIONS

Thanks to EPSRC(UK), MOD(UK), ARO(US).

Fig 1

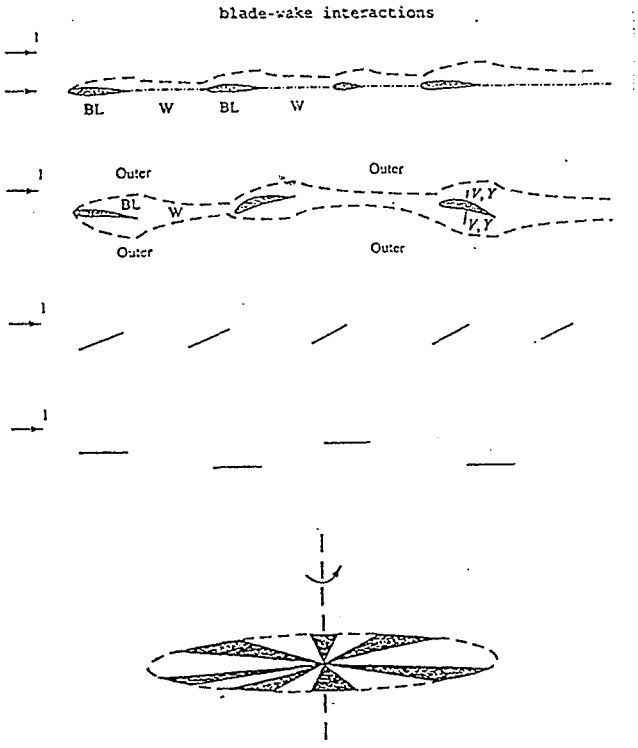
blade-wake interactions
BL
W
BL
W
Outer
Outer
BL
W
V,Y
V,Y
Outer
Outer

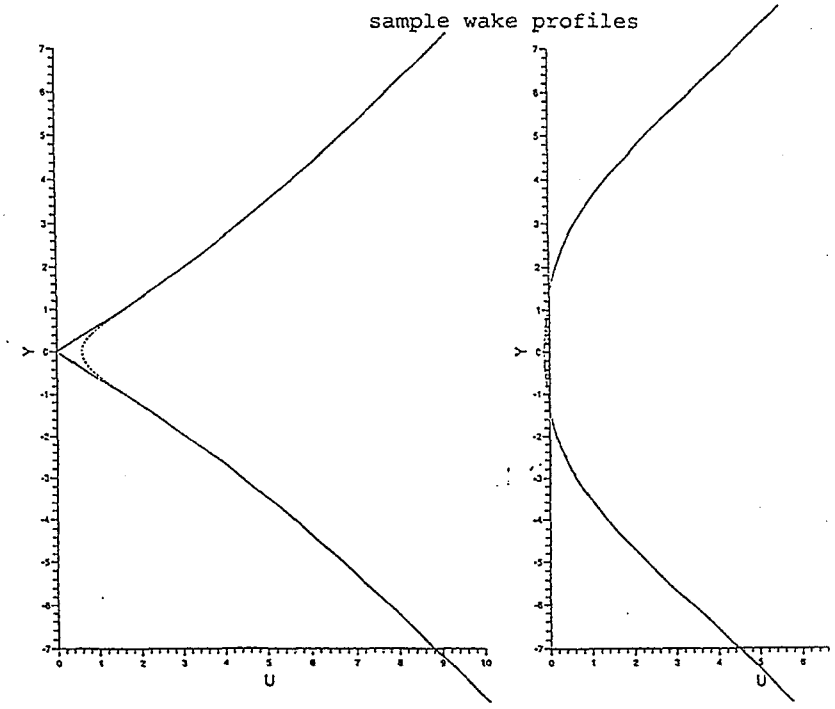
sample wake profiles
Y
U
Y
U

SECTION 1. BACKGROUND / MOTIVATION

- The present interest in near-wake transitions arose from recent research on rotary-blade-wake interactions. For example figure 1 shows there are many types of near-wake velocity profiles. Further, computations for many (typically more than 3) blades show two thickness scales, a thick boundary layer and, well inside the near-wall shear motion, a sublayer containing significantly distorted profiles.

- There is also interest in thin-wake instability generally : on model profiles (e.g. tanh-squared)(Drazin, Criminale, Miksad, ...) ; or on computed ones (e.g. Papageorgiou & Smith, Woodley & Peake) starting from say double-Blasius at the trailing edge. Is there absolute instability, and where is onset of inviscid instability, close to the trailing edge ? We find it can be very close indeed, depending on the induced local pressure gradient (theory and computations, figure 2).

- Thicker trailing edges : are the transition features in the wakes connected with those above ? (Hannemann,...,direct simulations, figure 3).

- The present work also has some impact regarding the modelling of turbulent structures using piecewise-constant vorticity (Drischel, Pullin,...). See simulations in figure 4.

Fig 2
Close to a thin trailing edge.

—— C. E. Jobe and O. R. Burggraf

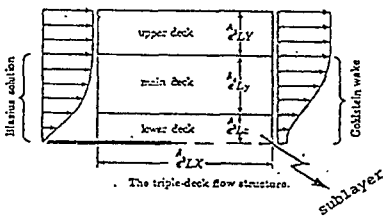

The triple-deck flow structure.

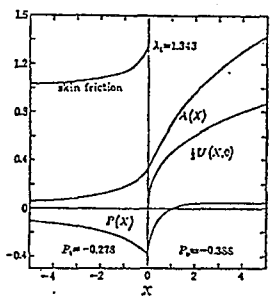

A summary of the numerical results.

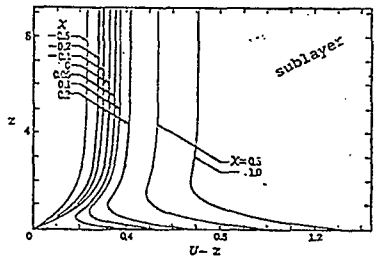

Velocity perturbation profiles.

Notice the induced pressure gradient is favourable upstream.
That's destabilizing for the wake.

Fig 3

Hannemann et al

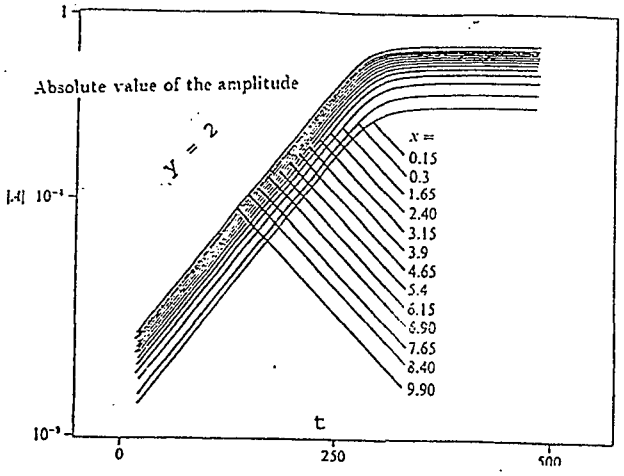

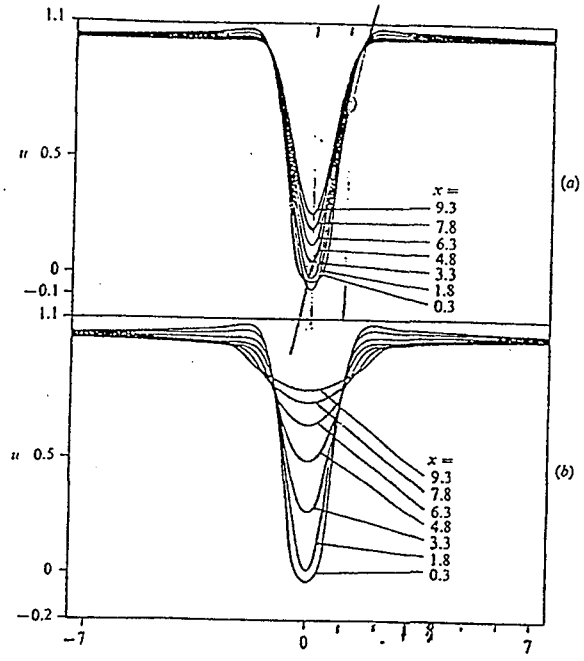

u-Velocity profiles of (a) the quasi-steady flow and (b) the mean flow in the saturation state.

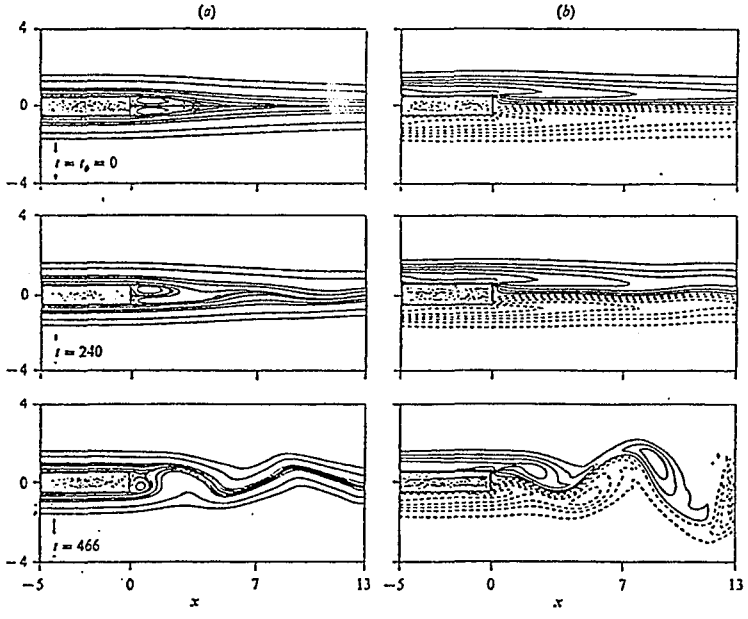

Temporal development of the wake in terms of (a) instantaneous streamlines and (b) lines of constant vorticity.

Fig 4

Pullin et al

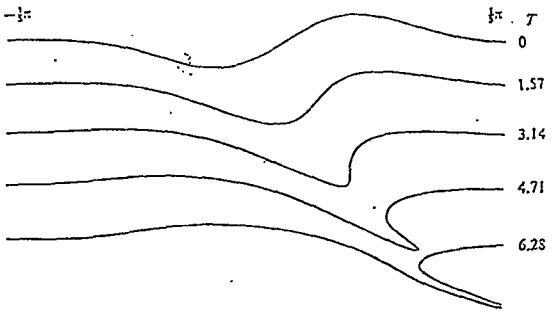

Evolution of portion of wave profile in $-\frac{1}{2}\pi < X < \frac{1}{2}\pi$ with antisymmetric almost isolated initial disturbance ( ). $A = \frac{1}{20}$, $m = 20$. Flow above interface is irrotational and flow below has unit vorticity.

Dritschel

Nonlinear evolution of rotating configurations of uniform vorticity

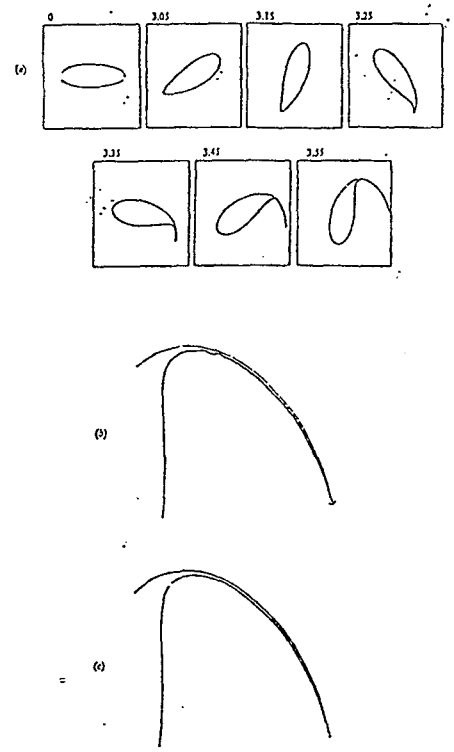

(a) 3:1 marginally stable ellipse with a superimposed marginal disturbance ($m = 3$). The first three rotations of the vortex are not shown, but the initial condition is displayed in the first frame. (b) Enlarged view of the last frame in (a) showing numerical instability. (c) As in (b) but with higher resolution (16 Gaussian points instead of 4).

COMMENTS AND ISSUES

- Genuine (calc'd) wake profiles should be used, rather than models ; similarly for related flows.
- The near-wake (where the flow is un-developed) may matter as much as the subsequent developed wake, whether thick or thin.
- Interest here is in initial-value problems (linear, nonlinear), of spots, for general initial conditions.
- Relevance of (linear/nonlinear) convective and absolute instability (Gaster, Drazin, Huerre,...)? Does the disturbance stay put? Or does it travel, and at what velocity?
- Sensitivity of turbulence-modelling computations above to smoothly varying vorticity?

FOCUS ON NEAR-WAKES: THERE THE BASIC FLOW IS UNDEVELOPED, AND SO DISTURBANCES CREATE A MOVING INTERFACE.

SECTION 2. LINEAR SPOT PROBLEMS

Basic-flow properties, as in (a) blade-wake profiles (figure 1) and (b) trailing edge of a single flat plate (figure 2), point to two special near-wakes, the Hakkinen-Rott (1965) and the Goldstein (1930). In each case locally the main velocity is

$$\bar{u} = \mathrm{mod}(y) + E * \bar{u}_1(y)$$

In case (b) above, for example, the particular value of E is 0.327 . In many cases it is useful (and accurate) to take E as small.

For spot initial-value problems, start with the Rayleigh equation and check sense of the results afterwards. In near-wakes (fig 5):

Fig 5

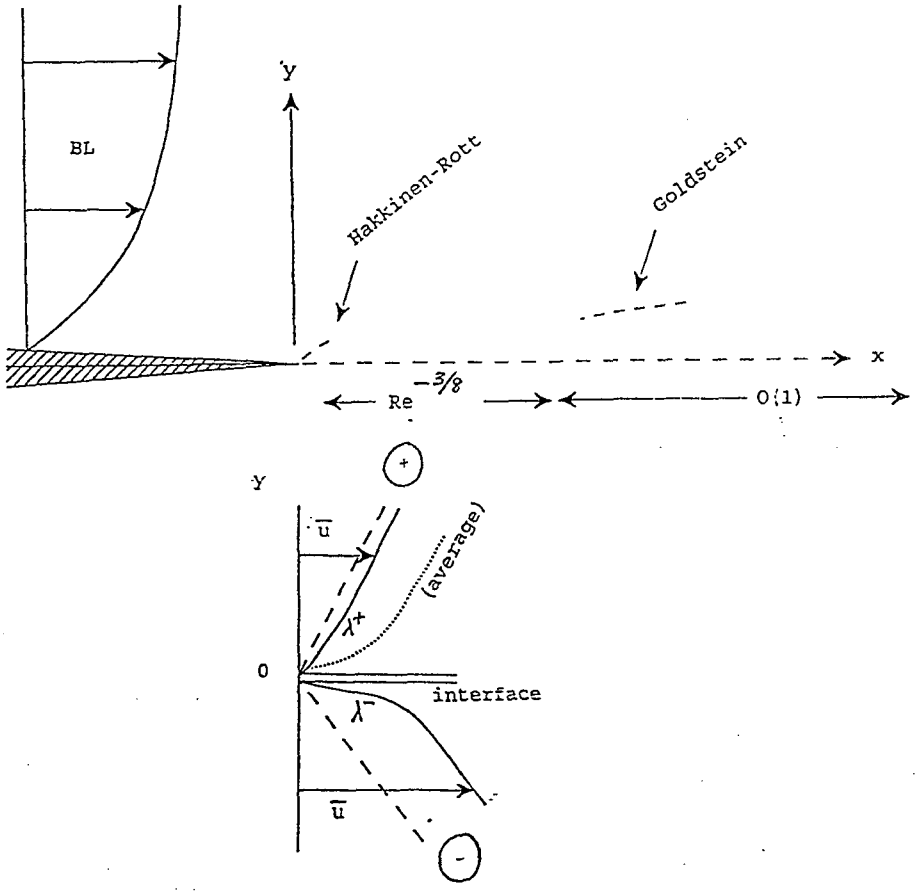

A linear disturbance $\propto \exp(i\alpha(x-ct)) + CC$ with wavenumber α (real) and wavespeed c is governed formally by the Rayleigh equation for the disturbance stream function $\tilde{\psi}(y)$,

$$(\bar{u}-c)(\tilde{\psi}''-\alpha^2\tilde{\psi}) = \bar{u}''\tilde{\psi},$$

subject to the boundary conditions

$$\tilde{\psi} \to 0 \text{ as } y \to \pm\infty, \qquad \text{(farfield)}$$

$$\tilde{\psi}^+ = \tilde{\psi}^- \text{ across } y = 0, \qquad \text{(interface)}$$

$$c(\tilde{\psi}^+)' + \lambda^+\tilde{\psi}^+ = c(\tilde{\psi}^-)' + \lambda^-\tilde{\psi}^- \text{ across } y = 0\ . \qquad \text{(interface)}$$

Results for two prime cases, the double-Blasius and the double-sublayer, are given in figure 6. In figure 7 a range of results is shown for E = 0 to 0.6 approx. These suggest that there is value in examining E << 1, partly because that yields explicit results but more especially for including nonlinear effects. When E is small, the Rayleigh results highlight two time scales, t of order unity (transient scale) and t large, of order 1/E, for the final growth in terms of T=Et.

Fig 6

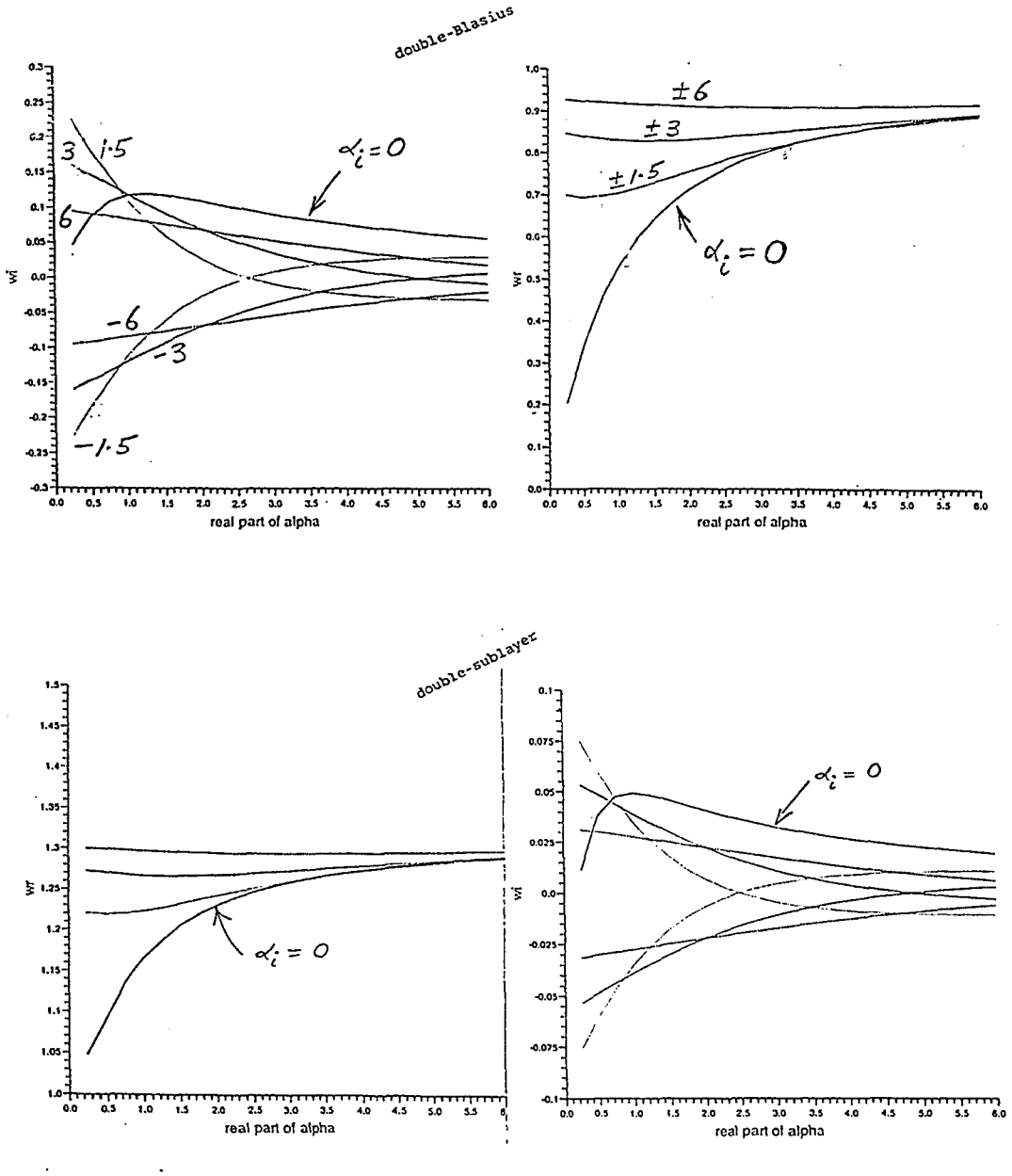

Fig 7

dotted: solutions of Rayleigh problem

dashed: small-E theory

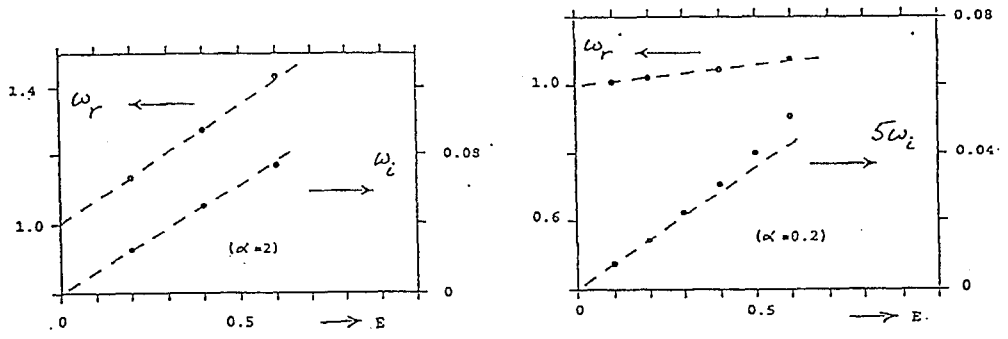

At the first approximation,

$$(\omega_0 =)\alpha c_0 = \mathrm{sgn}(\alpha)$$

as in Papageorgiou & Smith (1989), with $\omega(\equiv \alpha c) = \omega_0 + E\omega_1 + \ldots$ denoting the frequency response. So at this level the flow solution reacts at a fixed frequency of $(\pm)1$ for any wavenumber α.

At the next approximation,

$$\omega_i = E\alpha c_{1i}, \text{ with } \alpha c_{1i} = \frac{-\pi\{\bar{u}_1''(c_0) + \bar{u}_1''(-c_0)\}}{2e^2\gamma}$$

See immediately that negative profile curvature (favourable pressure gradient) is destabilizing for the near-wake.

Again, the above is taking only two-dimensional disturbances but figure 8 shows disturbance amplitude contours in the three-dimensional case. These induce a zone of effectively two-dimensional behaviour near the centre of the input, where the response is maximum, indicating that nonlinear effects enter first in two-dimensional manner (section 3 below).

Fig 8

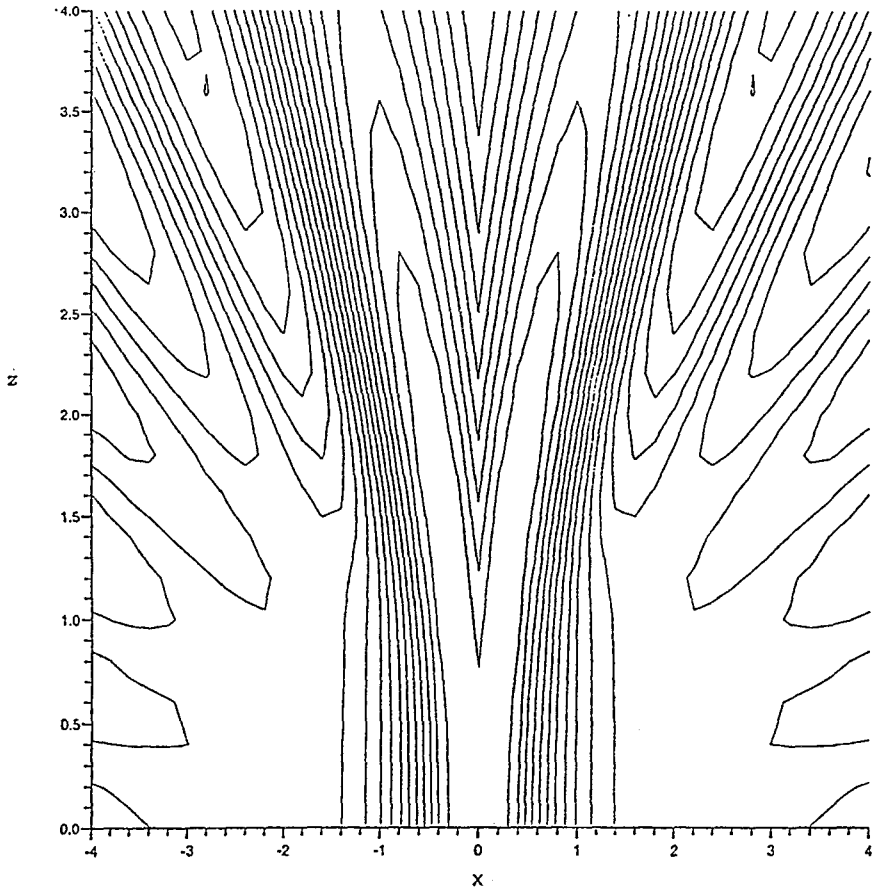

The case of a distortion profile $\bar{u}_1$ symmetric in y and a general initial condition symmetric in x about $x = x_1$ say seems representative, leading to the typical disturbance solution

$$\pi q(x,t) = \mathcal{J}_1 \cos t + \mathcal{J}_2 \sin t, \tag{2.11a}$$

$$\mathcal{J}_1 + i\mathcal{J}_2 = \int_0^\infty \hat{q}^*(\alpha) \exp\left[i\alpha x + (g_1(\alpha) + ig_2(\alpha))T\right] d\alpha \tag{2.11b}$$

interpreted in terms of a Fourier transform in $x(\rightarrow \alpha)$. In (2.11b), $\hat{q}^*$ is the initial transform, $t = \epsilon^{-1}T$ defines the slow time of stage II, and

$$g_1 = -\frac{\bar{u}_1''(\alpha^{-1})\pi\chi}{e^2\alpha}, \quad g_2 = \int_0^\infty \bar{u}_1''(y)\frac{e^{-2\alpha y}dy}{(\alpha y - 1)}, \tag{2.11c,d}$$

the effective slow complex frequency Ω being $-g_2 + ig_1$. In addition the same results (2.11a-d) apply for a nonsymmetric profile provided that $\bar{u}_1(y)$ in (2.11c,d) is replaced by the average profile $[\bar{u}_1(y) + \bar{u}_1(-y)]/2$, and likewise for $\bar{u}_1''(\alpha^{-1})$, $\bar{u}_1'(0)$

The precise behaviour at large times T depends on the specific distortion profile $u_1(y)$. There are two main points here, however. First, as a general rule unstable growth in the current regime is associated with $\bar{u}_1''$ being negative, and therefore more with a favourable streamwise basic pressure gradient than with an adverse one, in contrast with wall-bounded configurations; this change in stability characteristics as the flow leaves a trailing edge is in line with the curvature reversal which is implicit inside the thin Hakkinen-Rott or Goldstein viscous layer close to the centre-line. Furthermore,increasingly negative values of $y\bar{u}_1''$ can play a substantial role in the growth.

Some results giving absolute instability have been obtained for profiles of SYMMETRIC type, but mostly low-speed convective instability is found, e.g. figure 6. Profiles of NONSYMMETRIC type are much more likely to yield a.i., due to the average combination/addition mentioned earlier, e.g. as in figure 9. This a.i. is for instance from the large-T exponential behaviour obtained at the central location x = 0, exp(g1*T)

Fig 9

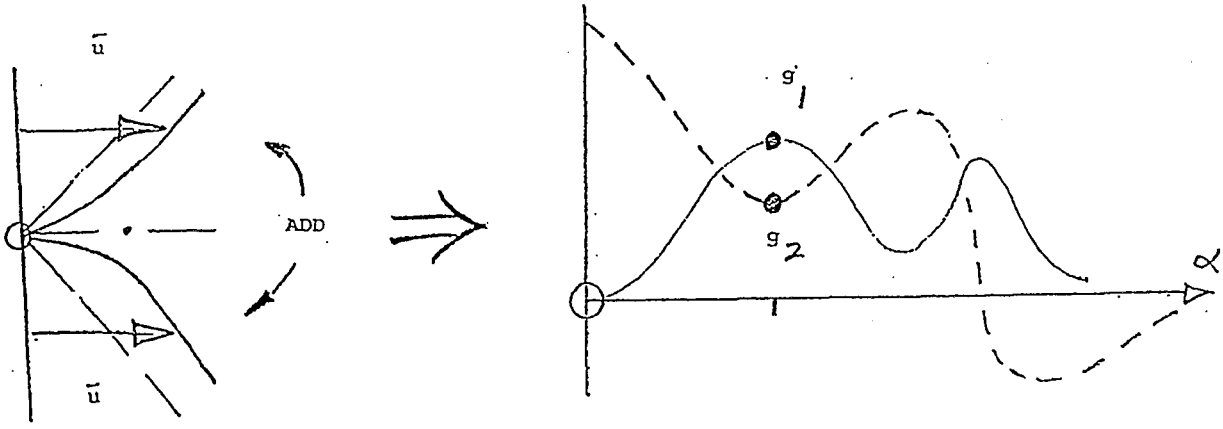

SECTION 3. FIRST NONLINEARITY IN SPOTS

At early times, nonlinear feedback produces E*t amplitude growth. Later times convert this to the main nonlinear response, which depends on the type of initial condition. Wave-like input leads to critical layers, more general input doesn't, and so we examine the latter, for which the nonlinear effect is more global and stems from the interface movement.
The amplitude equation here is found to be

$$4\frac{\partial Q_2}{\partial T} = \frac{2}{\pi}\int_{-\infty}^{\infty} Q_2^*(\alpha,T)\exp[i\alpha x + (g_1+ig_2)T]d\alpha$$

$$- D \frac{1}{2\pi}\int_{-\infty}^{\infty} \frac{(D\ D)_{\xi}}{(x-\xi)}\, d\xi \qquad + \text{other cubic terms},$$

with the relations $\partial Q_n/\partial x = -D_n$ for $n = 1,2$.

Results computed for zero E are shown in figure 10, for two different input conditions. The scales here and in section 2 agree with the direct simulations of figure 3 in orders of magnitude (e.g. the slow amplitude growth there, the saturation, the near-sawtooth response) and with figure 11 below at higher amplitudes.

Fig 10

(a)

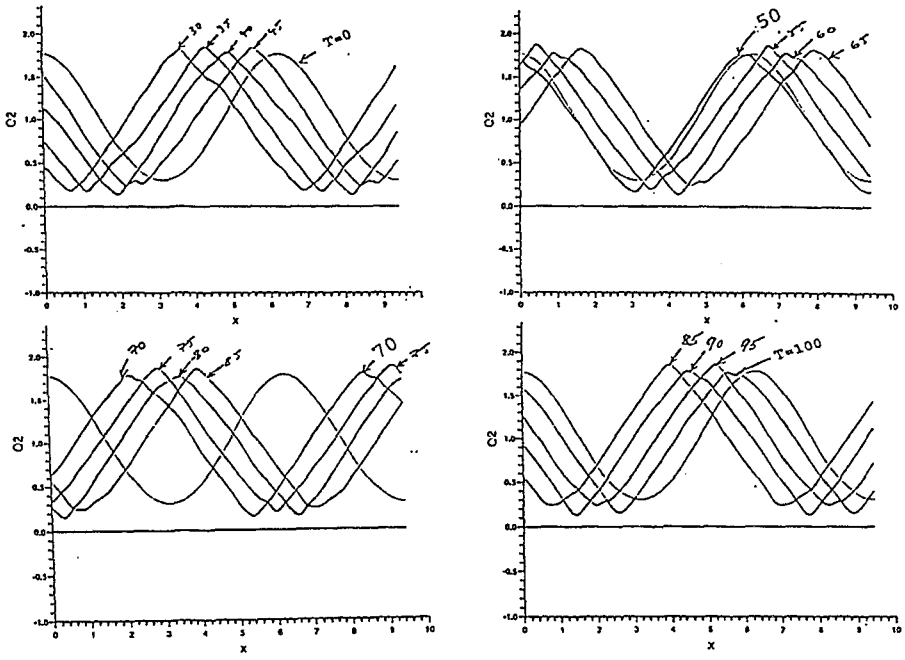

(b)

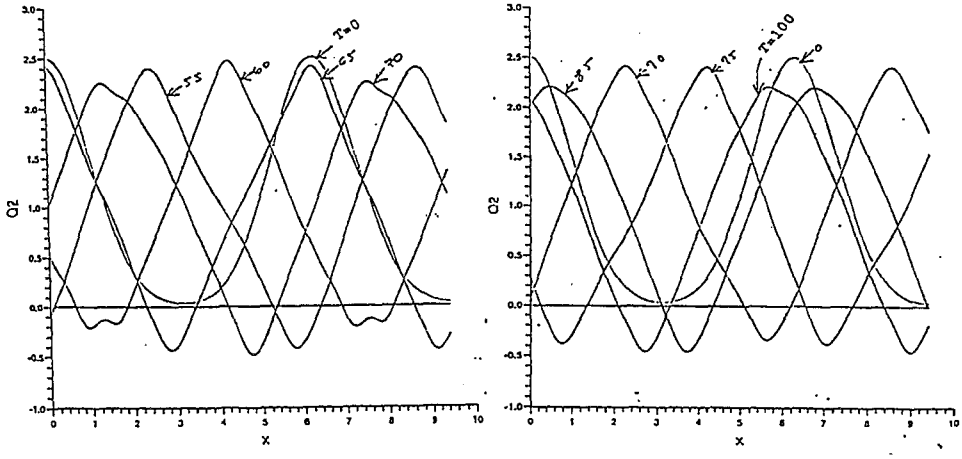

SECTION 4. STRONGER NONLINEAR RESPONSES

These were computed from the Euler equations, for zero E so far, using contour dynamics to handle the strong movement of the interface. Results are shown in figure 11. They agree with the earlier results, for reduced input amplitudes, but show also the appearance of vorticity squirts and other stronger processes at higher amplitudes. (Related results have been obtained for larger scale separating flows, in the amplitude ranges corresponding to sections 2-4).

Fig 11

(a) lower amps

(b) higher amps

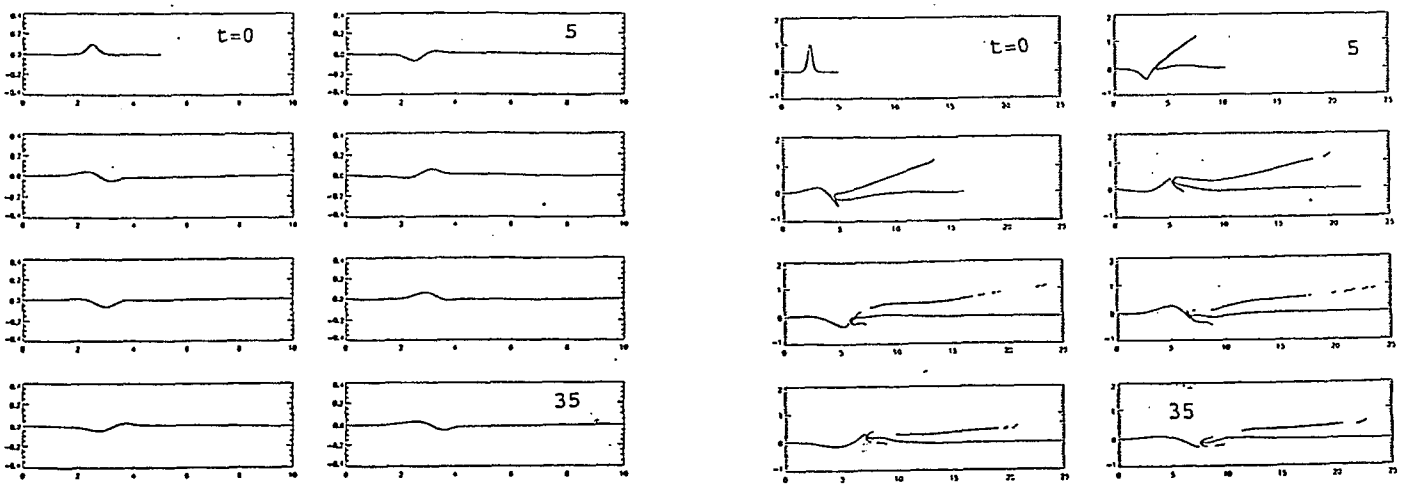

SECTION 5. CONCLUSIONS / QUESTIONS

(a) General initial conditions (linear/nonlinear) have been incorporated, for spot disturbances in near-wakes. And favourable pressure gradients have been found to be destabilizing in the near-wake.

(b) Linear:some absolute instab'ty, mostly (low-speed)convective.
Double-sublayer: seems low-speed convective, so far.
Double-Blasius: same.
Nonsymmetric near-wakes: more likely absolute instability.

(c) First nonlinear effects, for general input: blowup may occur when non-uniform vorticity (nonzero E) and/or high amps. are present.

(d) Strongly nonlinear effects: for zero E, contour-dynamic computations show persistent local oscillation.

(e) Move on to examine 3D disturbances more.

(f) Influence of adverse pressure gradients on spots in boundary layers is shown below (figure 12).

Fig 12 ADVERSE PRESSURE GRADIENTS ACTING ON SPOTS IN BOUNDARY LAYERS

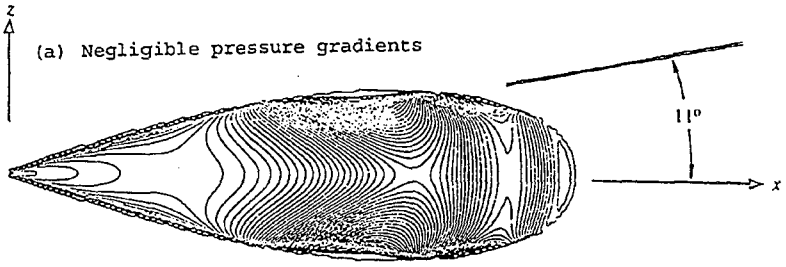

Theoretical spot solution from Bowles & Smith (1995) incorporating short-scale effects, and comparison with the typical 11° spread angle found experimentally.

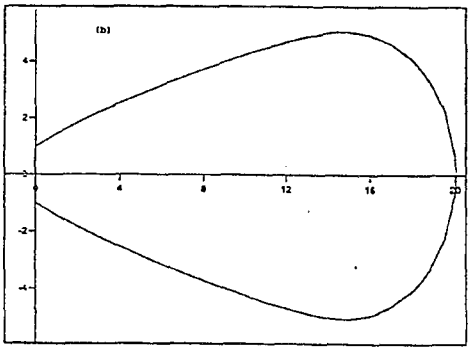

(b-d) Increasing adverse pressure gradient (Brown & Smith 1997)

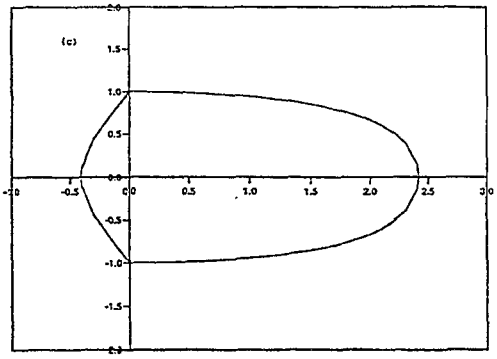

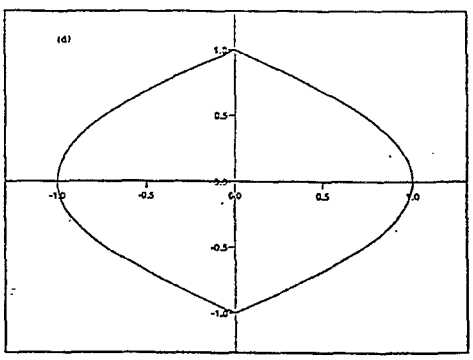

LAMINAR-TURBULENT TRANSITION IN PIPE POISEUILLE FLOW AND ITS SIMILARITY TO TRANSITION IN BOUNDARY LAYERS

S. Eliahou, G. Han, A. Tumin, and I. Wygnanski
Tel-Aviv University
Tel-Aviv, Israel

ABSTRACT

Transition in fully developed circular pipe flow was investigated experimentally by introduction of periodic perturbations. The simultaneous excitation of the azimuthal periodic modes $m = +2$ and $m = -2$ was chosen for detailed analysis. The experiments were carried out at three amplitudes. At the smallest amplitude the disturbances decayed in the direction of streaming. At the intermediate amplitude a transient growth of the disturbances was observed, and it was accompanied by higher harmonics. At still higher amplitudes transition occurred. A mean velocity distortion corresponding to azimuthal index of $m = 4$ was observed before occurrence of transition to turbulence. When four stationary jets were introduced through the wall to emulate a similar mean velocity distortion, transition was observed at smaller amplitudes of forcing at the same azimuthal modes (i.e. $m = \pm 2$). Thus, weak stationary longitudinal vortices provide an added instability needed to generate a secondary disturbance which, in turn, amplifies the steady vortical structures introduced by the jets.

The phenomenon described above is responsible for the concomitant development of azimuthal variations in mean velocity and in the amplitude of the disturbance. Peaks and valleys are generated as in "K"-type of breakdown in boundary layers. Analysis of temporal records of velocity disturbances revealed the presence of spikes prior to transition and these spikes are associated with the largest amplitudes observed. The spectrum of the spikes comprises of the fundamental frequency, its higher harmonics, and a geometric progression factor corresponds to the values obtained in boundary layers.

It follows that a similarity exists between the latest stages of transition in Poiseuille pipe flow and in boundary layers. The main difference is that the pipe flow is linearly stable and requires sufficiently large input to trigger a nonlinear mechanism.

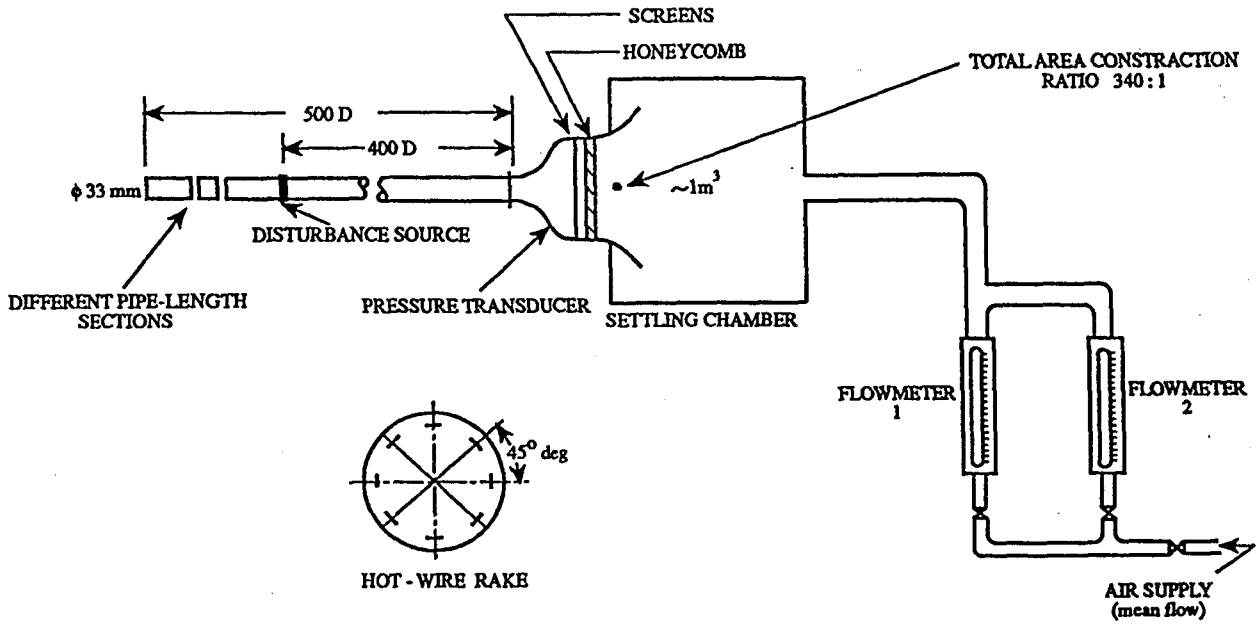

PIPE APPARATUS - GENERAL LOOK

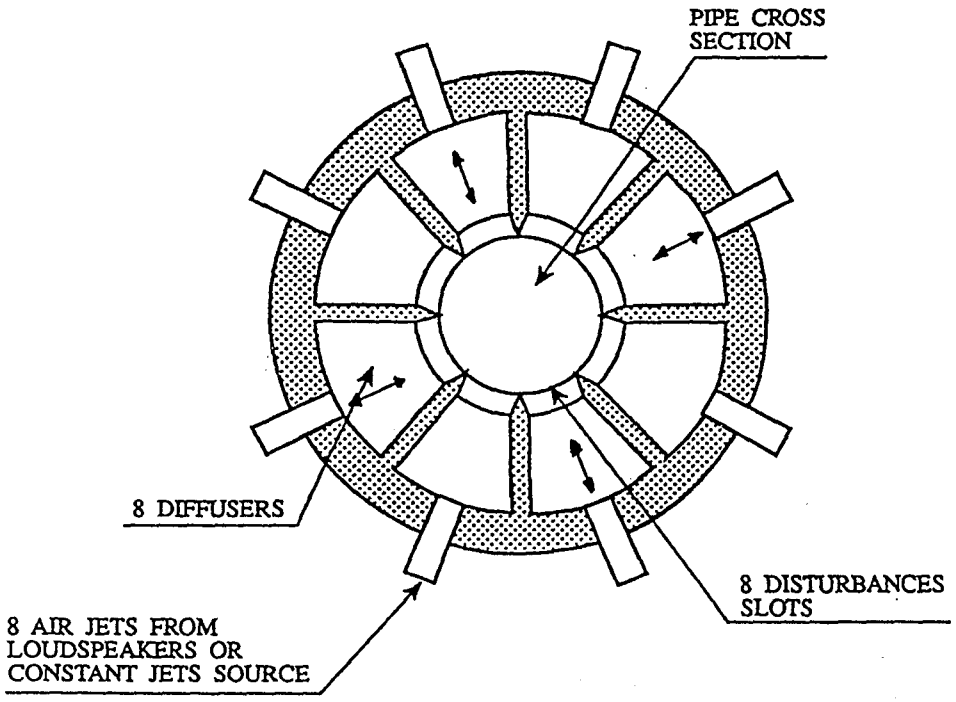

THE DISTURBANCES SOURCES - CROSS SECTION

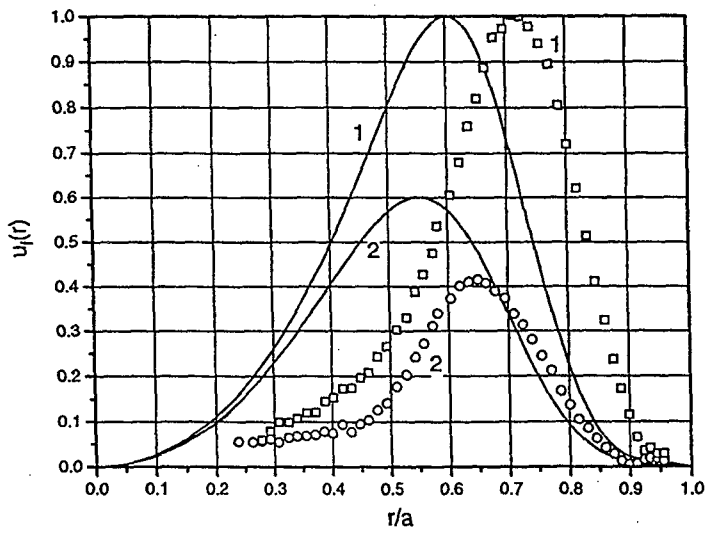

The disturbance of azimuthal index m = 2.
Small amplitude. f = 18.5 Hz. 1 - X/D=1.82;
2 - X/D=3.3. Symbols - experiment, lines - theory.

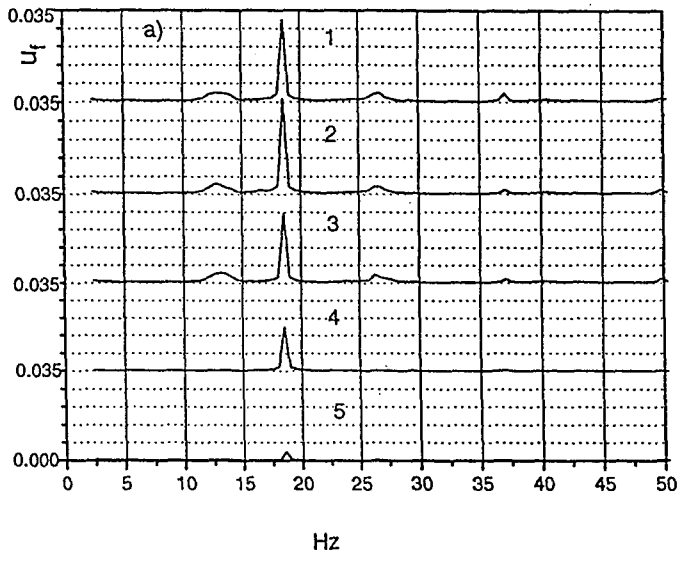

Spectra of longitudinal velocity disturbance. Small amplitude. r/a=0.7. 1,...,5 - X/D = 0; 0.61; 1.21; 1.82; 3.3. Re = 2280.

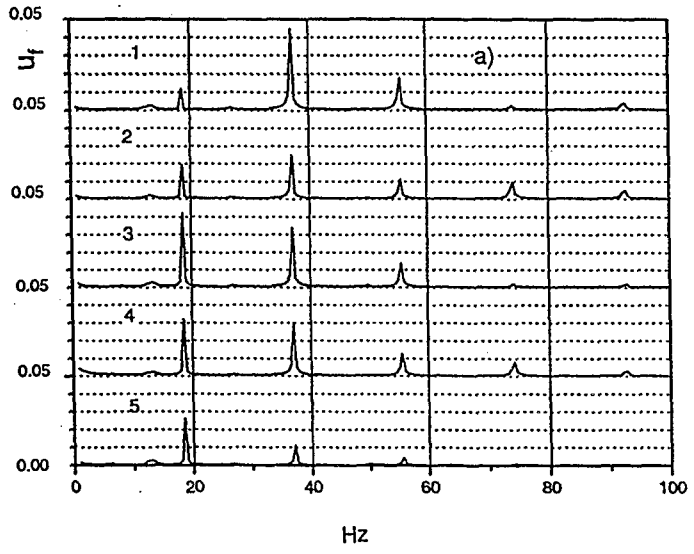

Spectra of longitudinal velocity disturbance in the meridional section of the active slots. Intermediate amplitude. r/a=0.5. 1,...,5 - X/D = 1.82; 3.3; 4.3; 5.23; 14. Re = 2280.

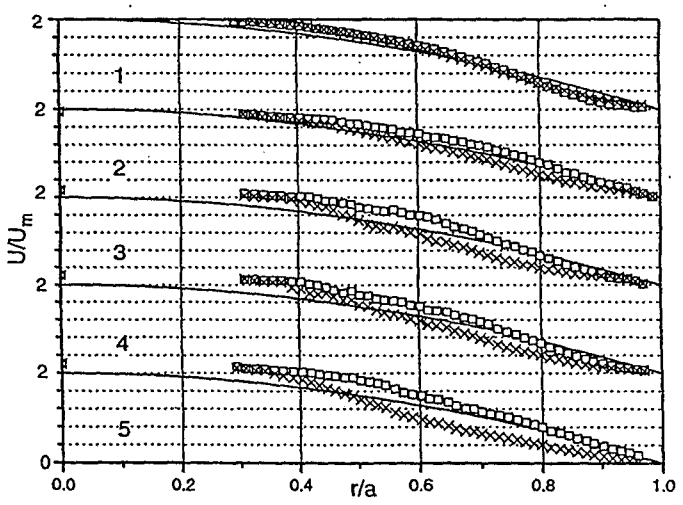

Mean velocity profiles in the two meridional sections. Intermediate amplitude of forcing. × - in the section opposite active slots; □ - opposite idle slots. 1,...,5 - X/D=1.82; 3.3; 4.3; 5.23; 14. Re = 2280. f = 18.5 Hz

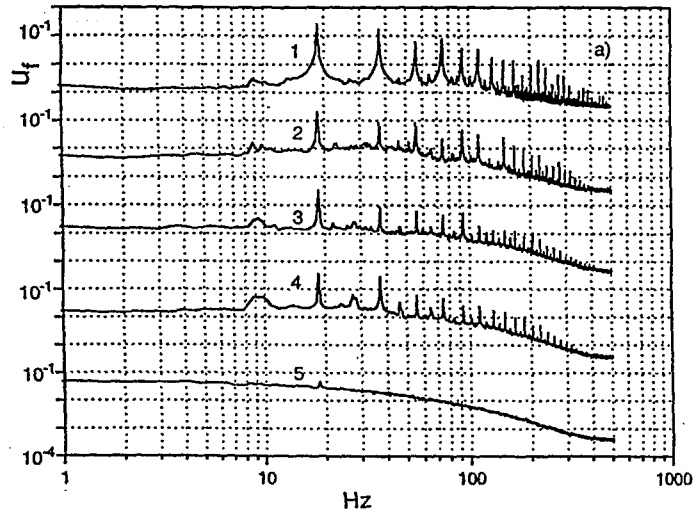

Spectra of longitudinal velocity disturbance in the meridional section of the active slots. High amplitude forcing. r/a=0.5. 1,...,5 - X/D = 1.82; 3.3; 4.3; 5.23; 14. Re = 2280.

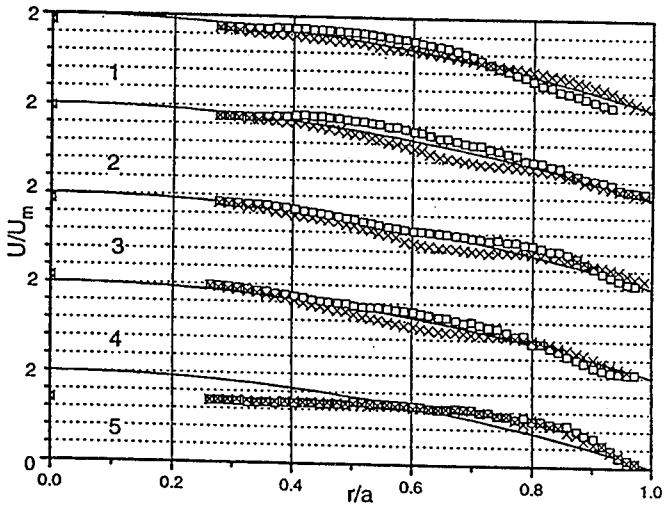

Mean velocity profiles in the two meridional sections. High amplitude of forcing. × - in the section opposite active slots; □ - opposite idle slots. 1,…,5 - X/D=1.82; 3.3; 4.3; 5.23; 14. Re = 2280. f = 18.5 Hz

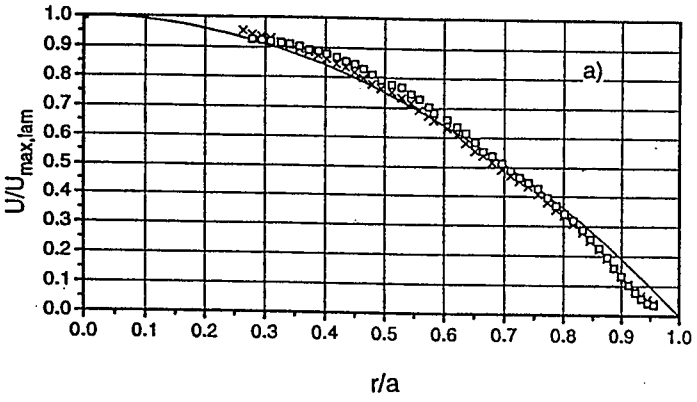

Mean velocity profiles at X/D = 7.3. × - in the section opposite active slots; □ - opposite idle slots. a) - four weak jets are induced to excite longitudinal rolls.

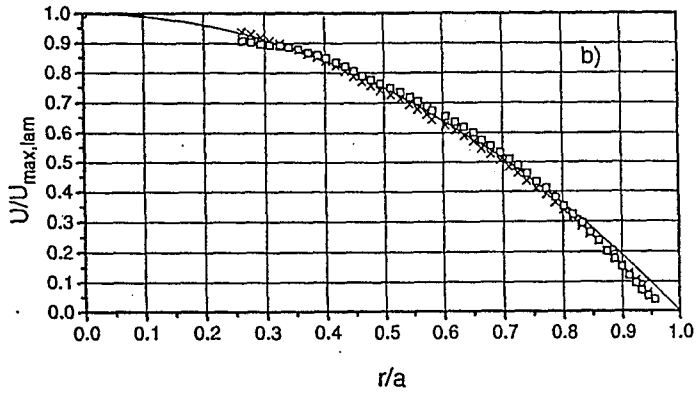

Mean velocity profiles at X/D = 7.3. × - in the section opposite active slots; □ - opposite idle slots. b) - only weak disturbances (m = +2 & m = -2) are induced.

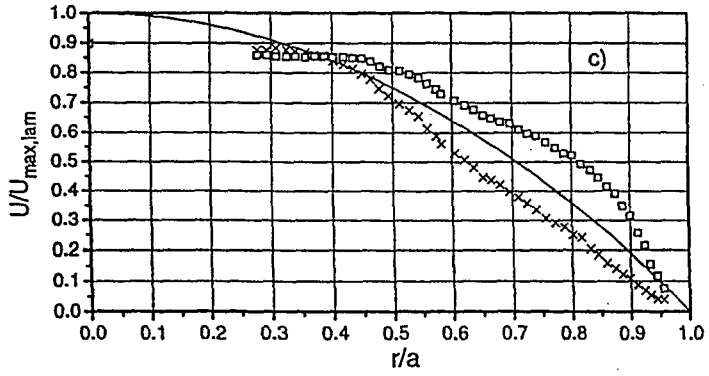

Mean velocity profiles at X/D = 7.3. × - in the section opposite active slots; □ - opposite idle slots. c) - four jets and the periodic disturbances (m = +2 & m = -2) are induced through the four slots.

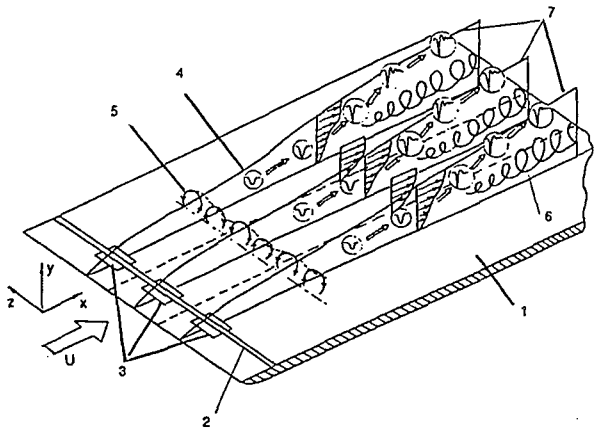

Sketch of experiment by Kelbanoff et al (1962) (from Kachanov, 1994). 1 - Plate, 2 - vibrating ribbon, 3 - spacers, 4 - boundary layer edge, 5 - pulsating streamwise vortices, 6 - local flow randomization, 7 - peak.

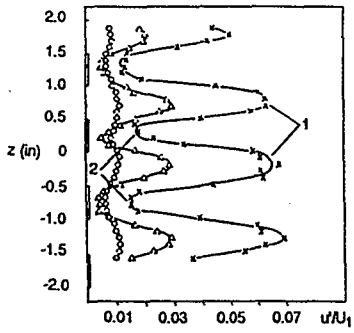

Spanwise distribution of u-fluctuation from Kelbanoff et al (1962)

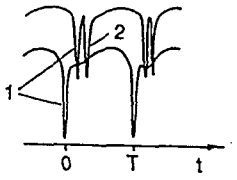

Typical single and double spikes. T - fundamental period

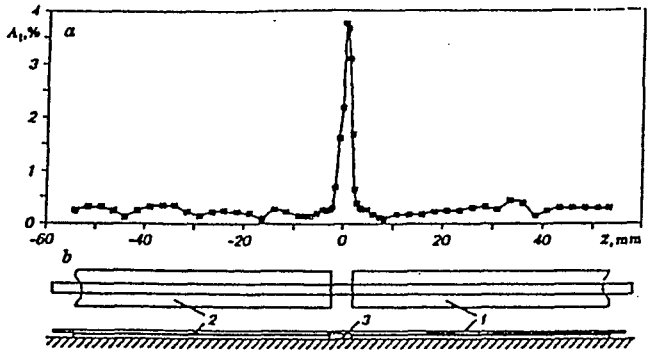

Sketch of disturbance generator and spanwise distribution of the amplitude of fundamental wave.
(from Borodulin & Kachanov, 1995)

x = 500 mm x = 550 mm x = 600 mm

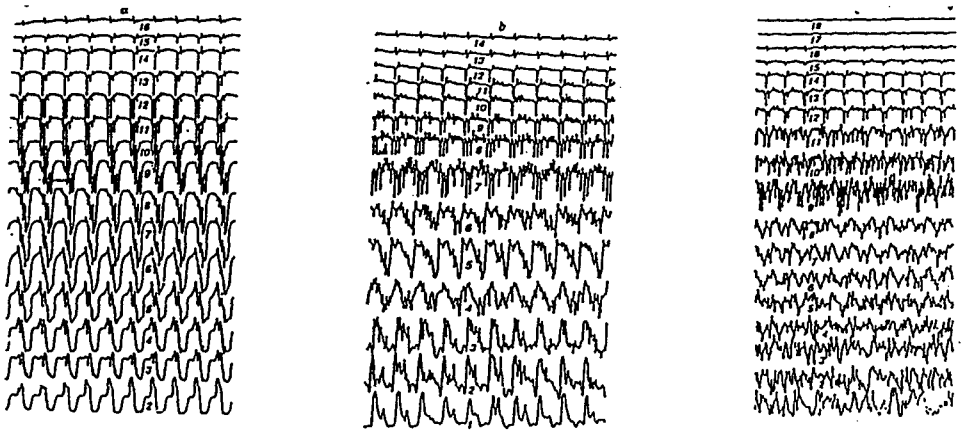

Development of the shape of disturbance oscilloscope traces on y (from the wall) at z=0.
(From Borodulin & Kachanov, 1995)

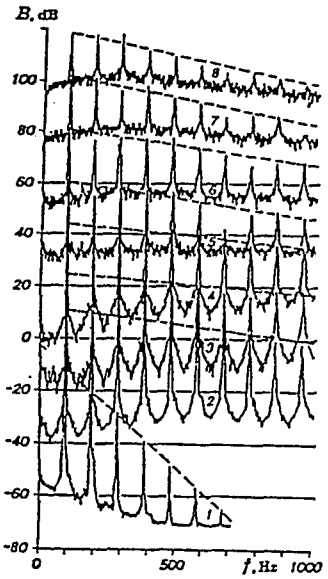

Development of disturbance amplitude spectra at y=ys , z=0 and various x- coordinates (from Borodulin & Kachanov, 1995)

X/D = 7.27

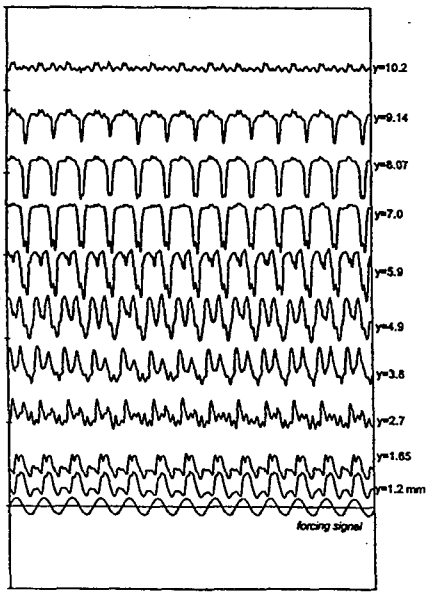

X/D = 8.27

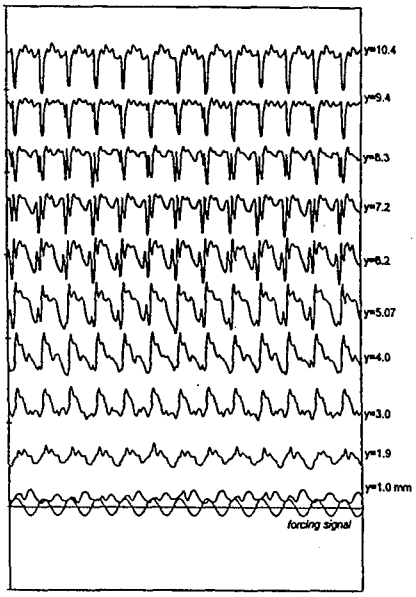

Development of the disturbance oscilloscope traces on y (from the pipe wall). Re = 2318.

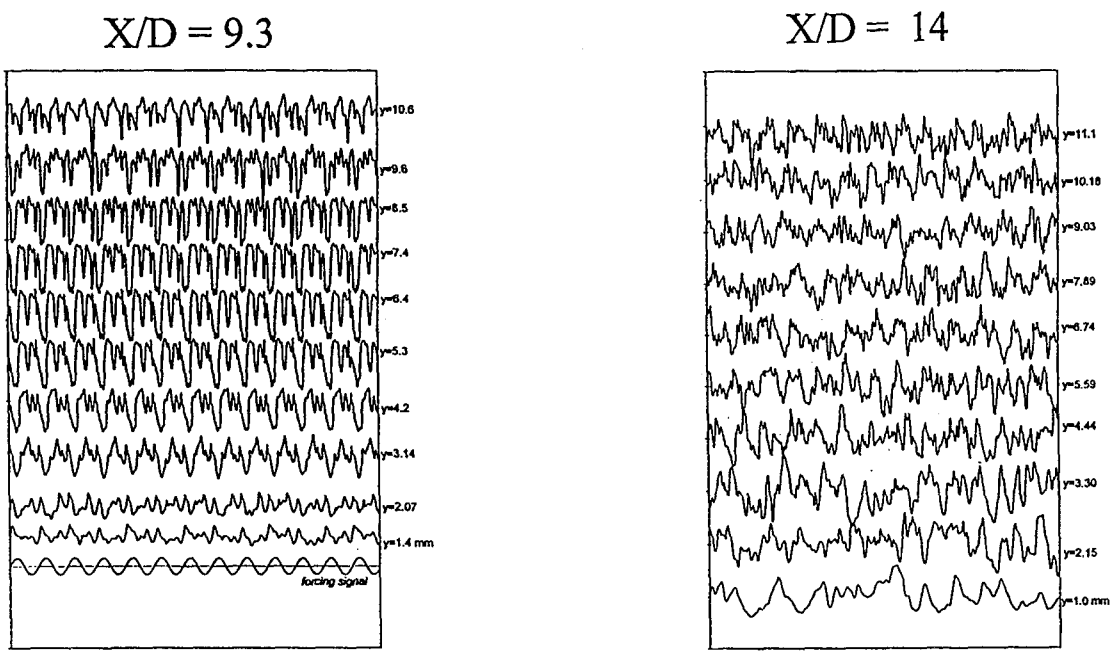

Development of the disturbance oscilloscope traces on y (from the pipe wall). Re = 2318.

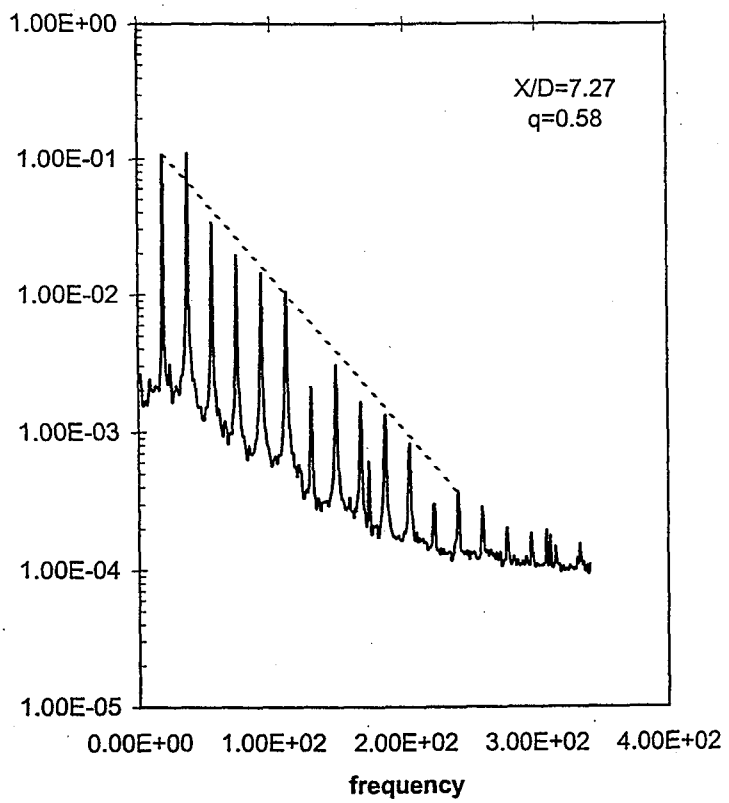

Amplitude spectra of the spike.
(q - progression factor)

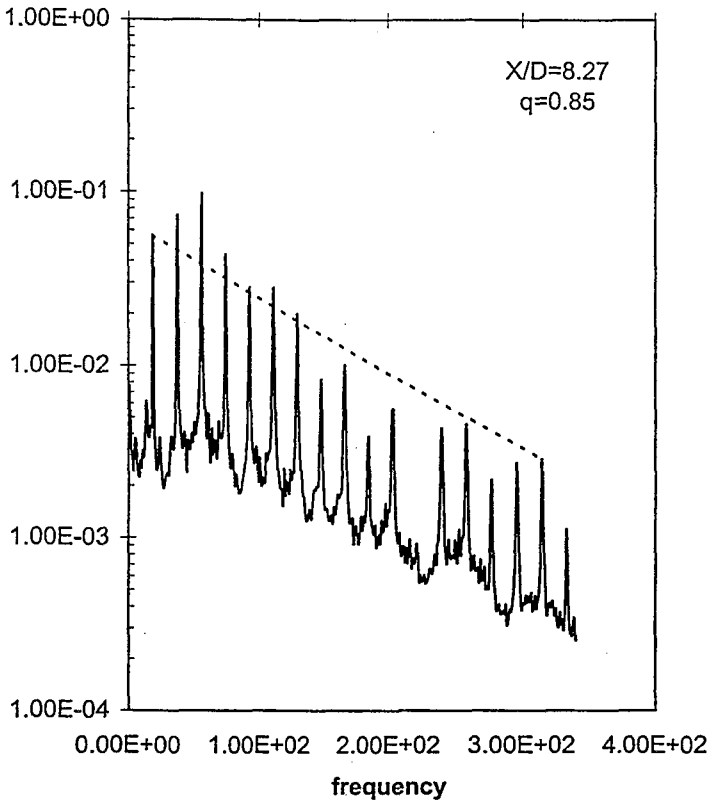

Amplitude spectra of the spike.
(q - progression factor)

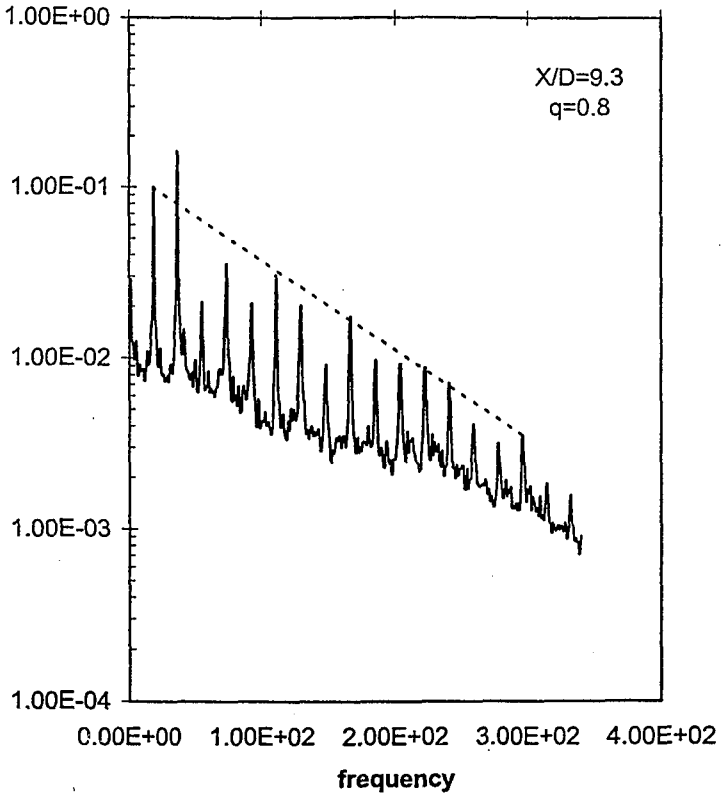

Amplitude spectra of the spike.
(q - progression factor)

Summary

- Transition in a fully developed Poiseuille pipe flow can occur only after the parabolic velocity profile got distorted by streamwise rolls
- A self-sustaining mechanism of transition was observed in the pipe flow:
  - Disturbances generate streamwise rolls;
  - The flow becomes unstable with respect to small azimuthal disturbances;
  - In turn, the streamwise rolls are amplified in presence of the disturbances.
- The transition is accompanied by appearance of spikes and the picture is similar to transition in K-regime of breakdown in boundary layers

SESSION 7

ADVANCED COMPUTATIONS

NASA/CP—1998-206958

PREDICTION OF UNSTEADY TRANSITIONAL LAYERS IN TURBOMACHINERY USING NAVIER-STOKES EQUATIONS*

B. Lakshminarayana, A. Chernobrovkin, and D.J. Kang
The Pennsylvania State University
University Park, Pennsylvania

Abstract

The objective of the research reported in this presentation is to develop computational techniques for the prediction of unsteady transitional flows associated with the rotor stator interaction in turbomachinery. Three low-Reynolds number turbulence models are incorporated in two unsteady Navier-Stokes codes (one is pressure based and the other is time marching with Runge-Kutta time stepping) and evaluated for accuracy in predicting the onset and the end of unsteady transitional patches due to wake passing. The best model is then used for modification and improvement for the leading edge effect. An existing steady Navier-Stokes code was modified to include pseudo-time stepping, which provided acceleration from 5 to 25 times that of the original code. A systematic validation procedure was implemented to assess the effects of the grid, artificial dissipation, physical, and the pseudo-time step for an accurate prediction of transitional flows resulting from the rotor-stator interaction. The ability of the Navier-Stokes code to predict the unsteady transitional flow on a turbomachinery blade is demonstrated. The unsteady pressure and velocity fields are in good agreement with the experimental data and the prediction from the Euler/boundary layer approach. The numerical solver was able to capture all zones (wake induced transitional strip, wake induced turbulent strip, calmed region, etc.) associated with wake induced transition in a compressor cascade.

Another significant step is the assessment of k-ε turbulence models, including the leading edge modifications. Best results were obtained from the FLB model[1]. The LB[2] model predicted earlier inception of the transition and shorter transition length. Modification of the k-ε model was found to be essential for an accurate prediction of the unsteady transtional flow in a compressor cascade. The CH[3] model failed to predict the unsteady transtional flow. Predicted boundary layer was turbulent from the leading edge, even with the modification of the k-ε model near the stagnation point. A comparison of the instantaneous shape factor, the skin friction coefficient, and the momentum thickness indicates that the Navier-Stokes predictions are reasonably good. Interaction between the upstream wake and stator wake results in shedding of unsteady vortices from the trailing edge and increased dissipation in the stator wake and, as a consequence, increased rate of decay of the stator wake. The procedure developed at Penn State should aid the designers of turbomachinery in allowing for the unsteady transitional flows due to rotor-stator interaction.

---

* Work supported by NASA Lewis Research Center (Grant no. NAG3-2025).

† Fan, S., Lakshminarayana, B., and Barnett, M., 1993, "Low Reynolds-Number k-ε Model for Unsteady Turbulent Boundary-Layer Flows," AIAA Journal, Vol. 31, No. 10, pp. 1777-1784.

‡ Lam C.K.G. and Bremhost, K., 1981, "A Modified Form of the k-ε Model for Predicting Wall Turbulence," Journal of Fluids Engineering, Vol. 103, September, pp. 456-460.

§ Chien, K.-Y., 1982, "Predictions of Channel and Boundary-Layer Flows With a Low Reynolds-Number Turbulence Model," AIAA Journal, Vol. 20, No. 1, pp. 33-38.

Outline

- SIGNIFICANCE AND OBJECTIVES
- EQUATIONS AND MODELS
- VALIDATION
- SIMULATION/PREDICTION OF TRANSITION
    - Rotor/Stator Interaction
        - Compressor cascade (Shultze et al.)
        - Compressor rotor (Halstead et al.)
    - Cascade-Laminar Separation Bubble
        - Turbine cascade - with laminar separation bubble (Qiu & Simon)
- CONCLUSIONS
- FUTURE PLANS

Objective

- Very few attempts have been made to simulate unsteady transitional flow with an emphasis on the unsteady boundary layer development.
- Development of the efficient and accurate numerical technique for the unsteady flow simulation, thorough and systematic assessment of the code.
- Assessment of the turbulence models for the prediction of the unsteady transitional flow, including leading edge effect.
- Numerical modeling of the unsteady transitional flow aimed at improved understanding of the flow physics

Numerical Technique

- Stage Runge-Kutta scheme for Favre average unsteady full Navier-Stokes equation.
- Pseudo-time acceleration to enable efficient modeling of the unsteady flow
- Non-reflecting boundary conditions
- Low Reynolds k-ε model for turbulence closer
    - Chien
    - Lam-Bremhorst
    - Fan-Lakshminarayana-Barnett (FLB)

Turbulence model

$$\frac{\partial(\bar{\rho}\tilde{k})}{\partial t}+\frac{\partial}{\partial x_j}\left(\bar{\rho}\tilde{k}\tilde{u}_j\right)=\frac{\partial}{\partial x_j}\left[\left(\mu_l+\frac{\mu_t}{\mathrm{Pr}_k}\right)\frac{\partial\tilde{k}}{\partial x_j}\right]+P-\bar{\rho}\tilde{\varepsilon}-\mathbf{D}$$

$$\frac{\partial(\bar{\rho}\tilde{\varepsilon})}{\partial t}+\frac{\partial}{\partial x_j}\left(\bar{\rho}\tilde{\varepsilon}\tilde{u}_j\right)=\frac{\partial}{\partial x_j}\left[\left(\mu_l+\frac{\mu_t}{\mathrm{Pr}_\varepsilon}\right)\frac{\partial\tilde{\varepsilon}}{\partial x_j}\right]+\left(f_1C_1P-f_2C_2\,\bar{\rho}\tilde{\varepsilon}\right)\frac{\tilde{\varepsilon}}{\tilde{k}}+\mathbf{E}$$

Low-Re number k-ε models:

Model	Code	f_μ
Chien	CH	$1-\exp(-0.0115y^+)$
Lam-Bremhorst	LB	$[1-\exp(-0.0165\mathrm{Re}_y)]^2(1+20.5/\mathrm{Re}_t)$
Fan-Lakshminarayana-Barnett	FLB	$0.4f_w/\sqrt{\mathrm{Re}_t}+(1-0.4f_w/\sqrt{\mathrm{Re}_t})[1-\exp(-\mathrm{Re}_y/42.63)]^3$

Code	f_1	f_2	D	E
CH	1.0	$1-0.22\exp(-\mathrm{Re}_t^2/36)$	$2\nu k/y^2$	$-2\nu(\frac{\varepsilon}{y^2})\exp(-0.5\,y_+)$
LB	$1+(0.06/f_\mu)^3$	$1-\exp(-\mathrm{Re}_t^2)$	0	0
FLB	1.0	$(1-2/9\exp(-\mathrm{Re}_t^2/36))f_w^2$	0	0

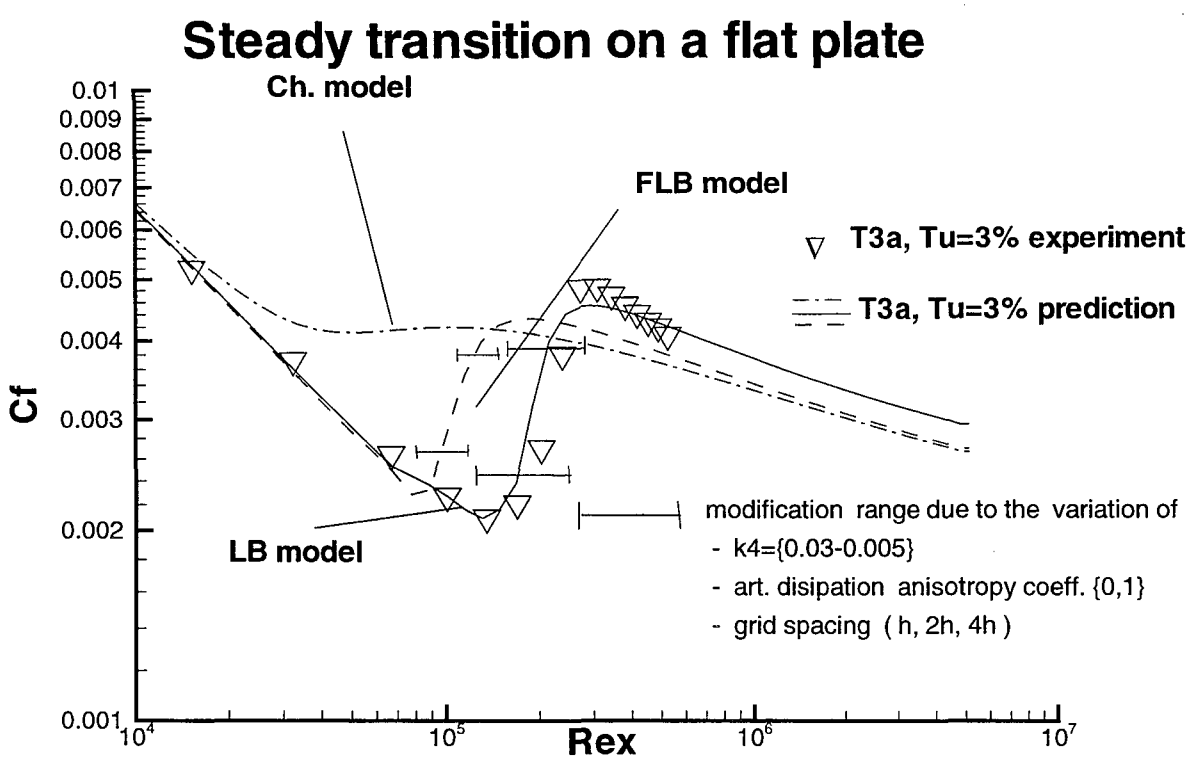
Steady transition on a flat plate
Ch. model
FLB model
T3a, Tu=3% experiment
T3a, Tu=3% prediction
LB model
modification range due to the variation of
- k4={0.03-0.005}
- art. disipation anisotropy coeff. {0,1}
- grid spacing (h, 2h, 4h)
Cf
Rex
0.01
0.009
0.008
0.007
0.006
0.005
0.004
0.003
0.002
0.001
10^4
10^5
10^6
10^7

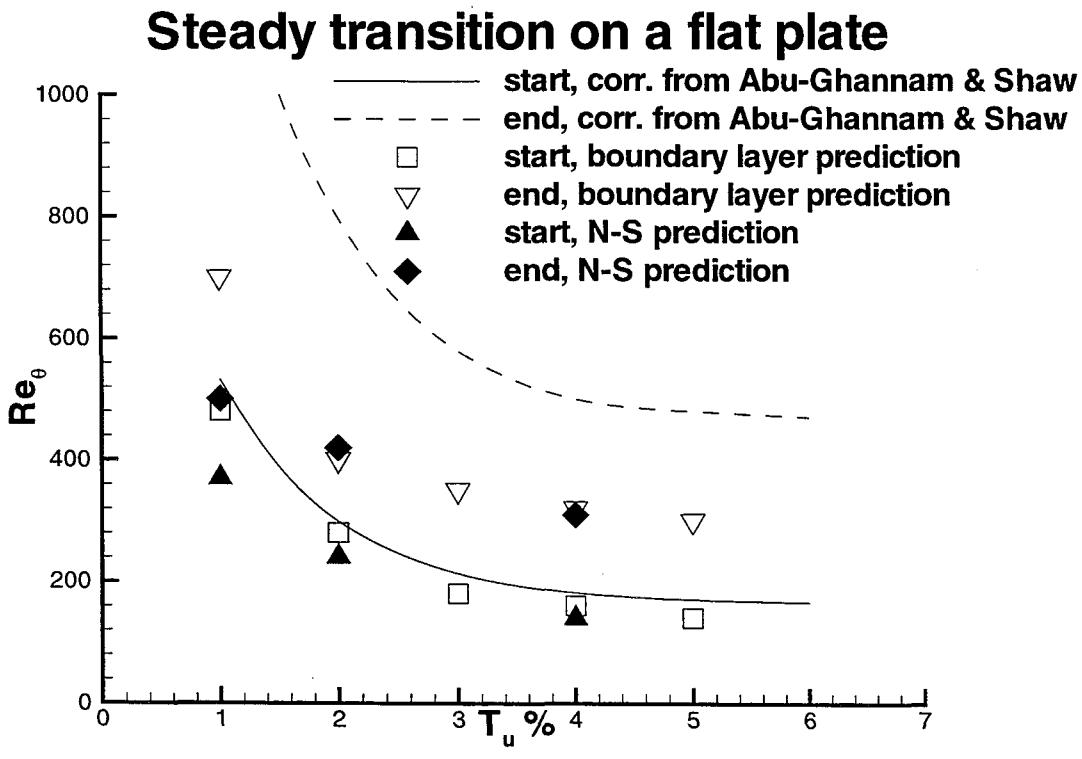
Steady transition on a flat plate
start, corr. from Abu-Ghannam & Shaw
end, corr. from Abu-Ghannam & Shaw
start, boundary layer prediction
end, boundary layer prediction
start, N-S prediction
end, N-S prediction
Re_θ
T_u %
1000
800
600
400
200
0
0
1
2
3
4
5
6
7

Modification of the k-ε model for stagnation point flow

- κ–ε model overpredicts increase of the turbulent kinetic energy at the stagnation point, this may lead to earlier transition.
- Modifications
  - Production term modification (Launder) $P = 2\nu_t \sqrt{(S_{ij})^2 \cdot (R_{ij})^2}$
  - Production term modification (Jin et al.) $P = 2\nu_t R_{ij} \cdot R_{ij}$
  - Modified constants in ε equation (Strahle et al.) $C_{\varepsilon 1} = C_{\varepsilon 2}$

Rotor-Stator Interaction Flows multi-stage compressor/turbine cascade

Halstead' Multi-stage compressor (Halstead et al 1995)

Three stage low speed compressor:

	IGV	ROTOR	STATOR
solidity	1.0	1.11	1.32
aspect ratio	1.36	1.25	1.44
chord, mm	83.8	91.2	79.1
stager angel (deg)	19.6	46.9	13.9
number of blades	53	54	74
axial gap, mm	98	25.4	
Reynolds number (x10^5)		4.24	3.07

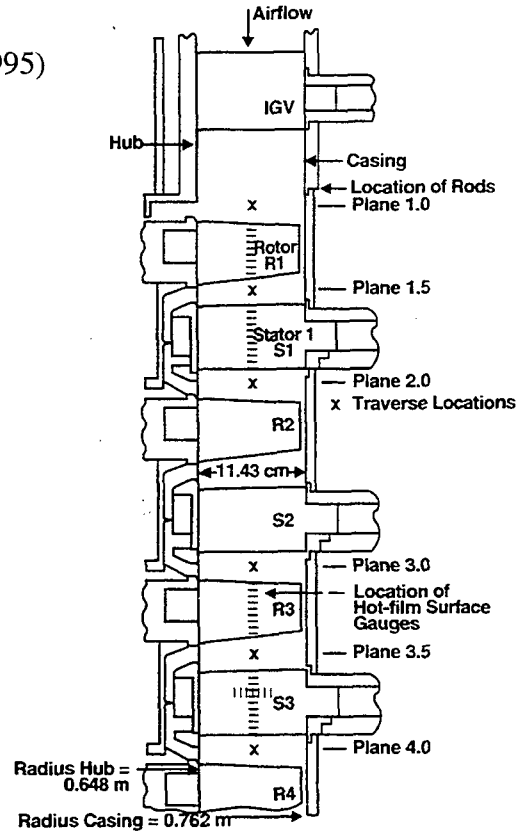

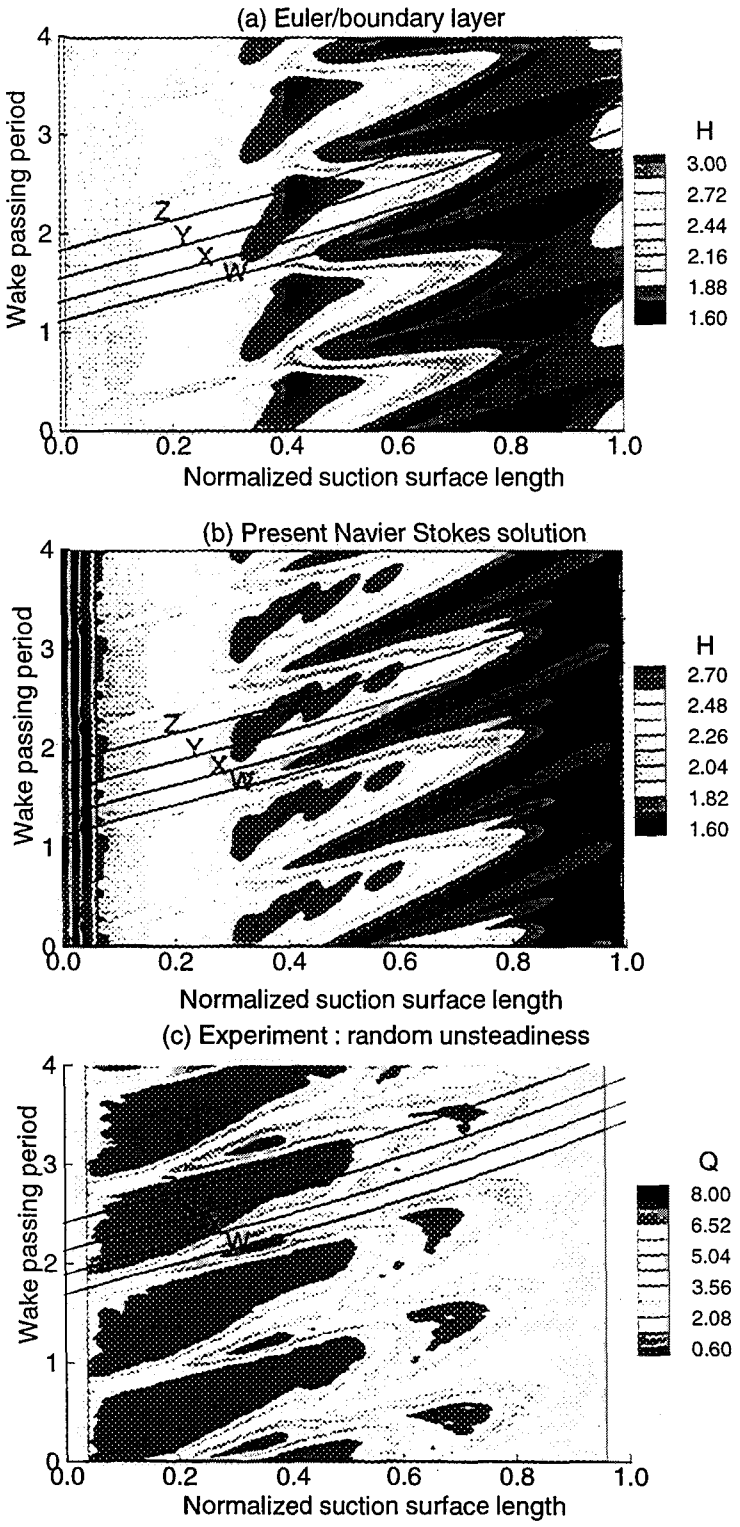

Fig. 7 Predicted distribution of instantaneous shape factor from unsteady NS and Boundary layer codes. The experimental data is random unsteadiness in skin friction coefficient in percent

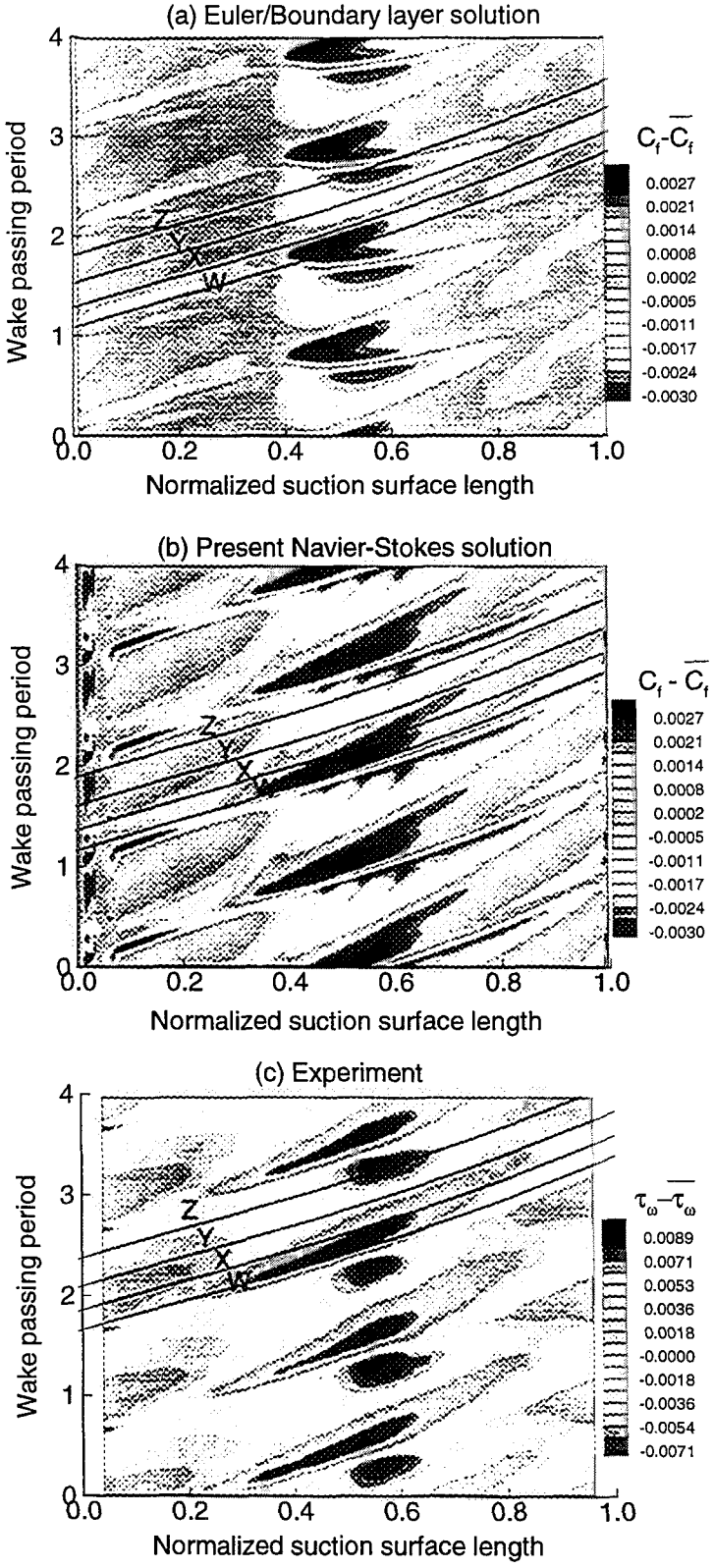

Fig. 12 Time history of measured and predicted fluctuations in skin friction coefficient

GROWTH OF A TURBULENT SPOT

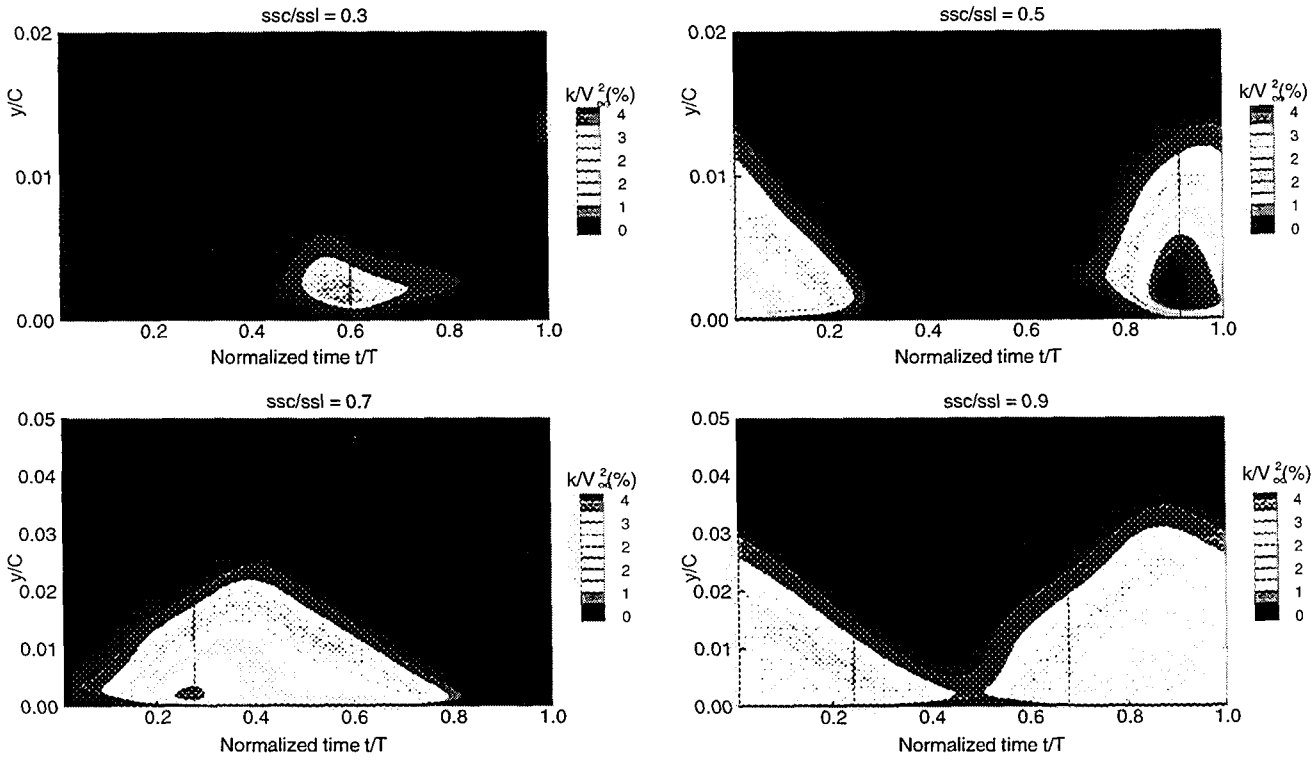

Fig. 14 Time history of turbulent kinetic energy in one period

Numerical simulation of the unsteady transitional flow in compressor cascade

- Cascade properties
  - 24 rods, 24 untwisted blades
  - rotation speed 3000 rpm — hub to tip ratio 0.7
  - tip diameter 428mm — hub diameter 321mm
  - aspect ratio 0.86 — solidity at midspan 0.78

IGV *Cylinder Rotor* *Measuring Cascade*

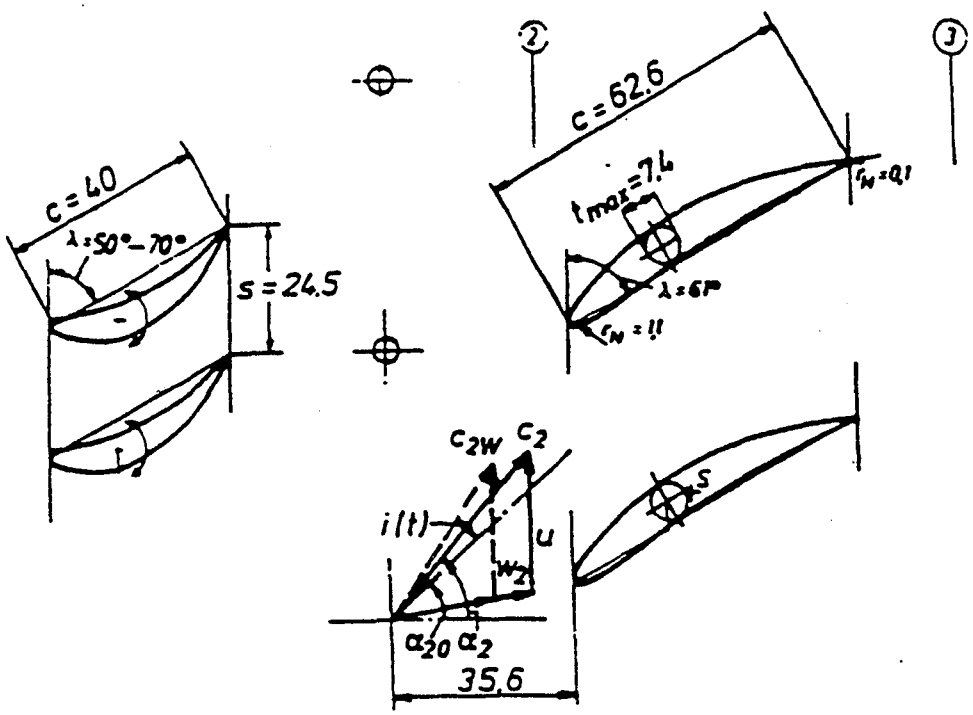

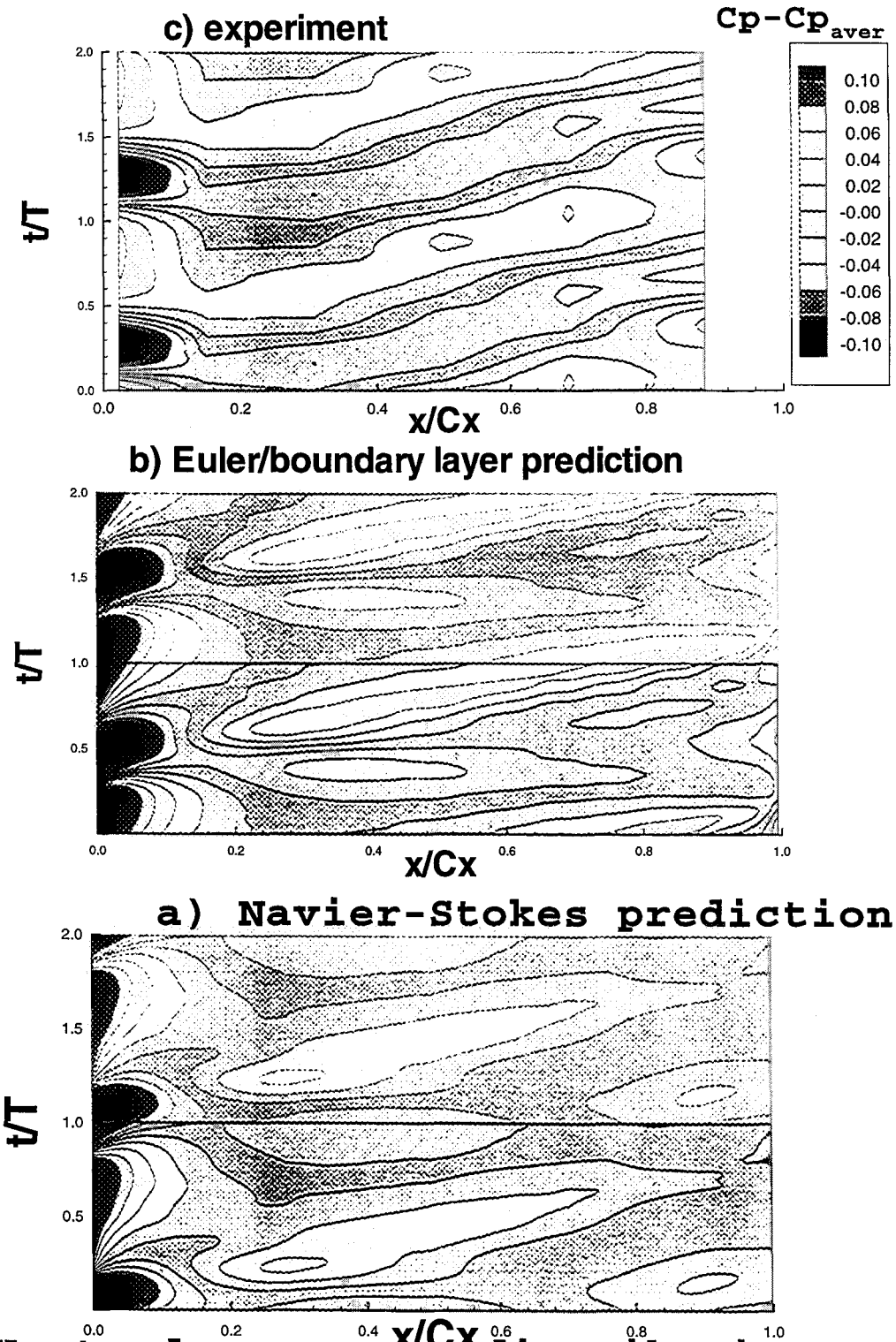

Unsteady pressure distribution, suction surface

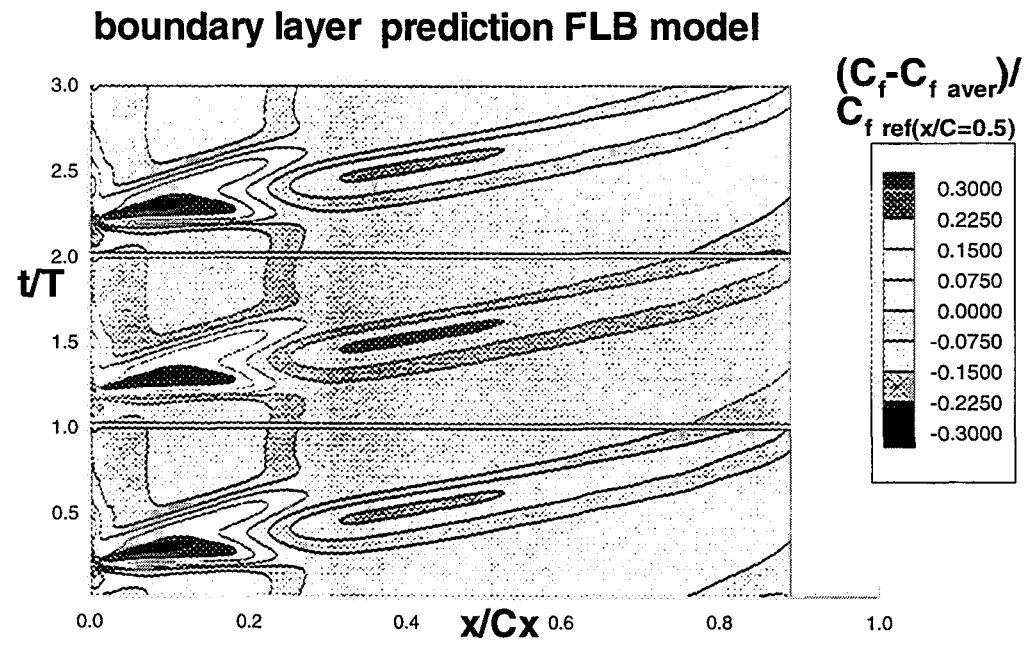

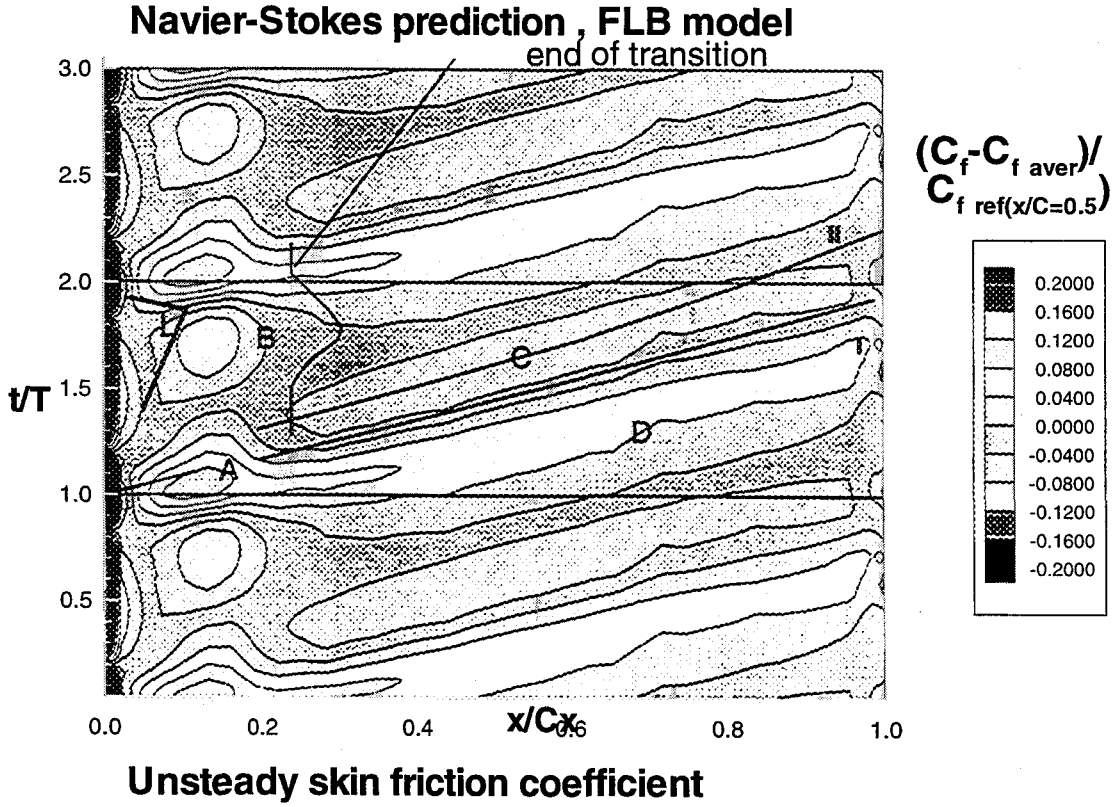

Unsteady skin friction coefficient

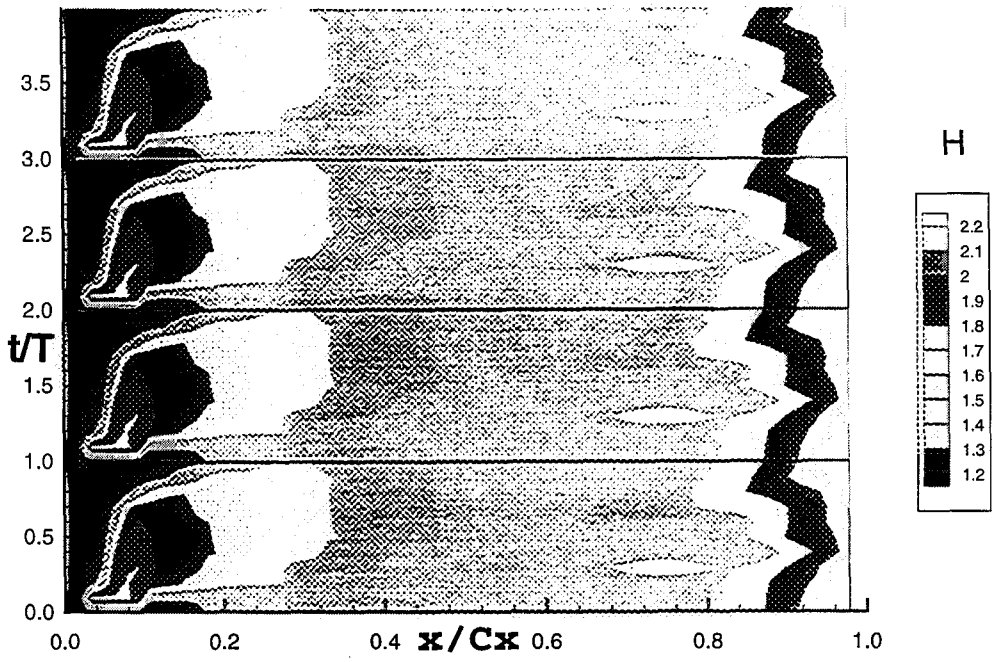

Shape factor, Navier-Stokes prediction LB model

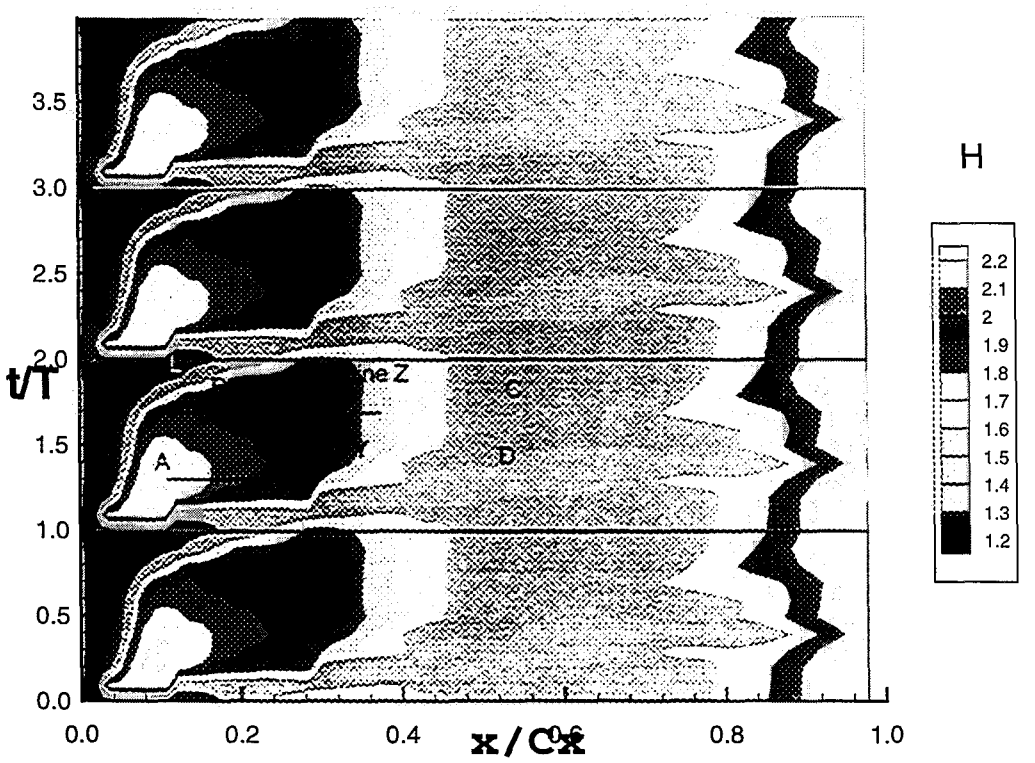

Shape factor, Navier-Stoked prediction , FLB turbulence model

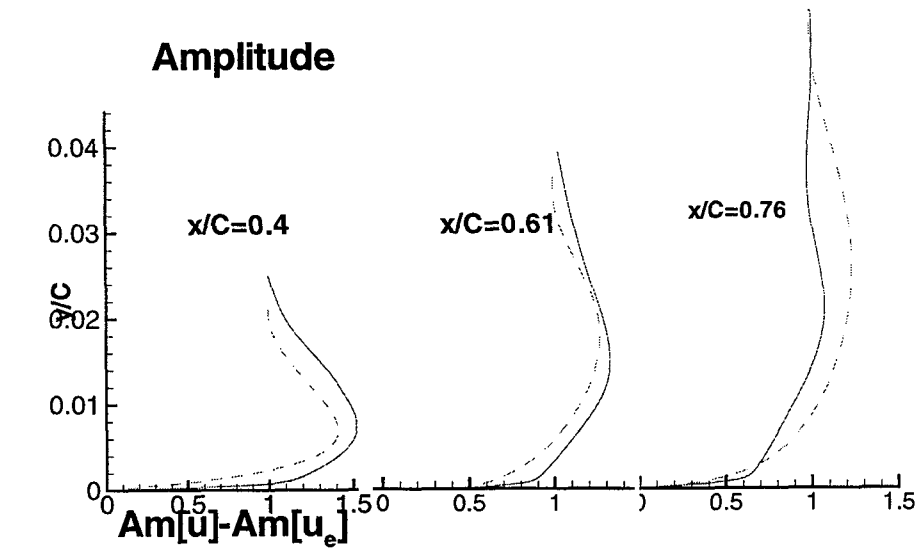

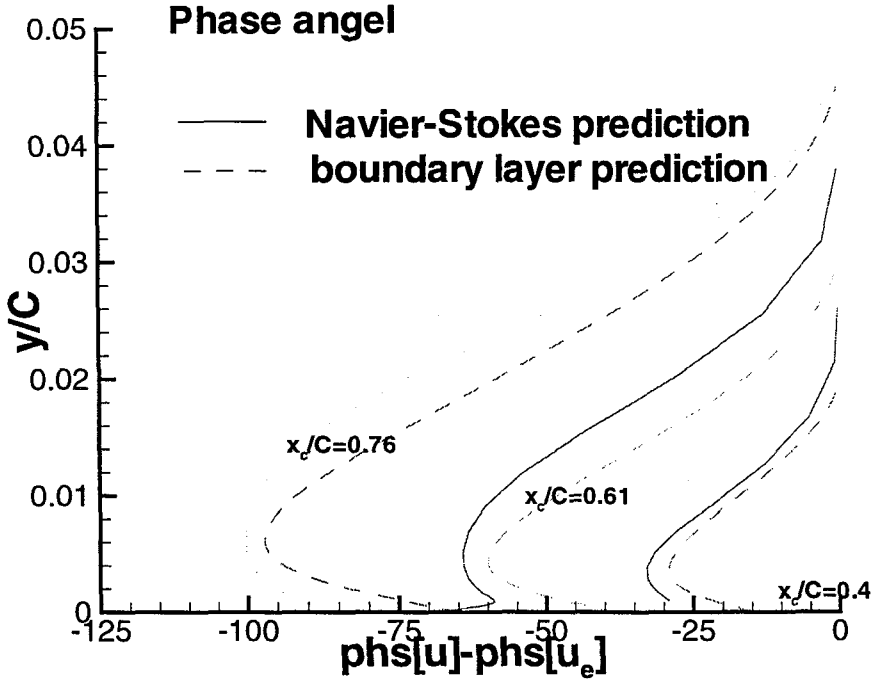

Unsteady velocity profiles

LP TURBINE TRANSITION
(Laminar Separation Bubble)

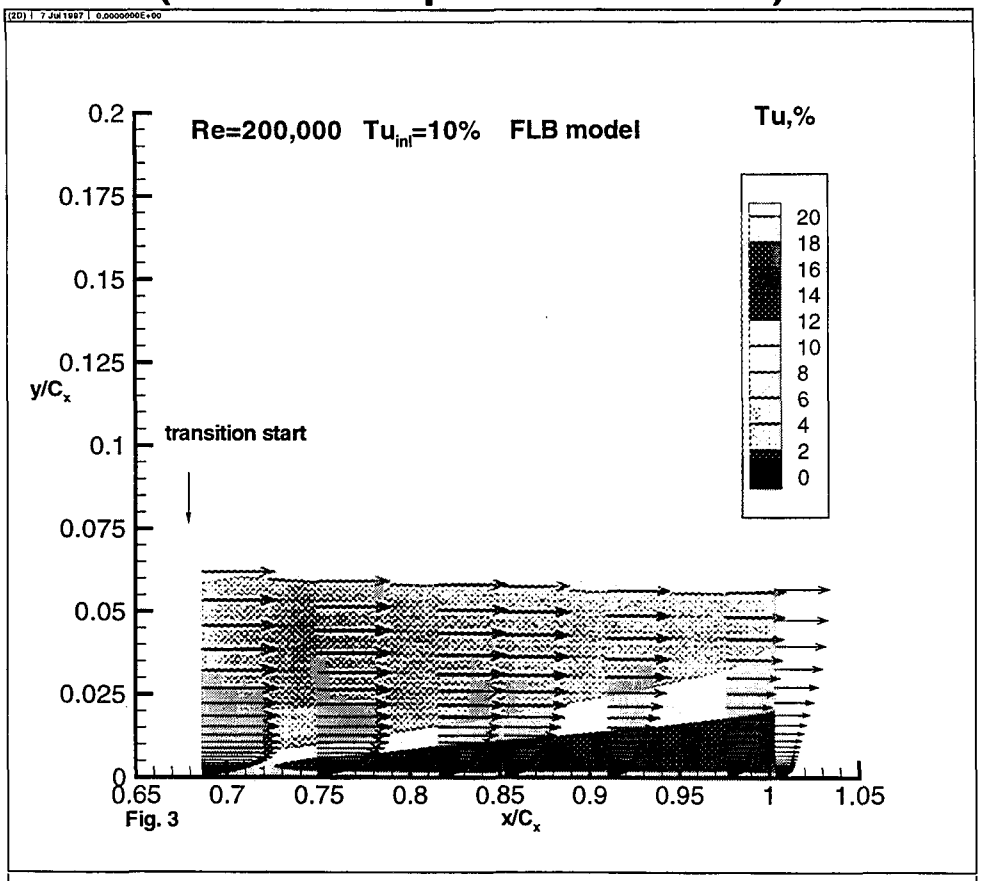

Fig. 3

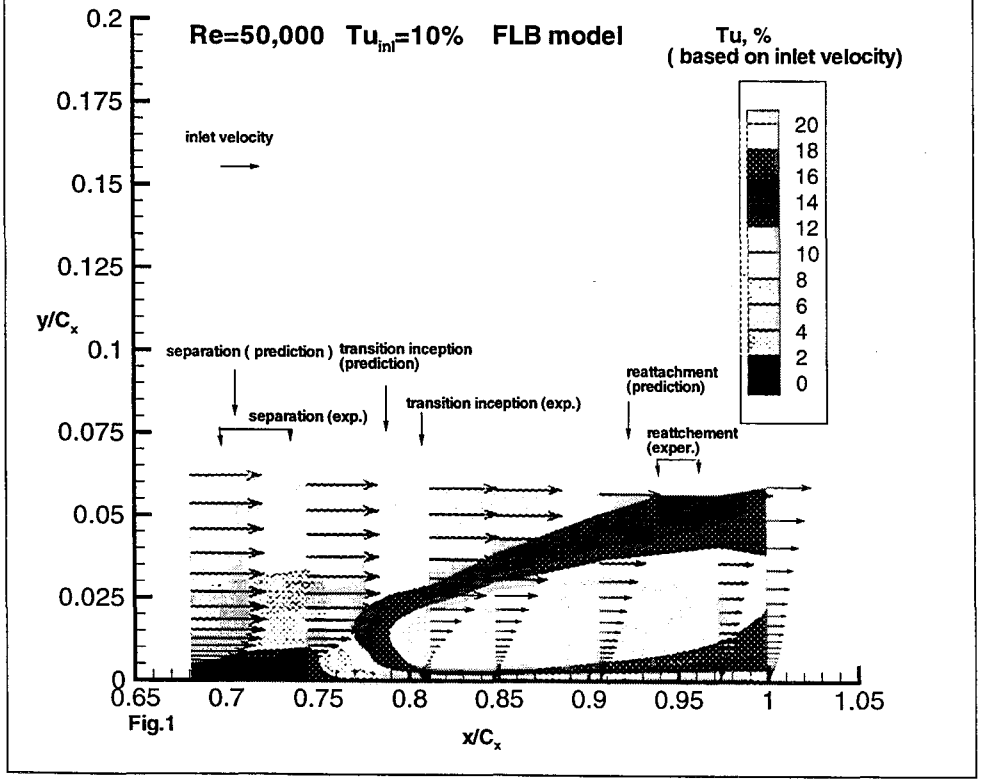

Fig.1

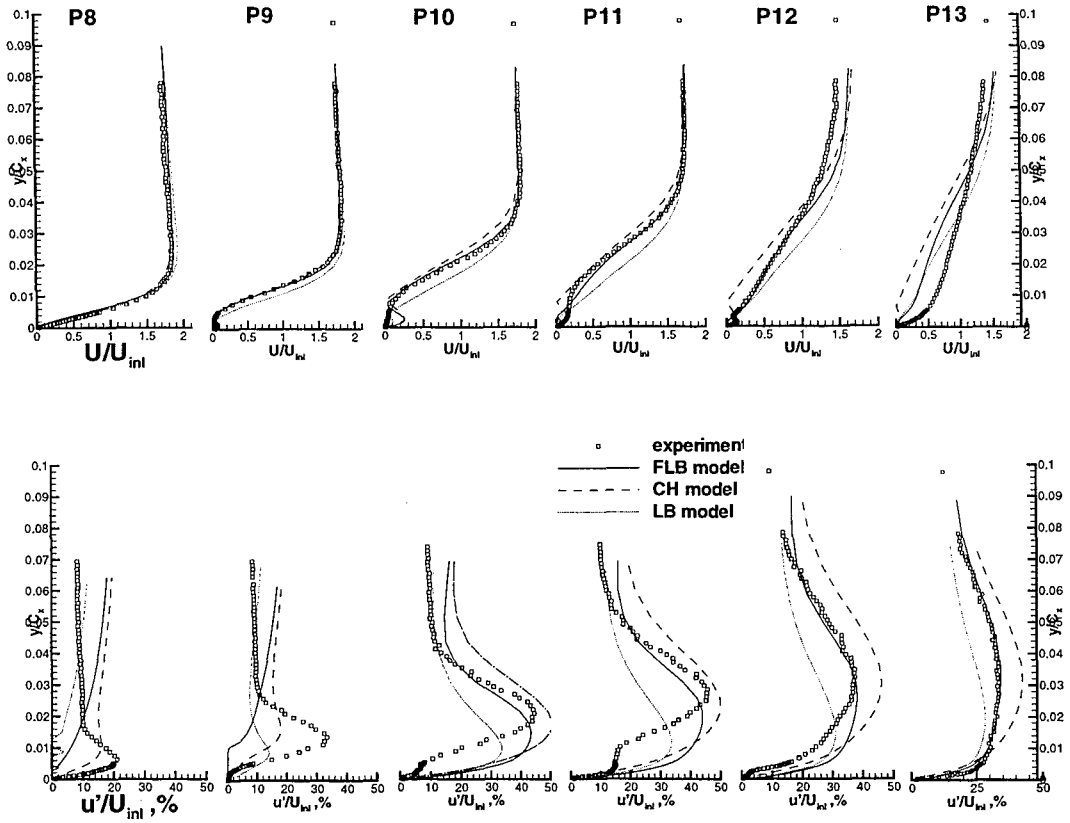

Velocity and turbulent intensity profiles Tu = 10 % Re =50000

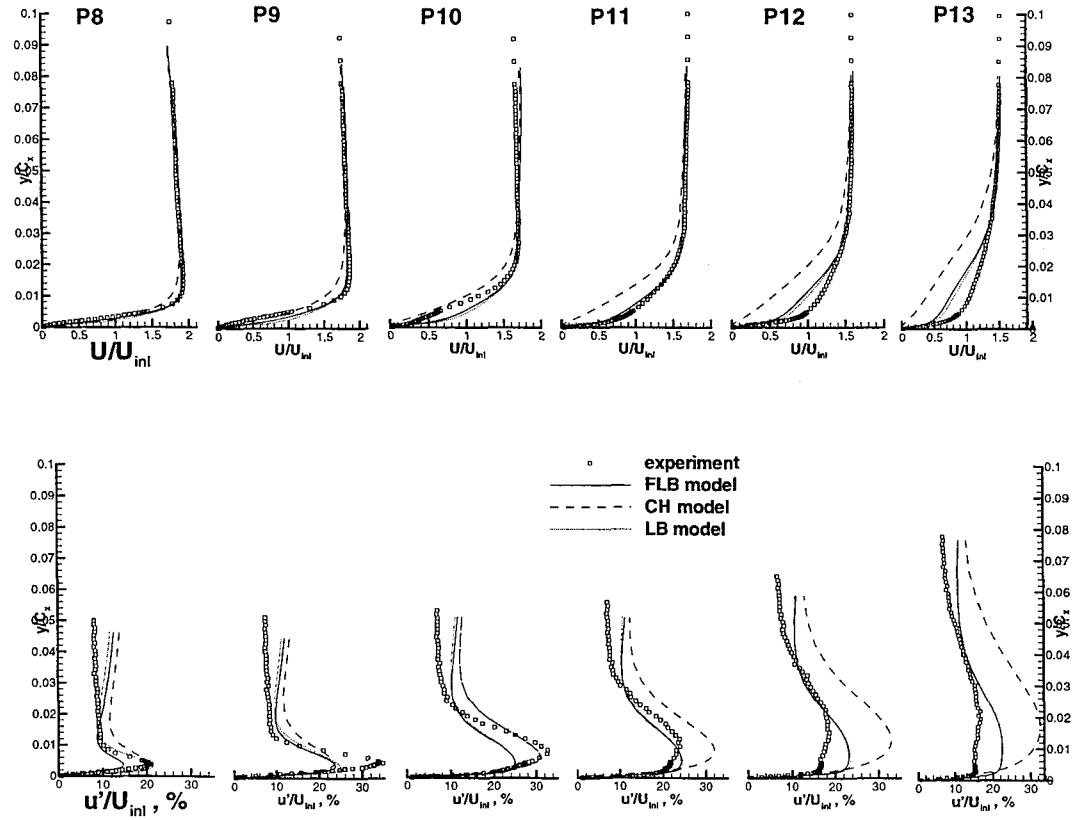

Velocity profiles and turbulence intensity, Tu = 10 % Re = 200000

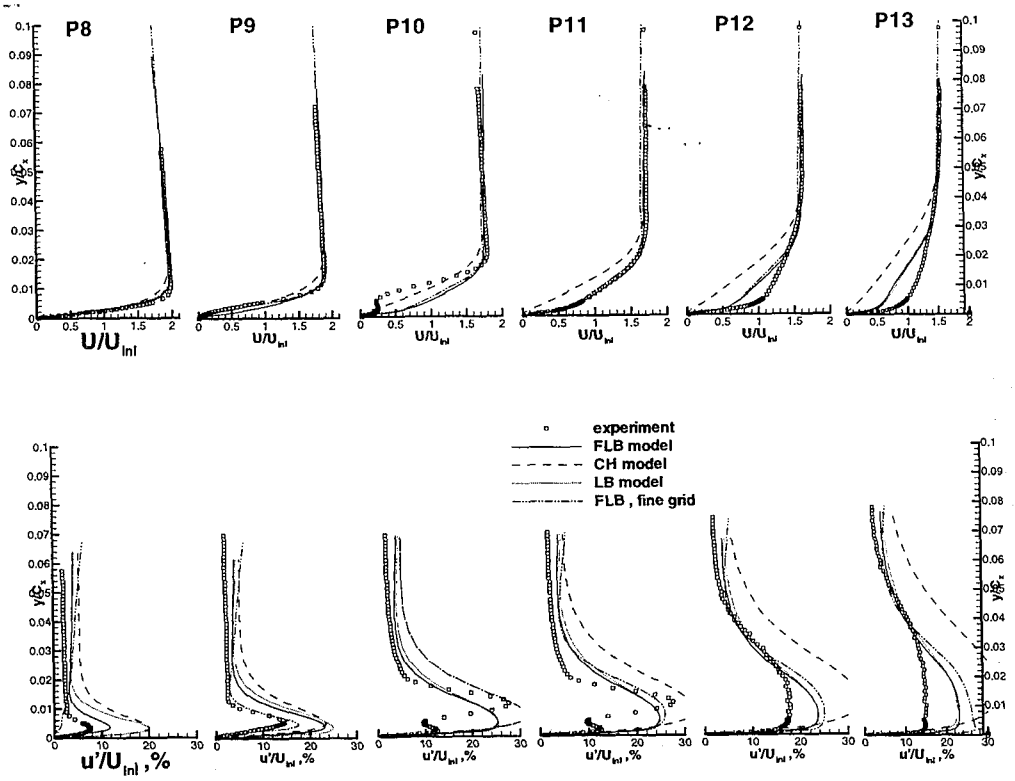

Velocity and turbulence intensity profiles,Tu = 2.5 % Re = 200000

Conclusion

- Incorporation of the pseudo-time step in conjunction with stability analysis enabled development of an efficient code for unsteady flow simulation
- Unsteady solver was successfully applied to simulation of the unsteady transitional flow in the compressor cascade. Good correlation was achieved with experimental data numerical analysis based on Euler/boundary layer procedure.
- N-S solver was able to predict main regions associated with wake induced transition: laminar region, calmed zone, wake induced transitional strip, wake induced turbulent strip.
- Fan-Lakshminarayna-Barnett low Reynolds k-e model gave best prediction. Lam-Bremhorst model predicted sharper transition with earlier inception. Computation based on Chien model failed to predict unsteady transition.
- A limited number of inner iteration is required to get unsteady pressure field. Correct prediction of unsteady boundary layer requires significantly more inner iterations. Based on this fact current N-S solver can be used as a replacement of the Euler solver in Euler/boundary layer technique with moderate increase in required computational resources.

DIRECT NUMERICAL SIMULATIONS OF BOUNDARY LAYER TRANSITION ON A FLAT PLATE

Man Mohan Rai
NASA Ames Research Center
Moffett Field, California

ABSTRACT

In recent years the techniques of computational fluid dynamics (CFD) have been used to compute flows associated with geometrically complex configurations. However, success in terms of accuracy and reliability has been limited to cases where the effects of turbulence and transition could be modeled in a straightforward manner. Even in simple flows, the accurate computation of skin friction and heat transfer using existing turbulence models has proved to be a difficult task, one that has required extensive fine-tuning of the turbulence models used. In more complex flows (for example, in turbomachinery flows in which vortices and wakes impinge on airfoil surfaces causing periodic transitions from laminar to turbulent flow) the development of a model that accounts for all scales of turbulence and predicts the onset of transition is an extremely difficult task.

Fortunately, current trends in computing suggest that it may be possible to perform direct simulations of turbulence and transition at moderate Reynolds numbers in some complex cases in the near future. This presentation will focus on direct simulations of transition and turbulence using high-order accurate finite-difference methods. The advantage of the finite-difference approach over spectral methods is that complex geometries can be treated in a straightforward manner. Additionally, finite-difference techniques are the prevailing methods in existing application codes. An application of high-order-accurate finite- difference methods to direct simulations of transition and turbulence in a spatially evolving boundary layer subjected to high levels of freestream turbulence will be presented.

OBJECTIVES

- EXTEND HIGH-ORDER ACCURATE FINITE-DIFFERENCE METHOD FOR INCOMPRESSIBLE FLOWS TO COMPRESSIBLE FLOWS

- INVESTIGATE REQUIREMENTS FOR COMPUTING TRANSITION AND TURBULENCE ON CURRENTLY AVAILABLE SUPERCOMPUTERS

- INVESTIGATE THE PHYSICS OF TRANSITION IN A HIGH FREESTREAM DISTURBANCE ENVIRONMENT

    - TURBOMACHINERY COMPUTATIONS
    - REDUCE COMPUTING REQUIREMENTS

APPROACH

- COMPRESSIBLE FLOW (SUBSONIC)

- NONCONSERVATIVE FORMULATION OF NAVIER-STOKES EQUATIONS

- HIGH-ORDER ACCURATE FINITE DIFFERENCES (5TH-ORDER FOR INVISCID TERMS AND 4TH-ORDER FOR VISCOUS TERMS)

- UPWIND-BIASING OF CONVECTIVE TERMS

- CENTRAL-DIFFERENCING OF VISCOUS TERMS

- ITERATIVE -IMPLICIT FRAMEWORK

- MULTIPLE ZONE DISCRETIZATION OF FLOWFIELD

- GENERATION OF NUMERICAL FREESTREAM TURBULENCE

COMPUTATIONAL METHOD

CONSIDER THE UNSTEADY EULER EQUATIONS IN ONE DIMENSION

$$Q_t + AQ_x = 0 \qquad (1)$$

USING A SIMILARITY TRANSFORM WE OBTAIN

$$A = T\Lambda T^{-1}$$

$$= T\Lambda^{+}T^{-1} + T\Lambda^{-}T^{-1}$$

$$= A^{+} + A^{-}$$

THE SECOND TERM IN EQ. 1 IS NOW WRITTEN AS

$$AQ_x = A^{+}Q_x^{-} + A^{-}Q_x^{+} \qquad \text{(SCM TECHNIQUE)}$$

WHERE Q_x^{+} AND Q_x^{-} ARE FORWARD AND BACKWARD DIFFERENCES RESPECTIVELY

COMPUTATIONAL METHOD.....CONTINUED

THE TERMS Q_x^{+} AND Q_x^{-} ARE EVALUATED AS

$$Q_x^{-} = \frac{-6Q_{i+2} + 60Q_{i+1} + 40Q_i - 120Q_{i-1} + 30Q_{i-2} - 4Q_{i-3}}{120\Delta x}$$

$$Q_x^{+} = \frac{4Q_{i+3} - 30Q_{i+2} + 120\,Q_{i+1} - 40Q_i - 60Q_{i-1} + 6Q_{i-2}}{120\Delta x}$$

THE FULLY IMPLICIT FINITE-DIFFERENCE REPRESENTATION OF EQ.1 BECOMES

$$\frac{Q_i^{n+1} - Q_i^{n}}{\Delta t} + (A^{+}Q_x^{-} + A^{-}Q_x^{+})^{n+1} = 0$$

A NEWTON LINEARIZATION YIELDS THE ITERATIVE-IMPLICIT FINITE-DIFFERENCE EQUATIONS

$$(I + \Delta t(\frac{A^{+}\nabla_x}{\nabla x_i} + \frac{A^{-}\Delta_x}{\Delta x_i}))^{p}(Q^{p+1} - Q^{p}) = -\Delta t(\frac{Q^{p} - Q^{n}}{\Delta t} + (A^{+}Q_x^{-} + A^{-}Q_x^{+})^{p})$$

SCHEMATIC OF COMPUTATIONAL REGION (NOT TO SCALE)

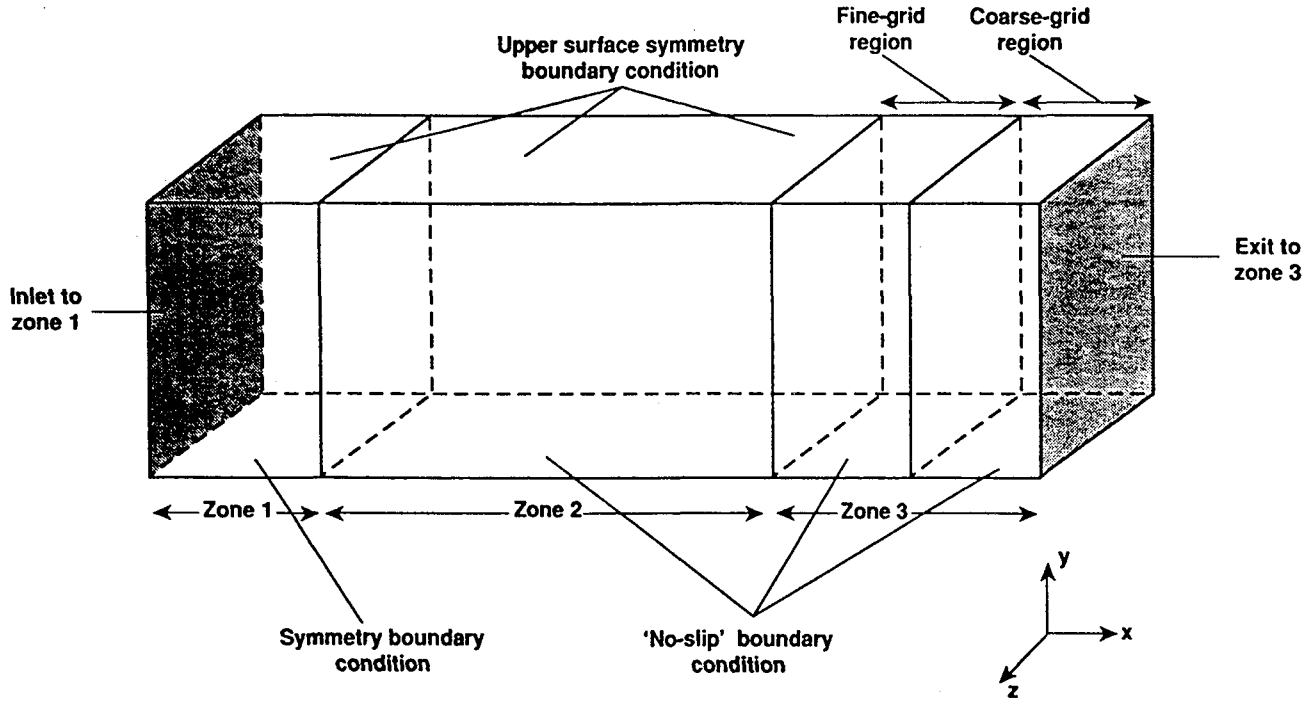

BOUNDARY CONDITIONS

LOWER SURFACE : ADIABATIC WALL / NO-SLIP

UPPER SURFACE : SYMMETRY

INLET BOUNDARY (ZONE 1) : VELOCITY PERTURBATIONS THROUGH RIEMANN INVARIANTS

EXIT BOUNDARY (ZONE 3) : PRESSURE REFLECTIVE CONDITION

SPANWISE BOUNDARY SURFACES : PERIODICITY

INLET BOUNDARY CONDITION

$$u_b + \frac{2c_b}{\gamma - 1} = (u_\infty + \tilde{u}) + \frac{2c_\infty}{\gamma - 1}$$

$$u_b - \frac{2c_b}{\gamma - 1} = u_2 - \frac{2c_2}{\gamma - 1}$$

$$v_b = \tilde{v}$$

$$w_b = \tilde{w}$$

$$p_b = P_\infty \left(1 + \frac{(\gamma - 1)(u_b^2 + v_b^2 + w_b^2)}{2 c_b^2}\right)^{-\gamma/(\gamma - 1)}$$

WHERE $\tilde{u}$, $\tilde{v}$ AND $\tilde{w}$ ARE THE PRESCRIBED PERTURBATIONS IN THE INLET VELOCITY

EVOLUTION OF SMALL AMPLITUDE DISTURBANCES

GROWTH RATES

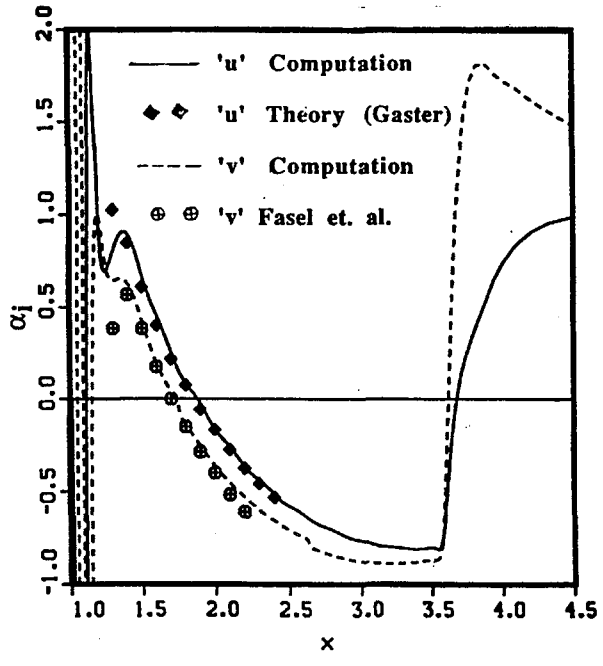

VELOCITY AMPLITUDES

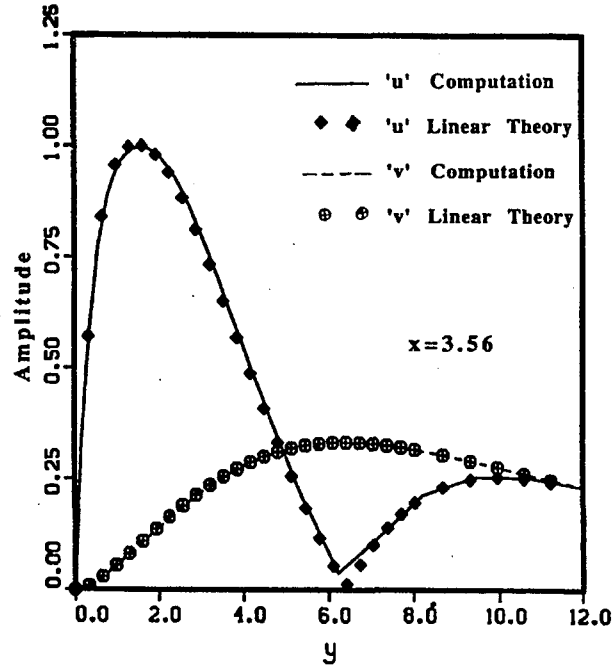

COMPUTATIONAL PARAMETERS

LENGTH OF PLATE = 24.0 INCHES / 13.0 INCHES

WIDTH OF PLATE = 1.5708 INCHES

HEIGHT OF COMPUTATIONAL REGION = 3.0 INCHES

INLET MACH NUMBER = 0.1

INLET REYNOLDS NUMBER = 50000.0 / INCH

FREESTREAM TURBULENCE LEVEL = 2.7 % (NEARLY ISOTROPIC)

SKIN FRICTION ALONG FLAT PLATE

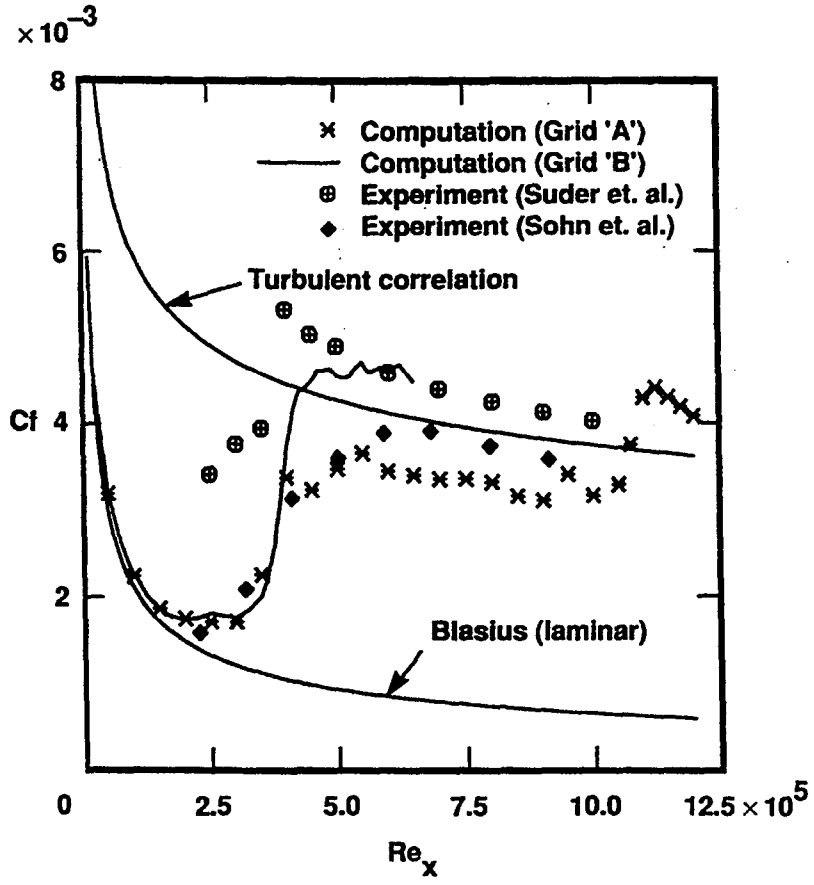

MEAN VELOCITY PROFILES

COMPUTATION

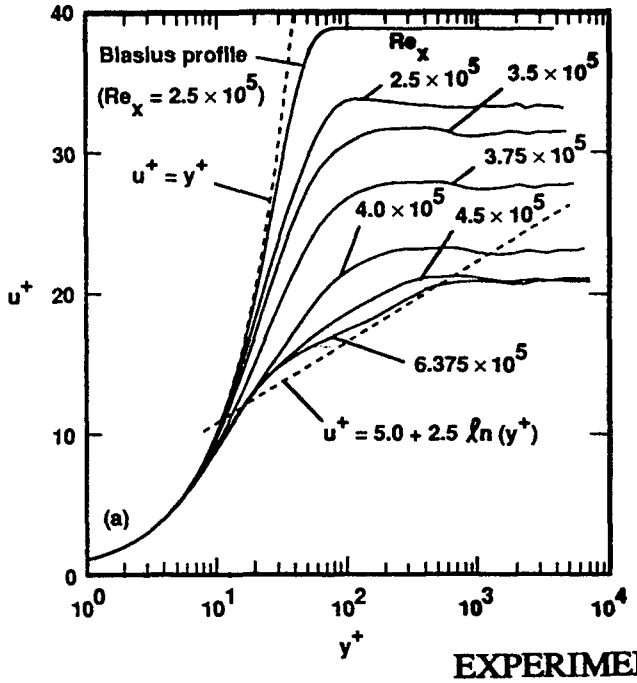

EXPERIMENT (SUDER ET. AL.)

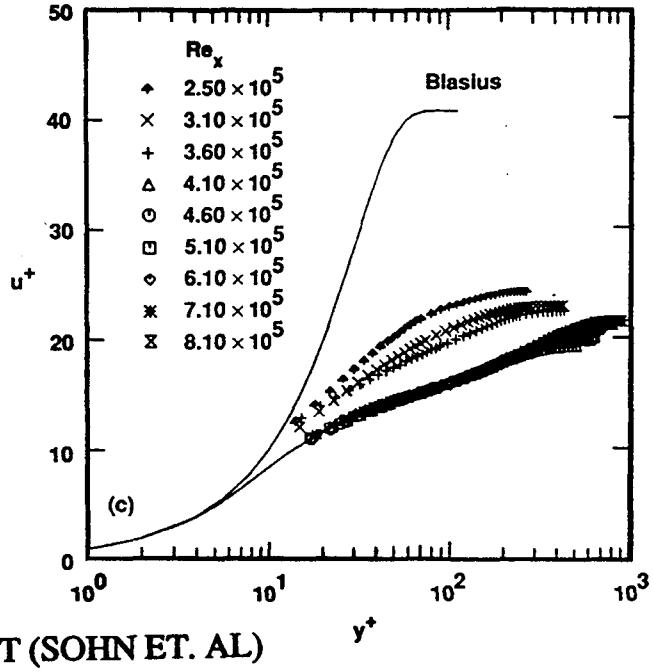

EXPERIMENT (SOHN ET. AL)

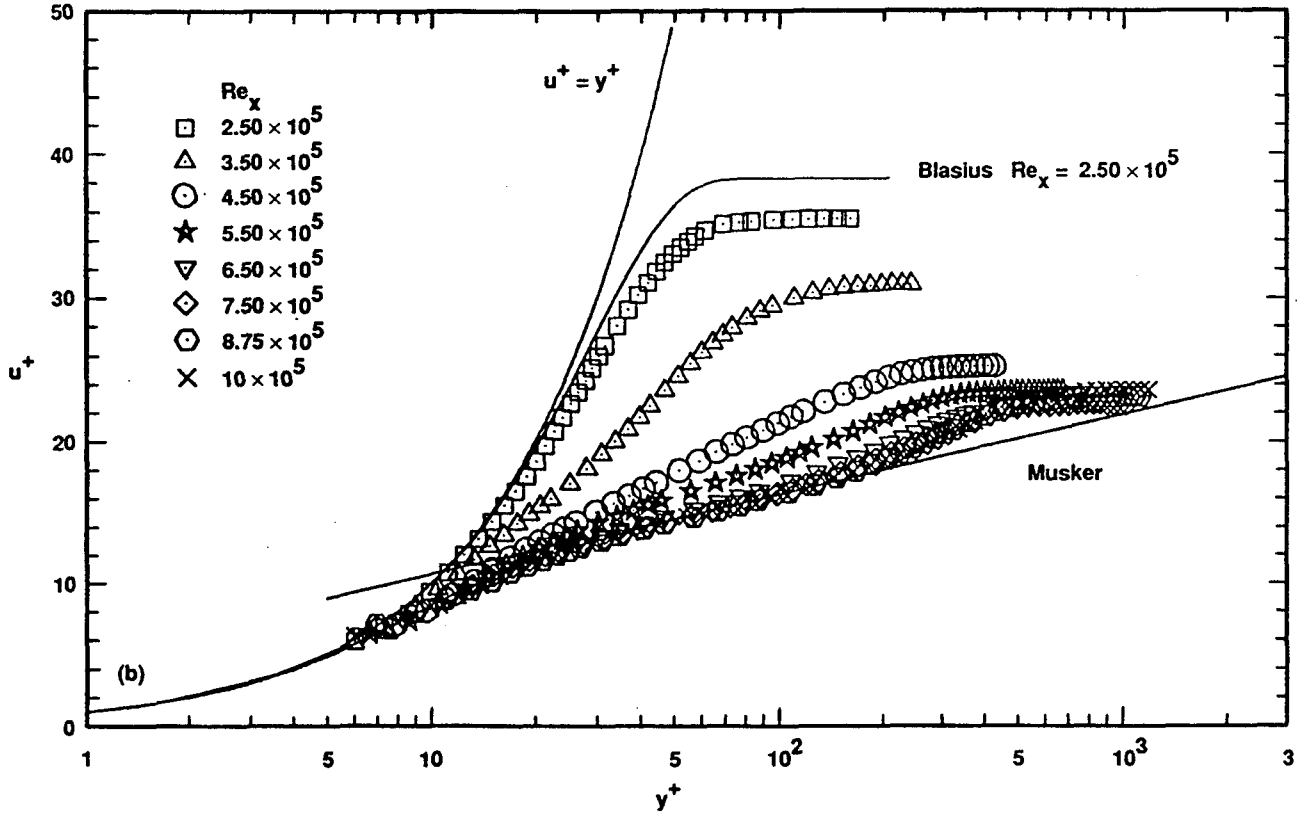

STREAMWISE COMPONENT OF TURBULENCE INTENSITY

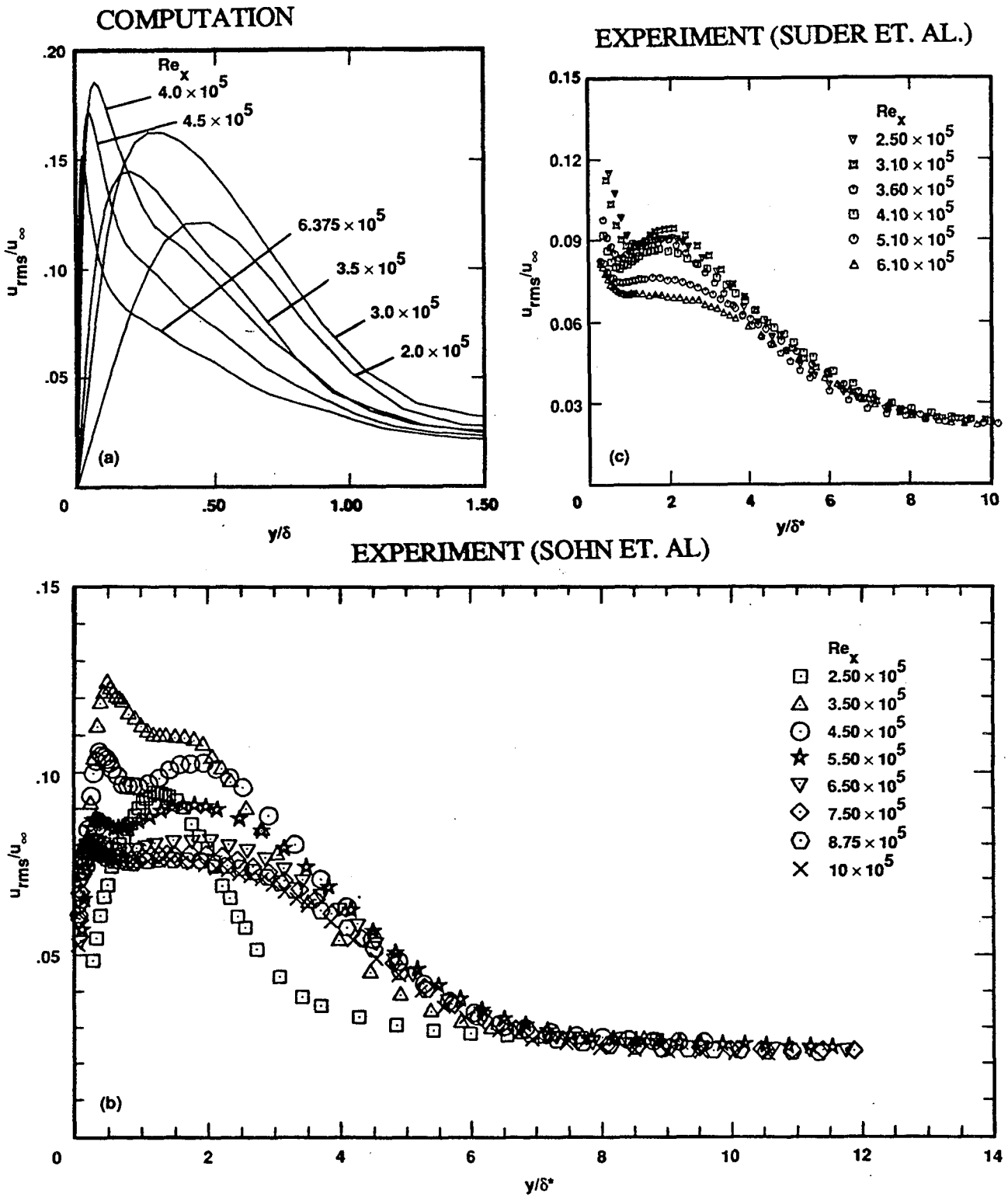

TURBULENCE INTENSITIES IN TURBULENT REGION (COMPARED WITH EXPT. OF KARLSON AND JOHANSSON)

NORMALIZED WITH WALL-SHEAR VELOCITY

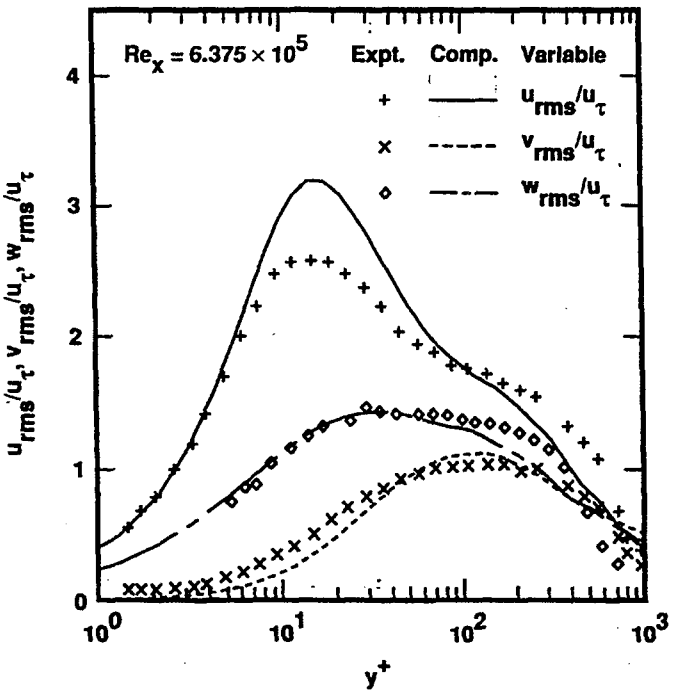

NORMALIZED WITH LOCAL MEAN VELOCITY

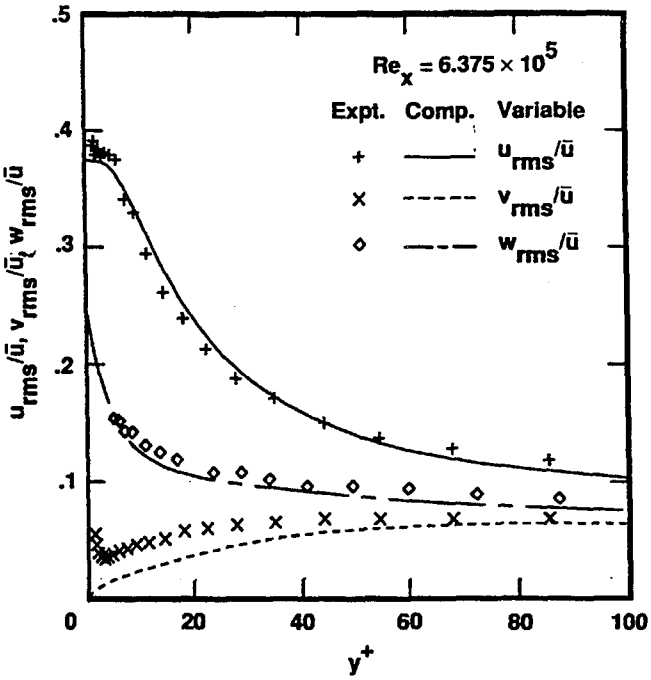

SUMMARY

- DEVELOPED A HIGH-ORDER-ACCURATE, UPWIND-BIASED, ITERATIVE-IMPLICIT, FINITE-DIFFERENCE APPROACH FOR DIRECT SIMULATIONS OF TRANSITION/TURBULENCE IN COMPRESSIBLE FLOW
- DEVELOPED AN ITERATIVE METHOD OF NUMERICALLY GENERATING FREESTREAM DISTURBANCES OF A PRESCRIBED NATURE
- DEVELOPED A CODE USING THE ABOVE TECHNIQUES FOR DIRECT SIMULATIONS OF FLAT-PLATE FLOW
- COMPUTED ONE CASE OF HIGH-FREESTREAM-TURBULENCE TRANSITION
- COMPUTED DATA AGREE QUALITATIVELY WITH EXPERIMENTAL DATA
- PRELIMINARY FLOW VISUALIZATION INDICATED THAT THE TRANSITION REGION WAS FOUND TO BE CHARACTERIZED BY DETACHED SHEAR LAYERS AND PAIRS OF COUNTERROTATING STREAMWISE VORTICES

SUMMARY.....CONTINUED

- RESULTS INDICATE THAT THE ESSENTIAL FEATURES OF THE TRANSITION PROCESS IN THIS PARTICULAR CASE HAVE BEEN CAPTURED
- JUDICIOUS USE OF ZONAL METHODOLOGY IS REQUIRED TO PERFORM SUCH COMPUTATIONS ON CURRENT SUPERCOMPUTERS
- A MORE REFINED GRID COMPUTATION WILL BE REQUIRED FOR DEMONSTRATING GRID INDEPENDENCE
- THE GRID B SAMPLE REQUIRED 800 HOURS OF SINGLE PROCESSOR CRAY-YMP HOURS
- THE COMPUTING REQUIREMENTS FOR HIGHER MACH NUMBER COMPUTATIONS WILL BE SIGNIFICANTLY LESS THAN THAT REQUIRED FOR THE CURRENT COMPUTATION
- THE FINITE-DIFFERENCE METHOD USED IN THE PRESENT STUDY CAN IN A STRAIGHTFORWARD MANNER BE EXTENDED TO CURVILINEAR GRIDS

DIRECT NUMERICAL SIMULATIONS OF TRANSITION TO TURBULENCE

N.D. Sandham
Queen Mary and Westfield College
London, England

ABSTRACT

Advances in computer hardware make direct numerical simulations (DNS) of the full Navier-Stokes equations a convenient source of data for studies of the final stages of transition to turbulence. The objective of this contribution is to review recent advances in techniques, outlining the range of problems that can currently be simulated, and to present results from some of the latest simulations.

Several of the earlier simulations followed the route to turbulence initiated by a vibrating ribbon, starting the simulations with quite large amplitude (e.g. 3%) two-dimensional disturbances. This was useful as the simulations could be validated against previous experiments and against the emerging theories of secondary instability. End-stage transition studies from such simulations have been reported in detail by Sandham & Kleiser (1993) for incompressible channel flow and by Sandham et al. (1994) and Adams & Kleiser (1996) for supersonic (Mach 2 and Mach 5 respectively) boundary layers. Such studies have focused primarily on the role of vorticity stretching and shear-layer roll-up as the physical mechanisms that lead from Lambda or quasi-streamwise vortices to the formation of a regeneration cycle of near-wall turbulence. Once the regeneration cycle is established a relaxation to the expected time-averaged statistics of turbulent flow is observed.

Simulations of transition induced by local disturbances are more computationally intensive, owing to the larger physical domains that must be used to capture the evolving turbulent spot. Simulations can be validated against theory for linear propagation and growth of a wave packet (Konzelmann & Fasel, 1991). The initial stages of turbulent spot formation have been studied in some detail by Singer (1994). Although the initiation, via fluid injection from the surface, is completely different from the vibrating-ribbon method, similarities occur in the end-stage of transition, as the turbulent spot establishes itself. Formation of new vortices can be followed using the same conceptual framework.

Another transition scenario that can be simulated by DNS is that of laminar separation bubbles. Alam & Sandham (1997) carry out spatial simulations with 256×128×120 grid points for separation of a laminar boundary layer, transition of the separated shear layer triggered by oblique disturbances, reattachment as a turbulent boundary layer with slow downstream relaxation to log-law behaviour. Such simulations do not require excessively long run times on current supercomputers as the problems parallelise very efficiently. Data from the simulations are being used to assess the capability of turbulence models to predict the reattachment and relaxation regions of the flow.

Direct simulation of transition scenarios:

- sequence of instabilities, beginning with 2D
- quasi-streamwise vortices
- separation of laminar boundary layer
- turbulent spot evolution

Transition via sequence of instabilities in channel flow
(Sandham & Kleiser 1991)

cyclical mechanism of near-wall turbulence arrived at via

- 2D primary instability
- secondary (K-type) instability
- Lambda vortices
- shear layer breakdown to vortices
- near-wall vortex
- first low-speed streak

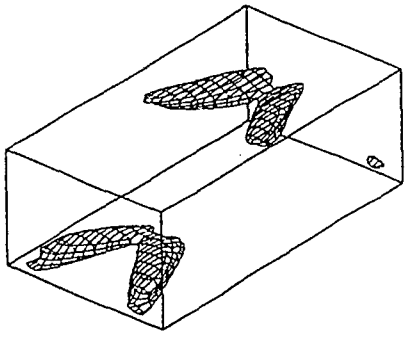

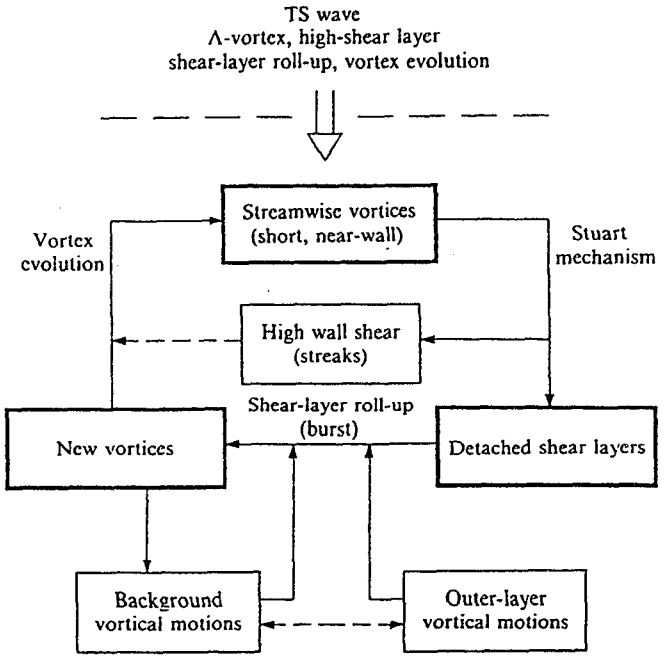

Transition via quasi-streamwise vortices in boundary layer at Mach 2
(Sandham, Adams and Kleiser 1995)

Oblique wave primary instability

- two-stage transition
- quasi-streamwise vortices
- non-zero angles of inclination and skewness crucial
- new streamwise vortices via stretching and tilting
- rapid breakdown into turbulent patches

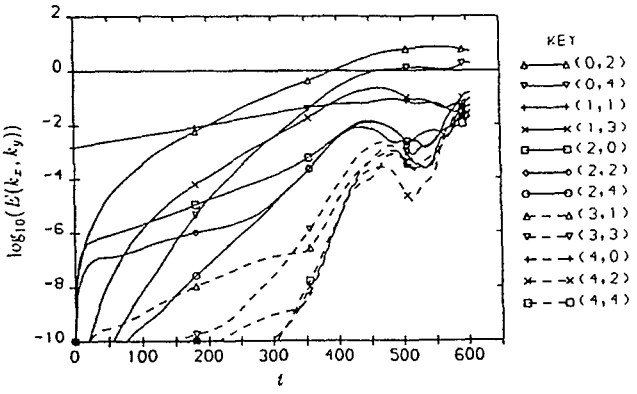

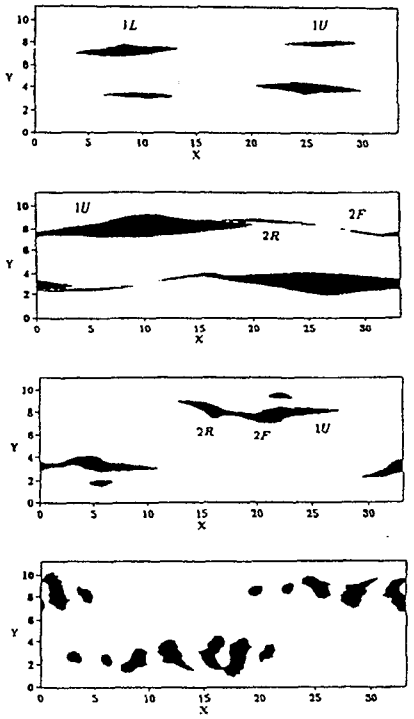

DIRECT NUMERICAL SIMULATION OF LAMINAR SEPARATION BUBBLES

(M. Alam and N. D. Sandham)

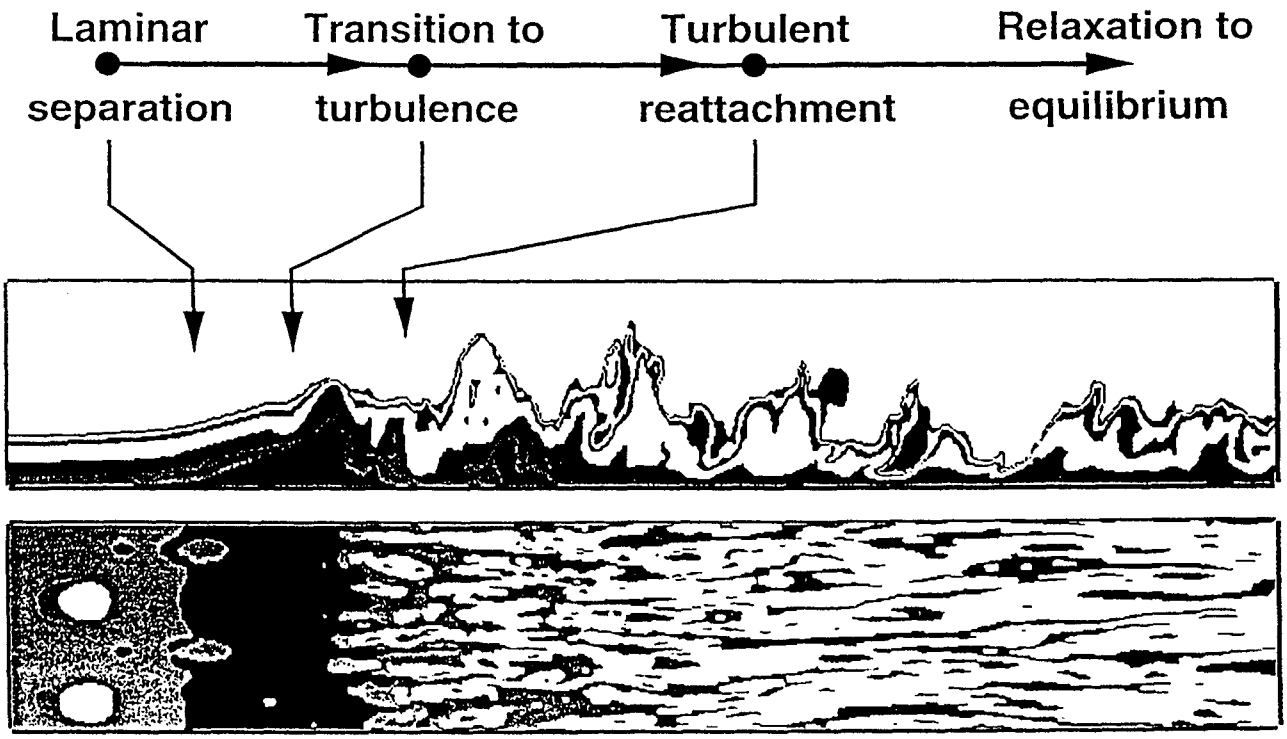

Numerical Methods

- Full three dimensional (3-D) time-dependent incompressible Navier-Stokes equations
- Fourier discretisation in spanwise and streamwise directions
- Compact third order Runge-Kutta method for time discretisation
- Crank-Nicolson method for viscous and pressure terms

- Blasius boundary layer specified at the inflow
- Gaussian profile for the upper boundary suction and the flat plate disturbances

128 PEs on Cray T3D
PVM } 90% Parallel eff.
MPI }
20600 PE hours
2-3 G-flops.

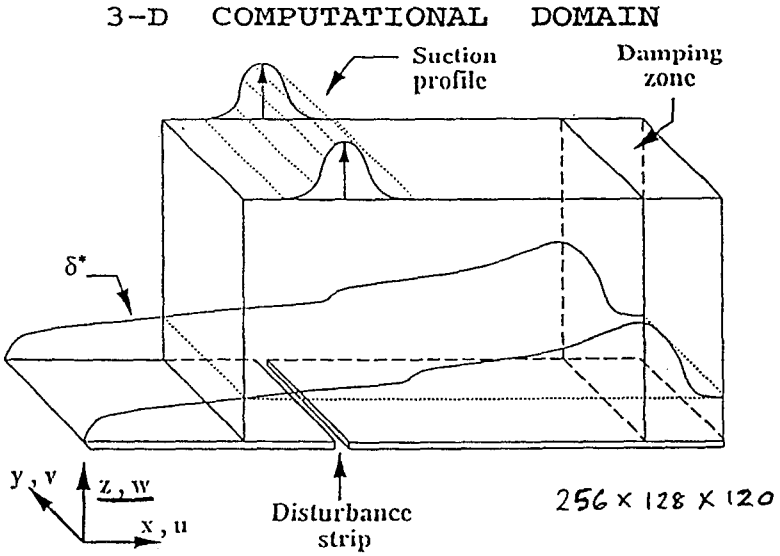

STREAMWISE VELOCITY PROFILES

DOWNSTREAM OF REATTACHMENT

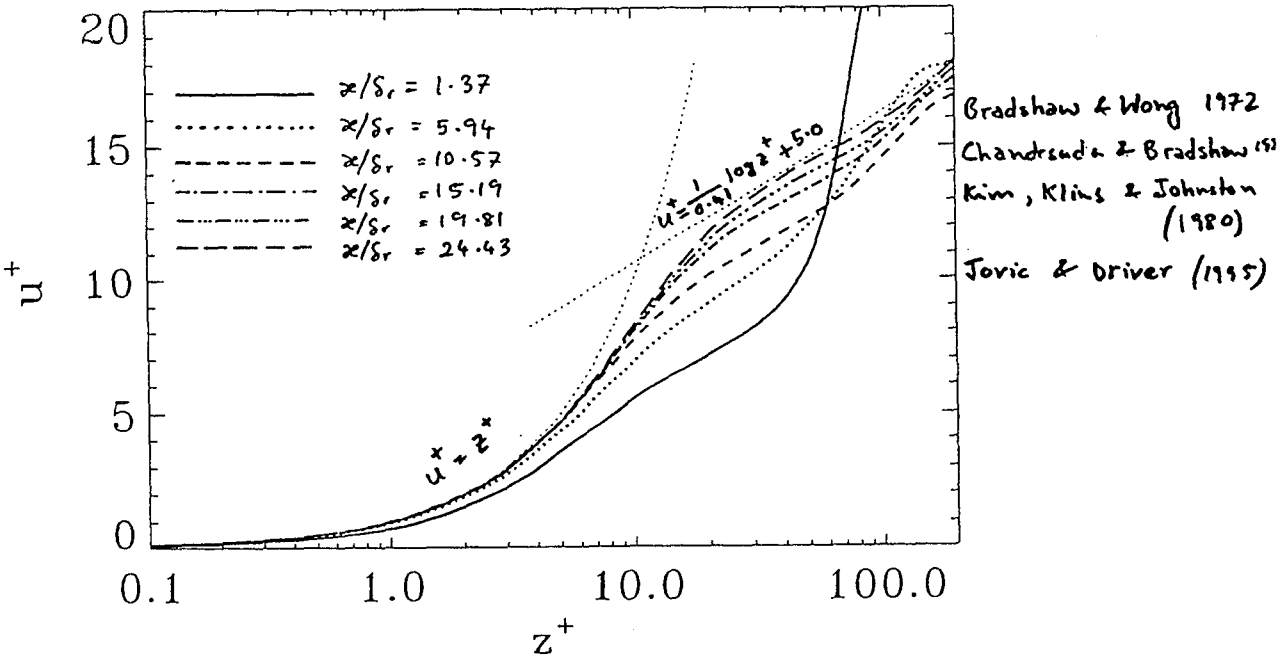

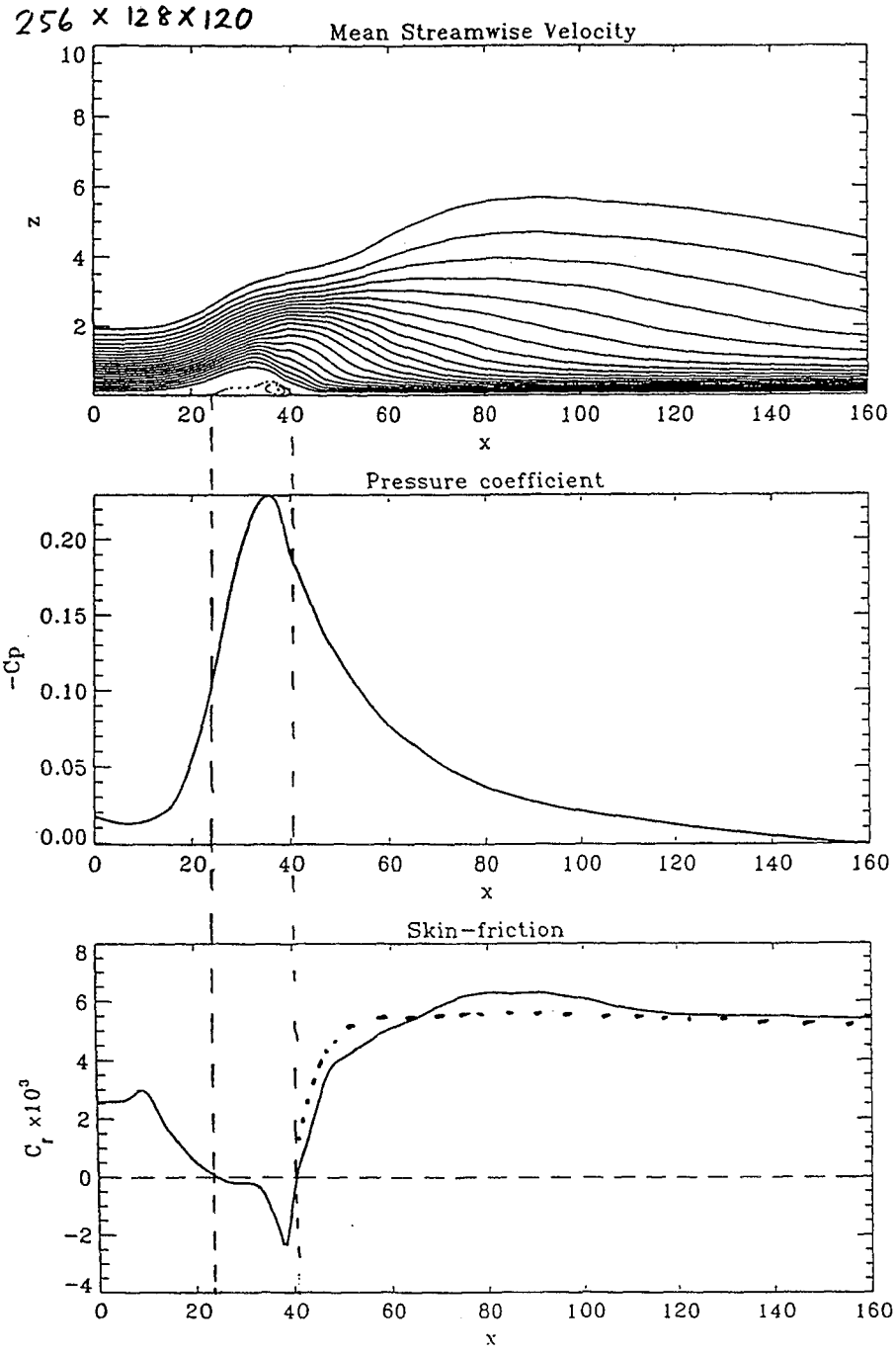
256 x 128x120
Mean Streamwise Velocity
z
x
Pressure coefficient
-Cp
x
Skin-friction
$C_f \times 10^3$
x

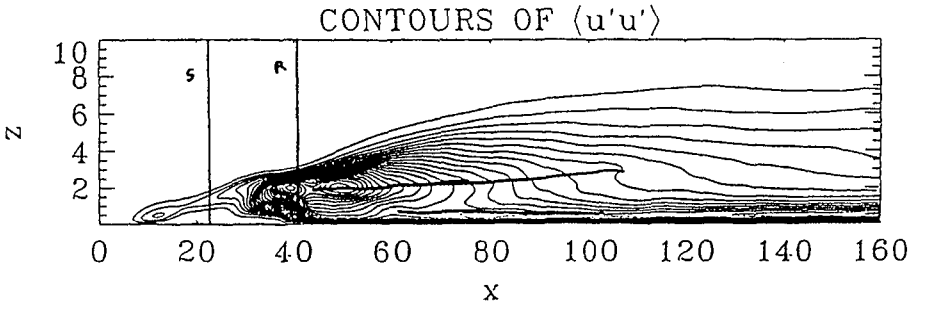
CONTOURS OF ⟨u'u'⟩
S
R
Z
10
8
6
4
2
0
20
40
60
80
100
120
140
160
X

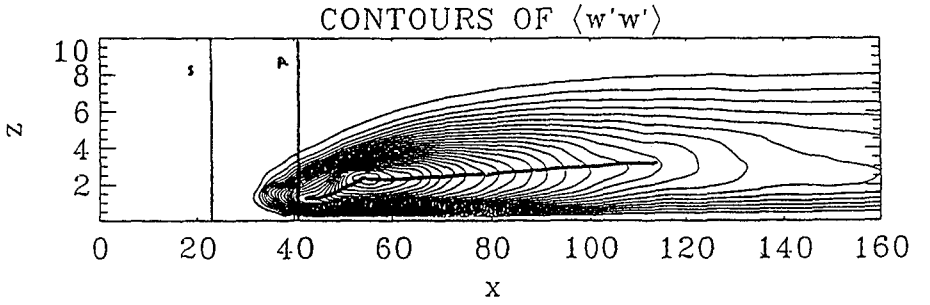
CONTOURS OF ⟨w'w'⟩
S
R
Z
10
8
6
4
2
0
20
40
60
80
100
120
140
160
X

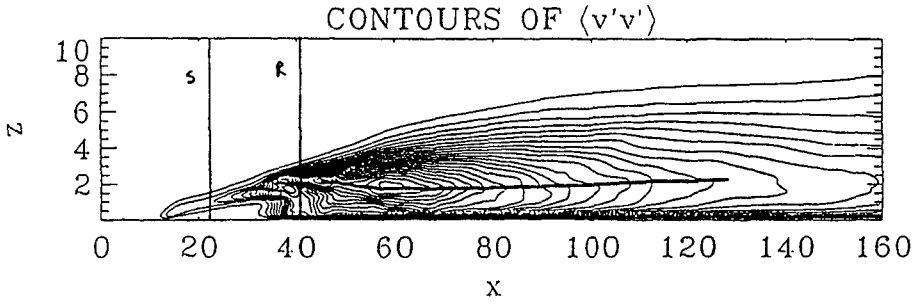
CONTOURS OF ⟨v'v'⟩
S
R
Z
10
8
6
4
2
0
20
40
60
80
100
120
140
160
X

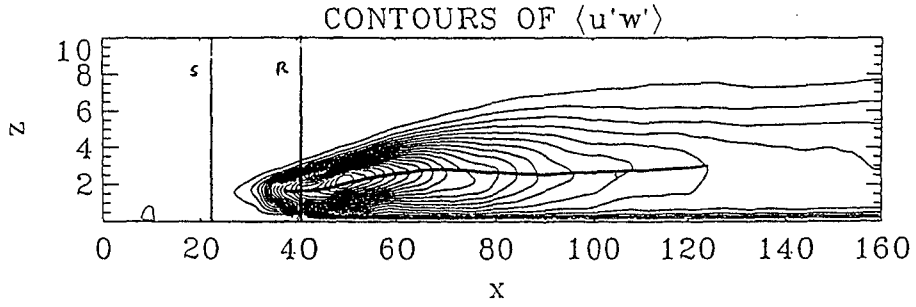
CONTOURS OF ⟨u'w'⟩
S
R
Z
10
8
6
4
2
0
20
40
60
80
100
120
140
160
X

EQUATIONS FOR THE TURBULENCE KINETIC ENERGY

$$\frac{\partial k}{\partial t}+\langle u_i\rangle\frac{\partial k}{\partial x_i}=P-\varepsilon-\frac{\partial}{\partial x_i}\left(J_i^u+J_i^p+J_i^v\right)$$

where:

$$P=-\langle u'_i u'_j\rangle\frac{\partial\langle u_i\rangle}{\partial x_j} \qquad \textbf{(Production)}$$

$$\varepsilon=\frac{1}{\mathrm{Re}}\langle\frac{\partial u'_i}{\partial x_j}\left(\frac{\partial u'_i}{\partial x_j}+\frac{\partial u'_j}{\partial x_i}\right)\rangle \qquad \textbf{(Dissipation)}$$

$$J_i^u=\langle u'_i u'_j u'_j\rangle/2 \qquad \textbf{(Turbulence transport)}$$

$$J_i^p=\langle p' u'_i\rangle \qquad \textbf{(Pressure transport)}$$

$$J_i^v=-\frac{1}{\mathrm{Re}}\left(\frac{\partial k}{\partial x_i}+\frac{\partial\langle u'_i u'_j\rangle}{\partial x_j}\right) \qquad \textbf{(Viscous transport)}$$

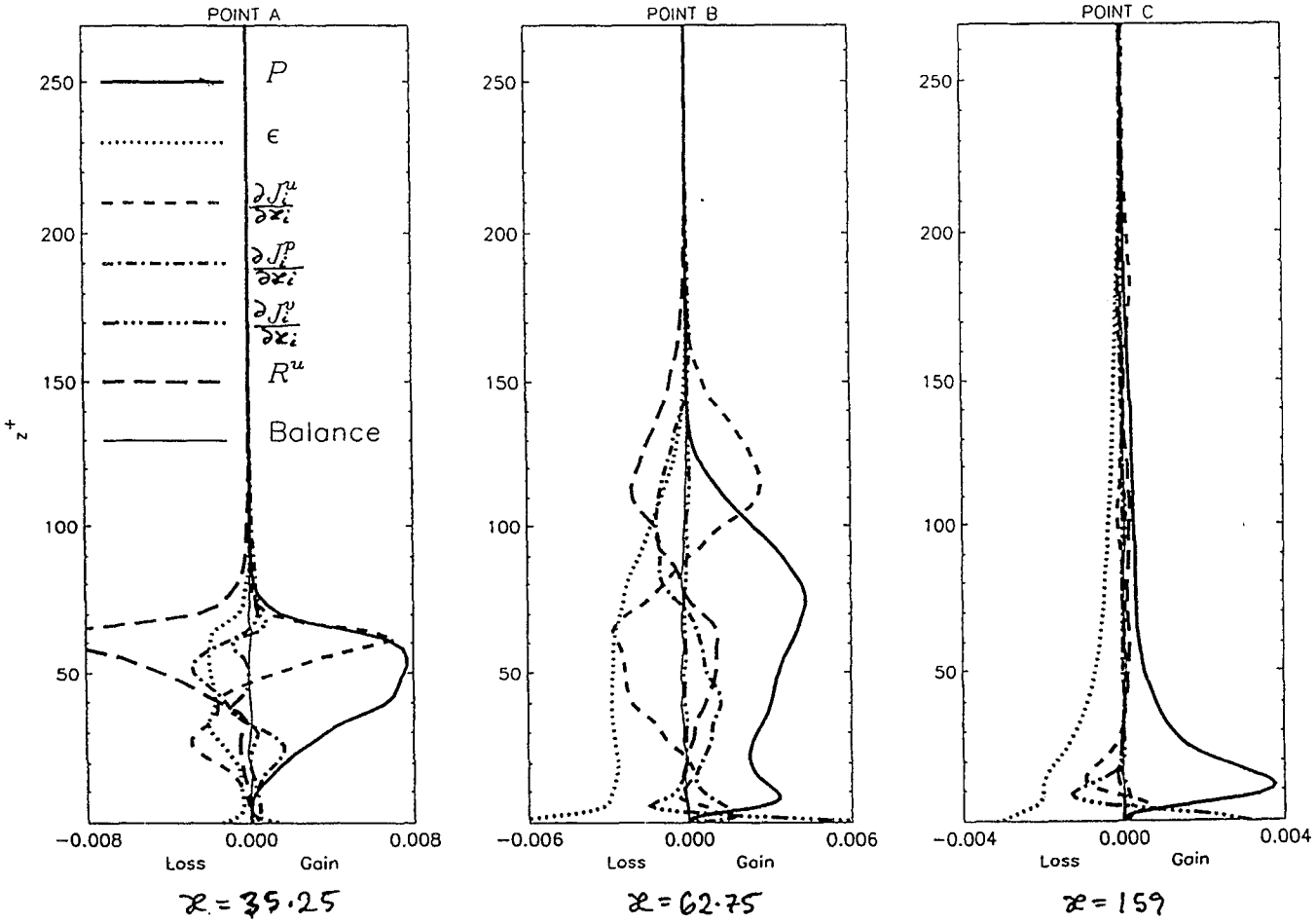

Summary

- fully-resolved DNS of separation bubbles now possible
- databases for RANS model validation for turbomachinery application
- efficient parallel DNS codes developed
- single and multiple turbulent spot calculations feasible

References

Alam, M. and Sandham, N.D. 1997 Simulation of laminar separation bubble instabilities. *Direct and Large Eddy Simulation II*, ed. Chollet, Voke and Kleiser, Kluwer, to appear

Alam, M. and Sandham, N.D. 1997 Numerical study of separation bubbles with turbulent reattachment followed by boundary layer relaxation. *Proc. Parallel CFD '97*, ed. Ecer et al. Kluwer, to appear.

Sandham, N.D. and Kleiser, L 1992 The late stages of transition to turbulence in channel flow *J.Fluid Mech.* **245**.

Sandham, N.D., Adams, N. and Kleiser, L. 1995 Direct simulation of breakdown to turbulence following oblique instability waves in a supersonic boundary layer. *Applied Scientific Research* **54**.

TRANSITION IN TURBINE FLOWS*

Thorwald Herbert
The Ohio State University
Columbus, Ohio

ABSTRACT

We have further developed our capabilities to analyze transition in turbine boundary layers from first principles by integrating the nonlinear parabolized stability equations (PSE) with improved initial and boundary conditions. With modified iteration schemes, we are able to proceed deeper into the transition region where skin friction coefficient and heat transfer coefficient significantly increase. Initial and boundary conditions at elevated turbulence levels can be derived by receptivity analysis. Test runs for ERCOFTAC test case T3A at 2.4\% turbulence level provide results in good agreement with the experimental data. The sharper minimum of the skin coefficient also shown by DNS results is likely due to the missing intermittency. The method has been applied to various experimentally studied turbine blades (UTRC, VKI, Zierke, Langston, Hippensteele, and others) (Work partially supported by NASA Lewis Research Center). The PSE results, though physically reasonable, do not agree as well as expected with the experimental findings. We have, therefore, performed an extensive search for the reasons of the seemingly systematic deviations.

A first source of uncertainty has been found in the often insufficient documentation of the experiments (e.g. on blockage by end-wall boundary layers). However, variation of the relevant parameters does not lead to more satisfactory agreement.

A second reason has been found in the "standard procedure" which considers a 2D flow at midspan and uses a panel code and subsequent boundary-layer code to obtain the laminar basic flow for the transition analysis. Comparison with the pressure distribution obtained with a 3D design code (RVC3D) shows significant three-dimensionality of the flow (e.g. in the UTRC experiments). The spanwise variation has been neglected in our original PSE code. To overcome this problem, we have developed the PSE/3D for fully 3D boundary layers to account for streamwise and spanwise variations. Since the design code does not provide the boundary-layer flow with sufficient resolution, we have generated the Euler solution and employed a 3D boundary-layer code to obtain the viscous basic flow. Although only the linear stability level of PSE/3D has been implemented so far, the discrepancies with the experiments change but do not disappear. We still find deviations between the computed and experimental variations of C_f and St along the blade for laminar flow.

The main reason can be seen by comparing the solution of the boundary-layer code with the viscous results of the design code. The conventional boundary-layer solution exhibits an asymptotic behavior appropriate in external aerodynamics but does not match the steep gradients of the inviscid flow through the passage and consequently provides biased results for C_f and St. An attempt is currently being made to correct this deficiency.

Before attempting to perform the transition analysis for the viscous flow provided by the design code, we have analyzed the implementation and "best possible" results. Code and results exhibit flaws that may negatively affect the design and are intolerable for transition analysis. Therefore, we have decided to develop a new code to obtain a reliable basis for stability and transition studies. We expect to report improved results by the time of the meeting.

---

* Work supported by NASA Lewis Research Center (SBIR Contract No. NAS3-27010).

Outline

PSE for Transition Analysis

Improvements since 1993

Results

PSE/3D for 3D Boundary Layers

Basic Flow Problems

Conclusions

Transition Analysis

At low turbulence levels (<3%), transition analysis based on stability characteristics appears most reliable

Stability theory and the e^N method are restricted to small (linear) disturbances and locally parallel flow

The parabolized stability equations (PSE) can be solved by efficient marching methods for linear and nonlinear disturbances and account for streamwise and (recently) spanwise changes of the flow

PSE solutions match the quality of DNS results at a small fraction of computer time and can be used in engineering design

Solving the PSE requires (i) a basic flow and (ii) initial and boundary conditions provided by "input models" to characterize the disturbance environment (scales and amplitudes)

Based on the PSE, a transition analysis package has been developed for applications in external aerodynamics (wings, tails, nacelles) and turbomachinery (compressor, low-pressure turbine)

Improvements (since 1993)

- Modified input models according to new receptivity results, extended models to swept-wing flows
- Implemented new results on Klebanoff modes that participate in K-type transition
- Increased speed by new numerics to enable more efficient e^N and nonlinear computations
- Improved iterative algorithms to converge up to higher amplitudes near breakdown
- Implemented a "stability synopsis" to automatically and reliably identify most dangerous modes of instability
- Connected the numerical code to a graphical user interface to simplify performing standard analysis tasks
- Increased robustness after experience with numerous test cases from aerodynamics
- Software was validated within a European comparison of similar codes

Results

External aerodynamics (flight tests)

- ATTAS
- Fokker F100 (G. Schrauf)

External aerodynamics (wind tunnel)

- Bippes
- Saric et al (swept wing)

Turbine and compressor experiments

- Dring et al (UTRC)
- Hippensteele et al
- Zierke et al (compressor)
- Hylton et al (C3X vane)
- Arts et al (VKI, transonic)
- Langston et al (strong 3D)

In external aerodynamic flows, the results are in good agreement with observations

In turbines/compressors, the results disagree with observations to minor or major extent, especially on the suction side

Why ?

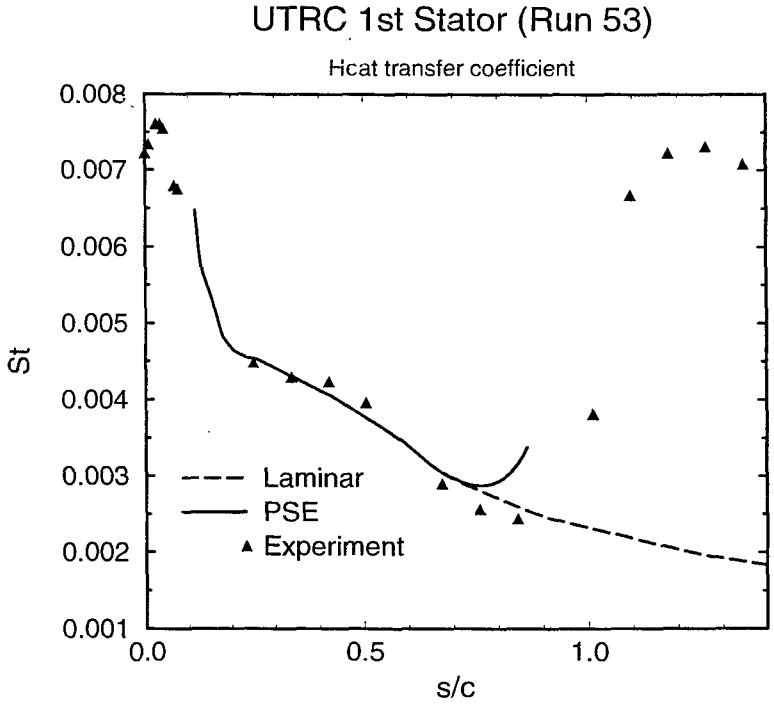

Check List for Possible Causes

- High free-stream turbulence (T3A)
- 3D flow
- Geometry: coordinates
- Experimental conditions
- Pressure distribution (PCPanel, RVC3D)
- Boundary-layer flow (WING)
- 3D inviscid/viscous solution (RVC3D)

ERCOFTAC Case T3A

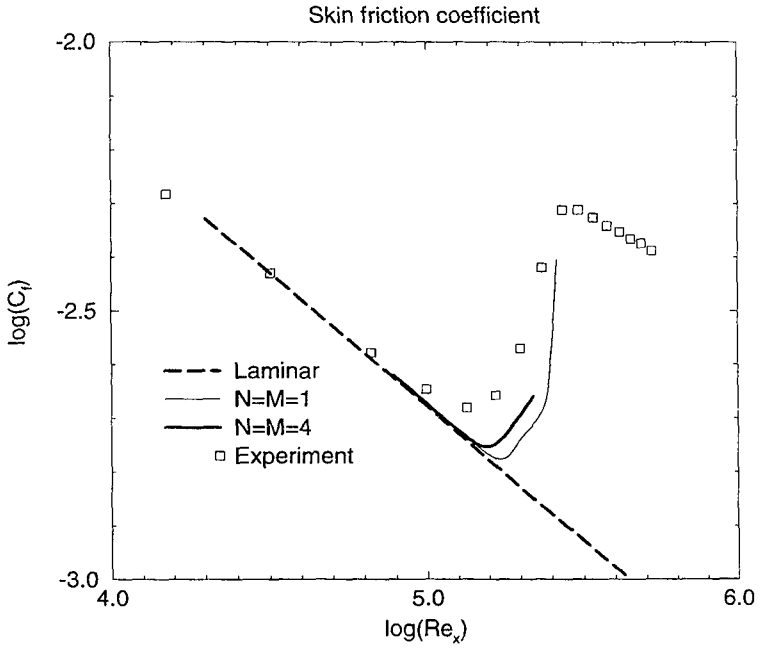

PSE/3D for 3D Boundary Layers

Solution

$$\mathbf{q}'(x,y,z,t) = \mathbf{q}(\xi,y,\zeta)\,\exp[i\theta(x,z) - i\omega t]$$

$$\xi = \varepsilon x,\ \zeta = \varepsilon z$$

$$\nabla\theta = (\alpha,\beta) = \mathbf{k}(\xi,\zeta)$$

Linear PSE/3D

$$[L_0 + \varepsilon(L_1+L_3)]\mathbf{q} + \varepsilon M_1 \frac{\partial \mathbf{q}}{\partial \xi} + \varepsilon M_3 \frac{\partial \mathbf{q}}{\partial \zeta} = 0$$

Norms in ξ and ζ

$$\int_\Omega \mathbf{v}^* \frac{\partial \mathbf{v}}{\partial \xi} dy = 0,\ \int_\Omega \mathbf{v}^* \frac{\partial \mathbf{v}}{\partial \zeta} dy = 0$$

Irrotationality condition (Mack 1977)

$$\nabla \times \mathbf{k} = 0 \text{ or } \frac{\partial \alpha}{\partial \zeta} = \frac{\partial \beta}{\partial \xi}$$

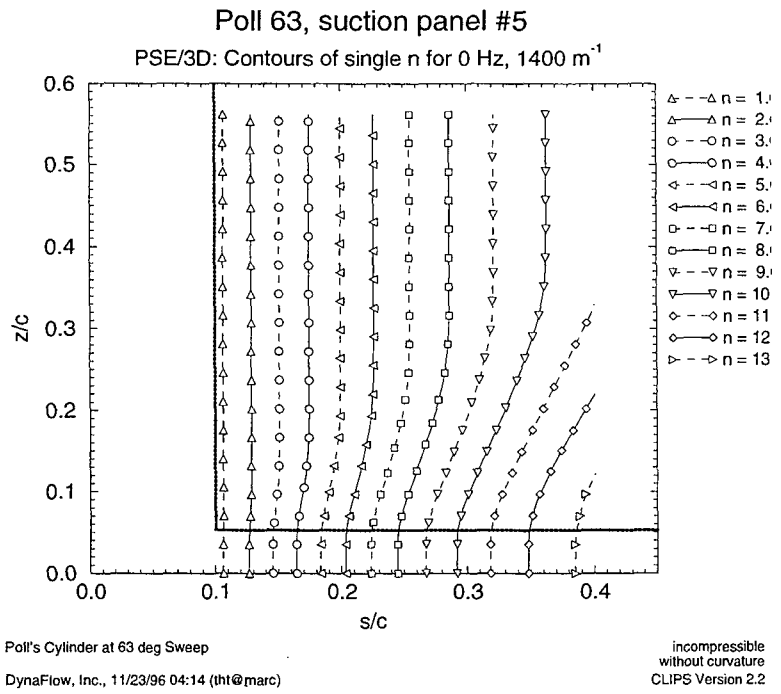
Poll 63, suction panel #5
PSE/3D: Contours of single n for 0 Hz, 1400 m-1
z/c
s/c
0.0
0.1
0.2
0.3
0.4
0.5
0.6
n = 1
n = 2
n = 3
n = 4
n = 5
n = 6
n = 7
n = 8
n = 9
n = 10
n = 11
n = 12
n = 13
Poll's Cylinder at 63 deg Sweep
DynaFlow, Inc., 11/23/96 04:14 (tht@marc)
incompressible
without curvature
CLIPS Version 2.2

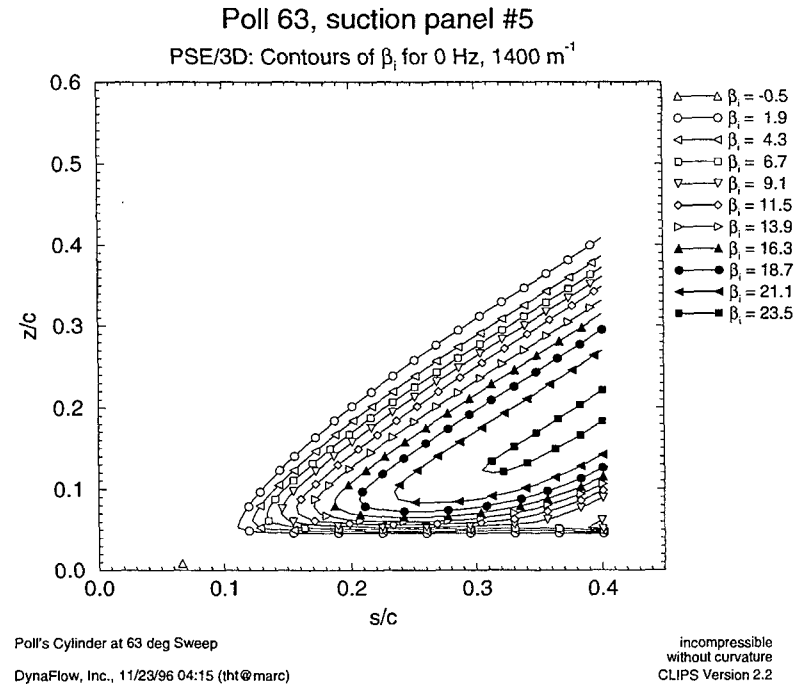
Poll 63, suction panel #5
PSE/3D: Contours of βi for 0 Hz, 1400 m-1
z/c
s/c
0.0
0.1
0.2
0.3
0.4
0.5
0.6
βi = -0.5
βi = 1.9
βi = 4.3
βi = 6.7
βi = 9.1
βi = 11.5
βi = 13.9
βi = 16.3
βi = 18.7
βi = 21.1
βi = 23.5
Poll's Cylinder at 63 deg Sweep
DynaFlow, Inc., 11/23/96 04:15 (tht@marc)
incompressible
without curvature
CLIPS Version 2.2

PSE/3D - Summary

The PSE/3D provide unexpected yet consistent and physically meaningful results. These are the first results for 3D boundary layers based on first principles.

The domain of influence of a spanwise change in the basic flow is limited by the group velocity path and the marching path of the boundary-layer computation.

The vector of growth rates (α_i, β_i) is not determined by the local flow characteristics.

The PSE/3D provide the basis for improved transition analysis in engineering design.

The computational effort for PSE/3D solutions is of the same order as for the section-by-section approach.

The PSE/3D analysis requires a 3D solution of boundary-layer or Navier-Stokes equations as input.

Geometry: Coordinates

- Sometimes too many coordinates are specified with insufficient number of digits, leading to wiggles and inaccuracies (UTRC data)
- Sometimes too few coordinates are specified and the geometry is not clearly defined, leading to errors (Hippensteele et al)
- Discrepancies between theoretical and experimental geometry are unknown (but likely)
- Agreement is typically better for "clean" data specifications (T3A, Zierke et al)

Experimental Conditions

- Important data are usually unavailable in reports on experiments, such as the blockage from the sidewalls, which has a strong effect on the pressure distribution

Pressure Distribution

- The computed pressure distribution disagrees with the experimental data (where available). Differences are largest on the suction side
- Similar results for the pressure distribution are found with the panel code PCPanel (McFarland) and the 3D solver RVC3D (Chima)

UTRC 1st Stator blade

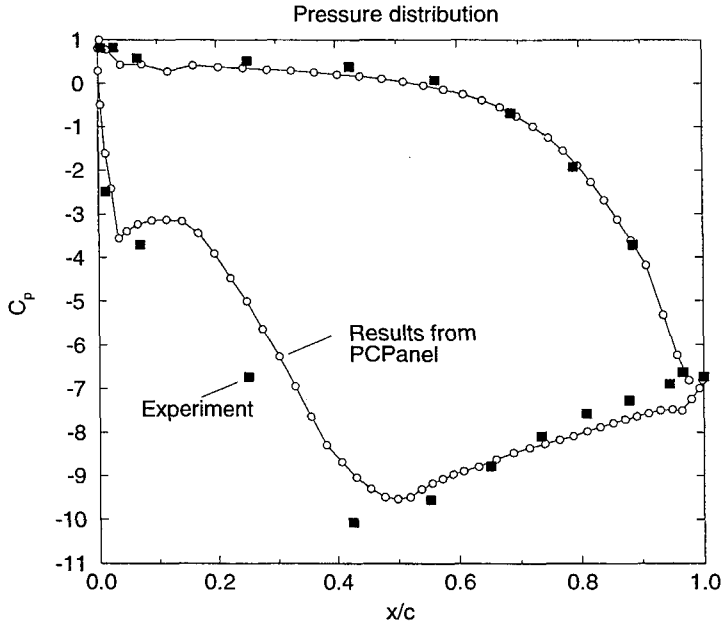

Langston/Graziani Cascade

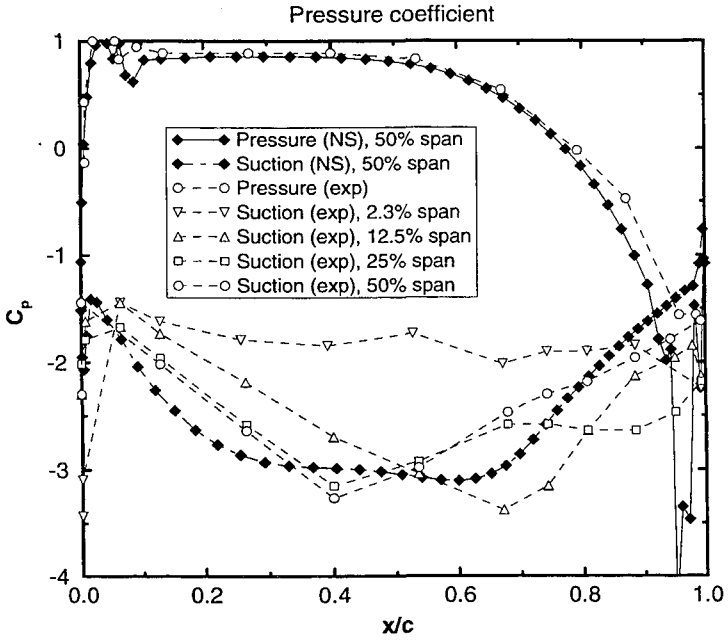

Boundary-Layer Flow

- Boundary-layer flows computed with standard boundary-layer codes (Kaups-Cebeci) disagree with those from the 3D viscous code RCV3D
- Standard codes cause a systematic error in skin-friction and heat-transfer coefficients
- The boundary-layer profiles $U \rightarrow const.$ as $y \rightarrow \infty$ do not match with the inviscid flow that has strong gradients
- The wall-normal pressure gradient is nonzero through the boundary layer. The term

$$\rho \frac{u^2}{r} = \frac{\partial p}{\partial y}$$

in the y-momentum equation must be taken into account

- It appears possible to overcome this problem with a new code that solves for both U and p and satisfies proper conditions as $y \rightarrow \infty$

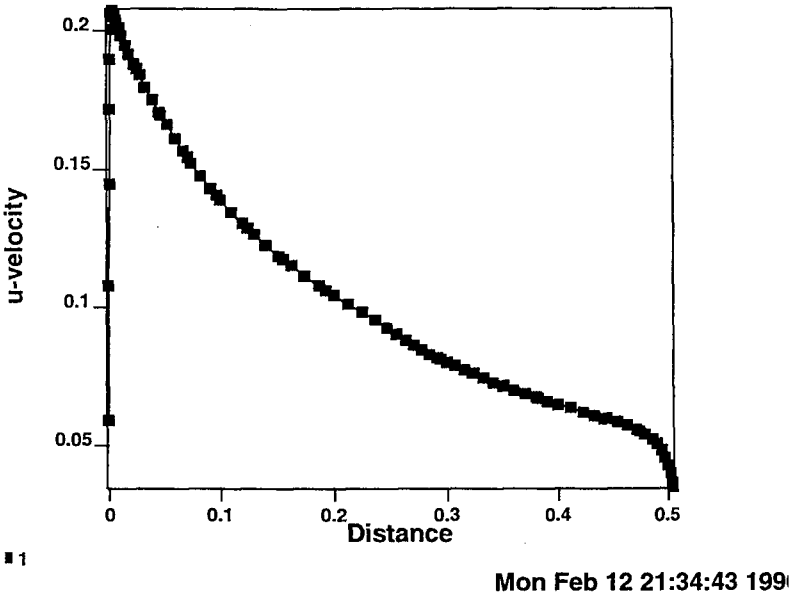

3D Inviscid/Viscous Solver

- The code RVC3D was used for the test case (Goldmann), 3D case (Langston et al) and the UTRC experiment
- In spite of grid refinement, we were unable to produce an acceptable solution and a satisfactory *St* distribution of the laminar viscous flow for the UTRC test
- The highly skewed grid especially on the suction side is not suited to produce an accurate solution
- Changes in the metric along the boundary between C grid and H grid and along the periodic boundary cause flaws in the solution
- The boundary layers were not sufficiently resolved to be used for transition analysis directly
- The boundary layer could not be computed from the inviscid pressure distribution on the suction side because it separated at the inlet to the cascade

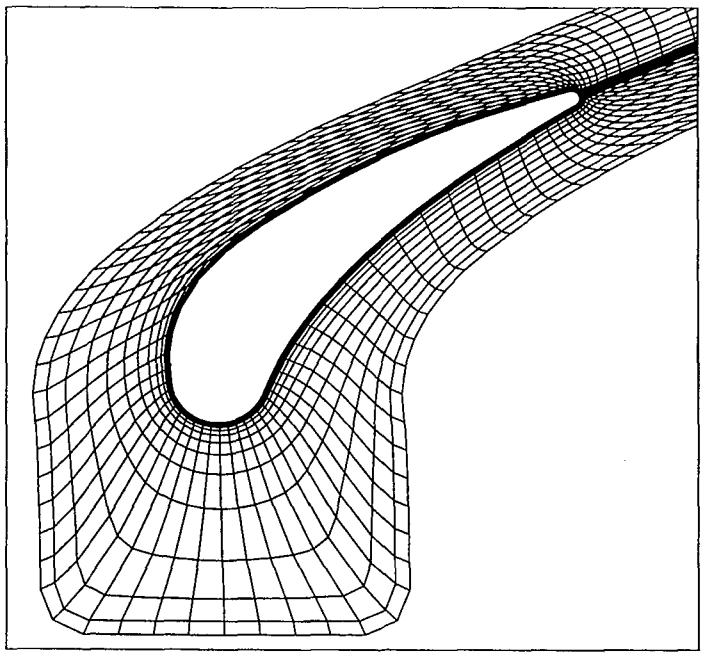

Conclusions

- We have developed a software package that uses linear stability theory and linear or nonlinear PSE to analyze transition in the engineering environment
- The results of the analysis are generally reliable and the software is successfully used by 50% of the major airplane companies
- For turbines and compressors, the agreement with experimental data is unsatisfactory
- The attempt to improve the agreement has caused major improvements of the software and the extension of the PSE to fully 3D boundary layers
- The reason for the disagreement was found in the poor capability to compute the viscous laminar flow as the basis for the analysis in agreement with the experiments
- Various deficiencies of boundary-layer code and 3D inviscid/viscous solver were found
- The lack of agreement between computed and measured pressure distribution is largely unexplained

SESSION 8

ADVANCED COMPUTATIONS II

VORTEX PARTICLE IN CELL COMPUTATIONS OF VORTEX-SURFACE INTERACTIONS

D.J. Doorly
Imperial College
London, England

ABSTRACT

The eruption process in a turbulent boundary layer is responsible for the production of turbulence. The problem is extremely complex, but certain essential features can be represented by studying model problems. Such model problems can provide inspiration and guidance for improved theoretical modelling of the essential dynamics. To start we consider the problem of an eddy modelled as a single region of vorticity in the outer flow interacting with a boundary layer. The problem is common to other areas, such as the interaction of trailing aircraft vortices with the ground and their behaviour in cross-flow. Hence we examine the role of the viscous and inviscid dynamics in the eruption of the shear layer.

In the work to be presented, a vortex particle-in-cell method based on the velocity-vorticity formulation of the Navier-Stokes equations is applied to the problem. The method is equally suitable for 2 or 3D flows, and since convection is treated as a Lagrangian particle move, the approach shares the favourable stability and low diffusive nature of the grid-free vortex particle method. The ability to track the evolution of strong vortical regions, and scalar concentrations which the procedure possesses are particularly important for these applications. The method is described and applied to the above problem. In particular the relative importance of viscous and inviscid effects in the initiation and subsequent development of the wall layer eruption are examined by contrasting the solutions of the full and reduced equations.

Acknowledgements:
B. T. Dodia and B.Peyrefitte helped produce these results at Imperial College

Outline:

- Vortex Particle-in-Cell (PIC) Method
- Wall-Layer Dynamics and Vortex-Surface Interactions
- Model Problem :

  Unsteady boundary layer due to 2D vortex above a wall

  Role of wall vorticity generation

- Relation to boundary-layer control

from: Haidari, AH and Smith CR, JFM 1994

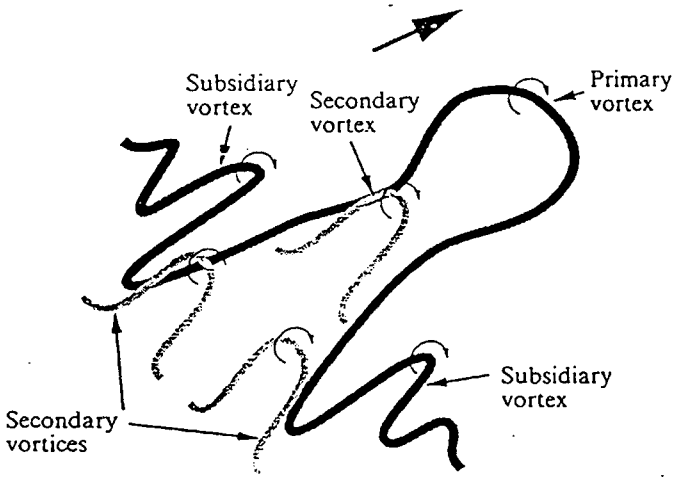

Schematic of the hierarchy of observed hairpin-like vortices.

Wall Region of Turbulent Boundary Layer:

from: Choi, K

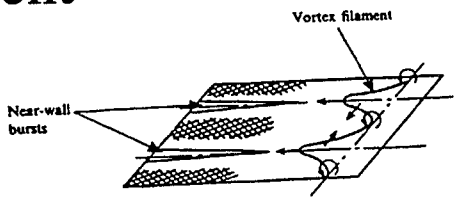

Stage 1

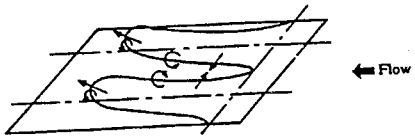

Stage 2

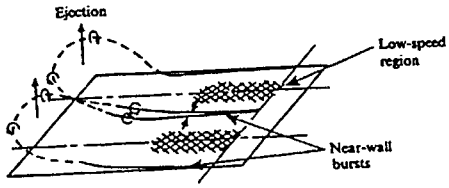

Stage 3

Vorticity-Velocity Formulation

$$\frac{\partial \vec{\omega}}{\partial t} + \vec{u} \cdot \nabla \vec{\omega} = \vec{\omega} \cdot \nabla \vec{u} + \frac{1}{Re} \nabla^2 \vec{\omega} \ , \tag{1}$$

where $\vec{u}$ is related to vorticity $\vec{\omega}$ by

$$\nabla^2 \vec{u} = -\nabla \wedge \vec{\omega} \ . \tag{2}$$

(2) follows from the definition,

$$\vec{\omega} = \nabla \wedge \vec{u}$$

and the zero divergence constraint

$$\nabla \cdot \vec{u} = 0.$$

In 3D, the computed $\vec{\omega}$ should satisfy

$$\nabla \cdot \vec{\omega} = 0.$$

Numerical Procedure

1. Map initial $\vec{\omega}$ (if any) to particles $\left\{ \vec{k}_p^o \right\}$:

$$\vec{\omega}^o \rightarrow \left\{ \vec{k}_p^o \right\} \ ; \tag{3}$$

project strengths of the particles onto the mesh, using volume-based weighting interpolation,

$$\left\{ \vec{k}_p^o \right\} \longrightarrow \vec{\omega}_{i,j,k}^o \ . \tag{4}$$

2. The mesh $\vec{u}$ field is found from,

$$\nabla_{\mathrm{D}}^2 \vec{u}_{i,j,k}^o = -\nabla_{\mathrm{D}} \wedge \vec{\omega}_{i,j,k}^o \ , \tag{5}$$

(subscript D represents discrete appprox.)

To advance the flow over one time step:

1. **interpolate** $\vec{u}_p^n$ from $\vec{u}_{i,j,k}^n$ and **move** particles

$$\vec{x}_p^{n+1} = \vec{x}_p^n + \vec{u}_p^n(\vec{x}_p).\Delta t \ ; \tag{6}$$

2. **project** particle strengths onto the mesh vorticity,

$$\vec{\omega}_{i,j,k}^* = P\left\{\vec{k}_p^n(\vec{x}_p^{n+1})\right\} \ ; \tag{7}$$

3. **solve on mesh** for diffusion and stretch/tilt of $\vec{\omega}$

$$\frac{\vec{\omega}_{i,j,k}^{n+1} - \vec{\omega}_{i,j,k}^*}{\Delta t} = L_D(\vec{\omega}_{i,j,k}^a) + L_S(\vec{\omega}_{i,j,k}^a) = \frac{\Delta\vec{\omega}^{n+1}}{\Delta t} \ , \tag{8}$$

L_D and L_S are discrete diffusion and stretch operators,
and level a may correspond to $*$, $n+1$ or some intermediate.

---

4. **backproject** change in nodal vorticity ($B\left\{\Delta\vec{\omega}\right\}$) to particles

$$\left\{\vec{k}_p^{n+1}(\vec{x}_p^{n+1})\right\} = \left\{\vec{k}_p^n(\vec{x}_p^{n+1})\right\} + B\left\{\Delta\vec{\omega}_{i,j,k}^{n+1}\right\} \ ; \tag{9}$$

5. **create** new particles on 'empty' nodes, if vorticity > tolerance,

$$\left\{\vec{k}_p^{n+1}\right\} \leftarrow \left\{\vec{k}_p^{n+1}\right\} \cup \left\{\vec{k}_p^c\right\}, \tag{10}$$

where $\vec{k}_p^c$ are newly created particles;

6. **solve for $\vec{u}$ field** corresponding to the new $\vec{\omega}$,

$$\nabla_{\text{D}}^2\vec{u}_{i,j,k}^{n+1} = -\nabla_{\text{D}} \wedge \vec{\omega}_{i,j,k}^{n+1} \ ; \tag{11}$$

7. **set boundary condition** for vorticity,

$$\vec{\omega}_{i,j,k}^{n+1}\Big|_{\text{surface}} = \nabla_{\text{D}} \wedge \vec{u}_{i,j,k}^{n+1} \ . \tag{12}$$

Vortex ring-wall impact

Normal and oblique impacts of vortex rings on a plane surface involve strong interactions between the external flow and the induced boundary layer, and are useful model problems to study boundary layer eruptions. The fig. shows isovorticity surfaces shaded according to vorticity

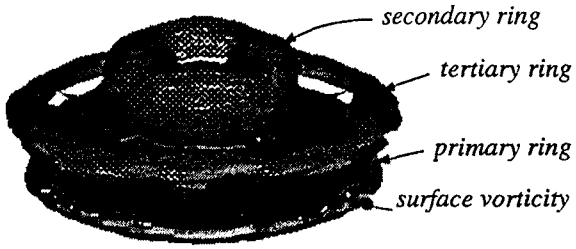

Figure 1: Normal ring impact, vortex PIC solution

orientation for a 3D computation; dark corresponds to impinging (primary) ring vorticity, light for secondary vorticity generated at the wall. The secondary vorticity ejected from the wall produces two successive rings (secondary and tertiary rings). The isolevel chosen shows the secondary ring (uppermost), but cuts away most of the tertiary ring to show more of the primary ring. (From Doorly Liu (1995)).

Model Problem: 2D Vortex suddenly imposed above a wall.

- Vortex induces an unsteady boundary layer; boundary layer solution eventually breaks down
- Eruption of boundary layer vorticity into outer flow then follows.

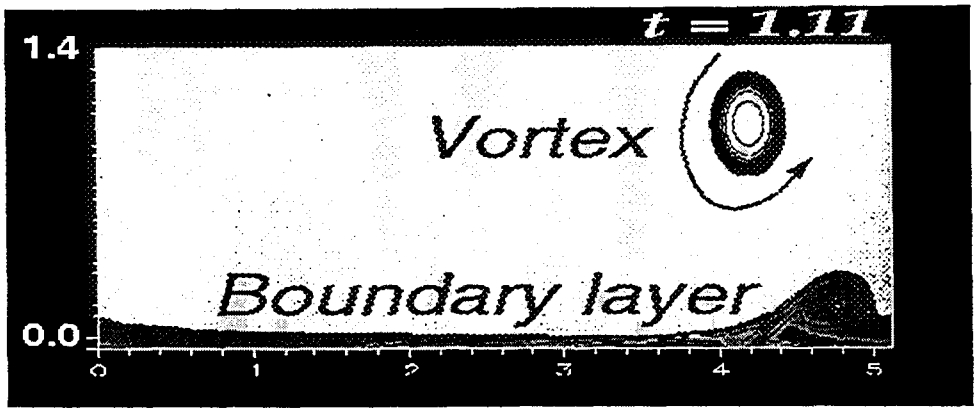

Boundary layer eruption:

- Sequence of snapshots showing boundary layer vorticity at successive instants

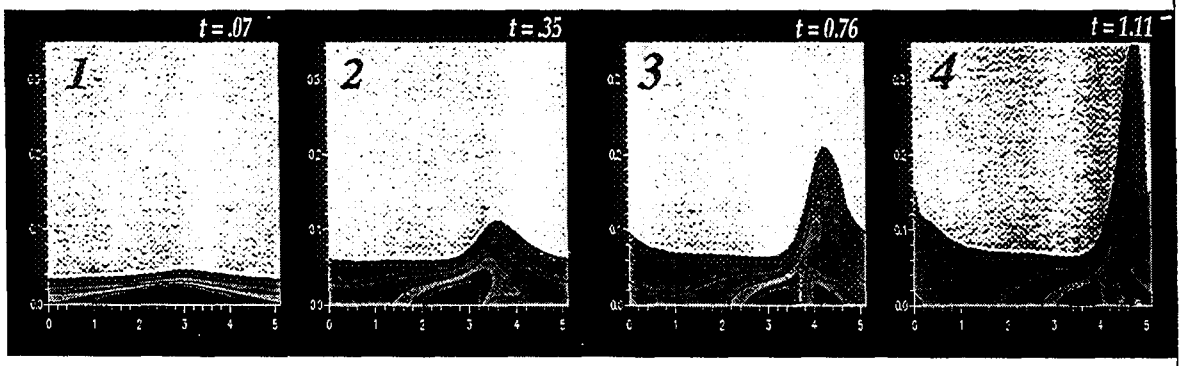

Boundary Layer Eruption: Role of wall vorticity generation

- Interaction of large core vortex with wall at Re = 500; snapshots of vorticity evolution.
- Sequences A and B continue from common initial condition, corresponding to snap 2
- Vorticity generation at the wall is turned off after 'snap' 2 in (lower) sequence 'B'

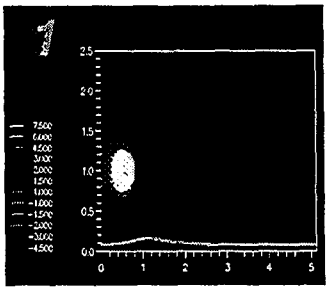

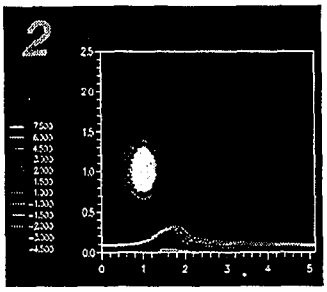

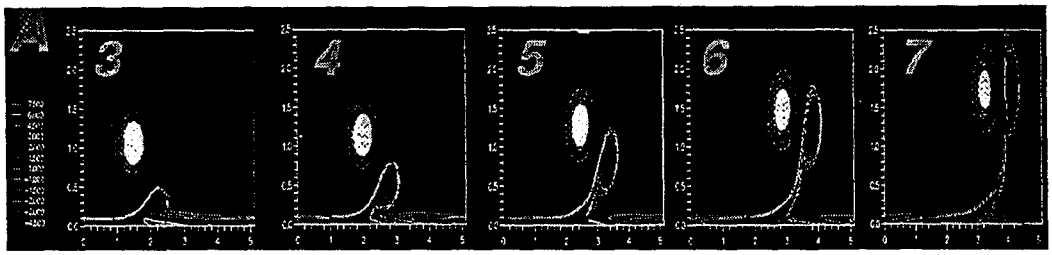

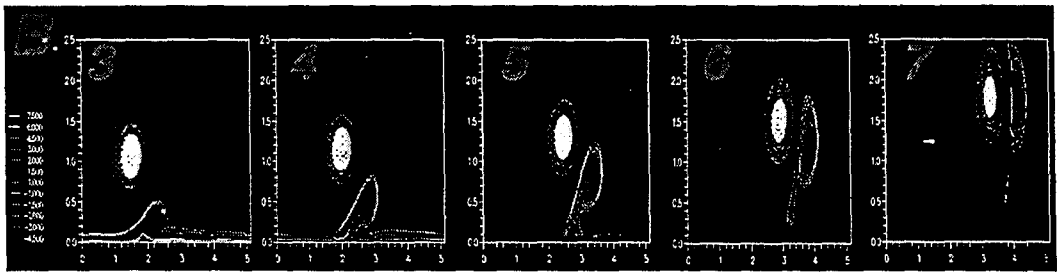

Control of eruption by wall blowing/suction:

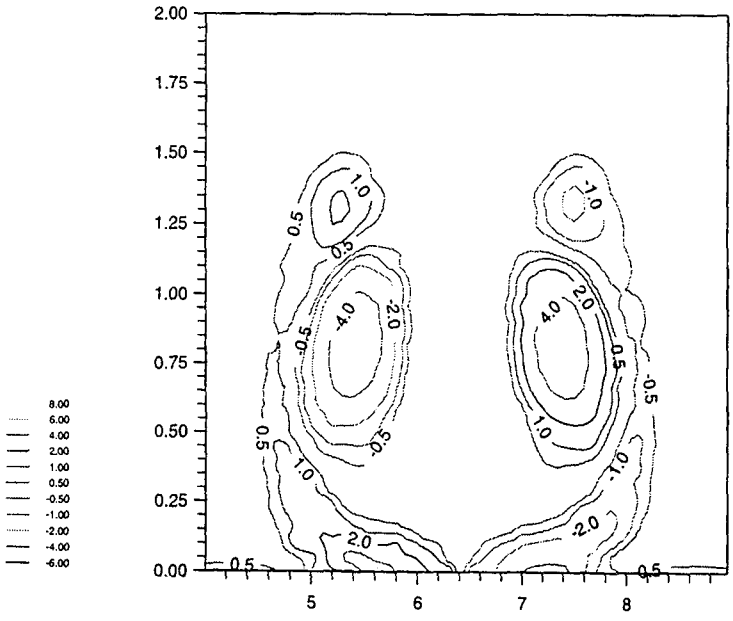

Dipole–wall interaction: no transpiration

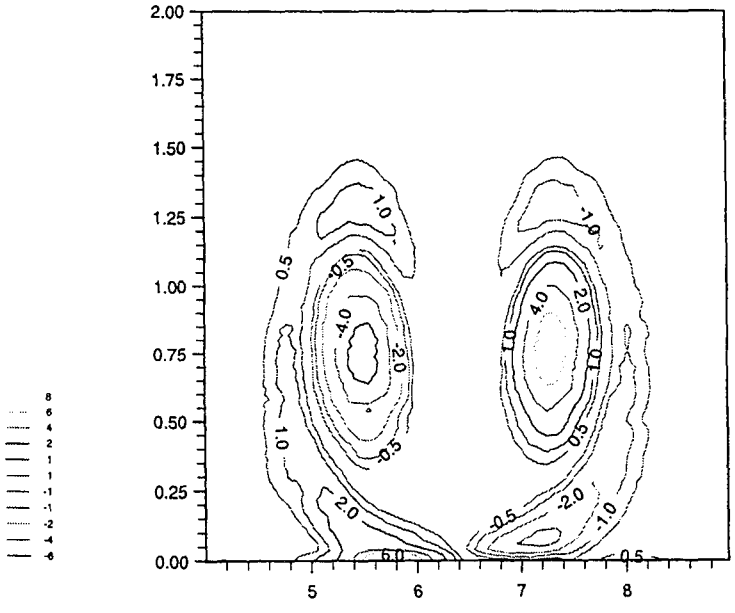

Dipole–wall interaction: transpiration

MODELLING OF BY-PASS TRANSITION WITH CONDITIONED NAVIER-STOKES EQUATIONS

J. Steelant and E. Dick
Universiteit Gent
Gent, Belgium

Abstract

By-pass transition emanates mainly from high free-stream turbulence and leads to a transition far further upstream than what would be expected for natural transition. From the start until the end of transition, the flow is characterized by changing gradually from laminar to turbulent flow. This intermittency zone can be evaluated by an intermittency factor γ which has an almost universal character for different flow patterns. Also, near the edge of the laminar boundary layer, the turbulence in the free stream interacts intermittently with the outer layer of the pre-transitional boundary layer. This behaviour can be evaluated by a freestream factor ω.
When modelling transition, it is essential to take these factors into account. Global time averaging used for classical turbulence modelling is not valid in intermittently changing flows. To describe the transitional zone and the outer layer zone, it is necessary to use conditional time averaging. These averages are taken during the fraction of time the flow is laminar or turbulent respectively. Conditionally averaged Navier-Stokes equations lead both for the laminar and turbulent part to a set of equations for mass, momentum and energy [1,2]. These conditioned equations differ from the original Navier-Stokes equations by the presence of source terms which are function of the weighting factor τ, which is the sum of the intermittency factor γ and the freestream factor ω:

$$\begin{aligned}
\frac{\partial \overline{U}_l}{\partial t} + \frac{\partial \overline{F}_l}{\partial x} + \frac{\partial \overline{G}_l}{\partial y} &= \frac{\partial \overline{F_{vl}}}{\partial x} + \frac{\partial \overline{G_{vl}}}{\partial y} + S_l^\tau, \\
\frac{\partial \overline{U}_t}{\partial t} + \frac{\partial \overline{F}_t}{\partial x} + \frac{\partial \overline{G}_t}{\partial y} &= \frac{\partial \overline{F_{vt}}}{\partial x} + \frac{\partial \overline{G_{vt}}}{\partial y} + S_t^\tau.
\end{aligned}$$

The evolution of the extra unknown τ depends mainly on the turbulence level, pressure gradient and Reynolds-number and is determined here by a transport equation:

$$\frac{\partial \overline{\rho}\,\tilde{u}\tau}{\partial x} + \frac{\partial \overline{\rho}\,\tilde{v}\tau}{\partial y} = D_\tau + P_\tau - E_\tau$$

where

$$\begin{aligned}
D_\tau &= \frac{\partial}{\partial x_i}[f_\mu \mu \frac{\partial \tau}{\partial x_i}] \\
P_\tau &= 2 f_\tau (1-\tau)\sqrt{-\ln(1-\tau)}\beta\overline{\rho}\sqrt{\tilde{u}^2+\tilde{v}^2} \\
E_\tau &= 2.5 f_\mu \mu \frac{|\,u\,|}{u_\infty^2}\frac{\partial u}{\partial n}\frac{\partial \tau}{\partial n}
\end{aligned}$$

where f_μ and β are the following functions:

$$\begin{aligned}
f_\mu &= 237 M^{6/7}[-ln(1-\tau)]^{-\frac{5}{6}} \\
\beta &= \sqrt{\hat{n}\sigma(K,Tu)}\frac{U_{\inf}}{\nu}
\end{aligned}$$

with K the pressure gradient parameter and Tu the turbulence intensity in the free stream. The terms $\tilde{u}$ and $\tilde{v}$ are global mean values of the velocity components ($\tilde{u} = \tau\tilde{u}_t + (1-\tau)\tilde{u}_l$). The

damping function f_τ models the distributed breakdown. The start of transition x_{tr} is determined from $Re_{\theta tr} = 420\ Tu^{-.69}$ where Tu is the turbulence level at the leading edge.

For the workshop, the above described method will be derived and tested on test cases with zero, favourable and adverse pressure gradient. The strength of the method will be demonstrated by comparison of experimental and numerical results on the basis of global $(C_f, \theta, ...)$ and detailed (u, k, γ) flow parameters.

Reference

[1] Steelant J., and Dick E., 'Modelling of Bypass Transition with Conditioned Navier-Stokes Equations Coupled to an Intermittency Transport Equation', *Int. J. of Numerical Methods in Fluids*, Vol. 23, 193-220, 1996.
[2] Steelant J., and Dick E., 'Calculation of Transition in Adverse Pressure Gradient Flow by Conditioned Equations', ASME 96-GT-160; 1996.

OUTLINE

1. Conditioned Flow Equations
2. Intermittency Equation
3. Applications
4. Conclusions

CONDITIONAL AVERAGED FLOW EQUATIONS.

Conditioned averages are defined as:

$$\overline{\phi} = (1-\gamma)\overline{\phi}_l + \gamma\overline{\phi}_t$$

Laminar and turbulent states determined by:

$$\frac{\partial \overline{U}_l}{\partial t} + \frac{\partial \overline{F}_l}{\partial x} + \frac{\partial \overline{G}_l}{\partial y} = \frac{\partial \overline{F_{vl}}}{\partial x} + \frac{\partial \overline{G_{vl}}}{\partial y} + S_l^\gamma$$
$$\frac{\partial \overline{U}_t}{\partial t} + \frac{\partial \overline{F}_t}{\partial x} + \frac{\partial \overline{G}_t}{\partial y} = \frac{\partial \overline{F_{vt}}}{\partial x} + \frac{\partial \overline{G_{vt}}}{\partial y} + S_t^\gamma$$

where S_l^γ and S_t^γ are interaction terms:

$$S_l^\gamma = f(\overline{U}_l, \overline{U}_t, \gamma)$$
$$S_t^\gamma = f(\overline{U}_t, \overline{U}_l, \gamma)$$

MASS EQUATION :

The turbulent conditioned mass equation is:

$$\frac{\partial \overline{\rho}_t}{\partial t} + \frac{\partial \overline{\rho}_t \tilde{u}_t}{\partial x} + \frac{\partial \overline{\rho}_t \tilde{v}_t}{\partial y} = \frac{1}{2\gamma} S_\gamma$$

The laminar conditioned mass equation is:

$$\frac{\partial \overline{\rho}_l}{\partial t} + \frac{\partial \overline{\rho}_l \tilde{u}_l}{\partial x} + \frac{\partial \overline{\rho}_l \tilde{v}_l}{\partial y} = \frac{1}{2(1-\gamma)} S_\gamma$$

with:

$$S_\gamma = (\overline{\rho}_l - \overline{\rho}_t)\frac{\partial \gamma}{\partial t} + (\overline{\rho}_l \tilde{u}_l - \overline{\rho}_t \tilde{u}_t)\frac{\partial \gamma}{\partial x} + (\overline{\rho}_l \tilde{v}_l - \overline{\rho}_t \tilde{v}_t)\frac{\partial \gamma}{\partial y}$$

INTERMITTENCY FACTOR γ

Algebraic description:

according to Dhawan and Narasimha:

$$\begin{cases} x < x_{tr} : \gamma = 0 \\ x > x_{tr} : \gamma = 1 - \exp\left[-\hat{n}\sigma(Re_x - Re_{x_{tr}})^2\right] \end{cases}$$

$$\gamma = 1 - \exp\left[-A(x - x_{tr})^2\right] \quad \text{with} \quad A = \frac{\hat{n}\sigma U^2}{\nu^2}$$

Transition point:

$$Re_{\theta_s} = 420 Tu^{-.69}$$

Dynamic equation for the weighting function τ:

$$\frac{\partial \overline{\rho}\,\tilde{u}\tau}{\partial x} + \frac{\partial \overline{\rho}\,\tilde{v}\tau}{\partial y} = D_\tau + P_\tau - E_\tau$$

where

$$\begin{aligned} D_\tau &= \frac{\partial}{\partial x_i}[f_\mu \mu \frac{\partial \tau}{\partial x_i}] \\ P_\tau &= 2 f_\tau (1-\tau)\sqrt{-\ln(1-\tau)}\beta\overline{\rho}\sqrt{\tilde{u}^2+\tilde{v}^2} \\ E_\tau &= 2.5 f_\mu \mu \frac{|\,u\,|}{u_\infty^2}\frac{\partial u}{\partial n}\frac{\partial \tau}{\partial n} \end{aligned}$$

where f_μ and β are the following functions:

$$\begin{aligned} f_\mu &= 237 M^{6/7}[-ln(1-\tau)]^{-\frac{5}{6}} \\ \beta &= \sqrt{\hat{n}\sigma(K,Tu)}\frac{U_{\inf}}{\nu} \end{aligned}$$

1. Without Diffusion
   - iso-τ lines: normal to the wall and streamlines
   - $\tau = 0$: everywhere upstream of transition point
   - $\tau = 1$: everywhere downstream of transition end

2. With Diffusion
   - iso-τ lines: normal to the wall but not to the streamlines
   - $\tau = 0$: upstream of transition point *near the wall*
   - $\tau = 1$: everywhere in *freestream*

TEST CASES

ZERO PRESSURE GRADIENT

- Clemson University [Kuan & Wang, 1990]
  - Flat Plate
  - Sharp Leading Edge
  - $U_\infty = 13.8 m/s$
  - $\frac{dp}{dx} = 0.$
  - $Tu_{le} = 1.1\%$
  - $x_{grid} - x_{le} = 0.9m$

FAVOURABLE PRESSURE GRADIENT

- ERCOFTAC: T3C5 [Rolls & Royce]
  - Flat Plate
  - Sharp Leading Edge
  - $U_\infty = 9.26 m/s$
  - $\overline{K} = 0.56 \times 10^{-6}$
  - $Tu_{le} = 3.0\%$
  - $x_{grid} - x_{le} = 0.61m$

ADVERSE PRESSURE GRADIENT

- SUG5K6 [Gostelow]
  - Flat Plate
  - Rounded Leading Edge
  - $U_\infty = 15.28 m/s$
  - $\overline{K} = -0.9 \times 10^{-6}$
  - $Tu_{le} = 3.9\%$
  - $x_{grid} - x_{le} = 1.2m$

CONCLUSIONS

- MODEL
  - Conditional averaging of NS-equations guarantees interaction between laminar and turbulent parts.
  - Dynamic equation for τ with normal variation realized
- TEST CASES
  - C_f: start and length
  - k-value:
    - too small at the start
    - peak well reproduced
  - velocity-profiles: good correspondence
  - H-profile: better with τ-diffusion
- IMPROVEMENTS
  - Model for laminar fluctuations
  - Start of transition

TRANSITION HEAT TRANSFER MODELING BASED ON THE CHARACTERISTICS OF TURBULENT SPOTS

Fred Simon and Robert Boyle
NASA Lewis Research Center
Cleveland, Ohio

ABSTRACT

While turbulence models are being developed which show promise for simulating the transition region on a turbine blade or vane, it is believed that the best approach with the greatest potential for practical is the use of models which incorporate the physics of turbulent spots present in the transition region. This type of modeling results in the prediction of transition region intermittency which when incorporated in turbulence models give a good to excellent prediction of the transition region heat transfer. Some models are presented which show how turbulent spot characteristics and behavior can be employed to predict the effect of pressure gradient and Mach number on the transition region. The models predict the spot formation rate which is needed, in addition to the transition onset location, in the Narasimha concentrated breakdown intermittency equation. A simplified approach is taken for modeling turbulent spot growth and interaction in the transition region which utilizes the turbulent spot variables governing transition length and spot generation rate. The models are expressed in terms of spot spreading angle, dimensionless spot velocity, dimensionless spot area, disturbance frequency and Mach number. The models are used in conjunction with a computer code to predict the effects of pressure gradient and Mach number on the transition region and compared with VKI experimental turbine data.

OBJECTIVE

Utilize Dynamic Characteristics of Turbulent Spots to Predict Transition Region Heat Transfer Dependency on Pressure Gradient and Mach Number

Two-Equation Turbulence Models Underpredict the transition Length, Unless.....

- Rate of Turbulence Production is Modified

or

- A Multi-Scale Approach is Used

or

- Provision is Made for the Intermittent Nature of Transition

Transition Physics & Intermittency

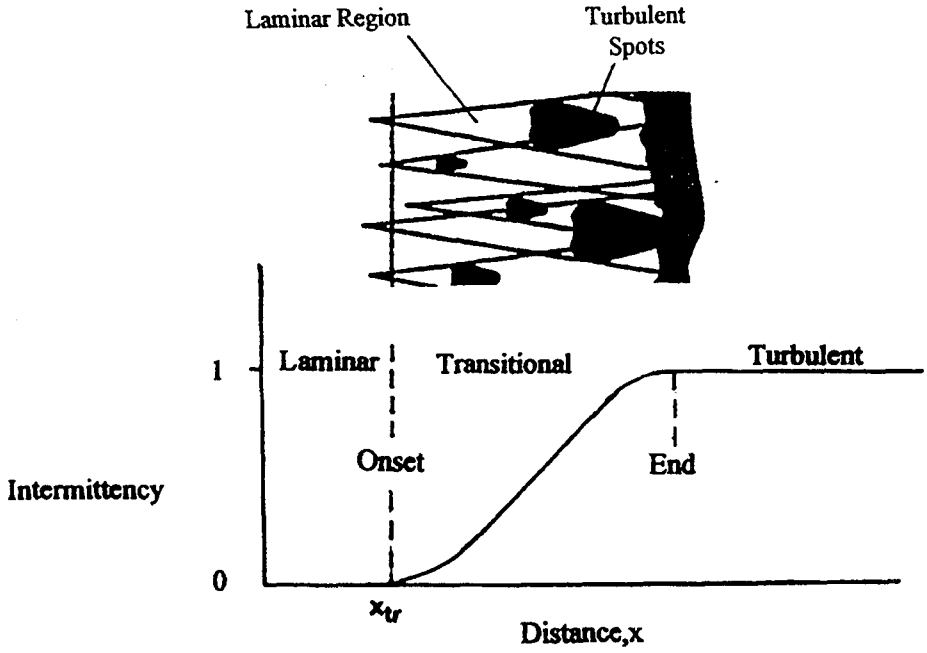

Use of Intermittency to Model Transition Region

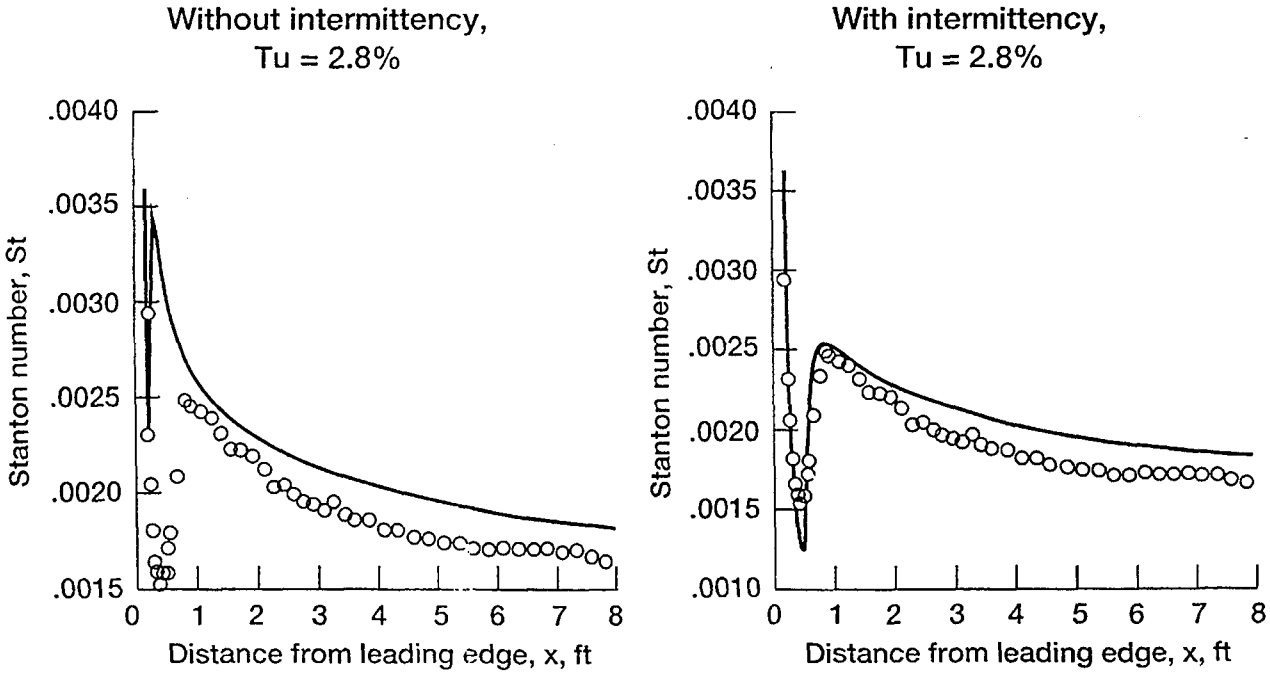

CD-96-72661

Intermittency Computation

Some Recent Methods

- Vancoillie & Dick,1988
- Simon & Stephens,1991
- Mayle,1991
- Simon,1994
- Solomon,Walker & Gostelow,1995
- Steelant & Dick,1994,1995,1996
- Johnson & Ercan,1996

Contentrated Breakdown Intermittency Equation

Narasimha,1957

$$\gamma = 1 - \exp\left[-\frac{n\sigma}{U_e}(x - x_{tr})^2 \right]$$

$$N = n\sigma\theta_{tr}^3/\nu$$

$$N = \frac{n\sigma\nu^2}{U_e^3} Re_{\theta_{tr}}^3$$

Intermittency Computation for a Variable Pressure Gradient

Solomon, Walker & Gostelow, 1995

$$\gamma = 1 - \exp\left[-n\int_{x_t}^{x} \frac{\sigma}{\tan\alpha}\left(\frac{dx}{U}\right)\int_{x_t}^{x} \tan\alpha \, dx\right]$$

$$\alpha = f(\lambda_\theta)$$

$$\sigma = f(\lambda_\theta)$$

$$N = n\sigma\theta_t^3/\nu = f(\lambda_{\theta_t}, Tu_t)$$

$$\lambda_\theta = \frac{\theta^2}{\nu}\frac{dU}{dx}$$

CD-96-72643

Turbulent Spot Inception/Growth Model

Method of Simon,1994

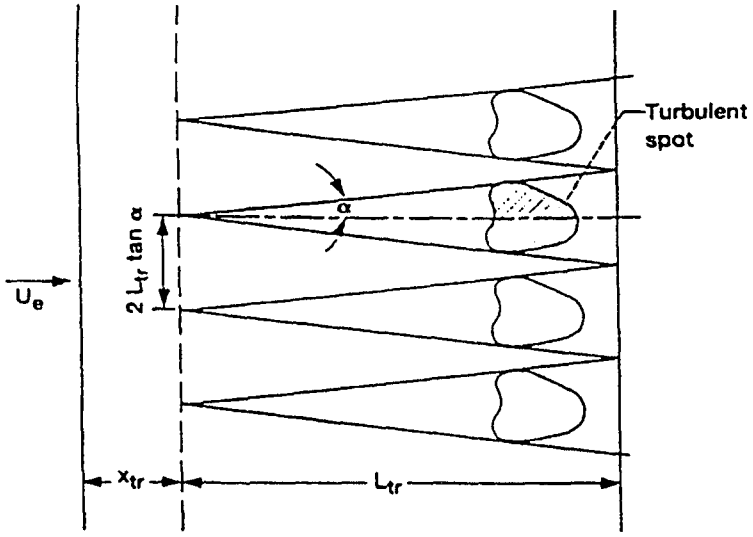

Turbulent Spot Inception/Growth Model

Resulting Equations(Simon,1994)

$$N = \left(\frac{f\nu}{U_e^2}\right)^2 \left(\frac{\Lambda \tan\alpha}{\beta}\right)^2 \mathrm{Re}^3{}_{\theta_{tr}} / 18.44$$

assume:

$$f\nu = \frac{0.7676 U_e^2}{2\pi \mathrm{Re}_{\theta_{tr}}^{3/2}}$$

Locus of Max. Disturbance Amplification Rate

$$N = 8.1x10^{-4}\left(\frac{\Lambda \tan\alpha}{\beta}\right)^2$$

Intermittency Computation

Method of Simon,1994

$$\mathrm{N} = \left(\frac{\Lambda \tan\alpha}{\beta}\right)^2 8.1\times10^{-4}$$

α	spreading angle of spot
β	velocity of center of spot/free-stream velocity
Λ	area of spot/square of half width

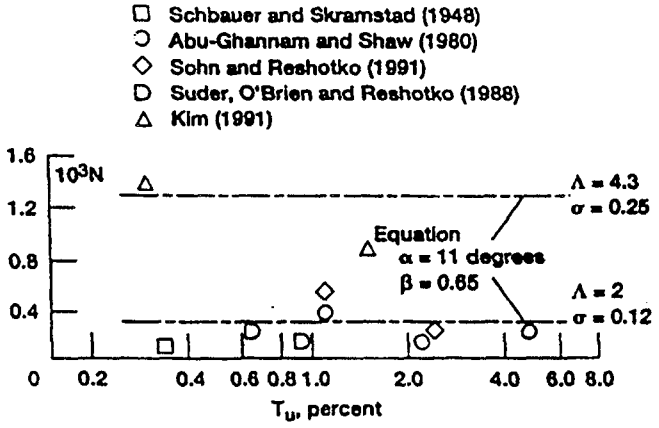

Non-Dimensional Spot Formation Rate Parameter

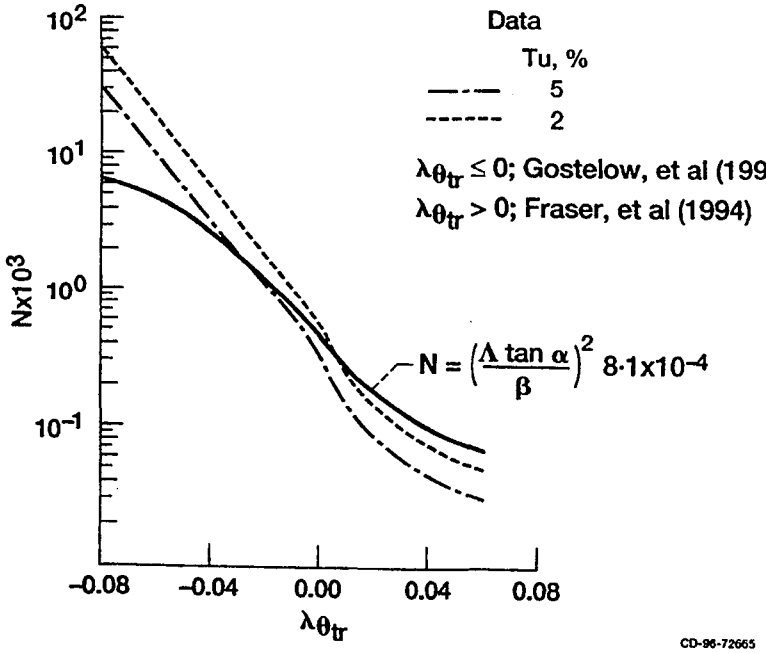

"Wedge-Flow" Model for Adverse Pressure Gradients

Clark(1993)
Wake-Induced
Wedge-Flow

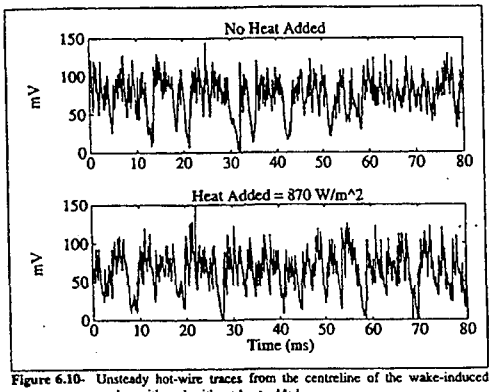

Figure 6.10- Unsteady hot-wire traces from the centreline of the wake-induced wedge with and without heat added.

Misley(1993)
Adverse Pressure
Gradient

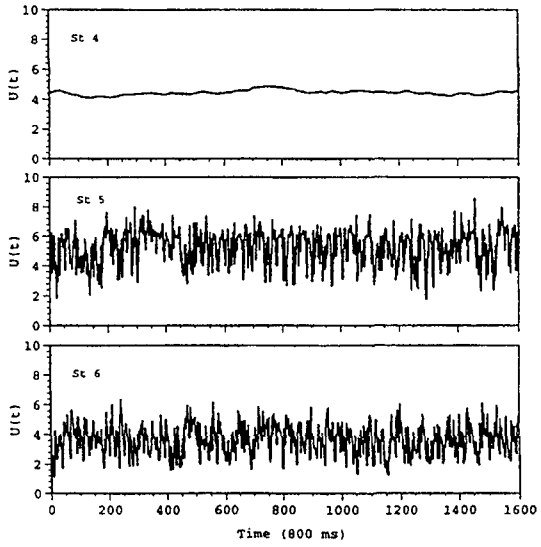

Figure 3.48. Velocity signals from 3-wire probe for $K1=-0.51 \times 10^{-6}$ taken at y/δ where u' is a maximum.

Transition Length Model

Method of McCormick, 1968

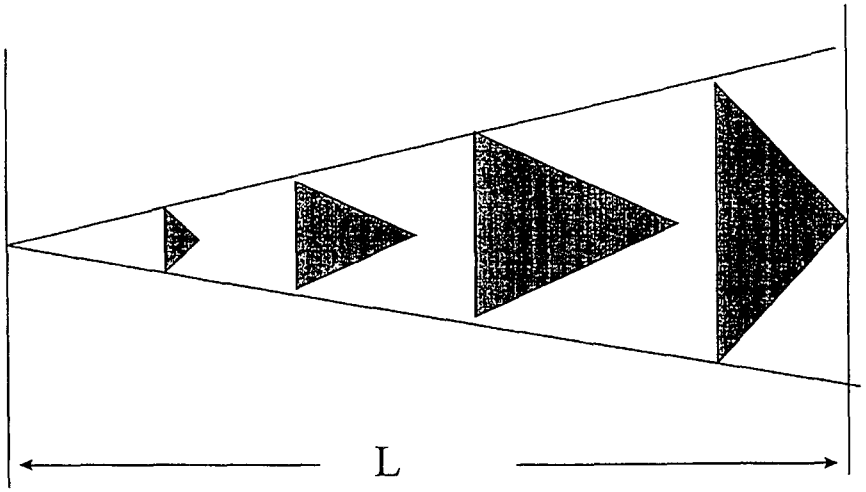

Transition Length Model

Method of McCormick,1968

$$N = \frac{0.0690}{\beta^2}$$

$$\beta = \frac{U_{te}}{1 - \frac{U_{te}}{U_{le}}}$$

Comparison of Prediction With Experiment

Favorable Pressure Gradient, $k = 0.75 \times 10^{-6}$, $\alpha = 5°$, $\beta = 0.8$

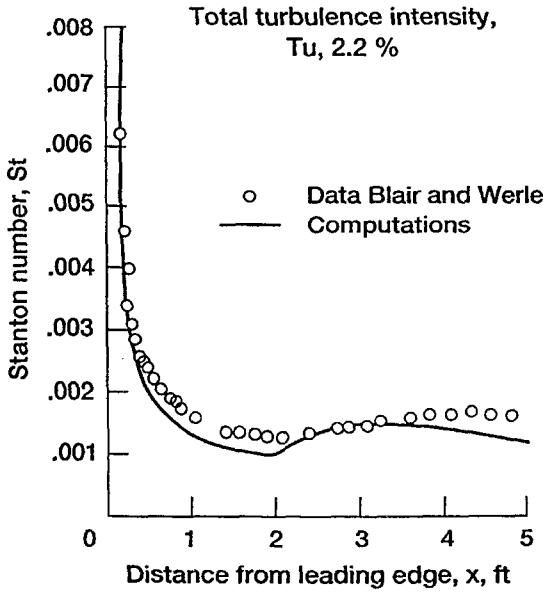

Spot Spreading Angle vs Mach Number for Zero Pressure Gradient

Clark,Jones& LaGraff,1994

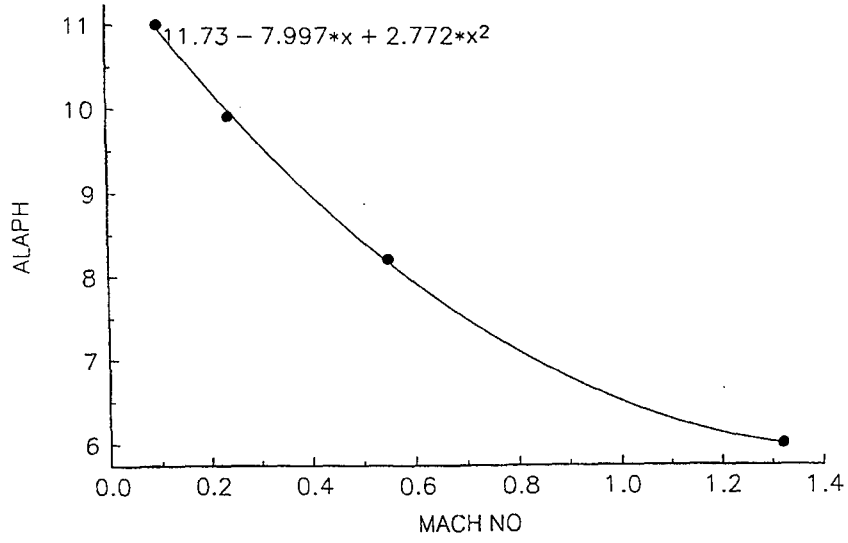

Mach Number Effect on N

$$N_{(M)} = N_{(0.1)}\, C_M$$

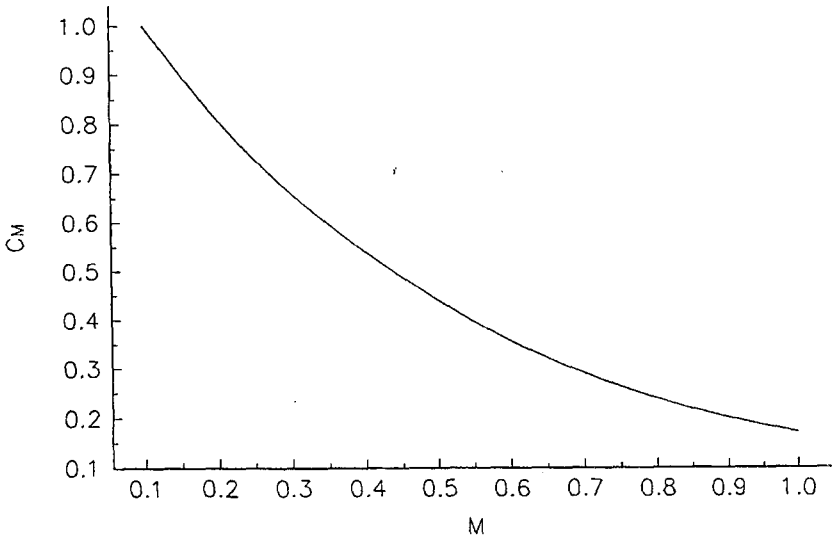

COMPUTATIONAL APPROACH

2D NAVIER–STOKES ANALYSIS – RVCQ3D (Chima – 1987)

THIN LAYER – TIME MARCHING APPROACH

DENSE C–GRIDS (321 X 53) (Arnone – 1992)

Mayle's (1991) TRANSITION START MODEL

Smith and Kuethe (1966) LEADING EDGE AUGMENTATION MODEL

ALGEBRAIC, (Baldwin–Lomax) TURBULENCE MODEL

CASES EXAMINED SO FAR

REQUIREMENT:

SIGNIFICANT TRANSITION LENGTH – IMPLIES MODERATE–TO–HIGH *Tu* LEVELS

STATOR – Arts et al. (1990) – 5 CASES

VARIATION in *Re, M,* and *Tu*

ROTOR – Arts et al. (1997) – 6 CASES

VARIATION in *Re, M, Tu,* and INCIDENCE,(PRESSURE GRADIENT)

TRANSITION LENGTH MODELS USED

SIMON

SOLOMON, WALKER, GOSTELOW, (SWG)

MACH NUMBER EFFECT on SURFACE HEAT TRANSFER

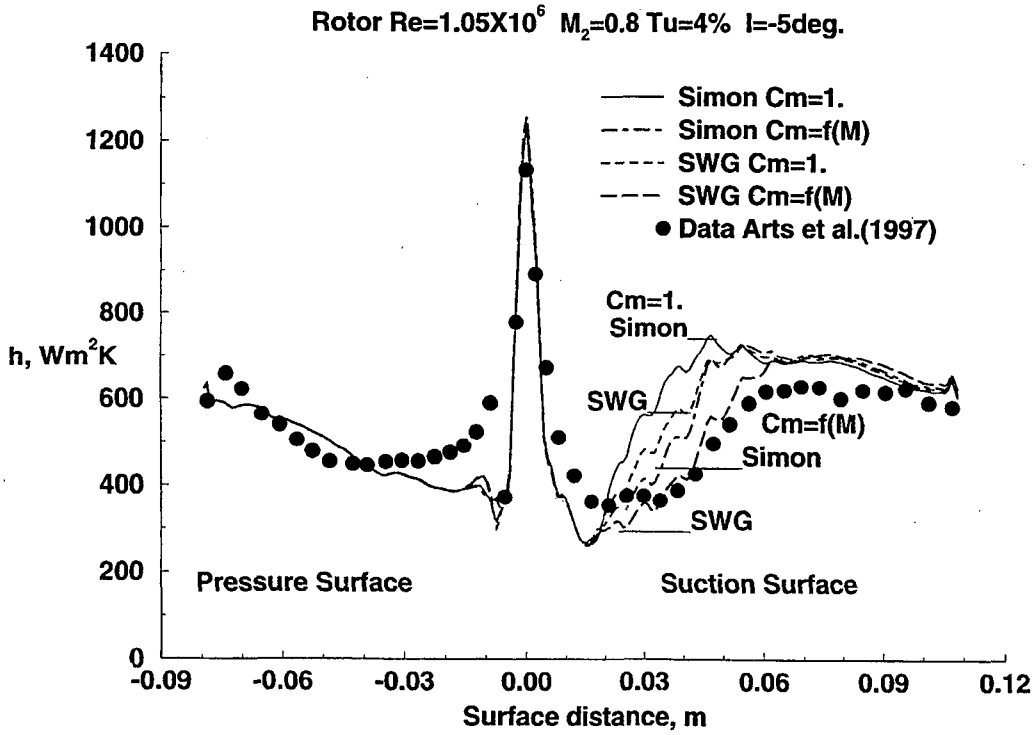

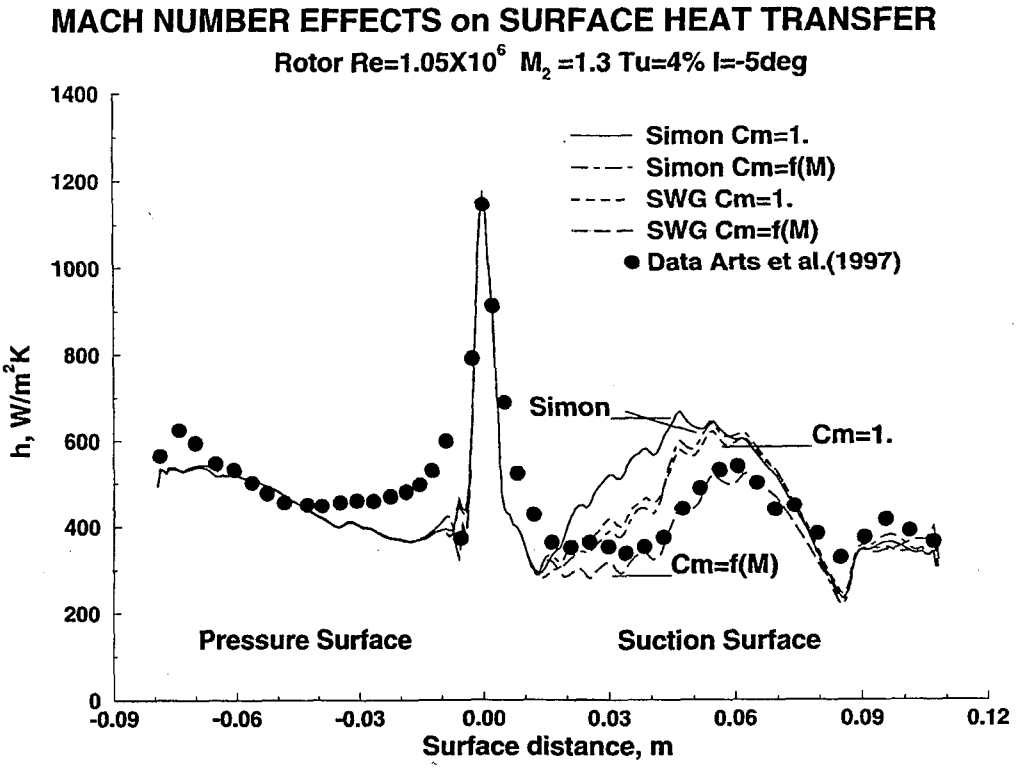
MACH NUMBER EFFECTS on SURFACE HEAT TRANSFER
Rotor Re=1.05X10^6 M2 =1.3 Tu=4% I=-5deg
Simon Cm=1.
Simon Cm=f(M)
SWG Cm=1.
SWG Cm=f(M)
Data Arts et al.(1997)
h, W/m^2K
Simon
Cm=1.
Cm=f(M)
Pressure Surface
Suction Surface
Surface distance, m

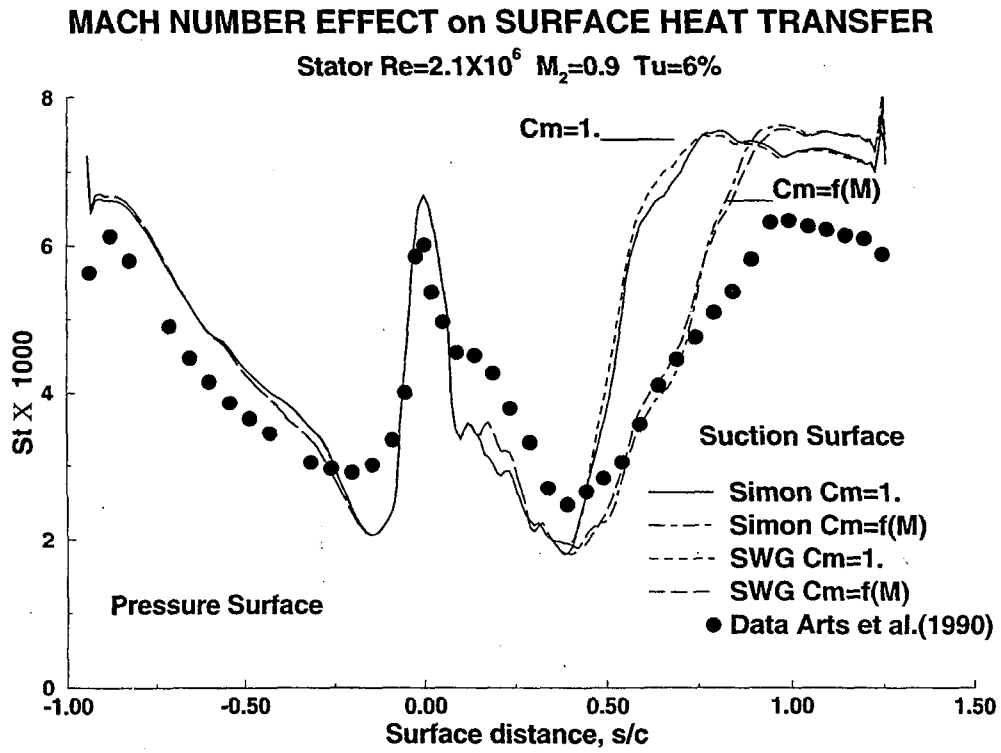
MACH NUMBER EFFECT on SURFACE HEAT TRANSFER
Stator Re=2.1X10^6 M2=0.9 Tu=6%
Cm=1.
Cm=f(M)
St X 1000
Suction Surface
Simon Cm=1.
Simon Cm=f(M)
SWG Cm=1.
SWG Cm=f(M)
Data Arts et al.(1990)
Pressure Surface
Surface distance, s/c

CONCLUSIONS

INCORPORATING a Mach NUMBER EFFECT GIVES IMPROVED AGREEMENT WITH EXPERIMENTAL DATA

GOOD TRANSITION LENGTH AGREEMENT FOR BOTH ROTOR AND STATOR DATA

SOLOMON, WALKER, GOSTELOW MODEL SHOWED BETTER AGREEMENT WITH DATA

RELATIVE CHANGES – INDEPENDENT OF MODEL USED

Use of Intermittency Results in a Good Prediction of Transition Region Heat Transfer for Turbines

Intermittency Prediction Obtained by Relating Spot Characteristics to Pressure Gradient & Mach Number

Intermittency Model of Solomon,Walker &Gostelow Performs Well in Accounting for Rapid Changes in Pressure Gradient

REFERENCES

Abu-Ghannam,B.J. and Shaw,R. 1980. Natural Transition of Boundary Layers-The Effects of Turbulence,Pressure Gradient, and Flow History, Journal of Mech. Engr. Sci., vol 22, No. 5,pp. 213-228.

Arnone,A., Liou,M.S. and Povinelli,L.A. 1992. Navier-Stokes Solution of Transonic Cascade Flows Using Non-periodic C-Type Grids, AIAA Journal of Propulsion and Power, vol. 8, no. 2, pp. 410-417.

Arts,T., Lambert de Rouvroit,M. and Rutherford,A.W. 1990. Aero-Thermal Investigation of a Highly Loaded Transonic Linear Turbine Guide Vane Cascade, von Karman Institute for Fluid Dyanamics, Technical Note 174

Arts,T., Duboue,J.-M., and Rollin,G. 1997. Aero-Thermal Performance Measurements and Analysis of a Two-Dimensional High Turning Rotor Blade, ASME paper 97-GT-120, International Gas Turbine Congress, Orlando

Blair,M.F. and Werle,M.J. 1981. Combined Influence of Free-Stream Turbulence and Favorable Pressure Gradients on Boundary Layer Transition, UTRC report R81-914388-17.

Chima,R.V. 1987. Expicit Multigrid Algorithm for Quasi-Three-Dimensional Flows in Turbomachinery, AIAA Journal of Propulsion and Power, vol. 3, no. 5, pp. 397-405.

Clark,J.P. 1993. A Study of Turbulent-Spot Propagation in Turbine-Representative Flows, D.Phil Thesis, Department of Engineering Science, University of Oxford, England.

Clark,J.P., Jones,T.V., and LaGraff,J.E. 1994. On the Propagation of Naturally-Occurring Turbulent Spots, Journal of Engineering Mechanics on Turbulent Spots, ed. F.T. Smith.

Fraser,C.J.,Higazy,M.G. and Milne,J.S. 1994. End-Stage Boundary Layer Transition Models for Engineering Calculations, Proceedings of the Institution of Mechanical Engineers, C208, 47-58.

Gostelow,J.P..Blunder,A.R. and Walker,G.J. 1994. Effects of Free-Stream Turbulence and Adverse Pressure Gradients on Boundary Layer Transition, ASME Journal of Turbomachinery, 116, 392-404.

Johnson,M.W. and Ercan,A.H. 1996. A Boundary Layer Transition Model, ASME paper 96-GT-444, International Gas Turbine Congress, Birmingham.

Kim,J. and Simon,T.W. 1991. Free-Stream Turbulence and Concave Curvature Effects on Heated, Transitional Boundary Layers, NASA CR-187150.

Mayle,R.E. 1991. The Role of Laminar-Turbulent Transition in Gas Turbine Engines, ASME paper 91-GT-261.

McCormick,M.E. 1968. An Analysis of the Formation of Turbulent Patches in the Transition Boundary Layer, ASME Journal of Applied Mechanics, vol. 35, pp. 216-219.

Mislevy,S. 1993. The Effects of Adverse Pressure Gradients on the Momentum and Thermal Structures in Transitional Boundary Layers, Clemson University M.S. Thesis

Narasimha,R. 1957. On the Distribution of Intermittency in the Transition Region of a Boundary Layer, J. Aeronautical Science, vol. 24, no. 9, pp. 711-712.

Schubauer,G.B. and Skramstad,H.K. 1948. Laminar-Boundary Layer Oscillations and Transition on a Flat Plate, NASA Report 909.

Simon,F. 1994. The Use of Transition Region Characteristics to Improve the Numerical Simulation of Heat Transfer in Bypass Transitional Flows, NASA TM 106445.

Simon.F.F. and Stephens,C.A. 1991. Modeling of the Heat Transfer in Bypass Transitional Boundary-Layer Flows, NASA TP-3170

Smith,M.C., and Kuethe,A.M. 1966. Effects of Turbulence on Laminar Skin Friction and Heat Transfer, Physics of Fluids, vol. 9, pp.2337-2344.

Sohn,K.H. and Reshotko,E. 1991. Experimental Study of Boundary Layer Transition with Elevated Freestream Turbulence on a Heated Flat Plate, NASA CR-187068.

Solomon,W.J.,Walker,G.J. and Gostelow,J.P. 1995. Transition Length Prediction for Flows with Rapidly Changing Pressure Gradients, ASME paper 95-GT-241, International Gas Turbine Congress, Houston.

Steelant,J. and Dick,E. 1994. Modelling of By-Pass Transition with Conditioned Navier-Stokes Equations and a k-e Model Adapted for Intermittency, ASME paper 94-GT-12, International Gas Turbine Congress, Netherlands.

Steelant,J. and Dick,E. 1995. Conditioned Navier-Stokes and k-e-Equations to Model Transition in Pressure Gradient Flow, ASME paper 95-GT-213, International Gas Turbine Congress, Houston.

Steelant,J. and Dick,E. 1996. Calculation of Transition in Adverse Pressure Gradient Flow by Conditioned Equations, ASME paper 96-GT-160, International Gas Turbine Congress, Birmingham.

Suder,K.L.,O'Brien,J.E. and Reshotko,E. 1988. Experimental Study of Bypass Transition in a Boundary Layer, NASA TM-100913

Vancoille,G. and Dick,E. 1988. A Turbulence Model for the Numerical Simulation of the Transition Zone in a Boundary Layer, Int. J. Eng. Fluid Mech.,vol 1, no. 1.

Walker,G.J.,1989. Modeling of Transitional Flow in Laminar Separation Bubbles, 9th Int. Sym. Air Breathing Engines, pp. 539-548.

PREDICTION OF TRANSITIONAL FLOWS IN THE LOW PRESSURE TURBINE*

George Huang and Guohua Xiong
University of Kentucky
Lexington, Kentucky

Abstract

Current turbulence models tend to give too early and too short a length of flow transition to turbulence, and hence fail to predict flow separation induced by the adverse pressure gradients and streamline flow curvatures [Huang and Xiong, 1998]. Our discussion will focus on the development and validation of transition models. The baseline data for model comparisons are the T3 series (Savill, 1993), which include a range of free-stream turbulence intensity and cover zero-pressure gradient to aft-loaded turbine pressure gradient flows. The method will be based on the conditioned N-S equations and a transport equation for the intermittency factor.

First, several of the most popular 2-equation models in predicting flow transition are examined: k-e (Launder-Sharma), k-w (Wilcox), Lien-Leschiziner and SST (Menter) models. All models fail to predict the onset and the length of transition, even for the simplest flat plate with zero-pressure gradient(T3A). Although the predicted onset position of transition can be varied by providing different inlet turbulent energy dissipation rates, the appropriate inlet conditions for turbulence quantities should be adjusted to match the decay of the free-stream turbulence.

Arguably, One may adjust the low-Reynolds-number part of the model to predict transition. This approach has so far not been very successful. However. We have found that the low-Reynolds-number model of Launder and Sharma [1974], which is an improved version of Jones and Launder [1972] gave the best overall performance. The Launder and Sharma model was designed to capture flow re-laminarization (a reverse of flow transition), but tends to give rise to a too early and too fast transition in comparison with the physical transition. The three test cases were for flows with zero pressure gradient but with different free-stream turbulent intensities. The same can be said about the model when considering flows subject to pressure gradient(T3C1).

To capture the effects of transition using existing turbulence models, one approach is to make use of the concept of the intermittency to predict the flow transition. It was originally based on the intermittency distribution of Narasimha [1957], and then gradually evolved into a transport equation for the intermittency factor. Gostelow and associates [1994, 1995] have made some improvements to Narasimha's method in an attempt to account for both favorable and adverse pressure gradients. Their approach is based on a linear, explicit combination of laminar and turbulent solutions. This approach fails to predict the overshoot of the skin friction on a flat plate near the end of transition zone, even though the length of transition is well predicted. The major flaw of Gostelow's approach is that it assumes the non-turbulent part being the laminar solution and the turbulent part being the turbulent solution and they do not interact across the transitional region.

The technique in condition averaging the flow equations in intermittent flows was first introduced by Libby [1975] and Dopazo [1977] and further refined by Dick and associates [1988, 1996]. This approach employs two set of transport equations for the

* Work supported by NASA Lewis Research Center (Grant no. NAG3-2018).

mean flow - one for the non-turbulent part and the other for the turbulent part. The advantage of this approach is that it allows the interaction of non-turbulent and turbulent velocities through the introduction of additional source terms in the continuity and momentum equations for the non-turbulent and turbulent velocities. However, the strong coupling of the two sets of equations has caused some numerical difficulties, which requires special attention. The prediction of the skin friction can be improved by this approach via the implicit coupling of non-turbulent and turbulent velocity fields.

Another improvement of the intermittency model can be further made by allowing the intermittency to vary in the cross-stream direction. This is one step prior to testing any proposal for the transport equation for the intermittency factor. Instead of solving the transport equation for the intermittency factor, the distribution for the intermittency factor is prescribed by Klebanoff's empirical formula [1955]. The skin friction is very well predicted by this new modification, including the overshoot of the profile near the end of transition zone. The outcome of this study is very encouraging since it indicates that the proper description of the intermittency distribution is the key to the success of the model prediction. This study will be used to guide us on the modeling of the intermittency transport equation.

References

Dopazo, C., 1977, "On conditioned averages for intermittent turbulent flows," J. Fluid Mech., vol. 81, part 3, pp. 433-438.

Gostelow, J. P., Hong, G., Walker, G. J., and Dey, J., 1994b, "Modeling of boundary layer transition in turbulent flows by linear combination integral method, " ASME Paper 94-GT 358.

Huang, P. G. and Xiong, G, "Transition and turbulence modeling of low pressure turbine flows," 36th AIAA Aerospace Science Meeting and Exhibit, Reno, NV, Jan 12-15, 1998.

Kelbanoff, P. S., 1955, "Characteristics of turbulence in a boundary layer with zero pressure gradient," NACA Rep. No. 1247.

Libby, P. A., 1975, "On the Prediction of intermittent turbulent flows," J. Fluid Mech., vol. 68, part 2, pp. 273-295.

Narasimha, R., 1957, "On the Distribution of Intermittency in the Transition Region of a Boundary Layer," Journal of Aerospace Sciences,Vol. 24, No. 9, pp. 711-712.

Savill, A. M., 1993, "Some Recent Progress in the Turbulence Modeling of By-Pass Transition," in Near-Wall Turbulent Flows, Ed. R. M. C. So, C. G. Speziale & B. E. Launder, Elsevier Science Publishers, pp. 829-848.

Solomon, W. J., Walker, G. J., and Gostelow, J. P., 1995, "Transition length prediction for flows with rapidly changing pressure gradients," ASME Paper 95-GT-241.

Steelant, J. and Dick, E., 1996, "Modeling of bypass transition with conditioned Navier-Stokes equations coupled to an intermittency transport equation," Int. J. for Num. Methods in Fluids, vol 23, pp. 193-220.

Vancoillie, G. and Dick, E., 1988, "A turbulent model for the numerical simulation of the transition zone in a boundary layer," J. Eng. Fluid Mech., 1, pp. 28-49.

Outline

- Simon and Qiu's Experiments
- Physics of Separation and Transition
- Modeling of Transitional Flows
- Summary

Simon and Qiu's experiments

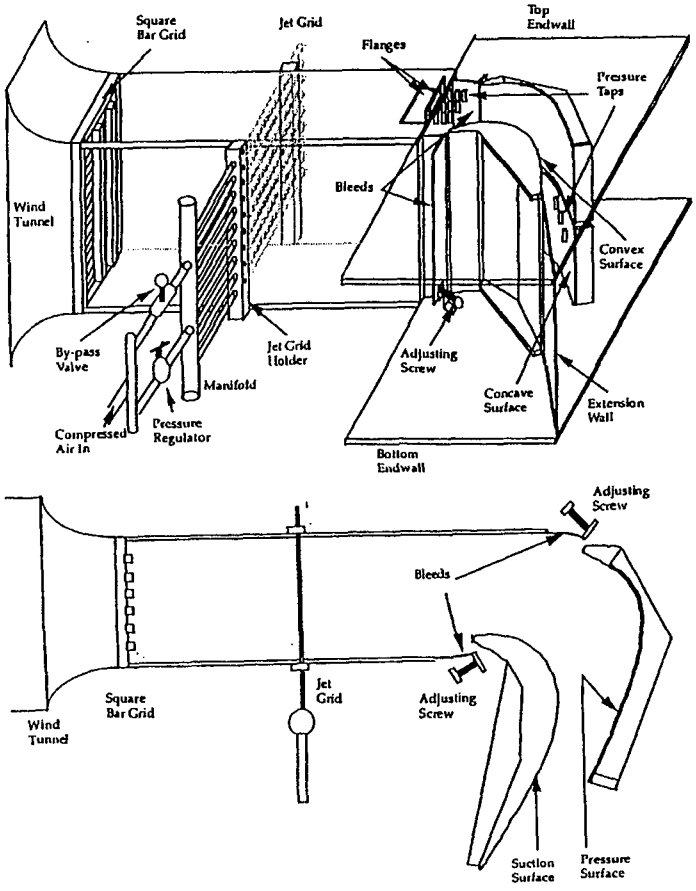

Re= 50,000
100,000
200,000
300,000

TI = 0.5%
2.5%
10%

NASA/CP—1998-206958

Comparison of Cascade and Non-cascade Flows

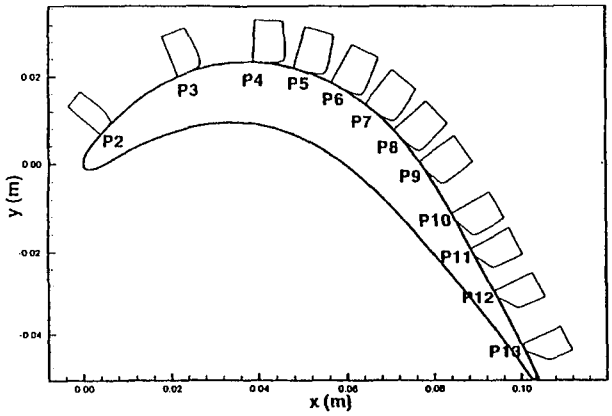

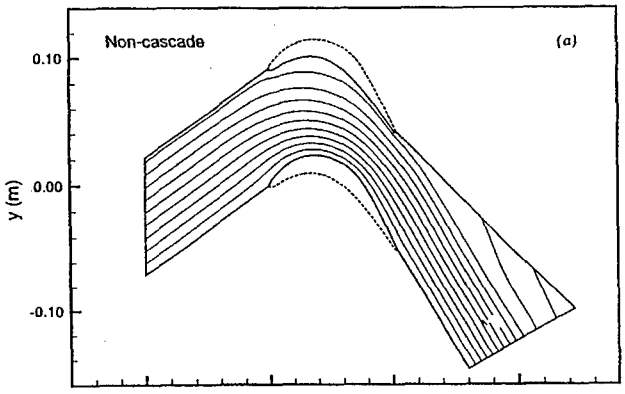

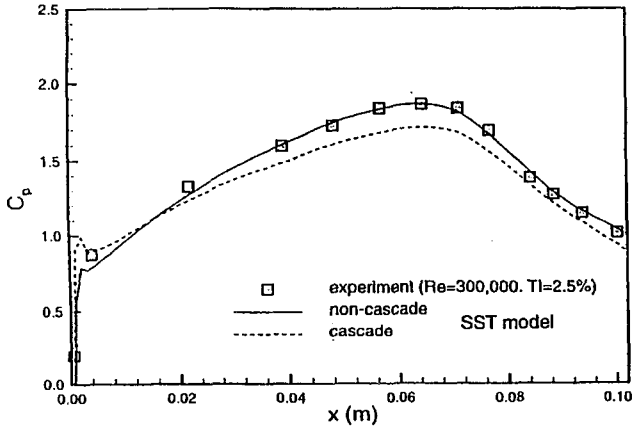

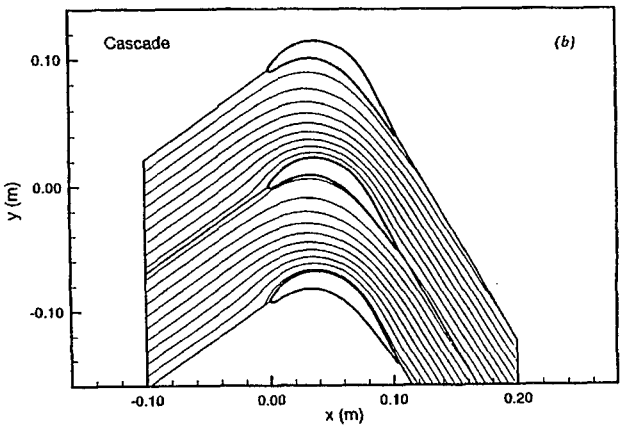

Separation and Transition

	Re = 50,000	Re = 100,000	Re = 200,000	Re = 300,000
TI=0.5%				
Height	full	4mm	1.6mm	0.6mm
Length	P8,9-	P8,9-P12,13	P8,9-P10,11	P8,9-P9,10
Transition	P12-	P10-P12	P9-P11	P9-P10
TI=2.5%				
Height	1.7mm	0.9mm	0.06mm	None
Length	P8,9-P11,12	P8,9-P10,11	P8,9-P9,10	----
Transition	P11-	P9,10-P12	P8-P10	<P8-P10
TI=10%				
Height	0.07mm	0.05mm	None	
Length	P8,9-P10,11	P8,9-P9,10	----	
Transition	P9,10-	P8,9-P11	<P8-P10	

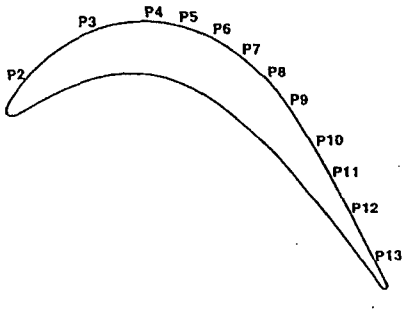

Numerical Predictions

Re	FSTI	Mach	Setup	Turbulent	Laminar	Inviscid
50,000	0.1%	0.015	experiment	X		
100,000	2.5%	0.03	experiment	X	X	
100,000	2.5%	0.03	cascade	X	X	
200,000	0.5%	0.06	cascade			X
300,000	2.5%	0.085	experiment	X	X	X
300,000	2.5%	0.085 - 0.3	cascade	X	X	X

Cases of Re=300k, TI=2.5% are chosen for detailed comparison

Re=300,000, TI=2.5% (I)

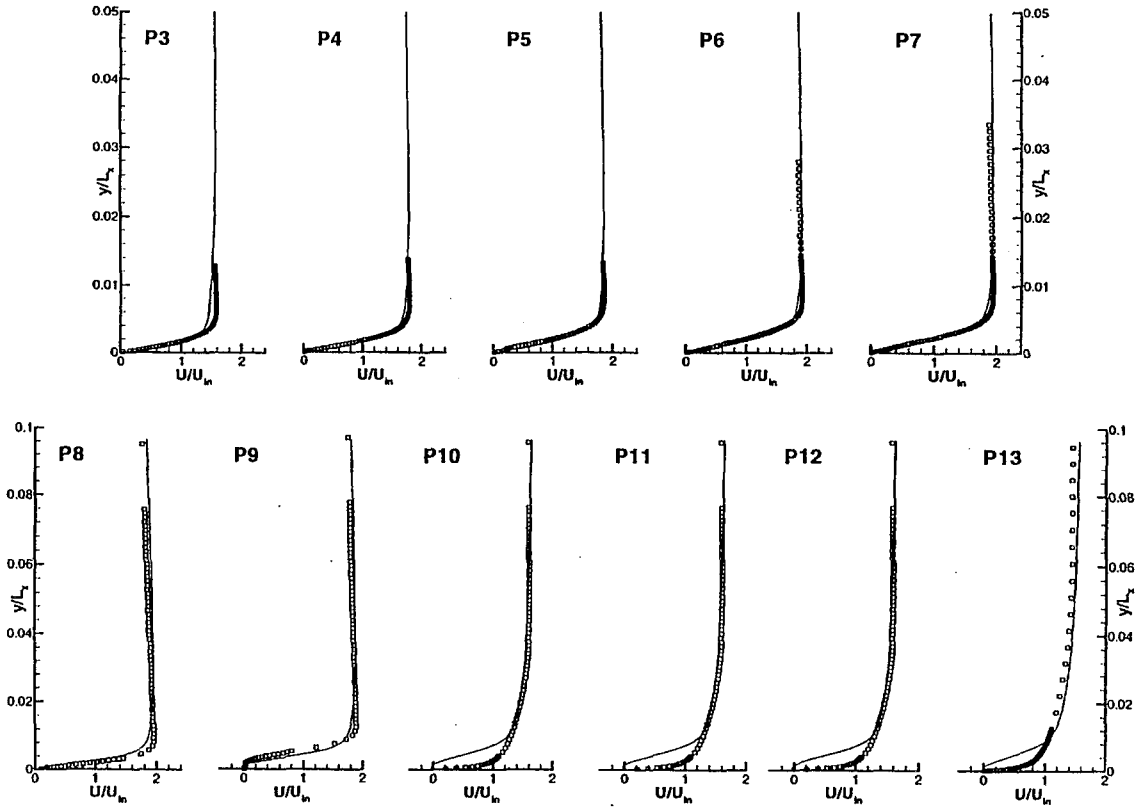

▫ experiment, —— laminar calculation

Re=300,000, TI=2.5% (II)

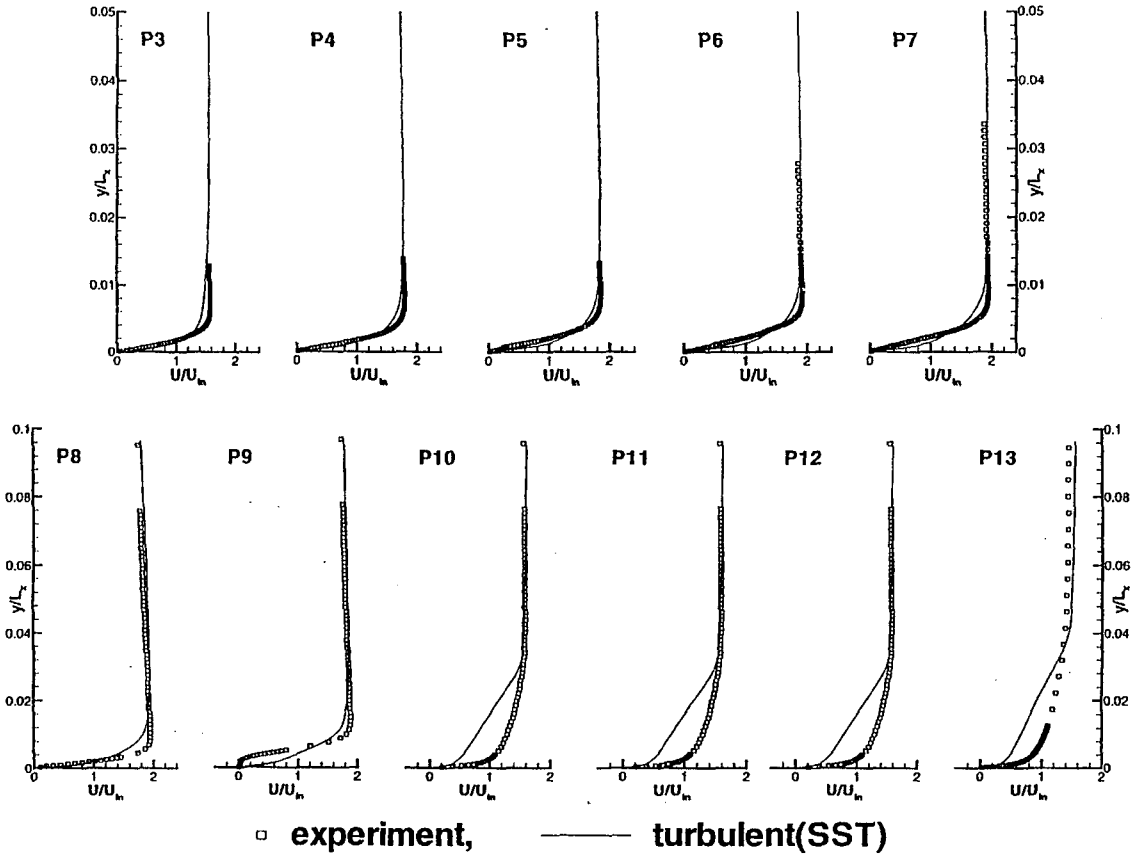

Re=100,000, TI=2.5%

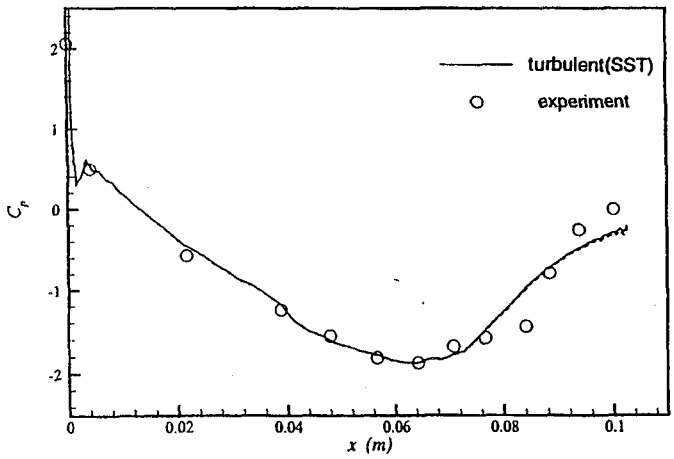

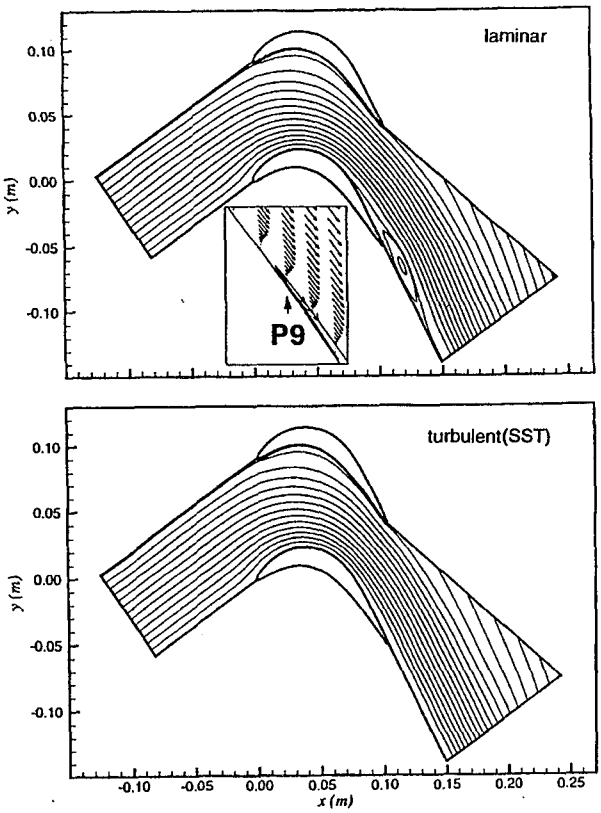

Transition: Key Point for Accurate Prediction

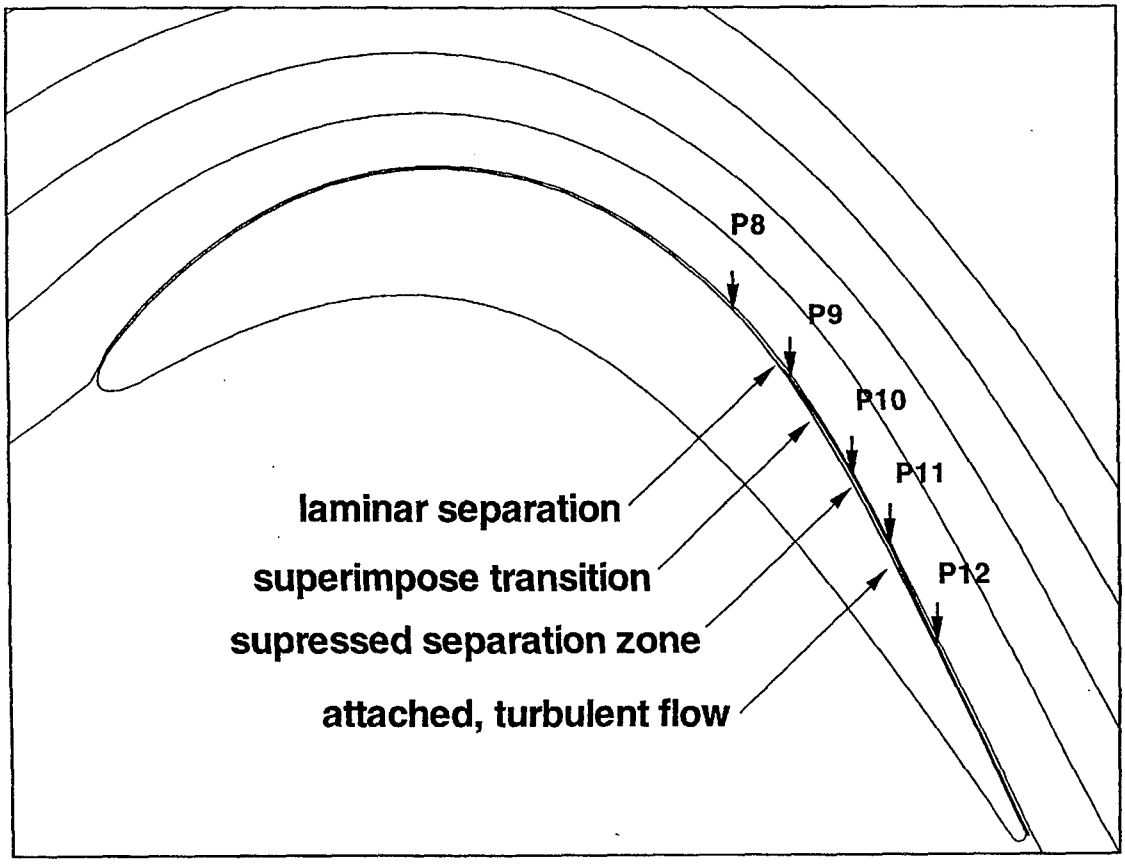

Modeling of Transitional Flows

- Adjustments of low-Re models
- k-ε-γ model for free shear flows
- Explicit method: (1-γ) Cf_{lam}+ γ Cf_{turb}
- Conditioned N-S equations + γ(x)
- Conditioned N-S equations + γ(x,y)

Predictions of Various Approaches for T3A experiment

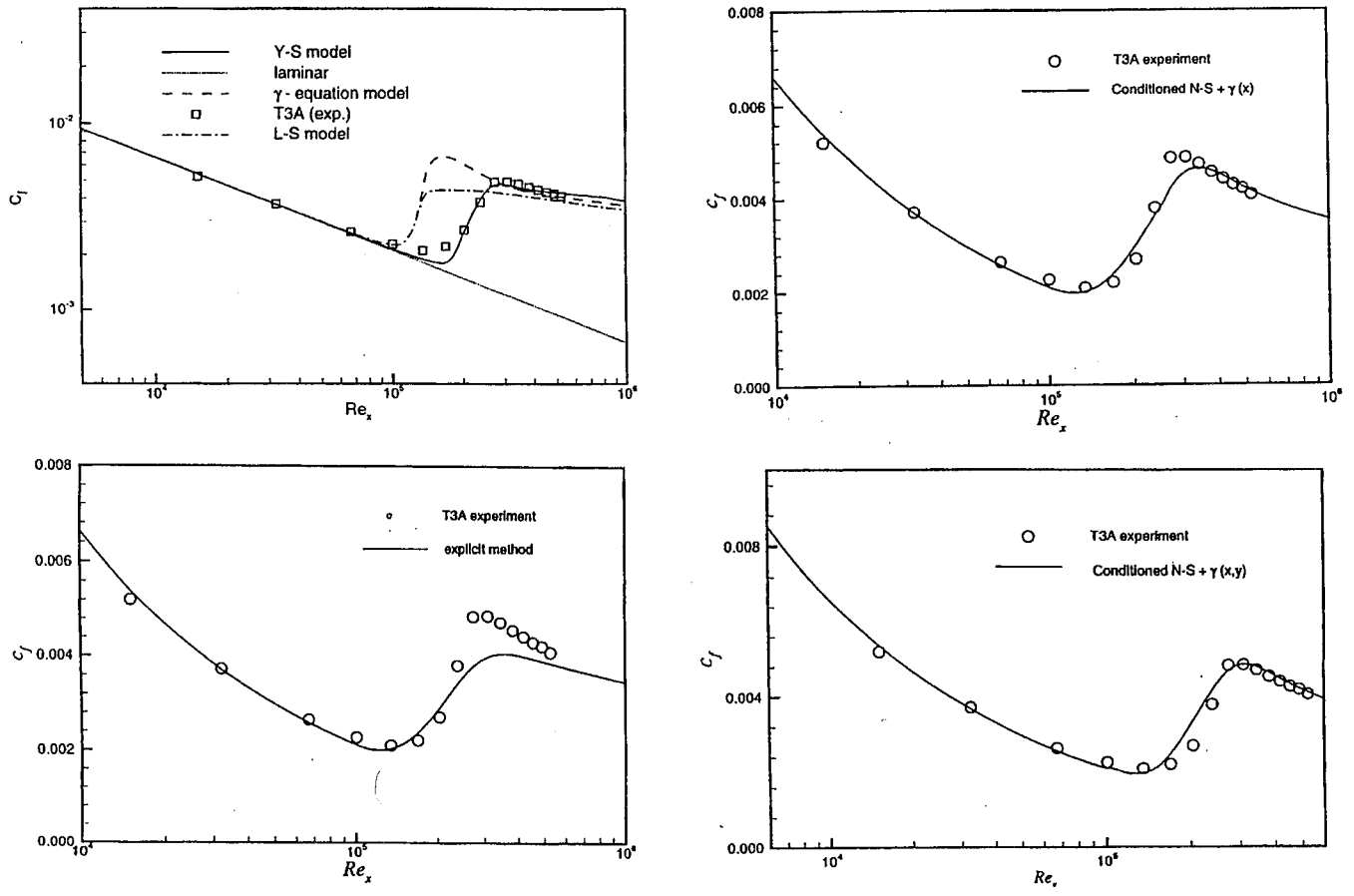

New Intermittency Model

Conditioning of N-S equations:

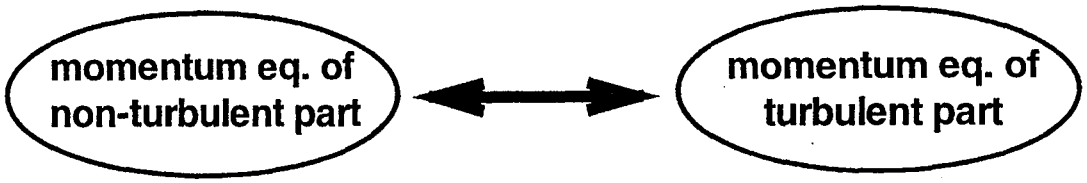

Interactions

$$= \frac{\partial \gamma}{\partial x_j}[(u_i^t u_j^t - u_i^l u_j^l) - \nu(\frac{\partial u_i^t}{\partial x_j} + \frac{\partial u_j^t}{\partial x_i} - \frac{\partial u_i^l}{\partial x_j} - \frac{\partial u_j^l}{\partial x_i})] + \frac{\partial \gamma}{\partial x_j}\overline{u_i u_j}^t$$

$$= (c_1^* + 1)(-\overline{u_i u_j}^t)\frac{\partial \gamma}{\partial x_j} + c_2^* \frac{2\gamma(1-\gamma)}{1-2\gamma}\frac{\partial(-\overline{u_i u_j}^t)}{\partial x_j}$$

Mean momentum equatiions for the transition zone:

$$\frac{\mathrm{d}U_i U_j}{\mathrm{d}x_j} = -\frac{\partial P}{\partial x_i} + \frac{\partial}{\partial x_j}(\nu(\frac{\partial U_i}{\partial x_j} + \frac{\partial U_j}{\partial x_i})) + c_1(\gamma)\frac{-\overline{u_i u_j}}{\partial x_j} + c_2(\gamma)\frac{\partial \gamma}{\partial x_j}(-\overline{u_i u_j})$$

$$c_1(\gamma) = \gamma^{3.0/\sqrt{TI}}, c_2(\gamma) = 0, \gamma = \gamma(x, y)$$

Preliminary Results: T3 Series Experiments

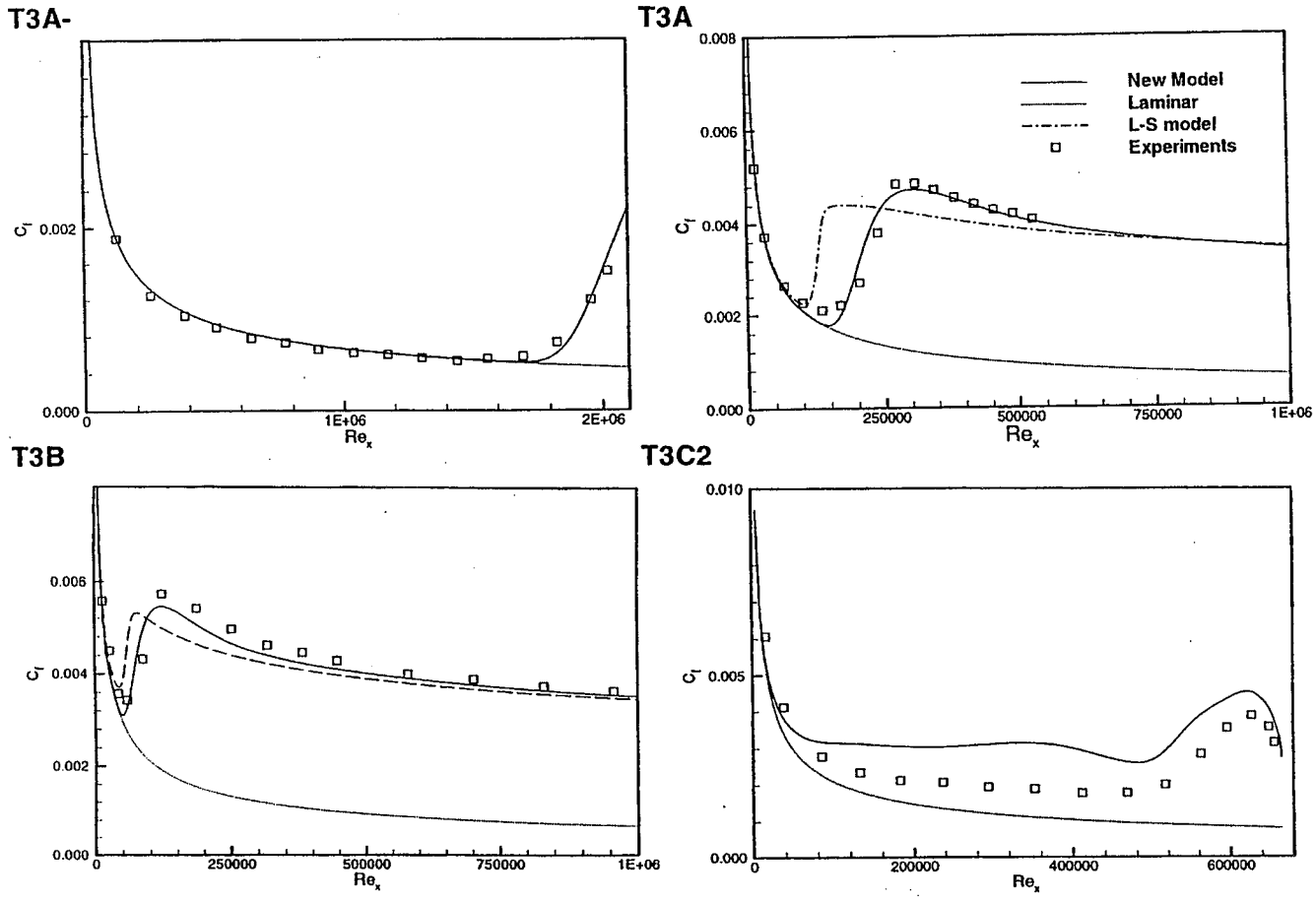

Preliminary Results: Re=300,000, Tl=2.5%

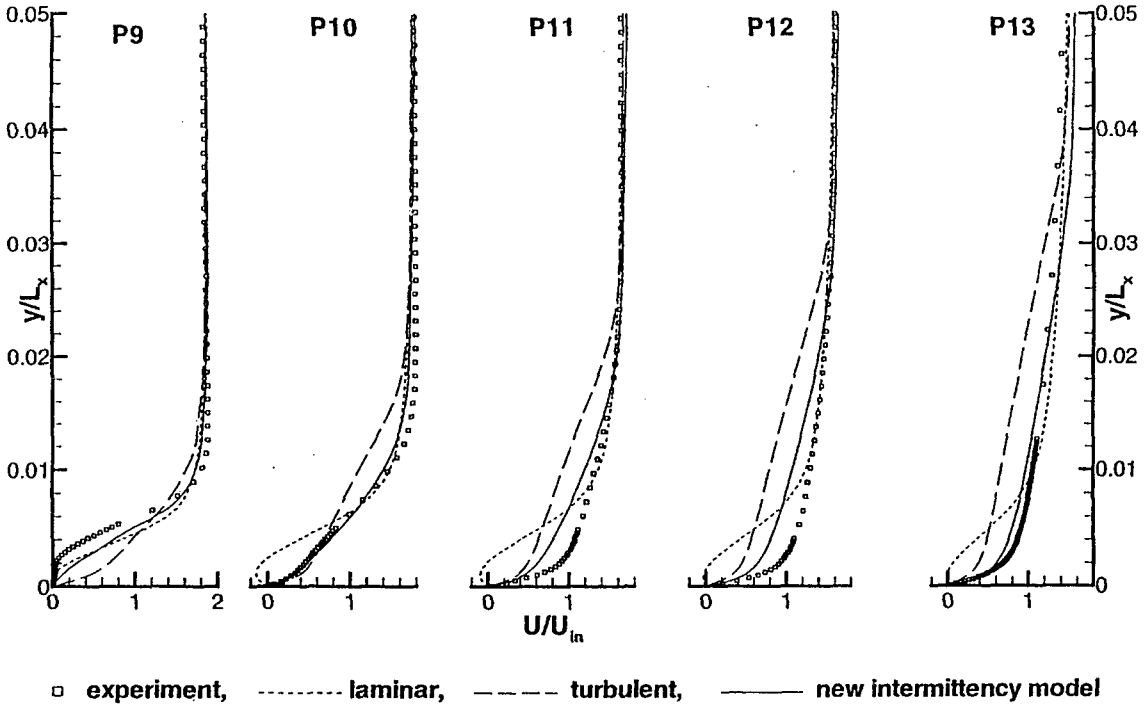

Summary

- To predict transition is the key to predict LPT flows
- Intermittency approach is very promising
- Refinement of the new model is in progressing

FINAL PLENARY SESSION

NASA/CP—1998-206958

MINNOWBROOK II - 1997 WORKSHOP ON BOUNDARY LAYER TRANSITION IN TURBOMACHINES
EDITORS: J.E. LAGRAFF AND D.E. ASHPIS, NASA CONFERENCE PUBLICATION 206958, 1998, PP. 467-482.

FINAL PLENARY SESSION TRANSCRIPT

J. Paul Gostelow
University of Leicester
Leicester UK

Gostelow Firstly this morning we will receive reports from the four working groups. Then Ted Okiishi will moderate a general discussion, finally Roddam Narasimha will give us his summing up of the meeting. I would firstly like to call on Terry Jones to report on the work of the group which considered the calmed region.

Calmed Region

Jones Two areas of interest relating to the becalmed region were considered. Firstly the origin and structure of the calmed region and then secondly we considered the use of the region in machines. The view that essentially it was a laminar region which was relaxing back in a relatively understandable manner to its steady state condition was to a large extent accepted. It was recognized, however, that there was some structure in the calmed region but that perhaps this was a remnant of structure in the spot which actually passed through into this region. The calming effect that this region has was still to be clarified. Maybe it was just the mean velocity profile which was doing it but maybe there were other properties of the region; that still is an area for ongoing work. A significant question was asked about the details of the flow at the rear of trailing edge of the spot. And the question of the flow around the spot, of where is the flow coming in and where is it going out, needs to be looked at in some detail and resolved I think. So that would be an area of work and clarification. But it was remembered that Professor Cumpsty said that the spot was actually a very flat object and the pictures that one sees are exaggerated in the normal direction and that has to be taken into account when picturing what goes on.

There was general consensus on the calmed region but these areas were highlighted for examination subsequently. And then we went on to the application of the spot. There were thought to be many possible applications of the calmed region and these were considered. The low pressure turbine was thought to be a prime candidate. The reason why it was beneficial, the calmed region representing a low source of entropy generation, there was the consequence of the calmed region on separation and acoustic and aeroelastic implications were raised. Those were highlighted as possible applications. Work needs to be done in all these areas.

Gostelow There is an important conceptual link between the turbulent spot and its calmed

region, which had previously been one area of study, and the calmed region on the blade in the real machine behind a wake interaction. There is clearly a strong suggestion that the two phenomena are basically one and the same. There is some limited experimental evidence which would indicate that. I think it is not demonstrated rigorously that the two are one and the same, I think that more experimental evidence is needed really to prove that. Nevertheless the circumstantial evidence is such that findings on the calmed region behind the spot could very reasonably be extended to the benefits that are being seen already in examples such as low pressure turbine design where you have this very extensive strip-like two dimensional calmed region behind the wake interaction with the blade surface.

Jones I think the general view was that it is one and the same phenomenon.

Gostelow Even if it is not proven rigorously.

Jones I suppose so. There was one other aspect of the calmed region and that was its prediction by DNS. We have been told that spots have been predicted and there was some question as to whether the calmed region had been predicted by DNS. I think Neil was going to discuss this, because that is an important conclusion. Those were just the broad outlines of what we discussed.

Gostelow One other thing we should say is that we felt we had a good understanding of the calmed region but that this didn't imply that we understood the turbulent spot itself which is a different question. Is that fair?

Jones Yes. The simple question of why the spot trailing edge goes at half the trailing edge velocity was not answered. This is a pretty fundamental question. If we can't predict that there is still a lot of work to do.

Gostelow Thank you Terry. Let's save any questions for the follow up session. Dave Ashpis will now report.

Low Pressure Turbines

Ashpis In the LPT group the discussion focused on LPT research programs without detailed discussion of technical issues. The technical discussions of other groups are very relevant to LPT, unfortunately they took place in parallel sessions.

The major recommendation that came out from the LPT group discussion is to initiate a project of measurement of the flow environment in an actual engine. The idea itself is a very good one. There is little known information about the turbulence and unsteadiness characteristics of the flow environment present in the engine. Numerous researchers are trying to solve the problem without fully knowing what is the input, so there is definitely a strong need. This project must involve industry, where actual engines and facilities to run them are available. The amount of funding involved was estimated to be of the order of 1-2 million dollars. The group encouraged me to try and secure NASA sponsorship for this project, which to my opinion, is quite a difficult task considering the severe budget constraints and priorities. The pre-competitive aspects of this project and the high cost involved make it very suitable for international collaboration with participation of industry in US and Europe. I will try to initiate a study of the technical requirements and feasibility of this proposed project and investigate the funding options.

The group general consensus was that NASA's LPT program is "doing the right things", and that generally its objectives and current and planned activities are balanced and on target.

In technical matters it was felt that the program should consider and adapt conclusions and recommendations from the other working groups, in particular the ones from the calmed region group. Additional specific technical suggestions were: Mach number effects are important and need to be studied; in particular effects on the turbulent spot. Another suggestion was to extend the Gostelow spot spreading rate celerities to a more relevant adverse pressure gradient parameter range as the present range is too narrow. Continuing work on attached boundary layer bypass transition was also suggested, as there is still a need for improved prediction methods.

Non-technical suggestions were to try to define short-term deliverables that can be used by industry in the near future, and to enhance the peer review process by adding outside experts to our workshops. There was a suggestion to establish international research collaborations on various topics. These are quite possible as long as proprietary data is not involved; and no funding is needed, we may be able to provide computer time, the only question is how to implement it.

Gostelow Thank you Dave. That keeps us moving.

End Users Group

T. Simon Most of this technical part came from the discussion the first evening. We were looking for a clear statement of where we would like to be, what we would like to provide, what would be useful to industry. We came up with this description. For the purpose of looking at off-design analysis and making their design choices in the early stages of their design, which is a very important part of the design cycle, a robust transition/turbulence model is needed for making these decisions, and that must include the calming effect. They also need a detailed analysis for being able to analyze their final candidates and, difficult to explain how it might be packaged, but it is important that we provide to them a clear description of the physics so that the designers and others within the company making these important early decisions in the design have a physical feel, and not just a program, for the processes taking place and how they might be able to use them.

It would be ideal if coming out of this work, or stemming from this work, a design could be developed that would be de-sensitized to strong Reynolds number effects. Designs that would not be quite so strongly changed by small changes in the shape of the blades or small changes off the regular design characteristic. It was stated that modeling attached flow is done satisfactorily but that for separated flow the models are not satisfactory. That was stated in the meeting but I heard beyond that meeting a number of comments saying that many feel that the analysis of attached flow transition is still in need of considerable development.

This group was very quick to frequently move off of the detailed technical part in thinking about the practical aspects of getting things going. There are two components to this. One which I call management and the other which I call funding. They aren't that different from each other but let's work with the management. In this text we use the word "we"; I want to be sure that we are not excluding industry. I mean by "we" that all of us working on this problem together are included and certainly that's an international group. We decided that NASA, AFOSR and maybe DOE ought to take on the responsibility of some long term planning to look farther into the future and decide what ought to be done now in preparation for the next generations of engines in a climate which is providing a lot of pressure to take care of the immediate needs. Somebody has to look over the long range issues. Dave Wisler explained to us about a gap which exists in industry now because there was a time when they

had people working on what was called the enabling technologies group - the people who would take the basic research and published information, massage it into the most useful form to be used in design, and then pass it onto the designers. These people have been re-assigned and these enabling technology groups are not such a clear entity any more. And so there's a gap. And we agreed in our group that people on both sides of that gap ought to be doing what they can to move the most useful information into that design setting, across that gap. This was mostly from Dave's early presentation in this group and then followed up by discussion in our group. Transition is important but there are a lot of important problems, and industry needs to consider all of those and transition work in that context. If we want to show the importance and value of what will be coming from this type of work we need to cast it in terms of things that describe the improved performance that comes about. There was quite a lot of discussion trying to see if we could get advocates out of the group that would advocate strongly for support. One agreement that we got was that there really needs to be a better understanding by people outside of industry of the industrial needs. The industrial people in our group agreed that they would be willing to explain to those of us who are interested and want to take the time to learn what the problems are in depth; they have offered that opportunity for us to learn more. They ask the academic people to do a better job of striving to understand the problems and needs that they have. This was a plea for mutual cooperation and understanding of the other side's problems.

Though I had an interest in the second day in trying to re-direct the group back into technology there was a long and very active and animated discussion about funding. Because again the practical aspect is - this work will probably not get done if is going to be a hobby. There is going to be a need for funding support to keep the activity going. So we talked a great deal about that. We would like to use the advancements that have been made in Minnowbrook I, and now Minnowbrook II to show that this work is showing progress. We wanted to show that all of us getting together from our so many different perspectives are truly providing the base that will eventually be addressing the needs that I showed on the slide. We need to clearly show the benefits to industry of these projects and I mentioned before how this would best be cast. We need to show specific gains in industry, we need to be able to show that the methods that we would propose, or the test programs that we would propose, can have a direct impact on the industry. We should be keeping that in mind as we talk about continued funding. There was certainly a lot more said about funding but I chose to highlight these aspects.

Gostelow Thank you Terry.

Direct Numerical Simulation

Sandham I am just trying to summarize some of the discussions of the group that met to talk about possible applications of DNS to flows with turbomachinery application that we can expect over the next few years. The background was really set by Roddam Narasimha in his opening talk. Turbomachinery Reynolds numbers are in the interesting range. You might substitute "difficult" for "interesting"- we have lots of phenomena associated with low Reynolds numbers, separation and transition but in a complex geometry environment. There are perceived problems with the models that are currently available to treat these flows. A question that we addressed in the group was "is DNS feasible at the moment and over what time scale is it feasible for really contributing to understanding the flow in turbomachinery applications"? One group of applications would be those that could be done over a time range of zero to three years - basically jobs that could be done on current supercomputers. We are

not insisting for these simulations on any great increase in computer power. Stuff that could be done straight away if the codes were available and if we developed proper boundary conditions to be able to run them. Our first group of simulations would be on spots. The first point is that some of this has already been done. There were simulations as long ago as the late 80's by Kim and Henningson at NASA Ames of spots in channel flow and temporally developing channel flow.[1] They didn't really get as far as a fully developed turbulent spot but even on computers of that time there was work on turbulent spots.

More recently we are not totally sure of progress made by Henningson; we suspect there is some recent work on spots being done in Sweden; also Bart Singer at NASA Langley had done an incipient spot simulation following blowing into a laminar boundary layer[2]. However what we suspect is that the range of pressure gradients that are interesting for turbomachinery application and also the range of Mach numbers, which was spoken about in a previous talk, has not been done and the data is certainly not widely available for any people who are interested to access that data and try to understand the physics of the spot flow. So certainly there is a need for a range of simulations. This would be a Falkner-Skan parameter, zero pressure gradient, -0.14 has already been done experimentally, this would be a good one to re-do computationally and the simulations could in principle be pushed further into the adverse pressure gradient up to separation whereas experiments are more difficult in that region. There was some discussion of the sensitivity to the particular trigger that you use to develop the spot. In a simulation you want the spot to develop quickly so that you are not wasting computational resources computing a laminar boundary layer. So to do this it is expensive to start with a very small perturbation leading to a linear response, a wave-packet response then developing very gradually into a fully-fledged turbulent spot. That's a limit of our expensive calculation. There are things that can be done much quicker. Putting in very big perturbations or even putting in artificial spots of turbulence from a simulation of turbulence that could give you a spot quicker. But there is a sensitivity issue; is there really a unique turbulent spot that we would get independently of how we start the process.

Separation bubbles are already feasible and work is in progress on looking at separation bubbles. There is also turbulent separation and a turbulent reattachment that has already been simulated. Spalart and Coleman have done this simulation of a small turbulent separation bubble. Peter Voke at Surrey has done the T3E test case -the laminar separation bubble around a semi-circular leading edge geometry and that has been done with Large Eddy Simulation. So there is work in progress on separation bubbles - what isn't really in progress at the moment is work on a single blade which from our discussions we really conclude is feasible on supercomputers. I certainly hadn't realized before this meeting that the Reynolds numbers were quite so low in turbomachinery applications in some situations. The obvious one to go for is an LP turbine blade with a chord Reynolds number around 50,000, a Mach number of 0.8 maybe; there is some interest among some of us who do DNS in applying compressible codes to turbine problems rather than incompressible codes. There was some discussion of geometry. I'm not certain of the details but Om suggested something with the same loading as the cascade B situation. This would be a uniform oncoming flow over a single turbine blade. Not looking at complicated effects of wakes. But this is really the first stage in developing DNS for turbomachinery applications - to do a single blade in conditions where experiments can be

---

1 Turbulent Spots in Channel Flow. D.S. Henningson et. Al., *Journal of Engineering Maths* 28 (1), 1994, pp. 21- 42.

2 Characteristics of a Young Turbulent Spot, B.A. Singer, *Phys. Fluids* 8 (2), Feb. 1996, pp. 509-521.

done for comparison or have perhaps already been done but maybe more data could be made available. The experiments need to be very well defined. We need as much data as can be measured to be able to set inflow boundary conditions sensibly. Spectra are not adequate by themselves. We really need a complete resolved flowfield of what is coming in. This is impossible to do experimentally but really spectra do not define a unique turbulent flowfield.

So that is what we think could be done right away. Then we had a think about what could be done over a longer time frame of 3-10 years. This is relying on improvements in supercomputer technology. We might expect over a ten year timeframe to see a factor of 10 increase every 3 years if previous increases carry on into the future. There is no guarantee that is going to happen. I was at a talk just before coming here by the people from Cray and what is driving high performance computer development is not applications to science. They make money by selling high performance machines to banks, to people setting up very fast web access and people who are trying to make money out of computers. It may be that the next generations of computers are not necessarily the kind of computers that we would want to do these applications. We may have to change the way we try to simulate these problems to fit the sort of computers and chips that we are going to have in the future. But if we project previous increases into the future this is the sort of increase that we could expect. Things that then could be done: The next stage in complexity is to have a wake impacting on that single turbine blade that we had already simulated. The wake could be from another blade, which involves doubling our computational cost. It could be a circular cylinder placed upstream, although Denis Doorly pointed out that circular cylinder simulations are very expensive at the moment. I suspect that it is actually cheaper to do a blade rather than a cylinder wake. There is a very wide range of length scales in a circular cylinder. To get an equivalent wake you have to resolve the very thin boundary layer at the leading edge of a very, very small circular cylinder. This makes the simulations more difficult. Then the next stage would be to multi-stage, to try to get into turbine applications. The big issue here is inflow boundary conditions. Can you measure what is coming in to a single stage with enough precision and data to give us a sensible initial condition? Thorwald Herbert's suggestion is that instead of starting in the LP turbine, which has the lowest Reynolds numbers, we should actually start in the HP turbine, where no one knows what the inflow is anyway. We can start with something reasonable there and by the time you have been through a few blade rows you lose the dependence on the initial condition. So really the building block, as Thorwald has pointed out, is the single blade calculation. Once you have that then parallel computing makes it very easy to replicate that same simulation to do different stages, static and rotating rows of blades and build up a complete simulation, over something like this ten year period, of a complete turbine.

End effects are things that could be looked at. Initially we would be looking at flows that were uniform in the radial direction. End effects have to be looked at. This makes the HP turbine easier to do because you have a narrower section. LP turbines are more difficult. Cooling etc. etc. Complexities can be added later. That is what we came up with as an overall strategy.

Jones You said you were going to say something about the calmed region.

Sandham I mentioned spots. The spot simulations would be fully developed spots that go as far as the laminar boundary layer surrounding the spot. This includes the relaxation back to laminar flow.

Jones Most of the cases, you said, were incipient.

Sandham Singer's spot was quite well developed (it is published in Physics of Fluids about 1994). He got quite a long way through the simulation in a spatially developing calculation

that was very expensive.

Gostelow Thank you to the four moderators. Let's pick anything else up in discussion. We will now move on to the summing up session. May I now hand the chair over to Ted Okiishi and Roddam Narasimha.

General Discussion

Narasimha Let's get your comments on what needs to be done. We need not proceed group by group.

Halstead I had one point concerning the DNS group. Was the consensus that in the next zero to three years we are in a position to do an LP cascade blade.

Sandham It is feasible now to start doing that problem. It doesn't need any more computer power.

Halstead There is a lot of laminar flow. You made the point of not wanting to expend a lot of computer time in a non-active flow. But you think this is do-able?

Sandham It is do-able but we haven't specified the initial conditions. That would need to be discussed later. There would be ways to trigger transition artificially just to give you something representative of a proper blade or you try to put high amplitude free stream turbulence in, both the experiments and the simulations, to make sure you get transition.

Okiishi Any other questions or comments?

T. Simon You said the power spectral distribution characterization of the flow approaching the test was not sufficient. Suppose we were able to measure long term velocity versus time wave-form records. Would you find that more useful? Could you use that instead of spectral distributions?

Sandham Possibly. I should refer this to Mohan Rai who has actually tried to replicate the spectrum by simulation. The way we try to do it is to do a separate simulation of the turbulence coming in that we would hope to match anything that you could measure.

Rai Actually what I have done in the past is to match the spectrum to some extent. Length scale and intensity. I wasn't sure what you meant when you said we need even more than that because right now I don't know how I would use more phase information. But that much, carefully documented, would be a good starting point.

Sandham My point is that it is a starting point but it does not describe uniquely the turbulence structure.

Rai Yes but you may not be able to reproduce that uniquely defined turbulence numerically. I think all you can do is reproduce the statistical properties as well as you want to depending on the number of iterations. Some of these discussions we had at our by-pass transition meeting at Lewis.

Reshotko Weren't your initial conditions actually velocity components versus time and space?

Sandham He needs velocity and pressure as a function of three-dimensional space. We don't have measurements of all that.

Reshotko No but Terry was suggesting getting that sort of thing. You can't get it at the actual nodes but you can presumably get a distribution of these quantities.

Rai But that's what you would need. You need to know all these quantities on the inlet grid. At every point the space and time distributions. Were you talking about something as detailed as that? And even then we would have to match the exit boundary conditions very closely with experiment. It can get pretty complicated.

T. Simon I wasn't thinking of that detail. I was thinking of a few representative points of the inflow. A detailed time record of the velocity.

Rai It would come in useful but I think you could do it with the spectrum and length scale as a starting point.

Okiishi I have a question for Terry, or anyone else. The acoustic and aeroelastic applications. You seemed a bit hesitant about the acoustics because probably not too much was known about that application as it relates to the calmed region or transition.

Jones It was one of the members of the group who brought this up. I will defer to them to explain the mechanism - Paul.

Gostelow This was a hypothesis. There is fundamental forcing behind the acoustics of turbomachinery. There is fundamental forcing physics behind the aeroelastic aspects of turbomachinery. I am not up with the current state of the art but, in the past certainly, there has been very much a cookbook approach to those basic questions of what are critical reduced frequencies and so on. What it is that separates the steady from the quasi-steady and unsteady behavior. That physics has always been kept in a black box, not understood. My suspicion is that the calmed region could be very important to that physics and therefore when looking at what we are expecting out of this increased recognition of the calming effect it is important to recognize that we are not just looking at efficiency; beyond that we are looking for improvements in separation resistance, tolerance, stall etc. and beyond that even we are looking to perhaps linking up some of the basic physics of the aerodynamics, the aeroacoustics, the aeroelasticity and that really, if we get it right, they should all be coming from the same basic physics. So it's a bit vague, general and long term. But it would be a big mistake to say the benefits of the calmed region are simply in efficiency. I don't believe that is the case - I think it goes way beyond that.

Okiishi Is there anything that those of you from the engine companies or those of you who work with the engine companies can say about this that will not get you into trouble?

Wisler I think that we can solve "nasty flow" separated regions of, for example, inlet guide vanes onto first stage rotors. We had one situation in the same engine family where a particular design A when they were off-design at low flows (start-up) produced a separated region that the rotor could tolerate. Design B, for reasons that we really don't understand, produced a two stripe instability that caused a near failure. This was not a flying engine but a development engine, it was repaired. We don't understand, in off-design conditions, the nasty flow. You start getting separation, where does the separation occur, how is it manifested downstream of the forcing functions to the next blade row. That is all aerodynamic and all highly tied to where the flow separates and the structures that occur afterwards. And so we are in the box of having to now run experiments to see if we can sort through and see how we can tune our models to the experimental data. That is a very important issue.

Reshotko Probably transition is the key.

Wisler Oh yes - absolutely. Transition, and where the separation occurs, and how the separation vortex leaves the airfoil.

Gostelow Can I throw in a question. Maybe the industry guys can shed some light on this. If there are calmed regions, let's say in compressors, from wake interaction effects, are there also calmed region effects to be observed, or something like that, from say circumferential inlet distortion situations? Should we be looking to see if there are implications there? Would it help our inlet distortion prediction capability?

Sharma I think the length scales may be much different for inlet distortion. The distortion may be of the order of 180 degrees. I think it is a different scale problem.

Gostelow But again there are cookbook approaches still to some extent. and maybe some of the basic physics of this could be explained if we were able to push some of these things on a little further.

Sharma That's on the point which Dave was making about trying to predict the off-design performance and I think that's what you were implying with the wake effect on the downstream rotor as well. More or less all simulations done to date, where Reynolds Averaged Navier Stokes were used the flow is assumed to be turbulent. We were just going from streamline codes to three-dimensional codes. So the transition aspect was not modeled and when you are off design you have leading edge separation bubbles and those models are not really there for getting robust calculations that we could use.

Okiishi Do you have a similar anecdote to offer, Om, relative to acoustic/ aeroelastic drivers in relationship to calmed regions and transition?

Sharma I would say it is not the calmed region. It is this progress in going from laminar to turbulent flow. The calmed region is a part of it really. If you think about it the only place where the flow doesn't want to separate, as the boundary layer grows, is during transition. Laminar flow increases in boundary layer thickness; if you diffuse it wants to separate, the same thing for turbulent flow. For the transitional flow the skin friction is increasing as the boundary layer is tightening up. The physics of transition is telling you that there is a calmed region, it is less susceptible to separation. I think that is a part of the transition modeling. As far as aeroelasticity is concerned it is driven, again, by laminar separation at the leading edge. Modeling that will be useful. On acoustics we have Nick here. I think noise generated at blade passing frequencies maybe manipulation of the boundary layer could generate calmed regions and may have beneficial effects.

Cumpsty I just think that the acoustics knowledge is too primitive to be able to say really. It is certainly not advanced enough to be able to take advantage of the calmed region in an explicit way.

Gostelow Is it worthwhile making that some kind of a goal?

Cumpsty I think it is fair to say that the whole study of acoustics in turbomachinery went into decline about twenty years ago and I think it is just coming out of that decline and building up. But it is probably premature for us to make a suggestion regarding transition.

Okiishi O.K., Don.

McEligot I have a question of clarification of one word that Terry used, and this is for Dave of course. What is the definition of "robust" as you see it in industry.

Wisler "Robust" in simple terms means that over a wide envelope of initial conditions or boundary conditions the code will function without going unstable or failing. It will function, it will give an accurate answer for the flowfield, both function and give good results. In such a way that the designer or user does not have to worry that his various knobs are tweaked in a specific flow range and take careful interactions with the program to keep it from going unstable. So it works accurately over a wide range of the envelope.

McEligot I wondered whether you just meant that the code would run?

Wisler No. It is stable over a wide range of incidence angles and Mach numbers and geometries.

Sharma I agree with Dave. Normally when you are doing a simulation you are doing a simulation of a large part. If you are doing a multistage calculation and one row of the solution becomes unstable this can cause problems in the modeling of the whole machine.

Norton We saw an example of a non-robust prediction at the workshop. That one where the transition location moved back and forth as the code tried to converge. It switched between using the attached flow criteria and the separated flow criteria. For a robust code we need to make sure this does not occur by looking at the turbulence models and then matching, for example, the separation transition criterion with the attached flow transition criterion to make sure that it is a continuous smooth function.

Gostelow This was one of the points that was made very early on the meeting, that we must have a smooth and robust move from the transition criterion to the laminar separation criterion and one that is comprehensive enough to take on board all of the conceivable modes that apply there. If we have a gap between the two, if we have separate physics for the two, it is a sure recipe for it not being robust.

Okiishi Other questions, comments? I wonder for the DNS group applications way out into the future if, in addition to blade end effects and cooling, clocking effects might be an important consideration. Clocking has been a hobby of mine for years; I keep thinking there is something there in the clocking but nobody has been able to show this definitively.

Cumpsty Ted. I would have thought that as far as compressors are concerned NASA have done that. There were those tests where they moved all the blades around. Yes they did find there was an effect but it was in the scatter band. If you took lots of measurements you could just perceive the trend. So, yes it is there, but having in mind that this was a special rig where all the blade numbers were the same so that you would expect the maximum effect I concluded that it had been definitively shown that it was too small to be interesting.

Okiishi I wasn't thinking so much of aero-performance as aero-elasticity. I wonder if there are some forcing functions that occur somewhere in the machine because of oddball clocking arrangements. A peculiar blade that is targeted for failure just because of the drivers.

Cumpsty Yes. I believe you there.

Halstead Isn't this possibly a bigger issue in turbines? Isn't that what Om's data has shown?

Okiishi You mean - getting back to performance?

Halstead Well yes. Performance and even the heat transfer characteristics.. Can certain blades be in a hotter area than others depending on the clocking of an upstream blade?

Okiishi I don't know. You did that work on the Space Shuttle Main Engine turbines and there the blade counts are identical.

Sharma I think clocking to a large extent we are doing it. I don't know what additional gains we could gain from DNS. I would rather apply DNS to some other problem like interaction between rotor and stator, identifying loss generation mechanisms. I think clocking is more mature technology.

Herbert If you talk about DNS there is no principal problem including fluid-structure interaction. The major problem is still to compute the fluid. So you could in principle include additional effects such as blade oscillations, loads on blades and so on.

Sharma That's a good point. That problem has not really been done. Because the blade has oscillations how does the stage characteristic change as a result?

Rai I think the Reynolds-averaged computations have been done, time accurate.

Sharma I don't remember what conclusions they reached.

Rai I can't remember; it's not one that I was involved in. But I think he brought it with him to Pratt. I don't think he was looking at transition - more blade-wake interaction in a traditional RANS type of situation.

Gostelow Can I pick up a question from Neil on DNS. He wonders about the expense of simulating a triggered spot, starting right at the beginning with linear development and so on. Nevertheless there is this real worry that the end result might be unduly sensitive to how it is started. If one infects the flow with turbulence there have to be methodological questions as to how this was done. Is it that much more expensive if one just has a minimal seeding or even looks for a naturally occurring spot and lets it develop through the various stages.

Sandham It really depends how low you start your initial fluctuation.

Gostelow I guess I'm suggesting that it would be worthwhile to take the time to go through the various stages of development, and on the way one would develop a very good feeling for how the spot came about.

Sandham It is feasible at the moment but you have to weigh up do I do one very big calculation like that or do I do five smaller calculation, for example over a range of pressure gradients. Do I do one large calculation and wait a year for the results or do many more runs?

Herbert You can speed it up by calculating an adverse pressure gradient.. Then you can go from very small to the end of the run in much shorter time than if you had a favorable pressure gradient.

McEligot Which situation is relevant to the turbine blade or the compressor blade? Isn't that the one you would like them to do the DNS for?

Gostelow I think you are really looking at the regions where there are adverse pressure gradients anyway, whether it is turbine or compressor.

McEligot But it's a specific blade you are talking about, either turbine or compressor.

Herbert At these relatively low Reynolds numbers you don't get any transition if there is a favorable pressure gradient. Typically for transition you have to support the Reynolds number by having an adverse pressure gradient. and then transition happens faster and the

computation happens faster too.

McEligot Don't we have a relatively high turbulence level that is likely to trigger transition?

Herbert That is usually only a small effect.

Narasimha I just wanted to raise a question that Neil Sandham already raised from his working group. If we were going to go ahead with the DNS exercise on a blade is there a good candidate for that blade? Namely one which has been widely studied experimentally, on which there is some experience, some data, so that one could validate the DNS with that data, or a blade which has interesting characteristics that are difficult to model, where DNS could immediately make an impact on the use that could be made of the solutions. Is there a blade like that of all the tests that have been made?

Okiishi Is it the Pack B blade?

Sharma The Pack B blade is the incompressible version of a compressible blade for which I have very detailed data. Skin friction, unsteady skin friction etc for two different turbulence levels. I have information over a range of Reynolds numbers for that same cascade and full span data.

Okiishi I think that is a very viable cascade.

Cumpsty We could also propose the compressor cascade tested at Monterey by Zierke and Deutsch. They did very careful laser measurements on those blades.

Okiishi They tested that in the large cascade at Monterey as well? So we have two, one turbine and one compressor.

Narasimha That would give a very focused objective to the DNS. We should quickly be able to clarify whether results are coming or not.

Okiishi Every detail you can imagine is available for that compressor blade.

Anyone want to take a crack at the synergies? As we listened to the four groups there were some obvious synergies came across, like the need to measure what is happening in the engine environment will impact on two or three of these groups. So are you all willing to pitch in a few dollars as you leave?

Gostelow Is that what synergy means?

Okiishi Haven't you learned that?

Laughter.

Concluding Remarks by Professor Narasimha

I have been asked to say a few words as this meeting draws to a close, and I don't intend to take more than ten minutes. What I am going to say is a personal reaction to this meeting following the first one we held here four years ago. First of all we could ask ourselves where are we in relation to the position as we saw it in 1993 when we met here for the first time. I think it is even clearer today than it was four years ago, that we are in the business of handling a very interesting flow situation. I think Greg Walker mentioned in his review that well known Chinese curse and the version of that that would apply to Minnowbrook is to say "May you

have a very interesting flow situation to tackle, without assured funding." It seems to me that this is the situation which is actually developing here. I would not be surprised if the kind of flow situation that prevails on turbomachinery blades is, in some sense, the most interesting fluid mechanical situation in a piece of technology. In what we have been calling this fluid mechanical zoo we have separation bubbles, we have reattachment, steady and unsteady transition, periodically-forced, stochastically-forced, re-laminarization; we didn't talk too much about that at this meeting but we did spend a great deal of time looking at the physics of the calmed region. We have turbulent spots, we have turbulent strips with growth of spots within those strips and so on.

But the people from industry have reminded us again and again that it is not enough to have a problem that is interesting, you actually have to have something which will make dollars for somebody. And it was pointed out, I think it was Dave Wisler who said, he would be very happy to have a half percent improvement in efficiency provided he didn't have to pay for making sure that that half percent emerged. So we have a situation here where there are a lot of interesting fluid dynamical problems but what is going to be done on those problems will be eventually judged by whether it leads to improvement in real turbomachines. There are other flows in the awkward Reynolds number range that turbomachines have to handle but these are either not so rewarding financially or maybe not even so interesting. I have in mind in particular birds and windmills. Keeping aside the issue of funding I would like to spend a few minutes on the physics of the problem and where we seem to be now, compared to four years ago.

On separation bubbles I think we heard here many interesting studies this time. Experimental there were presentations by Wygy, by Ting Wang, simulations by Neil Sandham, Nick Cumpsty's measurements and many others, and it looks to me that here, after a lull in the interest in separation bubbles, from the early days when people discovered those bubbles, some 30 or 40 years ago, it seems to me that now interest has picked up again and it would not be surprising if in another few years time, if there is going to be a Minnowbrook III, this problem will be under control. I think we are beginning to understand it, because all the elements required seem to be now getting in place.

Looking at spots, well I recall that ten or fifteen years ago there was very little work on spots after the first pioneering work by Schubauer and Klebanoff and some others. I myself at that time thought that if spots were studied under a variety of different arrangements and situations there would be many surprises. So it is very gratifying that during the last five years there have been many such studies on spots. Paul Gostelow and many others have looked at situations in which the observed behavior of the spot is falling into certain patterns. But I want to emphasize that observing and measuring what a spot does is still different from understanding it. Because I think that even fundamental questions about spots cannot be understood on the basis of principles here. We know what a spot does and we are getting to know what a spot does in a variety of different complex situations but I think our understanding of spots is still very primitive. I see that Frank Smith is the only brave attempt here to look at spots from a theoretical viewpoint and I think this is one area where we actually very badly need theory. I want to recall here what one great physicist said (Boltzman) "There is nothing more practical than a good theory" and on spots that is really what we lack now. A good theory I think would be a very practical thing. At the same time a complete theory is unlikely. I should say that also because after all a spot is turbulent and we still don't have any theories for turbulence either. There may be bits of spots which we may be able to understand. For example on the calming region the kind of analysis that Terry Jones presented will give us a feel for what is going on, provided we took the rest of the spot for granted. That is to say "If

the spot is this way, what is going to happen to the calming region?" But that is laminar flow, so we understand it. But why the spot was that way, still, I think, remains an open question.

There has been considerable emphasis in this meeting on the calmed region. This is the calm that follows the storm of the spot and it is getting to be observed, getting to be analyzed and many possibilities of its exploitation are also being assessed. There might indeed be something there. Howard Hodson showed how the calmed region lends itself to application, going back to a suggestion that was made he had a very appropriate quote from Schubauer and Klebanoff. I still remember that. They had noticed right away that there was this calming region and in fact there might be an advantage in triggering the spot so that you could make use of the calming region. It seems to me that there has similarly been very considerable progress on understanding (understanding is a dangerous word) in getting a grip on unsteady. periodically forced transition. The simplest situations here are getting sorted out; many experiments have been made, at G.E., the Whittle Lab., elsewhere, which are beginning to tell us what the nature of this animal is. One thing that we must realize is that periodically-forced transition will not, in general, be the same as what you might call statistically-forced transition. We use the words natural transition, free transition and so on but in fact there is no free transition in boundary layers. All boundary layer transition is forced in some way or the other. It's a question of whether you have control over the forcing or you don't have control over the forcing. Now basic intermittency distributions, the Emmons formula, the kind of distributions that we have used, all of these assume some kind of statistical forcing, so we must be careful not to use those ideas when the forcing is periodic rather than statistical.

Now the effect of wakes generated by upstream rows on transition has been studied quite a bit. I think there is a general feel for the strips that result from such forcing and the effect that they have on the boundary layer characteristics. There has been a lot of discussion about how this forcing would have to be taken into account if one were proposing to make detailed calculations on what happens on the blade, let's say in some n-th stage in some turbine. Now at first it would seem as if you really need to know everything that happens in all the stages upstream before you can actually get a handle on the situation. Now, I must confess to a prejudice here; I don't see that happening. I think that what is needed is a different way of describing the disturbance environment within the turbine. I therefore welcome the suggestion made by one of these working groups that there should be a special program on the turbine disturbance environment project. It seems to me that that would be very important from the point of view of applications and that should lead in my view to different ways of characterizing the disturbance environment. Now that's not just going to be the spectrum or correlation of scales, it might actually have to be an event-based statistics of the disturbance environment in the turbine stage. An interesting question would be how many stages have to pass before you can describe the environment with some kind of statistics, maybe new statistics, what that statistics is we will not know until we can find out how the characteristics of those blades are determined by this forcing environment. But I think an attempt to define those statistics and to characterize the disturbance in new ways is very urgently needed.

We go on to modeling. I think the situation now has changed very considerably in the last five years. There are now a very large number of models and I think the models are multiplying very fast. What happened in turbulent flows, which was that over a period of time you had a very large number of models (in my own personal view too many but I will not press that point of view too much here), may happen in transition in the following sense. First of all I must say that the formulation of these models should be welcomed. I think that it could tell us where the problems are likely to be. These models may appeal to the intermittency. That is you treat the intermittency either as a parameter or, in other cases, you treat the intermittency

as a dynamical variable. Both kinds of models now have been pursued and several presentations were made here showing what these models can do. I must confess to a personal prejudice for simpler models and not necessarily because they always perform better, but because if you wanted to consider how to manage a flow, how to control it, how to manipulate it, I think the simpler models give more insight than the more complex ones. Modeling unsteady transition is one of the major problems here that need to be pursued.

Let's come briefly to the situation regarding DNS. Neil Sandham has already made a presentation on behalf of this working group. While it is possible that our friends in industry will ask "what will you be able to deliver?" that would actually make more money at the end of so many years. I don't know whether the answers to that are very clear yet, but I would take a long term view, especially at a meeting like this. It seems to me that this is one fluid mechanical problem, not of technology and nature, where the Reynolds numbers are not impossibly high, in fact a Reynolds number of 50,000 on a blade is actually quite low, but if it were laminar flow on that 50,000 Reynolds number blade, it would not be worth simulating; we can handle that problem easily. What makes the turbomachinery problem so very interesting is that the Reynolds numbers are low but at the same time the flow is not easy to model. If one were to look at all the fluid mechanical situations in nature or in technology where there is a chance that DNS will give us real results I would say that turbomachinery is the prime candidate. Why? Because it is in that Reynolds number range and it is not something that can be easily handled by other models. So we must take a look, as Neil has done, at the next three years as well as the next five to ten years. So I would like to stick my neck out and make a prediction. Namely, that the first major technology field where DNS is going to make an impact is turbomachinery. Let's see whether that will happen or not. It seems to me that there is a good chance but I see a better chance in turbomachinery than in any other area. And therefore I think it is good to prepare ourselves for the future and, in fact, if it is at all possible to make it happen. I am not for a moment suggesting that one should make DNS for the full turbomachine. I do think that is well in the future and in fact it is not even that it would be worthwhile at the present stage. What is necessary however to do that kind of DNS, or parts of it, which would help us in defining what the designer needs to do and in giving us those insights which will actually help the designer. I do think we should keep the designer in industry in mind all the time. But there are many situations where the physics is not understood and I think one of the major objectives of such a program would be to give us insights into the physics and help the designer although not necessarily insisting that the full turbomachine will be designed by DNS. It will not need to be, not even desirable, because there is a lot of information in DNS which would probably never be used in applications.

Finally, I come to what one might call theory. And I think that Frank Smith's tribe needs to increase. As I said earlier theory is now badly needed. It doesn't necessarily follow that theory will automatically be available because it may need ideas which we have not thought up yet. The kind of approach that Frank described, and others, I think needs to be pursued. Stability issues, for example; he started by asking "is stability relevant for turbomachinery flows?" And I think the answer was "while it is not relevant in the same sense as it might be, let's say, to aircraft wing design stability will still give us considerable insight into what goes on on a turbine blade or on a compressor blade." There have been many approaches possible here. Thorwald had described PSE. We think we have other ways of looking at it. Eli Reshotko described how algebraic growth of transients can affect what happens on a blade. And I would like to emphasize again that we must make a distinction between the relevance of T-S waves and the relevance of linear response theory. These are really two different things and I think that linear stability theory, linear response theory, algebraic growth, all these things

will still give us considerable insight into what happens in certain aspects of turbomachinery flows. Also questions concerning absolute instability and convective instability, I see that they have not yet made a big impact on turbomachinery flows. Maybe once again because of this feeling that the large disturbances that one encounters in turbomachinery will make these not directly relevant. But I am saying if in fact there is a stage of linear response the situation may change there.

Well. Is there something missing in the scene just now? In which directions might things go in the coming four or five years? I thought I was a little surprised by how little mention there was of three-dimensional effects. By and large a lot of the work still seems to be on two-dimensional flows. Of course it is essential to study 2-D flows, I have nothing against that at all, it is the basic building block. But considering the very strong three-dimensionality of flows in turbomachinery it seems to me that that will require more attention. Neil Sandham presented this DNS work but once again looking at the Reynolds number range I would have thought that there would have been much more DNS and LES in turbomachinery applications. Talking about aircraft wings, there is no point in DNS, it is impossible. But in turbomachinery I would like to see more of this done. I already mentioned more theory. More on multiple stages. I don't know whether it is practical or not but it would seem to me that the experiments on which single blades or single blade rows or cascades have been investigated should now move on to installing multiple rows upstream. Try to see how things get more complicated as you install one, two, three and more rows upstream still making measurements only on that same set of blades. I would very much like to see an experimental program in which the blade row which you are investigating is fixed but upstream you keep on adding more and more complicating factors, and so on.

I must say that I have enjoyed this meeting very much. I think that this meeting is unique. Why is it unique? It is unique because it brings together in this atmosphere, apart from the fact that this place is lovely, people from industry and people doing basic research, together in an atmosphere that as far as I know has not been captured by any other meeting. One has attended other nice meetings but usually it is within closed communities. You are all talking to each other in a way that you have done for years. But here is an opportunity where people from industry, people from government labs, people from academic institutions can all get together but still look at one focused problem, namely in this particular case, turbomachinery. And I think that the organizers of this meeting have done a wonderful job getting this diverse group together and giving them an opportunity to talk to each other. And so I would like to take this opportunity if I may, to thank on behalf of all of you, the three people who organized this meeting, John LaGraff, Paul Gostelow and Terry Jones. Thank you very much for making this meeting so pleasant and so rewarding.

Gostelow I would like to thank Roddam most sincerely. First of all his clarity has taken on board and done justice to the meeting in a remarkable way. Those remarks that Roddam has made will be captured, will be printed, you will have copies of it all. I think that Roddam started the meeting in a challenging and a provocative way, that got discussion going. I think he has wrapped it up in a positive but also provocative way that will keep the work going. That is very important. And I would like to thank all of you for really having advanced the state of the art even over these couple of days. I think that you have all made a contribution to that. But especially let us thank Roddam for really summing up the meeting in a marvelously clear way. Thank you Roddam.

POST WORKSHOP SUMMARY

NASA/CP—1998-206958

MINNOWBROOK II - 1997 WORKSHOP ON BOUNDARY LAYER TRANSITION IN TURBOMACHINES
EDITORS: J.E. LAGRAFF AND D.E. ASHPIS, NASA CONFERENCE PUBLICATION 206958, 1998, PP. 485-495.

POST WORKSHOP SUMMARY

Roddam Narasimha

Fluid Dynamics Unit
Jawaharalal Nehru Centre for Advanced Scientific Research
and
Centre for Atmospheric and Oceanic Sciences
Indian Institute of Science
Bangalore, India

Almost exactly four years after the Workshop on End-Stage Transition [1, 2] (now seen as Minnowbrook I), nearly 50 participants gathered again at the same lovely site on the initiative of the same organizers (John LaGraff of Syracuse, Paul Gostelow of Leicester and Terry Jones of Oxford). As LaGraff reminded his audience in his opening remarks, the first workshop had sought to bring together two different communities involved in transition research: the JFM and ASME types, or high and low church, as Paul Gostelow had described them. The present workshop had a sharper focus on turbomachinery flows.

Roddam Narasimha (JNC/IISc, Bangalore) started the proceedings by reviewing what had transpired at and after Minnowbrook I. The distinguishing features of transition in turbomachinery flows are that they are unsteady on time scales longer than typical eddy turn-over times, occur in harsh and highly disturbed environments at awkward Reynolds numbers, and are generally three-dimensional (even in the mean). As a consequence the flow is a veritable fluid-dynamical "zoo", characterized by separation, reattachment, transition, relaminarization, retransition etc., all often occurring in the *same* flow. Greg Walker (Tasmania), in his keynote talk the next day, noted how "interesting" the problem was, and that this may be a version of the well-known Chinese curse about living in interesting times for turbo-machinery fluid dynamicists. Nevertheless, as Narasimha noted, there had been much progress on many fronts, but it was remarkable that ideas related to dynamical chaos, which at first appear so closely connected with transition to turbulent flow, had made so little impact on the subject they were going to discuss at the meeting: the reduction in the number of degrees of freedom that such ideas have till now provided is clearly not sufficiently significant to make a practical difference.

Minnowbrook I had been dominated by discussions on spots and modeling. Minnowbrook II saw much attention devoted to the characteristics of the calmed zone trailing a spot and the possibilities of its exploitation, and the understanding and management of separation bubbles and unsteady transition.

But how important is transition research for the turbomachinery industry? Walker cited GE compressor tests (made by Halstead) showing transition extending over 60% of the blade chord, and estimates of potential improvement in efficiency by several percentage points; considering how widely turbomachines are used in energy conversion and propulsion systems, significant economic and environmental benefits are possible. David Wisler (GE Aircraft Engines, Cincinnati) pointed out that the "lack of ability to predict the location of boundary layer transition for components in gas turbine engines is impeding our ability to gain maximum benefit from our design effort". If a complete CFD design tool incorporating transition were to be available, he foresaw airfoil designs with higher blade loading that would reduce part count and improve efficiency. He estimated that a 1 % improvement in the efficiency of a low pressure turbine would result in a saving of $52,000 per year on a typical airliner, but he was willing to accept even 1/2 %, provided it was reliable. Improved transition technology was thus very relevant. However Wisler thought it was unlikely to have a major impact on design: the gas turbine industry is now maturing, and is generally driven by cost and "error-proofing" the design rather than higher performance per se.

Apart from the gains that may be achieved if a reliable CFD design tool were to be available, where should one look to improve efficiencies now? The answer, as summarized by Greg Walker and widely endorsed during the meeting, appears to lie in the exploitation of the calmed region trailing a spot, understanding the time-dependent forcing of transition in a turbine row because of wakes from upstream rotor stages, and the management of separation bubbles.

Narasimha considered three-dimensionality important, and David Ashpis (NASA Lewis) listed 3D effects ("virtually unknown" in his words) as one of the barriers to progress. Several participants highlighted transition, separation and wake-boundary layer interaction as the major problems in turbomachinery boundary layers. Ashpis noted a 2% drop in efficiency from take-off to cruise (as the Reynolds number drops typically from about 300,000 to 80,000), and minimizing this loss was one of the objectives of the NASA Low Pressure Turbine Flow Physics Program (which involves aero-engine industries, several universities and government laboratories).

1. The Calmed Region

The possibility of exploiting the calmed region had been foreseen already in the pioneering work of Schubauer & Klebanoff, who wrote in 1955 (as Howard Hodson (Cambridge) reminded us) that "turbulence injected at the proper time intervals can in principle alleviate the severity of the turbulence 'disease'." As of today there is no clear demonstration of the efficacy of this "vaccination" principle - as we may call it - but there are now indications of how it might be done.

Terry Jones and John LaGraff described work showing that the behavior of the calmed region could be seen as the resumed growth of a disturbed laminar layer; the rate at which the calmed region trailing a spot grows is defined by the time for a new boundary layer to grow from the point where the spot was born. This view leads to a good prediction of the duration of calming, and a collapse of measured heat flux data as a function of time normalized by the duration so estimated.

Paul Gostelow pointed out that as the flow in the calmed region is more stable than the boundary layer it replaces, it delays separation and suppresses instability. In experiments on a flat plate subjected to strong adverse pressure gradients, Gostelow finds that the calm region behind a triggered spot is extensive. Its interaction with the natural boundary layer is complex, and depends on whether the boundary layer is laminar or turbulent. He introduces a new relaxation parameter to quantify and describe the calmed region, and uses the data obtained to validate his model for transition.

Hodson showed some experimental data indicating that a *higher* frequency of inducing transition spots could reduce the loss coefficient and trailing-edge momentum thickness.

Avi Seifert (Tel Aviv) reported on experiments showing that a train of spots generated some 200 momentum thicknesses *upstream* of the transition onset location can lengthen the transition zone and so significantly *reduce* the intermittency downstream in the transition zone; whether this would compensate for the *increase* in intermittency upstream and so actually reduce drag is not yet clear.

2. Unsteady Transition

The time-dependent forcing of transition already referred to attracted considerable attention at the meeting. Pavel Jonas (Prague) reported interesting measurements on the transition zone at different turbulence levels with superposed periodic oscillations of free-stream velocity (obtained by rotating a flap at the trailing edge of his test-surface). When the frequency of oscillation is low the final part of the transition zone is considerably longer, and the (average) skin friction shows non-monotonic variations in space; but if the frequency is high the transition is rapid as in a turbulent free stream. The changes appear to correlate with an unsteady Reynolds number directly proportional to the velocity amplitude and inversely to the frequency, with a critical value that determines whether the frequency is "high" or "low". Jonas also reported on the effect of turbulence length scale, which he could vary over a range of 1:15 in his facility without altering the turbulence intensity; he found a delay in the later stages of transition when the scales were small.

Hodson reported experiments using surface hot films from unsteady cascade as well as full-scale rig testing in an altitude test facility. David Halstead (GE Aircraft Engines, Cincinnati) showed detailed measurements of flow field unsteadiness in multi-stage compressors and turbines. These measurements provide not only the intensity and the spectrum, but also measurements of the length scales in a low-pressure turbine. The complexity of the unsteady flow field between blade rows was shown to increase markedly through the turbine. At the inlet of the second stage nozzle the unsteadiness correlates with the clocking position of the upstream nozzle blade row. (Such correlations might "select" particular blades for failure, as Halstead noted.) At the exit of the turbine, however, no such correlation could be found. It is clear that the wakes from stator and rotor blades upstream get chopped up, and that at some stage in the machine identification of the origin of various chunks of turbulence will become difficult, but it is not clear how deep into the machine one has to go before this happens. At the exit of the

turbine there is no discernible "free-stream" region, suggesting that experiments with moving wake generators upstream of a cascade or single stage will not simulate many features of the flow field in a multi-stage machine.

Om Sharma (Pratt & Whitney, E. Hartford) showed experimental data from an engine and a model rig to highlight current lack of understanding of the actual operating environment in the gas turbine engine. Analytical results showed the limitations of transition/turbulence models now in use in the low Reynolds number environment of low pressure turbines; this problem is important because of the loss in efficiency during cruise at altitude, where Reynolds numbers tend to be low relative to take-off conditions.

3. Separation Bubbles

Separation bubbles are another characteristic feature of many turbomachine blade flows. Ting Wang (Clemson) sketched three hypothetical modes of transition involving bubbles: (i) the short bubble at low Reynolds numbers (Re) and mild adverse pressure gradients, (ii) the long bubble - also at low Re but in strong adverse pressure gradients (in both cases the separating flow is laminar), and (iii) the transitional bubble. In the short laminar bubble, transition onset occurs at maximum displacement point, and maximum turbulence intensity (u') at (turbulent) reattachment. In the long bubble, there is a short, early transition region leading to the first reattachment type behavior, but the strong pressure gradient does not admit attached flow; a long and late transition occurs in the bubble before actual reattachment. The transitional bubble occurs at high Re and mild adverse pressure gradients. Here transition begins before separation and tends to house a long initial region (because of the constant pressure plateau induced by the bubble), and is followed by a short completion phase. Maximum u' occurs near the maximum displacement point. Ting Wang presented correlations for the Re values associated with bubble events as a function of an acceleration parameter for all three modes.

Nick Cumpsty (Cambridge) presented measurements showing how free stream turbulence and incidence have a large effect on the nature of the separation bubble. At low incidence no evidence of spot transition could be seen, but at higher incidence and low free stream turbulence spots were clearly visible in the bubble shear layer.

Fred Simon expressed surprise that even in separation bubbles the intermittency followed Narasimha's universal distribution, although the Emmons spot was presumably specific to wall-bounded flows. Narasimha explained that the universal distribution depended on three postulates: Poisson birth, linear propagation and concentrated breakdown; and if these were satisfied the universal distribution follows, whether or not the Emmons spot is involved. Thus, he had found that the temporal development of phase transition in metals followed the same or related distributions.

4. Stability

Eli Reshotko (Case Western) surveyed the role that transient growth (first invoked by Landahl in 1980 to explain the lift-up mechanism in boundary layers) can play, especially in roughness-induced transition (where there may be no evidence of TS waves), and presented a new picture of possible paths to turbulence in wall layers. In the

canonical TS route such transient growth (t.g.) is benign and insignificant. Other routes are that t.g. provides higher input to eigen-mode growth or directly excites secondary instabilities. Finally, t.g. can feed into the bypass mechanism. With very large forcing possessing a "crazy" spectrum, Reshotko thought bypass mechanisms can be directly excited without transient or eigen-mode growth. Interestingly he found evidence of transient growth in pipe experiments conducted at JPL in 1961!

Herbert reported that the PSE codes that work so well for external flows are less successful for turbomachinery blades. Among various possible causes, he found that there could be a serious problem even in the specification of the geometry of the blade (usually coordinates are given at too many points but to too few decimals). Further, computed pressure distributions do not agree with measurement (blockage corrections? gradients in outer inviscid flow? non-zero wall-normal pressure gradients?); these problems need to be first sorted out. Bob Boyle (NASA Lewis) emphasized the importance of using suitable grids for the turbomachinery base-flow calculations. At any rate, Herbert's codes have now seen various improvements like extension to swept-wing flows and inclusion of Klebanoff modes.

Narasimha briefly described work done with Rama Govindarajan (NAL, Bangalore) on a new formulation of boundary layer stability. This work leads to a hierarchy of three equations, most easily formulated for the Falkner-Skan similarity solutions. The highest member of the hierarchy is compatible with Herbert's PSE, but at this order consistency in approximation demands that account be taken of higher-order boundary layer theory, which presents difficulties and is therefore generally (but unjustifiably) ignored. The next member of the hierarchy is a lower order parabolic (LOP) P.D.E. that is simpler than the Herbert PSE; this is the *highest* order rational theory that can justifiably neglect higher order boundary layer effects. At sufficiently large Reynolds numbers this LOP theory reduces to an O.D.E. that is like Orr-Sommerfeld but not identical: two viscous O-S terms are absent but an additional term representing the transport of vorticity by the mean wall-normal velocity is present. All three members of the hierarchy apply to non-parallel flow. Results show significant differences from Orr-Sommerfeld only in strong adverse pressure gradients; in free shear flows the boundary of absolute instability can be substantially different, and this may be important for understanding separation bubbles.

Frank Smith (London) reported theoretical studies on near-wake transition, inspired by the need to understand rotary-blade/wake interactions. The near-wake may exhibit *two* length scales, because of the presence of a thin inner sublayer within a thicker boundary layer. He noted that a favorable pressure gradient may *destabilize* a near wake because of the negative profile curvature it induces. Smith highlighted various issues in which the stability characteristics of the wake - absolute or convective, linear or nonlinear - may be relevant to transition problems on blades.

5. Modeling

Models for the transition zone are now proliferating rapidly, and are being generalized to the unsteady situations prevailing in turbomachinery. Narasimha described briefly an improvement made by Dey (IISc, Bangalore) to linear-combination models, so that they can take account of the calming period and ensure better momentum conservation.

Fred Simon (with R. Boyle, NASA Lewis) presented models that utilize the dependence of spot characteristics on pressure gradient and Mach number for predictions of heat transfer; he uses the intermittency model of Solomon, Walker & Gostelow and correlations for the non-dimensional spot formation rate of Narasimha. He finds that relative changes can be estimated well independently of the model, but it is important to incorporate Mach number effects. His model gives good agreement with the data of Arts et al.

Johnson (Liverpool) uses a distributed breakdown model, postulating that spots are induced whenever the instantaneous velocity drops 50% below the mean - inducing transient local separation (an idea that I must point out goes back to G.I. Taylor). By making suitable assumptions on the proportion of minima that induce spots, Johnson provides a good fit to the intermittency near onset. With correlations for the spot formation rate parameter of Narasimha, he is able to get good agreement with the data of Abu-Ghannam & Shaw and Gostelow.

Fraser (Dundee) has implemented a transition model within the PHOENICS package. This is a linear-combination integral model, with correlations for the start of transition. The integral model is a set of coupled ordinary differential equations, generated from a K-ε type equation making certain simplifying assumptions. Comparisons were shown for several ERCOFTAC test cases, but I noted that the peak skin friction coefficient is always under-predicted.

Lakshminarayana (with Chernobrovkin, Penn State) described recent work on a low Reynolds number K-ε model; he found that the Fan-Lakshminarayana-Barnett (FLB) version gave the best results. The model is able to predict the occurrence of the major regions associated with wake-induced transition, including the calmed zone and the transition strip.

Steelant (Gent) has pursued the idea of modeling by-pass transition through conditionally averaged flow equations, each carrying interaction terms that depend on the conditionally averaged velocities as well as the intermittency γ, which is determined either algebraically (after Dhawan & Narasimha) or through a separate transport equation. Reasonable agreement was reported with the ERCOFTAC flow T3C5.

Guohua Xiong (with P.G. Huang, Kentucky) also uses conditioned K-ε equations with a transport equation for γ, to predict transitional flows in low-pressure turbines. When an allowance is made for the normal variation of γ through the Klebanoff distribution, Xiong finds good agreement with the ERCOFTAC turbine series of test cases.

Daniel Dorney (GMI Institute, Flint MI), using Baldwin-Lomax, K-ε and q-ω models, reported on both cascade and stage simulations of unsteady transition. The first two models give similar results on cascades. At a Reynolds number of 80,000 a transition limit-cycle appeared in the solutions. They remind me of Rotta's and Pantalu's observations in a pipe, but it is not clear if there is a connection.

Mark Savill (Cambridge, not present at the meeting) circulated a useful report about the coordinated European programme being promoted by the ERCOFTAC Transition Modeling Group. The programme now includes 15 groups outside Europe as well, and is becoming a major international force for assessment of transition models - often carried out "blind", i.e. without access to test data, or even in advance of its acquisition. A total of 15 test cases have so far been released to participants. Savill's report for Minnowbrook contains a detailed description of model performance in various cases.

6. DNS/LES

In his opening remarks Narasimha made what he called a "modest proposal", which was to do DNS on a realistic blade, but in the manner advocated in Minnowbrook I (i.e. in "mission mode"). He suggested beginning with the 2D case, with progressive "complexification" in the geometry (to 3D), specification of the disturbance environment (wake-passing), inclusion of compressibility effects, cooling etc. The current state of the art was discussed in several presentations. Man Mohan Rai (NASA Ames) simulates the spatially growing boundary layer on a heated flat plate in the presence of relatively high free-stream turbulence. The simulation involves 24×10^6 grid points. The basic physics of transition is captured, but computed onset is slightly downstream of observed onset in the experiments of Sohn & Reshotko (which Rai simulated). It is not clear why the fully turbulent boundary layer far downstream appears to originate at the leading edge, and has a profile without a wake region. Interestingly, Rai found no evidence of negative eddy thermal flux, of the kind that some experiments have (controversially) reported.

Neil Sandham (Queen Mary & Westfield) has now carried out simulations of separation bubbles showing laminar separation, transition and turbulent reattachment, on a 128-processor Cray T3D (achieving 90% parallelization efficiency and needing 20,000 processor-element hours at around 3 gigaflops). Sandham considered that fully-resolved DNS of separation bubbles, and single and multiple spot calculations, are now feasible.

D.J. Doorly (Imperial College) uses the vortex particle-in-cell method to study wall-layer dynamics and vortex-surface interactions. In a model problem a 2D vortex suddenly imposed on a wall is shown to lead to eruption of boundary-layer vorticity into the free stream.

7. Miscellaneous

William Saric (Arizona State, Tempe) summarized the detailed experiments being carried out in the ASU Unsteady Wind Tunnel to understand receptivity to free stream disturbances, in particular the large-amplitude noise characteristic of turbine engines; the problem cannot be handled through the usual linear mechanisms. Oblique and broad-band sound waves are used to determine how unstable waves are initiated. Acoustic

disturbances are produced in bursts, and the TS waves detected by a differential phase speed technique. Saric emphasized that theory, DNS and experiment are now in agreement, provided due care is exercised in defining receptivity coefficients.

As Walker pointed out, transition is most important in the LP turbine and compressor, where the blades have relatively high aspect ratio; low aspect ratio blades are largely immersed in the turbulent annulus wall boundary layer. This - and experimental convenience - have led to a large effort in 2D flows. But true 2D flows are rare, and 3D phenomena could be very significant. Narasimha showed results of measurements (made with Jahanmiri & Prabhu) on a spot in a divergent flow with no pressure gradient; it was found that the spot can cut across local streamlines at angles ranging from 3^0 to 13^0. On the other hand the spot wedge grows at an included angle of 20^0, about the same as in 2D flow. He concluded that divergence only produced a *geometric* distortion of the coherent structure in the spot (it was no longer symmetrical), but hardly affected its *dynamics*. Narasimha also mentioned the investigation of the 3D transition zone in the same diverging flow carried out by Ramesh, Dey and Prabhu (IISc).

Kohama (Sendai) reported detailed investigations of transition on a swept flat plate with a displacement body. He found two different instabilities apart from the well-known stationary mode: namely a traveling cross-flow instability and a high-frequency secondary instability propagating along the stationary vortex. The turbulent wedge triggered by this instability starts from the middle of the boundary layer on each cross-flow vortex. Kohama also reported on experiments at control using suction.

Tumin (with Eliahou, Han & Wygnanski at Tel Aviv) showed that transition in pipes begins with the distortion of the parabolic velocity profile, and proceeds through stream-wise rolls which amplify and finally break down following spikes as in the K-regime in boundary layers.

Jacques Lewalle (Syracuse) showed how wavelet analysis can be used on hot film time series data from Halstead experiments at GE to characterize and track structures in the flow.

McEligot described a new matched-index-of-refraction (MIR) facility that has been built at the Idaho National Engineering and Environmental Laboratory. The idea is that if fluid and model in a flow facility have the same refractive index, one can use LDV and PIV techniques to see through objects without disturbing the flow. Problems connected with transition on cascades and flow in cooling holes are proposed to be investigated.

8. Recommendations

As at Minnowbrook I, working groups were formed to look into selected areas and recommend directions for future research.

Terry Jones, who headed the Working Group on the Becalmed Region, pointed out that details at the trailing edge of the spot are not yet understood; e.g., why does it travel at half the free-stream speed? More work needs to be done on practical exploitation, not only to help manage separation, but possibly also aeroelasticity and acoustics.

The Low-Pressure Turbine Working Group report, presented by David Ashpis, called for an "Engine Flow Environment Measurement Project" to characterize the turbulence environment in the real engine. The discussions at Minnowbrook clearly brought out the serious need for such a project: the economic benefits of improved understanding of LPT flow physics, emerging from such initiatives as the NASA LPT program, are not only fuel savings but also reduced part count and weight, as well as a general improvement in design. It was further suggested that the project should be international due the complexity and high costs involved. Other recommendations highlighted the need for further studies of Mach number and (severe) adverse pressure gradient effects on spots. The group consensus was that NASA's LPT program objectives and implementation are on target.

Terry Simon reported on behalf of End-Users Working Group. What industry needs is robust transition/turbulence models for off-design analysis to evaluate design choices and determine optimum designs. ("Robustness" was defined by Wisler as the ability to work over a wide envelope of initial and boundary conditions, Mach and Reynolds numbers, and geometry, without needing special tuning.) Such models have to be integrated into the standard CFD codes. But, interestingly, the Group added that it is necessary to include a presentation of the physics of transition as well, to help engineers in design selection. Finally, the importance of desensitizing the engine to low-Re effects was emphasized.

The fourth Working Group on computations was chaired by Sandham. The Group identified the following DNS tasks as feasible in 3 years on current computer platforms:

- Spots - in a range of pressure gradients, with study of sensitivity of results to method of triggering.
- Separation bubbles on a single blade, at Re = 50,000 , M = 0.8 . Om Sharma offered "Cascade B" as a candidate, noting that further experiments with well-defined boundary conditions may need to be carried out.

In the 3-10 year time frame, assuming computer power increases 10-fold in 3 years, it might be possible to analyze wake-blade interactions. Doorly felt this would still be expensive. Herbert considered that the biggest problem would be to prescribe the appropriate inflow boundary conditions at the HP turbine.

There was much discussion on how all of this work was to be funded. Ashpis suggested that NASA, DOE and AFOSR need to formulate a joint strategy for supporting long term programmes. This is all the more necessary as there are now fewer people in industry working in "enabling technology groups", so the task has to be accomplished by academia, government and industry working together for visible benefits. Industry was willing to talk, Terry Simon said, if academics were willing to listen!

9. Conclusion

In his concluding remarks, Narasimha said it is even clearer today than it was in 1993 that turbomachinery boundary layers represent a very interesting and complex flow situation. There are other flows in the same-awkward Reynolds number range, such as

birds and windmills, but these do not present the complexity that arises from the multiple stages in turbomachinery. The industry is now mature, and costs seem to be driving everything: it is willing to consider even a half percent improvement in efficiency, but will not easily pay for attaining it.

As far as transition physics is concerned the increasing interest in separation bubbles is both timely and welcome. With the many interesting studies reported at the meeting, it was his assessment that in the coming few years the bubble problem would be largely sorted out, except of course for all those more basic questions that might remain in connection with spots and-turbulence.

With regard to spots it was gratifying that the studies that he had foreseen in 1985 as essential were now being conducted. The behavior of spots in pressure gradients, and the effect of Mach number, are slowly getting to be documented. But it is important to realize that we still do not *understand* spots. There is nothing more practical than a good theory, as Boltzmann had said, but one is not in sight yet: and Frank Smith is the only brave soul tackling this difficult problem.

The other interesting development over the last four years has been the considerable attention being devoted to "the calm that follows the storm". The possibilities of exploitation of the calm region trailing the spot, foreseen long ago by Schubauer & Klebanoff, are now being more quantitatively assessed.

The simpler situations in unsteady periodically forced transition are being sorted out. There is a big question regarding the disturbance environment in turbomachinery, and the proposed project on the subject was absolutely essential in his view. At the same time, as one moves deeper into the turbine and upstream wakes get chopped up, it is unlikely to be either necessary or desirable to follow each wake all the way through. Surely there must at some stage be a method of characterizing the disturbance environment statistically once again, although the statistics required would not be just the intensity, or even a length scale or a spectrum, but would have to be event-based: are there lumps of turbulence? at what rate do they arrive, how fat and intense are they? - and so on.

Transition models are now proliferating. Considering that even five to ten years ago there were only a few models around, growth has been rapid, and the subject is now becoming a minor industry. A major question that still remains is whether the models explicitly include the intermittency or not, and if they do whether it is treated as a parameter or as a dynamical variable. Models now exist adopting each of these options. Narasimha confessed to a personal preference for physical, integral methods, where one sees exactly what is being done, in contrast to the more elaborate multiple P.D.E. systems, the reason being that ideas for control, management, manipulation etc. are more obvious with the integral models. Of course the P.D.E. systems will perhaps integrate more easily with what is now being generally done with fully turbulent boundary layers, and if that route is followed, it would be essential in his view to follow the suggestion of David Ashpis and provide the designer with a presentation of the physics as well, so that he might be able to pick more intelligently the design options that should be explored.

Whatever model is adopted, it is clear now that it would have to include unsteady transition as well.

Narasimha was of the firm view that it was only a matter of time before DNS would start to be used in a practical way, even though it was not going to be easy and may not be immediately achievable. The main reason for this view was that the Reynolds numbers in turbomachinery are relatively low: even Re = 50,000 is of direct practical interest. He predicted that the first major field in technology where DNS will make a direct impact will be turbomachinery. It was therefore prudent to prepare for the future, and if possible to make it happen: after all, computer power will probably have increased about a thousand-fold or more in 10 years' time. He did not want to suggest that the full turbine or compressor should be handled by DNS, but there were various bits of the system that in his view should be, keeping always the designer's needs in mind.

He referred to questions often raised about the possible relevance of stability theory in turbomachinery. At first sight stability would seem unlikely to be a major consideration because of the high disturbance environment, but various presentations made at the meeting showed that such a conclusion might be hasty. Reshotko's work on algebraic growth showed the importance of analyzing transient disturbances. There was still the unresolved question about why e^N methods do not work as well on blades as on wings; Herbert had suggested several reasons that need to be investigated. Narasimha saw further use for the simpler alternatives that he and his colleagues at Bangalore had investigated. Questions of global and convective instability may play an important role in achieving a fuller understanding of the behavior of separation bubbles and of near wakes, as Frank Smith had suggested.

Narasimha finally listed what appeared to him to be conspicuous gaps in the present research scene. There is first of all too little work on three-dimensional flows, too little DNS/LES (done specifically for turbomachinery flows), and too little theory. A coordinated project on a given blade row as more and more stages are mounted upstream - coordinating between experiments and computation, if not theory - seemed to him to be a great need. Along the line of the suggestions made by Ashpis, international programmes on the disturbance environment in turbomachinery and on DNS/LES would seem highly worthwhile; ERCOFTAC and Minnowbrook have shown how such international programmes can be organized. With the funding situation becoming so difficult, there seemed to be no alternative. He concluded by thanking the organizers for putting together again such an interesting and pleasant meeting where industry, academics and government were all so well represented and interacted with such enthusiasm and frankness.

References

[1] J. E. LaGraff (ed.) 1993, Syracuse University Minnowbrook Workshop on End-Stage Boundary Layer Transition, August 15-18, 1993, Blue Mountain Lake, New York. Proceedings published by Syracuse University, Department of Mechanical, Aerospace and Manufacturing Engineering, Syracuse, New York 13244.

[2] R. Narasimha 1994, Report on the Workshop on End Stage Transition, *Current Science* 67:6-9.

APPENDIXES

APPENDIX A

Summary of Minnowbrook I

Reprint of "A Report on the Workshop on End-Stage Transition"*

Roddam Narasimha
Indian Institute of Science
Bangalore, India

*Cur. Sci. **67** (1), 10 July 1994. Reprinted, with permission, from the Indian Academy of Sciences.

A report on the workshop on end-stage transition

Nearly 40 invited participants gathered on the evening of 15 August 1993 in the Minnowbrook Conference Center on the shores of Blue Mountain Lake in the Adirondocks to discuss for the following two and a half days the late stages of transition in boundary layers. The Conference Center, run by Syracuse University, provided the ideal ambience for an informal and stimulating workshop on a subject that is at once scientifically challenging and technologically important. The workshop was unique in that it brought together, for the first time, those working on improving our understanding of transition phenomena with others concerned with handling and modelling transitional boundary layers in applications, especially in turbomachinery. Or, as Paul Gostelow (Sydney, who organized the meeting so effectively with John Lagraffe of Syracuse and Terry Jones of Oxford) put it, the intention was to bring the JFM and ASME types together (he mentioned high and low church as well!).

The point was pursued by Roddam Narasimha (Bangalore) in his opening talk (his theme was The Many Worlds of Transition Research). Transition is a complex subject, and its investigation is being pursued in many sub-communities, respectively concerned with stability, receptivity, breakdown, turbulent spots, modelling, direct numerical simulation (DNS), etc. It is remarkable that there is not a single experimental investigation of transition from laminar to turbulent flow in a boundary layer that goes the whole way—on any one of the many routes that everybody admits are possible.

The workshop was dominated by discussions on turbulent spots—their genesis, properties and consequences—although Tom Corke (Illinois) described how transition could occur *without* spots. This spot-less or 'scenic' route (as Narasimha called it—the road here is slow and long), discovered by the Novosibirsk group, was followed when a resonant interaction between a TS wave and a pair of oblique waves is arranged (this is done, in Corke's

experiment, by suitably programmed forcing through surface films excited thermally). There is in this case no evidence of rapid collapse into turbulent bursts, but only a gradual filling up of the spectrum. Although Corke finds that the route is followed even when there is some detuning, Narasimha felt that the spot-less route seemed contrived, and Mark Morkovin (Illinois Institute of Technology) questioned whether the disturbance field necessary was 'environmentally realizable'. Indeed, Morkovin emphasized that while the roads to turbulence are highly non-unique, the modes in which the final onset of bursting occurs are much less so.

Some very interesting discussion took place on the events leading to the birth of a spot. Jim Kendall (JPL) reported that the response of the boundary layer to weak free-stream turbulence (FST henceforth)—created in his tunnel by an array of 168 small jets directed upwind in the settling chamber—took three distinct forms. There is first of all a narrow Klebanoff mode peaking half way across the boundary layer (not to be confused with the peak-valley splitting also associated with his name); then there are wave packets, arising sporadically, narrower than Gaster's wave packet but with higher, randomly varying amplitude. Finally there are the TS waves. The dynamics of Kendall's wave packet is not clear. Mike Gaster (Cambridge), on the other hand, could track the birth of what appeared to be an Emmons spot within *his* type of wave packet, triggered by a surface-mounted microphone. Even when the input to the microphone is (deterministic) white noise, a modulated TS wave train appears, with a subsequent breakdown into a spot. Both experiments demonstrate incidentally how choosy the boundary layer is in picking out waves from whatever hash may be heaped on it.

While Gaster uses singular value decomposition and wavelet transforms to understand the time-frequency structure of the process of spot birth, a 3D view was presented by the flow visualization studies of Chuck Smith (Lehigh), who starts with a single hair-pin vortex generated by fluid injection at the surface. The key to the growth process, in his view, is strong vortex–surface interaction, which leads to more hair-pin vortices that amalgamate into a spot. Bart Singer (NASA Langley) could simulate similar primary and secondary vortices on the computer, but there is evidence of a counter-rotating wall vortex as well in his DNS results: the spot appears only after a rather long gestation period. Seifert (Tel Aviv) reported that two point disturbances separated spanwise, generated using Gaster's technique, interacted to *promote* transition.

Herbert's (Ohio State) parabolized stability equations (PSE) now take only 30 min on a work-station and so have potential for engineering calculations. As they are in excellent agreement with both experiment and Navier–Stokes solutions, they can provide flow to the late stages of transition before onset at modest cost; DNS can take off from there on. Encouraged by this experience PSE methodology has now been extended to 3D boundary layers in curvilinear coordinates from low to hypersonic speeds, in both linear and nonlinear regimes. The message was that if the disturbance can be specified properly, and the mean flow is known sufficiently accurately, PSE can take one quite far.

There was much discussion, incidentally, of the possibility of 'instability without eigenvalues', the title of a recent paper by Trefethen and coworkers (*Science*, 3 July 1993). Morkovin traced the history of related ideas; his assessment was that they were not particularly relevant to boundary layer transition, as the implied disturbances were again not 'environmentally realizable'.

How close to breakdown has basic theory been able to take us? Narasimha, in his opening remarks, was the only one to raise the question of the possible relevance of nonlinear dynamical-system theory to transition. He noted some broad similarities between a set of model equations he had studied with Bhat and Wiggins, and a set proposed by Herbert. These models do not of course reflect the full complexity of the 4-dimensional (3 space + time) forced nonlinear oscillator that the boundary layer is, so we cannot expect to encounter, in real-life transition, the relatively simple routes to chaos so familiar in dynamical system theory. Although no insight of predictive value could be said to have come from these developments yet, he thought it would be surprising if dynamical chaos had nothing to do with transition. The data analysis methods being developed by Gaster's group could throw light on the problem in coming years.

In any case, according to Narasimha, all the work being done on the different routes to turbulence would eventually have to be codified into appropriate basins of attraction, especially in disturbance space. In general the number of dimensions involved would be too high, but he made proposals for simpler sets of experiments that could help define the concept. Morkovin felt that the number of dimensions would be 10 to 20, and doubted whether the resources—funds, man-power—would be available for undertaking such a task. He was generally pessimistic about the usefulness of the dynamical system approach. Frank Smith (London) described the nonlinear theories currently being pursued, falling into three classes: vortex–wave interactions (important at low input amplitudes), pressure–displacement interactions (medium input) and Euler-scale motions (high input). These theories are very suggestive, and direct comparisons with experimental data in channel flow is encouraging; nevertheless, predictions for flows of the type presented at the Workshop still do not appear to be an immediate possibility.

Wygnanski reviewed what is known about the structure and propagation of fully developed spots. Beyond a critical Reynolds number the TS waves that trail the wing tips of a spot can break down, creating either apparently autonomous spots or 'spotlets' that eventually merge with the parent and so make it grow: he found no support for the alternative view of spot growth, namely that it consists of lambda vortices whose *numbers* grow in proportion to the size of the spot. It is now well-known that favourable pressure gradients inhibit spot growth—possibly because the wing-tip TS waves are suppressed. Further evidence of this inhibition was presented by Terry Jones (Oxford). Gostelow finds that in adverse pressure gradients, on the other hand, the turbulent region of a spot can spread at a half-angle of 20 degrees, and the attendant wave packet at 29 degrees! Narasimha showed that flow *distortion*—i.e. a situation in which the streamlines are *not* parallel but there is no pressure gradient—results in a curved spot trajectory, with spread rates not significantly altered; however the spot is asymmetrical, being thicker on the outside of the bend and not spreading *across* streamlines necessarily. It is gratifying that spots are

now beginning to be studied in more realistic environments, but clearly there may be many surprises in store as other situations are investigated. It is however important to remind ourselves that anomalous propagation is not read into a situation where the spot is not yet mature: the long gestation periods at low Reynolds numbers, known from the early Schubauer–Klebanoff work, can cause confusion in the interpretation of data if one is not careful.

In the real environment of applications, where are spots actually born? According to Morkovin locations are determined by sporadic extrema of the disturbances, but waves and wave packets act as mediators, at least under not highly disturbed conditions. Narasimha hypothesises concentrated breakdown, i.e. most spots are born in a relatively narrow band around transition onset. The resulting universal intermittency distribution finds support from many measurements, including those presented at the workshop by Fraser, Gostelow (in pressure gradients as well), Jones, Malkiel and Mayle (in a separation bubble, for the streamwise variation of the maximum value of the intermittency cross-stream, which occurs at the maximum vorticity point), among others. Ian Poll (Manchester) appeared to think that these distributions were being subjected to a rather heavy normalization process, but he also finds use for the same distributions in flow past swept wings, although his 'intermittency' is not necessarily the fraction of time that flow is turbulent, as it is for all others, but what one may call a transition progression index, which may be different for different parameters such as skin friction, heat transfer, boundary layer thickness, etc.

There is however no direct evidence for the hypothesis of concentrated breakdown, and Hodson (Cambridge) and Jones announced an Oxbridge 'spot-hunting' project, which now appears feasible with the development of liquid crystal and multi-gauge surface heat film probes that Jones described at the workshop. Such a project should in principle be able to track down each spot as it is born and as it propagates downstream. Spot-hunting should be a particularly enjoyable and rewarding exercise in pressure gradients so strong that intermittency distributions are not universal. The reason could be (as Narasimha has suggested) that growth rates vary with pressure gradient (as we know to be the case); but it could also be that breakdown is not sufficiently concentrated. Spot-hunting could throw light on the question, and seemed to receive the warm support of all assembled.

Hodson's catalogue of the woes that beset turbomachinery fluid dynamicists—harsh environment, high curvature, three-dimensionality, awkward Reynolds numbers and so on—were partly illustrated by Wisler (GE Aircraft Engines), who showed hot film traces from a cascade facility depicting the whole range of phenomena from transition after tripping through attachment, relaminarization and separation in a bubble, followed once again by transition and reattachment! The qualitative effects are so striking that it is not necessary to have the hot film properly calibrated to read shear stress. Ting Wang (Clemson) finds that acceleration may delay transition onset slightly, but can significantly affect transition zone lengths. Walker and Solomon (Tasmania) find that, on the stator blade of an axial compressor, with *adverse* pressure gradients that may cause laminar separation and intermittently turbulent reattachment, turbulent spots can appear periodically, following the growth of instability wave packets which *lag* behind wake passage. Lower FST does not alter the essential character of breakdown, confirming that FST is not the driving factor in adverse pressure gradients. Amidst all this talk of turbulence, Hodson reported some intriguing observations in a radial inflow turbine, where (in spite of relatively high Reynolds numbers and disturbance levels) the flow remains laminar or at worst intermittent.

Hypersonics was on many people's minds but did not attract too much attention at the workshop. Data obtained by Kimmel (Wright–Patterson), including shadowgraphs and spectra, show that transition onset, as indicated by deviation of boundary layer parameters from laminar values, occurs where the second stability mode (clearly seen in the spectra) saturates. Whether this onset is accompanied by turbulent bursts of any kind is still not clear.

Modelling efforts appeared to fall into two classes: those that take explicit account of streamwise intermittency and those that do not. In the first class Fraser (Dundee) has a model that introduces new correlations for Narasimha's non-dimensional spot formation rate, and shows good agreement with Sharma's experiments on turbine blades, and the data of Abu-Ghannam & Shaw and Dhawan & Narasimha. Ashworth (Rolls Royce), after an assessment of surface film-gauge data under realistic conditions, concludes that transition in turbomachinery flows can be adequately modelled on the basis of Emmons's spots. Eli Reshotko (Case Western), reviewing models, said that the intermittency distributions of Narasimha, Arnal and Chen and Thyson all appeared viable, and that their use was now spreading surprisingly fast. PSE, in combination with e^n methods, was proving very useful in quiescent streams (FST < 0.4%), although Herbert found that if stability conditions were rapidly alternating, e^n could be a poor guide.

What about 'by-pass'? There is a general tendency to use this word interchangeably with 'high disturbance', but this was questioned at the workshop. Are we on a by-pass if our hot-wire probes do not show TS waves? We cannot say yes, for Kendall can find TS waves in surface sensors when hot wires do not reveal them. Gaster thinks the TS mechanism may be operating even in the absence of recognizable TS waves: the boundary layer may still be responding through a TS transfer function even if it has not picked out relatively pure TS waves. There is on the other hand the observation of Blackwelder (USC) that, when rigid particulates are introduced into a laminar boundary layer, turbulent spots arise from the disturbances due to the resulting wake that 'scars' the boundary layer, rather than from the particulates themselves. Narasimha suggested that perhaps we should talk about a by-pass only if the mean flow were sufficiently modified to totally alter the transition mechanism. The issue was left hanging, and the participants found it convenient to ignore it for the moment, as they proceeded to talk of 'weak' bypass (FST between 0.4% and 2%) and 'strong' bypass (FST> 2%) as before (in spite of the fact that FST is not the dominating factor driving transition in adverse pressure gradient flows). By this definition all turbomachinery applications involve only by-pass routes: the disturbance environment is severe, with upstream blade rows often adding periodic wake-passage as another special dimension in disturbance space (as Hodson emphasized).

Reshotko considered the weak bypasses the most dangerous, and advocated PSE and correlations to tackle them. For strong bypasses he added the $K\varepsilon$ equations. Max Platzer (Monterey) uses a modified Chen–Thyson model to compute flow past airfoils with separation bubbles, and finds that the incorporation of a transition model is crucial for predicting the bubble. Crawford (Texas at Austin) is developing two-equation models, especially for strong by-pass. Neither the Launder–Sharma models nor Crawford's multiple time scale improvements seem able to predict the peak skin-friction and heat transfer parameters that are now well known to occur towards the end of the transition zone. My own feeling is that differential models for transitional flow, without a built-in intermittency, cannot yet perform as well as properly constructed integral-type methods.

There is one silver lining in the cloud in turbomachinery fluid dynamics: blade Reynolds numbers are low enough to make direct numerical solution at full-scale feasible. Thus Manmohan Rai (now at NASA Langley) is able to simulate flow in a spatially developing boundary layer on a flat plate all the way to full turbulence. He finds rather narrow and elongated spot-like regions, more Kendall than Emmons, it seemed to me. Perhaps the rather narrow plate width (only about 130 momentum thicknesses) constrains turbulent regions. Neil Sandham (Queen Mary & Westfield), working with Kleiser at DLR, simulates the complete transition process in a channel: from the intermediate stages involving shear layers, their roll-up, lambda vortices, and, later on, sublayer streaks, ejections etc. The role of the Emmons spot in these simulations remains rather vague yet. But the question was raised, especially by Steve Robinson (NASA Langley), whether all the 'captive' fluid mechanics produced on the computer is teaching us enough to be worthwhile? There was general agreement with Reshotko's proposal that DNS should now be done on a mission mode—planned like a flight experiment, say—and that the data must be easily available for interrogation by scientists through simple, well-understood procedures.

Transition control is in some sense an ultimate objective in applications, but was not much discussed. Hodson thinks there may be optimum wake-passing frequencies from the point of view of the boundary layer. If wake impact triggers transition through wave packets, and a wake-induced turbulent slab conceals within itself a number of turbulent spots (as some experimental evidence suggests), alteration of wake impact frequency may change transition zone parameters in interesting ways. Nosenchuck and Brown (Princeton) are trying a more direct active method, using a wall-normal Lorentz force in the flow of an electrolyte past a flat plate. The Lorentz force is generated by a spanwise magnetic field acting on a streamwise current, and acts by inhibiting lift-up and bursting in the wall layer. Control is exercised through 'tiles' consisting of permanent magnet and stainless steel surface-mounted electrodes. Laser sheet views and velocity traces show dramatic changes when control is on; e.g. stresses are down by up to 90% at a Reynolds number of 1700 (based on momentum thickness), with an applied field of 1000 G and current density of 10 mA/cm^2.

On the last day of the workshop, three working groups summarized their suggestions on what needs to be done. Apart from the question of where spots are born, there are many others that call for answers. Are celerities different from local free-stream velocities in pressure-gradient flows? Does spot growth occur by birth of offspring which amalgamate with the parent? How often do spots trigger the birth of other autonomous spots in the neighbourhood? How strong are spot-interaction effects? Do spot propagation parameters vary widely with pressure gradient? What happens in strongly curved and 3D flows? And so on.

On the routes leading to spots, the respective roles of narrow Kendall-type wave packets and the wider Gaster-type needs to be clarified. The damped Klebanoff mode needs serious consideration as it may be important in both moderate and high free-stream turbulence. Is it enough to consider free-stream turbulence frozen, or does its evolution need to be accounted for?—this remained an open question.

Frank Smith made a strong plea for greater attention to the physics of the end game. This needs theory, computation and experiment to go hand in hand, but the manpower to do it is not visible. The rewards, on the other hand, are many, and include better transition models and greater understanding of the multiple roads to turbulence, and, eventually, more efficient transition management.

The meeting was one of the most rewarding and stimulating I have attended on transition, because it got two till-now distant communities together, put them in an isolated spot where interaction was easy, kept the group small enough for intimate discussions and organized a programme that had just the right pace—neither overcrowded nor leisurely. I wish there were more meetings like this one.

Roddam Narasimha, Jawaharlal Nehru Centre for Advanced Scientific Research and Department of Aerospace Engineering, Indian Institute of Science, Bangalore.

NASA/CP—1998-206958

APPENDIX B

Written Submission of ERCOFTAC

COST-ERCOFTAC Transition SIG

Evaluation of Turbulence Models for Predicting Transition in Turbomachinery Flows

A.M. Savill
University of Cambridge
Cambridge, England

ABSTRACT

The primary aim of the SIG work has been and remains the evaluation and improvement of turbulence model predictions for by-pass transition and re-transition, with the initial emphasis on turbomachinery applications. Regular progress reports in the ERCOFTAC Bulletin have highlighted the success of the participants in establishing 'best practices' at all levels of model complexity. It is now planned to build on this by establishing a larger network activity involving 25 ERCOFTAC member groups (8 industrial, 3 research establishments, and 14 universities) and up to 6 Corresponding member groups from Eastern Europe.

The main aims will be:

(a) Expansion of the present work of SIG to consider other candidate model approaches of interest; validation of present 'best' model options at different levels of closure against a broader range of transition test cases, encompassing additional elements of complexity, rotation and unsteadiness.
[The emphasis will be on elliptic computations for finite leading-edge cases with the T3L case variants providing a new entry level of complexity].

(B) Establishment of definitive 'best choice' models at each level of closure from simple integral methods right through to Large Eddy Simulations: refinement and further development of these with reference to Direct Simulations and new experiments; as well as investigation of new schemes for linking turbulence modeling and stability analyses.

(C) The implementation of the established 'best' models in industrial codes for validation on practical 3D flow problems.

Participants will be divided into the following 5 linked sub-groups: (under overall coordination of Dr. Savill)

Sub- group 1: Integral/Intermittency Methods - Coordinator: Erik Dick (Ghent Univ.)
(Main aim: switch from standard correlation to intermittency transport modeling for current integral design methods, k-e and RST closures)

Sub- group 2: Eddy Viscosity Models & PSE/e^n - Coordinator: Ruud Henkes (Delft)
(Main aim: to define best choice model with widest predictive capabilities, but minimum mesh requirement for practical 3D problems and investigate if a combination stability methods with intermittency conditionalised turbulence modeling could provide a better design method).

Sub- group 3: Reynolds Stress Transport - Coordinator: Brian Launder (UMIST)
(Main aim: Validation SLYRST model in elliptic computations and comparison against alternative hybrid low-Re/2D-limit closure)

Sub- group 4: Transition Simulations - Coordiantor: Brain Launder (Surrey University)
(Main aim: Extension of LES to real engineering flow problems and wider used for generating databases to validate closure models).

Sub- group 5: Data input from real flows - Coordiantor Ferruccio Pittaluga (Genoa)
(Main aim: to extend and validate best models for real unsteady flows).

Evaluation of Turbulence Models for Predicting Transition in Turbomachinery Flows

A report on the ERCOFTAC Transition Modelling Group for the Minowbrook II Workshop on Boundary Layer Transition in Turbomachines

By: Eur.Ing.Dr.A.M.Savill
Senior Research Associate
Cambridge University Engineering Department
& Visiting Research Fellow
Mechanical Engineering Department UMIST (UK North PC)

During the last three years funding from the BRITE-EURAM Phase II AERO-CT92-0052 Project on Transition in Turbomachinery Flows has allowed Workshops to be held at UMIST (December 1993), VUB (September 1994), and lastly Aristotle University of Thessaloniki (September 1995). During the same period linking of the ERCOFTAC SIG with the 3D Viscous Flows COST Action F1 Transition Sub-group 7, resulted in an additional COST-funded Workshop at the Institute of Thermomechanics in Prague (April 1995). These meeting have allowed recent progress in the prediction of a progressively wider range of test cases to be reularly reviewed. Earlier work of the SIG, which was founded in 1990 shortly following two initial test case evaluations as part of the 1st ERCOFTAC Workshop at EPF Lausanne, has been discussed in a series of progress reports and review articles [1-11], published in a variety of Journals and Conference Proceedings, in addition to regular ERCOFTAC Bulletin reports. Results presented at the UMIST [12], VUB [13] and Prague [14] Workshops have also been separately reported and referenced. New results presented at the final Workshop in Thessaloniki [15] are attached to this summary which attempts to review all of the progress that has been made by the SIG during the full period of the BRITE-EURAM Project Sub-contract from 1993 to 1995 inclusive; with particular reference to the model evaluations that have been made against new test cases derived from data taken by the main Project partners. Additional details of the research work conducted by individual SIG participants can be found in the Theme Section on Transition of ERCOFTAC Bulletin 24 [16].

The primary aim of the SIG work remains the evaluation and improvement of turbulence model predictions for transition and re-transition, with the initial emphasis on turbomachinery applications, but gradually expanding to cover a wider range of flow conditions and varying degrees of free-stream disturbance relevant to internal and external aerodynamic applications.

It has to be stressed at the outset that all model validation is strictly controlled by insisting that Test Case computations are initially done 'blind' (i.e. without access to, or in some cases actually in advance of, the Test Case data); using only specified initial/boundary conditions, and high quality detailed experimental data, complimented by Simulations, to assess the predictions; with the necessary industrial input to ensure relevance of the comparisons. Subsequently participants are encouraged to perform tests of the sensitivity of their results to variations in the imposed conditions, model constants, and mesh resolution (which is particularly important since the very wide range of models being evaluated precludes the specification of fixed grids), and then to refine their model approaches before re-testing these on a wider range of cases.

Throughout the last three years the number of European SIG participants has remained approximately constant at around 25; the current breakdown being: Belgium(2), Czech Republic(1), France(2), Germany(3), Greece(1), Italy(1), Netherlands(2), Russia (2) Sweden(2), Ukraine (1) & UK(7). Of these 10 EU groups have been directly involved in sub-contracting to the BRITE-EURAM Project - see Table 2 - (NB. Changes in personnel/funding forced some changes in these). Approximately 15 other groups from outside Europe - including currently groups from Australia(1), Canada (1), China (1), Japan (4), Korea (1) & USA(8) - have also been contributing to the SIG activities.

Their involvement has helped to calibrate the European efforts and at the same time allowed the widest possible range of new models to be evaluated - again see Table 2 - since where possible the original developers of models have been encouraged to perform transition test case evaluations themselves rather than third parties. In this way the SIG has been able to examine the whole range of closure approaches from: modified correlation/integral methods; to turbulence models including one-equation q-l or k-l models, single/multi-scale two-equation low-Re k-ε or k-τ or k-ω schemes, 'partial' low-Re k-ε/k-l and strain-dependant non-linear/non-isotropic or RNG k-ε models, as well as various low-Re & 2D-limit RST turbulence schemes (including some models at all levels of closure with additional intermittency scaling); and various sub-grid scale model Large Eddy or even Direct (Fully-Resolved) Simulations.

The 1st BRITE-EURAM-funded Workshop at UMIST provided an opportunity to assess all of the calculations that had been performed for the initial entry series of parabolic flat plate **T3A-C** Test Cases since the SIG was first set up (work up to that point had been carried out purely be correspondence); to consider the first Simulations for the elliptic **T3D** Test Case and the first model predictions for two new parabolic **T3B+** and elliptic **T3L** Test Cases based on data acquired as part of a preceding BRITE-EURAM Pilot Phase Project AERO-0002 [see 12]; and thus to determine the best lines of modelling to concentrate on for the duration of the project.
The main tasks at the VUB (and Prague) Workshop were to review further parabolic and elliptic computations for the whole set of Test Cases considered at the 1st Workshop together with results for three new Test Cases **T3A+**, **T3E & T3K** (see Table 1 & [13]); to examine and discuss new alternative model developments and modifications; to consider in greater detail the validation and refinement of models by reference to the Transition Simulation Database; and to revise the modelling strategy accordingly.
New results considered at the the final Workshop in Thessaloniki include the first predictions for the **T3C+**, **T3F**, **T3L+ & T3N** Test Cases - see Table 1 & Appendices; further parabolic and elliptic results for the T3A-C series of Test Cases assessing both grid and model refinements; and further elliptic results for the **T3D ,T3L & T3K** Test Cases; allowing clarification of the best model options for current by-pass transition predictions across the complete range of closures - see attachment on 'Best' Current Transition Models.
Specifications for each of the new Test Cases were released 6 months prior to each Workshop.

The main conclusions arising from the 1st Workshop were as follows:

The k-ε level of closure appeared to be the minimum to achieve any generality in predictions.

At the k-ε (& RST) level of closure an R_t (or possibly R_L) dependent damping functions were required in oder to predict low-Re transitional flows with low-Re (near-wall) turbulence models and the Launder-Sharma-type low-Re formulation appeared to provide the best predictions for Tu=1-10%, at least for parabolic computations starting from specified starting conditions. Unfortunately there was some evidence that this particular low-Re transitional flow treatment was a little more sensitive to initial conditions and more demanding of grid resolution than many alternative low-Re formulations that work equally well or better for the near-wall regions of turbulent flows. However most of these models used Ry or y^+-dependent damping functions which could not correctly account for the x-wise variation of Re through transition regions - although very good results were obtained for the **T3A&B** Test Cases using a simpler Ry-dependent one-equation k-l model when a specific x-wise dependence was built in.

A further numerical disadvantage identified in the case of the Launder-Sharma model was that it introduced both additional D and E terms into the transport equations which were difficult to handle in 3D. It was noted that a primarily Rt-dependent Biswas-Fukuyama low-Re k-ε model avoided the use of both D and E factors and provided equally good predictions for the zero pressure gradient cases. Both models however exhibited significant discrepancies in their predictions for the effect of variable pressure-gradient on transition. This was a problem encountered with all eddy viscosity models for which correction factors needed to be introduced

to sensitise them to applied strain rates in transitional and turbulent flows and those tested, including the well-known UMIST Yap correction, were found to lack generality.
Two major advantages of moving up to the RST level of closure were found to be that stress transport models could largely capture the correct effect of applied strain rates without the need for any such additional corrections and could also correctly model Reynolds stress anisotropy. The Launder-Sharma-based Savill-Launder-Younis low-Re RST model was found to provide the best predictions for start and end of transition over the whole range of **T3A-B** zero pressure gradient Test cases and for the variable Reand favourable to adverse pressure gradients of the **T3C** series. In addition it reproduced the effects of weak free-stream turbulence anisotropy and captured the correct trends for strong anisotropy indicated by Simulations - which could not of course be achieved with any isotropic eddy-viscosity model.

The Launder-Sharma approach, even when applied at RST level, had two other important defects (which affected other similar low-Re schemes as well): it underpredicted the extent, and hence end, of transition and it required a large number of points across the boundary layer (>80) for grid independent solutions. It was found that the former deficiency could be rectified by introducing empirical PTM, transition function or (Narasimha-prescribed) intermittency scaling, although a better approach seemed to be to compute the intermittency variation directly using either a modelled transport equation or a surface-renewal-type model approach. The latter deficiency was less easily overcome, although it was demonstrated that equally good SLY RST model parabolic predictions could be obtained with a resolution close to the upper limit for current 2D blading computations (~20x200) on a carefully specified grid. This appeared to be a real difficulty in extending such transitional flow modelling to elliptic computations.

The first elliptic k-ε model results for the T3A&B Test Case indicated that enforced reduced resolution had the effect of shifting the predicted transition too far forwards even for the Launder-Sharma model, while preliminary computations for the finite leading-edge **T3L** Test Case revealed the need to suppress spurious generation of k due to irrotational straining in the stagnation region. It was suggested that a switch to the alternative k-ω or two-layer k-ε/k-l approach might allow some relaxation of the grid resolution requirement and that a multi-scale k-ε scheme could have other advantages, while intorduction of a suitable irrotational strain correction should avoid the excessive generation of k in impinging flows,but these possibilities remained to be demonstrated.

Separate parabolic computations performed by SIG partciipants for both transitional heat transfer and blading problems and results from a parallel NASA transition model evaluation project tended to confirm most of these findings - see [10 & 11] - so it was established that certain models had the best potential predictive capability at each closure level so the SIG participants were recommended to extend their model evaluation to the wider series of Test Case problems listed in Table 1, concentrating in particular on the following model approaches:

The modified integral methods of Gostelow, Solomon & Walker; Johnson; and Secundov & Vasiliev; the CIAM modified ν_t transport one-equation model; the Moores q-l model; and an (Rt-dependent) form of Grundmann's k-l model with additional x-wise damping; the Launder-Sharma k-ε model, alternative Biswas & Fukuyama k-ε model, or an Rt-dependent form of the Lam & Bremhorst model (all with UMIST Yap correction, Kato-Launder irrotational-strain extension, and a Production Transition Modification (PTM) or preferably prescribed intermittency scaling or a separate transport equation for γ); various two-layer k-ε/k-l approaches; a multi-scale k-ε scheme; the Craft-Launder-Suga non-linear k-ε & more advanced k-ε-A_2 models; variations on the Wilcox k-ω model; the SLY low-Re RST model (with additional intermittency transport) and alternative hybrid low-Re/2D-limit RST closure schemes; in addition to various Sub-Grid-Scale model Large Eddy Simulations.

Table 1: Test Cases for which specifications have so far been released to participants

T3A⁻: zero pressure gradient, 1% isotropic free-stream turbulence (theoretical or experimental initial conditions)
T3A: zero pressure gradient, 3% isotropic free-stream turbulence (theoretical or experimental initial conditions)
T3A⁺: zero pressure gradient, 3% isotropic fst, but variable Lue (theoretical or experimental initial conditions)
T3B: zero pressure gradient, 6% isotropic free-stream turbulence (theoretical or experimental initial conditions)
T3B$_{DNS}$: zero pressure gradient, 4.5% weakly anisotropic free-stream turbulence (Simulated initial conditions)
T3B⁺: zero pressure gradient, 10% weakly anisotropic free-stream turbulence (experimental initial conditions)
T3C1-5: pressure gradient representative of aft-loaded turbine blade, 3%fst (expt. initial conditions; various Re)
T3C⁺:compressor blade pressure gradient, 0-10%fst, circular & 2:1 ellipse leading edge (expt. initial conditions)
T3D1-3: zero pressure gradient, 0.1% isotropic fst, following laminar separation (expt. conditions; various Re)
T3E: strong favourable/adverse pressure gradient, 0.1% fst, relaminarisation/retransition (expt. initial conditions)
T3F: zero pressure gradient, 0.7% & 2% fst, mild&strong convex streamline curvature (expt. initial conditions)
T3L: semi-circular leading edge, 0-6% free-stream turbulence (expt. initial conditions; various Re, M, etc)
T3L⁺: as for T3L, but with imposed pressure gradient representative of aft-loaded turbine blade (expt. cond.)
T3K: Low-Speed (HP Rotor) Turbine Cascade, ~4% free-stream turbulence (expt. initial conditions)
T3N: zero pressure gradient, 5-20% fst generated by fixed cylinder wake (expt. initial conditions)s

Note: (1) The **T3A⁺** Test case data was taken as part of a COSTEC-funded project by the Prague group.
(2) The **T3B⁺**, **T3C⁺**, **T3L**, **T3L⁺** & **T3N** Test Cases have been derived directly from data taken as part of BRITE-EURAM Phase II Project or the earlier Pilot Phase Project AERO-0002.
(3) The **T3K** case is the same as ERCOFTAC Turbomachinery SIG 3D Test Case No.3, but has been adopted as a linking case because useful 2D computations could also be performed at mid-span using sufficiently high resolution to test turbulence and transition models.

Parabolic model calculations have now been made for all the **T3A,B,C, E, F & N** Test Cases and elliptic computational results have been obtained for the **T3A,B,C,D,L & K** Cases

As a result the following more detailed observations can be made regarding the performance of the selected models which, contrary to the initial conclusions, have produced some good predictions at all the following levels of closure:

Integral methods: Gostelow & Dey have found that a new correlation for Rel, based on a wider range of University of Sydney and Tasmania data, provides much better results for the **T3A&B** Test Cases than the standard Narasimha & Dey integral method [12]. Almost as good predictions were obtained for the **T3A⁻** & **T3C2** Test Cases and Prihoda et al. at Prague have obtained similar results for **T3A&B** with their own version of the UTS method. Agreement with experiment across this range of cases has proved to be superior to that reported by Vasiliev earlier [12], using an alternative modifed CIAM Integral Methods, and Solomon, Walker & Gostelow have subsequently shown that their results for the **T3C2** case can be significantly further improved if the correlations used in the revised UTS method are made a function of the local pressure gradient. An alternative integral method of Johnson, which introduces a specific model for free-stream turbulence pressure-field interactions, has also produced excellent predictions for **T3A,B & C1-5** Cases [13] and has now been shown to predict the **T3B$_{DNS}$** Test Case just as accurately. However his method predicts transition far too early for the **T3B⁺** Test Case, largely because it uses empirical information which is only valid up to 5-6% fst, and seems to exhibit too great a sensitivity to free-stream length scale variations for the **T3A⁺** Test Case. The model is currently being modified to correct these deficiencies and to introduce a pressure-gradient sensitive spot-generation model.

One-Equation Models: Grundmann and colleagues at VKI and Dresden have shown that even the simple (and incorrect) y-dependent Van-Driest damping treatment included in the Fish & MacDonald k-l model can be sufficiently improved by the introduction of additional x-wise transition scaling to produce good predictions for the **T3A,B&C2** Test Cases [12,13]. However variations of additional necessary model constants have not yet been well defined.

Researchers at CIAM have modified their ν_t - 90 eddy viscosity transport model, which surprisingly out-performed many other higher-level closure models across a wide range of

turbulent flow test cases considered by the 1990-94 Stanford Collaborative Testing of Turbuelnce Models exercise, to handle by-pass transition. Vasiliev has used this and their subsequent v_t - 92 model version, which also introduces a specific allowance for pressure-field effects to produce good predictions for the **T3A&B** Test Cases, but it appears the approach is rather too sensitive to the free-stream length-scale variations of the **T3A$^+$** Test case. Prihoda and colleagues have obtained better predictions for the **T3A$^-$,A &B** Test Cases using a two-layer model combining an outer k-l model with an inner layer prescribed length-scale which is scaled by an intermittency variation based on that of their modified UTS method.

Two-Equation Eddy-viscosity models:

The standard Launder-Sharma k-ε model has now been very widely evaluated by a number of SIG participants. In addition to confirming the earlier findings, parabolic computations performed for the **T3A$^+$** Test Case by Henkes & Westin at Delft have suggested that it shows approximately the correct sensitivity to free-stream length-scale variations, while some initial results obtained by Kang for his own variation of the **T3N** Test Case have again highlighted the far too sharp an increase of Cf through transition that all Rt-dependent models tend to produce.
The Karlsruhe groups, in conjunction with researchers from AUT, have made very good progress in developing a two-layer k-ε/k-l model, which avoids R_y dependency, and again employs an intermittency correlation to handle transition in a similar manner to Prihoda et al. This model has produced excellent predictions for **T3A$^-$,A, B & C2-5** Test Cases, particularly when v' is used in place of k as the most appropriate velocity scale for the inner layer. The results are even better than those they previously achieved using the PTM versions of the Launder-Sharma and a calibrated Lam & Bremhorst model. This is encouraging because further blading computations performed by the same researchers have indicated that even the PTM model versions fail to predict transition correctly when it occurs in a favourable pressure gradient (or in response to a shock-boundary layer interaction) [17]. In correctly predicting this feature the two-layer model appears to overcome a defficiency seen in all strain-dependent model versions so far tested at this level of closure (including the RNG k-ε model which has now been tested by researchers at KEMA who found that it was unable to predict transition correctly for the **T3A** Test Case).
Janour at Prague has also made considerable progress in developing his alternative and rather novel two-layer k-ε/surface-renewall model and produced some very good predictions for the **T3A&B** Test Cases [16]. His model also appears to capture the correct trends for relaminarisation and retransition in the **T3E** Test Case, and displays approximately the correct sensitivity to free-stream length scale variation of the **T3A$^+$** Test Case.

Steelant & Dick have shown that their conditionally zone-averaged k-ε model with prescribed intermittency can quite accurately predict the **T3A&B** Test Cases, but predicts transition too early for **T3A$^-$** and too late for **T3B$^+$** Test Cases. They have also now developed an alternative version, employing a simplified transport equation (ODE) for γ, which produces much better predictions for the **T3A&B** Cases and equally good new results for **T3C1&5**, but initial results for **T3A$^+$** suggest that their model may be insufficiently sensitive to variations in free-stream length-scale.

Elliptic model evaluations: The Launder-Sharma k-ε model has also now been tested on a wider range of elliptic computations for the **T3A&B** (Delft & UMIST), **T3C1,2,3&5** (UMIST) and the **T3D2** (Delft) & **T3L** (AUT,UMIST,Karlsruhe) Test Cases. The results confirm the tendency for transition to be predicted too early for all the flat plate test cases unless very high grid resolution, comparable with the best parabolic computations, is employed and careful discretisation adopted for both Advection and very near-wall terms. With a sufficiently fine grid Henkes has produced results for the laminar backstep **T3D2** Test Case which compare reasonably well with the experimental data and earlier LES results [11].

The first sets of Launder-Sharma k-ε turbulence model predictions for the semi-circular leading edge **T3L** Test Case proved to be in surprisingly good agreement with data from AUT, but it

now appears that turbulence levels in their separated shear laminar shear layer were artificialy raised by probe interference. Both the AUT and UMIST groups subsequently found that reasonable predictions could still be obtained for the highest free-stream turbulence levels considered in the Rolls-Royce and later AUT experiments, where probe interference effects were eliminated, but in order to correctly predict cases with much lower fst it was necessary first to suppress spurious model generation of k by irrotational strain in the impingement region. Both made use of the Kato-Launder irrotational strain correction to the Production terms in the turbulence equations (partly replacing the strain invariant by the vorticity invariant, which is zero in pure irrotational strain). The AUT group found that such a Kato-Launder-modified Launder-Sharma model produced reasonable predictions for the full range of fst cases in the immediate vicinity of the initial laminar separation bubble, but the unmodified Launder-Sharma scheme produced more accurate results in other parts of the flow, suggesting the need for a type of zonal modelling approach. The UMIST group in a similar manner found that a variable coefficient 'hybrid' model combination of the Launder-Sharma (or Lien-Leschziner) and Kato-Launder-modified schemes can also produce acceptable predictions.

The Craft-Suga-Launder two-equation non-linear k-ε treatment (which in principle should provide a more general method of handling irrotational straining than the Kato-Launder modification) has been found to provide as good results for the **T3A&B** Test Cases as the Launder-Sharma scheme (when a similar grid resolution was employed), and better results for **T3C** series (when the Yap correction was included; without this it too failed to correctly capture the variation in transition location). The same model has now produced good predictions for some of the **T3I** Test Case 2Dblading test cases, although convergence problems have been encountered when applying it to the **T3L** Test Case. Even better results have been achieved for **T3A&B** with the three-equation k-ε-A2 non-linear scheme, but convergence problems have then been encountered for the **T3C** Test Cases. It seems likely that both versions will require some reoptimisation to handle both variable pressure-gradients and 2D/3D flow curvatures.

It had been thought that there might be advantages in switching the dependent length-scale varaible to ω, since it is well established that the high-Re (Wilcox) k-ω model does not require a full low-Re treatment to describe the near-wall region of turbulent flows and can therefore be used with coarser meshes. However Wilcox has himself shown that specific low-Re damping factors are still required to handle transition regions, and some initial tests (conducted by Georgiades as part of MSc thesis work at UMIST) have indicated that the standard Wilcox (Rt-dependent) low-Re k-ω model fails to predict transition onset and length correctly for the **T3B** Test Case while a non-linear CLS-type k-ω model predicts transition length much better, but onset far too late. Despite this the k-ω approach may deserve further investigation because Zheng & Liu [18] have now proposed a simple transition 'fix' for the high-Re version which appears to work well for some cascade flows.

The first relatively low-resolution 3D computations were undertaken for the **T3K** Test Case, with the y-dependent Lam & Bremhorst k-ε model (at Durham), a modified version of this converted to Rt damping by Dawes (Cambridge/EPFL), and the Lien-Leschziner k-ε model (UMIST FLAIR group) prior to the VUB Workshop. All of these models overpredicted the total loss and mid-span loss downstream of the cascade, while underpredicting the degree of secondary flow. (In fact the best Turbomachinery SIG results have been obtained with a simple mixing length model, assuming laminar conditions throughout the passage up to 80% chord - the experimentally determined location of transition on the suction surface). The Dawes modified L&B model more accurately predicted the total loss, while the Lien-Leschziner model gave much better results for the secondary losses. Both groups have recently performed much higher resolution computations (>1.2M points/cells) and obtained far superior results, partcicularly for the secondary flow, irrespective of the modelling. A key advantage of the Dawes treatment for such complex flows appears to be that it employs a low-Re treatment purely to handle streamwise variations of Re and couples this with a type of modified wall-function approach where k^+ and ε^+ are prescribed below $y^+=10$, drastically reducing the near-

wall mesh requirements, while the Lien-Leschziner model attempts to achieve the same goal by constraining the near wall length-scale to be consistent with that produced by a two-layer approach. Both models together with other Rt versions of the L&B model and Biswas & Fukuyama model are still currently being evaluated on the **T3I** 2D blading Test Cases. The last of these at least appears to produce results equivalent to the Launder-Sharma scheme.
Grid resolution certainly remains a serious limiting factor in extending the best turbulence model approaches to predict transition in rreal engine flows - a view confirmed by a recent independent GE assessment of the Lam & Bremhorst low-Re k-ε model for Navier-Stokes code computations. In this respect it is encouraging that good results have now been obtained for the **T3D3 & T3L** Test Cases by Rodi & Papanicolaou with their version of the Karlsruhe two-layer model, which is also considerably less demanding of grid resolution.

Reynolds stress models: A re-evaluation of the low-Re SLY model against the **T3A** Test Case, performed in conjunction with Henkes & Westin at Delft, has clarified certain key features of the closure approximations, which have not been made clear before, and largely confirmed its relative insensitivity to initial and boundary conditions provided certain grid constraints are met. Interestingly, particularly in view of the attempts at UMIST & Delft to use the alternative 2D-limit approach to minimise the influence of wall-reflection terms, the same study has revealed that these can be omitted from the SLY model without significantly affecting the excellent Cf & H predictions for transition; although the development of the turbulence profiles and Reynolds stress budgets are then degraded - see attachment.
Preliminary computations performed with the original SLY model for the **T3A$^+$& T3E** Test Cases indicated a variation of transition onset with free-stream length scale for **T3A$^+$** consistent with other data and expectations based on earlier parametric studies performed with a variety of models, while the **T3E** predictions agreed well with the Test Case data up to onset of re-transition,but suggested further near-wall refinement was needed for the relaminarising section.
Parabolic computations have now also been performed for the exact **T3A$^+$** Test Case conditions and for the **T3C$^+$, T3F & T3N** Test Cases - again see separate attachments.
The **T3A$^+$** predictions have been compared with the first sets of experimental data just released by the Prague data-takers (see Appendices), and have confirmed that the SLY model does indeed predict the variation in transition with fst length scale at least as accurately as the Delft Launder-Sharma k-ε results and better than the Johnson Integral method, Vasilev one-equation model, Janour two-layer model and Steelant & Dick k-ε–γ model -the only models so far tested
No data or other predictions have so far been reported for the **T3C$^+$** Test Case (although computations for all three latest Test Cases are being undertaken at Delft by Hanjalic et al.), but the SLY model appears to correctly predict a rapid transition in the reattachment region.
The model also correctly predicts the effects of streamline curvature on transition in the **T3F** Test Case, at least at low free-stream turbulence levels, and seems to quite accurately predict the transition onset location for the fixed wake fst encountered in the **T3N** Test case.
These finding confirm the potential of this model for predicting more complex blading cases.

At the same time the original SLY RST model [12] has been refined by adding in model approximations for Pressure-Diffusion of the stresses and ε, together with other non-local transport effects, as indicated by the **T3B$_{DNS}$** Simulations in order to improve predictions for the Simulated Reynolds stress balances. As a result the Cf & H predictions for the **T3A$^-$, T3A, B & T3B$^+$**Test Cases (already the best overall) have been slightly further improved, together with the turbulence profile developement for **T3A&B**. In addition the modelled γ transport equation included in the SLY-γ version [13] has been modified to further improve intermittency predictions for both the **T3A$^-$& T3A** Test Cases.

In principle a hybrid low-Re/2D-limit approach should allow a clearer distinction to be drawn between the modelling of low-Re transitional and low-Re near-wall effects. Some good results for the **T3A&B** Test Cases have been reported by Cho & Launder at UMIST [16] (using a combination of the Launder-Shima low-Re RST model and 2D-limit Craft-Fu-Launder-

Tselepidakis RST scheme), and Henkes & Westin at Delft have now obtained equally good results for the T3B & C1 Test Cases (using the alternative 2D-limit RST model of Jakirlic, Hazdik & Hanjalic). However they found their scheme would not work for the lower fst of case **T3A**, and this approach still requires further development and evaluation against a wider range of test cases - especially **T3L**. The RST approach should prove superior for this Test Case also because such stress transport models correctly predict only a small growth in turbulence energy along stagnation streamlines and grid resolution may then be less of a problem.

Simulations: Besides the creation of the extensive $\mathbf{T3B_{DNS}}$ database, satisfactory Large Eddy Simulations have now been performed for the **T3A,T3B,T3C1,T3D2 & T3L** Test Cases. A detailed analysis of the Simulation $\mathbf{T3B_{DNS}}$ database has shown that the Launder-Sharma model provides a better represetation of the f_μ variation through transition, particularly when rescaled precisely as in the computer optimised E factor of the SLY model (a feature which contriubtes significantly to its success), although it now appears this is even better reproduced by the alternative Reynolds low-Re model Ry-dependent damping function which Dawes has converted to Rt form in his otherwise Rt-version of the Lam & Bremhorst scheme. The Simulations also indicate that the normal turbulent near-wall assumption used for such conversion,that Rt=0.4Ry, is altered through transition; a better approximation being Rt=0.6Ry Of more general significance is the fact that the Simulated Reynolds stress budgets indicate the need to include a specific allowance for necessarily non-local Pressure-diffusion effects, in the form of cross-diffusion terms for k & ε - only previously employed for the T3A &B Test Cases in the k-ε model of Abid [3] which suffered from other defficiencies - and at the RST level also for non-local Pressure-strain effects as well.
As noted above such modifications have been incorporated successfully in the non-local version of the SLY model, and surprisingly good predictions have also been obtained for the **T3A-C** Test cases using the much simpler Johnson integral methods and CIAM ν_t - 92 one-equation eddy-viscosity transport model when these were modified to include simpler allowances for such pressure field effects.

A number of LES numerical experiments have also been performed for variations on the $\mathbf{T3B_{DNS}}$ case in order to investigate further the mechanisms of transition and the effect of varying degrees of free-stream aniostropy. These have highlighted in particular the dominant role of vertical fluctuations in determining the actual location of transition for such unsheared free-stream turbulence (NB. For wake turbulence as in the **T3N** Test Case it is clear that uv should have an equally large effect) and thus helped to confirm the advantages of switching to v' for the velocity scale in the Karlsruhe two-layer model, and of adopting alternative non-linear k-ε or RST approaches. They have also served to re-emphasise the importance of allowing for interaction-at-a-distance pressure-field effects which are equally important as the Diffusion of external turbulence into the initial pseudo-laminar boundary layer that most low-Re treatments automatically assume is the primary controlling influence on by-pass transition.

The initial LES results have been obtained for the **T3L1** Test Case (0.2%fst at 5m/s) both with and without a symmetry boundary along the stagnation line and using different Sub-Grid-Scale models). The best of these appears to capture most of the expected mean and turbulent flow features, and shows a bubble which is only a little too short compared to nominally zero free-stream experimental conditions studied by Rolls-Royce researchers. Interestingly tests with different Sub-Grid-Scale models have provided support for the idea of adopting a kind of zonal or hybrid modelling approach [19]. Best agreement with experiment has so far been achieved not with a fixed Smagorinsky constant, but with value varying from approximately 0.23 (typical of a free-shear flow) for the initial bubble region, decreasing to 0.1 (typical of a wall-bounded layer, beyond reattachment). The Simulations also suggest that the important length and turbulence scales for the transition process are those associated with the reattaching shear layer rather than the imposed external fst and that the latter has only a rather indirect influence on the former whcih suggest that these additional scales should be accounted for in any truly predictive model.Work is now underway to perform a definitive database Simulation for this Test case using a simpler hybrid SGS model, and later to test a dynamic SGS treatment.

Other relevant work has been carried out by additional European SIG participants and affiliated members of the SIG in the USA and Australasia. A number of different studies suggest that the SIG should continue to consider the option of a model combining an R_y dependence for (low-Re) near wall regions and an R_t or R_L dependence for (low-Re) transition regions.

The alternative two-time-scale k-ε model of Yang & Shih (NASA Lewis), which uses a combination of R_t and a non-dimensional strain rate parameter to handle low-Re/near-wall damping, would also appear to merit further investigation. This model has been shown by the Cambridge group to provide the best k-ε model predictions for flow and separation around Tube-bundle rods, and the UMIST group have found that a modified version (including also elements of the Lien-Leschziner model) provides good predictions for 3D transition and separation on an elipsoid at an angle of attack. At the same time Crawford, working at Texas University and in conjunction with the Karlsruhe group, has obtained excellent predictions for both the onset and length of transition in the **T3A** Test Case using a modeified multi-scale k-ε scheme, which he is now extending to consider variable pressure gradient cases.

In view of the Simulation findings there is also good reason to believe that another good candidate for a transition prediction model may be that developed by Durbin [20] at NASA Ames/CTR, which both adopts v' as velocity scale and solves an elliptic relaxation equation to take specific account of the non-local damping influence of the wall on the external turbulence, and Durbin himself will shortly be testing this on the **T3A&B** Test Cases,

At the same time SIG participants in Lisbon and DRA/KTH are starting to pursue the possibility of extending the well-known e^n and Parabolised Stability Equation (PSE) approaches to the **T3A-B** series of zero p.grad. variable fst by-pass transition cases. There is some evidence that both methods can be used successfully to predict the onset of transition for non-zero fst, so coupling to the type of intermittency transport methods being developed within the SIG might provide a future alternative design method for predicting a wider range of transitional flows.

All the SIG findings have been used to draw up the attached 'Best' Current Transition Models list giving options at each level of closure, but it is perhaps appropriate to highlight the potential of the non-linear k-ε approach, two-layer models and perhaps especially the non-local SLY RST-γ and hybrid 2D-limit models for predicting both simple and more complex transitional test cases. These approaches in particular should now be thoroughly evaluated in elliptic computations for the **T3L** and blading Test Cases. It has to be recognised however that additional input from experimental and computation studies of much more complex Test Cases, including real engineering flows, will be required to further improve current physical modelling and ensure that the identified 'best' models really will be able to improve predictions when many more complicating factors have to be taken into account. Information is already being sought concerning the conditions that models need to be able to handle in practice and the effects which are likely to be the most difficult to predict, so that decisions can be taken regarding future test case selection.

The data taken by the BRITE-EURAM partners will provide a good foundation for the continued evaluation of transition models against progressively more complex test cases. The **T3L** Test Case has already become an important stepping stone from the simpler flat plate Test Cases considered by the SIG prior to the present project and the blading cases that need to be addressed for practical purposes. There is considerable scope for further analysis and refinement of models by comparison with both the experimental data and Simulations for **T3L**. Initial predictions for **T3L+** (with additional effect of imposed blading-type pressure-gradient) are expected shortly and the other **T3L** datasets (covering also variations in angle of attack, imposed mean shear, and fixed and moving wake turbulence) will provide allow successive evaluation of many of the factors influencing real blading flows.

These will be complemented by data from a further experimental investigation presently being conducted by Tain & Cumpsty at the Whittle Laboratory (which introduces also compressibilty effects), while further studies being conducted by Kang and colleagues in Korea on aerofoil wake/flat plate and aerofoil-wake/aerofoil-boundary-layer interactions will provide a useful further extension to the **T3N** Test Case.

It is intended that the success of the interaction between particularly the industrial BRITE-EURAM Project Partners/Endorsers and the SIG sub-contractors will be built upon by establishing a Thematic Network to provide direct access for a wider range of industries to the optimised transition capablilites being developed amongst the academic and research establishment contributors to the SIG. An outline of the proposed activity, involving up to 10 industries and 15 research groups, which it is hoped will form the core of an expanded SIG activity for 1998-2000, is included in the Appendices.

It is expected that a growing number of ERCOFTAC Corresponding Member groups from Easter Europe will become involved in this work in furture. Already groups in Poland and Roumania have applied to join the COSTEC-funded group in Prague, and funds have already been awarded for an INTAS-94-255 Project to allow the groups from CIAM and Institute for Problems in Mechanics in Moscow and the Institute for Engineering Thermophysics in Kiev to play a fuller role in the SIG activities during 1995-1997. As part of their work the Kiev group will provide data for a new **T3H** Test Case considering effects of turbulence on heat transfer. The COST Action is already providing complimentary data for two further Test Cases: **T3I** (2D Steam-Turbine Blading Case) and **T3J** (considering combined effect of 2D and 3D curvature), and has recently been approved for prolongation within Framework IV during 1996-1999. This will also allow an expansion of SIG activities to consider Taylor-Gortler-induced transition on concave surfaces (**T3G** Test Case) as a necessarily 3D extension to the **T3F** Test Case; natural transition as an extension to current intermittency modelling; hypersonic transition via the inclusion of the latest dilation model approximations; and transition on both moving and non-planar surfaces.

Data for the **T3A-C** series of Test Cases has already been included in the ERCOFTAC Database, set up with CEC SCIENCE funding, and it is hoped that data for all the other Test cases, and perhaps also model comparisons, will be added to this eventually. The Database can be accessed via internet from the server http://fluindigo.mech.surrey.ac.uk at Surrey University once an ERCOFTAC password has been obtained from Dr.Voke. The ERCOFTAC Coordination Centre has also set up a World Wide Web (WWW) Server http://imhefwww.epfl.ch/lmf/ERCOFTAC at EPFL to act as a Bulletin Board for the whole of ERCOFTAC and the SIGs in particular. A home page for the Transition SIG has already been established and it is intended that all the Test Case specifications and other SIG information will be available via this in furture.

References

[1] Various Authors (1992): Proceedings of the 1st ERCOFTAC Workshop on Numerical Simulation of Unsteady Flows, Transition to Turbulence and Combustion, Lausanne (Eds: O.Pironneau, W.Rodi, I.L.Ryhming, A.M.Savill & T.V.Truong; CUP) - see in particular A.M.Savill: A Synthesis of T3 Test Case Predictions.

[2]A.M.Savill (1991) Turbulence Model Predictions for Transition under Free-Stream Turbulence. Poster Paper at RAeS Transition and Boundary Layer Control Conference, Cambridge.

[3] A.M.Savill (1991) Predicting Transition Induced By Free-Stream Turbulence.Progress Report Poster Paper at 1st European Fluid Mechanics Conference, Cambridge.

[4] A.M.Savill (1992) Evaluating Turbulence Model Predictions of Transition - an ERCOFTAC Special Interest Group Project. In Advances in Turbulence (Ed: F.T.M.Nieuwstadt; Kluwer Academic Publishers), Applied Scientific Research 51 pp.555.

[5] A.M.Savill (1992) Predicting By-Pass Transition With Turbulence Models. Proc. 11th Australasian Fluid Mechanics Conf., Tasmania.

[6] A.M.Savill (1992) Transition Modelling for Turbomachinery. Invited Review Lecture on the ERCOFTAC Transition SIG Project in Proceedings of ERCOFTAC Turbomachinery SIG Seminar and Workshop on 3D Turbomachinery Flow Prediction, Vol.1.

[7] A.M.Savill (1993) Some recent progress in the turbulence modelling of by-pass transition. In Near-Wall Turbulent Flows (Eds: R.M.C.So & B.E.Launder; Elsevier B.V.), pp.829.

[8] A.M.Savill (1993) Further progress in the turbulence modelling of by-pass transition. In Engineering Turbulence Modelling and Experiments 2 (Eds:W.Rodi & F.Martelli; Elsevier Science Publishers B.V.), pp.583.

[9] A.M.Savill (1993) COST-ERCOFTAC Special interest Group on Transition. ERCOFTAC Bulletin 19 pp.22.
[10] A.M.Savill (1994) Invited Review Lecture on Transition Modelling for Turbomachinery - A summary of Transition SIG Progress. In Proceedings of the ERCOFTAC Turbomachinery SIG Seminar and Workshop on 3D Turbomachinery Flow Prediction II, Val D'Isere, Part II.
[11] A.M.Savill (1994) Invited Review Lecture on Transition Modelling for Turbomachinery - A summary of Transition SIG Progress. In Proceedings of the ERCOFTAC Turbomachinery SIG Seminar and Workshop on 3D Turbomachinery Flow Prediction II, Val D'Isere, Part II.
[12] A.M.Savill (1993) Transition Modelling for Turbomachinery. Summary Proceedings of the 1st ERCOFTAC Transition SIG Workshop of the BRITE-EURAM AERO-CT92-0052 Project Workshop on Transition in Turbomachinery, UMIST.
[13] A.M.Savill (1994) Transition Modelling for Turbomachinery II. Summary Proceedings of the 2nd ERCOFTAC Transition SIG Workshop of the BRITE-EURAM AERO-CT92-0052 Project Workshop on Transition in Turbomachinery, VUB.
[14] A.M.Savill (1995) Transition Modelling for Turbomachinery III. Summary Proceedings of the 3nd ERCOFTAC Transition SIG Workshop of the BRITE-EURAM AERO-CT92-0052 Project Workshop on Transition in Turbomachinery, AUT.
[15] A.M.Savill & F.Pittaluga (1995) Meeting Report: COST-ERCOFTAC Transition SIG COST Action F1 Workshop. ERCOFTAC Bulletin 25 pp.36-37.
[16] Various Authors (1995) Theme Section - Transition. ERCOFTAC Bulletin 24 pp.5-67.
[17] K.Sieger, R.Schiele, A.Schulz & S.Wittig (1994) Gas Turbine Blade Heat Transfer Calculations: An Assessment of Different Low-Reynolds Number k-ε Turbulence Models. Proc. 5th Int. Symp. on Transport Phenomena and Dynamics of Rotating Machinery, Hawaii.
[18] X.Zheng & F.Liu (1995) Staggered Upwind Method for Solving Navier-stokes and k-ω Turbulence Model Equations. AIAA J. 33 (6) pp.991.
[19] Z.Yang, P.R.Voke & A.M.Savill (1996) LES of Laminar Separation Bubble Induced Transition. To appear in Proc. Engineering Flow Modelling and Measurements 3, Crete.
[20] P.A.Durbin (1993) Application of a near-wall turbulence model to boundary layers and heat transfer. Int.J.Heat & Fluid Flow 14 (4) pp.316.

TABLE 2: ACTIVE PROJECT PARTICIPANTS, MODELS & PROGRESS
Europe {1-4 BRITE-EURAM Project Partners, 5-14 SIG Participant Sub-contractors}

					A^{-+}	B^{+}	C2	1	3	4	5	C^{+}	LL^{+}	B_{DNS}
*	ROLLS-ROYCE plc	(Coupland,Ho)	k-lε,k-ε [Hassid-Poreh/Birch,L&B][1]	E			X	X	X	X	X		p p	
*	ARISTOTLE Univ.	(Goulas et al.)	k-ε [Launder-Sharma] [3]	PE	p p		X		X	X	X		X	
+	CRANFIELD	(Elder et al.)	k-ε [4]	P								p	p	
	VUB	(Hirsch et al.)	k-ε [4] incl. Biswas&Fukuyama	E									p	
*	CAMBRIDGE Univ. & (Whittle/ EPFL)	(Savill / Brandt Dawes / Hustad	low-ReRST-γ [Savill-Launder-Younis] [1], k-ε [modified L&B]	P	X X	X	X	X	X	X	X	p	p	X
+	DRESDEN Univ.	(Grundmann et.al.)	k-lε [Fish & MacDonald] [6]	P	p	p	X	p	p	p	p			p
+	DELFT Univ.	(Henkes)	k-ε [7]	PE	X p	X	X						p	X
+	GHENT Univ.	(Dick & Steelant)	k-ε + γ + Intermittency] [5]	P	X X	p		X			X			p
*	KARLSRUHE Univ.	(Rodi et al.)	k-ε [Launder-Sharma,Lam Bremhorst] & k-ε/k-lε [1]	P			X						p	
+	&	(Sieger, Schulz & Wittig)	k-ε [PTM Launder-Sharma &Lam & Bremhorst, Chien, Myong-Kasagi, Nagano-Tagawa] [44,45]	P	X p	p	X	X	X	X	X			p
p	KTH & (FFA)	(Alfredsson /Henningson	k-ε,RST, DNS & PSE [Various approaches]	PE	p									
+	LIVERPOOL Univ.	(Johnson)	γ / Correlations [New pressure field model]	P	p X	X	X	X	X	X	X			X
+	LEICESTER Univ.	(Gostelow)	UTS Integral Method [27]	P	X	X	X	p	p	p	p			p
+	UMIST	(Launder & Cho)	RST [LaunderShima/CFLT10,11]	PE	X	X								X
+		(Lien,Leschziner & Chen) + (Suga)	k-ε [L-S/KL,L-L,CLS non-linear]	E			X	X	X		X		p p	
+			non-linear k-ε-A2	E			p	p	p		p		p	
*	SURREY Univ.	(Voke & Yang)	LES/DNS [Fully Resolved Simulation] [1]	E				X					X p	X
p	EDF	(Baron/Laurence)	k-ε & RST SLY or CFLT [1]	E										p
p	FLORENCE Univ.	(Martelli) (Michelassi)	k-ε [L&B,L-S+Rodi-Scheuerer]8] k-ε [Michelassi & Shih]	E										
+	PRAGUE Thermo.Inst.	(Prihoda & Janour)	Integral method, k-lε, k-ε-γ [Various formulations]	PE	X X									
p	Inst. Problem. Mech Moscow	(Aleksin)	k-ε, RST [Various model forms]	PE										
+	CIAM Moscow	(Vasiliev)	vt-90/92 & Integral Methods	P	X X	p	X	X	X	X	X	p		p
p	Inst.Thermophys Kiev	(Epik & Dyban)	Correlation/ Mixing Length	P										
	USA, Asia & Australia													
+	VIRGINIA P.I. & STATE U/Beijing	(Moores) (Jiang)	k-lε + correlations [Moores] [13]	P	p		p							
+	TEXAS Univ	(Stephens & Crawford) with Sieger at al.	k-ε [PTM Launder -Sharma], [Chien], [Lam & Bremhorst] [15] Multi-scale k-ε/k-lε	E	p p		p p							
+	NASA LANGLEY	(Gatski & Abid)	k-ε or k-τ [Speziale et al.] [17,18] RST [Launder-Shima] [10,18]	P										
p	NASA AMES/CTR	(Durbin)	k-ε-v Elliptic Relaxation Model											
+	NASA LEWIS	(Zhang & Shih)	k-ε/k-ε-γ [Shih & Zhang] [20]	E										
+	McGill Univ.	(Hedberg)	RST [Launder-Shima & SLY]	E									p	X
+	NAGOYA Univ.	(Nagano & Tagawa)	k-ε [Nagano-Hishida/Tagawa] [22,23]	P										
+	TOKYO Univ.	(Kasagi & Shikazono)	k-ε [Myong-Kasagi+mods] [24]	P			X							
*	GUNMA Univ.	(Fujisawa)	k-ε [Launder-Sharma+mods][25]	P			X							
+	TOSHIBA R&D	(BiswasFukuyama)	k-ε [Various+own new model]	PE	p	p	X		X	X	X			p
p	SEOUL Univ.	(Kang)	k-ε [Launder-Sharma]	PE										
p	KOREA Inst. Tech.	(Cho & Chung)	k-ε - γ [Intermittency] [26]	P										
+	Univ. TASMANIA	(Walker/ Solomon)	UTS Integral Method [27]	P	X	p	X	p	p	p	p			p

{*: Original Lausanne Workshop Computor for T3A&B Cases} {P: Parabolic Code, E:Elliptic Code}
{+: Have subsequently also computed original T3A&B Cases}
{X: Have made predictions for additional Test Cases as indicated}
{p: Computations in progress or planned}

NB Also: Surrey, Karlsruhe(Rodi), Delft: T3D2
Cambridge & Prague : T3E
Cambridge: T3F & T3K (with EPFL)
Cambridge & Seoul: T3N

References as in [9] or see [10,11]

'BEST' CURRENT TRANSITION MODELS
(ON BASIS OF TRANSITION SIG T3 TEST CASE EVALUATION)

Integral Methods
Johnson (Liverpool University) [including new Pressure-Field Model]

Validated for: zero pressure gradient 1-6%fst (not satisfactory for 10%fst, overpredicts effect of variable free-stream length-scale), 3-6% favourable/adv. p.grad &variable Re (unless laminar separation)

also: Gostelow (Leiceister University) [including UTS local parameter Correlation] & Walker & Solomon (University of Technology Sydney/Tasmania University)

Validated for: zero pressure gradient 1-6%fst (not tested for 10%fst/variable Lε) & 3% favourable/adv. p.grad. (only design Re tested)

One-Equation Models
Birch/Coupland (Rolls-Royce) - k-l model

Validated for: zero pressure gradient 3-6%fst (not tested for 1 &10%fst) &
(parabolic) variable Re (but not effect of variable pressure gradient)

also: Grundmann (Dresden University) modified Fish &MacDonald k-l model

Validated for: zero pressure gradient 3-6%fst (not tested for 1 or 10%fst) & 3% favourable/adv. p.grad (not tested for variable Re)

and: Vasiliev/Secundov (CIAM) - modified ν_t-90/92 model

Validated for: zero pressure gradient 1-3%fst (not as good for 6%fst & overpredicted effect of variable free-stream length scale)

'Standard' Two-Equation Models
Launder-Sharma k-ε model (independent verification by many SIG Participants)

Validated for: zero pressure gradient 3-6%fst (too early onset for 1 &10%fst) &
(parabolic) 3% favourable/adverse pressure gradient and variable Re
[with Fujisawa or Yap correction for adverse pressure gradient]
(but Fujisawa correction has wrong sign for favourable p. grad.)

(elliptic) finite leading edge/laminar separation bubble, variable fst & Re
[with: Kato-Launder irrotational Pk (and Yap) correction]
(earlier onset for zero or variable p.grad/sharp leading edge & need to scale K-L correction to predict correct bubble extent)

{But L-S maybe more grid sensitive than some other models}

also: Biswas & Fukuyama (Toshiba Research & Development) low-Re model
similar/better parabolic performance to L-S model [?with Rt f_2]
& avoids use of D & E factors + uses $d\varepsilon/dy=0$ wall b.c.

and: Lam & Bremhorst (with damping functions converted to Rt form?)
or Dawes (Reynolds/L&B model coverted to Rt-dependent form)
possibly better for elliptic computations and also have numerical advantages of avoiding use of D & E factors & uses $d\varepsilon/dy=0$ wall b.c.

{However L&B generally more sensitive to initial conditions}

{All tend to give too abrupt transition - zero p.grad improved with γ scaling;
zero and fav/adv p.grad and variable Re improved with PTM, but length then long}

Non-linear k-ε Schemes
Two-equation Craft-Suga-Launder k-ε model

Validated for:zero pressure gradient 3-6%fst (as good as L-S model)
(parabolic & elliptic) & 3% fst favourable/adverse pressure gradient &variable Re
(transition too early unless Yap correction also included)

and: Three-equation Suga-Launder k-ε-A_2 model

Validated for:zero pressure gradient 3-6%fst (better than L-S model)
(no good results yet obtained for variable pressure gradient)
(parabolic) {Problems encountered with elliptic implementation}

Second-Moment Closures
Savill-Launder-Younis or SLY (Cambridge/UMIST) - low-Re RST model

Validated for:zero pressure gradient 1-10%fst (transition length short for 1&10%);
variable free-stream length scale & convex curvature (trend only);
3-6% fst favourable/adverse pressure gradient,variable Re
(parabolic) & retransition following relaminarisation (trends correct);
weakly and strongly anisotropic 4.5%fst (only trends for strong)
& high intensity fixed free-stream wake turbulence.

{Equally good or better results with addition of non-local transport model approximations and/or intermittency transport, but needs elliptic code evaluation}

also: Launder, Tselepidakis & Cho - hybrid 2D-limit/Launder-Shima low-Re RST
and: Hanjalic & Jakirlic - alternative 2D-limit RST model approach

Validated for:zero pressure gradient 1-10%fst (transition length short for 1&10%)
(parabolic & elliptic) & weakly anisotropic 4.5% fst
(not tested for variable p.grad, Re or strongly anisotropic fst)

Other models currently under consideration:

Two-Layer k-ε/k-l model: validated for zero p.grad 1-6%fst
(Karlsruhe & Thessaloniki) & 3-6% fst favourable/adverse pressure gradient with variable Re
(results generally similar to L-S model, but very much better than L-S model when v' adopted as velocity scale - then predicts onset and extent of transition accurately without extra corrections)

Yang & Shih k-ε-γ (Narasimha)/ : validated for zero p. grad 1-10%fst
(Dick & Steelant γ transport model) (1% early, 10% late & underpredicts effect of variable free-stream length scale)
& 3-6% fst favourable/adverse pressure gradient (correct trends with variable Re only)

Launder-Sharma k-ε-γ /surface renewal: tested for zero p. grad 3%fst,variable Lε,
two-layer model and relaminarisation/retransition (correct trends)

Crawford multiscale k-ε : validated for zero p.grad 3%fst.

Durbin k-ε-v (elliptic relaxation equation) model - results awaited with interest.

Yang-Shih/Michelassi-Shih two-timescale k-ε : awaiting results, but tests for other flows including Turbulence Modelling SIG Tube Bundle Test case encouraging.

UMIST combined Lien-Leschziner/Yang-Shih (two-layer-type) model: has produced good results for 3D transition and spearation on an ellipsooid at angle of attack.

low-Re Wilcox k-ω & NASA LaRC k-τ : Tested for zero p.grad 3-6% fst with very variable results - alternative Zheng k-ω fix for transition may need investigation.

UMIST non-linear k-ω: Preliminary study suggests too late transition for 6%fst.

RNG k-ε : preliminary indications negative

{NB. All models predict mean flow/integral properties better than turbulence quantities. Non-local SLY RST model comes closest to predicting full set of data extracted from Simulation Database for zero p.grad, anisotropic, 5% fst. Implication that all models should include allowance for pressure-diffusion effects in addition to accounting for anisotropy, and both x-wise and y-wise Re variation}

COST-ERCOFTAC Transition SIG Update - August 1997

The primary aim of the SIG work still remains the evaluation and improvement of turbulence model predictions for by-pass transition and re-transition, with the initial emphasis on turbomachinery applications. Regular progress reports in the ERCOFTAC Bulletin have highlighted the success of the participants in establishing 'best practices' at all levels of model complexity. It is now planned to build on this by establishing a larger CEC Thematic Network activity involving 25 ERCOFTAC member groups (8 industrial, 3 research establishments, and 14 universities) and up to 6 Corresponding member groups from Eastern Europe.

The main aims will be:

(a) Expansion of the present work of the SIG to consider other candidate model approaches of interest; validation of present 'best' model options at different levels of closure against a broader range of transition test cases, encompassing additional elements of complexity encountered in real industrial flows - especially 2D & 3D curvature, compressibility, rotation and unsteadiness.
[The emphasis will be on elliptic computations for finite leading-edge cases with the T3L case variants providing a new entry level of complexity]

(b) Establishment of definitive 'best choice' models at each level of closure from simple integral methods right through to Large Eddy Simulations; refinement and further development of these with reference to Direct Simulations and new experiments; as well as investigation of new schemes for linking turbulence modelling and stability analyses.

(c) The implementation of the established 'best' models in industrial codes for validation on practical 3D flow problems.

Participants will be divided into the following 5 linked sub-groups:
(under overall coordination of Dr.Savill)

Sub-group 1: Integral/Intermittency Methods - Coordinator: Erik Dick (Ghent Univ.)
(Main aim: switch from standard correlations to intermittency transport modelling for current integral design methods, k-e and RST closures)

Sub-group 2 : Eddy Viscosity Models & PSE/e^n - Coordinator: Kemo Hanjalic (Delft)
(Main aim: to define best choice model with widest predictive capabilites, but minimum mesh requirement for practical 3D problems and investigate if a combination of stability methods with intermittency conditionalised turbulence modelling could provide a better design method)

Sub-group 3: Reynolds Stress Transport - Coordinator: Brian Launder (UMIST)
(Main aim: Validation SLY RST model in elliptic computations and comparison against alternative hybrid low-Re/2D-limit closure)

Sub-group 4: Transition Simulations - Coordinator: Peter Voke (Surrey University)
(Main aim: Extension of LES to real engineering flow problems and wider use for generating databases to validate closure models)

Sub-group 5: Data input from real flows - Coordinator: Ferruccio Pittaluga (Genoa)
(Main aim: To extend and validate best models for real unsteady flows)

The management of the SIG will revised accordingly - already Professor Dick has agreed to join Dr.Savill and Prof. Pittaluga (the present coordinator and deputy coordinator respectively) in a new management committee.
Funding of 700kecu has now been approved from the EU IMT Programme for an initial 3-year Thematic Network activity subject only to completion of Contract Negotiations this September for an expected start in Januaray 1998.

It is now planned to hold the next Workshop of the ERCOFTAC Transition Special Interest Group at Cambridge, hopefully at the Isaac Newton Institute, in April or June 1998.
The main aims of the Workshop will be to review recent model developments and further model validation against a broader range of established test cases for by-pass transition.
Related work carried out within Round II of the COST F1 Action and INTAS Project 94-255 will also be discussed, together with the expansion of activities within the EU Thematic Network on Transition Prediction.
In particular the emphasis will be on extending predictive capabilities to more complex turbomachinery flows, with heat transfer, and other aerodynamic applications.
As such the Workshop is likely to be of interest to a wide range of researchers. Members of the SIG will be circulated with further details later.
If any additional ERCOFTAC members or others wish to attend they should contact the Coordinator.

Eur. Ing. **Dr.A.M.Savill** Engineering Department,
University of Cambridge, Cambridge CB2 1PZ
& Visiting Research Fellow, Mech.Eng.Dept, UMIST.
UK North Pilot Centre
Tel: +44 1223 332704 Fax: +44 1223 332662
e-mail: ams3@eng.cam.ac.uk

APPENDIX C

Unscheduled Contribution to Workshop

The Effect of Freestream Turbulence on Separation and Its Possible Control

I. Wygnanski
University of Arizona
Tucson, Arizona

ABSTRACT

Turbulence has to be characterized by intensity, scale and coherence relative to the object on which it impinges. The characteristic features of a separation bubble on an airfoil (or on a deflected flap) are determined by the intensity and by the scale of the flow perturbations in the free stream. They can therefore be controlled by altering either one of these parameters. Particle Image Velocimetry (PIV) that provides an instantaneous quantitative picture of the flow-field in two dimensions helps one to understand and explain the physics of the phenomenon associated with separation and reattachment. Active introduction of small amplitude, periodic perturbations to the flow provides the diagnostic tool (i.e. phase reference) needed to capture the flow field at various stages of its development. It also provides a way to manipulate the flow and alter its characteristic features.

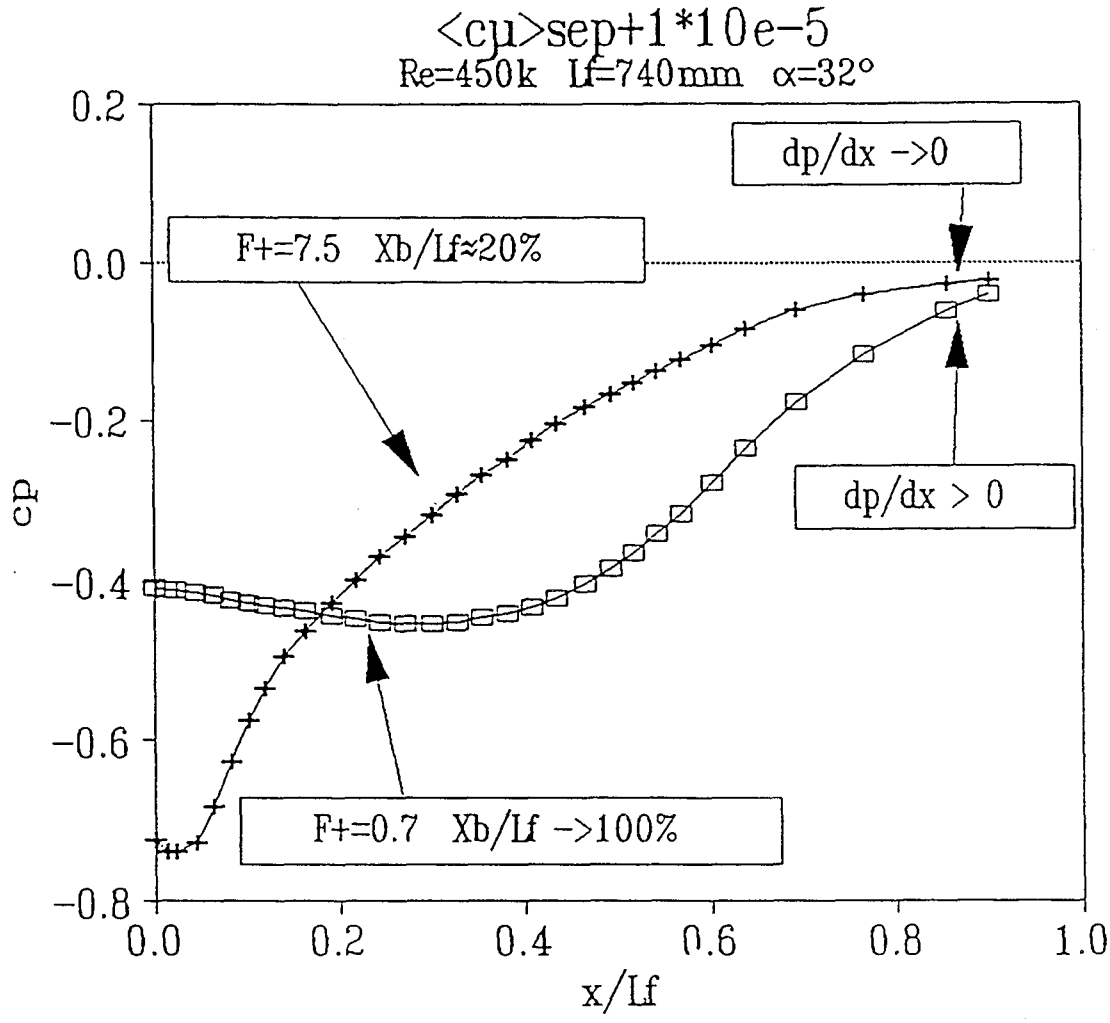
<cμ>sep+1*10e-5
Re=450k Lf=740mm α=32°
dp/dx ->0
F+=7.5 Xb/Lf≈20%
dp/dx > 0
F+=0.7 Xb/Lf ->100%
cp
x/Lf
0.2
0.0
-0.2
-0.4
-0.6
-0.8
0.0
0.2
0.4
0.6
0.8
1.0

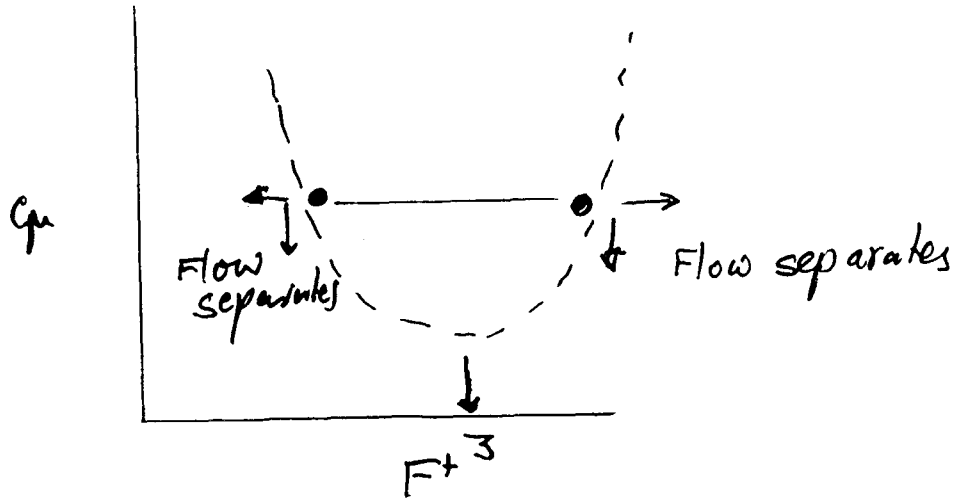
Cμ
Flow separates
Flow separates
F+3

MEAN VELOCITY

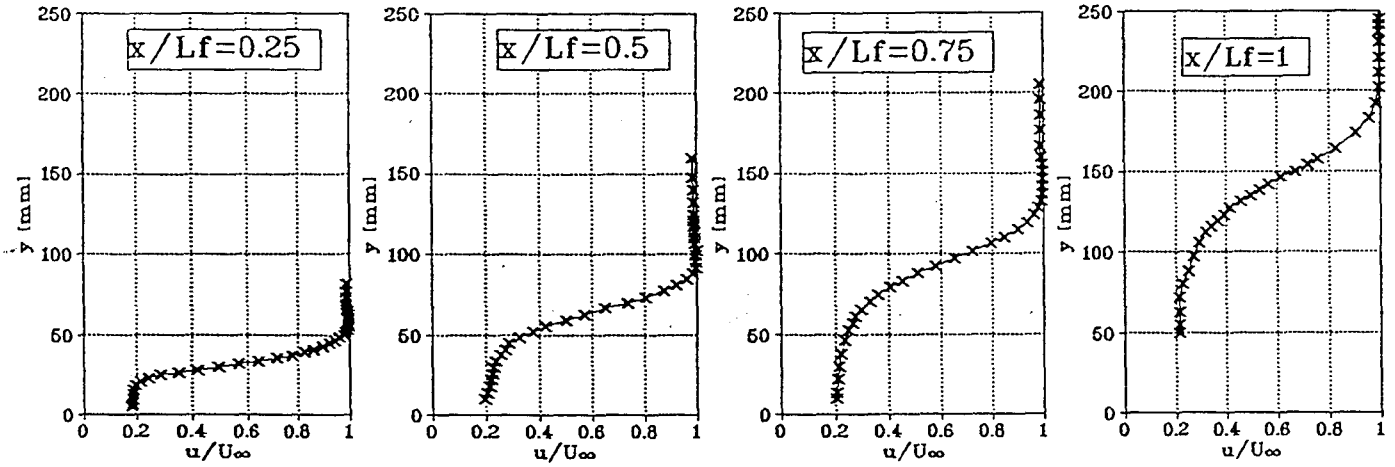

$C_\mu = 0.01\%$ $F^+ \sim 1$

AMPLITUDE

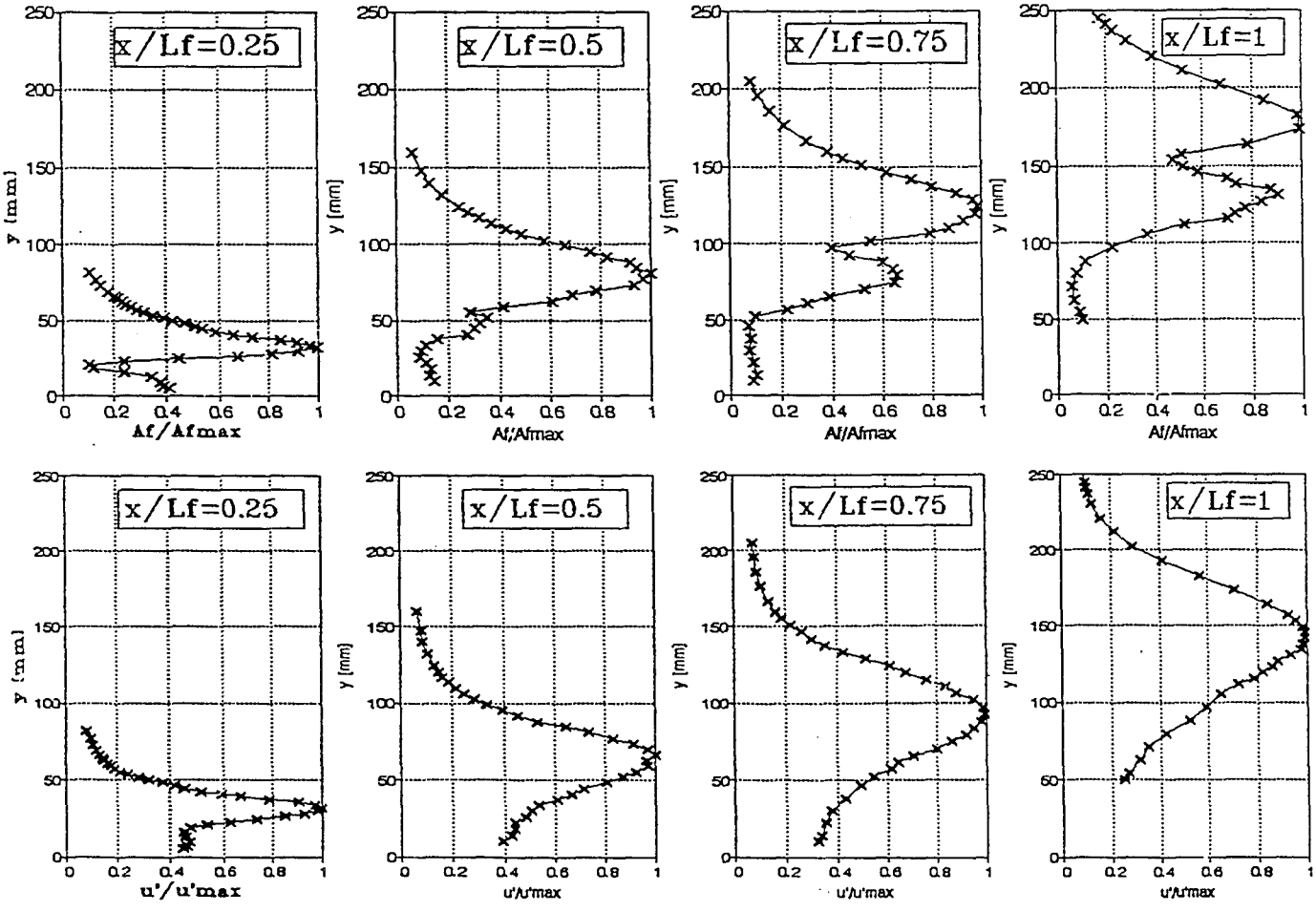

Mean vorticity

Re=165K , F^+=1.2 , α=26°

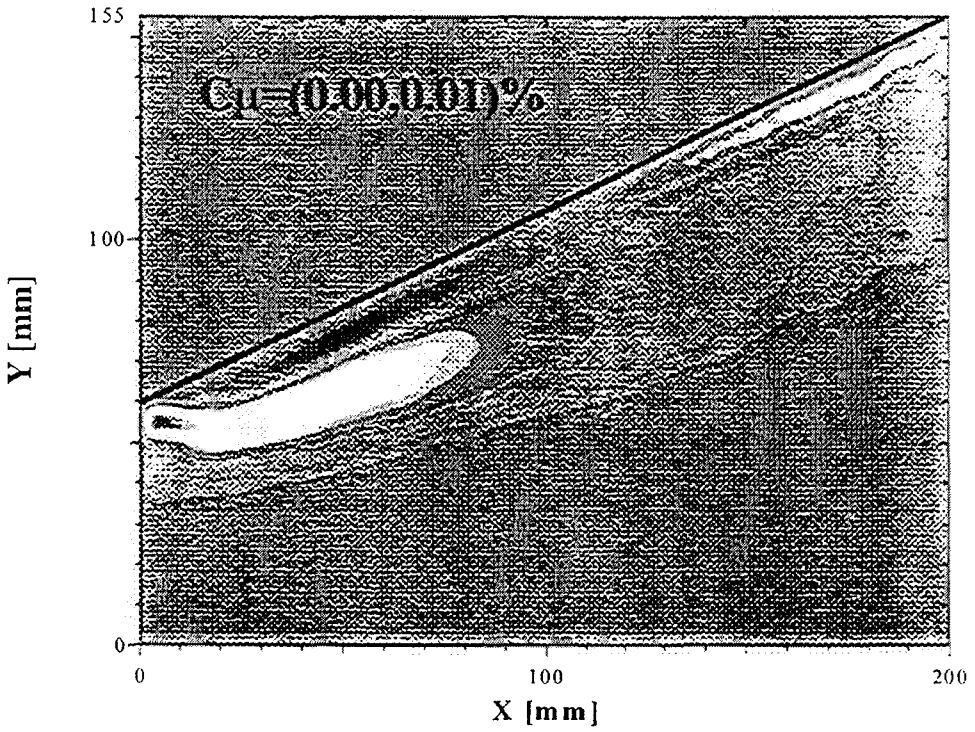

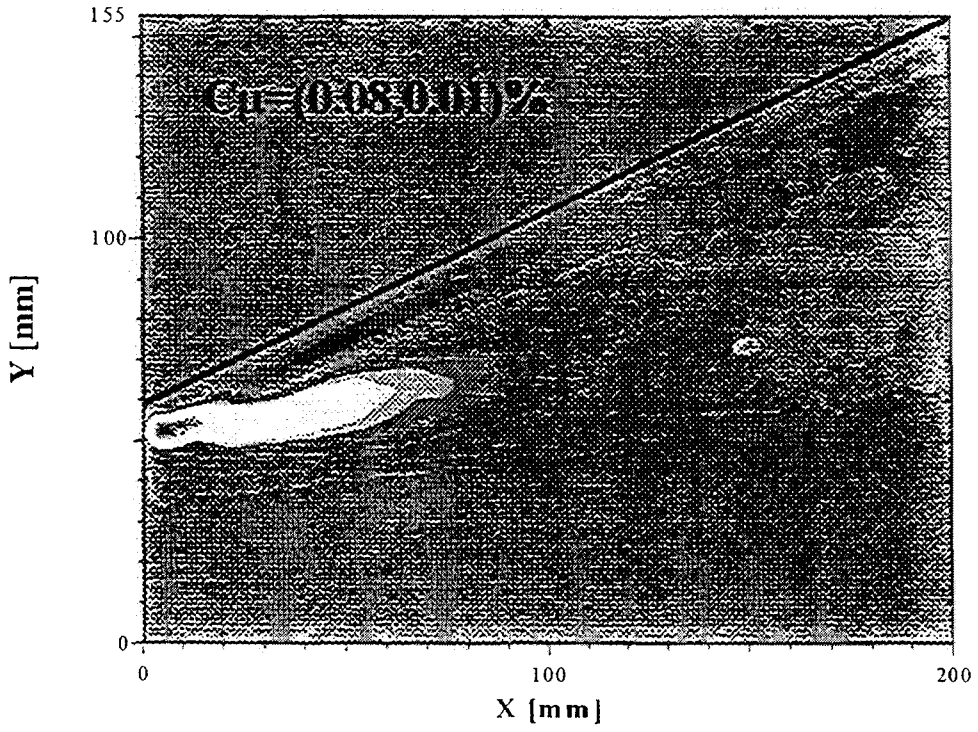

Phase Locked Vorticity and Straeklines

Re=165K , F^{+}=1.2 , α=26 deg

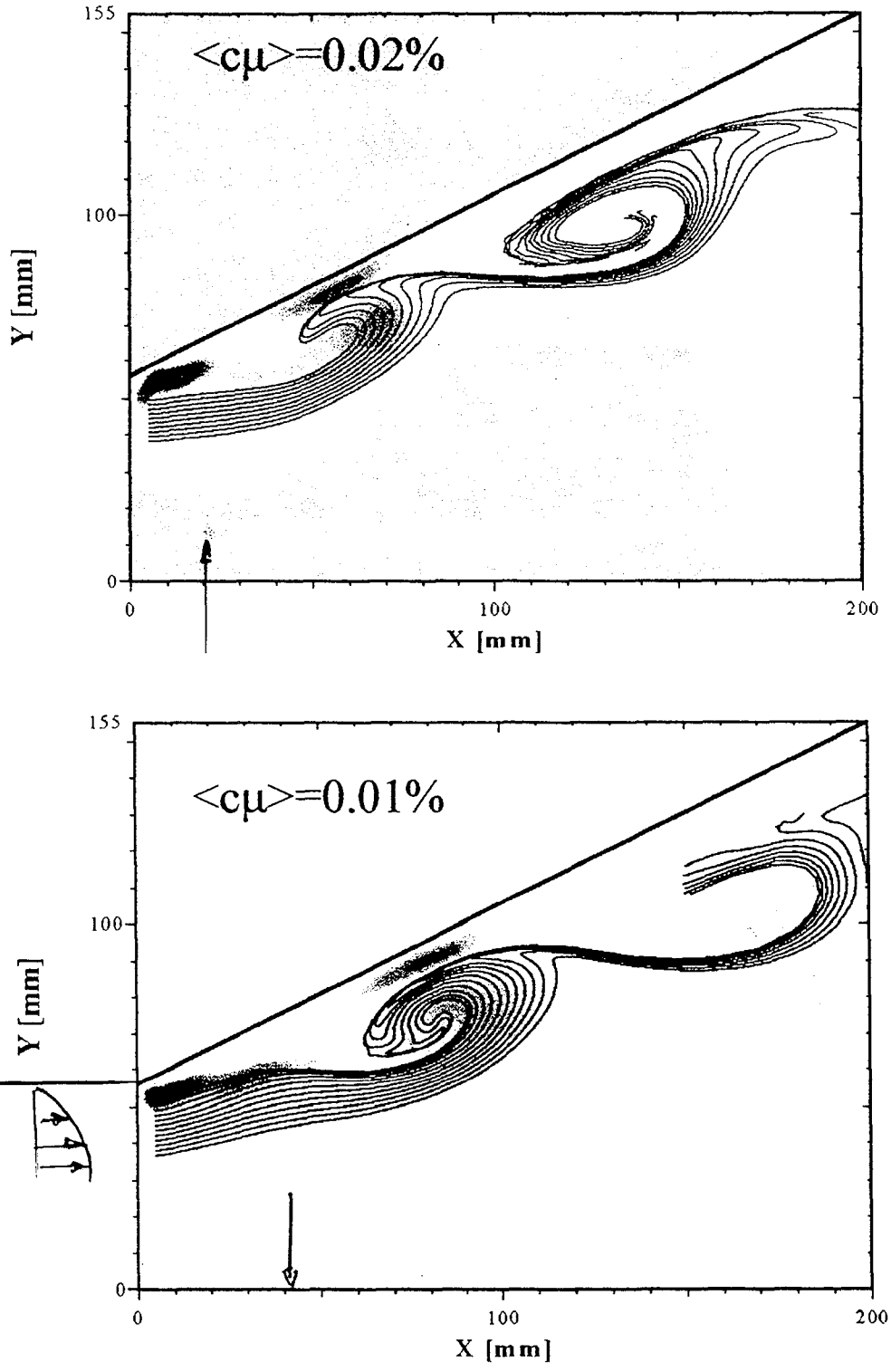

Phase-Locked Vorticity Through a Perturbation Cycle

$\langle c\mu \rangle = 0.01\%$; $F^{+}=1.2$; $\alpha_f=26°$; Re=165K

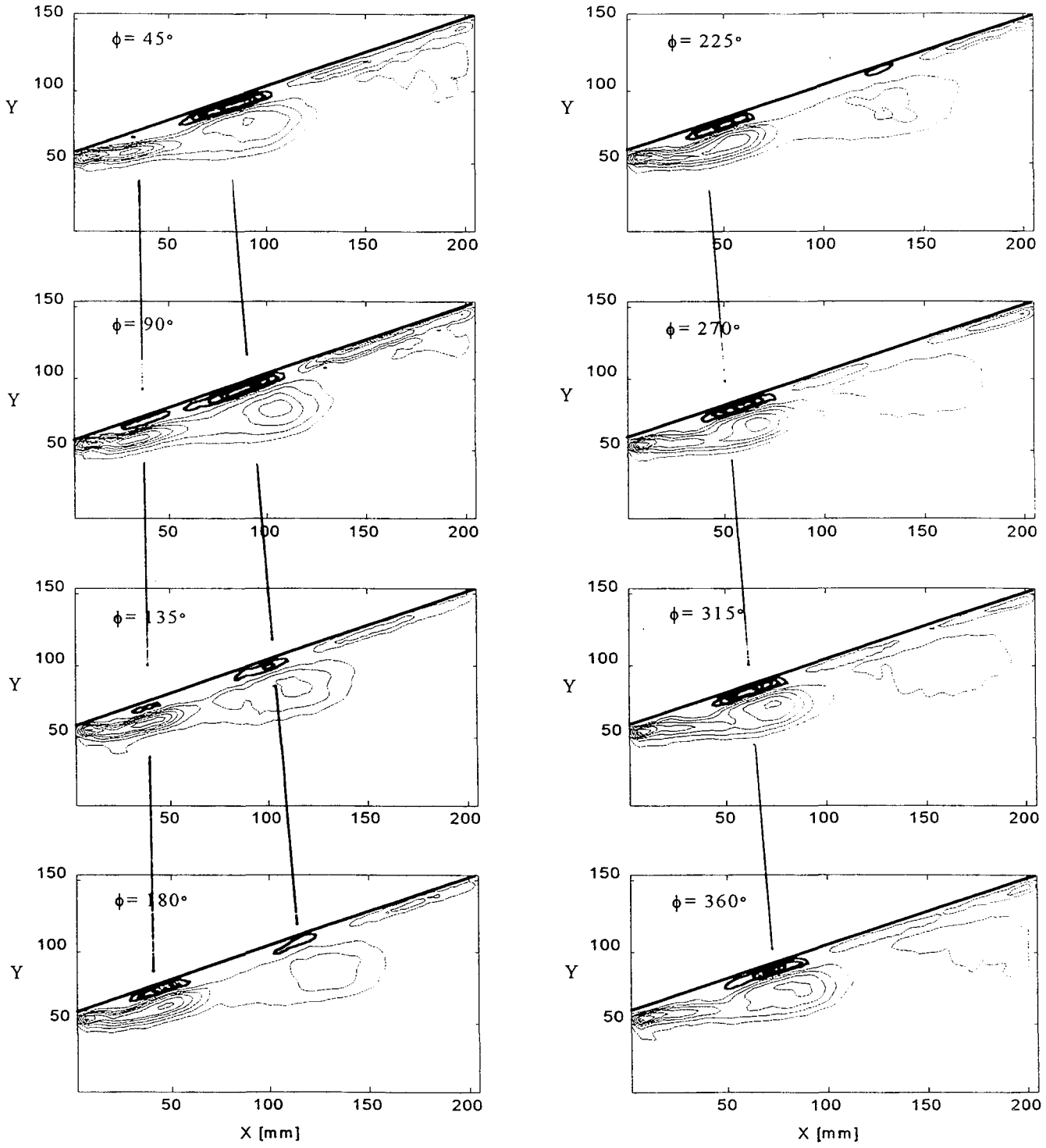

LIST OF PARTICIPANTS

Minnowbrook II
1997 Workshop on Boundary Layer Transition in Turbomachines
Syracuse University
7-10 September 1997

Dr. David Ashpis
NASA Lewis Research Center
21000 Brookpark Road, MS 5-11
Cleveland, OH 44135-3191
ashpis@lerc.nasa.gov.

Mr. Leonard Biagioni
Mech., Aero, & Mfg. Engr.
Syracuse University
151 Link Hall
Syracuse, NY 13244-1240
lbiagion@mailbox.syr.edu

Mr. Robert Boyle
NASA Lewis Research Center
21000 Brookpark Road, MS 5-11
Cleveland, OH 44135-3191
boyle@lerc.nasa.gov

Mr. Andrey Chernobrovkin
Penn. State University
153 Hammond Bldg.
University Park, PA 16802
acher@turbo3.psu.edu

Dr. Nick Cumpsty
Cambridge Univ.-Whittle Lab
Madingley Rd.
Cambridge CB3 0DY UK
cumpsty@eng.cam.ac.uk

Dr. Dan Dorney
GMI Engineering & Management Inst.
Dept. of Mechanical Engr.
1700 West Third Ave.
Flint, MI 48504-4898
ddorney@gmi.edu

Dr. Denis Doorly
Imperial College
Aeronautics Dept.
Prince Consort Way
London SW7-2BU UK
d.doorly@ic.ac.uk

Dr. Charles Fraser
School of Engineering
University of Abertay
Dundee DD5 4AR UK
cj.fraser@abertay-dundee.ac.uk

Dr. Mark Glauser
AFOSR/NA
Bldg. 410
Bolling AFB, DC 20332-6448
mark.glauser@afosr.af.mil

Dr. J. Paul Gostelow
Dept. of Engineering
Univ. of Leicester
Leicester, LE17 RH UK
jpg7@le.ac.uk

Dr. David Halstead
Mail Drop H92,
General Electric Aircraft Engines
One Neumann Way
Cincinnati, OH 45215-1988
david.halstead@ae.ge.com

Dr. Thorwald Herbert
Mechanical Engr. Dept.
206 West 18th Ave.
Ohio State University
Columbus, OH 43210-1107
herbert@dynaflow.com

Dr. Hiroshi Higuchi
Mech., Aero., & Mfg. Engr.
Syracuse University
151 Link Hall
Syracuse, NY 13244-1240
hhiguchi@syr.edu

Dr. Howard Hodson
Cambridge Univ.-Whittle Lab
Madingley Rd.
Cambridge CB3 0DY UK
hph@eng.cam.ac.uk

Dr. Lennart Hultgren
NASA Lewis Research Center
21000 Brookpark Road, MS 5-9
Cleveland, OH 44135-3191
hultgren@lerc.nasa.gov

Dr. Pavel Jonas
Institute of Thermomechanics
Dolejskova 5
CS 18200 Praha 8 Czech Republic
jonas@bivoj.it.cas.cz

Dr. Mark W. Johnson
Dept. of Mechanical Engr.
Univ. of Liverpool
PO Box 147
Liverpool L6938X UK
em22@liv.ac.uk

Dr. Terry V. Jones
Osney Labs-Oxford Univ.
Engineering Science
Oxford OX13PJ UK
terry.jones@eng.ox.ac.uk

Mr. Toshiro Kiura
Mech., Aero., & Mfg. Engr.
151 Link Hall
Syracuse University
Syracuse, NY 13244-1240
tkiura@syr.edu

Dr. Y. Kohama
Inst. of Fluid Sciences
Tohoku University
2-1-1 Katahira
Sendai, Japan
kohama@ifs.tohoku.ac.jp

Dr. John E. LaGraff
Mech., Aero., & Mfg. Engr.
151 Link Hall
Syracuse University
Syracuse, NY 13244-1240
jlagraff@syr.edu

Dr. Budugur Lakshminarayana
Penn. State University
153 Hammond Bldg.
University Park, PA 16802
b1Laer@engr.psu.edu

Dr. Jacques Lewalle
Mech., Aero., & Mfg. Engr.
151 Link Hall
Syracuse University
Syracuse, NY 13244-1240
jlewalle@syr.edu

Dr. Donald M. McEligot
Idaho National Engineering Lab
P.O. Box 1625
Idaho Fall, ID 83415-3890
dm6@inel.gov

Dr. Roddam Narasimha
Center for Atmospheric &
Ocean Sciences
Indian Institute of Science
Bangalore 560012 India
roddam@caos.iisc.ernet.in

Dr. Rob Norton
Allison Engine Co.
Box 420-Speed Code T10B
Indianapolis, IN 46206-0420
robert.j.g.norton@allison.com

Dr. Ted Okiishi
104 Marston Hall
Iowa State University
Ames, IA 50010
tedo@iastate.edu

Dr. Man Mohan Rai
NASA Ames Research Ctr.
Moffett Field, CA 94035-1000
mrai@mail.arc.nasa.gov

Dr. Eli Reshotko
Dept. of Mech. & Aero. Engr.
Case Western Reserve University
2109 Adelbert Rd.
Cleveland, OH 44106
exr3@po.cwru.edu

Dr. Neal D. Sandham
Queen Mary & Westfield College
Mile End Road
London E1 4NS UK
n.sandham@qmw.ac.uk

Dr. William Saric
Arizona State University
Dept. of Mech. & Aero. Engr.
Tempe, AZ 85287-6106
saric@asu.edu

Dr. Avi Seifert
MS 170
NASA Langley Research Center
Hampton, VA 23681
a.seifert@larc.nasa.gov

Dr. Om Sharma
Pratt & Whitney
400 Main St.
MS 163-01
East Hartford, CT 06108
sharmaop@pweh.com

Mr. Fred Simon
NASA Lewis Research Center
21000 Brookpark Road, MS 5-11
Cleveland, OH 44135-3191
frederick.f.simon@lerc.nasa.gov

Dr. Terry Simon
Mechanical Engr.
111 Church St.
Univ. of Minnesota
Minneapolis, MN 55455
tsimon@me.umn.edu

Dr. Frank Smith
University College-London
Dept. of Mathematics
Gower St.
London WC1E6BT UK
frank@math.ucl.ac.uk

Dr. William J. Solomon
General Electric Aircraft Engines
One Neumann Way
Cincinnati, OH 45215-6301
William.Solomon@ae.ge.com

Dr. Rolf Sondergaard
Turbine Branch, Aero., Prop. & Power
Wright Laboratory
WPAFB, OH 45433-6533
sonderr@typhoon.appl.wpafb.af.mil

Dr. J. Steelant
Dept. of Mechanical &
Thermal Engineering
St. Pietersnieuwastraat 41
B-9000 Gent Belgium
johan.steelant@rug.ac.be

Dr. Anatoli Tumin
Faculty of Engineering
Tel-Aviv University
Tel-Aviv 69978 Israel
tumin@eng.ac.il

Dr. Gregory J. Walker
Dept. Civil & Mech. Eng.
Univ. of Tasmania
GPO Box 252C
Hobart, Tasmania 7001 Australia
greg.walker@cmech.utas.edu.au

Dr. Ting Wang
Mechanical Engr.
109 Riggs Hall
Clemson Univ.
Clemson, SC 29634-0921
ting.wang@ces.clemson.edu

Dr. David Wisler
General Electric Aircraft Engines
Mail Drop A411
One Neumann Way
Cincinnati, OH 45215-6301
dave.wisler@ae.ge.com

Dr. Israel Wygnanski
Aerospace & Mechanical Engr.
University of Arizona
Tucson, AZ 85721
wygy@bigdog.engr.arizona.edu

Dr. Guohua Xiong
Dept. of Mechanical Engr.
Univ. of Kentucky
Lexington, KY 40506-0046
ghxiong@engr.uky.edu

REPORT DOCUMENTATION PAGE

Form Approved
OMB No. 0704-0188

1. AGENCY USE ONLY (*Leave blank*)	2. REPORT DATE	3. REPORT TYPE AND DATES COVERED
	June 1998	Conference Publication

4. TITLE AND SUBTITLE

Minnowbrook II
1997 Workshop on Boundary Layer Transition in Turbomachines

5. FUNDING NUMBERS

WU–522–31–23–00

6. AUTHOR(S)

John E. LaGraff and David E. Ashpis, editors

7. PERFORMING ORGANIZATION NAME(S) AND ADDRESS(ES)

National Aeronautics and Space Administration
Lewis Research Center
Cleveland, Ohio 44135–3191

8. PERFORMING ORGANIZATION REPORT NUMBER

E–11100

9. SPONSORING/MONITORING AGENCY NAME(S) AND ADDRESS(ES)

National Aeronautics and Space Administration
Washington, DC 20546–0001

10. SPONSORING/MONITORING AGENCY REPORT NUMBER

NASA CP—1998-206958

11. SUPPLEMENTARY NOTES

John E. LaGraff, Terry V. Jones, and J. Paul Gostelow, conference organizers. Responsible person, David Ashpis, organization code 5820, (216) 433–8317.

12a. DISTRIBUTION/AVAILABILITY STATEMENT

Unclassified - Unlimited
Subject Categories: 07, 34, and 02 Distribution: Nonstandard

This publication is available from the NASA Center for AeroSpace Information, (301) 621–0390.

12b. DISTRIBUTION CODE

13. ABSTRACT ***(Maximum 200 words)***

The volume contains materials presented at the Minnowbrook II - 1997 Workshop on Boundary Layer Transition in Turbomachines, held at Syracuse University Minnowbrook Conference Center, New York, on September 7–10, 1997. Workshop organizers were John E. LaGraff (Syracuse University), Terry V. Jones (Oxford University) and J. Paul Gostelow (University of Leicester). The workshop followed the informal format at the 1993 Minnowbrook I workshop, focusing on improving the understanding of late stage (final breakdown) boundary layer transition, with the engineering application of improving design codes for turbomachinery in mind. Among the physical mechanisms discussed were hydrodynamic instabilities, laminar to turbulent transition, bypass transition, turbulent spots, wake interaction with boundary layers, calmed regions, and separation, all in context of flow in turbomachinery, particularly in compressors and high and low pressure turbines. Results from experiments, DNS, computation, modeling and theoretical analysis were presented. Abstracts and copies of viewgraphs, a specifically commissioned summation paper prepared after the workshop, and a transcript of the extensive working group reports and discussions are included in this volume. They provide recommendations for future research and clearly highlight the need for continued vigorous research in the technologically important area of transition in turbomachines.

14. SUBJECT TERMS	15. NUMBER OF PAGES
Transition; Turbulence; Turbomachinery	541
	16. PRICE CODE: A23

17. SECURITY CLASSIFICATION OF REPORT	18. SECURITY CLASSIFICATION OF THIS PAGE	19. SECURITY CLASSIFICATION OF ABSTRACT	20. LIMITATION OF ABSTRACT
Unclassified	Unclassified	Unclassified	